

Advances in Geophysical and Environmental
Mechanics and Mathematics

AGEM²

Kolumban Hutter
Yongqi Wang
Irina P. Chubarenko

Physics of Lakes

Volume 1:
Foundation of the Mathematical
and Physical Background

 Springer

Advances in Geophysical and Environmental Mechanics and Mathematics

Series Editor: Professor Kolumban Hutter

Board of Editors

Aeolean Transport, Sediment Transport, Granular Flow

Prof. Hans Herrmann
Institut für Baustoffe
Departement Bau, Umwelt und Geomatik
HIF E 12/ETH Hönggerberg
8093 Zürich, Switzerland
hjherrmann@ethz.ch

Avalanches, Landslides, Debris Flows, Pyroclastic Flows, Volcanology

Prof E. Bruce Pitman
Department of Mathematics
University of Buffalo
Buffalo, N. Y. 14260, USA
Pitman@buffalo.edu

Hydrological Sciences

Prof. Vijay P. Singh
Water Resources Program
Department of Civil and Environmental Engineering
Louisiana State University
Baton Rouge, LA 70803-6405, USA

Nonlinear Geophysics

Prof. Efim Pelinovsky
Institute of Applied Physics
46 Uljanov Street
603950 Nizhni Novgorod, Russia
enpeli@mail.ru

Planetology, Outer Space Mechanics

Prof Heikki Salo
Division of Astronomy
Department of Physical Sciences
University of Oulu
90570 Oulu, Finland

Glaciology, Ice Sheet and Ice Shelf Dynamics, Planetary Ices

Prof. Dr. Ralf Greve
Institute of Low Temperature Science
Hokkaido University
Kita-19, Nishi-8, Kita-ku
Sapporo 060-0819, Japan
greve@lowtem.hokudai.ac.jp
<http://www.ice.lowtem.hokudai.ac.jp/~greve/>

Kolumban Hutter · Yongqi Wang ·
Irina P. Chubarenko

Physics of Lakes

Volume 1: Foundation of the Mathematical
and Physical Background

 Springer

Prof. Dr. Kolumban Hutter
ETH Zürich
c/o Versuchsanstalt für Wasserbau
Hydrologie und Glaziologie
Gloriastr. 37/39
8092 Zürich
ETH-Zentrum
Switzerland
hutter@vaw.baug.ethz.ch

PD. Dr. Yongqi Wang
Chair of Fluid Dynamics
Department of Mechanical Engineering
Darmstadt University of Technology
Petersenstr. 30
64287 Darmstadt
Germany
wang@fdy.tu-darmstadt.de

Dr. Irina P. Chubarenko
Russian Academy of Sciences
P.P. Shirshov Institute of
Oceanology
prospect Mira 1
236000 Kaliningrad
Russia
irina_chubarenko@mail.ru

ISSN 1866-8348 e-ISSN 1866-8356
ISBN 978-3-642-15177-4 e-ISBN 978-3-642-15178-1
DOI 10.1007/978-3-642-15178-1
Springer Heidelberg Dordrecht London New York

Library of Congress Control Number: 2010936078

© Springer-Verlag Berlin Heidelberg 2011

This work is subject to copyright. All rights are reserved, whether the whole or part of the material is concerned, specifically the rights of translation, reprinting, reuse of illustrations, recitation, broadcasting, reproduction on microfilm or in any other way, and storage in data banks. Duplication of this publication or parts thereof is permitted only under the provisions of the German Copyright Law of September 9, 1965, in its current version, and permission for use must always be obtained from Springer. Violations are liable to prosecution under the German Copyright Law.

The use of general descriptive names, registered names, trademarks, etc. in this publication does not imply, even in the absence of a specific statement, that such names are exempt from the relevant protective laws and regulations and therefore free for general use.

Cover design: deblik, Berlin

Printed on acid-free paper

Springer is part of Springer Science+Business Media (www.springer.com)

*This book series on Physics
of Lakes is dedicated
in memoriam to
Professor CLIFFORD H. MORTIMER (1911–2010)
and to
Professor LAWRENCE A. MYSAK
mentors, teachers and friends*

Preface to the Book Series

An integrated view of *Physics of Lakes* requires expert knowledge in different specialities which are hardly found in single scientists. Even in a team the overall subject must be restricted; this has also been done here, as we only treat in this book series the *geophysical aspects of fluid dynamics*. Being applied to very complicated natural objects and phenomena, this science traditionally uses three main complementary approaches: *theoretical description*, *field observation* and (numerical, laboratory and other kinds of) *modelling*. The present work extensively uses all three approaches, this way providing to the reader an opportunity to build a coherent view of the entire subject at once – from the introduction of governing equations to various field phenomena, observed in real lakes. Several features, we believe, will make the series of especial interest for a wide range of students and scientists of geophysical interest as well as specialists in physical limnology. Before plunging into the main focus of lake physics we start with a detailed introduction of the main mathematical rules and the basic laws of classical physics; this makes further work with equations and their solutions much easier for readers without solid knowledge in the common trade of the background of mathematics and physics of continuous systems – biologists, chemists and ecologists. These sciences are today the most active branches in limnology and are utterly needed for the development of modern society; thus, an easily available physical background for them cannot be overestimated. A feature of this treatise is a consolidated view expressed in its three books of a wide panoramic overlook of various lake phenomena, inherent in physical oceanography and a fairly thorough theoretical treatment of fluid mechanics. This way, the reader will find here both the mathematical background and general physical laws and considerations of natural phenomena with their driving mechanisms (waves, turbulence, wind action, convection, etc.) and also a zoo of field examples from many lakes on our Globe. Special attention is devoted to the dynamic response of lakes on their free surface and in their interior, perhaps best coined as the climatology in response to external driving mechanisms – wind action and seasonal input of solar energy. These subjects reflect the many years of professional interests of the authors.

The content of the books and the manner of the presentation are, of course, significantly influenced by the composition of the authors' team. Being professionals of slightly different branches of the same science (limnology, fluid dynamics and oceanography), we tried to present lake physics in the most coherent way, extracting

important kernels from all the mentioned fields. The differences in opinions, what procedure might be the optimal approach in presenting a certain topic have occasionally been quite extensive, requiring compromises, but we believe that the interference, rather than simple sum, of our knowledge contributed to an enhancement of the present product than would have been reached otherwise. An additional joy for us is national composition of our international team; translation of this Preface from English into our native languages can be directly understood by more than 70% of the Earth population.

The subjects of this treatise on *Physics of Lakes*, divided into three volumes, cover the following topics.

VOLUME 1: Physics of Lakes – Formulation of the Mathematical and Physical Background

It commences in the introduction with a general, word-only motivation by describing some striking phenomena, which characterise the motion of lake water on the surface, in the interior of lakes and then relate these motions to the density distribution. It lists a large number of lakes on the Earth and describes their morphology and the causes of their response to the driving environment.

Because physics of lakes cannot be described without the language used in mathematics and only limited college knowledge calculus and classical NEWTONian physics is pre-assumed, these subjects are introduced first by using the most simple approach with utmost care and continuing with increasing complexity and elegance. This process leads to the presentation of the fundamental equations of lake hydrodynamics in the form of ‘primitive equations’ to a detailed treatment of angular momentum and vorticity. A chapter on linear water waves then opens the forum to the dynamics in water bodies with free surface. Stratification is the cause of large internal motions; this is demonstrated in a chapter discussing the role of the distribution of mass in bounded water bodies. Stratification is chiefly governed by the seasonal variation of the solar irradiation and its transformation by turbulence. The latter and the circulation dynamics are built on input of wind shear at the surface. The early theory of circulation dynamics with and without the effect of the rotation of the Earth rounds off this first book into the dynamics of lakes. A chapter on turbulence modelling and a further chapter collecting the phenomenological coefficients of water complete this book on the foundations of the mathematics and physics of lakes.

VOLUME 2: Physics of Lakes – Lakes as Oscillators

The overwhelming focus in this volume of the treatise is on linear waves in homogeneous and stratified lakes on the rotating Earth. It comprises 12 chapters, starting with rotating linear shallow-water waves and demonstrating their classification into gravity and ROSSBY waves for homogeneous and stratified water bodies. This leads

naturally to the analysis of gravity waves in unbounded, semi-bounded and bounded domains of constant depth: KELVIN, inertial and POINCARÉ waves, reflection of such waves at the end of a gulf and their description in sealed basins as so-called inertial waves proper. The particular application to gravity waves in circular and elliptical basins of constant depth then builds further confidence towards the treatment of barotropic and baroclinic basin-wide wave dynamics affected by the rotation of the Earth. The classical analytical approach to the baroclinic motion in lakes is done using the two-layer approximation. Recent observations have focused on higher order baroclinicity, a topic dealt with in two chapters. Whole lake responses are illustrated in barotropic and baroclinic wave analyses in Lake Onega¹ and Lake Lugano, respectively, with detailed comparisons of field data. The final four chapters are then devoted to a detailed presentation of topographic ROSSBY waves and the generalized CHRYSTAL equations and their identification by field observations.

VOLUME 3: Physics of Lakes – Methods of Understanding Lakes as Components of the Geophysical Environment

Red line of this volume is the presentation of different methods of investigation of processes taking place in real lakes. Part I is devoted to numerical modelling approaches and techniques, applied to demonstrate the response of a lake to wind forcing. Numerical methods for convectively dominated problems are compared, as well as different numerical treatments of advection terms and subgrid turbulence parameterisation. Methods and tools of field measurements are laid down in Part II, including the presentation of principles of operation of commonly used current, temperature, conductivity, pressure and other sensors, along with modern techniques of measurement in the field. Basic rules of time series analysis are summarised. Laboratory experimentation, presented in Part III, is introduced by an account of dimensional analysis. Results of laboratory experiments on large-amplitude non-linear oscillations, wave transformation and meromixis and convective exchange flows in basins with sloping bottom are presented. Combined presentations of field, numerical and laboratory approaches build a general view of present-day methods of physical investigations in limnology.

Lake physics is a boundless subject embracing a great variety of questions. Some materials on the seasonal water cycle, stratification and various mixing and stirring mechanisms have been collected by us but are still not included in the treatise. It may hopefully be summarised in the fourth volume.

Zürich, Switzerland
Darmstadt, Germany
Kaliningrad, Russia
June 2010

Kolumban Hutter
Yongqi Wang
Irina P. Chubarenko

¹ In today's Russian, 'Onega' and 'Onego' are both in use. In this book we use 'Onega'.

Vorwort zur Buchreihe

Eine übergeordnete Betrachtungsweise von *Physik der Seen* verlangt überdurchschnittliche Kenntnisse in unterschiedlichsten Spezialgebieten, die man kaum in einer einzelnen Person vereinigt findet. Selbst innerhalb eines Teams muss das übergeordnete Thema eingeschränkt werden; das ist auch hier getan worden, da wir in diesen Bänden der Seenphysik nur *geophysikalische Belange* der *Fluiddynamik* behandeln. Dieses Gebiet der Strömungsmechanik, hier angewendet auf ziemlich komplizierte natürliche Objekte und Phänomene, verwendet traditionell drei unterschiedliche, aber komplementäre Vorgehensweisen: *Theoretische Beschreibungen*, *Feldbeobachtungen* und (numerische, Labor oder anderweitige) *Modellierung*. Das vorliegende Werk macht ausgedehnt Gebrauch von all diesen Methoden und gibt dem Leser so die Gelegenheit, eine kohärente Sichtweise über das gesamte Gebiet zu erarbeiten von einer Einführung in die Grundgleichungen bis zu den unterschiedlichsten Phänomenen, die man in realen Seen beobachten kann. Wir glauben, dass verschiedene Merkmale dieses Werk von speziellem Interesse macht für eine breite Leserschaft von Studierenden und Wissenschaftlern mit geophysikalischem Interesse, wie auch für Spezialisten der physikalischen Limnologie. Bevor wir jedoch eintauchen in das Zentrum der Seenphysik, starten wir mit einer detaillierten Einführung in die mathematischen Voraussetzungen und die grundlegenden Gesetze der klassischen Physik; dieses Vorgehen macht das Arbeiten mit Gleichungen und ihren Lösungen wesentlich leichter für all jene Leser, welche keine gründlichen Kenntnisse in der üblichen Anwendung der Mathematik und Physik von kontinuierlichen Systemen mitbringen, in der Regel angewandte Biologen, Chemiker und Ökologen. Diese Wissensgebiete gehören heute zu den aktivsten Gruppen der Limnologie und bilden daher die Spezialwissensgebiete, die für die Entwicklung der modernen Gesellschaft von großer Bedeutung sind. Eine leicht zugängliche Darbietung des physikalischen Hintergrundes kann nicht überschätzt werden. Ein Hauptzug dieses Werkes ist eine über drei Bände verteilte Betrachtungsweise, welche eine Übersicht über verschiedene Phänomene in Seen schafft, welche der physikalischen Ozeanographie zugeordnet sind und auf einer streng theoretischen Handhabung der Methoden der Fluidmechanik beruhen. So findet der Leser hier sowohl den mathematischen Hintergrund, die allgemeinen physikalischen Gesetze und deren Anwendung auf die natürlichen Phänomene der Seenphysik mit ihren Anregungsmechanismen (Wellen, Turbulenz, Windantrieb, Konvektion, etc.), wie

auch eine ganze Palette von Feldbeispielen vieler Seen dieser Erde. Spezielle Beachtung findet die dynamische Reaktion von Seen auf ihrer freien Oberfläche und in ihrem Innern, das Klima des Sees als Antwort der äusseren Antriebsmechanismen Wind-Antrieb, jahreszeitlicher Eintrag der Sonnenenergie. Diese Thematik umfasst die jahrelange Erfahrung der beruflichen Interessen der Autoren.

Der Inhalt der Bücher und die Art und Weise der Darstellung des Stoffes sind offensichtlich stark von der Zusammensetzung des Autorenteam beeinflusst. Als Repräsentanten von (leicht) unterschiedlichen Spezialgebieten derselben Wissenschaft (Limnologie, Fluidodynamik und Ozeanographie), haben wir uns bemüht, die Seenphysik in kohärenter Weise darzustellen und wichtige Elemente aller oben erwähnten Gebiete zu extrahieren. Meinungsunterschiede, wie ein Thema am optimalsten darzustellen sei, waren gelegentlich recht heftig und verlangten Kompromisse; wir glauben hingegen, dass die Interferenz unseres Wissens im Gegensatz zu einer einfachen Summe mehr zur Qualität des gegenwärtigen Produktes beigetragen hat als dies andernfalls der Fall gewesen wäre. Ein zusätzlicher Gewinn für uns ist die internationale Zusammensetzung des Teams. Die Übersetzung dieses Vorwortes aus dem Englischen in unsere Muttersprachen kann direkt verstanden werden von mehr als 70% der professionellen angesprochenen Bevölkerung dieser Erde.

Der Inhalt dieser Abhandlung über Seenphysik, aufgeteilt in drei Bände, umfasst die folgenden Themen:

BAND 1: Physik der Seen – Formulierung des mathematischen und physikalischen Hintergrundes

Der Band beginnt in der Einführung mit einer allgemeinen, formelfreien Motivation durch Beschreibung von gewissen, treffenden Phänomenen, welche die Bewegung des Seewassers an der Oberfläche und im Seeinnern betreffen und ordnen letztere der Verteilung der Dichte des Seewassers zu. Es wird zudem eine große Zahl von Seen auf dieser Erde gelistet und ihre Morphometrie charakterisiert, einschließlich der Beschreibung ihrer Verhaltensweise auf Grund der Reaktion auf die antreibenden Mechanismen.

Da die Physik von Seen nicht ohne die mathematische Sprache beschrieben werden kann, und da nur gerade die einfachsten Kenntnisse der Hochschulanalyse und der klassischen Physik vorausgesetzt werden, erfolgt eine Einführung in diese Themen anfänglich in der einfachsten möglichen Art und mit größter Sorgfalt; mit wachsender Gewöhnung und fortschreitender Komplexität wird dann aber schrittweise auf eine elegantere Schreibweise übergegangen. Dieser Prozess führt so (i) zur Darstellung der Grundgleichungen der Seen-Hydrodynamik in Form der primitiven Gleichungen, die direkt den physikalischen Bilanzen entsprechen, und (ii) zu einer detaillierten Behandlung des Drehimpulssatzes und der Wirbelbilanzgleichungen. Ein Kapitel über lineare Wasserwellen öffnet danach das Forum für die Dynamik von wassergefüllten Becken mit freier Oberfläche. Die Dichteschichtung ist Ursache für große interne Bewegungen, was in einem Kapitel demonstriert wird, in welchem

die Rolle der Verteilung der Masse in endlichen Becken untersucht wird. Schichtung wird hauptsächlich durch die jahreszeitliche Variation der Sonneneinstrahlung und deren Umformung durch Turbulenz gesteuert. Letztere sowie die Zirkulationsdynamik werden durch den Eintrag von Windschub an der Seeoberfläche gesteuert. Die frühe Theorie der Zirkulationsdynamik mit dem, bzw. ohne den, Einfluß der Erdrotation schließen dann den Themenkreis dieses ersten Bandes der Seendynamik. Ein Kapitel über turbulente Modellierung und ein weiteres Kapitel, das die phänomenologischen Koeffizienten von Wasser behandelt, vervollkommen diesen ersten Band über die Grundlagen der mathematischen und physikalischen Behandlung der Physik von Seen.

BAND 2: Physik der Seen – Seen als Oszillatoren

Das hauptsächliche Thema in diesem zweiten Band der Monographie *Physik der Seen* betrifft lineare Wellen in homogenen und geschichteten Seen auf der rotierenden Erde. Er umfasst zwölf Kapitel und beginnt mit linearen Wasserwellen auf der rotierenden Erde. Es werden Klassifikationen eingeführt, welche die Schwerewellen und ROSSBY-Wellen im begrenzten homogenen und im Schichtmedium charakterisieren. Dies führt in natürlicher Weise zur mathematischen Analyse von Schwerewellen im unbegrenzten und endlichen Medium mit konstanter Tiefe: KELVIN, Inertial- und POINCARÉ Wellen, Reflektion solcher Wellen am Ende eines Golfes und deren Beschreibung in vollkommen geschlossenen Becken als sogenannte eigentliche Inertialwellen (inertial waves proper). Die Anwendung von Gravitationswellen in kreisförmigen und elliptischen Becken konstanter Tiefe führt in natürlicher Weise zur interpretationsgerechten Behandlung von barotroper und barokliner beckenweiter Wellendynamik auf der rotierenden Erde. Das klassische analytische Vorgehen zur Beschreibung der baroklinen Bewegung in Seen wird mit der Zweischichten-Approximation gemacht. Neuere Beobachtungen an Seen haben sich jedoch auf das Erfassen der höheren Baroklinizität konzentriert. Diesem Thema werden zwei Kapitel gewidmet. Beckenweite Dynamik wird anhand von barotropen und baroklinen Studien des Onega Sees und Luganersees vorgenommen und mit ausgedehnten in-situ Messungen verglichen. Die letzten vier Kapitel werden der detaillierten Darstellung topographischer ROSSBY Wellen und den verallgemeinerten CHRYSTAL Gleichungen und deren Identifikation anhand von Feldmessungen gewidmet.

BAND 3: Physik der Seen – Methoden, die Seen als Komponenten des geophysikalischen Umfeldes verstehen

Der rote Faden in diesem Band ist die Entwicklung unterschiedlicher Methoden zur Charakterisierung von physikalischen Prozessen in natürlichen Seen. Teil I ist numerischen Modellierungsmethoden und -techniken gewidmet, welche

die Reaktion eines Sees auf die äusseren Windkräfte bestimmen. Numerische Methoden für verschiedene, von Konvektion dominierten Problemen, werden untereinander verglichen. Desgleichen werden unterschiedliche Schemata für die advektiven Terme in den bestimmenden partiellen Differenzialgleichungen und die Subgrid-Parametrisierung der Turbulenz getestet. In Teil II werden Methoden und Werkzeuge für Feldmessungen erläutert, und es werden die Arbeitsweisen von üblichen Strömungs-, Temperatur-, Leitfähigkeits-, Druck- und anderen Messgeräten vorgestellt bis hin zu den modernen Messtechniken, welche bei Feldmessungen eingesetzt werden. Die Grundregeln der Zeitreihenanalyse und statistischen Datenauswertung werden ebenfalls zusammengefaßt. Laborexperimentiertechniken werden im Teil III dargelegt und auf die Grundlage der Dimensionsanalyse abgestützt. Es werden Resultate vorgestellt von Laborexperimenten betreffend nichtlineare Schwingungen mit großer Amplitude, und es wird ihre Instabilität und Umwandlung durch Meromixis und konvektiven Austausch in Becken mit geneigten Topographien entlang ihrer Küstenlinien behandelt. Kombinierte Darstellung von Feldbeobachtungen, numerischen und Labormessdaten-Analysen stellen heute ganz allgemein den methodischen Zugang zur Interpretation von physikalischen Prozessen der Limnophysik her.

Physik der Seen ist ein sehr breites Gebiet, welches ein großes Spektrum von Fragestellungen umfasst. Gewisse Besonderheiten des jahreszeitlichen Wasserzyklus, Schichtung und unterschiedliche Mischungs- und Vermengungsmechanismen sind von uns studiert und angegangen worden, aber in diesem Werk noch nicht enthalten. Es ist zu wünschen, dass wir die Zeit und Energie aufbringen, diese in einem vierten Band zusammen zu fassen.

Zürich, Switzerland
Darmstadt, Germany
Kaliningrad, Russia
June 2010

Kolumban Hutter
Yongqi Wang
Irina P. Chubarenko

Предисловие к серии

Интегральное представление физики озер требует глубокого знания целого ряда различных специальностей, что вряд ли может быть достигнуто одним ученым. Даже коллективу авторов столь общую тему пришлось ограничить: в этой монографии рассматриваются только *геофизические* аспекты *динамики жидкости*. Имея дело со сложными природными объектами и явлениями, физическая лимнология традиционно использует три взаимодополняющих подхода: *теоретическое описание*, *натурные наблюдения* и (численное, лабораторное и другие виды) *моделирования*. Представленная работа в значительной степени использует все три подхода, давая читателю таким образом возможность построить максимально полное и согласованное представление о предмете – от вывода основных уравнений до исследования разнообразных явлений, наблюдаемых в реальных озерах.

Некоторые особенности этой серии, мы надеемся, сделают ее особенно привлекательной для широкого круга студентов, исследователей геофизической гидродинамики, специалистов в физической лимнологии. Прежде чем погрузиться в описание собственно физики озер, мы начинаем с детального введения основных математических правил и основополагающих законов классической физики; это облегчит дальнейшую работу с уравнениями тем читателям, у кого нет специального образования в математике и физике сплошных сред – биологов, химиков, экологов. Именно эти области лимнологии сегодня развиваются наиболее активно и особенно нужны для развития современного общества; следовательно, доступность изложения для них физических основ трудно переоценить.

Характерной чертой этой серии является обобщенный подход к изложению материала, сочетающий широкий панорамный обзор явлений, присущий физической океанографии, с глубоким и тщательным теоретическим рассмотрением, свойственным механике жидкости. Таким образом, читатель найдет здесь и математические основы, и основополагающие физические законы, и рассмотрение конкретных природных явлений вместе с их движущими механизмами (волны, турбулентность, действие ветра, конвекция и т.д.), и широкий спектр примеров натурных наблюдений во многих озерах нашей планеты. Особое внимание уделяется динамическому отклику озер и их свободной

поверхности на внешние факторы – действие ветра и сезонное поступление солнечной энергии, что обусловлено многолетним профессиональным интересом авторов.

Содержание книг и манера представления материала, конечно, существенно зависит от состава авторского коллектива. Будучи представителями разных школ и профессионалами в нескольких различных аспектах одной и той же науки – в лимнологии, механике жидкости и океанологии – мы пытались представить физику озер наиболее гармоничным образом, извлекая ценные зерна из каждой области знаний. Разница мнений о том, какой путь мог бы быть оптимальнее в представлении того или иного материала, была иногда довольно значительна, требуя компромиссов; мы искренне надеемся, что результатом явилась не простая сумма, а реальная интерференция наших знаний, и финальный продукт от этого заметно выиграл. Еще один штрих к возникающей объемной картине добавляет национальный состав нашего интернационального коллектива: перевод этого Предисловия с английского на наши родные языки может быть непосредственно понят более чем 70% населения Земли.

Материал, изложенный в монографии **Физика Озер**, разделен на три тома:

ТОМ 1: Физика Озер – Математические и Физические Основы

Введение начинается с описания поразительных явлений, связанных с движением воды в озере и на его поверхности; затем эти движения соотносятся с распределением плотности. Далее перечисляются наиболее крупные озера Земли, описывается их морфология и характеризуются основные причины их отклика на воздействие окружающей среды.

Поскольку физика озер не может быть описана без языка математики, а у читателя предполагаются только ограниченные школьные знания об исчислении и классической НЬЮТОНовой физике, эти области вводятся сначала максимально просто, а затем исследование продолжается с нарастающей сложностью и элегантностью. Этот процесс приводит к представлению фундаментальных уравнений Гидродинамики Озер в форме так называемых 'примитивных уравнений', вплоть до детального описания вращательного момента и завихренности. Затем обсуждение динамики вод в бассейнах со свободной поверхностью открывается главой о свойствах линейных волн. Присутствие стратификации является основным условием возникновения движений вод внутри озера; это демонстрируется в главе, обсуждающей роль распределения масс в ограниченных бассейнах. Стратификация вод в значительной степени управляется сезонными вариациями солнечной радиации и ее трансформацией турбулентностью.

Последняя, так же как циркуляция вод, обусловлена главным образом действием ветра на поверхность. Изложение основ теории циркуляции вод с учетом и без учета влияния вращения Земли включает рассмотрение динамики вод в озерах. Главы о методах моделирования турбулентности и феноменологических свойствах воды заканчивают эту книгу об основах математики и физики озер.

ТОМ 2: Физика Озер – Озера как Осцилляторы

Основная тема этого тома серии – линейные волны в однородных и стратифицированных озерах на вращающейся Земле. Он содержит 12 глав. Сначала рассматриваются линейные волны на мелкой воде во вращающейся жидкости и дается их классификация на гравитационные волны и волны РОССБИ в однородных и стратифицированных бассейнах. Это естественным образом приводит к анализу гравитационных волн в неограниченных, полуограниченных и ограниченных бассейнах с постоянной глубиной: волн КЕЛЬВИНА, инерционных волн и волн ПУАНКАРЕ, отражения этих волн от закрытого конца залива и их описания в закрытых бассейнах как так называемых ‘собственно инерционных волн’. Приложение к гравитационным волнам в круглых и эллиптических бассейнах постоянной глубины продолжает обсуждение баротропной и бароклинной динамики волн во вращающемся бассейне. Классический аналитический подход к бароклиным движениям в озерах продемонстрирован с использованием двухслойной аппроксимации. Современные работы фокусируются на исследовании бароклинности более высоких порядков, что рассматривается в последующих двух главах. Отклик озера как целого проиллюстрирован анализом баротропных и бароклиных волн в озерах Онежском и Лугано и сопровождается детальным сравнением с натурными данными. Последние четыре главы посвящены подробному анализу топографических волн РОССБИ и обобщенных уравнений КРИСТАЛА и их идентификации в натурных данных.

Том 3: Физика Озер – Методы Исследования Озер в их Геофизическом Окружении

Представление различных *методов исследования* процессов, протекающих в реальных озерах, является основной темой этого тома. Часть I посвящена подходам и техникам *численного моделирования*, используемым для демонстрации отклика озер на действие ветра. Сравниваются численные методы, используемые для описания движений, доминируемых конвекцией; рассматриваются разные численные алгоритмы для расчета адвективного члена и параметризация подсеточной турбулентности. Методы и средства

натурных измерений изложены в Части II, включая описание принципов действия типичных сенсоров для измерения течений, температуры, электропроводности, давления и других, а также современные техники полевых измерений. Отдельная глава суммирует основные правила анализа временных рядов. *Лабораторное моделирование*, представленное в Части III, вводится началами анализа размерностей. Представлены результаты лабораторных экспериментов по нелинейным колебаниям большой амплитуды, трансформации волн и частичному перемешиванию, обменным течениям конвективной природы в бассейнах с наклонным дном. Совместное представление натурных, численных и лабораторных подходов позволяет в результате выстроить общий вид современных методов физических исследований в лимнологии.

Физика озер – тема, не имеющая границ, охватывающая огромный круг разнообразных вопросов. Собранный нами материал о сезонном цикле, различных механизмах перемешивания, размешивания и установления стратификации не включен в трехтомник, и, мы надеемся, может быть суммирован в четвертом томе серии.

Цюрих, Швейцария
Вена, Австрия
Калининград, Россия
июнь 2010

Колумбан Хуттер
Йонгки Ванг
Ирина Чубаренко

本书系列序言

湖泊物理学的综述，需要本领域不同专业的知识，这对于一个单独著述的学者是很难兼备的。甚至对于三人作者团队，我们也必须限制所著述研究的范围。本书系列专注于地球物理学的流体动力学研究。目前科学界对复杂自然现象的研究，通常采用三种互补的研究方法，即：理论描述，场观测和(数值的，试验的和其它方式的)模拟。本专著亦充分运用这三种方法，以期提供给读者一个机会，从理论方程的引入到真实湖泊中所观看到的各种自然现象，建立一套对该领域清晰连贯的看法。我们相信本书系列的一些特色主题将吸引湖泊物理学专家们，以及众多对地球物理学有特别兴趣的学生和学者。

在进入湖泊物理的核心之前，我们先从详细的数学前提和基本物理定律的引入开始，这将使进一步的方程建立及求解变得容易理解，特别是对生物学家，化学家，生态学家而言，而他们从事的正是目前湖泊物理学研究中最具活力并对现代社会的发展深具影响的领域。在这些科学学者看来是高深的物理知识应成为容易利用的工具。本书系列分为三部，目的是要获得对湖泊中各种物理现象的一个全面了解。所采用的方法是建立在对流体力学精确的理论基础上。读者可以从中找到相关的数学基础，普遍的物理定律，也包括他们在湖泊物理中对自然现象上的应用和理解，以及这些现象产生的力学原理(比如：水波，湍流，风驱动，对流等)，从而得到对湖泊物理场的一个宏观印象。湖泊对其自由表面和内部特性的动力学响应，以及对外部驱动，如风力和太阳能的季节性摄入气象现象的反应也会被专门讨论。这些方面均涉及作者多年的相关工作经验和兴趣。

本系列所涉及的内容及描述的方式受到作者组合的深刻影响。由于各自不尽相同的专业背景(湖泊动力学，流体力学和海洋力学)，我们尝试以一个协调一致的方式介绍湖泊物理学和萃取所有上面提及领域的重要基础。作者因意见不同，比如怎样更好地描述一个相关的主题，有时甚至会有激烈的争辩，亦需要相互妥协。然而我们相信与所有作者知识的简单叠加相比，这样的交叉互补对本专著的质量是一个重要的贡献。对我们来说，这其中更大的乐趣是一个国际合作团队的形成。本序言从英语到我们各自母语的翻译将使得地球上超过 70% 的人们可以直接理解。

这个三部曲的系列将涵盖湖泊物理学的以下方面：

第一部：湖泊物理学 ----- 数学和物理学基础的构成

本书将从一些相关现象的描述开始。这些现象与湖水在表面和内部的运动及水密度分布紧密相关。地球上许多湖泊被一一罗列，它们的地貌特征及对驱动力的响应特点也会被描述。

由于不通过数学语言，人们无法描述湖泊物理特性，并且我们假设读者仅具备最基本的大学数学解析和牛顿物理学基础，湖泊物理描述首先以一种尽可能简单的方式小心地被引入，其理论描述的复杂性将逐步增加。湖泊水力学的基本方程，物理学平衡和角动量守恒及涡流守恒方程随之被导出。关于线性波的章节将引出含有自由表面水体的动力学讨论。水的密度分层是产生强烈内部运动的原因，一个讨论在水体中质量分布影响的章节将论证这个特性。这样的水密度分层主要是由于太阳辐射的季节性变化以及由湍流产生的输运所控制，后者以及水环流动力学是由风力在水表面的作用而产生。早期环流动力学理论的引入，包括和不包括地球自转影响，将带领读者进入这本书的湖泊动力学部分。本系列书的第一部将以阐述湍流模拟和水的表征参数为结束。

第二部：湖泊物理学 ----- 作为振荡器的湖泊

本书系列第二部将主要涉及受地球自转影响的匀质和密度分层湖泊中的线性波。包括 12 个章节，从在转动地球上的线性浅水波的讨论开始，引入波的分类，以便描述在均质和分层水体中的重力波和 Rossby 波。这将自然引出在无限大，半有限和有限的等深水域中重力波的分析: Kelvin, 惯性 Poincare 波。也包括波在港湾端部的反射和在全封闭水域里惯性波的描述。重力波在圆形或椭圆形等深水域中的应用自然引入了在旋转地球上正压和斜压波的动力学处理。在湖泊中斜压运动将首先用二层近似这种经典方法来分析。观测主要集中在高阶斜压性的捕捉上。两个章节将涉及此内容。湖泊作为一个整体的特性，将通过在 Onega 湖和 Luganer 湖的正压和斜压运动的研究来讨论，相关测量数据将被仔细地对比。本部书最后四章将讨论地貌产生的 Rossby 以及它们在场观测中的识别。

第三部：湖泊物理学 ----- 了解湖泊的方法

本部书聚焦于介绍研究天然湖泊物理过程的不同方法。第一部分涉及数值方法和技术。这些被用来研究湖泊对外部风力的响应。针对各种对流起主导作用的问题，不同的数值方法被加以对比，不同的数值格式将被应用到给定偏微分方程的对流项和湍流的模拟上，并加以测试。第二部分包括有关测量的

方法和仪器。传统的在大规模场观测中使用的流速，温度，传导，压力和其它测量仪器的操作原理将会被介绍。其中也包括一些现代的测量仪器。时间序列分析和统计数据处理的基本规则将被总结。第三部分阐述了一些建立在量纲分析基础上的实验室试验技术。该部分也介绍和讨论了与大幅值的非线性波动相关的实验结果，以及与其相关的稳定性，在倾斜底部的局部混合和对流等。场观测，数值和实验数据分析构成了当今理解湖泊物理现象的一个通用方法。

湖泊物理学是一个广泛的学科，我们也搜集了比如季节性循环，密度分层及各种混合机制等的相关材料。但是本书系列没有包括这些内容。我们希望，在有时间和精力基础上，能出版这个系列的第四部书，以期对这些内容加以总结。

瑞士 Zurich,
德国 Darmstadt
俄罗斯 Kaliningrad
2010年6月

K. Hutter
王永奇
I. Chubarenko

Acknowledgements

This book series is an outgrowth of more than three decades of research and teaching activities, and so, the institutions which supported these activities deserve an early word of appreciation. The precursors to the books started as lecture notes on hydrodynamics of lakes, in particular ‘Waves in the Ocean and Lakes’ which KH held since the early 1980s of the last century in the Department of Mechanics of Darmstadt University of Technology and for some years also at the Swiss Federal Institute of Technology (ETH) in Zurich to upper level students of Earth Sciences, Physics, Engineering and Mathematics. Advanced courses, addressed to graduate students and postdoctoral fellows, were also held on subtopics of lake physics at the International Centre for Mechanical Sciences (CISM) in Udine, Italy (1983), and published as ‘Lake Hydrodynamics’ [1] and as an Article in the Encyclopedia of Fluid Mechanics [2]. During the teaching and research years 1987–2006, considerable activity was devoted to physics of lakes, which is documented in the reference list for diploma theses [9–18], doctoral dissertations [19–21, 25–28] and habilitation theses [29, 30]. Out of this grew a particularly fruitful collaboration with Dr.-Ing. habil YONGQI WANG (YW), who serves as second author of this book series. The incentive to write a broader text on the subject grew during a research project in the years 2001–2004 in the Physical Limnology Group of the Limnology Institute of Constance University, Germany, in its Collaborative Research Projects ‘Transport Processes in Lake Constance’ and ‘Littoral of Lake Constance’. In the field campaigns conducted by the Limnological Institute, external research Institutes were also involved. Collaboration was initiated with Drs. IRINA (IC) and BORIS CHUBARENKO from the Atlantic Branch of the P. P. Shirshov Institute of Oceanology of the Russian Academy of Sciences, Kaliningrad, who were leading in the conduction of systematic experiments, data analysis and interpretation, mostly executed by IC, who joined the book series as third author.

In the mid-1970s of the last century, KH’s activities within the Laboratory of Hydraulics, Hydrology and Glaciology (VAW), at the Swiss Federal Institute of Technology, Zurich, were shifted from glaciology to physical limnology. A new small research unit, dealing with hydrodynamics of lakes, was created. Generous financial support was provided. The group received expert advice from Prof. J. SÜNDERMANN at the University of Hannover (later Centre for Ocean and Climate Research, University of Hamburg), the late Prof. W. KRAUSS, formerly at the

Leibnitz Institute for Ocean Sciences, University of Kiel, and in particular, the late Prof. C.H. MORTIMER, Centre for Great Lakes Studies, University of Wisconsin, Milwaukee. The synoptic field campaigns, conducted in Lake Zurich, 1978; Lake of Lugano, 1979 and 1984; Lake Constance, 1993, were greatly influenced by them. In the late 1970s and early 1980s Prof. MORTIMER spent several visiting assignments with the group, looking at the Lake Zurich data of 1978 and teaching us his outstanding graphical and statistical methods by which time series data, taken synoptically at several moorings with thermistor chains and current meters, could be combined to extract the physics and thus find an understanding of the underlying physical processes. Later, during the academic year 1982/1983, Prof. L.A. MYSK, now at Department of Atmospheric and Ocean Sciences at McGill University, Montreal, spent his sabbatical with the group; his influence was of equal significance as that of Prof. C.H. MORTIMER, but complementary. The papers on barotropic, baroclinic gravity and ROSSBY wave dynamics in Alpine lakes, summarised in this book, owe much to Profs. C.H. MORTIMER's and MYSK's advice. The work of the lake group at VAW has also greatly benefited from Dr. D.J. SCHWAB of NOAA's Great Lakes Environmental Research Laboratory (GLERL), Ann Arbor, Michigan, and from associations with doctoral students (now Dr.) GABRIEL RAGGIO [22] (now Dr. Prof.), THOMAS STOCKER [6, 24] (now Dr.), JOHANNES SANDER [23] and research assistant GORDON OMAN [3, 4] as well as Dr. Mike Laska [5] with whom gravity waves, topographic ROSSBY waves, non-linear internal waves in channels and wind-induced currents in stratified and homogeneous Lake Zurich were studied. Moreover, a long and very fruitful early collaboration ought to be mentioned with a group of community college teachers in Lugano and Melide in the South (Italian) Canton of Switzerland: Dr. F. ZAMBONI, Dr. C. SPINEDI and Mr. G. SALVADÈ, with whom a very active collaboration existed between 1978 and 1987 on research of physical limnology in Lake of Lugano. It is seldom that such a collaboration between research professionals and 'hobby scientists' leads to a considerable surge of substantial results. Volume 2 of this treatise will demonstrate in several chapters that this collaboration has been very fruitful.

In the Department of Mechanics at Darmstadt University of Technology in (1987–2006), the focus of lake research was on laboratory experimental techniques and theoretical–numerical methods of non-linear internal waves and barotropic and baroclinic circulation dynamics. A fortunate association with the Limnological Institute of the University of Constance initiated by Prof. M. TILZER, first casually and later more formally, within the collaborative research programs 'Transport Processes in Lake Constance' and 'Littoral of Lake Constance', led by Profs. P. BÖGER and K.O. ROTHHAUPT, made it possible that field work could be pursued, though at a somewhat moderate pace. Much of the fundamental work, which was done in Darmstadt in diploma (M.Sc), Ph.D. and habilitation dissertations (cf. the mentioned references), has been motivated by this collaboration, as well as collaboration within this program with Drs. B. and I. CHUBARENKO from the Atlantic Branch of the P.P. Shirshov Institute of Oceanology, Russian Academy of Sciences, Kaliningrad, who had visiting assignments within this program. Throughout this 'Constance Period'

Dr. E. BÄUERLE and (until 1997) Dr. K. JÖHNK [29] were very supportive through their own work, but also in many helping discussions, field work planning and measuring assignments.

In addition to all the above-mentioned scientists Drs. N. STASHCHUK and V. VLASENKO, now at the School of Earth, Ocean and Environmental Sciences, Plymouth University, UK, ought to be mentioned as well. They spent more than four years, from 1999 to 2003, in the fluid mechanics research group within the Department of Mechanics at Darmstadt University of Technology, working on a project funded by the Deutsche Forschungsgemeinschaft, mainly concentrating on non-linear wave dynamics and convection in the baroclinic ocean. Their work, which was begun already in their Ph.D. dissertations and V. VLASENKO's doctoral thesis (corresponding to the habilitation or D.Sc. in the West) in the Institute of Oceanology, Ukrainian Academy of Sciences, Sevastopol, provided a substantial boost to the lake research of the small group at that time. Apart from a number of important peer-reviewed papers in oceanographic periodicals the collaboration with them led to the book 'Baroclinic Tides – Theoretical Modeling and Observational Evidence' [8]. V. VLASENKO also took the initiative to formulate with KH an INTAS project (funded from 03.2004 to 02.2007, grant Nr. 03-51-37 28) on 'Strongly Nonlinear Internal Waves in Lakes: Generation, Transformation, Meromixis' with collaboration of KH from Darmstadt, V. VLASENKO and N. STASHCHUK from Plymouth, Prof. V. MADERICH and associates (from the Institute of Mathematical Machine and System Problems) and Prof. V. NIKISHOV and associates (from the Institute of Hydrodynamics), both of the Ukrainian Academy of Sciences in Kiev, Prof. N. FILATOV (and associates) from the Northern Water Problems Institute, Russian Academy of Sciences, Petrozavodsk, Prof. E. PELINOVSKY (and associates), Institute of Applied Physics, Russian Academy of Sciences, Nizhny Novgorod. The work of this INTAS project will be reviewed in a separate book, co-authored by the above-mentioned scientists, one reason why topics covered in that book are treated less systematically in this book series.

Our work has generously been supported through the years by the Institutions by which we were applied. KH and YW were additionally funded by the Swiss National Science foundation (KH, 1975–1987); by the German Research Foundation (Deutsche Forschungsgemeinschaft) (KH and YW, 1987–2006); German Academic Research Exchange Service (Deutscher Akademischer Austauschdienst); Alexander von Humboldt Foundation (1987–2006); INTAS, Brussels (2004–2007). B. & I. Ch.'s visits to the Limnological Institute, Constance University were funded by the German Research Foundation; further collaboration was supported by the German Academic Exchange Service, by a Collaborative Linkage Grant by NATO and the Russian Foundation for Basic Research. To all these funding agencies we express our sincere thanks. Only such sources make it possible that research ideas can effectively and efficiently be put into practice.

In writing this treatise, KH as a retired member of Darmstadt University of Technology wishes to acknowledge the generosity offered by Profs H.-E. MINOR and R. BOES for the free access to the institute's facilities at VAW-ETH, of which

KH is not a member. He also thanks all the other members of VAW for their endurance to cope with his presence. He particularly acknowledges the help received from BRUNO NEDELA, who drew a great many of the illustrations in the second volume from hand-drafted and scanned ‘originals’. His input is explicitly visible in the quality of these illustrations. Moreover, Drs. E. VASILIEVA and S. KELITAREVA helped in TEXing some manuscript elements and the production of Indices.

Finally, we all thank Springer Verlag for the support, in particular Dr. C. BENDALL and A. OELSCHLÄGER for their efforts in the publication process of the books.

Zürich, Switzerland
Darmstadt, Germany
Kaliningrad, Russia
June 2010

Kolumban Hutter
Yongqi Wang
Irina P. Chubarenko

References

Books, Reports

1. Hutter, K.: *Lake Hydrodynamics*. CISM Courses and Lectures No 286, Springer New York, NY, 341 p. (1984)
2. Hutter, K.: Hydrodynamic modeling of lakes. Chap. 22. In: *Encyclopedia of Fluid Mechanics* (ed. Chermesinoff). Gulf Publishing Company Houston, 6, 897–998 (1987)
3. Oman, G.: *Das Verhalten des geschichteten Zürichsees unter äusseren Windlasten. Resultate eines numerischen Modells. Sein Vergleich mit Beobachtungen*. Mitteilung Nr 61, der Versuchsanstalt für Wasserbau, Hydrologie und Glaziologie and der ETHZ 185 p. (1982)
4. Hutter, K., Oman G. and Ramming, H.-G.: *Wind-bedingte Strömungen des homogenen Zürichsees*. Mitteilung Nr 60 der Versuchsanstalt für Wasserbau, Hydrologie und Glaziologie and der ETHZ, 123 p. (1982)
5. Laska, M.: *Characteristics and modelling of the physical limnology processes*. Mitteilung Nr 54, der Versuchsanstalt für Wasserbau, Hydrologie und Glaziologie and der ETHZ 290 p. (1982)
6. Stocker, T. and Hutter, K.: *A model for topographic Rossby waves in channels and lakes*. Mitteilungen der Versuchsanstalt für Wasserbau, Hydrologie und Glaziologie, ETH Zürich, No 76, 1–154 (1985)
7. Stocker, T. and Hutter, K.: *Topographic waves in channels and lakes on the f-plane*. Lecture Notes on Coastal and Estuarine Studies, Vol. 9, Springer, Berlin (1987)
8. Vlasenko, V., Stashchuk, N. and Hutter, K.: *Baroclinic Tides – Theoretical Modelling and Observational Evidence*. Cambridge University Press, Cambridge (2004)

Diploma (M. Sc.) Theses

9. Bauer, G.: *Windangeregte Strömungen im geschichteten Bodensee–Modellrechnungen und Feldbeobachtungen*. Diplomarbeit am Fachbereich Mechanik, Darmstadt University of Technology, 169 p. (July 1993)

10. Franke, V. *Physikalisch-biologische Kopplung zur Modellierung des Algenwachstums in Seen*. Diplomarbeit am Fachbereich Mechanik, Darmstadt University of Technology, 112 p. (November 1996)
11. Güting, P.: *Windgetriebene Strömungen und Diffusion eines Tracers* Diplomarbeit am Fachbereich Mechanik, Darmstadt University of Technology, 61 p. (Februar 1994)
12. Hüttemann, H.: *Modulation interner Wasserwellen durch Variation der Bodentopographie* Diplomarbeit am Fachbereich Mechanik, Darmstadt University of Technology, 110 p. (September 1997)
13. Maurer, J.: *Skaleneffekte bei internen Wellen im Zweischichtenfluid mit topographischen Erhebungen*. Diplomarbeit am Fachbereich Mechanik, Darmstadt University of Technology, 112 p. (November 1993)
14. Salzner, E.: *Energieeinträge in Seen*. Diplomarbeit am Fachbereich Mechanik, Darmstadt University of Technology, 98 p. (Dezember 1996)
15. Umlauf, L.: *Strömungsdynamik im Ammersee*. Diplomarbeit am Fachbereich Mechanik, Darmstadt University of Technology 151 p. (November 1993)
16. Wessels, F.: *Wechselwirkung interner Wellen im Zweischichtenfluid mit topographischen Erhebungen*. Diplomarbeit am Fachbereich Mechanik, Darmstadt University of Technology, 69 p. (November 1993)
17. Weimar, V.: *Nichtlineare, durch Randschwingung angeregte Wellen im Zweischichtenfluid*. Diplomarbeit am Fachbereich Mechanik, Darmstadt University of Technology, 65 p. (April 1995)
18. Zeitler, M.: *Vergleich zweier eindimensionaler Turbulenzmodelle der Seenphysik* Diplomarbeit am Fachbereich Mechanik, Darmstadt University of Technology, 112 p. (November 1996)

Doctoral Dissertations

19. Diebels, S.: *Interne Wellen – Ein Modell, das Nichtlinearität, Dispersion, Corioliseffekte und variable Topographie berücksichtigt*. Doctoral Dissertation, TH Darmstadt, 1–173, TH Darmstadt (1991)
20. Güting, P.: *Dreidimensionale Berechnung windgetriebener Strömungen mit einem $k - \epsilon$ -Modell in idealisierten Becken und dem Bodensee*. Doctoral Dissertation, TU Darmstadt, 1–343 (1998)
21. Lorke, A.: *Turbulenz und Mischung in einem polymiktischen See – Untersuchungen auf der Basis von Mikrostrukturmessungen*. Doctoral Dissertation, TU Darmstadt 1–85 (1998)
22. Raggio, G.: *A channel model for curved elongated homogeneous lakes*. Mitteilung Nr 49 der Versuchsanstalt für Wasserbau, Hydrologie und Glaziologie and der ETHZ, 1–222 (1981)
23. Sander, J.: *Weakly nonlinear unidirectional shallow water waves generated by a moving boundary*. Mitteilung Nr 105 der Versuchsanstalt für Wasserbau, Hydrologie und Glaziologie and der ETHZ, 1–199 (1990)
24. Stocker, T.: *Topographic Waves. Eigenmodes and reflection in lakes and semi-infinite channels*. Mitteilung Nr 93 der Versuchsanstalt für Wasserbau, Hydrologie und Glaziologie an der ETHZ, 1–170 (1987)
25. Schuster, B.: *Experimente zu nichtlinearen internen Wellen großer Amplitude in einem Rechteckkanal mit variabler Bodentopographie*. Doctoral Dissertation, TH Darmstadt vii + (1–165) (1991)
26. Umlauf, L.: *Turbulence parameterisation in hydrobiological models for natural waters*. Doctoral Dissertation, TU Darmstadt, XVI + 1–228 pp. (2001)
27. Wang, Y.: *Windgetriebene Strömungen in einem Rechteckbecken und im Bodensee*. Band I: Text 1–186, Band II: Abbildungen 187–432, Doctoral Dissertation, TH Darmstadt (1995)
28. Weis, J.: *Ein algebraisches Reynoldsspannungsmodell*. Doctoral Dissertation, TU Darmstadt, 1–111 (2001)

Habilitation Theses

29. Jöhnk, K. D.: *Ein-dimensionales hydrodynamische Modelle in der Limnophysik. Turbulenz-Meromixis-Sauerstoff*. Fachbereich Mechanik, TU Darmstadt, XII + 1–235 (2000)
30. Wang, Y.: *From lake dynamics to granular materials – Two aspects of environmental mechanics*. Department of Mechanics, Darmstadt University of Technology, 277 p. (2001)

Preface to Volume I

At an early planning stage of this book series – almost 10 years ago – the intention was to write a treatise on lake physics or physical limnology, designed to be understandable by limnologists of all kinds, those with a basic training in physics and mathematics: physical oceanographers, physicists, applied mathematicians and engineers, as well as classical limnologists with principal training in biology, chemistry and ecology. This approach requested a layout of the fundamental mathematical and physical background in a form accessible with only basic tools of college calculus as is generally taught in a two semester course in undergraduate analysis. Analogously, the fundamental laws of classical physics – only mechanics and thermodynamics – could not be assumed to be fully known, perhaps once learned but (partly) forgotten. Therefore, these basic axioms of classical physics also needed to be laid out.

This is the reason why this first book contains after a brief introduction into the subject of *lakes on the Earth* a chapter on *mathematical prerequisites* and a further chapter on the *thermodynamical laws of classical physics*. These chapters are primarily tutorial to those for whom the topic seems novel and others who feel weak in the mentioned subjects and need to rehearse the perhaps new material. These chapters lay the foundations of mathematics and physics and set the language that is freely used in the ensuing developments.

The knowledge acquired in these fundamental chapters is in the subsequent chapter on the *fundamental equations of lake hydrodynamics* applied to the laws of conservation of mass, momenta, energy and species mass. This is done in the conceptually most simple form, which, we believe, transmits the substantive content of these laws in an intellectually transparent form by using infinitesimal material elements; this approach of derivation, we admit, becomes technically rather involved when, e.g., applied to the energy equation and calls for more elegance, which is introduced concurrently with the development by a transformation from the Cartesian notation to a symbolic, coordinate-free notation of the governing equations. We think that this approach enlightens the learning process and is likely apt for considerable removal of the anxiety of formal mathematics, which cannot be avoided when deriving the ‘primitive’ equations used in the description of dynamic and thermal behaviour in the physics of lakes. The same equations, incidentally, are also applicable in physical oceanography and meteorology. The chapter ends

with the presentation of two approximations: one is known as the *BOUSSINESQ approximation* – it holds when the density variations are small – and the other is the *shallow-water approximation*, in which the lake geometries and water currents are large in the horizontal directions as compared to corresponding values in the vertical direction.

For an inviscid fluid under so-called adiabatic conditions the global form of the conservation law of angular momentum ([Chap. 5](#)) can be taken as a basis for a number of elegant vorticity theorems which allow general inferences regarding the behaviour of these idealised hydrodynamic processes. They give qualitative pictures, which are slightly modified for viscous fluids under non-adiabatic conditions. The role played by the rotation of the Earth is explicitly apparent in these vorticity theorems, which provide a particularly deep understanding of the vorticity-laden fluid motion.

Turbulence, considered in [Chap. 6](#), entered the science of fluid mechanics when REYNOLDS in 1883 performed his steady pipe flow experiments and demonstrated that two characteristically different flow patterns exist in such motions, one in which streak lines are essentially rectilinear (called *laminar*) and a second in which they are torn and tangled with an apparent random structure (the turbulent flow). Technically, the turbulent flow is made accessible by restricting considerations to certain mean behaviour, characterised by length and timescales, and accounting for the sub-scale processes by parameterising the correlation products (which are averages of products of fluctuation quantities) accordingly. The computational procedure to this approach is achieved by introducing filter operations to the primitive equations. The emerging class of turbulent equations then depends on the mathematical properties of the filter operations and the degree of complexity of the parameterisation of the correlation terms. The classes of theories depend on the filter properties and are called *Reynolds-averaged Navier–Stokes (RANS)* or *large eddy simulation (LES)* equations, and the complexity of the parameterisations of the correlation terms is known as zeroth, first and higher order closure, also denoted *gradient-type* closure, *one or two equation models*, e.g. *k – ε closure* and *Reynolds stress models*, etc. A brief account on these turbulence parameterisations is given.

The approach to turbulent closure in the pre-computer time and occasionally still today is to use the classical eddy viscosity and eddy diffusivity (for heat and mass diffusion) if thought appropriate anisotropically for these to distinguish the difference between the turbulent intensities in the horizontal and vertical directions. We give an outline of this procedure from a more fundamental point of view and delineate its applicability.

Whereas the above-treated subjects are fundamental to most processes in lake physics (and physical oceanography, meteorology and geophysical fluid mechanics, in general), the remainder of the book ([Chaps. 7, 8 and 9](#)) is devoted to special topics, which are further studied in more detail in volumes 2 and 3. In geophysical fluid dynamics, the fact that phenomena are taking place in a non-inertial frame of reference makes the fluid motions a great deal richer than otherwise. Moreover, flow properties in lakes, the ocean and the atmosphere are characteristically different depending upon whether the fluid is homogeneous or stratified, and finally, all

these motions possess some degree of randomness in their turbulent structure. In the hydrodynamic response of lakes the cause for the pulsating nature of the current and temperature fields is due to internal flow instabilities and due to the stochastic nature of the driving wind.

Waves at the surface and in the interior of lakes are an important topic in physical limnology, because they are permanently generated by wind and have distinctively different behaviour when the lake water is, respectively, homogeneous and stratified. In [Chap. 7](#) an account is given on linear water waves in constant depth containers with free surface when the rotation of the Earth is ignored. Deep-water and shallow-water linear waves and their dispersive and non-dispersive nature are studied. The reflection properties at walls are explained. The eigen oscillations of the water motion in a rectangular basin of constant depth terminate this introductory chapter on linear water waves.

Since the density distribution in lakes varies continually with an annual period and the dynamics of free and bounded water motions depends chiefly on the density structure, [Chap. 8](#) is devoted to distinctive physical implications of the mass distribution in a lake (or ocean). At first, typical vertical temperature profiles are discussed as they are transformed in lakes within the temperate belt of the Earth from homo-thermal conditions in late winter/early spring to primarily vertically stratified configurations generated by solar irradiation and possibly transformed by turbulent mixing. The unstratified and stratified configurations give rise to the existence of two different *barotropic* and *baroclinic* flow states, respectively. Moreover, the sign of the vertical density gradient gives rise for the identification of stable and unstable stratification of water masses. Depending on the stratification within a lake, either internal wave dynamics or convective flow features are established and may thus contribute to the transport of species and the ventilation of the deeper regions of a lake. A detailed study of linear oscillations illustrates how the density distribution affects these motions.

The vertical distribution of the horizontal current in open waters or a bounded lake, presented in [Chap. 9](#), belongs to the central challenges which were studied by mathematicians and physical oceanographers in the first half of the 20th century. The analytical methods designed by them were continued in the 1970s and 1980s and have found applications in rather sophisticated early computer software of wind-induced motions of the free surface of lakes under stormy meteorological conditions, known as *storm surges*. The chapter commences with the analysis of steady flow in a narrow rectangular basin of constant depth subject to uniform wind in its long direction, first for unstratified waters and then for two-layered configuration. For homogeneous waters the wind shear stress at the surface generates downwind near-surface current, surface set-up and an upwind return flow at depth. In the two-layer system the free surface set-up is counter-balanced by a strong opposite slope of the interface of the layers. The surface current at the free surface is again with the wind, but the return current is in the vicinity of the interface. The corresponding downwind flow in the lower layer depends strongly upon whether and how the interface and basal friction forces are operating. Details are discussed.

The role played by turbulent friction is studied in [Chap. 9](#) by solving the so-called EKMAN problem; this is the response of an infinitely deep homogeneous water mass in a horizontally infinite ‘ocean’ subject to a constant uniform wind on a frame rotating with constant angular velocity. This problem was first solved by EKMAN in 1905 on the assumption that the (eddy) viscosity is constant and only shear stresses τ_{xz} and τ_{yz} (x, y horizontal, z vertical) would be significant.

This original EKMAN problem was later generalised in various respects. For instance, the vertical eddy viscosity was assumed to vary with depth according to prescribed functional relations (chosen to allow an analytical solution of the emerging problem) and the infinite depth ocean was replaced by a finite depth ocean. Moreover, the horizontally infinite domain was replaced by a finite bounded domain, and in a further generalisation the steady-state conditions were replaced by time dependence to allow storm surge evolutions due to time-dependent wind. All these formulations are based on the assumption that only τ_{xz} and τ_{yz} must be accounted for in the construction of the solutions, and these solutions had been found by HIDAKA in 1934 and by WELANDER in 1957. The solution procedures were, however, too complicated, even when computers were already available. In 1963 PLATZMAN came forward with a very elegant approximation of the basal shear stress and constructed first numerical solutions of the governing equations for the time-dependent, wind-induced current and set-up problem. To various given North American storms between 1940 and 1959 he compared computed time series of the set-up at various limnigraph stations around Lake Erie with the corresponding measured time series and found surprising agreement. This linear and stress-approximated, wind-induced current determination in homogeneous water is generalised in volume 3 to non-linear stratified situations with modern high-powered numerical techniques.

[Chapter 10](#) of this first volume of *Physics of Lakes* gives a collection of the thermomechanical coefficients of water, in the temperature range $T \in [0, \sim 30]^\circ\text{C}$. This chapter is technically useful as it provides quantitative information that is useful for the entire book series.

Zürich, Switzerland
Darmstadt, Germany
Kaliningrad, Russia
June 2010

Kolumban Hutter
Yongqi Wang
Irina P. Chubarenko

Acknowledgements for Copyright Permission

Grateful acknowledgement is made to the following publishers, organisations and authors for permission to use previously published copyrighted figures. Most figures were scanned and redesigned, sometimes with slight changes. Some figures are compositions of several figures of the source manuscript.

American Geophysical Union

Journal of Geophysical Research

Figs. 9.13, 9.14, 9.16 – reproduced from R. T. GEDNEY & W. LICK (1972)

American Meteorological Society

Journal of Physical Oceanography

Fig. 8.4 – adopted from U. SEND & J. MARSHALL (1975)

Fig. 9.10 – reproduced from O. S. MADSEN (1977)

American Meteorological Society

Meteorological Monographs

Figs. 9.18–9.21 – reproduced/adopted from G. PLATZMAN (1963)

Archives of the City of Constance

Fig. 1.1 – adopted from E. HOLLAN (1980)

Gauthier-Villars

Fig. 9.12 – reproduced from H. LACOMB (1965)

Gebrüder Borntraeger, Berlin, Stuttgart

Mitt. Int. Verh. Theor. Angew. Limnol.

Fig. 1.3 – reproduced from C. H. MORTIMER (1974)

Houille Blanche

Fig. 7.7 – reproduced from A. WALLET & F. RUELLAN (1950)

Mitteilungen der Versuchsanstalt für Wasserbau, Hydrologie und Glaziologie an der Eidgenössischen Technischen Hochschule, Zürich

Fig. 8.18 – reproduced from W. HORN, Internal Report (1981)

Fig. 9.7 – reproduced from M. LASKA, Mitt. Nr. 54 (1981)

Figs. 10.2, 10.6, 10.7, 10.8, 10.9 – reproduced from K. HUTTER and J. TRÖSCH, Mitt. Nr. 20 (1975)

Nauka Publishing House

Fig. 1.9, – reproduced from A. I. TIKHINOV (1982)

Dr. rer. nat. habil. K. JÖHNK

Figs. 1.3, 1.8 – adopted from the Habilitation Thesis (2000)

Dr. rer. nat. M. MAISS

Fig. 2.6 – adopted from the Doctoral Dissertation (1992)

Royal Society, London

Fig. 6.1 – adopted from O. REYNOLDS (1885)

Fig. 10.11 – reproduced from D. J. JEFFREY (1974)

Zürich, Switzerland

Darmstadt, Germany

Kaliningrad, Russia

June 2010

Kolumban Hutter

Yongqi Wang

Irina P. Chubarenko

Contents

1	Introduction	1
1.1	Motivation	1
1.2	Lakes on Earth	10
1.3	Lakes Characterised by Their Response to the Driving Environment	14
1.3.1	Seasonal Characteristics	14
1.3.2	Characteristics by Mixing	15
1.3.3	Boundary-Related Processes	18
1.3.4	Characterisation by Typical Scales	20
	References	22
2	Mathematical Prerequisites	25
2.1	Scalars and Vectors	26
2.2	Tensors	38
2.3	Fields and Their Differentiation	41
2.4	Gradient, Divergence and Rotation of Vector and Tensor Fields	50
2.5	Integral Theorems of Vector Analysis	60
2.5.1	GAUSS Theorems	60
2.5.2	STOKES Theorems	62
	References	65
3	A Brief Review of the Basic Thermomechanical Laws of Classical Physics	67
3.1	Underlying Fundamentals – General Balance Laws	67
3.2	Physical Balance Laws	73
3.2.1	Balance of Mass	73
3.2.2	Balance of Linear Momentum	74
3.2.3	Balance of Moment of Momentum	76
3.2.4	Balance of Energy	77
3.2.5	Second Law of Thermodynamics	79
	References	82

4	Fundamental Equations of Lake Hydrodynamics	83
4.1	Kinematics	84
4.2	Balance of Mass	100
4.3	Balances of Momentum and Moment of Momentum, Concept of Stress, Hydrostatics	110
4.3.1	Stress Tensor	113
4.3.2	Local Balance Law of Momentum or Newton's Second Law	118
4.3.3	Material Behaviour	123
4.3.4	Hydrostatics	128
4.4	Balance of Energy: First Law of Thermodynamics	136
4.5	Diffusion of Suspended Substances	141
4.6	Summary of Equations	146
4.7	A First Look at the Boussinesq and Shallow-Water Equations	150
	References	155
5	Conservation of Angular Momentum–Vorticity	157
5.1	Circulation	157
5.2	Simple Vorticity Theorems	167
5.3	Helmholtz Vorticity Theorem	170
5.4	Potential Vorticity Theorem	177
	References	184
6	Turbulence Modelling	185
6.1	A Primer on Turbulent Motions	185
6.1.1	Averages and Fluctuations	185
6.1.2	Filters	187
6.1.3	Isotropic Turbulence	190
6.1.4	REYNOLDS Versus FAVRE Averages	192
6.2	Balance Equations for the Averaged Fields	194
6.2.1	Motivation	194
6.2.2	Averaging Procedure	195
6.2.3	Averaged Density Field $\langle \rho \rangle$	197
6.2.4	Dissipation Rate Density $\langle \phi \rangle$	198
6.2.5	Reynolds Stress Hypothesis	198
6.2.6	One- and Two-Equation Models	201
6.3	k – ε Model for Density-Preserving and Boussinesq Fluids	203
6.3.1	The Balance Equations	203
6.3.2	Closure Relations	204
6.3.3	Summary of $(k - \varepsilon)$ -Equations	206
6.3.4	Boundary Conditions	207
6.4	Final Remarks	210
6.4.1	Higher Order RANS Models	210

6.4.2	Large Eddy Simulation and Direct Numerical Simulation	211
6.4.3	Early Anisotropic Closure Schemes	212
	References	219
7	Introduction to Linear Waves	221
7.1	The Linear Wave Equation and Its Properties	222
7.2	Surface Gravity Waves Without Rotation	234
7.2.1	Short-Wave Approximation	245
7.2.2	Long-Wave Approximation	246
7.2.3	Standing Waves – Reflection	247
7.3	Free Linear Oscillations in Rectangular Basins of Constant Depth	252
7.4	Concluding Remarks	258
	References	261
8	The Role of the Distribution of Mass Within Water Bodies on Earth ..	263
8.1	Motivation	263
8.2	Processes of Surface Water Penetration to Depth	268
8.3	Homogenisation of Water Masses Requires Energy	274
8.3.1	Constant Density Layers	275
8.3.2	Continuous Density Variation	280
8.3.3	Influence of the Thermal Expansion	283
8.4	Motion of Buoyant Bodies in a Stratified Still Lake	285
8.4.1	Influence of Friction	290
8.5	Internal Oscillations – The Dynamical Imprint of the Density Structure	294
8.5.1	Fundamental Equations	297
8.5.2	Eigenvalue Problem for the Vertical Mode Structure in Constant Depth Basins	301
8.6	Closure	315
	References	317
9	Vertical Structure of Wind-Induced Currents in Homogeneous and Stratified Waters	319
9.1	Preview and Scope of This Chapter	319
9.2	Hydrodynamic Equations Applied to a Narrow Lake Under Steady Wind	322
9.2.1	Wind-Induced Steady Circulation in a Narrow Homogeneous Lake of Constant Depth	322
9.2.2	Influence of Bottom Slip on the Wind-Induced Circulation	328
9.2.3	Wind-Induced Steady Circulation in a Narrow Lake Stratified in Two Layers	330

9.3	Ekman Theory and Some of Its Extensions	340
9.3.1	Ekman Spiral	341
9.3.2	Steady Wind-Induced Circulation in a Homogeneous Lake on the Rotating Earth	358
9.3.3	Wind-Driven Steady Currents in Lake Erie	364
9.3.4	Time-Dependent Wind-Induced Currents in Shallow Lakes on the Rotating Earth	369
9.3.5	The Dynamical Prediction of Wind Tides on Lake Erie	376
9.4	Final Remarks	384
	References	385
10	Phenomenological Coefficients of Water	389
10.1	Density of Water	390
10.1.1	Natural Water and Sea Water	393
10.1.2	Suspended Matter	398
10.2	Specific Heat of Water	399
10.2.1	Specific Heat of Salty Water	399
10.3	Viscosity of Water	404
10.3.1	Pure Water	405
10.3.2	Sea Water	406
10.3.3	Natural Water	409
10.3.4	Suspended Matter	410
10.4	Molecular Heat Conductivity of Water	412
10.4.1	Heat Conductivity of Salt Water	413
10.4.2	Impurities	414
	References	416
	Name Index	419
	Lake Index	423
	Subject Index	425

Notations

Only the principal symbols are listed. A scalar is written in italic type, a vector generally in lower case italic bold type, whilst a second-rank tensor is written in upper case italic bold type.

Roman Symbols

$\mathbf{a}, \mathbf{b}, \mathbf{c}$	General vectors
$\mathbf{A}, \mathbf{B}, \mathbf{C}$	General tensors of second rank
\mathbf{A}^T	Transpose of \mathbf{A}
\mathbf{A}^{-1}	Inverse of \mathbf{A}
\mathbf{A}^{-T}	Transpose of inverse of \mathbf{A}
$ \mathbf{A} $	Norm of \mathbf{A} : $ \mathbf{A} = (\text{tr } \mathbf{A}^2)^{1/2}$
a	Semi-major axis of an ellipse
$\mathbf{a}, \mathbf{a}_{\text{abs}}, \mathbf{a}_{\text{rel}}$.	Acceleration vector, absolute, relative
\mathbf{a}_c	CORIOLIS acceleration
\mathbf{A}	Turbulent anisotropy tensor: $\mathbf{A} = \mathbf{R} + \frac{2}{3}\rho k \mathbf{1} - 2\rho v_t \langle \mathbf{D} \rangle$
\mathcal{A}_L	Aspect ratio $\hat{=}$ typical vertical to horizontal <i>length</i>
\mathcal{A}_V	Aspect ratio $\hat{=}$ typical vertical to horizontal <i>velocity</i>
$\mathcal{A} = \mathcal{A}_L = \mathcal{A}_V$		Aspect ratio for length <i>and</i> velocity
\mathcal{B}	Body
\mathcal{B}_R	Reference configuration of the body
\mathcal{B}_t	Present configuration of the body
\mathbf{B}	Left CAUCHY–GREEN deformation tensor (B_{ij}): $\mathbf{B} = \mathbf{V}^2 = \mathbf{F} \mathbf{F}^T$
\mathbf{B}, B	Buoyancy force, modulus (in the ARCHIMEDEAN principle)
b	Semi-minor axis of an ellipse
$b(x, y, t)$	Function defining the bottom topography of a lake, $z = b(x, y, t)$
\mathbf{C}	Right CAUCHY–GREEN deformation tensor ($C_{\alpha\beta}$): $\mathbf{C} = \mathbf{U}^2 = \mathbf{F}^T \mathbf{F}$

c_v, c_p	Heat capacities or specific heats at constant volume and constant pressure, respectively.
\mathcal{C}	Pressure work parameter
$c_0 = \left. \frac{dp}{d\rho} \right _0$...	Speed of sound at density ρ_0
$c_{\text{ph}} = \frac{\omega}{ k } \frac{k}{ k }$	Phase velocity
$c_{\text{gr}} = \frac{d\omega}{dk}$	Group velocity
d	Differential symbol
$d(\mathbf{x}, \mathbf{y})$	Distance function between \mathbf{x} and \mathbf{y}
div	Divergence operator
dA	Areal increment
$d\ell$	Vectorial length increment
$d\mathbf{x}, d\mathbf{y}$	Vectorial position increments in the present configuration at \mathbf{x} and \mathbf{y}
$d\mathbf{X}, d\mathbf{Y}$	Vectorial position increments in the reference configuration at \mathbf{X} and \mathbf{Y}
dV	Volume increment
$\frac{d\mathbf{a}}{dt}$	Total or ‘material’ time derivative of \mathbf{a} in an inertial frame
D	Layer thickness, EKMAN depth
DNS	Direct numerical simulation
$D^{\alpha\beta}$	Diffusivity of tracer α due to tracer β
$\mathbf{D} = \text{sym } \mathbf{L}$..	Strain rate tensor ($D_{i,j}$) $\hat{=}$ rate of strain tensor $\hat{=}$ stretching tensor
\mathbf{e}_i or $\hat{\mathbf{e}}_i$	Basis vectors ($i = 1, 2, 3$) of length 1 and orthogonal to one another
\mathbf{E}	Distortion (rate) tensor: $\mathbf{E} = \mathbf{D} - \frac{1}{3}(\text{tr } \mathbf{D})\mathbf{1}$
\mathcal{E}_V^k	Kinetic energy of the body with volume V
\mathcal{E}_V^i	Internal energy of the body with volume V
f	General symbol for a function
f'	Derivative or perturbation of f
f, \tilde{f}	First, second CORIOLIS parameter
\mathbf{f}	Specific volume (body) force
$\mathbf{F} = \frac{\partial \mathbf{X}}{\partial \mathbf{X}}$	Deformation gradient
$F(\mathbf{x}, t) = 0$..	Equation for a general surface in three-dimensional space
F_{fric}	Frictional force in a STOKESian approximation
$\mathcal{F}_{\partial V}^{\mathcal{G}_V}$	Flux of \mathcal{G}_V through ∂V of V
$\mathcal{F}_{\partial V}^{\mathcal{P}} = \mathcal{K}_{\partial V}$..	Sum of forces acting on the surface ∂V of V
$\mathcal{F}_{\partial V}^{\mathcal{L}} = \mathcal{M}_{\partial V}$	Sum of all moments acting on the surface ∂V of V
$\mathcal{F}_{\partial V}^{\mathcal{E}}$	Flow of the total energy through the boundary of ∂V of V : $\mathcal{F}_{\partial V}^{\mathcal{E}} = \mathcal{L}_{\partial V} + \mathcal{Q}_{\partial V}$

g, \mathbf{g}	Gravity constant, specific gravity force
grad	Gradient operator
$\mathbf{G} = \int_V \rho \mathbf{g} \, dV$	Weight of a body with volume V
\mathcal{G}_V	General physical quantity defined for a material volume V
h_m	Typical thickness of a layer subject to large changes of a physical variable across it
H, H_E, H_H ..	Depth, water depth of epilimnion, water depth of hypolimnion
\mathcal{H}	Entropy of a body
i	Imaginary unit ($= \sqrt{-1}$)
i, j, k	Identifiers for components of a vector or a tensor
$\mathbf{i}, \mathbf{j}, \mathbf{k}$	Unit vectors of the Cartesian system in three dimensions
\mathbf{I}	Second-order unit tensor (generally in three dimensions)
I_A, II_A, III_A ..	First, second and third invariant of a second-order tensor in three-dimensional space
$J = \det \mathbf{F}$...	Determinant of the deformation gradient \mathbf{F}
\mathbf{j}^α	Diffusive mass flux of tracer α : $\mathbf{j}^\alpha = \rho^\alpha (\mathbf{v}^\alpha - \mathbf{v})$
$\mathbf{j}_t := \langle \mathbf{v}' \mathbf{c}' \rangle$..	Turbulent (species) mass flux
k	Friction (drag) coefficient
$k = \frac{1}{2} \langle \mathbf{v}' \cdot \mathbf{v}' \rangle$	Turbulent kinetic energy
\mathbf{k}	Force vector in three-dimensional space, wavenumber vector
$\hat{\mathbf{k}}$	Unit vector in the z -direction
$k^{(1)}$	Friction velocity, a measure of diffusion across the layer with thickness: $k^{(1)} = \frac{v}{h_m} [\text{m s}^{-1}] h_m$
\mathbf{K}	(Resultant) force acting on a body
\mathcal{K}_V	Sum of volume forces acting on the body with volume V
$\mathcal{K}_{\partial V}$	Sum of forces acting on the surface ∂V of V
ℓ	PRANDTL mixing length
$\boldsymbol{\ell}$	Specific body couple
L	Length, characteristic length
LES	Large eddy simulation
$\mathbf{L} = \text{grad } \mathbf{v}$..	Spatial velocity gradient
\mathcal{L}_V	Power of working of the body forces acting in V
$\mathcal{L}_{\partial V}$	Power of working of the surface forces acting on ∂V
\mathcal{L}_V	Moment of momentum of the body V
\mathbf{M}_O^a	Moment of the vector \mathbf{a} with respect to the point O
\mathbf{M}_n	Couple stress traction on a surface with unit normal vector \mathbf{n}
\mathcal{M}_V	Sum of all moments acting within the body V
$\mathcal{M}_{\partial V}$	Sum of all moments acting on the surface ∂V of the body V
n	Porosity, fluid volume fraction
$\mathbf{n}, \mathbf{n}_\sigma$	Unit normal vector (general) on the surface σ
$\mathbf{n}^b, \mathbf{n}^s$	Unit normal vectors (general) on the basal surface and free surface, respectively

N	Buoyancy frequency, BRUNT-VÄISÄLÄ frequency: $N = -\frac{g}{\rho_0(z)} \frac{d\rho_0(z)}{dz}$
O	Point in three-dimensional space, origin of a Cartesian coordinate system in three-dimensional space.
\mathbf{O}	General orthogonal transformation ($\mathbf{O}\mathbf{O}^T = \mathbf{1}$)
\mathcal{O}	Order symbol
p	Pressure
$p_{\perp}^s = -\mathbf{n} \cdot \mathbf{t}\mathbf{n}$	Normal stress vector (pressure) perpendicular to the surface with normal vector \mathbf{n}
P	Power of working of the wind stress on the lake surface
\mathbf{P}_V	Momentum of a body with volume V
$\mathcal{P}_V^{\mathcal{G}_V}$	Production of \mathcal{G}_V in the material volume V
$Q = Q_x + iQ_y$	Complex valued vertically integrated volume flux (EKMAN problem)
Q_{\perp}^{geoth}	Geothermal heat flux perpendicular to the basal surface
\mathbf{Q}	Orthogonal transformation
$\dot{\mathbf{Q}}$	Rate of \mathbf{Q}
Q_n	n th-order velocity correlation function. $Q_n = \underbrace{\mathbf{Q} \otimes \cdots \otimes \mathbf{Q}}_{n\text{-times}}$
	$Q_2 = \langle \mathbf{v}' \otimes \mathbf{v}' \rangle$
Q_V	Energy supplied to the body by radiation
$Q_{\partial V}$	Total non-mechanical energy (heat) flow from the environment to the body
\mathbf{q}	Heat flux vector
$\mathbf{q}_t = \rho c_v \langle \mathbf{v}' \theta' \rangle$	Turbulent heat flux vector
RANS	Reynolds-averaged navier-stokes simulations
\mathbf{R}	Rotation matrix in the polar decomposition of the deformation gradient \mathbf{F}
$\mathbf{R} = -\rho \langle \mathbf{v}' \mathbf{v}' \rangle$	REYNOLDS stress tensor
$\mathbf{R} = \mathbf{Q} \dot{\mathbf{Q}}$	General rotation matrix of an orthogonal transformation \mathbf{Q}
\mathbb{R}_e	REYNOLDS stress tensor
\mathbb{R}_i	RICHARDSON number
$\mathbb{R}_i^{\text{scale}}$	Scaled RICHARDSON number
\mathbb{R}_0	ROSSBY number
r	Radiation density (per unit mass)
s	Arc length
\mathbf{s}	Specific spin vector
$S, \Delta S$	Surface, surface area
\mathbb{S}	BURGER number
$\mathcal{S}_V^{\mathcal{G}_V}$	Supply of \mathcal{G}_V to a material volume V
$\mathcal{S}_V^{\mathcal{P}} = \mathcal{K}_V$...	Sum of volume forces acting on the material volume V
$\mathcal{S}_V^{\mathcal{L}} = \mathcal{M}_V$..	Sum of all moments acting within the body V

$\mathcal{S}_V^{\mathcal{E}} = \mathcal{L}_V + Q_V$	Body energy supply $\hat{=}$ power of working of the body forces plus energy supply by radiation
t, t_0	Time
\mathbf{t}	Stress vector, traction
\mathbf{t}_n	Traction vector on a surface with unit normal vector \mathbf{n}
\mathbf{t}_{\parallel}^b	Traction vector at the basal surface parallel to the surface $z = b(x, y, t)$
u	x component of the velocity vector, longitudinal velocity
\hat{u}	Scaled dimensionless longitudinal water velocity
U	Characteristic horizontal velocity,
U	Depth-integrated volume flow in the x -direction
$\mathbf{U} = \mathbf{U}^T$	Right stretch tensor (in the polar decomposition of \mathbf{F})
\mathbf{v}	Velocity vector in three-dimensional space
$\dot{\mathbf{v}}$	Acceleration vector
\mathbf{v}'	Fluctuation of the velocity vector \mathbf{v}
\mathbf{v}''	FAVRE fluctuation of the velocity function
$v_{\perp}^s, v_{\parallel}^s$	Velocities at the surface with label s perpendicular and parallel to the surface
$\langle \mathbf{v} \rangle$	Average of the velocity function $\mathbf{v}(\mathbf{x}, t)$
$\{\mathbf{v}\} = \frac{\langle \rho \mathbf{v} \rangle}{\langle \rho \rangle}$..	FAVRE average of the velocity function
V	Depth-integrated volume flow in the y -direction
$\mathbf{V} = \mathbf{V}^T$	Left stretch tensor (in the polar decomposition of \mathbf{F} , (V_{ij}))
w	Vertical water velocity
\hat{w}	Scaled dimensionless vertical water velocity
\mathbf{W}	Complex velocity ($\mathbf{W} = u + iv$)
$\mathbf{w} = \text{curl } \mathbf{v}$...	Vorticity vector
W	Wind speed immediately above lake surface
$W(\mathbf{k})$	Wavenumber function, defining the dispersion relation ($\omega = W(\mathbf{k})$)
\mathbf{W}	Depth-integrated complex horizontal velocity: $\mathbf{W} = Q_x + iQ_y$
$\mathcal{W}(x, y)$	Complex velocity for lake bottom EKMAN layer
$\mathbf{W} = \text{skw } \mathbf{L}$..	Vorticity tensor ($= -\frac{1}{2}\boldsymbol{\varepsilon}\boldsymbol{\omega}$)
$\mathbf{W}_m(t)$	Horizontal wind velocity at shore near stations of Lake Erie enumerated by m
x	Horizontal coordinate of a Cartesian system in three dimensions
\mathbf{x}	Position vector in the present configuration
$\ \mathbf{x}\ $	Norm of \mathbf{x} : $\ \mathbf{x}\ = \sqrt{\mathbf{x} \cdot \mathbf{x}}$
x	Dimensionless length coordinate ($x = x/\ell$)
\mathbf{X}	Position vector in three-dimensional space of the reference configuration
y	Horizontal coordinate of a Cartesian system in three-dimensional space
\mathbf{y}, \mathbf{Y}	Position vectors in the present and reference configurations

z	Vertical coordinate of a Cartesian system in three-dimensional space
z_{hom}	Centre of mass of a homogeneous lake
z_{strat}	Centre of mass of a vertically stratified lake
\mathfrak{z}	Dimensional depth coordinate ($\mathfrak{z} = z/h$)
$\mathcal{Z}_n(z)$	Eigenfunction of the linear baroclinic internal oscillation of the vertical fluid velocity in a constant depth basin

Greek Symbols

α	Heat transfer coefficient
$\alpha_T = -\frac{1}{\rho} \frac{d\rho}{dT}$	Coefficient of thermal expansion
α'	Wind factor (in the EKMAN problem)
$\beta = \frac{df}{d\phi}$	Beta factor in the β -plane
γ	Friction coefficient
Γ	Symbol for circulation integral
δ	Symbol for a small number
δ_{ij}	KRONECKER delta ($\delta_{ij} = 1$ if $i = j$ and $\delta_{ij} = 0$ if $i \neq j$).
δ_{ij}	Components of the unit matrix
$\Delta = \nabla^2 = \nabla \cdot \nabla$	LAPLACE operator, symbol for the difference of two numbers
$\Delta\rho$	Density difference
$\Delta\pi_{\text{hom}}$	Change in gravity potential of a water column stratified in two homogeneous layers
$\Delta\Pi_{\text{hom}}$	Change in gravity potential of a water column stratified in two homogeneous layers
ε	Symbol for a small positive number
ε	Specific internal energy
$\boldsymbol{\varepsilon}, \varepsilon_{ijk}$	LEVI-CIVITÀ tensor, alternating symbol
$\varepsilon_{ijk} = \begin{cases} 1 & : \text{ if } i, j, k \text{ are an even permutation of } 1, 2, 3 \\ -1 & : \text{ if } i, j, k \text{ are an odd permutation of } 1, 2, 3 \\ 0 & : \text{ if } i, j, k \text{ are no permutation of } 1, 2, 3 \end{cases}$	
$\varepsilon = 4\nu\langle \Pi_{D'} \rangle$	Turbulent dissipation rate
ζ	Vertical displacement of an isolated water particle in a stratified still fluid
$\zeta(x, y, t)$	Function defining the free surface of a lake or ocean: ($z = \zeta(x, y, t)$)
ζ	Dynamic bulk viscosity
$\zeta = (\text{curl } \mathbf{v})_z$	Vertical component of the vorticity vector, simply called vorticity

$\zeta_{\text{abs}}, \zeta_{\text{rel}}$	Vertical component of the absolute and relative vorticity vector
$\eta, \eta_{\text{water}}, \eta_{\text{air}}$	Dynamic shear viscosity [$\text{kg m}^{-1} \text{s}^{-1}$]
η	Specific entropy
θ	Empirical, later also absolute temperature [in degree CELSIUS and KELVIN]
$\theta = \mathbf{k} \cdot \mathbf{x} - \omega t$	Phase of a wave with wavenumber \mathbf{k} and frequency ω
$\theta = \pi \frac{z}{D} + \frac{\pi}{4}$	Phase angle (in the EKMAN problem)
κ	Thermal conductivity
κ	von Kármán constant ($= 0.41$)
$\kappa = \frac{d^2 \rho}{d\theta^2} \langle \theta \rangle$	Curvature of the density as a function of θ (turbulence theory)
λ	LAGRANGE parameter, eigenvalue of the stretching tensors \mathbf{U}, \mathbf{V}
λ	Scalar parameter associated with the potential vorticity π_λ
μ	Dynamic shear viscosity
ν	Kinematic viscosity ($\nu = \eta/\rho$ or $\nu = \mu/\rho$)
π^α	Production rate density of constituent α
π_λ	Potential vorticity associated with λ
$\langle \pi \rangle_{\text{bt}}$	Depth-averaged barotropic potential vorticity
$\pi_{\text{bt}}^\varepsilon$	Barotropic potential vorticity in the shallow-water approximation
π_{bc}	Baroclinic potential vorticity
$\pi_{\text{bc}}^{\text{app}}$	Approximate baroclinic potential vorticity
Π_V	Entropy production within the material body V
ρ	Mass density
ρ^*	Density of water at normal pressure and 4°C CELSIUS
$\rho_0 = \rho_0(z)$	Density function of water varying only with z
ρ_E, ρ_H	Epilimnion density, hypolimnion density
$\rho \mathbf{v}$	Specific momentum density
σ	Singular surface, boundary surface
$\sigma_c = \frac{\nu_t}{\chi_t^{(c)}}$	Turbulent SCHMIDT number
$\sigma_\theta = \frac{\nu_t}{\chi_t^{(\theta)}}$	Turbulent PRANDTL number
$\sigma = \frac{\rho - \rho^*}{\rho^*}$	Density anomaly
Σ_V	Supply of entropy to the body V
$\boldsymbol{\tau}$	(Shear) stress tensor
$\tau_{xy}, \tau_{yz}, \tau_{zx}$	Shear stress components
$\boldsymbol{\tau}_s$	Shear stress field due to wind at the surface of a lake
ϕ	Latitude angle
$\phi = \varphi(\mathbf{x}, t)$	Physical quantity, represented as a function $\varphi(\mathbf{x}, t)$ in the EULERIAN representation

$\phi = \Phi(X, t)$	Physical quantity, represented as a function $\Phi(X, t)$ in the LAGRANGian representation
$\Phi_{\partial V}$	Flow of entropy through the surface ∂V of a material body V
ϕ^k	Flux of turbulent kinetic energy
ϕ^ε	Flux of turbulent dissipation rate
χ	Thermal diffusivity
$\chi_t^{(\theta)}, \chi_t^{(c)}$	Eddy diffusivities of heat and mass, respectively
$\chi(X, t)$	Motion, motion function
ψ	Stream function, transport stream function
Ψ	Force potential
$\Psi = \frac{ \Omega ^2 \tilde{r} ^2}{2}$	Potential of the centripetal acceleration at a distance $ \tilde{r} $ from the rotation axis
ω	(Circular) frequency
ω	Turbulent vorticity
$\omega = \frac{\mathbf{w}}{\rho}$	Vectorial vorticity per unit mass
$\omega = \boldsymbol{\varepsilon} \cdot \mathbf{W}$	Dual vector of the skew-symmetric tensor \mathbf{W}
Ω	Frequency, angular velocity of the Earth
$\boldsymbol{\Omega}$	Vector of angular velocity Ω

Miscellaneous Symbols

$\frac{d(\cdot)}{dt} = (\cdot)'$	Material time derivative, keeping the LAGRANGian position fixed
$\frac{\partial (\cdot)}{\partial t}$	Local time derivative, keeping the spatial position fixed
$\frac{\delta (\cdot)}{\delta t}$	Total or material time derivative in a non-inertial frame
\times	Multiplication sign (in general text)
\times	Cross (vector) product between two vectors in three-dimensional space, e.g. $\mathbf{a} \times \mathbf{b}$
\cdot	Multiplication sign in general text
\cdot	Scalar multiplication of two vectors or two matrices, e.g. $\mathbf{a} \cdot \mathbf{b} \hat{=} a_i b_i$, $\mathbf{A} \cdot \mathbf{B} = \mathbf{A}\mathbf{B}^T \hat{=} A_{ij} B_{ij}$
ϕ, φ	Symbols for angles, e.g. geographical latitude
\otimes	Dyadic (tensor) product between vectors and tensors, e.g., $\mathbf{a} \otimes \mathbf{b} \hat{=} a_i b_j$, $\mathbf{A} \otimes \mathbf{b} \hat{=} A_{ij} b_k$, $\mathbf{A} \otimes \mathbf{B} \hat{=} A_{ij} B_{kl}$
$[H], [V]$	Scales for H and V , i.e. typical values for H and V
$\text{curl } \mathbf{A}$	Curl operator (corresponding to the operator not in German-speaking countries: $\text{curl } \mathbf{A} = \nabla \times \mathbf{A} \hat{=} \varepsilon_{ijk} A_{k,j}$)
$\text{div } \mathbf{A} = \nabla \cdot \mathbf{A}$	Divergence of \mathbf{A} : $\text{div } \mathbf{A} \hat{=} A_{i,i}$

$(\operatorname{div} \mathbf{T})_\ell, (\operatorname{div} \mathbf{T})_r$	Left and right divergence operators of \mathbf{T}
$\operatorname{grad} \mathbf{A}$	Gradient operator: $\operatorname{grad} \mathbf{A} = \nabla \mathbf{A} \hat{=} A_{ij,k}$
$\operatorname{tr} \mathbf{A}$	Trace of $\mathbf{A} = A_{ii}$
$\langle \mathbf{v} \rangle_T$	Temporal average of the pulsating function $\mathbf{v}(\mathbf{x}, t)$ at fixed \mathbf{x} : $\langle \mathbf{v} \rangle_T(\mathbf{x}, t) = \frac{1}{T} \int_{t-T/2}^{t+T/2} \mathbf{v}(\mathbf{x}, \tau) d\tau$
$\langle \mathbf{v} \rangle_s$	Spatial average of the pulsating function $\mathbf{v}(\mathbf{x}, t)$ at fixed t
$\llbracket f \rrbracket = f^+ - f^-$	Jump of f across a singular surface

Chapter 1

Introduction

1.1 Motivation

Limnology, the science of lakes, has been in the past primarily a field of activity of the biological and chemical sciences with only limited interaction with physics. This fact has its historical justification as the study of lakes has primarily been motivated by questions of biological concern, and these are deeply rooted in the life sciences among which biology and chemistry play an important role. A certain significance of physics has nevertheless always been accepted – for instance, the seasonal variation of the temperature distribution in a lake has always been recognised to be the result of solar radiation and wind action at the water surface. This as such is natural and nearly self-evident, since all processes occurring in nature are interconnected and cannot be divided into separate pieces. Lake physics, as a field of science by its own, is, however, a very effective approach, rich in the variation of methods and powerful in its effectiveness of explaining the observed phenomena. It often lies in the background of the biological and chemical processes, not only affecting their performances but also acting as their initiating nucleus. This makes it worth to study lake physics, to understand the related phenomena and thus to gain a more integrated view of the science of lakes.

The topic of this book is thus physics of lakes, commonly called *physical limnology*. It embraces by and large the science of fluid dynamics of lakes and is therefore sometimes also called *hydrodynamics of lakes* but includes special topics that lie beyond common hydrodynamics. Such extensions are for instance the couplings of the purely mechanical processes with the thermal fields, and, indeed, because of the solar irradiation the lake water is heated from spring to summer but cools in fall and winter. This seasonal variation of the thermal regime of a lake has an obvious effect on the life cycle of all living creatures in the water bodies on Earth. It has an equally dramatic effect in most lakes on the water motions because lakes are often homo-thermal in winter, i.e. they have the same temperature and thus the same density¹ everywhere. The fluid motion, induced by the wind, the variations of

¹ In lake waters the density is in many cases negligibly affected by the content of the minerals – the salts. This is not so in the ocean, in fjords and lagoons, as well as in salty lakes. The density structure is physically important.

the atmospheric pressure and the inflow and outflow of tributaries are quite different in a lake with uniform water density from the corresponding motion when the lake is *stratified*. It is evident that if the water motion is so different in the two cases, the biochemical processes will also depend on it. Biology, chemistry and lake physics are necessarily coupled via the different transports of the *tracers* such as nutrients, oxygen, phytoplankta.

The fact that the water motion in lakes or the ocean under homogeneous and stratified conditions is so different is manifested in the depth distribution of induced water disturbances and their typical wave speeds. In a homogeneous water body with free surface the largest displacements of the water occur at the free surface – centimetres to at most metres – and the motion is attenuated as one moves from the surface down to larger depth. The speed of propagation of such signals along the surface is several tens of metres per second. This implies that typical timescales of the re-occurrence of an event in a lake of 10–100 km extent are in the order of one to several hours. Alternatively, it will be seen that in a water body with typical stratification the largest vertical displacement of the water particles arises inside the lake, not at the surface, namely at the location where the vertical density variations are largest. For the same external wind forcing as in a homogeneous lake, these vertical excursions of the water body at depth are several metres, much larger than typical amplitudes of surface displacements in a homogeneous lake, and accompanied surface traces are very small. Moreover, such signals typically travel with a speed of several tens of centimetres per second so that re-occurrences of an event in a lake of 10–100 km extent must be of the order of several days – not minutes to hours as for a signal in a homogeneous lake. In this sense, adjustments of the current regime in a homogeneous lake to changes in the external driving mechanisms may be called *fast*, while those in a stratified lake are *slow*.

The solar irradiation enters a lake or the ocean as an electromagnetic wave at various wavelengths. In the visible range we call it *light*, in the infrared range as *heat* and *ultra-violet radiation* in the short-wave range. All are attenuated with depth with a rate of extinction that, in the visible range, is affected by the *turbidity* of the water. Obviously, since photosynthesis of the phytoplankta depends on the availability of light and also the vitality of the zooplankta and many other living species, expressed in their rate of reproduction, depends on the water temperature, the heat and light budgets in the water are important qualifications that affect the life cycles within natural waters. Since most microspecies in water follow more or less the water motion – they essentially ride on the water particles and only perform a comparably small motion relative to them – the slow and large vertical excursions of the internal water particles in a stably stratified water body will expose the phytoplankta to a variable light field with a 24-h day–night period as well as periods dictated by the internal oscillations due to the peculiar stratification. Since the periods of the waves depend on the density stratification as well as the geometry of a lake basin, the living species in each lake have their own ‘physical climate’. More precisely, this is to say that the physical processes of each lake affect the biological and biochemical responses in their own way. Properly understanding lake physics in the context of its biological impact is therefore important, because differences

of otherwise identical situations may be due to such differences in the physical conditions.

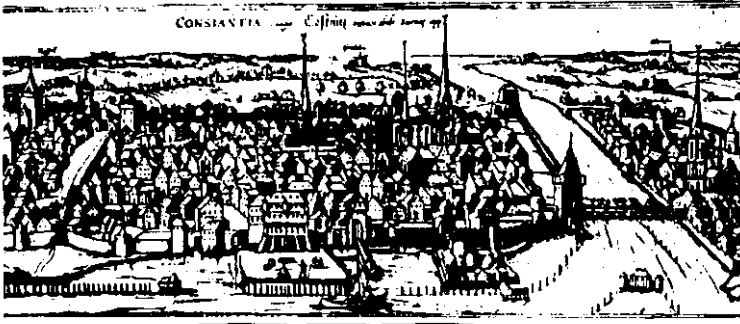
The above succinct description of physical processes in lakes should have made it clear that the structure of the water temperature and consequently density governs a large portion of the coupling between biology and physics. This variation is by and large vertical; models that describe the seasonal variation of the temperature and thus density fields are therefore one dimensional and express the formation and destruction of a certain stratification as results of solar irradiation, destabilisation by cooling and turbulence due to wind input. Biological coupling to this balance is achieved by appending oxygen, nutrient species and light field balances, eventually yielding a one-dimensional vertical model of the seasonal variation of the biophysical fields through depth.

Such a one-dimensional vertical model possesses the potential to constitute a fairly accurate description of the ‘global’ biophysical processes in lakes; however, it ignores their horizontal spatial dependence, which is so conspicuously visible in the differences of the *pelagial* – far from shore – and *littoral* – near shore – biological processes. If these differences are to be accounted for in a biophysical description, then a three-dimensional description is necessary in which the distinction between the behaviour in the pelagial and littoral zones can be accounted for. Modern physical limnology operates to a large extent with full spatially three-dimensional modelling.

These and similar subjects form the principal topics of this book. It is hoped that the preceding description provided an intelligible outline of the major ideas that are covered in this book. To be a bit more specific, let us give a more concrete description of a few phenomena that conspicuously influenced the early development and then led – via the application of hydrodynamics championed in meteorology and oceanography – to the modern understanding of physical limnology.

The physics of lakes has been a subject of human curiosity for many centuries. We do not wish to give here an accurate historical account, but reports of the Jesuits who inhabited the Wisconsin shore of Lake Michigan in the 17th and 18th centuries demonstrate a number of observations of the lake surface motion induced by the position of the moon. Father LOUIS describes in 1672 the water-level oscillation at the head of Green Bay and ascribes it to the variation of the gravitational attraction by the moon, but the phenomenon was only satisfactorily explained by HEAPS et al. [10] in 1982 as a combination of the response to the semi-diurnal tide and a resonance of the Green Bay to the free oscillations of the entire Lake Michigan.

Another exceptional incidence of lake physics is the so-called wonder of the rising water at the medieval town Constance described by C. SCHULTHAISS in 1549 [19]. According to the report, the 5-km-long River Rhine connecting the upper and lower Lake Constance was for about an hour not monotonously flowing from the upper lake to the lower lake but oscillating forth and back between the two otherwise dynamically separated lake basins for several times with a period of approximately 12 min, see Figs. 1.1 and 1.2. At that time, since no one was able to rationally explain the phenomenon, the event was called a wonder. There are no historical records that would indicate a repetitive occurrence of the phenomenon; however, HOLLAN et al.



WUNDER ANLOFFEN DES WASSERS

Uff disen tag, was Sant Mathyß
abend, mongens fröh, ist der
see an und abgeloffen, wol
einer ellen hoch, der gestalt, so
der see angeloffen, so ist er in
der wette¹ schier bis zu der
Spittals Egk² heruff gangen;
so er abgeloffen, ist er schier
by der siegen an der Visch-
prugk³ erwunden, und so er
so klain worden, so ist er bald
mit ainem ruschen, als ob das
gwoill von dem wind (welcher
doch nit was) getriben wüld,
wider angeloffen. Und sölsch
ist etwa in ainer stund vier
oder fünf mal geschehen (wie
ich selbst gesehen hab). Das
hat also bis nach mittag ge-

wert, aber je speter es worden,
je minder er an- und abgelof-
fen ist. Glicher gestalt ist auch
im Rheyn hinab geschehen. Es
habend ettlich Paradies⁴ ire
rüschen im Rheyn wellen bü-
ren oder hoben, die habend
befunden, daß der Rheyn uff-
wärts dis tags gegen der statt
und Rheynprugk⁵ geloffen,
wie er sunst hinab loufft. Ist
ouch dis tags an und abgelof-
fen zugleich wiederseeoben by
dem Dam und Vischprugk⁶.
Das hat menigklich ain gross
verwunderung gehabt, den
niemant gwesen, der ie gehört
hab, das der gleichen vor mer
hie geschehensyge.

Fig. 1.1 (a) Wooden engraving of the city of Constance from 1570 with a bird's-eye view from east to west © Archives of the city of Constance. The text is the description of the peculiar event when the river Rhine seen in the picture must have flown forth and back between the upper and lower Lake Constance with a period of approximately 12 min. The old text reads as follows (according to HOLLAN et al. [11], and also provides an interpretation of medieval units. For the numbered sites, see the map from approximate 1700 in Fig. 1.2):

The wonder of the rising water. 'In the morning of this day, February 23 in 1549, the surface of the lake rose and fell by about one ell (59 cm). At high water the level rose up to the corner of the hospital 1, at low water it fell so far that the water was swirling around the bases of the piles of the fishermen's jetty 3. As soon as it had sunk this far it came surging back as if the waves had been driven by the wind (though there was no wind). This happened four or five times in about an hour as I saw myself. This continued until after noon, but decreased as time went on. The same thing happened further down in the Rhine. Several people from Paradise 5 wanted to raise their fish traps and found the Rhine was flowing on this day upstream towards the town and the Rhine bridge 4, whereas it normally flows away from them. It also flowed backwards and forwards at the same time as the lake at the landing place 2 and the fishermen's jetty 3. This caused great astonishment among the people, since there was nobody who had ever before heard of such a thing happening.'

HOLLAN et al. [11] converted the observed wave height of 1 ell into centimetres according to the definition of the old unit mentioned by JÄNICHEN [14]. He reported that the unit of a short ell was

[11] firmly believe that it could be explained as a resonance mode of the bight of Constance of a seiching motion² of the entire upper Lake Constance.

Seiches, the eigen-oscillations of lakes that are primarily initiated by the wind, were among the first phenomena to which physicists focused their interest in the second half of the 19th century. FOREL's study of the surface seiches of LAC LÉMAN and of other lakes – together with the measurements of SARASIN, a physics professor at the University of Geneva – are well known and documented in FOREL's monographs [9] and many annual reports of the local chapters of the Swiss Academy of Sciences (Jahresschriften der Naturforschenden Gesellschaft zu Zürich, Luzern, Geneva). The physicists of the 19th century were also deeply involved with thermometry of lakes and with lake morphology. The life climate of the lake was also studied, but this biochemical activity was basically disjoint from the physics of lakes or connections were thought to be weak and of qualitative nature. More precisely, the question of the direct interaction of lake physics and lake biochemistry was not raised or it was set aside.

This stayed and remained so for much of the first half of the 20th century and even for sometime of its second half. Lake physics made considerable advances, mainly because it is structurally essentially the same science as *physical oceanography*, its bigger and elder sister. Prior to the 1960s, physical limnologists kept themselves primarily busy with explaining the surface traces of the water motion within lakes. Stratification began to play a crucial role, as it was the key to the explanation of the considerable motion of the water in the interior of the lake, while the free surface remained essentially flat. Internal wave dynamics was recorded – probably for the first time systematically by MORTIMER in LAC LÉMAN in 1953 [16], 1963 [17] when he collected the 1950 records of the time series of the water level at eight stations around the lake and the Geneva waterworks intake temperature and filtered from these the short periodic (barotropic) oscillations, Fig. 1.3 [16]. What remained were long periodic variations of the water level at the sites that would be



Fig. 1.1 (continued) in use in Constance in 1534. It was defined by the following relation between three linear measures:

$$1 \text{ Rute} = 6 \text{ ells} \text{ minus } 1 \text{ Zoll},$$

where 1 Rute equals 3.5141 m and 1 Zoll represents the length of an inch, which is not precisely known for that time. If we assume the actual definition of an inch, i.e. 1 Zoll = 2.54 cm, the length of an ell results in 58.98 cm. Since the unit of 1 Zoll had the same small magnitude in former times, it is apparent from the above equation that the derived value of an ell depends only slightly on this quantity. For instance, if we introduce 1 badischer Zoll = 3 cm used in Constance until 1877, one ell amounts to 59.07 cm, which differs negligibly from the previous value

² The word 'seiche' derives from old French as spoken in the Roman part of Switzerland 'sec' and means 'dry'. It has been used in the 19th century (by FOREL [9] and earlier) in the region of Lake Geneva to denote the surface oscillation of the water level along the shore, drying periodically a strip of the shoreline. Today by 'seiche' a periodic lake oscillation is generally meant. According to FOREL, the word 'seiche' characterising lake oscillations, is due to FATIO DE DUILLIER [4] and occurred in his paper in 1730.

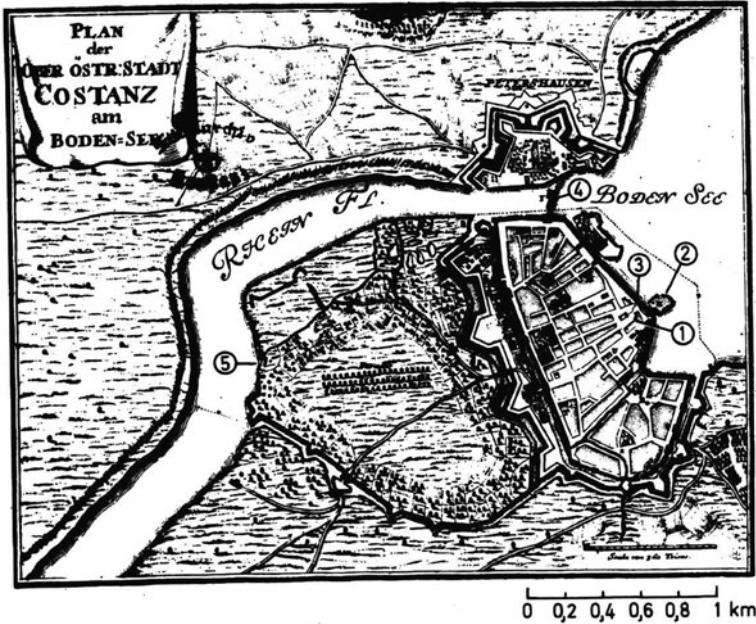


Fig. 1.2 Map of the city of Constance and surroundings ca. 1700. Locations denoted by numbers: 1 Heilig Geist hospital, 2 landing place, 3 site of the fishermen's jetty, 4 Rhine bridge, 5 site of the former village of Paradise. The scale given in toise has been converted to kilometres using the following definitions of former French linear measures quoted by WEISBACH [24]: 1 toise = 6 old feet, 1 old foot = 0.324839 m (reproduction of the map by courtesy of the Archives of the City of Constance)

interpreted as the fundamental mode of the internal seiche in LAC LÉMAN. In the subsequent years, especially in the 1970s and 1980s of the 20th century, internal wave dynamics was the major concern of research by physical limnologists. This research was, however, soon supplemented by analytical and numerical analyses of the current and temperature distributions induced by wind. This latter problem still constitutes one of today's most important research topics of physical limnology. It forms the cornerstone of explaining the transport of pollutants and nutrients in large water bodies such as lakes and ponds and is the basis where lake physics and lake biochemistry can be coupled together.

Another topic of even more central interest to the biological limnologists is the description of the seasonal variation of the mass distribution within the water body, i.e. the temperature distribution throughout the year, if the solar radiation, the long-wave energy fluxes at the water surface and the wind forcing through the year are prescribed, Fig. 1.4. The solution to this problem is very complicated because, obviously, *turbulence*³ plays an important role. Needless to say that the latter is a

³ Turbulence arose from the recognition that the flow of water, e.g., in a pipe can have two distinct appearances: (i) *laminar* flow, in which the flow is smooth and *streaklines* from a point source are maintained as small filaments and (ii) *turbulent* flow, in which the filaments are torn apart and

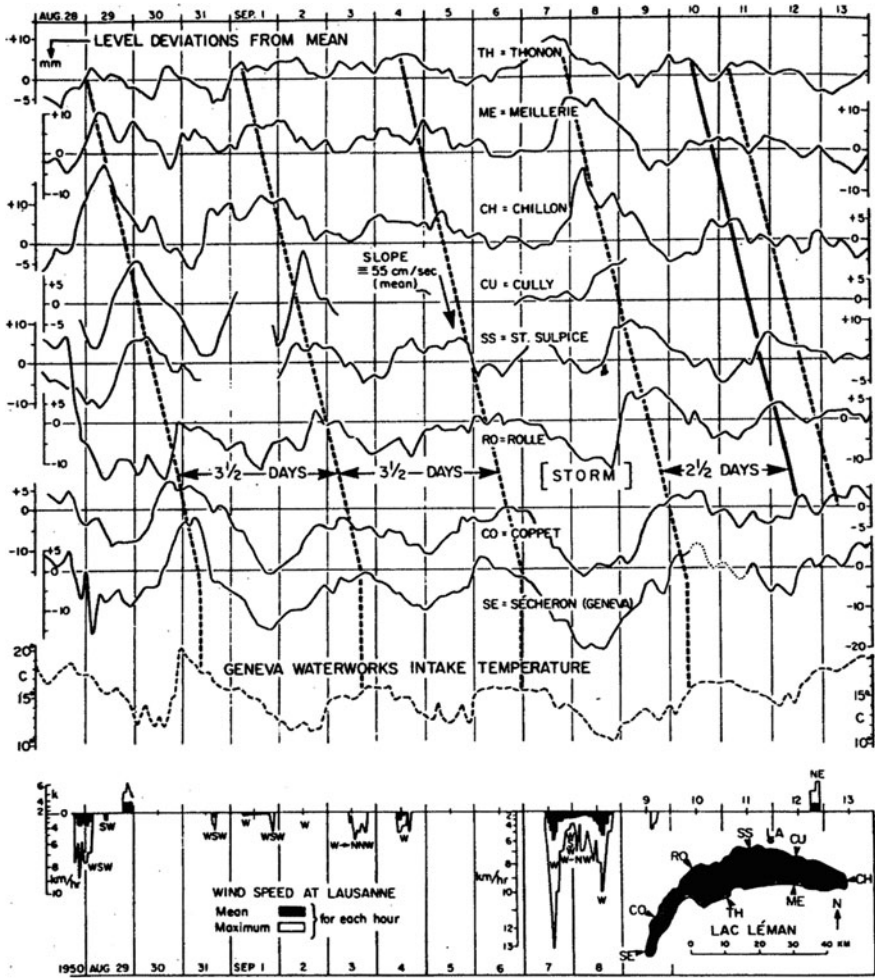


Fig. 1.3 LAC LÉMAN, 1950: fluctuations of smoothed water levels at eight stations, arranged in counterclockwise order around the basin and compared with temperature at the City of Geneva waterworks intake and with wind observations at Lausanne (reproduced from MORTIMER [16]. © Gebrüder Bornträger, Berlin, Stuttgart)

notoriously difficult problem. Turbulent activity is imported into a lake mostly by the wind stress at the free surface. It leads to the shearing of the uppermost water layers and destabilises these layers. Intuition tells us that the turbulent activity cannot in general penetrate to all depths but must attenuate with depth. There is likely

spread over larger regions of the domain of the fluid. For instance, the streakline of the smoke of a still cigarette is smooth and narrowly confined for a certain distance and then suddenly torn apart and wound in complicated gyres or eddies. Such eddies of many sizes are a typical characteristic of turbulent flow, and they affect fluid mechanics of lakes substantially.

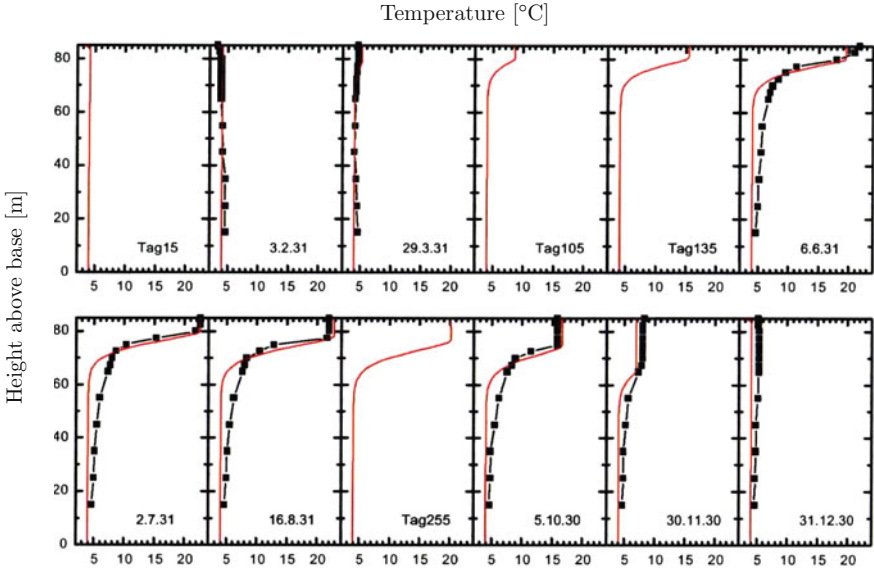
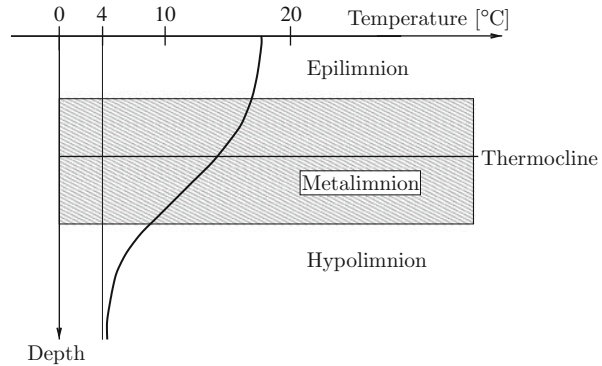


Fig. 1.4 Temperature profiles at the deepest position in the Ammersee (Bavaria) as measured between 15 April and 20 November 1996 and as computed by JÖHNK [15] (reproduced with permission)

a maximum depth to which the turbulence can penetrate; it may be called the *turbocline*. A process counteracting the destabilisation of the wind-induced turbulence is the stratification due to near-surface absorption of solar irradiation. The more the heat radiated into the lake, the higher the water temperature and the less dense the corresponding water. This is also a process that is attenuated with depth, but contrary to wind action, it stabilises the water masses. The arguments should make it clear that the state of stability (or the potential of water overturning to occur or not) is the interplay between input of momentum (i.e. motion) by wind and radiation by the sun.

The answer to the question of how the water masses are distributed in a lake is of utmost significance to biological limnologists both on timescales of internal wave dynamics and on seasonal variation of the thermocline. This is simply so because it is known that phyto- and zooplankta react very sensitively to the thermal conditions, i.e. the climate of a lake. The surface with the largest vertical gradient in a temperature profile, called the *thermocline*, separates the upper lake – *epilimnion* – from the lower lake – *hypolimnion* – and the biological activity primarily takes place in the vicinity of the thermocline – the *metalimnion* – and above (Fig. 1.5). The availability of light, restricted to the upper layers, governs the *photosynthesis* of the phytoplankton, and the amount of dissolved oxygen O_2 and nutrients (phosphates, nitrates, etc.) determines the growth rate of the phyto- (and hence zoo) plankton and how they metabolise. Oxygen largely enters mechanically into the lake through the free surface by wind action and turbulence, and the stratification (i.e. the density

Fig. 1.5 Typical temperature distribution in a lake during summer, defining epi-, meta- and hypolimnion and the thermocline. The latter is the location of the (absolutely) maximum temperature gradient



difference between epi- and hypolimnion) determines how oxygen is transported across the thermocline to the hypolimnion. It is obvious that the physical processes share their role in determining whether a lake may be classified as *aerobic* or *anaerobic* and how the biochemical decay processes take place.

This brief introduction to physical limnology should provide to the novel reader an adequate impression of what *physical limnology* constitutes. *It aims at a detailed understanding of the physical processes as they occur in lakes.* They form the result of the motion of the water masses in the gravity field of the rotating Earth under external driving mechanisms such as the solar irradiation and the dynamical action of the atmospheric processes, mostly exerted on lakes at their free surfaces as shear tractions due to wind and atmospheric pressure. These processes ought to be analysed always with a view on their impact on lake biology and chemistry. In what follows, the concepts will be presented in a form that discloses their significance with regard to lakes at four different levels.

- *Firstly*, there are the laws of classical physics; they describe those parts of the knowledge which are common to all material bodies. These laws are known as the conservation laws of mass, momentum, moment of momentum, energy and entropy. Still at this first level are those statements that characterise water as a particular form of matter which distinguishes it from other materials (e.g. ice).
- *Secondly*, these laws will be applied to water bodies with free surface to elucidate how the general laws of physics may be applied to situations pertinent to lakes. At this level, a first, basic understanding will be established that explains why the distribution of the water masses, i.e. the variation of the density within the water body, is significant, what effects the wind may exert on a lake and how the solar irradiation influences the thermomechanical state of a lake. Of such nature are also first analyses of how waves propagate in a homogeneous and stratified water body with free surface, and finally to what extent the rotation of the Earth affects the physical processes, primarily waves and the general circulation, arising in lakes.
- *Thirdly*, while the analyses at this second level attempt to build an understanding by avoiding as much as possible complicated mathematical formulae, the

latter can at last not be avoided. Mathematical models will be deduced from the fundamental equations by simplification due to physical reasoning, and these often allow the construction of analytical results, thus providing answers to the ‘what and why things happen in lakes’ and giving reasons of the effects that are observed and expressed analytically. Frequently such analyses corroborate the physical behaviour previously surmised by plausibility arguments. More often, however, these analytical results provide only the basis for a proper understanding of the quality of the processes and need to be known in detail to interpret observational data.

- Once a general understanding has been reached, it is advisable to analyse at the *fourth* level the full description exploring the three dimensionality of the processes and the coupling with biological and chemical processes. The knowledge gained with analytical models will greatly aid the interpretability of the results obtained via computation and field measurements. In much the same way it will also help when biology is coupled to lake physics.

Finally, a remark may be of help to the reader when trying to judge physical limnology against limnology in general. Specifically, while a large number of physical processes can be explained without consideration of biological components, it seems very difficult to draw correct biological inferences by excluding considerations of physics. This means that the coupling is by and large one sided: the physics affects in many respects the biological processes but much less vice versa. This implies that lake physics can be studied ‘in isolation’ free from the peculiarities of the biological processes. Future advances in the ecology of lakes will, however, largely depend upon a deeper understanding of lake physics and its implementation in biological modelling. These books are an attempt to lay the foundations to this end, a fascinating interdisciplinary subject.

1.2 Lakes on Earth

A *lake*, by definition, is a large body of usually freshwater surrounded by land. The main distinctive feature of a lake is the absence of an influence of the World Ocean. However sometimes, large lakes are referred to as ‘inland seas’ and small seas are sometimes referred to as lakes, for example, the Dead Sea. As the fates decree, the largest lake in the world is called the Caspian Sea.⁴

Apart from this common feature – the separation from the World Ocean – the Earth’s lakes enjoy a great variety of natural conditions. In order to illustrate this diversity, we mention a few examples: Lake Tianchi in northeast China, the highest volcanic lake in the world, is located at an altitude of 2,189.1 m above sea level (a.s.l.), while the surface of the Dead Sea is the lowest point on the Earth’s surface at an elevation of 417 m below sea level. More than 70 lakes in Antarctica are

⁴ Data in this section have been collected mainly by consulting sources in the Internet, e.g. <http://www.ilec.or.jp>.

buried below 3–4 km of ice, and large underground lakes were discovered recently in Namibia and China. The deepest (1636 m) Lake Baikal in Siberia contains one-fifth of the World's freshwater resource, and Lake Eyre in Australia is dry most of the time but becomes filled under seasonal conditions of heavy rainfall. Water from Lake Constance is drinkable, while in the Dead Sea, depending on the position, it is 5–10 times as salty as the World's Oceans. The water near its bottom is so saturated that salt precipitates out of the solution onto the sea floor. It is called 'dead' because its high salinity allows no fish or macroscopic aquatic organisms to live in it. No one knows how any organism, cut off from air, sunlight or any apparent source of life-sustaining energy, could survive below 4-km-thick ice in Lake Vostok under crushing pressure of more than 360 times the atmospheric pressure at sea level. The highest and the world's second largest inland saltwater Lake Qinghai in China (3195 m above sea level), despite its salinity, has an abundance of fish, while warm tropical Lake Victoria – the largest lake in Africa and the second largest freshwater lake in the World – has an extremely weak ecosystem. The enormous depth of another tropical Lake Tanganyika (maximum depth 1470 m) contains so-called 'fossil water' with almost constant temperature of about 23.3°C throughout the year, with a remarkable variety of fish fauna in the upper layer, much of it unique. It never mixes throughout the entire depth because of stable water stratification and soft climate conditions. At the same time, the always cold water of Lake Baikal is ventilated throughout its depth due to specific mechanisms of thermal convection, and only a few lakes may compete with Lake Baikal in biotic diversity.

All the fantastic variety of the Earth's lakes, however, can be described in terms of physical processes taking place in various large water bodies on the rotating Earth under different boundary conditions. Which of the processes are of importance for a particular lake objectively depends on the lake size, its bathymetry, the characteristics of its water masses and external conditions like the location, climate, tributaries. Table 1.1 contains the main morphometric characteristics of the World's largest lakes: their areas, maximum depths, volumes and latitudes.

Figures 1.6 and 1.7 present these data graphically. For convenience, the shapes are plotted at the same scale, and some lake volumes (in cubic kilometre) from Table 1.1 are also recorded. The diagram of Fig. 1.7 shows the maximum depth (in metres) and the latitudes of the largest lakes. The area of the circle is proportional to the surface area (in thousands of square kilometre) of the corresponding lake. Later in the book, we will refer to these figures when discussing different physical processes taking place in lakes: wind-induced motions, internal waves, seasonal variations of the thermocline, etc. For example, the dynamics of a very shallow large lake like Lakes Chad (maximum depth 11m), Winnipeg (18 m) or Balaton (12 m) can be completely changed by strong winds. On the other hand, in a very deep lake, the water compressibility becomes important for mixing processes, even though it is naturally very small. It was first shown for the deepest Lake Baikal, and one may then expect this influence also in the Caspian Sea, Lake Vostok and Lake Tanganyika.

It is convenient for the further description and investigation to select 'the most universal' example of a lake for which one can find the widest range of physical

Table 1.1 Morphometric characteristics of the largest lakes on Earth arranged according to their surface area

Lake	Continent	Area $\times 10^3 \text{ km}^2$	Max.depth m	Volume km^3	Latitude
Caspian Sea	Europe	376	1024	78200	41° 50' N
Superior	N. America	82.4	406	11600	47° 45' N
Victoria	Africa	68	82	2700	1° 10' S
Huron	N. America	59.6	229	3580	44° 55' N
Michigan	N. America	57.8	281	4680	44° N
Aral Sea	Asia	51.1	55	1020	45° 15' N
Tanganyika	Africa	34	1470	18900	6° 15' S
Baikal	Asia	31.5	1636	23000	53° 30' N
Nyasa	Africa	30.8	726	7725	12° 10' S
Great Bear	N. America	30.2	446	1010	66° N
Great Slave	N. America	28.6	614	1070	61° 55' N
Erie	N. America	25.7	64	545	42° 15' N
Winnipeg	N. America	24.4	18	127	52° 20' N
Balkhash	Asia	22	26	112	46° 15' N
Vostok	Antarctica	19.6 ^a	1000 ^a	4900 ^a	72° S
Ontario	N. America	18.8	243	1710	43° 45' N
Ladoga	Europe	17.7	225	908	60° 55' N
Chad	Africa	16.3	11	44	13° 25' N
Eyre	Australia	15 ^b	20	1 ^b	28° 30' S
Maracaibo	S. America	14.2	250		9° 45' N
Tonle Sap	Asia	10	14	40	12° 50' N
Onega	Europe	9.8	127	295	61° 50' N
Amadeus	Australia	8.7			24° 45' S
Rudolf	Africa	8.6	73	360	3° 30' N
Titicaca	S. America	8.3	304	710	
Volta	Africa	8.3	74	165	7° 40' N
Nicaragua	N. America	8.1	70	108	11° 35' N
Athabaska	N. America	7.9	60	110	59° 10' N
Issyk Kul	Asia	6.3	702	1732	42° N
Reindeer	N. America	6.3	60		57° 15' N
Tung Ting	Asia	6	10		
Urmia	Asia	5.8	15		37° 35' N
Torrens	Australia	5.7	8		34° 50' S
Venern	Europe	5.6	100		58° 55' N
Edward	Africa	5.4	58		0° 25' S
Winnipegosis	N. America	5.4	12		52° 20' N
Mweru	Africa	5.2	15		9° S
Gairdner	Australia	4.7	0		34° 17' S
Manitoba	N. America	4.6	28		50° 55' N
Qinghai	Asia	4.6	33		36° 55' N
Great Salt	N. America	4.4	15		41° 10' N
Dead Sea	Asia	1	330		31° 30' N
Geneva	Europe	0.6	310		46° 25' N
Balaton	Europe	0.6	11		46° 50' N
Constance	Europe	0.5	252		47° 40' N
Zürich	Europe	0.09	143		47° 15' N

^a Estimation^b Seasonal maximum

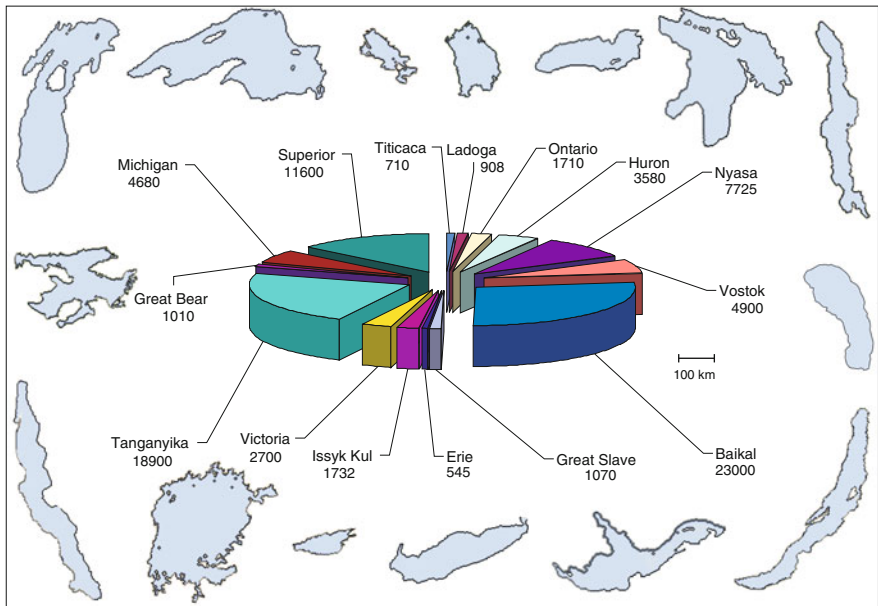


Fig. 1.6 Shapes of the largest lakes on Earth, plotted on a common scale, with their relative volumes indicated in cubic kilometres

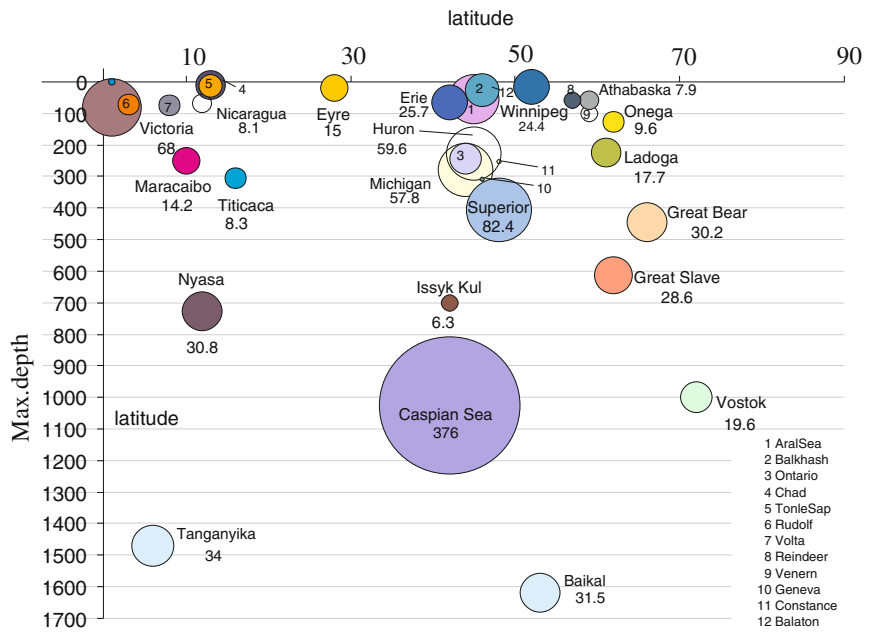


Fig. 1.7 Diagram showing maximum depth (in metres) and latitudes of the World's largest lakes. The area of the circle is proportional to the surface area (in thousands of square kilometres) of the corresponding lake

phenomena. One of the key features here is vertical water *stratification*. Relatively deep lakes at mid-latitudes typically have a well-pronounced stratification and, as a consequence, experience wealthy internal wave dynamics. Mid-latitude lakes possess also a specific type of seasonal water mixing during the spring and autumn transition periods, which relates to the nonlinear thermal expansion of water with its 4°C *water density maximum*.⁵ For lakes of the size of a few kilometres and more, *the Earth's rotation* becomes an important factor, increasing with latitude, which supports their general cyclonic water circulation. Thus, the largest variety of physical processes can be found in *large lakes at mid-latitudes*.

1.3 Lakes Characterised by Their Response to the Driving Environment

Lakes are exposed to the atmosphere and the weather as it evolves through the seasons. Thus they are subject to wind, solar radiation, atmospheric temperature, the flux of tributaries, etc. All these exert some influence, and depending on their relative 'weight' and the size and form of the lake itself, typical behaviors can be identified. For instance, depending upon the location of the lake on the globe, different climates prevail that determine the seasonal characteristics of a lake. Similarly, the amounts of solar radiation, atmospheric temperature and wind are important components for the characterisation of mixing. Furthermore, because of the boundedness of the basins, shores restrict and guide the motion of the water, implying boundary-related processes, not envisaged in the open ocean. Finally, the various distinct processes can also be typified by scale analysis. A brief outline of what is meant by these characterisations is given below.

1.3.1 Seasonal Characteristics

In the course of a year, a large lake, situated at medium geographical latitude, changes its temperature distribution drastically. This happens on the basis of both seasonal and daily (diurnal) variations of the external activities, primarily wind and solar irradiation. In summer, the upper water layer becomes warmer and less dense due to solar heating so that a strong *summer stratification* is established with the typical *stable* temperature profile: lighter water above heavier water throughout. The hydrological autumn in a lake begins with the seasonal cooling from the surface (compare also Fig. 1.4); it produces the upper homogeneous mixed layer, which grows with time, usually also supported by a seasonal increase of the wind activity. When mixing from the surface due to these mechanisms reaches the lake bottom, the *winter homothermy* is established. With further cooling and mixing throughout

⁵ For pure water the density maximum is reached at 3.8°C, but many parameterisations use 4°C instead.

the entire depth, the temperature of the water column decreases simultaneously throughout the entire depth down to 4°C. At this temperature, the water density is maximum, and further cooling from the surface makes the upper layer lighter than the lower ones: the water column becomes again more and more thermally stably stratified. So, the top layer continues to cool without thermally induced convective mixing with lower layers. The water surface may eventually start to freeze, thus blocking also wind-induced mixing and further cooling of deeper layers (which is of importance for lake inhabitants). This phase, characterised by *inverse stable* temperature stratification, is called *winter stagnation*. The spring begins with warming up the surface so that the water again, as in autumn, becomes heavier; it then has the tendency to fall to larger depth and to mix with the underlying water, called now the *spring circulation*. The entire water body finally reaches again a uniform temperature of 4°C. Subsequently, and often supported by a few days with calm and warm weather, a stable direct temperature profile is built, which becomes stronger as the summer proceeds.

This seasonal behaviour does not hold for all lakes but is adequate for most deep lakes in moderate climate zones, e.g. the Alpine lakes such as Lake Constance. In Fig. 1.8, monthly averaged temperature profiles for Lake Constance are shown through the year 1987. It allows to identify and corroborate the above explained behaviour. The figure displays the results obtained by averaging temperature profiles, taken every 20 min in the middle of the north-western part of Lake Constance at the depths from 3 to 139 m. The very profiles are shown as solid lines, the areas of shading columns are proportional to their heat content and the intensity of the shadowing is related to the density of the water. Thus according to data collected in [2] in the year 1987, the water body of Lake Constance had a *stable direct summer stratification* from April to September; an upper mixed layer, increasing in depth, exists from October to December; January, February, and March are months of *winter stagnation* when the water column is *inversely stably stratified*. During certain time periods in late December and late March, conditions of *winter homothermy* and *spring circulation* prevail when the entire water body throughout the whole depth has the same uniform temperature (density), and any small wind or heat loss generates deep mixing.

One easily recognises in many of these curves the transition from the (more or less well) mixed upper layer (*epilimnion*; Greek: *epi*, above; *limnon*, lake) via an intermediate layer with strong vertical temperature gradient (*metalimnion*; *meta*, in-between) to a lower layer above the lake bottom with nearly constant temperature (*hypolimnion*; *hypo*, below). The (horizontal) surface in a lake with *maximum temperature gradient* is called *thermocline* (from: thermal inclination).

1.3.2 Characteristics by Mixing

Lakes are often classified according to their scheme of circulation. If the mixing reaches at any one time during the year the lake bottom, then it is called *holomictic* (*holo*, entire; *mictic*, mixing). In deep lakes or in lakes with a lower layer containing

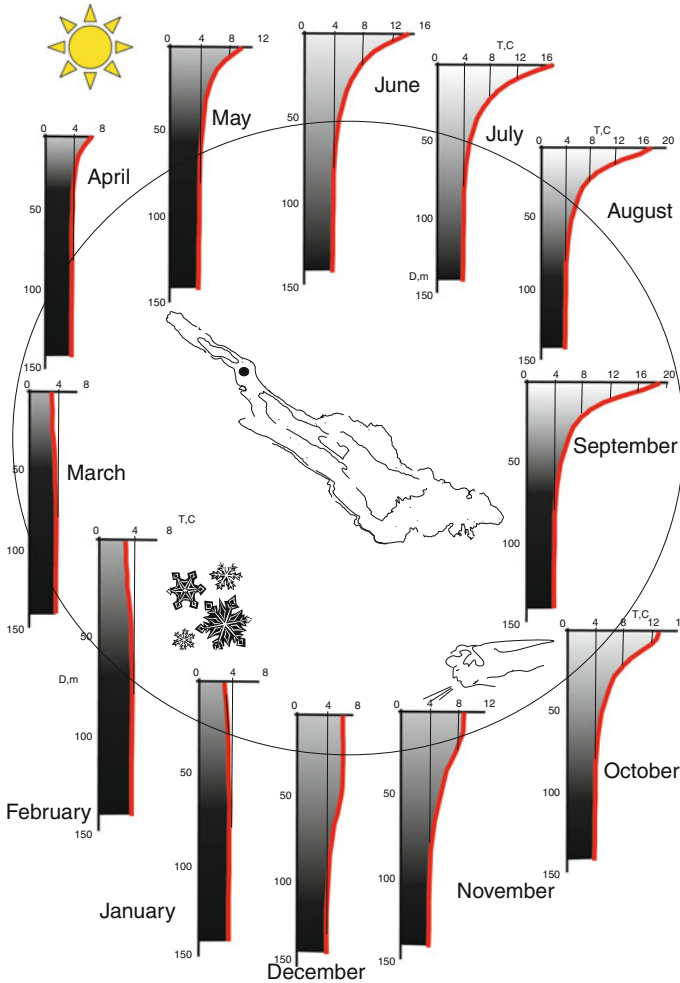


Fig. 1.8 Monthly averaged temperature profiles for Lake Constance through the year 1987, taken from thermistor recordings at the indicated station (Constance Data Band) [2]

increased salinity, the heavy water may, on occasion, not participate in the mixing processes; in those cases the lake is called *meromictic* (*mero*, partly). In such waters in which virtually no deep water exchange occurs, a shortage of available oxygen usually arises.

The above described mixing and heating processes are typical of *holomictic* lakes, especially for *dimictic* ones (*di*, two, double), which mix twice per year. The classification of lakes according to their mixing behaviour goes back to works by FOREL [9] and was extended and updated by FINDENEGG [6–8] and HUTCHINSON and LÖFFLER [12] to its present used form. In general, one may differentiate three classes: *holomictic* lakes, which are mixed once or several times during a year down

to the bottom; *meromictic* lakes, which mix only to a certain depth, which chiefly depends on how much a lake is exposed to wind; these lakes never (or only very seldom) mix to the ground; and, finally, *amictic* lakes which never mix. Amictic lakes for instance arise in Antarctica where a whole-year ice cover attenuates the energy fluxes into the water body, and thus generation of turbulent intensity is blocked.

Holomictic lakes – they are the rule – are further differentiated according to how often they mix during a year. At moderate latitudes, one often encounters *dimictic* lakes, which experience a complete circulation in spring and in autumn; in spring the inverse (but stable) temperature profile goes through a complete circulation and then establishes a stable (and normal) stratification; in fall the opposite phenomenon arises, namely the transition from a direct to an inverse temperature profile. If the density maximum (i.e. the 4°C temperature) is never crossed, then this lake is *monomictic*, it mixes only once per year. If the temperature remains always below the temperature corresponding to the density maximum, then one speaks of a *cold monomictic* lake, in the reverse case of a *warm monomictic* one.

If in the course of a year several mixing events take place – e.g. because frequent wind events trigger complete mixing in a shallow lake or because only a weak stratification has formed and the air temperature is subject to strong variations (which often occurs in the tropics) – then the lake is called *polymictic* (*poly*, many). If a lake mixes in irregular intervals, e.g. in intervals more than a year, it is called *oligomictic* (*oligo*, several).

Essential conditions which make the various states likely are the geographical position (latitude, altitude), exposition to wind in connection with the lake surface and depth and a possible chemical stratification. Some characterisations of such lake types are illustrated in Fig. 1.9.

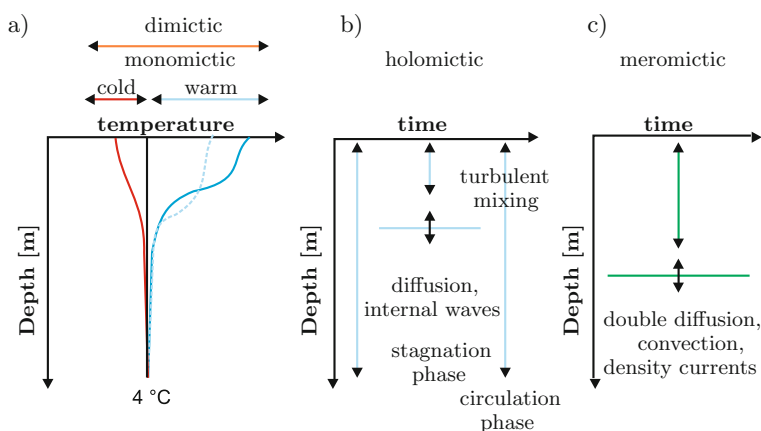


Fig. 1.9 Lake types characterised according to how they mix. (a) Mono- and dimictic lakes are characterised by the vertical temperature profile and how it varies near the surface; (b), (c) holomictic and meromictic lakes are characterised by the fact whether the mixed layer may reach the bottom or not (courtesy K. JÖHNK [15])

The mixing type of a lake is the result of global external conditions such as climate, location, water inflow and outflow, and lake morphometry. So, it is a very conservative lake feature and difficult to influence. However, it can be changed if some of these conditions are altered. For example, the hypersaline Dead Sea was during the past 300 years a meromictic lake: the freshwater input from the Jordan and Yarmuk rivers created a light (freshened) upper layer above the extremely salty lake waters so that winter cooling or any wind could overcome such a strong stratification. However, since the 1960, an increasing fraction of freshwater has been diverted for irrigation, the thickness of the less-saline surface layer decreased and since 1979 the meromictic structure is variable. The Dead Sea can now turn over during winter depending on the strength, timing, duration of the river inflow, evaporation, and cooling [1, 13].

Another – natural – change of mixing type occurs in Lake Constance of which the seasonal circle for the year 1987 is given in Fig. 1.8. This lake is typically classified as warm monomictic, the only one of this mixing type among European lakes to the north of the Alpine chain. Its ‘winter homothermy’ typically meets its ‘spring circulation’ so that the lake has its long *winter holomixis* from late December until March with a water temperature of about $4.5 - 5 - 6^{\circ}\text{C}$. However, it can on occasion be completely ice covered; the last such extraordinary event was observed in winter 1962/1963 [3, 23]. Thus, this lake is actually oligomictic.

1.3.3 Boundary-Related Processes

In contrast to the large open ocean, various boundary-related processes are significant for lake dynamics at large. For instance, strong wind that is steady for a certain time may generate a *wind set-up*⁶ of the water masses, which after secession of the wind induces an oscillating motion of which the periods are dictated by the size, shape and bathymetry of the basin. Moreover, one encounters the generation of boundary-related turbulence, internal wave reflection from the bottom slope, down-sloping gravity currents, inflows of tributaries, etc., which are all essential processes. At the scale of seasonal and diurnal lake dynamics, boundary-related *thermal* processes are remarkable. They produce horizontal temperature gradients between the *littoral area*⁷ (located near the shore) and the *pelagial* or *limnetic* (open water, away from the bottom⁸ and not in close proximity to the shoreline) regions

⁶ *Wind set-up* is used to mean the inclination of the lake surface set-up under the action of a steady (uniform) wind blowing along a lake surface.

⁷ Henceforth, we shall use the denotations ‘littoral’ and *pelagial* to denote these disjoint zones. This is used in limnology, while in oceanography, ‘littoral’ means ‘a coastal zone between high and low tide marks’.

⁸ The sediments, free of vegetation, that lie below the pelagial zone are referred to as the *profundal zone*.

and generate a specific littoral–pelagial water exchange. Such littoral–pelagial water exchanges are the likely source of the ventilation of the deep layers in Lake Baikal [20, 21, 25]. Effectively, in a diurnal circle, shallow waters near the coast experience faster heating during daytime and faster cooling at night. This process is especially well pronounced in summer when one easily observes daily heating of waters near shore. Actually, this horizontal inhomogeneity generates a weak diurnal circulation (with the characteristic speed of units of millimetre per second) directed offshore/onshore, which is physically similar to the sea/land or lake/land breezes in the atmosphere of coastal land areas.

On seasonal timescales, namely during the *spring and fall transition periods*, due to the different speeds of the cooling/heating processes in the littoral and pelagial regions, the horizontal temperature gradients become especially large and may affect the entire lake dynamics. Indeed, when the upper mixed layer is formed in a lake under autumn cooling (or during the spring circulation period), the littoral waters become heavier than the surface limnetic water masses; they slowly sink down the coastal slope beneath the upper mixed layer and generate a (more or less) permanent cooled water cascade from the coastal zone into deeper and deeper layers of the pelagial region. Since this process may last for months, it then adjusts to the Earth's rotation so that general cyclonic circulation is typically reported for large lakes in autumn, with velocities of the order of a few centimetres per second. An even more conspicuous influence on lake-scale water dynamics and associated exchange of water masses is exerted when water reaches the 4°C barrier: it always happens first near the coast. With ongoing cooling in autumn, one observes in a lake an inversely and thus stably stratified area near the coast and, simultaneously, a still mixing unstably stratified limnetic region. To accentuate this difference in the structure of mixing, the three-dimensional surface in-between, where the water has the maximum density, is called the *structural front* (or *thermal bar* in freshwater lake).

It possesses a specific water circulation, see Fig. 1.10; when it is just formed, the 4°C densest water tends to sink down; the lake surface experiences an (very small) inclination towards the bar, water from both sides flows to the barrier, sinks and returns back in the deeper layers. With time, horizontal temperature/density gradients between littoral and limnetic areas increase, driving the horizontal exchange flows: offshore flow in the upper layers of the heated shallow region, onshore flow at intermediate depths and again offshore cascading flow further down in the still cold limnetic area. Thus, the lake body becomes divided into nearly separated littoral and limnetic circulatory cells. This process is most profitable for the lake biota in spring: being separated from the cold lake body, the littoral waters are warming up much faster and thus providing favourable living conditions. This specific circulation stops when the stratified volumes that move from opposite shores meet one another in the middle of the lake; a stable stratification is then established all over the lake. These processes definitely develop in lakes at mid-to-high latitudes, where the water temperature in its seasonal cycle crosses the 4°C point, at least near the shore. It has been observed and described for the first time by FOREL [9] in Lake

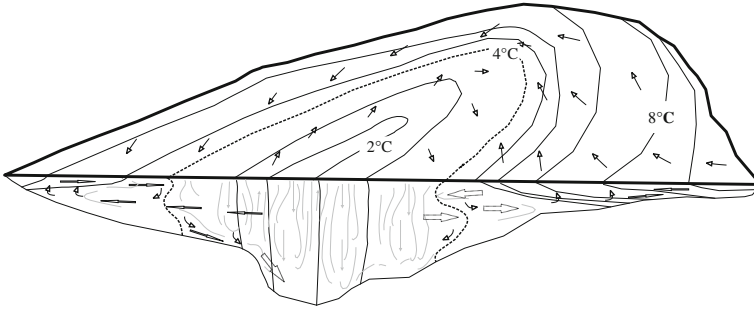


Fig. 1.10 *Spring thermal bar and related structure of the field of currents.* The dashed line on the horizontal free surface and on the front cross-sectional area marks the 4°C isotherm shell-like surface. Under the same conditions of spring heating, mixing regimes in water columns are different at both sides of the 4°C isotherm; there is a stable vertical density stratification in the shallow littoral region and an unstable stratification (vertical convective mixing) in the deep area. This leads to the horizontal circulation shown by *arrows*. CORIOLIS forces, acting on the water particles, drive their motion towards the right on the northern hemisphere and lead to a cyclonic (anticyclonic) circulation in the littoral (limnetic) surface sub-regions, a pattern that is reverse in the southern hemisphere (after TIKHOMIROV [22] with changes)

Geneva; it regularly crosses the Great Lakes of America [17] and Lake Baikal in Siberia [20] twice a year; it lasts 1–1.5 months in spring and about the same time in autumn in Lakes Ladoga and Onega in northern Europe [5, 18, 22].

1.3.4 Characterisation by Typical Scales

When approaching a physical description of a lake, one should quantify both the very object and the phenomena in focus. Nowadays, many characteristics of particular lakes are available via data banks in the Internet (as for example, databank of the International Lake Environment Committee Foundation; <http://www.ilec.or.jp>). An obvious parametre connected with the topography of a lake is the ratio of a characteristic depth to a typical horizontal distance. As such one often takes the maximum depth to the square root of the surface area. Any one of these ratios is called *aspect ratio*, and typical values are of the order of 10^{-3} . Thus, the horizontal scale is much larger than the vertical scale, and this suggests the obvious supposition that the large-scale motions are also predominantly horizontal, with relatively large horizontal and correspondingly small vertical velocities. This will later be made mathematically formal by the so-called *shallow-water approximation*. For instance, the aspect ratio for the large mountain Lake Constance is rather big – of the order of 10^{-2} . However, reducing this lake (the maximum length of about 60 km) to the size of a desk (1.5 m), its maximum depth would be about 6 mm. Similarly, the maximum depth of the World's deepest Lake Baikal (1636 m) scaled to the size of a desk is about 1.5 cm. However, unlike in the ocean, for many physical processes in lakes the three dimensionality is very significant, primarily as a result of the

influence of the sloping boundaries. In this connection it is also important to note that typical values of the bottom slope in lakes are of the same order as the aspect ratio, i.e. 10^{-3} , i.e. 1 m of difference in depth per 1 km of horizontal distance, or about 0.5° . A bottom slope of 3° is already steep, susceptible to the development of turbidity currents, and a slope of 6° is considered very steep since sandy sediments slide down along it and internal waves can be reflected. Thus, the *aspect ratio and bottom slope in lakes are typically small parameters*.

An important parametre in lake dynamics (as well as in the ocean) is the ROSSBY number. It characterises *how significant for a given process is the rotation of the Earth*. If the length scale for some motion is L and the characteristic velocity is U , then the time required to pass the distance L is L/U . If this time is significantly smaller than the period of rotation of the Earth, the flow will hardly experience an influence of the latter. The ROSSBY number measures this as it is the ratio of the timescale of the rotation of the Earth, i.e. 24 h, to the timescale typical for the given process. Denoting this ratio by \mathbb{R}_0 , we obtain

$$\mathbb{R}_0 = \frac{1/\Omega}{L/U} = \frac{U}{\Omega L},$$

where $\Omega = 2\pi/(24 \text{ h}) = 7.3 \times 10^{-5} \text{ s}^{-1}$. If $\mathbb{R}_0 \ll 1$, then the motion is of small scale, and effects of the rotation of the Earth may be ignored.

A measure for the *significance of the water stratification* is the so-called BURGER number \mathbb{S} :

$$\mathbb{S} = g \frac{\Delta\rho}{\rho} \frac{D}{f^2 L^2},$$

where D and L are typical vertical and horizontal scales, $\Delta\rho/\rho$ is a characteristic density difference, measured at the *vertical scale* of a motion D (for instance, between the epi- and the hypolimnion), g is the gravity acceleration and $f = 2\Omega \sin\phi$ is the CORIOLIS parametre. \mathbb{S} may be interpreted as the ratio of two squared velocities $g \Delta\rho/\rho D$ and $f^2 L^2$, respectively, or two squared lengths $\mathbb{S} = (L_D/L)^2$, where $L_D = \frac{1}{2}(g \Delta\rho/\rho D)^{1/2}$ is called the ROSSBY radius of deformation. Physically, it gives an estimate of the length scale of a motion, for which the Earth's rotation becomes the main driving force. Using the characteristic lake width B as the scale of motion, we obtain a dimensionless parametre $\mathbb{S}^{1/2} = R = L_D/B$, indicating a potential influence of the rotation of the Earth on general lake circulation. If $R \geq 1$, planetary rotation is a significant factor for basin-scale motion.

There are many more dimensionless numbers that are defined in physical limnology. The reader may in other contexts already have encountered the REYNOLDS number RICHARDSON number and others. They all can be expressed as ratios of quantities having the same physical dimension and expressing an order of magnitude of a physical quantity describing a subprocess of the system that is analysed. The value of the dimensionless characteristic number then allows to estimate how significant the two subprocesses are relative to one another. If, e.g., the characteristic

number is very small or very large, then this expresses that one of the subprocesses plays an insignificant role in comparison with the other. For instance, the FROUDE number can be viewed as the ratio of the kinetic energy to the gravitational potential energy. With ρ , U , g and D denoting density, typical velocity, gravity and depth scale, respectively, one may write

Typical kinetic energy $\sim \rho U^2$,

Typical potential energy due to gravity $\sim \rho g D$,

and so

$$\mathbb{F}r = \frac{\rho U^2}{\rho g D} = \frac{U^2}{g D}.$$

$\mathbb{F}r \ll 1$ means that kinetic effects are much smaller than gravity effects and so inertia plays an insignificant role in comparison to gravity forces. On the other hand, when $\mathbb{F}r \gg 1$, it is reverse; gravity effects may be ignored but not inertia.

A large part of the working methods of physical limnology consists in establishing equations that describe the processes in focus in mathematical terms. When these equations are suitably scaled, i.e. written in dimensionless form by introducing for each physical variable, a typical order of magnitude and using this to non-dimensionalise the equations, the equations will appear in a form in which dimensionless characteristic numbers appear as parameters. If for some limnological process some of these are very small or very large, approximations are suggested which simplify the equations and make analysis and physical interpretation simpler. We will encounter this in a number of situations.

References

1. Anati, D.A., Stiller, M., Shasha, S. and Gat, J.R.: Changes in the thermohaline structure of the Dead Sea: 1979–1984. *Earth Planet. Sci. Lett.* **84**, 109–121 (1987)
2. Bäuerle, E., Chubarenko, B., Chubarenko, I., Halder, J., Hutter, K. and Wang, Y.: Autumn Physical Limnological Experimental Campaign in the Mainau Island Littoral Zone of Lake Constance (Constance Data Band) 12 October – 19 November 2001. *Report of the 'Sonderforschungsbereich 454 Bodenseelittoral'*, 85 p. (2002)
3. Bäuerle, E., Ollinger, D. and Ilmberger, J.: Some meteorological, hydrological, and hydrodynamical aspects of upper lake constance. In: *Arch. Hydrobiol. Spec. Issues Advanc. Limnol. Lake Constance: Characterization of an ecosystem in transition.* (eds. Bäuerle, E. and Gaedke, U.), **53**, 31–83 (1998)
4. Fatio de Duillier, J.-C.: Remarques sur l'histoire naturelle du Lac de Genève. In Spon, *Histoire de Genève* **II**, 463 (1730)
5. Filatov, N.N.: *Dynamics of Lakes*. Leningrad, Hydrometeoizdat, 165p. (1983) (In Russian)
6. Findenegg, I.: Die Schichtungsverhältnisse im Wörthersee. *Arch. Hydrobiol.* **24**, 253–262 (1932)
7. Findenegg, I.: Zur Naturgeschichte des Wörthersees. *Carinthia II, Sonderheft* **2**, 1–63 (1933a)
8. Findenegg, I.: Alpenseen ohne Vollzirkulation. *Int. Rev. Hydrobiol.* **28**, 295–311 (1933b)
9. Forel, F.A.: *Le Léman: monographie limnologique*, (F. Rouge, Librairie de l'Université de Lausanne Vol. 1, 1892, 539p.; Vol. 2, 1895, 651p.; Vol. 3, 1904, 715p.)

10. Heaps, N.S., Mortimer, C.H. and Fee, E.J.: Numerical models and observations of water motion in Green–Bay, Lake Michigan. *Phil. Trans. Royal. Soc., London* **A306**, 371–398 (1982)
11. Hollan, E., Rao, D.B. and Bäuerle, E.: Free surface oscillations in Lake Constance with an interpretation of the “Wunder of the rising water at Konstanz” 1549. *Arch. Met. Geophys. Biokl. A* **29**, 301–315 (1980)
12. Hutchinson, G.E. and Löffler, H.: The thermal classification of lakes. *Proc. Natl. Acad. Sci.* **42**, 84–86 (1956)
13. Imboden, D.M. and Wüest, A.: Mixing mechanisms in lakes. In: *Physics and Chemistry of Lakes* (eds. Lerman, A., Imboden, D.M. and Gat, J.R.), Springer Verlag, Berlin, 83–138 (1995)
14. Jänichen, H.: Wirtschaft und Verkehr. In: *Der Landkreis Konstanz, amtliche Kreisbeschreibung*. Hrsg. Staatliche Archivverwaltung Baden-Württemberg. **1**, 361–404 (1968)
15. Jöhnk, K.: *Ein eindimensionales hydrodynamisches Modell in der Limnophysik. Turbulenz–Meromixis–Sauerstoff*. Habilitationsschrift, Fachbereich Mechanik, Technische Hochschule Darmstadt, Darmstadt, 235 p. (2000)
16. Mortimer, C.H.: Lake hydrodynamics. *Mitt. Int. Ver. Limnol.* **20**, 124–197 (1974)
17. Mortimer, C.H.: Frontiers in physical limnology with particular reference to long waves in rotating basins. *Proc. 5th Conf. Great Lakes Res. Univ. Mich. Publ.* **9**, 9–42 (1963)
18. Naumenko, M.A.: Some aspects of the thermal regime of large lakes: Lake Ladoga and Lake Onega. *Water Poll. Res. J. Can.* **29**, (2–3), 423–439 (1994)
19. Schulthaiss, C.: Wunder anloffen des Wassers. *Collectaneen*, **VI**, 80–81. Stadtarchiv Konstanz (1549)
20. Shimaraev, M.N., Granin, N.G. and Zhdanov, A.A.: The role of spring thermal bars in the deep ventilation of Lake Baikal water. *Limnol. Oceanogr.* **38**(5), 1068–1072 (1993)
21. Shimaraev, M.N., Verbolov, V.I., Granin, N.G. and Sherstyankin, P.P.: *Physical limnology of Lake Baikal: A Review*. (eds. Shimaraev, M.N. and Okuda S.), Baikal International Center for Ecological Research Irkutsk-Okayama. 89 p. (1991)
22. Tikhomirov, A.I.: *Thermics of Large Lakes*. Leningrad, Nauka Publishing House, 232 p. (1982) (In Russian)
23. Wagner, G.: Untersuchungen am zugefrorenen Bodensee. *Schweiz. Z. Hydrol.* **26**, 52–68 (1964)
24. Weisbach, J.: *Der Ingenieur. Sammlung von Tafeln, Formeln und Regeln der Arithmetik, der theoretischen und praktischen Geometrie sowie der Mechanik und des Ingenieurwesens*. 3. Aufl. F. Vieweg & Sohn, Braunschweig, 862 p. (1860)
25. Wüest, A., Ravens, T.M., Granin, N.G., Kocsis, O., Schurter, M. and Sturm, M.: Cold intrusions in Lake Baikal: Direct observational evidence for deep-water renewal. *Limnol. Oceanogr.* **50** (1), 184–196 (2005)

Chapter 2

Mathematical Prerequisites

Lake physics cannot be described let alone understood without tailoring the statements in mathematical expressions and deducing results from these. We now wish to lay down the mathematical prerequisites that are indispensable to reach quantitative results. A systematic presentation will not be given because it is assumed that the reader is (or once has been) familiar with the subjects and only needs to be reminded of knowledge that may be somewhat dormant. Let us begin with mathematics.¹

The objects in question are material bodies; these are the lake waters filling the entire lake or parts of it, tracers or species that are mixed with the water as suspended matter (plankton, sediments) or matter in solution (oxygen, phosphate, nitrate), etc. Henceforth, when dealing with these subjects, we simply refer to them as *material bodies* or *bodies* which occupy a certain region or volume of the three-dimensional space, the *space of the physical world*. Euclidean geometry describes correctly all the geometric, kinematic quantities that need to be considered when describing the motion of bodies within this space, with which the reader is essentially supposed to be familiar. In short, in such a space one can measure distances, lengths and angles. Mathematical entities that arise in the formulation of physical laws are *scalars*, *vectors* and *tensors*. These are mathematical objects defined by the mathematical operations which one may perform among such objects.

¹ The mathematical prerequisites and the knowledge of physics required to follow the ensuing developments are those of a basic education in engineering or natural sciences at universities that is generally acquired in two or three semesters of calculus, linear algebra, differential equations and vector and matrix calculus. However, while the elements of these subjects are taught, they do not lie in the centre of the syllabi of the mentioned fields of study. Likewise, as far as the background of physics is concerned, only the fundamentals of classical physics are needed which are generally taught at universities to engineers and natural scientists in a one or two semester course during their basic education. To lay a common ground of this knowledge and to outline the ‘language’ used we shall repeat subsequently elements of both fields. There are many books on basic physics and on calculus, and each university seems to teach these subjects from its own lecture notes. A very popular set of physics books are The FEYNMAN Lecture Notes [8]. Well-known calculus books are [2, 12, 15–17]. Readers familiar with the calculus of vectors and tensors – here only the Cartesian tensor notation is used – may omit a careful reading of this chapter and directly pass to Chap. 3. Nevertheless, a quick glance through this section may be helpful, since the notation used throughout the entire text is introduced.

2.1 Scalars and Vectors

Scalars are quantities that behave like real or complex numbers; four operations, addition, subtraction, multiplication and division, are defined for them, and we generally are so familiar with them that we use the mathematical operations without further thought. In fact, addition (subtraction) and multiplication (division) obey the commutative, associative and distributive laws. This means that if x, y, z are scalars, then

$$\left. \begin{array}{l} x + y = y + x \\ xy = yx \end{array} \right\} \quad \text{commutative law,}$$

$$\left. \begin{array}{l} (x + y) + z = x + (y + z) \\ (xy)z = x(yz) \end{array} \right\} \quad \text{associative law,}$$

$$(x + y)z = xz + yz, \quad \text{distributive law}$$

also define scalars. Furthermore, there is a zero, 0, and unit, 1, scalar such that

$$\begin{aligned} x + 0 &= x, & 0x &= 0, & 1x &= x, \\ x + (-x) &= 0, & x \left(\frac{1}{x} \right) &= 1. \end{aligned}$$

In these operations only the division by 0 is special, i.e. $x(\frac{1}{y})$ is defined only for $y \neq 0$. Should $y = 0$, then we declare $x(\frac{1}{y}) = \infty$ if $x \neq 0$. If a set of scalars possesses the property that any two or three scalars, which are combined according to the above declared operations, yields a number of the set, then this set is called a *field*. We speak of the field of the real numbers \mathbb{R} or complex numbers \mathbb{C} because adding or multiplying two real numbers again yields a real number, etc. A field is therefore also said to be a set of scalars that is *closed* under addition and multiplication.

Vectors are quantities that behave like directed segments. Mathematically, we have the following:

Definition 2.1 A vector space is a set of objects $\mathbf{x}, \mathbf{y}, \mathbf{z}$ called **vectors** that is closed under vector addition and multiplication with scalars. One vector is distinguished, called zero vector, and denoted by $\mathbf{0}$, and for each vector \mathbf{x} , there is a vector $-\mathbf{x}$, called the negative of \mathbf{x} . The following axioms are assumed to hold:

(A) For any vectors $\mathbf{x}, \mathbf{y}, \mathbf{z}$ we have

$$\begin{aligned} (A_1) \quad \mathbf{x} + \mathbf{y} &= \mathbf{y} + \mathbf{x}, & \text{commutative law,} \\ (A_2) \quad \mathbf{x} + (\mathbf{y} + \mathbf{z}) &= (\mathbf{x} + \mathbf{y}) + \mathbf{z}, & \text{associative law,} \\ (A_3) \quad \mathbf{x} + \mathbf{0} &= \mathbf{x}, \\ (A_4) \quad \mathbf{x} + (-\mathbf{x}) &= \mathbf{0}. \end{aligned}$$

(M) For each scalar λ and each vector \mathbf{x} the multiple of \mathbf{x} with λ , denoted by $\lambda\mathbf{x}$, exists with the properties

$$\left. \begin{aligned} (M_1) \quad \lambda(\mathbf{x} + \mathbf{y}) &= \lambda\mathbf{x} + \lambda\mathbf{y}, \\ (M_2) \quad (\lambda + \mu)\mathbf{x} &= \lambda\mathbf{x} + \mu\mathbf{x}, \end{aligned} \right\} \quad \text{distributive law,}$$

$$(M_3) \quad (\lambda\mu)\mathbf{x} = \lambda(\mu\mathbf{x}), \quad \text{associative law,}$$

$$(M_4) \quad 1\mathbf{x} = \mathbf{x}.$$

■

This definition does not assign to vectors the property to have a length. To this end, a further operation between two vectors must be defined.

Definition 2.2 The **scalar product** between two vectors \mathbf{x} and \mathbf{y} , denoted by $\mathbf{x} \cdot \mathbf{y}$, assigns to \mathbf{x} and \mathbf{y} a real number and obeys the following rules²:

$$\begin{aligned} (P_1) \quad \mathbf{y} \cdot \mathbf{x} &= \mathbf{x} \cdot \mathbf{y}, \\ (P_2) \quad (\mathbf{x} + \mathbf{y}) \cdot \mathbf{z} &= \mathbf{x} \cdot \mathbf{z} + \mathbf{y} \cdot \mathbf{z}, \\ (P_3) \quad (\lambda\mathbf{x}) \cdot \mathbf{y} &= \lambda(\mathbf{x} \cdot \mathbf{y}), \\ (P_4) \quad \mathbf{x} \cdot \mathbf{x} &> 0, \text{ when } \mathbf{x} > \mathbf{0}. \end{aligned}$$

We use the dot between two vectors to denote the scalar product. ■

In three dimensions the scalar product is defined in a slightly different form, one that is likely more familiar to the reader (but also less general). All rules defined above may, however, be corroborated.

Definition 2.3 With the scalar product the **length** or the **norm** of a vector can be defined as

$$\|\mathbf{x}\| = +\sqrt{\mathbf{x} \cdot \mathbf{x}},$$

and it is obvious that $\|\lambda\mathbf{x}\| = |\lambda| \|\mathbf{x}\|$. ■

Clearly, because of the property (P_4) , $\|\mathbf{x}\| > 0$ when $\mathbf{x} \neq \mathbf{0}$ and $\|\mathbf{x}\| = 0$ if and only if $\mathbf{x} = \mathbf{0}$. As an exercise to familiarise himself, the reader may also prove the following facts:

² We restrict here considerations to real numbers. If $\mathbf{x} \cdot \mathbf{y}$ can be a complex number, then P_1 is defined as $\mathbf{x} \cdot \mathbf{y} = (\mathbf{y} \cdot \mathbf{x})^*$, where $*$ denotes the conjugate complex number.

Problem 2.1 Using the definition of the norm, prove that

$$(1) \quad \| \mathbf{x} + \mathbf{y} \|^2 + \| \mathbf{x} - \mathbf{y} \|^2 = 2(\| \mathbf{x} \|^2 + \| \mathbf{y} \|^2) \quad (\text{Parallelogram law})$$

$$(2) \quad | \mathbf{x} \cdot \mathbf{y} | \leq \| \mathbf{x} \| \| \mathbf{y} \| \quad (\text{Cauchy-Schwarz inequality})$$

$$(3) \quad \| \mathbf{x} + \mathbf{y} \| \leq \| \mathbf{x} \| + \| \mathbf{y} \| \quad (\text{Triangle inequality})$$



Definition 2.4 The **scalar product** of two vectors \mathbf{a} and \mathbf{b} in \mathbb{R}^3 is a scalar (i.e. real number) c given by the formula

$$c := \mathbf{a} \cdot \mathbf{b} = |\mathbf{a}| |\mathbf{b}| \cos \varphi_{ab}. \quad (2.1)$$

In words: The scalar product c of two vectors \mathbf{a} and \mathbf{b} is the product of the lengths of the two vectors $|\mathbf{a}|$ and $|\mathbf{b}|$, respectively, times the cosine of the angle spanned by the two vectors. ■

In order to define the angle between two vectors, one may in imagination have to move the two vectors to a common point of attack as shown in Fig. 2.1. Notice, moreover, that in the above we have used the point \cdot to symbolise the scalar product and defined $|\mathbf{a}|$ to be the length of the vector \mathbf{a} (and similarly for the vector \mathbf{b}), and we have introduced φ_{ab} to denote the angle between the two vectors, see Fig. 2.1. For an acute angle ($-90^\circ \leq \varphi < 90^\circ$) c is positive, while for an obtuse angle ($90^\circ < \varphi \leq 270^\circ$) c is negative. It follows from (2.1) that if two vectors \mathbf{a} and \mathbf{b} are orthogonal, then $c = 0$ since φ is then 90° . Mathematically this statement may be written as

$$\mathbf{a} \perp \mathbf{b} \implies \mathbf{a} \cdot \mathbf{b} = 0, \quad (2.2)$$

but (2.2) cannot be read in the opposite (\Leftarrow) direction; if $\mathbf{a} \cdot \mathbf{b} = 0$, then either \mathbf{a} or \mathbf{b} is a zero vector or \mathbf{a} is perpendicular to \mathbf{b} . Thus the reverse statement is

$$\left\{ \begin{array}{l} \mathbf{a} = \mathbf{0} \text{ or} \\ \mathbf{b} = \mathbf{0} \text{ or} \\ \mathbf{a} \perp \mathbf{b} \end{array} \right\} \Leftarrow \mathbf{a} \cdot \mathbf{b} = 0. \quad (2.3)$$

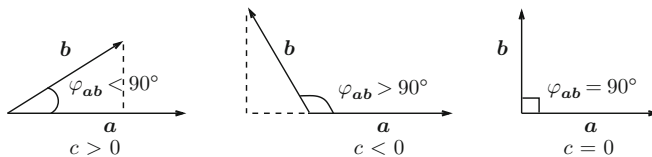


Fig. 2.1 Explaining the scalar product of two vectors $c = |\mathbf{a}||\mathbf{b}| \cos \varphi_{ab}$

Problem 2.2 Prove that Definition 2.4 satisfies the properties (P_1) – (P_4) . \blacklozenge

For two vectors \mathbf{x} , \mathbf{y} , we call $\|\mathbf{x} - \mathbf{y}\|$ the *distance* from the endpoint of \mathbf{x} to the endpoint of \mathbf{y} and denote it sometimes by $d(\mathbf{x}, \mathbf{y})$. With the above definitions and properties, it is easy to show that

$$\begin{aligned} d(\mathbf{x}, \mathbf{y}) &> 0, \text{ when } \mathbf{x} \neq \mathbf{y}, \\ d(\mathbf{x}, \mathbf{y}) &= 0, \text{ if and only if } \mathbf{x} = \mathbf{y}, \\ d(\mathbf{x}, \mathbf{y}) &= d(\mathbf{y}, \mathbf{x}), \\ d(\mathbf{x}, \mathbf{z}) &\leq d(\mathbf{x}, \mathbf{y}) + d(\mathbf{y}, \mathbf{z}). \end{aligned}$$

The last relation says that the sum of the length of two triangle sides is always larger than or equal to the third side.

Two vectors, \mathbf{x} and \mathbf{y} , are called *collinear* (to one another) if $\mathbf{y} = \lambda\mathbf{x}$, $\lambda \neq 0$. The two vectors are then parallel (or antiparallel) and the length of \mathbf{y} is $|\lambda|$ times the length of \mathbf{x} . If $\mathbf{y} \neq \lambda\mathbf{x}$ for any real λ , then \mathbf{x} and \mathbf{y} are not collinear. We also call two non-trivial vectors, \mathbf{x} and \mathbf{y} , *orthogonal* if the scalar product between them vanishes, explicitly,

$$\mathbf{x} \text{ and } \mathbf{y} \text{ are orthogonal} \implies \mathbf{x} \cdot \mathbf{y} = 0.$$

If, in addition, the length of the two vectors is unity, $\|\mathbf{x}\| = 1$, $\|\mathbf{y}\| = 1$, and $\mathbf{x} \cdot \mathbf{y} = 0$, then these two vectors are called *orthonormal*. It is obvious that two nontrivial vectors which are orthogonal cannot be collinear. Two non-trivial vectors which are not collinear are called *linearly independent*. It can be proved that in a vector space there is a set $\{\mathbf{b}_1, \dots, \mathbf{b}_n\}$ of linearly independent vectors which is maximal, i.e. possesses n elements \mathbf{b}_j ; the maximum number of such independent elements n is unique and defines the *dimension* of the vector space; it can be finite or infinite. Any independent maximum set $\{\mathbf{b}_1, \dots, \mathbf{b}_n\}$ is called a *basis*, and an arbitrary vector \mathbf{x} can be represented as a linear combination of the basis elements

$$\mathbf{x} = x^1\mathbf{b}_1 + \dots + x^n\mathbf{b}_n = \sum_{j=1}^n x^j\mathbf{b}_j.$$

Moreover, in a vector space with scalar product, there exist orthonormal bases $\{\hat{\mathbf{e}}_1, \hat{\mathbf{e}}_2, \dots, \hat{\mathbf{e}}_n\}$ consisting of n elements with the properties that

$$\hat{\mathbf{e}}_i \cdot \hat{\mathbf{e}}_j = \begin{cases} 1, & i = j, \\ 0, & i \neq j. \end{cases}$$

If such a basis is constant, i.e. the same for all \mathbf{x} , it is called *Cartesian*.

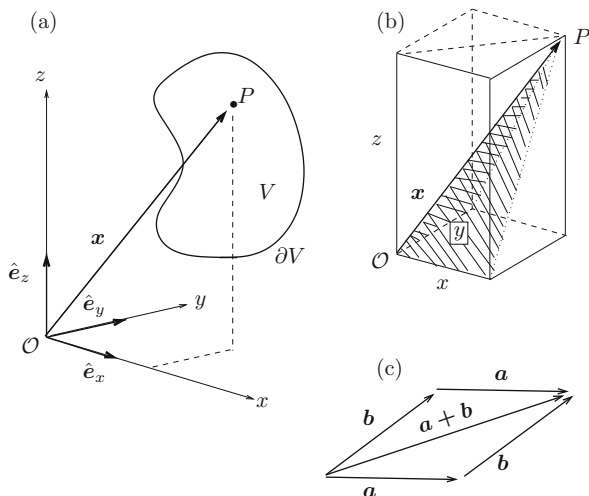


Fig. 2.2 (a) Three-dimensional EUCLIDIAN space equipped with an origin \mathcal{O} and an orthonormal basis $\{\hat{e}_x, \hat{e}_y, \hat{e}_z\}$, defining a Cartesian coordinate system. Embedded in this space is a material body with volume V and boundary ∂V ; the position P of a point is described by the vector \mathbf{x} . (b) The orthogonal projections of \mathbf{x} onto the directions of the basis vectors defining the coordinates x, y, z of \mathbf{x} . (c) Parallelogram for the addition of vectors \mathbf{a} and \mathbf{b} , demonstrating that $\mathbf{a} + \mathbf{b} = \mathbf{b} + \mathbf{a}$

In what follows, we shall interpret the physical space as a three-dimensional vector space. In particular, to describe the various points of a material body that occupies a certain region V in this space, one chooses a particular point as the origin \mathcal{O} and selects a basis $\{\hat{e}_x, \hat{e}_y, \hat{e}_z\}$ defining three non-co-planar directions, see Fig. 2.2. The elements $\{\hat{e}_x, \hat{e}_y, \hat{e}_z\}$ may be chosen to be orthogonal, and their lengths can be chosen to be unity on a selected length scale (e.g. 1 m, 1 km). If they are so chosen, the basis $\{\hat{e}_x, \hat{e}_y, \hat{e}_z\}$ is called an *orthonormal basis* and the corresponding coordinate system is called a Cartesian coordinate system. The position of a body point P is then given by the vector $\overrightarrow{\mathcal{O}P}$ which in Fig. 2.2 is written as \mathbf{x} , and inspection shows that

$$\mathbf{x} = x\hat{e}_x + y\hat{e}_y + z\hat{e}_z, \quad (2.4)$$

in which x, y, z are the components³ of \mathbf{x} relative to the base vectors \hat{e}_x, \hat{e}_y and \hat{e}_z , respectively. Alternatively, since $x = \mathbf{x} \cdot \hat{e}_x$, $y = \mathbf{x} \cdot \hat{e}_y$, $z = \mathbf{x} \cdot \hat{e}_z$, x, y and z are the projections of \mathbf{x} onto \hat{e}_x, \hat{e}_y and \hat{e}_z , respectively. As the reader has certainly realised, vectors are drawn in the graphs as arrows and their symbols are set in bold

³ In a general basis, these components can be constructed parallel to the base vectors or orthogonal to them. In a Cartesian system the two different projections coincide.

type. Moreover, in (2.4) we have assumed that the vector $x\hat{e}_x$ points in the direction of \hat{e}_x and has a length which is x times the length of \hat{e}_x , etc., and we have used the so-called *parallelogram rule*, according to which the vectors \mathbf{a} and \mathbf{b} are added together by arranging their arrows in sequence and by connecting the point of origin of the first with the end point of the second to obtain $\mathbf{a} + \mathbf{b}$. It is immediately seen that this addition is independent of the order in which it is performed, so $\mathbf{a} + \mathbf{b} = \mathbf{b} + \mathbf{a}$, see Fig. 2.2c.

The symbolic notation of vectors as bold faced letters, such as $\mathbf{a}, \mathbf{b}, \mathbf{c}, \dots$, or as italic letters with an overhead arrow $\vec{a}, \vec{b}, \vec{c}$ is standard, but some authors use fancy notations, e.g. $\mathfrak{a}, \mathfrak{b}, \mathfrak{c}, \dots$. In handwritten manuscripts, $\vec{a}, \vec{b}, \vec{c}$ or $\underline{a}, \underline{b}, \underline{c}, \dots$ are used. Important is that vectors are differentiated symbolically from scalars (which are simple real or complex numbers, and are generally italicised). There is, however, also a different, very popular way of writing vectors, but it is less general and based on a particular choice of a basis $\{\hat{e}_x, \hat{e}_y, \hat{e}_z\}$, for our purposes always chosen as an orthonormal Cartesian basis. This notation for (2.4) would be

$$\mathbf{x} \hat{=} (x, y, z), \quad (2.5)$$

i.e. one only writes down the Cartesian components as an *ordered triplet*. In (2.5) we have not written an equal sign but ' $\hat{=}$ ' instead to emphasise that the ordered triplet is not identical to the vector but *equivalent* or, as mathematicians say, *isomorphic* to the vector. For two vectors \mathbf{a} and \mathbf{b} we would write $\mathbf{a} \hat{=} (a_x, a_y, a_z)$ and $\mathbf{b} \hat{=} (b_x, b_y, b_z)$, and we leave it as an exercise to the reader to prove, using simply the parallelogram rule, that

$$\mathbf{a} + \mathbf{b} \hat{=} (a_x + b_x, a_y + b_y, a_z + b_z). \quad (2.6)$$

The elements a_x, a_y, a_z in (a_x, a_y, a_z) are called the components of the vector \mathbf{a} (with respect to the Cartesian basis $\{\hat{e}_x, \hat{e}_y, \hat{e}_z\}$).

There is yet another common rule of notation for vectors, and it is based on the fact that a three-dimensional EUCLIDIAN space can be '*spanned*' by three mutually non-co-planar base vectors which may be selected to be orthonormal. Instead of calling the three directions x, y, z , they may be called x_1, x_2, x_3 or simply x_i ($i = 1, 2, 3$). Instead of (2.4) we then can write

$$\begin{aligned} \mathbf{x} &= x_1\hat{e}_1 + x_2\hat{e}_2 + x_3\hat{e}_3, \\ &= \sum_{i=1}^3 x_i\hat{e}_i \stackrel{(1)}{=} \sum x_i\hat{e}_i \stackrel{(2)}{=} x_i\hat{e}_i, \end{aligned} \quad (2.7)$$

$$\mathbf{x} \hat{=} (x_1, x_2, x_3) \text{ or simply } \mathbf{x} \hat{=} x_i. \quad (2.8)$$

In these equations the expression in the first line and the first expression in the second line need no further explanation; the step indicated by ' $\stackrel{(1)}{=}$ ', simply omits

the explicit mentioning that the summation is carried over the indices from 1 to 3 and in $\text{‘}\stackrel{(2)}{=}\text{’}$, the summation is not even written down any longer and the convention is used that over doubly repeated indices i the expression must be summed over i from 1 to 3.

In the second expression of (2.8) the vector \mathbf{x} is simply replaced by an unspecified component x_i , where one tacitly implies that with i any one of the three components is meant.

The properties (P_1) – (P_4) provide us with the presentation of a very easy evaluation of the scalar product of two vectors using the notation (2.5). To this end, let $\mathbf{a} = \sum_i a_i \hat{\mathbf{e}}_i$, $\mathbf{b} = \sum_j b_j \hat{\mathbf{e}}_j$. Then,

$$\begin{aligned} \mathbf{a} \cdot \mathbf{b} &= \left(\sum_i a_i \hat{\mathbf{e}}_i \right) \cdot \left(\sum_j b_j \hat{\mathbf{e}}_j \right) \\ &\quad \text{(rules } (P_1)\text{--}(P_3) \text{ are used)} \\ &= \sum_{ij} a_i b_j \underbrace{\hat{\mathbf{e}}_i \cdot \hat{\mathbf{e}}_j}_{\delta_{ij}} \\ &= \sum_{ij} a_i b_j \delta_{ij} = \sum_i a_i b_i \\ &= a_1 b_1 + a_2 b_2 + a_3 b_3. \end{aligned} \tag{2.9}$$

Here, we have introduced a new symbol δ_{ij} . Its meaning can be understood if the reader recalls that for an orthonormal basis the vectors $\hat{\mathbf{e}}_i$ have unit length and are orthogonal so that $\hat{\mathbf{e}}_i \cdot \hat{\mathbf{e}}_j = 1$ if $i = j$ but $\hat{\mathbf{e}}_i \cdot \hat{\mathbf{e}}_j = 0$ if $i \neq j$. Therefore we define

$$\delta_{ij} = \begin{cases} 1 & \text{for } i = j, \\ 0 & \text{for } i \neq j, \end{cases} \quad \text{or } (\delta_{ij}) \hat{=} \begin{pmatrix} 1 & 0 & 0 \\ 0 & 1 & 0 \\ 0 & 0 & 1 \end{pmatrix}. \tag{2.10}$$

The symbol δ_{ij} is called **KRONECKER delta**, and (δ_{ij}) is its matrix representation. We shall later see that the **KRONECKER delta** may be interpreted as a (second rank) tensor that is equivalent to the unit tensor. Symbolically, one therefore writes $\mathbf{1}$ and not δ since $\mathbf{1}\mathbf{a} = \mathbf{a}$; in other words the unit tensor $\mathbf{1}$ maps every vector into itself $\mathbf{1} : \mathbf{a} \mapsto \mathbf{a}$.

The last line in (2.9) provides us with the computationally useful formula to evaluate the scalar product, namely if \mathbf{a} and \mathbf{b} are referred to a Cartesian basis

$$\mathbf{a} \hat{=} (a_1, a_2, a_3), \mathbf{b} \hat{=} (b_1, b_2, b_3), \tag{2.11}$$

then to obtain the scalar product of the two vectors, one must multiply their corresponding components $a_1 b_1$, $a_2 b_2$, $a_3 b_3$ and add the results together. This rule can best be remembered by the graphical arrangement

$$\begin{array}{c}
 \boxed{\begin{array}{c} b_1 \\ b_2 \\ b_3 \end{array}} \downarrow \\
 \boxed{\begin{array}{ccc} a_1 & a_2 & a_3 \end{array}} \rightarrow \boxed{\mathbf{a} \cdot \mathbf{b}}
 \end{array} \tag{2.12}$$

The arrows indicate that the elements in the first, second and third positions, respectively, must be multiplied together and then added.

The scalar product is one form of product connections between two vectors. There are two more, and one is the vector product which is defined only for three-dimensional vector spaces.

Definition 2.5 The **vector product** of two vectors \mathbf{a} and \mathbf{b} is a vector \mathbf{c} with the following properties:

- The direction of \mathbf{c} is perpendicular to \mathbf{a} and \mathbf{b} and the three vectors form (in the order $\mathbf{a}, \mathbf{b}, \mathbf{c}$) a right-handed system of vectors.⁴
- The length of \mathbf{c} equals $|\mathbf{c}| = |\mathbf{a}||\mathbf{b}| \sin \varphi_{ab}$. ■

The symbol used for the vector product is a cross, viz. $\mathbf{c} = \mathbf{a} \times \mathbf{b}$. For this reason, the vector product is sometimes called the cross product. The following properties are straightforward consequences of the above definition:

$$\begin{aligned}
 (1) \quad & \mathbf{a} \times \mathbf{b} = -\mathbf{b} \times \mathbf{a}, \\
 (2) \quad & \mathbf{a} \times \mathbf{a} = \mathbf{0}, \\
 (3) \quad & (\alpha \mathbf{a}) \times \mathbf{b} = \alpha(\mathbf{a} \times \mathbf{b}), \quad \mathbf{a} \times (\beta \mathbf{b}) = \beta(\mathbf{a} \times \mathbf{b}), \\
 (4) \quad & \mathbf{a} \times \mathbf{b} = \mathbf{0} \implies \begin{cases} \mathbf{a} = \mathbf{0} \text{ or } \mathbf{b} = \mathbf{0} \\ \mathbf{b} = \beta \mathbf{a}, \beta \neq 0, \end{cases} \\
 (5) \quad & (\mathbf{a} + \mathbf{b}) \times \mathbf{c} = \mathbf{a} \times \mathbf{c} + \mathbf{b} \times \mathbf{c}.
 \end{aligned} \tag{2.13}$$

Property (1) follows since for a right-handed system, $\{\mathbf{a}, \mathbf{b}, \mathbf{c}\}$, $\{\mathbf{b}, \mathbf{a}, \mathbf{c}\}$ forms a left-handed system of vectors, but $\{\mathbf{b}, \mathbf{a}, -\mathbf{c}\}$ would be a right-handed system, so $\mathbf{b} \times \mathbf{a} = -\mathbf{c}$. Property (2) is trivial since $\sin \varphi_{aa} = 0$. Property (3) follows, since multiplying a vector with a positive scalar does not change its direction. On the other hand, if the scalar is negative, the resulting vector changes the direction and the orientation of the triad $\alpha \mathbf{a}, \mathbf{b}, \mathbf{c}$ changes. Property (4) follows immediately once (2) and (3) have been proved. The proof of property (5) is less trivial and left to the reader as an exercise.

⁴ If the thumb, index finger and the middle finger of the right hand are stretched out such that they form a triad of non-co-planar vectors such that thumb, index finger and middle finger are identified with \mathbf{a}, \mathbf{b} , and \mathbf{c} , respectively, then those ‘arrows’ form a right-handed system of vectors.

To find the computational rule that must be applied to evaluate the vector product of two vectors \mathbf{a} and \mathbf{b} , we refer these vectors to the basis $\hat{\mathbf{e}}_1, \hat{\mathbf{e}}_2, \hat{\mathbf{e}}_3$ of a Cartesian coordinate system. This yields

$$\begin{aligned}\mathbf{a} \times \mathbf{b} &= \left(\sum_i a_i \hat{\mathbf{e}}_i \right) \times \left(\sum_j b_j \hat{\mathbf{e}}_j \right) \\ &= \sum_{ij} a_i b_j (\hat{\mathbf{e}}_i \times \hat{\mathbf{e}}_j) \quad (\text{properties 2 and 5 used}).\end{aligned}\quad (2.14)$$

To evaluate this summation, the reader must convince him/herself that

$$\begin{aligned}\hat{\mathbf{e}}_1 \times \hat{\mathbf{e}}_2 &= \hat{\mathbf{e}}_3, & \hat{\mathbf{e}}_2 \times \hat{\mathbf{e}}_1 &= -\hat{\mathbf{e}}_3, \\ \hat{\mathbf{e}}_2 \times \hat{\mathbf{e}}_3 &= \hat{\mathbf{e}}_1, & \hat{\mathbf{e}}_3 \times \hat{\mathbf{e}}_2 &= -\hat{\mathbf{e}}_1, \\ \hat{\mathbf{e}}_3 \times \hat{\mathbf{e}}_1 &= \hat{\mathbf{e}}_2, & \hat{\mathbf{e}}_1 \times \hat{\mathbf{e}}_3 &= -\hat{\mathbf{e}}_2,\end{aligned}\quad (2.15)$$

and, of course, $\hat{\mathbf{e}}_1 \times \hat{\mathbf{e}}_1 = \mathbf{0} = \hat{\mathbf{e}}_2 \times \hat{\mathbf{e}}_2 = \hat{\mathbf{e}}_3 \times \hat{\mathbf{e}}_3$. The double summation in (2.14), when written out in long hand, involves a linear combination of the above nine terms (three of which are zero). The remaining six can be condensed to three terms so that after this condensation

$$\mathbf{a} \times \mathbf{b} = (a_2 b_3 - a_3 b_2) \hat{\mathbf{e}}_1 + (a_3 b_1 - a_1 b_3) \hat{\mathbf{e}}_2 + (a_1 b_2 - a_2 b_1) \hat{\mathbf{e}}_3. \quad (2.16)$$

In the notation (2.5), this becomes

$$\mathbf{a} \times \mathbf{b} \hat{=} [(a_2 b_3 - a_3 b_2), (a_3 b_1 - a_1 b_3), (a_1 b_2 - a_2 b_1)]. \quad (2.17)$$

This is the formula that holds when the vectors \mathbf{a} and \mathbf{b} are referred to a Cartesian coordinate system.

There is a thumb rule which allows us to easily memorise formula (2.17). To this end, we write the components of \mathbf{a} and \mathbf{b} in lines one over the other and repeat the first two components at the end of the rows as follows:

$$\begin{array}{cccccc} a_1 & a_2 & a_3 & a_1 & a_2 \\ b_1 & b_2 & b_3 & b_1 & b_2 \end{array}$$

Then we omit the first column and perform the product and sums as indicated by the arrows

$$\begin{array}{ccccccc} a_2 & & a_3 & & a_1 & & a_2 \\ & \nearrow & & \nearrow & & \nearrow & \\ b_2 & & b_3 & & b_1 & & b_2 \\ & \nwarrow & & \nwarrow & & \nwarrow & \\ & & & & & & \end{array}$$

$$a_2 b_3 - b_2 a_3 \quad a_3 b_1 - b_3 a_1 \quad a_1 b_2 - b_1 a_2$$

Products of downward pointing arrows have to be taken positive and those of upward pointing arrows must be taken negative. The result in the third line lists the Cartesian components of the cross product $\mathbf{a} \times \mathbf{b}$.

The following problem deals with a vector product of two vectors that is very important for many problems of fluid flow on the Globe. In ensuing flow-problem formulations it will often arise. In the problem formulation, *velocities* and *accelerations* of particles will arise. In anticipation of a careful treatment of these quantities, we state that both are elements of vector spaces with their own scalar products. Accepting this the problem reads as follows:

Problem 2.3 Consider the Globe as a sphere. Isolate an arbitrary point on the surface of the northern hemisphere and let this point be the origin of a Cartesian coordinate system in which the x -axis points towards east, the y -axis points towards north and the z -axis points towards the zenith, see Fig. 2.3. Let ϕ be the angle of geographical latitude. The angular velocity of the Earth can be represented as a vector $\mathbf{\Omega}$ parallel to the direction of the rotation axis of the Earth.

- Show that in the chosen coordinate system $\mathbf{\Omega}$ has the representation $\mathbf{\Omega} \hat{=} (0, |\mathbf{\Omega}| \cos \phi, |\mathbf{\Omega}| \sin \phi)$.
- The Coriolis acceleration \mathbf{a}_c is defined as the vector product

$$\mathbf{a}_c = 2\mathbf{\Omega} \times \mathbf{v}, \quad \mathbf{v} = \mathbf{v}(\mathbf{x}, t), \quad (2.18)$$

where \mathbf{v} is the velocity vector at point \mathbf{x} and time t as measured by an observer on the Earth. Show that in this coordinate system

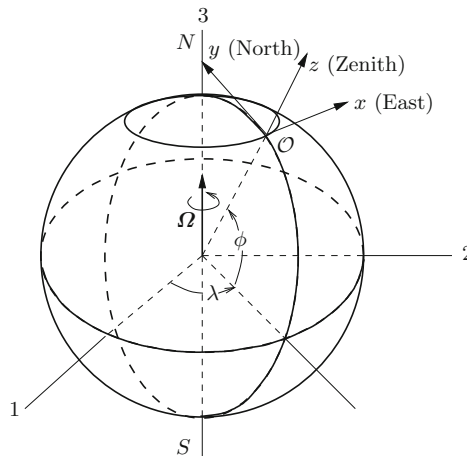


Fig. 2.3 Perspective view of the Earth modelled as a sphere. λ and ϕ are the geographical longitude and latitude, respectively, and $\mathbf{\Omega}$ is the angular velocity of the Earth [$= 7.272 \times 10^{-5} \text{ s}^{-1}$]. The local Cartesian coordinate system $\mathcal{O}xyz$ fixed with the Earth has axes pointing towards east (x), north (y) and the zenith (z). This is the standard coordinate system used in oceanography

$$\mathbf{a}_c \hat{=} (\tilde{f}w - fv, fu, -\tilde{f}u), \quad (2.19)$$

in which we have chosen $\mathbf{v} \hat{=}(u, v, w)$ and where

$$f = 2|\boldsymbol{\Omega}| \sin \phi, \quad \tilde{f} = 2|\boldsymbol{\Omega}| \cos \phi. \quad \blacklozenge$$

Definition 2.6 Let $\boldsymbol{\Omega}$ be the vector of angular velocity of the rotation of the Earth and ϕ the angle of geographical latitude, positive (negative) on the northern (southern) hemisphere. Then

$$f = 2|\boldsymbol{\Omega}| \sin \phi, \quad \tilde{f} = 2|\boldsymbol{\Omega}| \cos \phi \quad (2.20)$$

are called **first and second Coriolis parameters**. ■

Problem 2.4 Find orders of magnitudes for the components of \mathbf{a}_c and give reasons why in most processes of physical limnology the contributions involving \tilde{f} can be ignored as compared to the others. If so, it follows that the second Coriolis parameter \tilde{f} is far less important than the first, f . ◆

To solve this problem, only order-of-magnitude arguments are needed. Simple observations from a boat or measurements show that horizontal components of the water velocity are much larger than the vertical component. Typical values in lakes are perhaps $10^{-1}(\text{m s}^{-1})$, and $10^{-3}(\text{m s}^{-1})$, respectively. On the other hand, f and \tilde{f} are of the same order of magnitude and vary from 0 to $1.46 \times 10^{-5}[\text{s}^{-1}]$. Thus in (2.19) $\tilde{f}w$ can be ignored relative to fv (except close to the equator where f vanishes). Furthermore $-\tilde{f}u$, the third component, has a magnitude of, perhaps, $1.46 \times 10^{-5}(\text{m s}^{-2})$ which is negligible when compared with the acceleration due to gravity, $g \simeq 9.81(\text{m s}^{-2})$. These estimations are the reason why in later chapters we shall often approximate the Coriolis acceleration by

$$\mathbf{a}_c \hat{=} (-fv, fu, 0). \quad (2.21)$$

It is easy to infer from Fig. 2.3 that this approximation corresponds to the neglect of the component of the vector of angular velocity of the rotation of the Earth that lies within the xy -plane.

Problem 2.5 Prove the rule (5) in (2.13) ◆

Forces are *vectors*. They have a material point of attack and point in a direction along their line of action. In rigid bodies a force can be arbitrarily moved along its line of action, but it is intuitively clear that in a deformable body the point of attack is important. Referred to an origin of a (Cartesian) coordinate system, the force on a body is thus defined by the position vector \mathbf{x} of its point of attack and the vector \mathbf{k} defining the length and orientation of the force at the point of attack, see Fig. 2.4a. Let us define now the *moment of a force* or more generally the moment of a vector \mathbf{a} bound to a line of action.

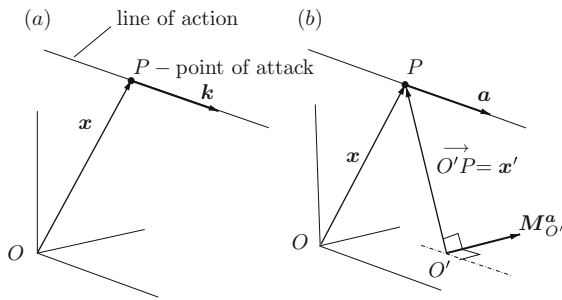


Fig. 2.4 (a) Force \mathbf{k} with point of attack P and line of action. (b) Explaining the definition of the moment of a vector \mathbf{a} relative to a point O' in three-dimensional space

Since forces in rigid bodies can be arbitrarily shifted along their lines of attack, they are vectors and can be added and subtracted and multiplied with real numbers in accordance with the rules listed in Definitions 2.1, 2.2 and 2.4. Physical quantities defined as scalar or vector products of a force and another vector can also be formed and may have a deeper physical meaning. The *moment of a force* or more generally the moment of a vector relative to a point is one such quantity.

Definition 2.7 Let \mathbf{a} be a vector bound to a line of action and having a point of attack P . Let, moreover, O' be an arbitrary point in the three-dimensional space. The moment $\mathbf{M}_{O'}^{\mathbf{a}}$ of the vector \mathbf{a} relative (or with respect) to the point O' is the vector product of the vectors $\overrightarrow{O'P} = \mathbf{x}'$ and \mathbf{a} , see Fig. 2.4b,

$$\mathbf{M}_{O'}^{\mathbf{a}} = \mathbf{x}' \times \mathbf{a}. \quad (2.22)$$

According to this definition, $\mathbf{M}_{O'}^{\mathbf{a}}$ is a vector perpendicular to both vectors \mathbf{x}' and \mathbf{a} , and $\mathbf{M}_{O'}^{\mathbf{a}}$, \mathbf{x}' , \mathbf{a} in this order form a right-handed system of vectors. If the point relative to which the moment of a force is computed is chosen to be the origin of the Cartesian coordinate system, then

$$\mathbf{M}_O^{\mathbf{a}} = \mathbf{x} \times \mathbf{a}$$

is the moment of the vector \mathbf{a} relative to the point O .

Problem 2.6 The formula of the moment of a vector involves the point of attack but of importance is alone the line of action. So prove

- that $\mathbf{M}_{O'}^{\mathbf{a}}$ is independent of where the point of attack P is positioned along the line of action.
- geometrically that if \mathbf{a} and \mathbf{b} are two vectors on different lines of action, but which have one common point

$$\mathbf{M}_{O'}^{\mathbf{a}} + \mathbf{M}_{O'}^{\mathbf{b}} = \mathbf{M}_{O'}^{\mathbf{a}+\mathbf{b}}.$$

[This is nothing else than the distributive law given in (2.13)].

Given a number of vectors \mathbf{a}_j and their lines of action which may not mutually intersect, we may for each define its own moment with respect to point O' , $\mathbf{M}'_j = \mathbf{x}'_j \times \mathbf{a}_j$. Then we simply define the total moment (relative to O') as the sum of the individual moments

$$\mathbf{M}_{O'} = \sum_{i=1}^n \mathbf{x}'_j \times \mathbf{a}_j = \sum_{j=1}^n \mathbf{M}'_j.$$

If the vectors \mathbf{a}_j are identified with the forces \mathbf{k}_j , then the ‘reduction’ of these forces to the point O' is given by the resultant force $\mathbf{K}' = \sum_{j=1}^n \mathbf{k}_j$ and the resultant moment $\mathbf{M}'_O = \sum_{j=1}^n \mathbf{x}'_j \times \mathbf{k}_j$.

Problem 2.7 Let O' and O'' be two points in the three-dimensional space and let $\mathbf{k}_j, \mathbf{x}_j$ ($j = 1, 2, \dots, n$) be forces with their points of attack \mathbf{x}_j . Prove that

$$\mathbf{K} = \mathbf{K}'' = \mathbf{K}' = \sum_{j=1}^n \mathbf{k}_j, \quad \mathbf{M}_{O''} = \mathbf{M}_{O'} - \mathbf{r} \times \mathbf{K},$$

where $\mathbf{r} = \overrightarrow{O'O''}$. ◆

Thus, \mathbf{K} is invariant under changes of reference points, but \mathbf{M} is not.

2.2 Tensors

In the above we dealt with scalars and vectors; here we will briefly deal with tensors of second order or second rank but we shall not have the occasion to deal with tensors of higher order than rank 2. For this reason we mean in this text by a tensor a second-rank tensor. The reader familiar with matrices may think of these when second-rank tensors are meant.⁵

Definition 2.8 A tensor \mathbf{A} is a linear transformation from the vector space V into itself. Specifically, \mathbf{A} assigns to an arbitrary vector \mathbf{a} a vector denoted by \mathbf{Aa} in such a way that

$$\mathbf{A}(\alpha \mathbf{a} + \beta \mathbf{b}) = \alpha(\mathbf{Aa}) + \beta(\mathbf{Ab}),$$

for all scalars α, β and all vectors \mathbf{a}, \mathbf{b} . ■

⁵ Some readers may feel the desire for complementary reading. Books on tensor analysis are, e.g., BETTEN [3], BLOCK [4], BOWEN and WANG [5] and KLINGBEIL [11]. Books on continuum mechanics containing chapters on tensors are by CHADWICK [7], GURTIN [9], SPENCER [18], HUTTER and JÖHNK [10] and LIU [13]. This is only a selection of many.

Two tensors are equal if and only if their actions on an arbitrary vector are identical. The rules for additions, scalar multiplication and multiplication (or composition) of tensors are

$$\begin{aligned}(A + B)a &= Aa + Ba, \\ (\alpha A)a &= \alpha(Aa), \\ (AB)a &= A(Ba).\end{aligned}$$

The zero tensor \mathbf{O} assigns to \mathbf{a} the zero vector, $\mathbf{O}\mathbf{a} = \mathbf{0}$, and the *identity tensor* $\mathbf{1}$ assigns to \mathbf{a} the vector \mathbf{a} itself, $\mathbf{1}\mathbf{a} = \mathbf{a}$. The following properties can be easily verified:

$$\begin{aligned}(i) \quad A + B &= B + A, \\ (ii) \quad \alpha(AB) &= (\alpha A)B = A(\alpha B), \\ (iii) \quad A(B + C) &= AB + AC, \\ (A + B)C &= AC + BC, \\ (iv) \quad A(BC) &= (AB)C, \\ (v) \quad AO &= OA = O, \quad A\mathbf{1} = \mathbf{1}A = A.\end{aligned}$$

Associated with an arbitrary tensor A there is a unique tensor A^T , called the *transpose* of A , such that

$$\mathbf{a} \cdot (A^T \mathbf{b}) = (A\mathbf{a}) \cdot \mathbf{b} = \mathbf{b} \cdot (A\mathbf{a}).$$

It follows from this definition and the rules, previously defined and derived, that

$$\begin{aligned}(\alpha A + \beta B)^T &= \alpha A^T + \beta B^T, \\ (AB)^T &= B^T A^T.\end{aligned}$$

The *inverse* of A , if it exists, is denoted by A^{-1} such that

$$AA^{-1} = A^{-1}A = \mathbf{1}.$$

Having introduced second-rank tensors we can now introduce another product between vectors, which neither yields a scalar nor a vector but a tensor of rank 2.

Definition 2.9 To a pair of vectors (\mathbf{u}, \mathbf{v}) we can assign a tensor, denoted by $\mathbf{u} \otimes \mathbf{v}$ and called the **tensor product** or the **dyadic product** of \mathbf{u} and \mathbf{v} ; it is defined through its action on an arbitrary vector \mathbf{a} by

$$(\mathbf{u} \otimes \mathbf{v})\mathbf{a} = (\mathbf{a} \cdot \mathbf{v})\mathbf{u}.$$

■

The reader may easily deduce the properties

$$\begin{aligned}
 (i) \quad & (\alpha \mathbf{u} + \beta \mathbf{v}) \otimes \mathbf{w} = \alpha(\mathbf{u} \otimes \mathbf{w}) + \beta(\mathbf{v} \otimes \mathbf{w}), \\
 & \mathbf{u} \otimes (\alpha \mathbf{v} + \beta \mathbf{w}) = \alpha(\mathbf{u} \otimes \mathbf{v}) + \beta(\mathbf{u} \otimes \mathbf{w}), \\
 (ii) \quad & (\mathbf{u} \otimes \mathbf{v})^T = \mathbf{v} \otimes \mathbf{u}, \\
 (iii) \quad & (\mathbf{u} \otimes \mathbf{v})(\mathbf{w} \otimes \mathbf{x}) = (\mathbf{v} \cdot \mathbf{w})(\mathbf{u} \otimes \mathbf{x}), \\
 (iv) \quad & \mathbf{A}(\mathbf{u} \otimes \mathbf{v}) = (\mathbf{A}\mathbf{u}) \otimes \mathbf{v}, \\
 & (\mathbf{u} \otimes \mathbf{v})\mathbf{A} = \mathbf{u} \otimes (\mathbf{A}^T \mathbf{v}).
 \end{aligned}$$

Let $\{\hat{\mathbf{e}}_1, \hat{\mathbf{e}}_2, \dots, \hat{\mathbf{e}}_n\}$ be an orthonormal basis. Then for any $p (= 1, \dots, n)$ we have

$$(\hat{\mathbf{e}}_p \otimes \hat{\mathbf{e}}_p)\mathbf{a} = (\mathbf{a} \cdot \hat{\mathbf{e}}_p)\hat{\mathbf{e}}_p = a_p \hat{\mathbf{e}}_p = \mathbf{a} \cdot \mathbf{1} \mathbf{a},$$

which implies

$$\hat{\mathbf{e}}_p \otimes \hat{\mathbf{e}}_p = \mathbf{1}.$$

In this equation, summation over p from 1 to n is understood. Thus, the tensor $\hat{\mathbf{e}}_p \otimes \hat{\mathbf{e}}_p$ is equal to the $n \times n$ -dimensional unit tensor.

We now wish to find the representation of \mathbf{A} with respect to the orthonormal basis $\{\hat{\mathbf{e}}_1, \hat{\mathbf{e}}_2, \dots, \hat{\mathbf{e}}_n\}$. To this end, let A_{ij} be the components of the vector $\mathbf{A}\hat{\mathbf{e}}_j$ relative to $\hat{\mathbf{e}}_i$, so that

$$\mathbf{A}\hat{\mathbf{e}}_j = A_{pj}\hat{\mathbf{e}}_p \quad \text{and} \quad A_{ij} = \hat{\mathbf{e}}_i \cdot (\mathbf{A}\hat{\mathbf{e}}_j).$$

Then, let $A_{pq}\hat{\mathbf{e}}_p \otimes \hat{\mathbf{e}}_q$ and \mathbf{a} be given and form

$$\begin{aligned}
 (\mathbf{A} - A_{pq}\hat{\mathbf{e}}_p \otimes \hat{\mathbf{e}}_q)\mathbf{a} &= (\mathbf{A} - A_{pq}\hat{\mathbf{e}}_p \otimes \hat{\mathbf{e}}_q)a_r \hat{\mathbf{e}}_r \\
 &= a_r \left(\underbrace{\mathbf{A}\hat{\mathbf{e}}_r}_{A_{pr}\hat{\mathbf{e}}_p} - A_{pq} \underbrace{(\hat{\mathbf{e}}_r \cdot \hat{\mathbf{e}}_q)}_{\delta_{qr}} \hat{\mathbf{e}}_p \right) = a_r (A_{pr} - A_{pq}\delta_{qr}) \hat{\mathbf{e}}_p = \mathbf{0}.
 \end{aligned}$$

This implies, since $\{\hat{\mathbf{e}}_r\}$ is a basis,

$$\mathbf{A} = A_{pq}\hat{\mathbf{e}}_p \otimes \hat{\mathbf{e}}_q$$

and so $\{\hat{\mathbf{e}}_p \otimes \hat{\mathbf{e}}_q; p, q = 1, \dots, n\}$ is a basis for \mathbf{A} , and A_{pq} are the tensor components with respect to this basis.

The above calculations also indicate that the vector $\mathbf{A}\mathbf{a}$ has the components $A_{ip}a_p$ and that the components of \mathbf{A}^T are A_{ji} if those of \mathbf{A} are A_{ij} . Furthermore, if $\mathbf{A} = A_{pq}\hat{\mathbf{e}}_p \otimes \hat{\mathbf{e}}_q$ and $\mathbf{B} = B_{rs}\hat{\mathbf{e}}_r \otimes \hat{\mathbf{e}}_s$, then

$$\begin{aligned}
\mathbf{AB} &= (A_{pq}\hat{\mathbf{e}}_p \otimes \hat{\mathbf{e}}_q)(B_{rs}\hat{\mathbf{e}}_r \otimes \hat{\mathbf{e}}_s) = A_{pq}B_{rs} \underbrace{(\hat{\mathbf{e}}_p \otimes \hat{\mathbf{e}}_q)(\hat{\mathbf{e}}_r \otimes \hat{\mathbf{e}}_s)}_{\delta_{qr}\hat{\mathbf{e}}_p \otimes \hat{\mathbf{e}}_s} \\
&= A_{pq}B_{qs}\hat{\mathbf{e}}_p \otimes \hat{\mathbf{e}}_s.
\end{aligned}$$

This formula can be easily proved by recognising that $(\mathbf{AB})\mathbf{a} = \mathbf{A}(\mathbf{Ba})$, for all \mathbf{a} . It follows that \mathbf{AB} has the components $A_{iq}B_{qj}$ relative to the basis $\{\hat{\mathbf{e}}_1, \dots, \hat{\mathbf{e}}_n\}$.

Many physical quantities such as mechanical stress, strain and strain rate behave as tensors. They are indispensable tools in the ensuing analysis. The reader is therefore encouraged to familiarise himself/herself with their properties. In the subsequent analysis we need these representations for the three-dimensional vector space.

2.3 Fields and Their Differentiation

In ensuing chapters we shall encounter *fields* of scalar, vector and tensor-valued physical quantities. By fields we mean mathematical objects which can vary in space and time. If f is such a quantity, then $f = f(\mathbf{x}, t)$ is a field if its value can be computed for all \mathbf{x} in the region V of the body and for some time t in a non-vanishing interval. f can mean the temperature and then constitutes a scalar field, or the velocity field within the body in which case it is a vector-valued field. In this latter case

$$\mathbf{v} \doteq (u(\mathbf{x}, t), v(\mathbf{x}, t), w(\mathbf{x}, t)),$$

i.e. each component of the vector \mathbf{v} is a scalar field. Finally, \mathbf{f} may be tensor valued, and then $\mathbf{f}(\mathbf{x}, t)$ defines a tensor field for all those points (\mathbf{x}, t) of which evolution of $\mathbf{f}(\mathbf{x}, t)$ is meaningful.

We assume that the reader is familiar with the elements of differentiation of a function of several variables. It is not our intention here to develop this theory, we rather shall present some highlights with the intention to refresh the reader's memory.

Definition 2.10 *A function of a single variable $f(x)$ is differentiable in a closed interval $x \in [x_1, x_2]$ if it is continuous and possesses a continuous tangent. Then its derivative is uniquely defined by*

$$f'(x) = \frac{df}{dx} = \lim_{\Delta x \rightarrow 0} \frac{f(x + \Delta x) - f(x)}{\Delta x}. \quad (2.23)$$

At $x = x_1$ ($x = x_2$) this definition applies for $\Delta x > 0$ ($\Delta x < 0$) only and delivers the derivation from the right and left, respectively. ■

The reader may use this definition to corroborate by proof the following rules of differentiation of two differentiable functions $f(x)$ and $g(x)$:

$$\begin{aligned}
(f(x) + g(x))' &= f'(x) + g'(x), \\
(f(x)g(x))' &= f'(x)g(x) + f(x)g'(x), \\
(g^{-1}(x))' &= \left(\frac{1}{g(x)}\right)' = -\frac{1}{g^2(x)}g'(x), \\
\left(\frac{f(x)}{g(x)}\right)' &= \frac{1}{g^2(x)}[f'(x)g(x) - f(x)g'(x)], \\
(f(g(x)))' &= f'(g)g'(x).
\end{aligned}$$

For instance

$$\begin{aligned}
(g^{-1}(x))' &= \lim_{\Delta x \rightarrow 0} \frac{1}{\Delta x} \left\{ \frac{1}{g(x + \Delta x)} - \frac{1}{g(x)} \right\} = \lim_{\Delta x \rightarrow 0} \frac{1}{\Delta x} \frac{g(x) - g(x + \Delta x)}{g(x + \Delta x)g(x)} \\
&= \lim_{\Delta x \rightarrow 0} \frac{1}{g(x + \Delta x)g(x)} \lim_{\Delta x \rightarrow 0} \left\{ -\frac{g(x + \Delta x) - g(x)}{\Delta x} \right\} \\
&= -\frac{1}{g^2(x)}g'(x).
\end{aligned}$$

The reader is equally supposed to know the derivatives of typical functions, e.g.

$$\begin{aligned}
\frac{d}{dx}(\sin x) &= \cos x, & \frac{d}{dx}(\cos x) &= -\sin x, \\
\frac{d}{dx}(x^n) &= nx^{n-1}, & \frac{d}{dx}(e^x) &= e^x.
\end{aligned}$$

These may simply be derived by using the definition (2.23) or, else, by consulting mathematical tables, e.g. [1, 6]. We also assume that the reader is familiar with the fact that in the graph of $f(x)$ the derivative $f'(x)$ or df/dx evaluated at x is the slope of the function $f(x)$ at x , i.e. the tangence of the angle between the x -axis and the tangent to the curve at the point x .

A function may be repetitively differentiable, and then we write for its first-, second-, etc., order derivative

$$\begin{aligned}
\frac{df}{dx}, \quad \frac{d}{dx}\left(\frac{df}{dx}\right) &= \frac{d^2f}{dx^2}, \quad \dots, \quad \frac{d}{dx}\left(\frac{d^{n-1}f}{dx^{n-1}}\right) = \frac{d^n f}{dx^n}, \\
f', \quad (f')' &= f'', \quad \dots, \quad (f^{(n-1)})' = f^{(n)}.
\end{aligned} \tag{2.24}$$

Next we wish to consider derivatives of functions of several variables. In preparation for these, let us first rewrite (2.23) slightly differently as follows:

$$\lim_{\Delta x \rightarrow 0} (f(x + \Delta x) - f(x)) = f'(x)\Delta x. \tag{2.25}$$

This equation may be interpreted to say that the limit of the difference of the two function values on the left-hand side as $\Delta x \rightarrow 0$ is proportional to Δx with a

coefficient of proportionality which equals $f'(x)$. In this connection, $f'(x)$ is often also called the *gradient* of $f(x)$, and one writes $f'(x) = \text{grad } f(x)$.

Formula (2.23) and (2.25) also provide us with a formula for the second-order derivative of a function f if this derivative exists. Indeed, simply by using (2.23) repetitively, we may deduce an expression for f'' :

$$\begin{aligned} f''(x) &= \lim_{\Delta x \rightarrow 0} \frac{f'(x + \Delta x) - f'(x)}{\Delta x} \\ &= \lim_{\Delta x \rightarrow 0} \frac{\frac{f(x + 2\Delta x) - f(x + \Delta x)}{\Delta x} - \frac{f(x + \Delta x) - f(x)}{\Delta x}}{\Delta x} \\ &= \lim_{\Delta x \rightarrow 0} \frac{f(x + 2\Delta x) - 2f(x + \Delta x) + f(x)}{(\Delta x)^2}. \end{aligned}$$

Solving this for $f(x + 2\Delta x)$ and replacing in the emerging equation Δx by $\Delta x/2$ yields⁶

$$\begin{aligned} \lim_{\Delta x \rightarrow 0} f(x + \Delta x) &= 2 \lim_{\Delta x \rightarrow 0} \left[f\left(x + \frac{\Delta x}{2}\right) - f(x) \right] \\ &\quad + f(x) + \frac{1}{4} f''(x) \lim_{\Delta x \rightarrow 0} (\Delta x)^2 \\ &= f(x) + f'(x) \Delta x + \frac{1}{2} f''(x) (\Delta x)^2, \end{aligned}$$

which is an approximation formula for a differentiable function $f(x)$ in the neighbourhood of the point x :

$$f(x + \Delta x) = f(x) + f'(x) \Delta x + \mathcal{O}(|\Delta x|^2), \quad (2.26)$$

in which $\mathcal{O}(|\Delta x|^2)$ is a symbol that gives an order of magnitude for the error. It is proportional to $|\Delta x|^2$. As is known to a reader familiar with the properties of analytic functions, the right-hand side of (2.26) comprises the first two terms of a Taylor series expansion

$$f(x + \Delta x) = \sum_{n=0}^{\infty} \frac{f^{(n)}(x)}{n!} (\Delta x)^n. \quad (2.27)$$

⁶ We use

$$\begin{aligned} \lim_{\Delta x \rightarrow 0} 2 \left[f\left(x + \frac{\Delta x}{2}\right) - f(x) \right] &= \lim_{\Delta x \rightarrow 0} f' \left(x + \frac{\Delta x}{4} \right) \Delta x \\ &= \lim_{\Delta x \rightarrow 0} \left(f'(x) \Delta x + f''(x) \frac{(\Delta x)^2}{4} \right). \end{aligned}$$

For a function of several variables, e.g. a scalar-valued $f(\mathbf{x})$, where \mathbf{x} is the position vector in three-dimensional space, the function $f(\mathbf{x})$ may change differently in different directions. Thus we select the vectorial length increment $\Delta\mathbf{x}$ and generalise (2.25) as follows:

Definition 2.11 *Let $f(\mathbf{x})$ be a scalar-valued function of the vector-valued variable \mathbf{x} . Then $\text{grad } f$ is a linear transformation such that*

$$\lim_{|\Delta\mathbf{x}| \rightarrow 0} (f(\mathbf{x} + \Delta\mathbf{x}) - f(\mathbf{x})) = (\text{grad } f) \cdot \Delta\mathbf{x}, \quad (2.28)$$

in which $\text{grad } f$ is called the gradient of f . ■

When the left-hand side of (2.28) is computed, its result is a real number, since $f(\mathbf{x})$ is a scalar-valued function; so, the right-hand side must also be a scalar. Consequently, since $\Delta\mathbf{x}$ is a vector, $\text{grad } f$ must be a vector as the only scalar formed by $\Delta\mathbf{x}$ that is linear in $\Delta\mathbf{x}$ is its scalar multiplication with another vector. Referred to a Cartesian basis, we thus have

$$\text{grad } f = \sum_i (\text{grad } f)_i \hat{\mathbf{e}}_i; \quad (2.29)$$

note here that $\text{grad } f$ on the left-hand side is a vector, while $(\text{grad } f)_i$ on the right-hand side is a scalar. There remains to find an interpretation of the components

$$\text{grad } f \triangleq ((\text{grad } f)_1, (\text{grad } f)_2, (\text{grad } f)_3). \quad (2.30)$$

To find these, we simply write down (2.28) for an increment in the direction of a base vector $\hat{\mathbf{e}}_j$ and use (2.29):

$$\begin{aligned} \lim_{\Delta x \rightarrow 0} (f(\mathbf{x} + \Delta x \hat{\mathbf{e}}_j) - f(\mathbf{x})) &= \sum_i ((\text{grad } f)_i \hat{\mathbf{e}}_i) \cdot \hat{\mathbf{e}}_j \Delta x \\ &= \sum_i (\text{grad } f)_i \Delta x \underbrace{(\hat{\mathbf{e}}_i \cdot \hat{\mathbf{e}}_j)}_{\delta_{ij}} = (\text{grad } f)_j \Delta x. \end{aligned}$$

This may also be written in the form

$$\lim_{\Delta x \rightarrow 0} \frac{f(\mathbf{x} + \Delta x \hat{\mathbf{e}}_j) - f(\mathbf{x})}{\Delta x} = (\text{grad } f)_j. \quad (2.31)$$

The left-hand side is the definition of the derivative of $f(\mathbf{x})$ in the direction of the base vector $\hat{\mathbf{e}}_j$ and is commonly written as $\partial f / \partial x_j$ and called the *partial derivative of $f(\mathbf{x})$ in the direction of $\hat{\mathbf{e}}_j$* . So, (2.30) can also be written as

$$\text{grad } f \hat{=} \left(\frac{\partial f}{\partial x_1}, \frac{\partial f}{\partial x_2}, \frac{\partial f}{\partial x_3} \right). \quad (2.32)$$

This result is sufficiently important to be highlighted by

Definition 2.12 *Let $f(\mathbf{x})$ be a scalar-valued differentiable function of the vector-valued variable \mathbf{x} . Then (2.31) defines its derivative in the direction of the base vector $\hat{\mathbf{e}}_j$; it is commonly written as*

$$(\text{grad } f)_j = \frac{\partial f}{\partial x_j}$$

and called the partial derivative of $f(\mathbf{x})$ with respect to x_j or the partial derivative of $f(\mathbf{x})$ in the direction of $\hat{\mathbf{e}}_j$. ■

In much the same way we can also find an approximation formula for $f(\mathbf{x} + \Delta\mathbf{x})$ to second order in $\Delta\mathbf{x}$; it is structurally built as (2.26) and reads

$$f(\mathbf{x} + \Delta\mathbf{x}) = f(\mathbf{x}) + (\text{grad } f) \cdot \Delta\mathbf{x} + \mathcal{O}(|\Delta\mathbf{x}|^2), \quad (2.33)$$

in which $\mathcal{O}(|\Delta\mathbf{x}|^2)$ again denotes the order of magnitude of the error if $\Delta\mathbf{x}$ does not tend to the zero vector but has a finite value. A particular case of (2.33) is

$$\begin{aligned} f(\mathbf{x} + \Delta x_j \hat{\mathbf{e}}_j) &= f(\mathbf{x}) + (\text{grad } f \cdot \hat{\mathbf{e}}_j) \Delta x_j + \mathcal{O}((\Delta x_j)^2) \\ &= f(\mathbf{x}) + \frac{\partial f}{\partial x_j} \Delta x_j + \mathcal{O}((\Delta x_j)^2). \end{aligned} \quad (2.34)$$

This is a formula that shall be used in subsequent chapters over and over again.

Let us give a geometric interpretation of the gradient of a function $f(\mathbf{x})$ in the three-dimensional space. To this end, consider the equation $f(\mathbf{x}) = c$, where c is a constant. It is easy to see that the equation $f(\mathbf{x}) = c$ defines a surface in three-dimensional space. For instance, the relation

$$\begin{aligned} &(x_1 - a_1)^2 + (x_2 - a_2)^2 + (x_3 - a_3)^2 = R^2 \\ \text{or} \quad &(\mathbf{x} - \mathbf{a}) \cdot (\mathbf{x} - \mathbf{a}) = R^2, \end{aligned} \quad (2.35)$$

in which \mathbf{a} is a constant vector and \mathbf{x} is variable, defines a sphere with centre at $\mathbf{x} \hat{=}(a_1, a_2, a_3)$ and radius R , see Fig. 2.5. Thus, in this example, R^2 corresponds to the constant c in the equation $f(\mathbf{x}) = c$ and $f(\mathbf{x})$ is $(\mathbf{x} - \mathbf{a}) \cdot (\mathbf{x} - \mathbf{a})$. It is evident from this example that by changing the value of the constant c , (2.35) describes concentric spheres with centre at $\mathbf{x} \hat{=}(a_1, a_2, a_3)$ and different radii; making R larger leads to larger spheres, like the various shells of an onion. Obviously, if we imagine to move on one of the ‘onion shells’, we keep c in the equation $f(\mathbf{x}) = c$ constant; the value

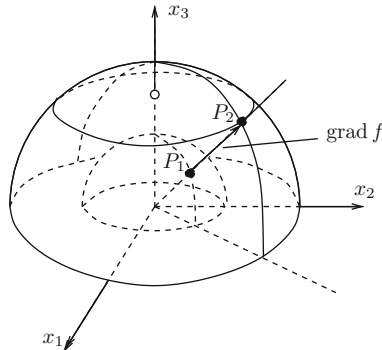


Fig. 2.5 Perspective view of two concentric spheres with centres at $\mathbf{a} = \mathbf{0}$. Thus their equations read $\mathbf{x} \cdot \mathbf{x} = R_i^2$ ($i = 1, 2$). At any point P_1 of the small sphere, the segment connecting P_1 with any point on the second sphere is smallest when it is orthogonal to the two surfaces. This is obviously the radial direction which is given by $\text{grad } f = 2\mathbf{x}$

of $f(\mathbf{x})$ does not change, even though the value of \mathbf{x} changes as one moves within the shell surface. Alternatively, if we move \mathbf{x} from one shell to its neighbouring shell, the function value changes since c changes its value. However, while we may move from a point of the first shell to any arbitrary point on the second shell, the change Δc of the value c in the equation $f(\mathbf{x}) = c$ is the same. The shortest path connecting a point of the first shell with one of the second shell is obtained if it is orthogonal to the shell. If \mathbf{n} is the unit vector orthogonal to the surface $f(\mathbf{x}) = c$, then

$$\begin{aligned} \lim_{\Delta x \rightarrow 0} (f(\mathbf{x} + \Delta x \mathbf{n}) - f(\mathbf{x})) &= (\text{grad } f) \cdot \mathbf{n} \Delta x \\ \text{or} \quad \frac{\partial f}{\partial \mathbf{n}} &:= \lim_{\Delta x \rightarrow 0} \frac{f(\mathbf{x} + \Delta x \mathbf{n}) - f(\mathbf{x})}{\Delta x} = \text{grad } f, \end{aligned} \quad (2.36)$$

according to Definition (2.28). Thus, *the vector $\text{grad } f$ points in the direction perpendicular to the surface $f(\mathbf{x}) = c$. Its length is a measure of how fast the value of $f(\mathbf{x})$ changes in the direction perpendicular to the surface $f(\mathbf{x}) = c$.*

Let us give a geometrically obvious application. So let $\mathbf{x} \hat{=} (x_1, x_2)$ be the position vector in the horizontal plane of a three-dimensional Euclidean space, and let $x_3 = f(x_1, x_2)$ represent a surface. For instance,

$$f(x_1, x_2) = x_3 \quad (2.37)$$

may represent the bathymetry of Lake Constance and the topography of the surrounding landscape, see Fig. 2.6a. Let us, moreover, agree that $x_3 = 0$ identifies the level of the lake surface and $x_3 > 0$ the landscape and $x_3 < 0$ the bathymetry. Assigning a constant value to x_3 defines the level lines of the topography and bathymetry, respectively. Thus the gradient

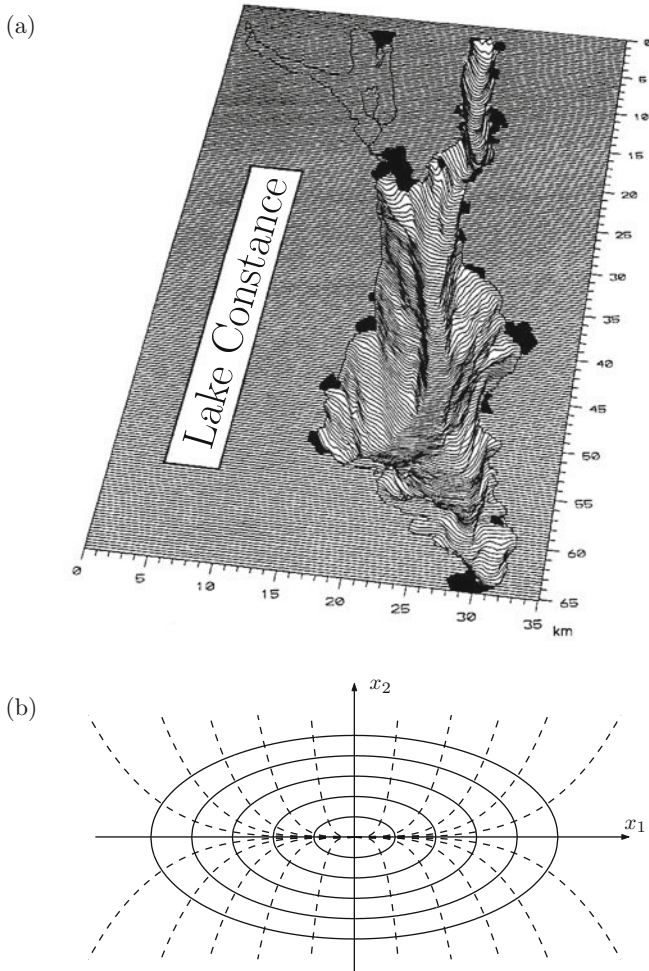


Fig. 2.6 (a) Bird's-eye view of the bathymetry of Lake Constance (© MAISS (1992) [14]); (b) an elliptical basin with parabolic bottom with lines of constant depth (*solid lines*) and lines of steepest descent (*dashed lines*)

$$\text{grad } f \hat{=} \left(\frac{\partial f}{\partial x_1}, \frac{\partial f}{\partial x_2} \right)$$

defines at a point $\mathbf{x} \hat{=}(x_1, x_2)$ the direction in which the value of x_3 changes fastest. These directions are the directions of steepest ascent. Limnologically more significant are the directions of *steepest descent*, because cold and dense water will approximately move along these lines.

Problem 2.8 Let $x_3 = f(x_1, x_2)$ describe the bathymetric profile of a lake. Determine the lines of steepest descent. ♦

The solution of this problem is obtained if it is recognised that the vector $(\text{grad } f)$ defines in each point (x_1, x_2) the direction of steepest ascent. The lines of steepest descent or steepest ascent are therefore the integral curves which in each point are tangential to this direction; thus

$$dx_1 = -d\sigma \frac{\partial f}{\partial x_1}(x_1, x_2), \quad dx_2 = -d\sigma \frac{\partial f}{\partial x_2}(x_1, x_2),$$

where $d\sigma$ is this coefficient of proportionality. The above equations may also be written as

$$\begin{aligned} \frac{dx_1}{d\sigma} &= -\frac{\partial f}{\partial x_1}(x_1, x_2) = g_1(x_1, x_2), \\ \frac{dx_2}{d\sigma} &= -\frac{\partial f}{\partial x_2}(x_1, x_2) = g_2(x_1, x_2). \end{aligned} \quad (2.38)$$

The functions $g_1(x_1, x_2)$ and $g_2(x_1, x_2)$ are known if $f(x_1, x_2)$ is prescribed. The system (2.38) is a system of ordinary differential equations (ODEs) and can be integrated if initial conditions are given. One can for instance prescribe the point on the shore through which one wishes to construct the line of steepest descent. Therefore, one may request

$$x_1 = x_1^{(0)}, x_2 = x_2^{(0)}, \text{ for } \sigma = 0. \quad (2.39)$$

Solving the ODE initial-value problem (2.38), (2.39) will yield the lines of steepest descent; in a similar way, level-line maps are constructed.

As an example, consider the ellipse with parabolic bottom given by

$$x_3 = \frac{x_1^2}{a^2} + \frac{x_2^2}{b^2} - H_0 = f(x_1, x_2).$$

Its directions of steepest descent are given by the differential equations

$$\frac{dx_1}{d\sigma} = -\frac{2x_1}{a^2}, \quad \frac{dx_2}{d\sigma} = -\frac{2x_2}{b^2}$$

and possess the solution

$$\frac{x_2}{x_2^{(0)}} = \left(\frac{x_1}{x_1^{(0)}} \right)^{a^2/b^2},$$

where $(x_1^{(0)}, x_2^{(0)})$ defines a reference point on the selected line of steepest descent.

Figure 2.6b shows the lines of constant depth for an ellipse having $a = 10$, $b = 5$, $H_0 = 1$ and corresponding lines of steepest descent.

Problem 2.9 Let $\mathbf{v}(x_1, x_2, x_3, t)$ be the velocity field within a lake domain, and let $-h(x_1, x_2) = x_3$ be its bathymetric surface. If the bottom is impermeable to the water, then there is no loss of water through the bottom and, consequently, the water flow must at any point of the bottom surface be tangential to it or vanish. If \mathbf{n} is the exterior unit normal vector to the bottom surface, then this tangentiality implies

$$\mathbf{v} \cdot \mathbf{n} = 0, \text{ on } x_3 = -h(x_1, x_2). \quad (2.40)$$

Derive a differential equation for h expressing this. ◆

Let us derive the equation that guarantees the tangentiality of the velocity field to the bottom surface. To solve this problem, we note first that

$$F(x_1, x_2, x_3) := -h(x_1, x_2) - x_3 = 0$$

defines the surface of the lake bottom, and its gradient is a vector orthogonal to it:

$$\text{grad } F \triangleq \left(-\frac{\partial h}{\partial x_1}, -\frac{\partial h}{\partial x_2}, -1 \right);$$

however, it does not have unit length; indeed

$$|\text{grad } F| = \sqrt{\text{grad } F \cdot \text{grad } F} = \sqrt{1 + \left(\frac{\partial h}{\partial x_1} \right)^2 + \left(\frac{\partial h}{\partial x_2} \right)^2}.$$

Thus

$$\mathbf{n} \triangleq \frac{\left(-\frac{\partial h}{\partial x_1}, -\frac{\partial h}{\partial x_2}, -1 \right)}{\sqrt{1 + \left(\frac{\partial h}{\partial x_1} \right)^2 + \left(\frac{\partial h}{\partial x_2} \right)^2}} \quad (2.41)$$

is of unit length. If we write \mathbf{v}

$$\mathbf{v} \triangleq (u(x_1, x_2, x_3, t), v(x_1, x_2, x_3, t), w(x_1, x_2, x_3, t)),$$

we obtain

$$\mathbf{v} \cdot \mathbf{n} = \mathbf{v} \cdot \frac{\text{grad } F}{|\text{grad } F|} = 0 \implies \mathbf{v} \cdot \text{grad } F = 0, \quad (2.42)$$

or when referred to a Cartesian basis

$$\frac{\partial h}{\partial x_1} u + \frac{\partial h}{\partial x_2} v + w = 0 \quad \text{at } x_3 = -h(x_1, x_2). \quad (2.43)$$

This equation is a very important boundary condition arising in lake hydrodynamics. It expresses *tangency of the velocity field of the lake water to the bottom surface* and may for this reason be called *condition of impermeability*.

2.4 Gradient, Divergence and Rotation of Vector and Tensor Fields

In the above the gradient field was defined only for a scalar field $f(\mathbf{x})$. It is possible to define gradient fields for differentiable vector- and tensor-valued functions $\mathbf{v}(\mathbf{x})$ and $\mathbf{T}(\mathbf{x})$, respectively. In the fundamental equations of lake hydrodynamics, such expressions are needed and thus must be derived. We do it with the minimum of mathematical requirement by reducing the problem of finding the gradient of a vector- or a tensor-valued function to that of a scalar. So, let \mathbf{a} be an arbitrary constant vector. Then, $\mathbf{a} \cdot \mathbf{v}$ is a scalar for which the gradient operator was defined in formulae (2.25), (2.26), (2.27), (2.28), (2.29), (2.30), (2.31) and (2.32). With respect to a Cartesian basis we may write

$$\mathbf{a} \cdot \mathbf{v} = a_1 v_1 + a_2 v_2 + a_3 v_3, \quad (2.44)$$

and therefore, in view of the results (2.32)

$$\begin{aligned} \text{grad } (\mathbf{a} \cdot \mathbf{v}) &\hat{=} \left\{ \frac{\partial (\mathbf{a} \cdot \mathbf{v})}{\partial x_1}, \frac{\partial (\mathbf{a} \cdot \mathbf{v})}{\partial x_2}, \frac{\partial (\mathbf{a} \cdot \mathbf{v})}{\partial x_3} \right\} \\ &= \left\{ \left(a_1 \frac{\partial v_1}{\partial x_1} + a_2 \frac{\partial v_2}{\partial x_1} + a_3 \frac{\partial v_3}{\partial x_1} \right), \left(a_1 \frac{\partial v_1}{\partial x_2} + a_2 \frac{\partial v_2}{\partial x_2} + a_3 \frac{\partial v_3}{\partial x_2} \right), \right. \\ &\quad \left. \left(a_1 \frac{\partial v_1}{\partial x_3} + a_2 \frac{\partial v_2}{\partial x_3} + a_3 \frac{\partial v_3}{\partial x_3} \right) \right\} \\ &= (a_1, a_2, a_3) \begin{pmatrix} \frac{\partial v_1}{\partial x_1} & \frac{\partial v_1}{\partial x_2} & \frac{\partial v_1}{\partial x_3} \\ \frac{\partial v_2}{\partial x_1} & \frac{\partial v_2}{\partial x_2} & \frac{\partial v_2}{\partial x_3} \\ \frac{\partial v_3}{\partial x_1} & \frac{\partial v_3}{\partial x_2} & \frac{\partial v_3}{\partial x_3} \end{pmatrix}, \end{aligned} \quad (2.45)$$

where in the last expression the classical matrix–vector notation has been used. The above result now suggests the definition of the gradient of a vector field $\mathbf{v}(\mathbf{x})$. It is customary to define the right-hand side of (2.45) as $\mathbf{a} \text{ grad } \mathbf{v}(\mathbf{x})$.

Definition 2.13 Let $\mathbf{v}(\mathbf{x}, t)$ be a differentiable vector-valued field, and let \mathbf{a} be a constant vector; both defined in a three-dimensional Euclidean space; then

$$\text{grad } (\mathbf{a} \cdot \mathbf{v}(\mathbf{x}, t)) =: \mathbf{a} \text{ grad } \mathbf{v}(\mathbf{x}, t) \text{ for any } \mathbf{a} \quad (2.46)$$

defines the gradient of $\mathbf{v}(\mathbf{x}, t)$ and its representation in a Cartesian coordinate system is given by a second-rank tensor

$$\text{grad } \mathbf{v}(\mathbf{x}, t) \hat{=} \begin{pmatrix} \frac{\partial v_1}{\partial x_1} & \frac{\partial v_1}{\partial x_2} & \frac{\partial v_1}{\partial x_3} \\ \frac{\partial v_2}{\partial x_1} & \frac{\partial v_2}{\partial x_2} & \frac{\partial v_2}{\partial x_3} \\ \frac{\partial v_3}{\partial x_1} & \frac{\partial v_3}{\partial x_2} & \frac{\partial v_3}{\partial x_3} \end{pmatrix}. \quad (2.47)$$

■

We remark that a second possibility of defining the gradient operator would be by the equation

$$\text{grad } (\mathbf{a} \cdot \mathbf{v}(\mathbf{x}, t)) = (\text{grad } {}_2\mathbf{v}(\mathbf{x}, t))\mathbf{a} \quad \text{for any } \mathbf{a}, \quad (2.48)$$

and its representation in a Cartesian coordinate system is easily shown to be given by

$$\text{grad } {}_2\mathbf{v}(\mathbf{x}, t) \hat{=} \begin{pmatrix} \frac{\partial v_1}{\partial x_1} & \frac{\partial v_2}{\partial x_1} & \frac{\partial v_3}{\partial x_1} \\ \frac{\partial v_1}{\partial x_2} & \frac{\partial v_2}{\partial x_2} & \frac{\partial v_3}{\partial x_2} \\ \frac{\partial v_1}{\partial x_3} & \frac{\partial v_2}{\partial x_3} & \frac{\partial v_3}{\partial x_3} \end{pmatrix} =: (\text{grad } \mathbf{v}(\mathbf{x}, t))^T. \quad (2.49)$$

It is obvious that $\text{grad } {}_2\mathbf{v}(\mathbf{x}, t) = (\text{grad } \mathbf{v}(\mathbf{x}, t))^T$, where $(\cdot)^T$ denotes the transposed matrix. In the literature both forms are used. We shall employ the form defined in (2.46) and not (2.48), but the reader is cautioned to be aware of the two possibilities when consulting other books.

With the above defined gradient operator of a differentiable vector field, we may now introduce further operators of this vector field. Two of them are simply obtained by observing that the matrix representation of $\text{grad } \mathbf{v}(\mathbf{x})$ does not, in general, possess symmetry properties. Such properties are defined for higher order tensors, and here we confine attention to second-rank tensors. So, let $\mathbf{T}(\mathbf{x})$ be such a differentiable tensor field. It is defined as a linear transformation and maps any vector \mathbf{a} into a new vector \mathbf{b} , and depending on whether \mathbf{T} operates on \mathbf{a} from the left or the right the resulting vector may be different:

$$\begin{aligned} \mathbf{b}_1 &= \mathbf{T}\mathbf{a} = T_{ij}\hat{\mathbf{e}}_i \otimes \hat{\mathbf{e}}_j a_k \hat{\mathbf{e}}_k = T_{ij}a_k \delta_{jk} \hat{\mathbf{e}}_i = T_{ij}a_j \hat{\mathbf{e}}_i, \\ \mathbf{b}_2 &= \mathbf{a}\mathbf{T} = a_i \hat{\mathbf{e}}_i T_{jk} \hat{\mathbf{e}}_j \otimes \hat{\mathbf{e}}_k = a_i T_{jk} \delta_{ij} \hat{\mathbf{e}}_k = a_i T_{ik} \hat{\mathbf{e}}_k. \end{aligned} \quad (2.50)$$

These results suggest the following definition:

Definition 2.14 Let \mathbf{T} be a tensor and \mathbf{a} and \mathbf{b} two arbitrary vectors. Then, the *transpose* of \mathbf{T} is the tensor \mathbf{T}^T defined by the relation

$$\mathbf{a} \cdot (\mathbf{T}^T \mathbf{b}) = \mathbf{b} \cdot (\mathbf{T} \mathbf{a}). \quad (2.51)$$

■

It is easy to show that if $[\mathbf{T}]$ is the matrix representing \mathbf{T} in a Cartesian coordinate frame, the matrix of \mathbf{T}^T is obtained from $[\mathbf{T}]$ by interchanging rows and columns, i.e.

$$\mathbf{T} \triangleq \begin{bmatrix} T_{11} & T_{12} & T_{13} \\ T_{21} & T_{22} & T_{23} \\ T_{31} & T_{32} & T_{33} \end{bmatrix} \implies \mathbf{T}^T \triangleq \begin{bmatrix} T_{11} & T_{21} & T_{31} \\ T_{12} & T_{22} & T_{32} \\ T_{13} & T_{23} & T_{33} \end{bmatrix}. \quad (2.52)$$

With the definition of the transpose \mathbf{T}^T of \mathbf{T} , we now define a symmetric \mathbf{T} and a skew-symmetric \mathbf{T} as follows:

Definition 2.15 A tensor \mathbf{T} is called **symmetric** if $\mathbf{T} = \mathbf{T}^T$. Alternatively, \mathbf{T} is called **skew-symmetric** if $\mathbf{T} = -\mathbf{T}^T$. ■

This suggests the following definition for an arbitrary tensor

Definition 2.16 Let \mathbf{T} be an arbitrary tensor; then

$$\text{sym } \mathbf{T} := \frac{1}{2}(\mathbf{T} + \mathbf{T}^T), \quad \text{skew } \mathbf{T} := \frac{1}{2}(\mathbf{T} - \mathbf{T}^T) \quad (2.53)$$

are the symmetric and skew-symmetric parts of \mathbf{T} , respectively, and

$$\mathbf{T} = \text{sym } \mathbf{T} + \text{skew } \mathbf{T} \quad (2.54)$$

can be additively decomposed by its symmetric and skew-symmetric parts. This decomposition is unique. ■

These definitions imply that $(\text{sym } \mathbf{T})^T = \text{sym } \mathbf{T}$ and $(\text{skew } \mathbf{T})^T = -\text{skew } \mathbf{T}$ and thus justify the notation. The definitions may be applied to the gradient of a differentiable vector field. Because of its importance later on, we write it in the form of a definition.

Definition 2.17 The gradient of a differentiable vector field $\mathbf{v}(\mathbf{x}, t)$ can be additively decomposed, viz.

$$\text{grad } \mathbf{v}(\mathbf{x}, t) = \mathbf{D}(\mathbf{x}, t) + \mathbf{W}(\mathbf{x}, t), \quad (2.55)$$

where

$$\begin{aligned} \mathbf{D}(\mathbf{x}, t) &:= \text{sym grad } \mathbf{v}(\mathbf{x}, t) = \frac{1}{2} (\text{grad } \mathbf{v}(\mathbf{x}, t) + \text{grad}^T \mathbf{v}(\mathbf{x}, t)), \\ \mathbf{W}(\mathbf{x}, t) &:= \text{skew grad } \mathbf{v}(\mathbf{x}, t) = \frac{1}{2} (\text{grad } \mathbf{v}(\mathbf{x}, t) - \text{grad}^T \mathbf{v}(\mathbf{x}, t)) \end{aligned} \quad (2.56)$$

are its symmetric and skew-symmetric parts, respectively, viz. $\mathbf{D} = \mathbf{D}^T$ and $\mathbf{W} = -\mathbf{W}^T$. One often writes $\mathbf{L} = \text{grad } \mathbf{v}$. ■

Problem 2.10 Show that the representations in Cartesian coordinates of $\mathbf{D}(\mathbf{x}, t)$ and $\mathbf{W}(\mathbf{x}, t)$ are given by

$$\mathbf{D}(\mathbf{x}, t) \hat{=} \begin{pmatrix} \frac{\partial v_1}{\partial x_1} & \frac{1}{2} \left(\frac{\partial v_1}{\partial x_2} + \frac{\partial v_2}{\partial x_1} \right) & \frac{1}{2} \left(\frac{\partial v_1}{\partial x_3} + \frac{\partial v_3}{\partial x_1} \right) \\ & \frac{\partial v_2}{\partial x_2} & \frac{1}{2} \left(\frac{\partial v_2}{\partial x_3} + \frac{\partial v_3}{\partial x_2} \right) \\ \text{sym} & & \frac{\partial v_3}{\partial x_3} \end{pmatrix}, \quad (2.57)$$

$$\mathbf{W}(\mathbf{x}, t) \hat{=} \begin{pmatrix} 0 & \frac{1}{2} \left(\frac{\partial v_1}{\partial x_2} - \frac{\partial v_2}{\partial x_1} \right) & \frac{1}{2} \left(\frac{\partial v_1}{\partial x_3} - \frac{\partial v_3}{\partial x_1} \right) \\ & 0 & \frac{1}{2} \left(\frac{\partial v_2}{\partial x_3} - \frac{\partial v_3}{\partial x_2} \right) \\ \text{skew} & & 0 \end{pmatrix}, \quad (2.58)$$

in which the two matrices are symmetric and skew-symmetric, respectively. Prove, moreover, that the decomposition is unique. ◆

With the symmetric and skew-symmetric parts of the gradient of a differentiable vector field $\mathbf{v}(\mathbf{x}, t)$ being defined, we now introduce two further operators, the *divergence* and the *rotation*, also called *curl*. To define the former, let us recall the scalar product of two second-rank tensors \mathbf{A} and \mathbf{B} given by

$$\begin{aligned} \mathbf{A} \mathbf{B}_i^T &= \mathbf{A} \cdot \mathbf{B} = A_{ij} \hat{\mathbf{e}}_i \otimes \hat{\mathbf{e}}_j \cdot B_{lk} \hat{\mathbf{e}}_k \otimes \hat{\mathbf{e}}_l = A_{ij} B_{lk} \hat{\mathbf{e}}_i \otimes \underbrace{\hat{\mathbf{e}}_j \cdot \hat{\mathbf{e}}_k}_{\delta_{jk}} \otimes \hat{\mathbf{e}}_l \\ &= A_{ij} B_{lj} \underbrace{\hat{\mathbf{e}}_i \cdot \hat{\mathbf{e}}_l}_{\delta_{il}} = A_{ij} B_{ij}. \end{aligned} \quad (2.59)$$

This suggests the definition for the trace operator.

Definition 2.18 Let \mathbf{A} be a second-rank tensor and $\mathbf{1}$ the second-rank unit tensor. Then, the **trace operator**, written $\text{tr}[\mathbf{A}]$, is defined as

$$\text{tr}[\mathbf{A}] = \mathbf{1} \cdot \mathbf{A} = \delta_{ij} A_{ij} = A_{ii}. \quad (2.60) \quad \blacksquare$$

Note that the representation of $\text{tr} [\mathbf{A}]$ in a Cartesian coordinate system is the sum of the diagonal elements of the matrix of \mathbf{A} : $\text{tr} [\mathbf{A}] = A_{11} + A_{22} + A_{33}$, as shown in (2.60). Furthermore, according to (2.47), (2.56) and (2.59)

$$\begin{aligned}\text{tr} [\mathbf{A}\mathbf{B}^T] &= \mathbf{1} \cdot \mathbf{A}\mathbf{B}^T = \delta_{ij} A_{ik} B_{jk} = A_{ik} B_{ik}, \\ \text{tr} [\text{grad } \mathbf{v}(\mathbf{x}, t)] &= \frac{\partial v_i}{\partial x_i} = \frac{\partial v_1}{\partial x_1} + \frac{\partial v_2}{\partial x_2} + \frac{\partial v_3}{\partial x_3}, \\ \text{tr} [\mathbf{D}(\mathbf{x}, t)] &= \text{tr} [\text{grad } \mathbf{v}(\mathbf{x}, t)], \\ \text{tr} [\mathbf{W}(\mathbf{x}, t)] &= 0.\end{aligned}\tag{2.61}$$

All these special applications of the trace operator have important hydrodynamical interpretations if $\mathbf{v}(\mathbf{x}, t)$ is the velocity field, as will soon be seen. However, $\text{tr} [\text{grad } \mathbf{v}(\mathbf{x}, t)]$ and $\mathbf{W}(\mathbf{x}, t)$ are so significant that they carry their own names.

Definition 2.19 The **divergence** of the differentiable vector field $\mathbf{v}(\mathbf{x}, t)$ is defined by

$$\text{div } (\mathbf{v}(\mathbf{x}, t)) \triangleq \text{tr} [\text{grad } \mathbf{v}(\mathbf{x}, t)] \triangleq \frac{\partial v_1}{\partial x_1} + \frac{\partial v_2}{\partial x_2} + \frac{\partial v_3}{\partial x_3}.\tag{2.62}$$

■

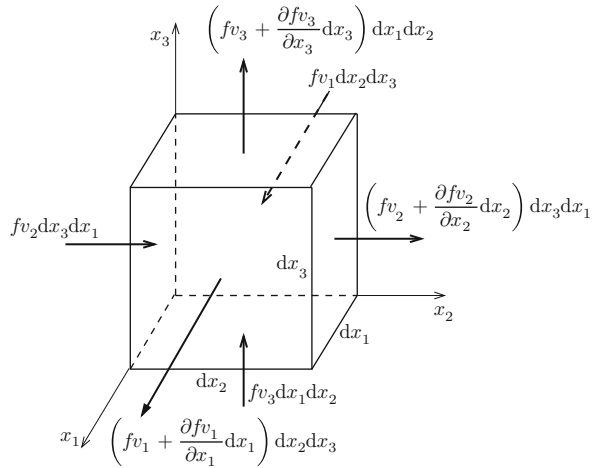
To find the geometrical interpretation of the divergence of a differentiable vector field, consider an infinitesimal stationary cube with side lengths dx_1 , dx_2 and dx_3 parallel to the coordinate axes of a Cartesian coordinate system, Fig. 2.7. Let $f(\mathbf{x}, t)$ and $\mathbf{v}(\mathbf{x}, t)$ be differentiable scalar and vector fields and think of $\mathbf{v}(\mathbf{x}, t)$ to be the velocity field of a fluid occupying the three-dimensional space which is carrying the property f . The flow of the quantity f into and out of the cube through its bounding surfaces is graphically displayed in Fig. 2.7 and can be recorded in tabular form as follows:

	In	Out
faces $\perp x_1$	$f v_1 dx_2 dx_3$	$\left(f v_1 + \frac{\partial(f v_1)}{\partial x_1} dx_1 \right) dx_2 dx_3$
faces $\perp x_2$	$f v_2 dx_3 dx_1$	$\left(f v_2 + \frac{\partial(f v_2)}{\partial x_2} dx_2 \right) dx_3 dx_1$
faces $\perp x_3$	$f v_3 dx_1 dx_2$	$\left(f v_3 + \frac{\partial(f v_3)}{\partial x_3} dx_3 \right) dx_1 dx_2$

Adding all the contributions, counting a flow *into* the cube as *positive*, yields

$$- \left(\frac{\partial f v_1}{\partial x_1} + \frac{\partial f v_2}{\partial x_2} + \frac{\partial f v_3}{\partial x_3} \right) \underbrace{dx_1 dx_2 dx_3}_{d \text{ Vol}} = - (\text{div } f \mathbf{v}) d \text{ Vol}.\tag{2.63}$$

Fig. 2.7 Stationary cubic volume element with side lengths dx_1 , dx_2 , dx_3 and indicated flows of the quantity f into and out of the side faces of the cube. The total flux of f into the volume element is obtained by adding all inflows and subtracting all outflows together



This must be equal to the growth of f per unit time $(\partial f / \partial t) d \text{ Vol}$ so that

$$\frac{\partial f}{\partial t} + \text{div}(f \mathbf{v}) = 0. \quad (2.64)$$

Thus, $\text{div}(f \mathbf{v})$ may be interpreted as the loss per unit volume and unit time of the quantity f at position \mathbf{x} and time t . A positive value of $\text{div}(f \mathbf{v})$ therefore means that the quantity is decreased at \mathbf{x} and t , a negative value means that f is increased and $\text{div}(f \mathbf{v}) = 0$ means that f is stationary.

In the above analysis, the divergence operator was defined for a differentiable vector field. In the physical laws to be derived in [Chap. 4](#), however, a divergence operator for a second-rank tensor field is also needed. So, let $\mathbf{T}(\mathbf{x}, t)$ be a differentiable tensor field. Such a field is a linear transformation and maps any vector \mathbf{a} into a new vector: $\mathbf{b} = \mathbf{aT}$. Since $\mathbf{b}(\mathbf{x}, t)$ is a differentiable vector field, its divergence is well defined as follows:

$$\begin{aligned} \text{div}(\mathbf{aT}) &= \frac{\partial}{\partial x_1} (\mathbf{aT})_1 + \frac{\partial}{\partial x_2} (\mathbf{aT})_2 + \frac{\partial}{\partial x_3} (\mathbf{aT})_3 \\ &= \frac{\partial}{\partial x_1} (a_1 T_{11} + a_2 T_{21} + a_3 T_{31}) + \frac{\partial}{\partial x_2} (a_1 T_{12} + a_2 T_{22} + a_3 T_{32}) \\ &\quad + \frac{\partial}{\partial x_3} (a_1 T_{13} + a_2 T_{23} + a_3 T_{33}) \\ &= a_1 \frac{\partial T_{11}}{\partial x_1} + a_2 \frac{\partial T_{21}}{\partial x_1} + a_3 \frac{\partial T_{31}}{\partial x_1} + a_1 \frac{\partial T_{12}}{\partial x_2} + a_2 \frac{\partial T_{22}}{\partial x_2} + a_3 \frac{\partial T_{32}}{\partial x_2} \\ &\quad + a_1 \frac{\partial T_{13}}{\partial x_3} + a_2 \frac{\partial T_{23}}{\partial x_3} + a_3 \frac{\partial T_{33}}{\partial x_3} \end{aligned} \quad (2.65)$$

for any constant vector \mathbf{a} . This suggests the following definition of $(\operatorname{div} \mathbf{T})$:

$$\operatorname{div} (\mathbf{aT}) = \mathbf{a} \cdot (\operatorname{div} \mathbf{T})_r, \quad (2.66)$$

which implies

$$(\operatorname{div} \mathbf{T})_r \hat{=} \left\{ \left(\frac{\partial T_{11}}{\partial x_1} + \frac{\partial T_{12}}{\partial x_2} + \frac{\partial T_{13}}{\partial x_3} \right), \left(\frac{\partial T_{21}}{\partial x_1} + \frac{\partial T_{22}}{\partial x_2} + \frac{\partial T_{23}}{\partial x_3} \right), \right. \\ \left. \left(\frac{\partial T_{31}}{\partial x_1} + \frac{\partial T_{32}}{\partial x_2} + \frac{\partial T_{33}}{\partial x_3} \right) \right\}. \quad (2.67)$$

We wish to add the following remark: There is a second combination of \mathbf{a} and \mathbf{T} , namely $\mathbf{c} = \mathbf{Ta}$, defining a vector different from \mathbf{b} . Repeating the above computation for the evaluation of $\operatorname{div} \mathbf{c}$ suggests an alternative definition of the divergence of \mathbf{T} , namely

$$\operatorname{div} (\mathbf{Ta}) = (\operatorname{div} \mathbf{T})_l \cdot \mathbf{a}, \quad (2.68)$$

which leads to the representation in Cartesian coordinates

$$(\operatorname{div} \mathbf{T})_l \hat{=} \left\{ \left(\frac{\partial T_{11}}{\partial x_1} + \frac{\partial T_{21}}{\partial x_2} + \frac{\partial T_{31}}{\partial x_3} \right), \left(\frac{\partial T_{12}}{\partial x_1} + \frac{\partial T_{22}}{\partial x_2} + \frac{\partial T_{32}}{\partial x_3} \right), \right. \\ \left. \left(\frac{\partial T_{13}}{\partial x_1} + \frac{\partial T_{23}}{\partial x_2} + \frac{\partial T_{33}}{\partial x_3} \right) \right\}. \quad (2.69)$$

Comparing (2.67) and (2.69), it is seen that in the definition $(\operatorname{div} \mathbf{T})_r$ differentiation is with respect to the second right index, whereas in the definition $(\operatorname{div} \mathbf{T})_l$ this differentiation is with respect to the first left index. In the literature both definitions are used to define the divergence operator; in the physics and engineering literature the divergence of a tensor field \mathbf{T} is mostly defined with $(\operatorname{div} \mathbf{T})_l$; in the mathematical literature $(\operatorname{div} \mathbf{T})_r$ is employed instead. It is also easily seen that there is no difference between the two definitions if $T_{ij} = T_{ji}$ (for $i, j = 1, 2, 3$), i.e. if \mathbf{T} is symmetric. We shall mostly encounter symmetric tensors in this book for which the two definitions $(\operatorname{div} \mathbf{T})_l$ and $(\operatorname{div} \mathbf{T})_r$ do not differ from one another.

To define the *curl* of a differentiable vector field, observe that in three dimensions a skew-symmetric tensor possesses only three independent components, as, e.g., explicitly shown for $\mathbf{W}(\mathbf{x}, t) = \operatorname{skw} \operatorname{grad} \mathbf{v}(\mathbf{x}, t)$ in (2.58). Thus, it must be possible to assign to each skew-symmetric second-rank tensor a vector, its so-called *dual vector*.

Definition 2.20 Let \mathbf{W} be a skew-symmetric second-rank tensor and $\boldsymbol{\varepsilon}$ the epsilon (third order) tensor defined by

$$\boldsymbol{\varepsilon} = \varepsilon_{ijk} \hat{\mathbf{e}}_i \otimes \hat{\mathbf{e}}_j \otimes \hat{\mathbf{e}}_k \quad (i, j, k = 1, 2, 3)$$

with⁷

$$\varepsilon_{ijk} = \begin{cases} 1 & ijk = 123, 231 \text{ or } 312, \\ -1 & ijk = 132, 213 \text{ or } 321, \\ 0 & \text{if at least two of the three indices are equal;} \end{cases}$$

then $\boldsymbol{\omega}$, the **dual vector** corresponding to \mathbf{W} , and \mathbf{W} are related by the formulae

$$\boldsymbol{\omega} := \boldsymbol{\varepsilon} \cdot \mathbf{W} \quad \text{and} \quad \mathbf{W} = -\frac{1}{2} \boldsymbol{\varepsilon} \boldsymbol{\omega}. \quad (2.70)$$

These are the transformation rules from one into the other. ■

Problem 2.11 Show that the representations of $\boldsymbol{\omega}$ and \mathbf{W} in a Cartesian coordinate system are

$$\boldsymbol{\omega} = \varepsilon_{ijk} W_{kj} \hat{\mathbf{e}}_i, \quad \mathbf{W} = -\frac{1}{2} \varepsilon_{ijk} \omega_k \hat{\mathbf{e}}_i \otimes \hat{\mathbf{e}}_j \quad (2.71)$$

or

$$\boldsymbol{\omega} \hat{=} (W_{32} - W_{23}, W_{13} - W_{31}, W_{21} - W_{12}) \quad (2.72)$$

$$\mathbf{W} \hat{=} \frac{1}{2} \begin{pmatrix} 0 & -\omega_3 & \omega_2 \\ \omega_3 & 0 & -\omega_1 \\ -\omega_2 & \omega_1 & 0 \end{pmatrix}. \quad (2.73)$$

◆

An immediate application of Definition 2.20 and Problem 2.11 is obtained if $\mathbf{W} = \text{skw grad } \mathbf{v}(\mathbf{x}, t)$.

Definition 2.21 Let $\mathbf{v}(\mathbf{x}, t)$ be a differentiable vector field and $\mathbf{W}(\mathbf{x}, t) = \text{skw grad } \mathbf{v}(\mathbf{x}, t)$. Then

$$\boldsymbol{\omega} = \boldsymbol{\varepsilon} \cdot \mathbf{W} = \text{curl } \mathbf{v}(\mathbf{x}, t) \quad (2.74)$$

is called the **curl** or the **rotation** of $\mathbf{v}(\mathbf{x}, t)$. Alternatively, $\mathbf{W}(\mathbf{x}, t)$ is called the **spin tensor** of $\mathbf{v}(\mathbf{x}, t)$. ■

Problem 2.12 Show by using (2.58) and (2.72) that the coordinate representation of $\text{curl } \mathbf{v}(\mathbf{x}, t)$ is given by

$$\text{curl } \mathbf{v}(\mathbf{x}, t) = \boldsymbol{\omega}(\mathbf{x}, t) \hat{=} \left[\left(\frac{\partial v_3}{\partial x_2} - \frac{\partial v_2}{\partial x_3} \right), \left(\frac{\partial v_1}{\partial x_3} - \frac{\partial v_3}{\partial x_1} \right), \left(\frac{\partial v_2}{\partial x_1} - \frac{\partial v_1}{\partial x_2} \right) \right]$$

⁷ One also says that the components of the ε tensor have value 1 when the indices i, j, k are evenly permuted between 1, 2 and 3; they have value (-1) when the indices i, j, k are odd permutations of 1, 2 and 3; and they have value 0 if i, j, k are no permutation of 1, 2 and 3.

and corroborate that $\text{div} [\boldsymbol{\omega}(\mathbf{x}, t)] = 0$ as well as $\text{curl} [\text{grad } f] = 0$ for any twice differentiable \mathbf{v} and f . Furthermore, write coordinate representations of $\text{div} [\text{grad } f]$ and $\text{grad} [\text{div} (\mathbf{v}(\mathbf{x}, t))]$. \blacklozenge

To find a geometrical, kinematic interpretation of $\text{curl } \mathbf{v}(\mathbf{x}, t)$, consider a vector field $\mathbf{v}(\mathbf{x}, t)$ at a fixed time and its line integral around a simply connected closed path (Fig. 2.8)

$$\Gamma = \oint \mathbf{v} \cdot d\mathbf{l}, \quad (2.75)$$

where $d\mathbf{l}$ represents the vectorial differential arc length along the path. In the evaluation of (2.75) it is tacitly assumed that the line along which the integration is performed never leaves the region of definition of $\mathbf{v}(\mathbf{x}, t)$. The line integral of \mathbf{v} is called the *circulation*. If the circulation is zero, the vector field \mathbf{v} is said to be *irrotational*. If the surface bounded by the closed curve is ΔS and $\Delta S \rightarrow 0$ in such a way that the length of the path enclosing ΔS also approaches zero,⁸ then the ratio of the circulation Γ to the surface element ΔS

$$\lim_{\Delta S \rightarrow 0} \frac{\Gamma}{\Delta S} = \lim_{\Delta S \rightarrow 0} \frac{1}{\Delta S} \oint \mathbf{v} \cdot d\mathbf{l} \quad (2.76)$$

gives the circulation per unit area at a space point in the field. Its value depends in general on the orientation of the surface element ΔS . The orientation is specified by the unit normal \mathbf{n} , where the rotation of $d\mathbf{l}$ along the closed curve ℓ around \mathbf{n} is related in the right-handed sense as shown in Fig. 2.8. If \mathbf{n} is oriented along the x_1 , x_2 and x_3 axes in turn, then three different values are obtained for the circulation per unit area. The three values form the components of a vector called the *curl* of \mathbf{v} . If \mathbf{n} points in some arbitrary direction, then the circulation per unit area is equal to the component of the curl in the direction of \mathbf{n} . Thus,

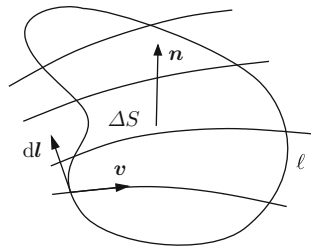


Fig. 2.8 Area ΔS with unit normal \mathbf{n} bounded by a closed curve ℓ with the vectorial arc element $d\mathbf{l}$ lying in a vector field \mathbf{v} . The three vectors \mathbf{v} , $d\mathbf{l}$ and \mathbf{n} form a right-handed basis

⁸ When shrinking this area to zero, it is tacitly assumed that the closed curve does not leave the region of definition of $\mathbf{v}(\mathbf{x}, t)$. A region for which this reduction can be done, starting with any curve and reducing it to any point of the region, is called simply connected. An annulus in two dimensions is not simply connected, but the exterior of a cavity in three dimensions is simply connected.

$$\mathbf{n} \cdot \text{curl } \mathbf{v} = \lim_{\Delta S \rightarrow 0} \frac{1}{\Delta S} \oint \mathbf{v} \cdot d\mathbf{l} \quad (2.77)$$

defines the curl of \mathbf{v} . The value of this expression is a maximum when \mathbf{n} and $\text{curl } \mathbf{v}$ are parallel. Thus, the curl of \mathbf{v} is a vector in the direction of \mathbf{n} when \mathbf{n} is oriented so that the circulation per unit area is a maximum. The magnitude of the curl \mathbf{v} is equal to this maximum circulation per unit area.

It must still be demonstrated that the definition in (2.77) is consistent with that in (2.74). To find the x_1 component of $\text{curl } \mathbf{v}$ from (2.77), one calculates the circulation per unit area around the surface element $\Delta S = \Delta x_2 \Delta x_3$ which lies in the $x_2 x_3$ -plane as shown in Fig. 2.9. Since the element is small, the average of \mathbf{v} along each side can be taken as the value of \mathbf{v} at the central point.⁹ Therefore,

$$\begin{aligned} (\text{curl } \mathbf{v})_1 &= \lim_{\Delta S \rightarrow 0} \frac{1}{\Delta S} \oint \mathbf{v} \cdot d\mathbf{l} \\ &= \lim_{\Delta x_2, \Delta x_3 \rightarrow 0} \frac{1}{\Delta x_2 \Delta x_3} \left[v_3^{(1)} \Delta x_3 - v_2^{(2)} \Delta x_2 - v_3^{(3)} \Delta x_3 + v_2^{(4)} \Delta x_2 \right], \end{aligned} \quad (2.78)$$

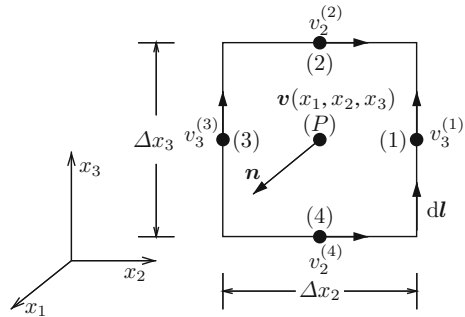
where $v_i^{(j)}$ denotes the x_i component of the vector \mathbf{v} at the point j and their values can be found in terms of \mathbf{v} at the central point P of the area from the first terms of a TAYLOR series expansion. Thus, to orders linear in Δx_i ,

$$\begin{aligned} v_3^{(1)} &= v_3(x_1, x_2, x_3) + \frac{\partial v_3}{\partial x_2} \frac{\Delta x_2}{2}, & v_2^{(2)} &= v_2(x_1, x_2, x_3) + \frac{\partial v_2}{\partial x_3} \frac{\Delta x_3}{2}, \\ v_3^{(3)} &= v_3(x_1, x_2, x_3) - \frac{\partial v_3}{\partial x_2} \frac{\Delta x_2}{2}, & v_2^{(4)} &= v_2(x_1, x_2, x_3) - \frac{\partial v_2}{\partial x_3} \frac{\Delta x_3}{2}. \end{aligned} \quad (2.79)$$

Substituting these values into (2.78), one obtains

$$(\text{curl } \mathbf{v})_1 = \frac{\partial v_3}{\partial x_2} - \frac{\partial v_2}{\partial x_3}. \quad (2.80)$$

Fig. 2.9 Area element with side lengths Δx_2 , Δx_3 and indicated components of the vector field \mathbf{v} at each side along the direction of the side line. The x_1 component of the curl \mathbf{v} is obtained by the line integral of \mathbf{v} along the element sides divided by the area element



⁹ Strictly, according to the mean-value theorem, it is a point between the two edge points. The difference to the value at the central point is, however, of higher order small.

Similarly, the x_2 and x_3 components of $\text{curl } \mathbf{v}$ can be found:

$$(\text{curl } \mathbf{v})_2 = \frac{\partial v_1}{\partial x_3} - \frac{\partial v_3}{\partial x_1}, \quad (\text{curl } \mathbf{v})_3 = \frac{\partial v_2}{\partial x_1} - \frac{\partial v_1}{\partial x_2}. \quad (2.81)$$

Thus, the vector $\text{curl } \mathbf{v}$ in terms of its Cartesian components is given by

$$\text{curl } \mathbf{v} = \left(\frac{\partial v_3}{\partial x_2} - \frac{\partial v_2}{\partial x_3} \right) \hat{\mathbf{e}}_1 + \left(\frac{\partial v_1}{\partial x_3} - \frac{\partial v_3}{\partial x_1} \right) \hat{\mathbf{e}}_2 + \left(\frac{\partial v_2}{\partial x_1} - \frac{\partial v_1}{\partial x_2} \right) \hat{\mathbf{e}}_3. \quad (2.82)$$

Hence the two definitions (2.77) and (2.74) for the curl of a vector field coincide.

2.5 Integral Theorems of Vector Analysis

2.5.1 GAUSS Theorems

In Chap. 4, Sect. 4.2 on mass balances, GAUSS' *Divergence Theorem* is derived. It reads as follows: *If \mathbf{f} is a differentiable vector field in a given volume V with bounding surface ∂V with exterior unit normal vector \mathbf{n} , then*

$$\int_{\partial V} (\mathbf{f} \cdot \mathbf{n}) \, dA = \int_V (\text{div } \mathbf{f}) \, dV. \quad (2.83)$$

Later, again in Chap. 4, Sect. 4.3, when discussing the *Archimedean principle*, a similar formula was derived: *If p is a differentiable scalar field in a given volume V with boundary surface ∂V and unit exterior normal vector \mathbf{n} , then*

$$\int_{\partial V} p \mathbf{n} \, dA = \int_V (\text{grad } p) \, dV. \quad (2.84)$$

These integral theorems are derived in Chap. 4, framing them by physical motivations paired with mathematical arguments. This is done so for motivating reasons to tailor the mathematics. Incidentally, (2.83) implies (2.84) and vice versa. Indeed:

(2.83) \rightarrow (2.84): Let $\mathbf{f} = p \mathbf{a}$, where \mathbf{a} is a constant vector. Then, (2.83) implies

$$\int_{\partial V} p \mathbf{a} \cdot \mathbf{n} \, dA = \int_V \left(\frac{\partial p}{\partial x} a_x + \frac{\partial p}{\partial y} a_y + \frac{\partial p}{\partial z} a_z \right) dV.$$

If we select here, in turn, $\mathbf{a} = \{\mathbf{e}_x, \mathbf{e}_y, \mathbf{e}_z\}$, we obtain

$$\begin{aligned}\int_{\partial V} p n_x dA &= \int_V \frac{\partial p}{\partial x} dV, \\ \int_{\partial V} p n_y dA &= \int_V \frac{\partial p}{\partial y} dV, \\ \int_{\partial V} p n_z dA &= \int_V \frac{\partial p}{\partial z} dV,\end{aligned}\tag{2.85}$$

from which follows

$$\int_{\partial V} p(n_x, n_y, n_z) dA = \int_V \left(\frac{\partial p}{\partial x}, \frac{\partial p}{\partial y}, \frac{\partial p}{\partial z} \right) dV,\tag{2.86}$$

which directly corresponds to (2.84).

(2.84) \rightarrow (2.83): Choose p in (2.85) to be, in turn, the x, y, z components of \mathbf{f} : f_x, f_y, f_z . Then

$$\begin{aligned}\int_{\partial V} f_x n_x dA &= \int_V \frac{\partial f_x}{\partial x} dV, \\ \int_{\partial V} f_y n_y dA &= \int_V \frac{\partial f_y}{\partial y} dV, \\ \int_{\partial V} f_z n_z dA &= \int_V \frac{\partial f_z}{\partial z} dV.\end{aligned}\tag{2.87}$$

Adding these relations yields

$$\int_{\partial V} f_i n_i dA = \int_V \left(\frac{\partial f_x}{\partial x} + \frac{\partial f_y}{\partial y} + \frac{\partial f_z}{\partial z} \right) dV,$$

which is isomorphic to

$$\int_V \mathbf{f} \cdot \mathbf{n} dA = \int_V \operatorname{div}(\mathbf{f}) dV,\tag{2.88}$$

which is (2.83).

In a similar and obvious way one may also prove the relations

$$\int_{\partial V} (\mathbf{v} \times \mathbf{n}) dA = \int_V (\operatorname{curl} \mathbf{v}) dV,\tag{2.89}$$

$$\int_{\partial V} (\mathbf{v} \otimes \mathbf{n}) dA = \int_V (\operatorname{grad} \mathbf{v}) dV.\tag{2.90}$$

Both (2.89) and (2.90) can be proved by writing them in Cartesian component form, e.g.

$$\int_{\partial V} v_i n_j dA = \int_V \frac{\partial v_i}{\partial x_j} dV. \quad (2.91)$$

GREEN's identities also follow from adequate application of the Divergence Theorem. The *first* GREEN's identity is obtained by choosing in (2.83) $\mathbf{f} = \phi \mathbf{v}$. This yields

$$\begin{aligned} \int_{\partial V} \phi \mathbf{v} \cdot \mathbf{n} dA &= \int_V \operatorname{div}(\phi \mathbf{v}) dV \\ &= \int_V \{\phi \operatorname{div} \mathbf{v} + \mathbf{v} \operatorname{grad} \phi\} dV. \end{aligned} \quad (2.92)$$

If we substitute here $\mathbf{v} = \operatorname{grad} \psi$ and observe that $\operatorname{div} \mathbf{v} = \operatorname{div} \operatorname{grad} \psi = \Delta \psi$, where Δ is the LAPLACE operator, then

$$\int_V \{\operatorname{grad} \phi \cdot \operatorname{grad} \psi\} dV = - \int_V \phi \Delta \psi dV + \int_{\partial V} \phi \frac{\partial \psi}{\partial n} dA, \quad (2.93)$$

which is GREEN's *first identity*.

If in (2.93) the roles of ϕ and ψ are interchanged, we obtain

$$\int_V \{\operatorname{grad} \psi \cdot \operatorname{grad} \phi\} dV = - \int_V \psi \Delta \phi dV + \int_{\partial V} \psi \frac{\partial \phi}{\partial n} dA. \quad (2.94)$$

Subtracting (2.93) and (2.94) from one another leads to

$$\int_V \{\phi \Delta \psi - \psi \Delta \phi\} dV = \int_{\partial V} \left\{ \phi \frac{\partial \psi}{\partial n} - \psi \frac{\partial \phi}{\partial n} \right\} dA, \quad (2.95)$$

which is GREEN's *second identity*.

2.5.2 STOKES Theorems

Let \mathbf{f} be a differentiable force field in \mathbb{R}^3 . Then, $\mathbf{f} \cdot d\mathbf{x}$ is the infinitesimal work done by \mathbf{f} if the point of attack of \mathbf{f} is displaced by the vectorial displacement increment $d\mathbf{x}$.

Definition 2.22 The rotor or rotation of a vector (here force) field \mathbf{f} is defined as¹⁰

¹⁰ The symbol for 'curl' in continental Europe is 'rot'.

$$\begin{aligned}
\text{curl } \mathbf{f} &= \nabla \times \mathbf{f} \\
&\hat{=} \left(\frac{\partial f_z}{\partial y} - \frac{\partial f_y}{\partial z}, \frac{\partial f_x}{\partial z} - \frac{\partial f_z}{\partial x}, \frac{\partial f_y}{\partial x} - \frac{\partial f_x}{\partial y} \right) \\
&\hat{=} \varepsilon_{ijk} f_{k,j} = \varepsilon_{ijk} \frac{\partial f_k}{\partial x_j}.
\end{aligned} \tag{2.96}$$

Figure 2.10 shows a right angle triangle with side length $2dx$ and $2dy$ parallel to the x - and y -axes of the rectangular coordinates and surface area $dA_z = 2dx \, dy$. If the point of attack of the force field is displaced in the indicated orientation, then the work done by \mathbf{f} along the margin of the triangle is given by

$$\begin{aligned}
dW_z &= \frac{\partial f_x}{\partial y} dy (-2dx) + \frac{\partial f_y}{\partial x} dx (2dy) \\
&= \left(\frac{\partial f_y}{\partial x} - \frac{\partial f_x}{\partial y} \right) (2dx \, dy) = (\text{curl } \mathbf{f})_z dA_z.
\end{aligned} \tag{2.97}$$

If we generalise this two-dimensional situation to the infinitesimal triangle of Fig. 2.10b with surface increment dA and orientation indicated by the normal vector \mathbf{n} , it is seen that this work can be composed as the sum of the work done by the force field along the three triangles in the coordinate parallel planes (xy) , (yz) , (zx) . (In this process the work done along the coordinate parallel axes cancels out, because these lines are traversed twice in opposite directions). Therefore,

$$\begin{aligned}
dW &= dW_x + dW_y + dW_z \\
&= (\text{curl } \mathbf{f})_x dA_x + (\text{curl } \mathbf{f})_y dA_y + (\text{curl } \mathbf{f})_z dA_z \\
&= (\text{curl } \mathbf{f}) \cdot \mathbf{n} \, dA,
\end{aligned} \tag{2.98}$$

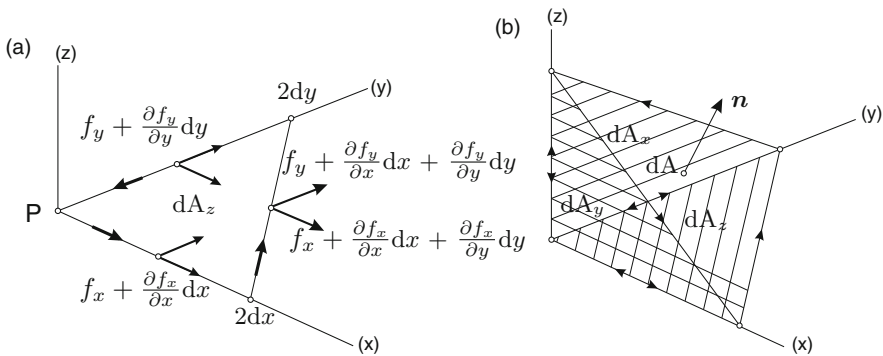


Fig. 2.10 (a) Infinitesimal triangle in the (xy) -plane with sides $2dx$ and $2dy$ along the x - and y -axes. Components of the force field \mathbf{f} parallel to the x - and y -axes are indicated at the midpoints of the triangle, explaining the evaluation of the work done by \mathbf{f} around the triangle. (b) The work done by \mathbf{f} along an infinitesimal triangle with unit normal \mathbf{n} can be evaluated by adding the work of \mathbf{f} along the triangles in the (xy) -, (yz) - and (xz) -planes

where we have used the obvious geometric property

$$dA_j = n_j dA \quad \longleftrightarrow \quad d\mathbf{A} = \mathbf{n} dA.$$

Consider next a closed double-point free curve C in a region of \mathbb{R}^3 in which the force field \mathbf{f} is defined and span this loop by a smooth surface, which does not leave this domain. This area is filled with a connected grid of infinitesimal triangles as shown in Fig. 2.11. It is easy to see that the work done along the closed loop can be calculated by evaluating the work around all triangles in the same orientation as that spanned by C . The work done along the interior triangle sides cancels out as these sides are traversed twice in opposite directions. The work done along an infinitesimal triangle is given by $dW = (\text{curl } \mathbf{f}) \cdot \mathbf{n} dA$, and so, the total work performed by \mathbf{f} on the surface is given by

$$W = \int_{A_C} (\text{curl } \mathbf{f}) \cdot \mathbf{n} dA = \oint_C \mathbf{f} \cdot d\mathbf{x}. \quad (2.99)$$

This is STOKES' theorem in \mathbb{R}^3 . It holds for any differentiable field \mathbf{v} ,

$$\oint_C \mathbf{v} \cdot d\mathbf{x} = \int_{A_C} (\text{curl } \mathbf{v}) \cdot \mathbf{n} dA \quad (2.100)$$

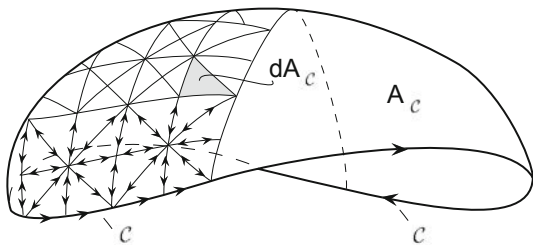
and states that *the circulation of a differentiable vector field around a closed double-point free loop equals the flux of its rotation normal to and through the surface A_C spanned by C .*

STOKES' theorem has a number of corollaries:

- If we set in (2.100) $\mathbf{v} = \phi \mathbf{e}_x$, $\mathbf{v} = \phi \mathbf{e}_y$, $\mathbf{v} = \phi \mathbf{e}_z$, in turn, one obtains

$$\begin{aligned} \int_C \phi dx &= \int_{A_C} (\text{curl}(\phi \mathbf{e}_x)) \cdot \mathbf{n} dA \hat{=} \int_{A_C} \left(\frac{\partial \phi}{\partial z} n_y - \frac{\partial \phi}{\partial y} n_z \right) dA, \\ \int_C \phi dy &= \int_{A_C} (\text{curl}(\phi \mathbf{e}_y)) \cdot \mathbf{n} dA \hat{=} \int_{A_C} \left(\frac{\partial \phi}{\partial x} n_z - \frac{\partial \phi}{\partial z} n_x \right) dA, \\ \int_C \phi dz &= \int_{A_C} (\text{curl}(\phi \mathbf{e}_z)) \cdot \mathbf{n} dA \hat{=} \int_{A_C} \left(\frac{\partial \phi}{\partial y} n_x - \frac{\partial \phi}{\partial x} n_y \right) dA, \end{aligned}$$

Fig. 2.11 Surface A_C spanned by a smooth double-point free closed curve C . The work done by a differentiable force field \mathbf{f} around C is composed of the summation of the work around all infinitesimal triangles dA_C



which, when combined, yields

$$\int_C \phi \, d\mathbf{x} = - \int_{A_C} (\text{grad } \phi) \times \mathbf{n} \, dA. \quad (2.101)$$

- If ϕ in (2.101) is the i th component of a vector field, then it also implies

$$\int_C \mathbf{v} \otimes d\mathbf{x} = - \int_{A_C} (\text{grad } \mathbf{v}) \times \mathbf{n} \, dA. \quad (2.102)$$

- A further interesting formula is obtained by selecting

$$\mathbf{e}_i \times \int_C v_i \, d\mathbf{x} = \oint_C \mathbf{v} \times d\mathbf{x} = - \int_{A_C} \underbrace{\mathbf{e}_i \times \text{grad } v_i}_{-\text{curl } \mathbf{v}} \times \mathbf{n} \, dA$$

so that

$$\oint_C \mathbf{v} \times d\mathbf{x} = \int_{A_C} (\text{curl } \mathbf{v}) \times \mathbf{n} \, dA. \quad (2.103)$$

References

1. Abramowitz, M. and Stegun, I.A.: *Handbook of Mathematical Functions*. Dover, New York, NY (1964) (and later)
2. Arfken, G.B. and Weber, H.J.: *Mathematical Methods for Physicists* (6th Edition). Wiley Danvers, MA (2005)
3. Betten, J.: *Tensorrechnung für Ingenieure*. B.G. Teubner, Stuttgart 320 p. (1987)
4. Block, H.D.: *Introduction to Tensor Analysis*. Charles E. Merrill Books, Columbus, OH, 62 p. (1962)
5. Bowen, R.M. and Wang, C.C.: *Introduction to Vectors and Tensors*, Vol. 1: *Linear and multi-linear Algebra*, Vol. 2: *Vector and Tensor Analysis*. Plenum New York, NY, 434 p. (1976)
6. Bronstein, I.N., Semendjajew, K.A., Musiol, G. and Mühlig, G.: *Taschenbuch der Mathematik*. Verlag Harri Deutsch, Germany 1. Aufl. 848 p. (1993)
7. Chadwick, P.: *Continuum Mechanics, Concise Theory and Problems*. George Atten & Unwin Ltd. 174 p. (1976), also Dover, New York, NY, 187 p. (1999)
8. Feynman, R.P., Leighton, R.B. and Sand, M.: *The Feynman Lectures on Physics*. Vol. 1, 2, 3 Addison-Wesley, Reading, MA (1966)
9. Gurtin, M.E.: *An Introduction to Continuum Mechanics*. Academic, New York, NY, 265 p. (1981)
10. Hutter, K. and Jöhnk, K.: *Continuum Methods of Physical Modeling*. Springer, Berlin, 635 p. (2004)
11. Klingbeil, E.: *Tensorrechnung für Ingenieure*. B. I. Wissenschaftsverlag, Mannheim 197 p. (1989)
12. Kreyszig, E.: *Advanced Engineering Mathematics* (9th Edition). Wiley, Hoboken, NJ, USA, (2006)
13. Liu, I.-S.: *Introduction to Continuum Mechanics*. Springer, Berlin, 297 p. (2002)

14. Maiss, M.: *Schwefelhexafluorid (SF₆) als Tracer für Mischungsprozesse im westlichen Bodensee*. PhD Thesis, Ruprecht-Karls-Universität Heidelberg (1992)
15. Papula, L.: *Mathematik für Ingenieure und Naturwissenschaftler*, Band 3 (3. Auflage), Vieweg, Braunschweig, Wiesbaden (1999)
16. Papula, L.: *Mathematik für Ingenieure und Naturwissenschaftler*, Bände 1,2 (9. Auflage). Vieweg, Braunschweig, Wiesbaden (2000)
17. Sokolnikoff, I.S. and Redheffer, R.M.: *Mathematics of Physics and Modern Engineering* (2nd Edition). McGraw-Hill, New York, NY (1966)
18. Spencer, A.J.M.: *Continuum Mechanics*. Longman, New York, NY, 183 p. (1980)

Chapter 3

A Brief Review of the Basic Thermomechanical Laws of Classical Physics

3.1 Underlying Fundamentals – General Balance Laws

As far as physics is concerned, the required background knowledge is by and large classical physics. Its basis is long-lasting human experience with the surrounding physical world; it pertains to the properties of the space in which the physical objects exist; it is concerned with the processes which these physical objects undergo and searches for the reasons behind their occurrence. This experience must not depend on the observer; it should be *objective* and ought to be expressed in an observer-independent fashion, verified only by real physical experiments. To express this knowledge, physicists use *concepts* (such as space, time, motion, energy), *laws* (such as the law of gravity, NEWTON's second law of motion, conservation of energy) and *postulates* [for instance, that time progresses only in one direction from the past to the future (monotonicity of the time) and that only events in the past can influence those at present (principle of determinism), expressed sometimes by the contradictorily sounding statement that 'the future cannot be remembered'].

Some of these postulates are expressed in classical physics only as general ideas, taken for granted, but not at all obvious from a more philosophical point of view. For example:

- *time is unidirectional*, it can only proceed from the past to the present and future, and it is *homogeneous*, i.e. it does not contract or extend;
- the universe, i.e. the *physical space* is *homogeneous* – has in all its points the same properties, *isotropic* – has at a point the same behaviour in all directions and can be assumed to be *three dimensional*;
- this space is filled with material bodies that are equipped with physical properties such as mass, momentum. The *interaction* of such bodies manifests itself through the appearance of *forces*. For a pair of bodies they are of the same origin, equal in value and opposite in direction;

- the interaction of a body with a second (real physical) body is the only reason for its acceleration relative to an *inertial reference system*¹;
- there are *favourable directions* of all physical processes as they develop in the universe: a gas has the tendency to fill the entire space available to it; a fluid may form droplets and can only support pressures when it is at rest, but moves otherwise, while a solid is at rest when it is subject to any equilibrated external force system; a thermodynamic body reaches uniform temperature in thermal equilibrium, etc.

Neither classical nor modern physics are able to provide more fundamental reasons for these *postulates and concepts*; they are features of nature, must be viewed as axioms and can only be replaced by other statements, equivalent to them. And some of these postulates have been shown to be false in modern physics. Nevertheless we will take them for granted here and use them in everyday practice of classical physics without further notice. These general concepts define the basis of the language in which our physical ideas are phrased. To quantify them, they must be complemented by well-defined *physical quantities*, such as mass, momentum, energy, in terms of which the physical processes are quantified. To give an example, energy is a physical concept and is made concrete as kinetic, potential and internal energy which are the physical quantities. Moreover, time is a fundamental concept; to measure it we need a clock by which intervals can be measured. Furthermore, a stick with a length unit allows to measure distances. The fact that we apply the same clock and the same stick with the same units in all inertial systems is the expression of our tacit assumption that time and length in classical physics are absolute quantities.

To understand and describe the physical processes correctly, both physical concepts and physical quantities are needed. The latter being measurable or derivable from measurable quantities offers the possibility to establish dependencies between them. Often, the mathematical relations defining these dependencies are called *physical laws*. Examples are the general balance laws and their specifications known as the physical *conservation laws* treated below.

Except for the physics of radiation, physics of lakes makes use only of NEWTONian or GALILEan mechanics and *thermodynamics*. The development of the respective laws embraced approximately four centuries and involved the most prominent scientists. Without going into any depth it is probably fair to say that it needed NEWTON (1643–1724), EULER (1707–1783) and CAUCHY (1789–1857) until a clear understanding of the balance laws of mass, linear momentum (NEWTON's second law) and moment of momentum (EULER's law of angular

¹ In this list of qualitative properties, tacit knowledge of 'obvious' facts is assumed which actually requires deep understanding. The concept of an inertial reference system is one of these concepts of classical mechanics. It means that for a body in isolation that it cannot be decided whether it is at rest or moves with constant velocity. Two such systems thus move relative to one another with a constant velocity, and no such system can be found that would *absolutely* be at rest. All these systems are called inertial reference systems and the inability to single out one as being at rest is referred to as the *classical principle of relativity*.

momentum) was safely established for a continuous body (CAUCHY's law of motion). The 19th century was the domain of the development of basic thermodynamics. The first law of thermodynamics, now simply expressed as the conservation law of energy, is attributed to have first been spelled out in 1841/1843 by R. MAYER (1814–1878), and Lord KELVIN (1824–1907) introduced the concept of *absolute temperature*, also called *KELVIN temperature*. Loosely speaking, this means that temperature can be measured in a body as an 'absolute' quantity not influenced in itself by the body in which it is measured. The second law of thermodynamics traces back in its fundamentals to CARNOT (1796–1832), CLAUSIUS (1822–1888), and DUHEM (1861–1961) and found its culmination in the 20th century with the work of CARATHEODORY (1873–1950), TRUESDELL (1919–2000) and the many researchers of the 'Rational Thermodynamics' school. The second law of thermodynamics expresses the fact that *all physical processes are irreversible*, and reversibility is an idealisation that will never be realised. One form how this postulate of irreversibility of all physical processes can be expressed is the *concept of entropy*, introduced by CLAUSIUS, of which the production in a physical process is required to be non-negative.

The thermomechanical physical laws, the fundamental laws of classical physics that describe the processes which material bodies can undergo, are thus the following statements:

- *Conservation of mass* of a material body; in a material body, mass can neither be produced nor created.
- *Conservation of linear momentum*. This law is the second of Newton's laws as stated in Fig. 3.1. For Newton's biographical sketch, see Fig. 3.3.
- *Conservation of moment of momentum*. This law was first spelled out by Euler; for a biographical sketch, see Fig. 7.1.
- *Conservation of energy* or the first law of thermodynamics. This law expresses the fact that the union of all energies of a material body is a conserved quantity, i.e. cannot be produced.
- *Balance of entropy* states that its production in a material body is non-negative for whatever process that is occurring in the body.

These laws must be accepted as such; they cannot be proved and therefore have an axiomatic status, but they can be and have been verified over and over again (as long as effects of relativity and quantum mechanics are negligible). None of the statements in this list is made sufficiently explicit to the extent that they would allow quantification as outlined above. This is the intention in the remainder of this chapter and in the subsequent chapter. The presentation will provide examples of what was meant in the introductory paragraphs when physical quantities were mentioned to be needed, which can be related to one another to form dependences. The five laws of the above list establish such dependences in a fashion of particular depth, because these laws enjoy universal qualifications; within classical physics they are valid for all processes, fast or slow, and all material bodies, be they gaseous, fluid or solid.

Before stating these laws, it is advantageous to first explain the concept *balance law* in a general form; it is valid for processes in everyday life as well as in physics

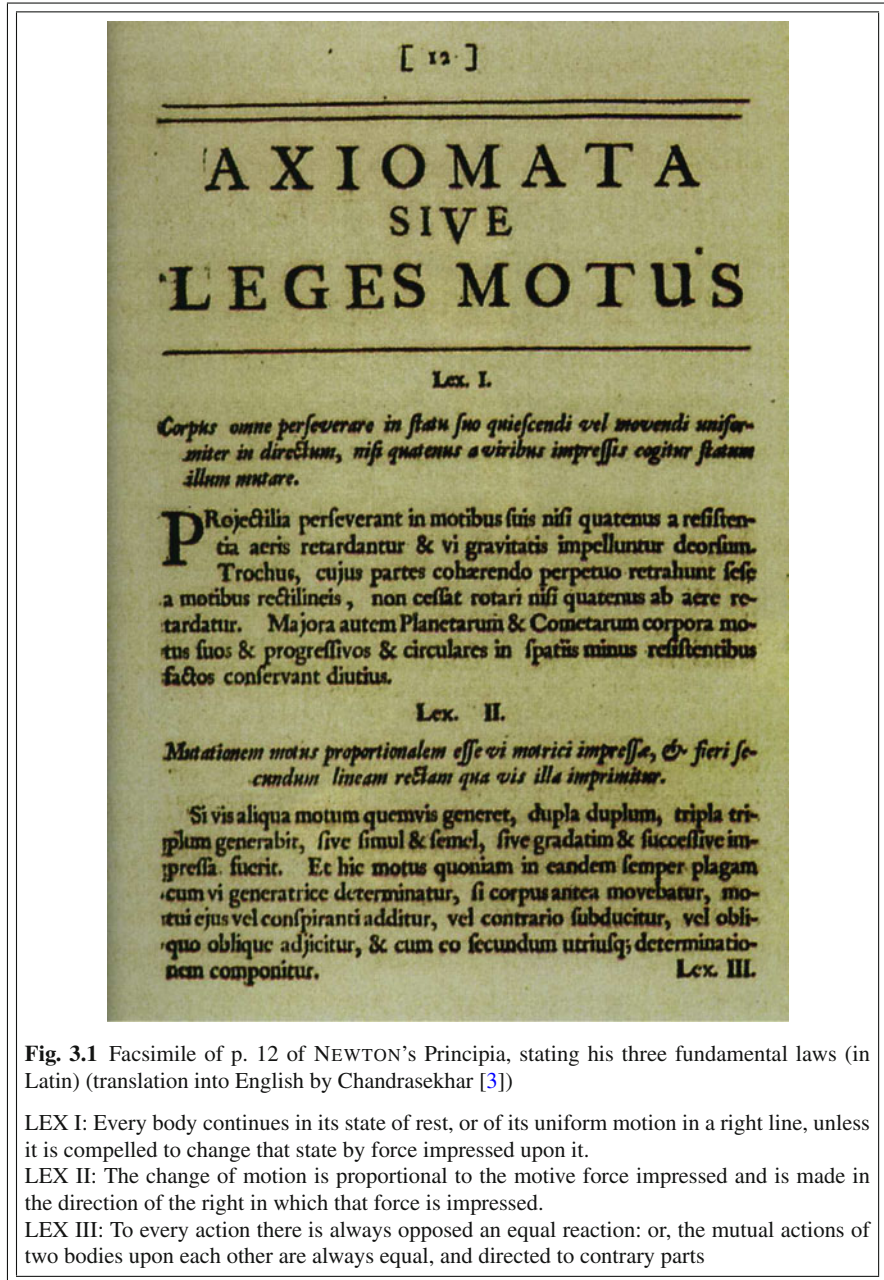


Fig. 3.1 Facsimile of p. 12 of NEWTON's Principia, stating his three fundamental laws (in Latin) (translation into English by Chandrasekhar [3])

LEX I: Every body continues in its state of rest, or of its uniform motion in a right line, unless it is compelled to change that state by force impressed upon it.

LEX II: The change of motion is proportional to the motive force impressed and is made in the direction of the right in which that force is impressed.

LEX III: To every action there is always opposed an equal reaction: or, the mutual actions of two bodies upon each other are always equal, and directed to contrary parts

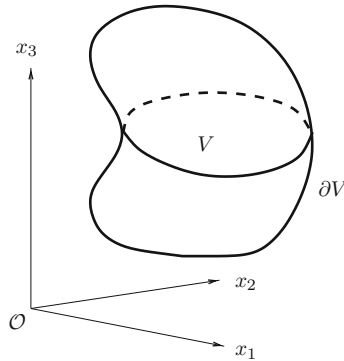


Fig. 3.2 Material body V with surface ∂V in the three-dimensional space equipped with orthogonal Cartesian coordinates x_1, x_2, x_3

and actually forms a triviality. To this end, we single out in physical space a material volume² V with boundary ∂V . Since this volume is supposed to be material, so is its boundary. Trivial as this may be, we wish to emphasise it here, because in future developments we shall often cut in imagination a body into smaller parts which occupy certain volumes with bounding surfaces. These parts are obviously material, may be represented as in Fig. 3.2, and they move with time. The body parts may be a house or part of it, a lake or simply a certain fluid mass which we imagine to be held together by an imaginary massless skin. Subsequently, we call this simply an arbitrary body. The complement of this body in physical space is then the outside of V , or its *environment*.

Let \mathcal{G}_V be any physical quantity (e.g. mass, momentum or energy) defined for a body instantaneously occupying the volume V and consider its time rate of change, $d\mathcal{G}_V/dt$. How can we describe this change of \mathcal{G}_V in V ? Quite naturally, this change (a growth if it is positive) is given by the following individual contributions:

- Flux of \mathcal{G}_V per unit time through the surface ∂V : $\mathcal{F}_{\partial V}^{\mathcal{G}_V}$;
- Supply of \mathcal{G}_V within V per unit time from the environment: $\mathcal{S}_V^{\mathcal{G}_V}$;
- Production of \mathcal{G}_V within V per unit time: $\mathcal{P}_V^{\mathcal{G}_V}$.

² A *material volume* is here understood to be a region in the three-dimensional physical space that is continuously filled with matter and bounded by a surface through which no mass flows. To denote this, we use the word ‘*body*’. We differentiate between ‘volume’ as a region in physical space that is fixed and ‘material volume’ or body that may move with time through physical space.

Adding these three contributions together, we thus are led to the following *Concept of a balance law*:

Time rate of change of a physical quantity
in a material body of volume V

= **Flux** of this quantity through the boundary of the material volume
 + **Supply** of the quantity to the body within the volume V from the environment
 + **Production** of the quantity within the volume V .

Here, ‘flux’, ‘supply’ and ‘production’ are understood to be those quantities per unit time. When formulated mathematically as a balance equation for \mathcal{G}_V , this reads

$$\frac{d\mathcal{G}_V}{dt} = \mathcal{F}_{\partial V}^{\mathcal{G}_V} + \mathcal{S}_V^{\mathcal{G}_V} + \mathcal{P}_V^{\mathcal{G}_V}. \quad (3.1)$$

We shall see that the five above-stated physical laws can be written in this form. This is very convenient, because it makes the amount of knowledge which one must learn rather economical. Let us give a few simple examples that make the understanding of (3.1) more transparent.

Example 3.1 *Let V be the downtown office in a German town or City of the Deutsche Bank and let \mathcal{G}_V be all the money stored in coins, notes, computer accounts of all the customers in this office. Then \mathcal{G}_V is changing in time: Customers will enter the bank through the door; they carry money with them, and they may make a deposit to or withdraw money from their accounts and leave again. This defines $\mathcal{F}_{\partial V}^{\mathcal{G}_V}$. It is positive if the customers have made a deposit and negative if they have withdrawn money. On the other hand, one of their debtors may advise his debt amount in another bank to an account at this downtown office; or an outside bank may withdraw money from an account of an account holder by mutual agreement. This corresponds to $\mathcal{S}_V^{\mathcal{G}_V}$, a source or a sink whose origin is external. Thirdly, the downtown office of the bank may (illegally) print notes or press coins, or they may destroy old bank notes which are a production or annihilation of money, $\mathcal{P}_V^{\mathcal{G}_V}$. So we have been able to assign a definite interpretation to all the terms in (3.1). •*

Example 3.2 *Consider a microwave oven with a bowl of cauliflower to be heated. Let \mathcal{G}_V be the heat content in the cauliflower and $d\mathcal{G}_V/dt$ its time rate of change. In the microwave oven the source of heat is the electromagnetic wave with a frequency that agrees with the eigenfrequency of the water molecules. Because of a resonance reaction the water molecules in the cauliflower start to oscillate as soon as the microwave oven is turned on. Because the oscillation of the molecules is felt as heat, the cauliflower becomes hot. This term in (3.1) is $\mathcal{S}_V^{\mathcal{G}_V}$. There is essentially no heat flow by conduction across the surface of the cauliflower and so $\mathcal{F}_{\partial V}^{\mathcal{G}_V} \sim 0$.*

And neither is there any internal heat production, $\mathcal{P}_V^{G_V}$, unless the cauliflower is radioactively contaminated or rotten. Alternatively, consider the cauliflower in a pan that is filled with water and heated on a stove. In this case, almost all heat growth is due to conduction across the surface, $\mathcal{F}_{\partial V}^{G_V}$. There is no production as before, $\mathcal{P}_V^{G_V} = 0$, but very small radiation as long as the water and cauliflower have different temperatures, $\mathcal{S}_V^{G_V} \sim 0$. •

We shall come back to the formulation of balance laws at several places. In fact the concept of balance laws is the most useful concept throughout the entire book.

Problem 3.1 *The reader is encouraged to find his/her own real-world example of a process forming a balance law.* ♦

Before we apply the concept of balance laws to formulate the physical laws we wish to introduce the following definition³:

Definition 3.1 *A balance law whose production term vanishes, $\mathcal{P}_V^{G_V} = 0$, is called a **conservation law**. Similarly, a physical quantity \mathcal{G}_V whose production term vanishes is called a **conserved quantity**.* ■

In the above two Examples 3.1 and 3.2 the second defines a conserved quantity, whereas the first does not, if the bank prints or destroys money.

3.2 Physical Balance Laws

All physical laws of mechanics and thermodynamics are conservation laws except the second law of thermodynamics, which is a balance law with non-negative production. This *non-negative entropy production* is the manifestation of the *irreversibility* of the physical processes. We shall not explicitly be involved with the second law of thermodynamics by any constructive means in this book, but the other conservation laws of mass, momenta and energy will be explicitly explained.

3.2.1 Balance of Mass

The mass of a body is conserved; this is a physical law holding by experience and cannot otherwise be proved. Moreover, a body mass cannot be supplied by outside sources, and neither can there be any mass flow through a material surface. So all terms on the right-hand side of (3.1) vanish and the balance law of mass reduces to the simple statement

³ This is not the only way in which a conserved quantity is defined in physics and mathematics. We restrict the definition here to quantities of which the production vanishes.

$$\frac{d\mathcal{M}_V}{dt} = 0, \quad (3.2)$$

where we have set $\mathcal{G}_V = \mathcal{M}_V$ and \mathcal{M}_V denotes the total mass within V . So the conservation of mass reads: *The mass of a material body does not change.*

3.2.2 Balance of Linear Momentum

The law of balance of linear momentum is the first dynamical law that enables us to write down equations describing the motion of a body. It corresponds to *Newton's second law* (1687) [10] even though this is historically not strictly correct, because the corresponding statements for continuous media were spelled out later by EULER (1755) [5] (for a fluid) and CAUCHY (1823) [2] (for a solid continuum)⁴. Nevertheless it is convenient for us to think in terms of NEWTON's law for which a colloquial version reads as follows:

Newton's second law: *The time rate of change of the momentum of a body equals the sum of all external forces that are acting on this body.*

This is its correct modern formulation, but more popular is the following variant: *Mass times acceleration equals the sum of the external forces.* In this form it is less precise, correct for most cases but not for all. We shall encounter NEWTON's second law in many occasions when dynamics is involved. Firstly, simple examples will be given in the next section.

NEWTON's second law is a statement involving forces acting on a body, and forces are vectors in the three-dimensional space; thus NEWTON's second law corresponds to three scalar statements, one in each direction of the three-dimensional physical space. To see that it possesses balance law structure we make the following identifications:

$\mathcal{G}_V = \mathcal{P}_V$ momentum of the body V ,

$\mathcal{F}_{\partial V}^{\mathcal{P}} = \mathcal{K}_{\partial V}$ sum of forces acting on the surface ∂V of V ,

$\mathcal{S}_V^{\mathcal{P}} = \mathcal{K}_V$ sum of volume forces acting on the volume V .

There is no momentum production inside the body, because momentum can be produced only by external forces (axiom). So the physical quantity is momentum; its flux into the body – the momentum flux – comprises all the surface forces, and the supply of momentum from outside is the sum of the volume forces:

$$\frac{d\mathcal{P}_V}{dt} = \mathcal{K}_{\partial V} + \mathcal{K}_V. \quad (3.3)$$

We remark that we use \mathcal{P}_V to denote the momentum of a body with volume V as is customary in physics even though $\mathcal{P}_V^{\mathcal{G}_V}$ was used earlier for the production of \mathcal{G}_V (Fig. 3.3). Since \mathcal{P}_V as a vector-valued quantity is written in bold face, confusion

⁴ For biographical sketches for EULER and CAUCHY see Fig. 7.1 and Fig. 4.10, respectively.

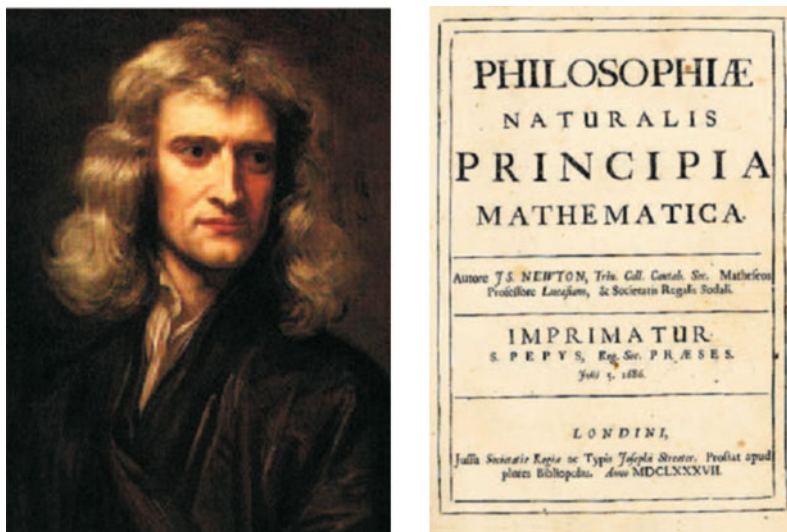


Fig. 3.3 Godfrey KNELLER's 1689 portrait of Isaac NEWTON (aged 46) (<http://www.library.usyd.edu.au/>) and NEWTON's *Principia*, the most important book on natural philosophy published in the early modern period

Sir Isaac NEWTON (4 January 1643 – 31 March 1727) was an English physicist, mathematician, astronomer, natural philosopher, alchemist, and theologian who is considered as one of the most influential people in human history. His 1687 publication of the *Philosophiæ Naturalis Principia Mathematica* (usually called the *Principia*) is among the most influential books in the history of science, laying the groundwork for most of classical mechanics. In this work, NEWTON described universal gravitation and the three laws of motion which dominated the scientific view of the physical universe for the next three centuries. NEWTON showed that the motions of objects on the Earth and of celestial bodies are governed by the same set of natural laws by demonstrating the consistency between KEPLER's laws of planetary motion and his theory of gravitation, thus removing the last doubts about heliocentrism and advancing the scientific revolution.

NEWTON also built the first practical reflecting telescope and developed a theory of colour based on the observation that a prism decomposes white light into the many colours that form the visible spectrum. He also formulated an empirical law of cooling and viscous friction and studied the speed of sound.

In mathematics, NEWTON shares the credit with Gottfried LEIBNIZ for the development of the differential and integral calculus, but LEIBNIZ published his work first. For years there was friction between the two countries over priority. Moreover, the science of fluxions (NEWTON's terminology) and differential calculus (LEIBNIZ's terminology) differed in notation. Today the latter is favoured. He also demonstrated the generalised binomial theorem, developed NEWTON's method for approximating the roots of a function and contributed to the study of power series.

LAGRANGE once said that NEWTON was the greatest genius who ever lived, and once added that NEWTON was also 'the most fortunate, for we cannot find more than once a system of the world to establish'. NEWTON himself had been rather more modest of his own achievements, famously writing in a letter to Robert HOOKE in February 1676: 'If I have seen further it is by standing on the shoulders of Giants.'

The text is based on: <http://en.wikipedia.org/>

should not arise. Furthermore, \mathcal{K}_V and $\mathcal{K}_{\partial V}$ represent the sum of *external* forces. The external source for both should be clear by their very definition as flux and supply terms. Finally, we have divided the external forces into two categories, \mathcal{K}_V and $\mathcal{K}_{\partial V}$, respectively. \mathcal{K}_V denotes those forces which apply at each material volume element, such as the gravity forces, and their sum constitutes the volume force; alternatively, $\mathcal{K}_{\partial V}$ applies at the boundary and constitutes the surface forces. The latter are often loads or reactive forces introduced when, in imagination, cutting a body free from its surroundings.

It is the understanding of continuum mechanics that *any part of the body is itself a body* and that NEWTON's second law also applies to such material parts if at the newly formed surface the corresponding action of the surface cut away is properly taken into account at the newly formed surface. This leads to new definitions of $\mathcal{K}_{\partial V}$ for the new surface, but equally also to a newly defined momentum \mathcal{P}_V and volume force \mathcal{K}_V . According to this principle a body may be cut, e.g., into infinitesimal cubic elements, and to each such element (3.3) may be applied. This will be done in Chap. 4.

3.2.3 Balance of Moment of Momentum

Balance of moment of momentum is the second dynamical law that determines the motion of a body of finite extent. More generally, it is also called the balance of *angular or rotational momentum*. NEWTON in his seminal work 'Principia' (1687) [10] did not principally deal with angular momentum. The historically first encounter of the necessity of this second dynamical law is with L. EULER in 1750 [4, 11]. The law says that angular momentum is a conserved quantity for a material body and can be changed only by external forces (axiom). In the restricted application dealt with in this book we shall use the law as literally stated, namely 'moment of the momentum',⁵ and the law of momentum is NEWTON's second law. So, literally translating this, yields the following:

Euler's law of moment of momentum: see EULER (1750) [4] and TRUESDELL (1964) [11]. *The time rate of change of the moment of momentum of a body equals the sum of all moments of the external forces that are acting on this body.*

With the identifications

$$\begin{aligned}\mathcal{G}_V &= \mathcal{L}_V && \text{moment of momentum of the body } V, \\ \mathcal{F}_{\partial V}^{\mathcal{L}} &= \mathcal{M}_{\partial V} && \text{sum of all moments acting on the surface of the body,} \\ \mathcal{S}_V^{\mathcal{L}} &= \mathcal{M}_V && \text{sum of all moments acting within the body } V\end{aligned}$$

⁵ The more general form of the balance law of *angular momentum* is based on the supposition that angular momentum is composed of two contributions, namely *spin* and *moment of momentum* so that its flux would equally be split into a flux of spin plus moment of flux of linear momentum, and supply of angular momentum would be composed of supply of spin plus moment of supply of linear momentum.

and vanishing production, the balance of moment of momentum takes the form

$$\frac{d\mathcal{L}_V}{dt} = \mathcal{M}_{\partial V} + \mathcal{M}_V. \quad (3.4)$$

We have here given a verbal form of the balance of moment of momentum. To fill it with physical content a clear understanding of the term ‘moment’ must be given. This has been done in [Definition 2.7](#). Accordingly, the law (3.4) holds if the respective moments are taken relative to an *arbitrary* fixed point in space. Because the result can be shown to be independent of the point of reference one usually chooses the origin of a Cartesian coordinate system. Moreover, \mathcal{M}_V and $\mathcal{M}_{\partial V}$ are the *external* body and surface moments, i.e. the moments of the external body and surface forces just as for NEWTON’s law. Moreover, (3.4) is understood to hold true for any body part as was already the case for the balance of linear momentum.

Finally, let us observe and emphasize that the left-hand sides in (3.2), (3.3) and (3.4) are *state variables* of the body defining ‘conditions’ to which the body is subjected. Alternatively, the right-hand sides are ‘agents’ externally applied to the body causing evolutionary changes. They may therefore be interpreted as *process variables*. This same division into state and process variables characterises the next physical law also.

3.2.4 Balance of Energy

This is the fourth of the physical principles of classical physics and it states that energy, when consisting of all forms arising in a body, is conserved (axiom). Because the various forms that may arise also involve thermal contributions, this balance law yields an equation that, under usual conditions, allows us to determine the temperature within a body. Temperature is, however, not the fundamental variable⁶; this variable is the *internal energy*, and its change may be due to the internal deformation of a body, the agitation of the molecules in the body – which is normally interpreted to constitute the temperature – electromagnetic actions, etc. It is the expression of the *first law of thermodynamics that kinetic energy and internal energy together are conserved quantities*.

It follows then that the time rate of change of the total energy (a state variable) is balanced by external surfacial and bulk process quantities. These are also due to two contributions – the mechanical work per unit time of the external forces, $\mathcal{L}_{\partial V}$ and \mathcal{L}_V , and the non-mechanical contributions $Q_{\partial V}$ and Q_V , respectively. If the origin of the latter is due to thermal effects alone, then $Q_{\partial V}$ is called the *heat flow* from the environment to the body through its bounding surface and Q_V the *heat supply* by *radiation*. Both are external and may thus be considered as process quantities.

⁶ Historically, temperature (or an empirical measure for the hotness of a body) has been introduced prior to the internal energy. That the latter is the fundamental variable has been the recognition of the first law of thermodynamics. So the true physical quantity expressing how much energy is stored in a body as heat, deformation, electricity, etc. is the internal energy, while temperature is a measure of the hotness.

In summary we thus have the following:

First law of thermodynamics (also called the **balance law of energy**):

The time rate of change of the total energy (comprising kinetic and internal energy) is balanced by the power of working of the (external) volume and surface forces plus the (external) non-mechanical energy flow (heat flow) through the surface of the body plus the external non-mechanical energy supply (radiation) to the body volume.

Explicitly, let

$\mathcal{G}_V = \mathcal{E}_V^k + \mathcal{E}_V^i$	be the physical quantity in focus, the kinetic plus internal energy within V ,
$\mathcal{F}_{\partial V}^{\mathcal{E}} = \mathcal{L}_{\partial V} + \mathcal{Q}_{\partial V}$	be the flow of total energy through the boundary ∂V of V , the sum of the power of working of the surface forces and the non-mechanical energy (heat) flow from the environment to the body,
$\mathcal{S}_V^{\mathcal{E}} = \mathcal{L}_V + \mathcal{Q}_V$	be the body energy supply, the power of working of the body forces plus the energy supplied by radiation.

Then the first law of thermodynamics reads

$$\frac{d}{dt}(\mathcal{E}_V^k + \mathcal{E}_V^i) = \mathcal{L}_{\partial V} + \mathcal{Q}_{\partial V} + \mathcal{L}_V + \mathcal{Q}_V. \quad (3.5)$$

The first law of thermodynamics says that heat can in principle be transformed into mechanical energy or vice versa, but it does not say whether it is ‘easier’ to transform heat into mechanical energy or vice versa. This non-symmetry is spelled out by the second law of thermodynamics, and both laws were developed in the 19th century when it was for the first time recognised that heat is a form of energy. Strangely, this cognition came long after the realisation of the steam engine, which in fact does nothing else than transforms heat into work. Its first construction is ascribed to the French physicist DENIS PAPIN (1647–1712). However, it was Nicolas Léonard Sadi CARNOT (1796–1832) who first wrote systematically about the production of usable work from heat. He created a construct, the perfect machine and its performance in perfect cyclic processes, now called *CARNOT processes*. They tell us the optimum of this energy transfer from heat to work. In these processes, some heat is always lost to the environment.

CARNOT’s scientific works were in large parts published only more than 40 years after his death. This is the reason why most of today’s thermodynamicists ascribe the merit of having spoken out for the first time the hypothesis of the equivalence of heat and energy to Robert MAYER (1814–1878), a physician from Heilbronn (Baden-Württemberg, Germany), see Fig. 3.4. Between 1841 and 1843 he published two papers expressing the fact that in a material body the total energy was conserved.

Note that the law (3.5) does not contain any potential energy, and in fact potential energy does not belong to it. Potential energy can enter the first law of thermodynamics under special circumstances only. For instance, some of the external body and surface forces may be *conservative*⁷ and derivable from a potential. Under such circumstances, one may show that

$$\mathcal{L}_V + \mathcal{L}_{\partial V} = \mathcal{L}'_V + \mathcal{L}'_{\partial V} - \frac{d}{dt}(\mathcal{U}),$$

so that (3.5) may take the alternative form

$$\frac{d}{dt}(\mathcal{E}_V^k + \mathcal{E}_V^i + \mathcal{U}) = \mathcal{L}'_{\partial V} + \mathcal{Q}_{\partial V} + \mathcal{L}'_V + \mathcal{Q}_V. \quad (3.6)$$

Here, \mathcal{U} is the potential energy of the conservative forces and $\mathcal{L}'_V + \mathcal{L}'_{\partial V}$ is the power of working of the body and surface forces to which no potential has been assigned.

3.2.5 Second Law of Thermodynamics

There is yet a fifth law of physics, the so-called *second law of thermodynamics*. It expresses in mathematical form what experience has shown and proved to be correct, namely that all physical processes are irreversible. In other words, if a process to which a body is subjected takes place from time t_1 to time $t_2 > t_1$, then the second law of thermodynamics states that this process is accompanied by a non-recoverable loss of energy, except, of course, if nothing happens at all. It also means that a process obtained by traversing the given process backward in time is not physically realisable, because the non-recoverable energy would have to be provided as an input. The second law gives the physical processes an orientation and is tantamount to the assumption that all motion of a body is associated with *dissipation* or loss of energy into heat that is eventually transferred to the environment. It was CARNOT who first recognised this loss of mechanical energy when studying the performance of heat engines. Julius Emanuel CLAUSIUS (1822–1888) introduced a scalar-valued state variable, which he called *entropy*, which would measure the amount of irreversibility that physical processes generate in a body. It needed almost an additional century of research, involving the most prominent physicists⁸ of the time, until the second law of thermodynamics was established as a balance law of entropy as follows:

⁷ A force \mathcal{F} is called conservative if the work done by the force along a trajectory from a point A to a point B only depends on the positions of A and B and not on the trajectory connecting A and B . It can be proved that such a force is derivable from a potential \mathcal{U} such that $\mathcal{F} = -\text{grad}(\mathcal{U})$ and $\mathcal{L}_{\mathcal{F}} = -\frac{d}{dt}(\mathcal{U})$.

⁸ Maurice Marie DUHEM (1861–1961), Max PLANCK (1858–1947), Constantine CARATHEODORY (1873–1950), Lord KELVIN (1824–1907), Clifford TRUESDELL (1919–2000) and many others.

Second law of thermodynamics: *Let*

$\mathcal{G}_V = \mathcal{H}_V$ *be the entropy of the body V ,*

$\mathcal{F}_{\partial V}^{\mathcal{H}} = \Phi_{\partial V}$ *the flux of entropy through the surface ∂V of V ,*

$\mathcal{S}_V^{\mathcal{H}} = \Sigma_V$ *the supply of entropy to the body V ,*

$\mathcal{P}_V^{\mathcal{H}} = \Pi_V$ *the production of entropy within the body V .*

These quantities obey the balance law

$$\frac{d\mathcal{H}}{dt} = \Phi_{\partial V} + \Sigma_V + \Pi_V, \quad (3.7)$$

and it is the expression of the irreversibility of the physical processes that the entropy production

$$\Pi_V \geq 0 \quad (3.8)$$

is non-negative for all processes obeying the conservation laws of mass, momentum, moment of momentum and energy as well as the material equations.

According to this law, any process of a body obeying the conservation laws but violating inequality (3.8) is unphysical and therefore physically unrealisable. The above formulation of the second law, however, also involves an additional quality, namely the *material equations* or *constitutive relations*. These are those statements beyond the conservation laws of mass, momenta and energy which distinguish different materials from one another, e.g. water from ice or vapour. The second law of thermodynamics is viewed as a statement which constrains the material behaviour such that the entropy imbalance is never violated for any process satisfying the physical conservation laws and the material equations.

An important achievement of thermodynamics of the 19th century is the discovery of a ‘universally’ valid measure of the hotness of a material point. This ‘universal’ quantity is the so-called *absolute* or *KELVIN temperature*, and its existence is a consequence of the second law of thermodynamics (Fig. 3.4). To explain it, recall that temperature is measured by instruments, and these measure the volume of a given mass of liquid (mercury thermometer), the pressure of a gas contained in a fixed volume (ideal gas thermometer) or the electrical resistivity of a metallic specimen. In these instruments, addition of heat to the thermometer changes (monotonically) the volume of the liquid, the pressure of the gas and the electrical resistivity of the metallic specimen, respectively. The instruments may be calibrated such that volume, pressure and resistivity correspond to temperature, but even if they exactly reproduce the freezing and boiling points of water at normal pressure, there is no guarantee that they also reproduce the same values for the temperature θ in-between. This is so because the value of θ depends on the material properties of the fluid, gas or metal of which the thermometer is made. So, these thermometers measure so-called empirical temperatures. The second law of thermodynamics shows that all ideal gas thermometers measure exactly the same temperature in the entire range of measurable temperature irrespective of which ideal gas is used.

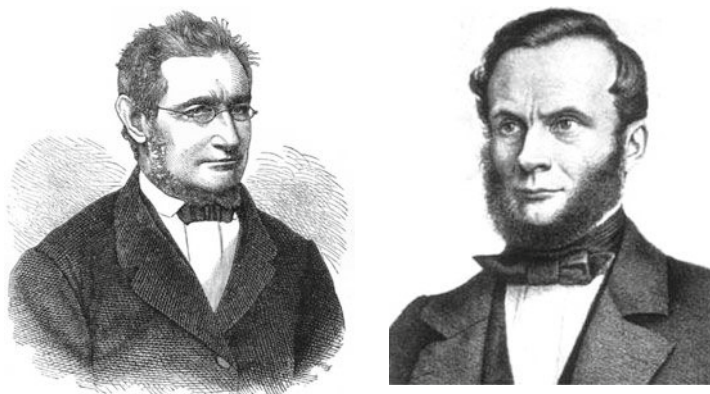


Fig. 3.4 Julius Robert von MAYER and Rudolf Julius Emmanuel CLAUSIUS (<http://en.wikipedia.org/>, <http://www-groups.dcs.st-and.ac.uk/>)

Julius MAYER (25 November 1814 – 20 March 1878) was a learned German physician and self-made physicist and one of the founders of thermodynamics. He studied medicine and once travelled as a ship's physician on a Dutch three-mast sailing ship to Jakarta. Although he had hardly been interested before this journey in physical phenomena, his observation that storm-whipped waves are warmer than the calm sea started him thinking about the laws of nature, in particular about the physical phenomenon of warmth and the question: whether the directly developed heat alone or the sum of the amounts of heat developed in direct and indirect ways contributes to the temperature. After his return during February 1841 MAYER dedicated his efforts to this problem. MAYER was the first person to state the law of conservation of energy, one of the most fundamental tenets of modern day physics. During 1842, MAYER described oxidation as the primary source of energy for any living creature. His achievements were overlooked and priority for the discovery of the mechanical equivalent of heat was attributed to James JOULE in the following year. He also proposed that plants convert light into chemical energy. A truly original scientist, much of his work was belittled or ignored by his contemporaries because of his stilted style of writing.

Rudolf Julius Emmanuel CLAUSIUS (2 January 1822 – 24 August 1888), a physicist of the University of Berlin in 1844 with doctorate from the University of Halle in 1848 taught physics in Berlin, Zürich, Würzburg and Bonn. His doctorate aimed at explaining the blue colour of the sky, the red colours seen at sunrise and sunset, and the polarisation of light. His first and most famous paper is on the mechanical heat *Über die bewegende Kraft der Wärme und die Gesetze, welche sich daraus selbst ableiten lassen*, *Annalen der Physik*, 155 (1850) [On the motive power of heat, and on the laws which can be deduced from it for the theory of heat] and established his fame. This paper marks the foundation of thermodynamics, as it states for the first time the basic idea of the second law of thermodynamics. CLAUSIUS also formulated the second law in terms of a quantity expressing the nature of irreversibility which he called 'entropy'. After 1875, CLAUSIUS concentrated on electrodynamics. He gave a principle of conservation of energy in electrodynamics related to a force law of action at a distance. Despite the difficulties in the theory, which resulted in a charge at rest on the Earth being subjected to a force due to the motion of the Earth, it played an important role in the development of electrodynamics.

The text is based on the article by J. J. O'Connor and E. F. Robertson (<http://www-groups.dcs.st-and.ac.uk/>), the book I. Müller, *A History of Thermodynamics*, Springer 2007, and <http://en.wikipedia.org/>

The temperature measured by these thermometres is called *absolute temperature* or *KELVIN temperature*. Lord KELVIN introduced it around 1850. It enjoys some notion of universality among all ideal gas thermometres and is therefore sometimes called *universal temperature*.

We shall not need in detail to work with the entropy inequality here. All equations that will be used will automatically fulfil it. We have stated it here to present the complete set of all thermomechanical equations of classical physics. Interested readers may consult the specialised literature.⁹

References

1. Carnot, S.: Réflexions sur la puissance motrice du feu et sur les machines propres développer cette puissance. *Annales scientifiques de l' École Normale Supérieure* **Sèr. 2**, (1), 393–457 (1872)
2. Cauchy, A.-L.: Recherches sur l'équilibre et le moment intérieur des corps solides ou fluides, élastiques ou nonélastiques. *Bull. Soc. Philomath., Paris*, 9–13 = Oevres (2) **2**, 300–304 (1823)
3. Chandrasekhar, S.: *Newton's Principia for the Common Reader*. Clarendon, Oxford, 593 p. (1995)
4. Euler, L.: *Mémoires de l'Académie des Sciences de Berlin* **5**, 185–217 (1750) printed 1752, also in L. Euleri Opera Omnia, ser. Sec. **5**, 81–108
5. Euler, L.: *Mémoires de l'Académie des Sciences de Berlin* **11**, 274–315 (1755) also in: Opera Omnia, ser. Sec. **12**, 54–91
6. Gurtin, M.E.: *An Introduction to Continuum Mechanics*. Academic, New York, NY (1981)
7. Haupt, P.: *Continuum Mechanics and Theory of Materials*. Springer, Berlin (1999)
8. Hutter, K. and Jöhnk, K.: *Continuum Methods of Physical Modeling*. Springer, Berlin, 635 p. (2004)
9. Müller, I.: *Thermodynamics*. Pitman (1985)
10. Newton, I.: *Philosophiae naturalis principia mathematica*. London (1687) (1st edition) (1703) (2nd edition) (1726) (3rd edition)
11. Truesdell, C.A.: Die Entwicklung des Drallsatzes. *Zeitschrift für angewandte Mathematik und Mechanik (ZAMM)* **44**, 149–158 (1964)

⁹ See, e.g., [6–9, 11] and others.

Chapter 4

Fundamental Equations of Lake Hydrodynamics

Having laid down in the previous chapters the foundations of NEWTONian mechanics, classical thermodynamics and elements of mathematics, indispensable to anyone dealing with lake physics, we shall now attempt to formulate the basic laws in a mathematical form appropriate for direct use in the ensuing chapters.¹

Firstly, the notion of kinematics will be introduced; this is the science of the geometry of the motion of bodies in three-dimensional physical space; velocity, acceleration and deformation are particular aspects of the geometry of deformable bodies in motion. Subsequently, the focus will be on the mathematical specification and physical interpretation of the balance laws of mass, momentum, moment of momentum and energy. This entails in particular the introduction of the concepts of the ‘stress vector’ and ‘stress tensor’, of which a clear understanding is vital if the various forms of the balance of momentum are to be understood. The balance laws of mass, momenta and energy are physical laws common to all bodies irrespective of whether they are solids or fluids or gases. The characterisation of this distinction is a matter of material science; we shall here not dwell upon a systematic presentation of this so-called constitutive theory; we are rather satisfied with a typical characterisation of a fluid and the presentation of the material equation of ideal and linearly viscous fluids – so-called NEWTONian fluids. For both the material equations will be derived and their response in hydrostatic equilibrium will be presented. Finally, the first law of thermodynamics will be explained, and it will be shown how from its application as a balance law the heat equation can be derived.

The subject content of the entire chapter is large; however utmost care is taken to present the concepts as simple as possible, and indeed no further mathematics is used than was introduced in [Chap. 2](#).

¹ There are many books on continuum mechanics and thermodynamics of continuous systems where alternative presentations of these derivations are given, e.g. [\[1, 5, 6, 9, 15\]](#).

4.1 Kinematics

The *purpose of Physics of Lakes* is the investigation of the main physical *processes* arising in the Earth's lakes and the analysis of their causes and consequences in order to reach an estimation of their importance for the physical and ecological variabilities that may occur in a lake. This entails determination of the field variables that are in focus. These are primarily the velocity and temperature fields, but also other physical quantities such as the O_2 content, the phosphate content of the water, the concentrations of the phytoplankta and other field quantities. Because the motion of the water is central, we focus in this section upon quantities defining the motion.

Basic to the description of the motion of water bodies is the notion of a *material particle*. By this we mean a point in three-dimensional space, which carries along with it the properties of the body under consideration: mass, momentum, energy densities, etc. The particles are identified by their position vectors \mathbf{x} . If a particle is in motion, its position will continuously change with time. Thus, \mathbf{x} can be viewed as a function of its initial position, \mathbf{X} and of time t , viz. see Fig. 4.1

$$\mathbf{x} = \chi(\mathbf{X}, t), \quad (4.1)$$

and this function – called *motion* or *motion function* – is assumed to be continuously differentiable and invertible. This means that to a single \mathbf{X} , there belongs a single \mathbf{x} and vice versa. Sometimes one simply writes $\mathbf{x} = \mathbf{x}(\mathbf{X}, t)$. Because $\mathbf{X} = \chi(\mathbf{X}, 0)$ identifies the particle in its initial position, one may use \mathbf{X} as the name of the particle.

All particles of a body at time $t = 0$ define the body in its initial position. All these points comprise what is called the *reference configuration* of the body. Alternatively, all position vectors \mathbf{x} are the unique maps of the material points \mathbf{X} of the body at time t and constitute the so-called *present configuration* of the body.

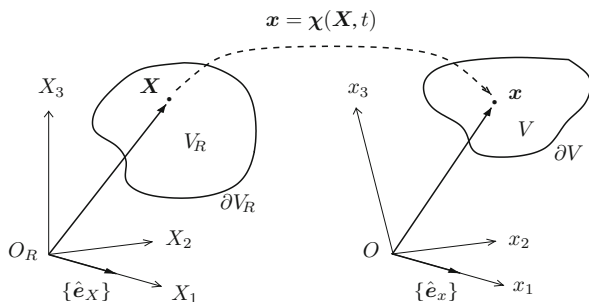


Fig. 4.1 Body in its *reference configuration* (left) at time $t = 0$ and in its *present configuration* (right) at an arbitrary time $t > 0$. A material particle in the former is represented by \mathbf{X} and referred to a Cartesian coordinate system $O_R X_1 X_2 X_3$; in the latter the particle's position is \mathbf{x} , referred to $O x_1 x_2 x_3$, a second Cartesian origin and basis. The motion is the map $\mathbf{X} \mapsto \mathbf{x}$ written as $\mathbf{x} = \chi(\mathbf{X}, t)$. The two origins O_R, O and the bases $\{\hat{\mathbf{e}}_X\}$ and $\{\hat{\mathbf{e}}_x\}$ are chosen to be distinct in this figure, but in practice they are often the same. In those cases, of course, \mathbf{X} and \mathbf{x} are still different vectors in general

Notice that the reference configuration is fixed once and for all when it is chosen, but the present configuration changes in general with time; the motion of a body is *steady* if the present configuration does not change with time. The positions \mathbf{X} in the reference configuration are referred to an origin O_R with Cartesian basis $\{\hat{\mathbf{e}}_X\}$ so that $\mathbf{X} = \sum_{\alpha} X_{\alpha} \hat{\mathbf{e}}_{X_{\alpha}}$. Similarly, the locations \mathbf{x} of the particles in the present configuration are referred to an origin O with Cartesian basis $\{\hat{\mathbf{e}}_x\}$ so that $\mathbf{x} = \sum_i x_i \hat{\mathbf{e}}_{x_i}$. In Fig. 4.1 the two origins and bases are distinct; however, often they are chosen to be the same. Under such restrictive assumptions, one may identify \mathbf{X} and \mathbf{x} with (X_1, X_2, X_3) and (x_1, x_2, x_3) because the two vectors are in this case referred to the same Cartesian basis.

With the motion defined in (4.1), we may now introduce the velocity and acceleration fields.

Definition 4.1 *Let $\mathbf{x} = \chi(\mathbf{X}, t)$ be the motion of a material particle. Then velocity and acceleration are the change of position per unit time and the change of velocity per unit time, respectively; mathematically, they are the first and second time derivatives² of the motion, keeping the particle fixed, viz.*

$$\begin{aligned} \mathbf{v} &:= \frac{\partial \chi(\mathbf{X}, t)}{\partial t} = \hat{\mathbf{v}}(\mathbf{X}, t) \quad (\text{velocity}) \\ \mathbf{a} &:= \frac{\partial^2 \chi(\mathbf{X}, t)}{\partial t^2} = \hat{\mathbf{a}}(\mathbf{X}, t) \quad (\text{acceleration}). \end{aligned} \tag{4.2}$$

These formulae define both fields as functions of the reference (initial) positions and time. This is so because the motion is already defined as a function of these variables. ‘Keeping the particle fixed’ means that the derivatives of the function $\chi(\mathbf{X}, t)$ must be so taken that the particle \mathbf{X} is held constant during differentiation; this corresponds exactly to the partial derivatives of $\chi(\mathbf{X}, t)$ with respect to time as expressed in (4.2).

The functions $\hat{\mathbf{v}}(\mathbf{X}, t)$ and $\hat{\mathbf{a}}(\mathbf{X}, t)$ are not convenient representations in fluid mechanics. More adequate would be to express the velocity and acceleration as functions of \mathbf{x} and t . Such representations can be obtained if the function (4.1) is inverted, i.e. if \mathbf{X} is expressed as a function of \mathbf{x} and t . If the inverse function is denoted by χ^{-1} , then³

$$\mathbf{x} = \chi(\mathbf{X}, t) \text{ is equivalent to } \mathbf{X} = \chi^{-1}(\mathbf{x}, t). \tag{4.3}$$

² We do not explicitly state here the degree of smoothness of a function; any needed degree of smoothness is simply tacitly assumed to exist by stating and performing the operations of differentiation. This is very often done so in topics where mathematics is applied. Functions are assumed to be differentiable as many times as needed for the computations that are performed.

³ If $x = X^n$, then the inverse function is $X = x^{1/n}$. Generally, for an invertible function $f(x)$ the graph of the inverse function is the image mirrored at the 45° line. Furthermore, it is tacitly assumed that in performing this inversion, possible multi-valuednesses are automatically eliminated by restricting considerations to principal values of the inverse function.

Substituting (4.3) into (4.2) yields

$$\begin{aligned} \mathbf{v} &= \hat{\mathbf{v}}(\mathbf{X}, t) \stackrel{(4.3)}{=} \hat{\mathbf{v}}(\chi^{-1}(\mathbf{x}, t), t) = \tilde{\mathbf{v}}(\mathbf{x}, t), \\ \mathbf{a} &= \hat{\mathbf{a}}(\mathbf{X}, t) \stackrel{(4.3)}{=} \hat{\mathbf{a}}(\chi^{-1}(\mathbf{x}, t), t) = \tilde{\mathbf{a}}(\mathbf{x}, t). \end{aligned}$$

The above two different representations of the velocity and acceleration – once as functions of \mathbf{X}, t and once as functions of \mathbf{x}, t – raise the more general question, how any field quantity, defined for a material particle,⁴ is best represented as a function of the particle's initial position \mathbf{X} and time t , $\phi = \Phi(\mathbf{X}, t)$, or as a function of its present position \mathbf{x} and time t , $\phi = \varphi(\mathbf{x}, t)$. The two representations are so different in approach and so significant that we shall list them here in the form of a definition:

Definition 4.2 *Let ϕ be a physical quantity of a particle.*

- *If $\phi = \Phi(\mathbf{X}, t)$, i.e. if ϕ is represented as a function of the reference position \mathbf{X} and time t , then this is called the **Lagrangian representation**.*
- *If $\phi = \varphi(\mathbf{x}, t)$, i.e. if ϕ is represented as a function of the position \mathbf{x} in the present configuration and time t , then this is called the **Eulerian representation**. ■*

Because of the significance of these descriptions let us illustrate them by an example. Imagine, we wish to measure the water current field in a certain region of a lake. This can be done by deploying current metres at moorings fixed in space. Because the moorings are for all time at the same position, the measured velocity components represent the functions $v_j(\mathbf{x}, t)$ and thus register functions in the EULERian description. If, however, the velocities are inferred from registered positions of drifting buoys, then one identifies the varying positions of the buoys with the varying positions of a fluid particle and thus encounters the LAGRANGEan description. Of course, identifying the motion of a buoy with that of a material fluid particle is still a conjecture subject to criticism, but its supposition is quite common in physical limnology.

The choice of representation – EULERian or LAGRANGEan – influences the operation of time differentiation keeping the particle fixed.

Definition 4.3 *Let ϕ be a physical quantity. Its **material time derivative** is the time rate of change of ϕ , holding the particle fixed. It is denoted by an overhead point $\dot{\phi}$, or by the straight differentiation symbol, d/dt . ■*

⁴ Note that we define here a physical quantity for a particle even though a physical property (mass, momentum, etc.) in Chap. 3 was only defined for a body. The difference in viewpoint is based upon the tacit assumption that any part of a body – even infinitesimally small – equally constitutes a body.

With this definition, one obtains in the *Lagrangian description*

$$\dot{\phi} = \frac{d\phi}{dt} \Big|_{X=\text{fix}} = \frac{\partial \Phi(X, t)}{\partial t}. \quad (4.4)$$

The material derivative is here obtained simply as the partial derivative of the function $\Phi(X, t)$ with respect to time t . In the EULERian description, one has $\phi = \varphi(\mathbf{x}, t)$, whereby \mathbf{x} itself is given by the motion (4.1). Therefore, \mathbf{x} is itself varying with time (if the particle is held fixed), and the material time derivative has to be obtained by employing the chain rule of differentiation of the function $\varphi(\mathbf{x}, t)$; to be sure

$$\dot{\phi} = \frac{\partial \varphi(\mathbf{x}, t)}{\partial t} + \sum_i \frac{\partial \varphi(\mathbf{x}, t)}{\partial x_i} \tilde{v}_i(\mathbf{x}, t), \quad (4.5)$$

in which we have set $\partial \chi_i(X, t)/\partial t = \tilde{v}_i(\mathbf{x}, t)$ and where we have assumed that \mathbf{x} in the argument of $\varphi(\mathbf{x}, t)$ is given by its three components referred to a Cartesian basis. Other forms of writing (4.5) are⁵

$$\dot{\phi} = \frac{\partial \varphi}{\partial t} + \frac{\partial \varphi}{\partial x_1} v_1 + \frac{\partial \varphi}{\partial x_2} v_2 + \frac{\partial \varphi}{\partial x_3} v_3 = \underbrace{\frac{\partial \varphi}{\partial t}}_{\text{local}} + \underbrace{(\text{grad } \varphi) \cdot \mathbf{v}}_{\text{convective derivative}}, \quad (4.6)$$

as already shown in Chap. 2. Here we have not repeated the independent variables \mathbf{x} and t , as they are implicitly clear. In the EULERian description the material (or total) time derivative of a physical quantity – this is the time rate of change of a quantity that is experienced along the trajectory of the particle – is composed of the local derivative – this is the derivative function one can infer from a physical quantity measured at a fixed mooring – and the convective derivative.

Let ϕ be the velocity field \mathbf{v} ; then its material time derivative is the acceleration and application of (4.6) yields

$$\tilde{\mathbf{a}}(\mathbf{x}, t) = \dot{\mathbf{v}}(\mathbf{x}, t) = \frac{\partial \mathbf{v}}{\partial t} + (\text{grad } \mathbf{v}) \mathbf{v}. \quad (4.7)$$

Written in component form of a Cartesian coordinate system, this yields

$$\begin{aligned} a_1 &= \frac{dv_1}{dt} = \frac{\partial v_1}{\partial t} + \frac{\partial v_1}{\partial x_1} v_1 + \frac{\partial v_1}{\partial x_2} v_2 + \frac{\partial v_1}{\partial x_3} v_3, \\ a_2 &= \frac{dv_2}{dt} = \frac{\partial v_2}{\partial t} + \frac{\partial v_2}{\partial x_1} v_1 + \frac{\partial v_2}{\partial x_2} v_2 + \frac{\partial v_2}{\partial x_3} v_3, \\ a_3 &= \frac{dv_3}{dt} = \frac{\partial v_3}{\partial t} + \frac{\partial v_3}{\partial x_1} v_1 + \frac{\partial v_3}{\partial x_2} v_2 + \frac{\partial v_3}{\partial x_3} v_3. \end{aligned} \quad (4.8)$$

⁵ Here (and henceforth often), we have omitted the overhead tilde characterising the EULERian description. This we shall regularly do when the functional dependencies are clear from the context.

Introducing the matrix representation of the gradient [see Chap. 2, (2.47)]

$$\text{grad } \mathbf{v} \hat{=} \begin{pmatrix} \frac{\partial v_1}{\partial x_1} & \frac{\partial v_1}{\partial x_2} & \frac{\partial v_1}{\partial x_3} \\ \frac{\partial v_2}{\partial x_1} & \frac{\partial v_2}{\partial x_2} & \frac{\partial v_2}{\partial x_3} \\ \frac{\partial v_3}{\partial x_1} & \frac{\partial v_3}{\partial x_2} & \frac{\partial v_3}{\partial x_3} \end{pmatrix}, \quad (4.9)$$

the convective derivative takes the form

$$(\text{grad } \mathbf{v})\mathbf{v} \hat{=} \begin{pmatrix} \frac{\partial v_1}{\partial x_1} & \frac{\partial v_1}{\partial x_2} & \frac{\partial v_1}{\partial x_3} \\ \frac{\partial v_2}{\partial x_1} & \frac{\partial v_2}{\partial x_2} & \frac{\partial v_2}{\partial x_3} \\ \frac{\partial v_3}{\partial x_1} & \frac{\partial v_3}{\partial x_2} & \frac{\partial v_3}{\partial x_3} \end{pmatrix} \begin{pmatrix} v_1 \\ v_2 \\ v_3 \end{pmatrix}, \quad (4.10)$$

and (4.8) becomes

$$\begin{pmatrix} \dot{v}_1 \\ \dot{v}_2 \\ \dot{v}_3 \end{pmatrix} = \begin{pmatrix} \frac{\partial v_1}{\partial t} \\ \frac{\partial v_2}{\partial t} \\ \frac{\partial v_3}{\partial t} \end{pmatrix} + \begin{pmatrix} \frac{\partial v_1}{\partial x_1} & \frac{\partial v_1}{\partial x_2} & \frac{\partial v_1}{\partial x_3} \\ \frac{\partial v_2}{\partial x_1} & \frac{\partial v_2}{\partial x_2} & \frac{\partial v_2}{\partial x_3} \\ \frac{\partial v_3}{\partial x_1} & \frac{\partial v_3}{\partial x_2} & \frac{\partial v_3}{\partial x_3} \end{pmatrix} \begin{pmatrix} v_1 \\ v_2 \\ v_3 \end{pmatrix}. \quad (4.11)$$

Formulae (4.7) and (4.11) list two forms of representation of the acceleration in the EULERian description. The former gives the acceleration in symbolic notation when the velocity field is given as a function $\mathbf{v}(\mathbf{x}, t)$, the latter shows how it is evaluated when it is referred to a Cartesian basis, i.e. (4.11) tells us how the three components of the acceleration are computed when the components of the velocity field are given in the EULERian description.

Problem 4.1 *Prove that another formula for the acceleration of the velocity field is*

$$\tilde{\mathbf{a}}(\mathbf{x}, t) = \frac{\partial \mathbf{v}}{\partial t} + \text{grad} \left(\frac{\mathbf{v} \cdot \mathbf{v}}{2} \right) - \mathbf{v} \times \text{curl } \mathbf{v}. \quad (4.12)$$

(This proof can most easily be performed by writing each term of the right-hand side in Cartesian component form.) ♦

In texts on continuum mechanics the spatial gradient of the velocity field is often denoted by \mathbf{L} , $\text{grad } \mathbf{v} = \mathbf{L}$, and its Cartesian components L_{ij} ($i, j = 1, 2, 3$) are given in (4.9). Furthermore, \mathbf{L} is a second-rank tensor and the scheme (4.9) is its

matrix representation referred to a Cartesian coordinate system. It is evident that this matrix is not symmetric, because its transpose is, in general, not the same as the matrix itself.

Definition 4.4 Let $\mathbf{L} := \text{grad } \mathbf{v}(\mathbf{x}, t)$ be the spatial gradient of the velocity field. The symmetric and skew-symmetric parts of \mathbf{L} are defined as

$$\begin{aligned}\mathbf{D} &= \frac{1}{2} (\mathbf{L} + \mathbf{L}^T) = \frac{1}{2} (\text{grad } \mathbf{v} + (\text{grad } \mathbf{v})^T), \\ \mathbf{W} &= \frac{1}{2} (\mathbf{L} - \mathbf{L}^T) = \frac{1}{2} (\text{grad } \mathbf{v} - (\text{grad } \mathbf{v})^T).\end{aligned}\quad (4.13)$$

\mathbf{D} is called the **stretching or strain rate tensor** with $\mathbf{D} = \mathbf{D}^T$, while \mathbf{W} is called the **vorticity tensor or spin tensor** with $\mathbf{W} = -\mathbf{W}^T$. Moreover

$$\boldsymbol{\omega} = \boldsymbol{\varepsilon} \cdot \mathbf{W} = \text{curl } \mathbf{v}(\mathbf{x}) \quad (4.14)$$

is called the **vorticity vector**, or simply the **vorticity**. ■

These quantities were already introduced in Chap. 2, (2.70), where also the component representations

$$\mathbf{D} \hat{=} \begin{pmatrix} \frac{\partial v_1}{\partial x_1} & \frac{1}{2} \left(\frac{\partial v_1}{\partial x_2} + \frac{\partial v_2}{\partial x_1} \right) & \frac{1}{2} \left(\frac{\partial v_1}{\partial x_3} + \frac{\partial v_3}{\partial x_1} \right) \\ & \frac{\partial v_2}{\partial x_2} & \frac{1}{2} \left(\frac{\partial v_2}{\partial x_3} + \frac{\partial v_3}{\partial x_2} \right) \\ \text{sym} & & \frac{\partial v_3}{\partial x_3} \end{pmatrix}, \quad (4.15)$$

$$\mathbf{W} \hat{=} \begin{pmatrix} 0 & \frac{1}{2} \left(\frac{\partial v_1}{\partial x_2} - \frac{\partial v_2}{\partial x_1} \right) & \frac{1}{2} \left(\frac{\partial v_1}{\partial x_3} - \frac{\partial v_3}{\partial x_1} \right) \\ & 0 & \frac{1}{2} \left(\frac{\partial v_2}{\partial x_3} - \frac{\partial v_3}{\partial x_2} \right) \\ \text{skw} & & 0 \end{pmatrix}, \quad (4.16)$$

and

$$\boldsymbol{\omega} \hat{=} \left[\left(\frac{\partial v_3}{\partial v_2} - \frac{\partial v_2}{\partial x_3} \right), \left(\frac{\partial v_1}{\partial x_3} - \frac{\partial v_3}{\partial x_1} \right), \left(\frac{\partial v_2}{\partial x_3} - \frac{\partial v_3}{\partial x_2} \right) \right] \quad (4.17)$$

were given, in which sym and skw indicate that the matrix elements must be symmetrically and skew-symmetrically repeated.

The motion function (4.1) also gives rise to the definition of a material (rather than) spatial gradient. Let $d\mathbf{X}$ be a material line element in the reference configuration and $d\mathbf{x}$ its image in the present configuration. Then according to (4.1), we have

$$d\mathbf{x} = \mathbf{F} d\mathbf{X} \quad \text{or} \quad dx_i = F_{i\alpha} dX_\alpha. \quad (4.18)$$

The tensor

$$\mathbf{F} = \frac{\partial \chi(\mathbf{X}, t)}{\partial \mathbf{X}} = \text{grad } \chi(\mathbf{X}, t), \quad F_{i\alpha} = \frac{\partial \chi_i(\mathbf{X}, t)}{\partial X_\alpha} \quad (4.19)$$

is known as the *deformation gradient*. It maps vectors from the reference configuration to the present configuration and is therefore also known as a *two-point tensor*, which is expressed in coordinate form relative to both bases $\{\hat{\mathbf{e}}_{x_i}\}$ and $\{\hat{\mathbf{e}}_{X_\alpha}\}$ in the present and reference configurations, respectively, as

$$\mathbf{F} = F_{i\alpha} \hat{\mathbf{e}}_{x_i} \otimes \hat{\mathbf{e}}_{X_\alpha}. \quad (4.20)$$

Every second-rank tensor may be product decomposed into two parts, one an orthogonal tensor and the other a positive definite symmetric tensor. This so-called *polar decomposition* can also be carried out for the deformation gradient; it will yield a closer interpretation of the local deformation that will be of importance later on.

The theorem reads as follows:

Polar decomposition theorem *Every second-rank tensor \mathbf{F} with $\det \mathbf{F} \neq 0$ permits two polar decompositions, namely*

$$\mathbf{F} = \mathbf{R}\mathbf{U} = \mathbf{V}\mathbf{R}, \quad (4.21)$$

with the following properties:

- \mathbf{V} and \mathbf{U} are symmetric,

$$\mathbf{V} = \mathbf{V}^T, \quad \mathbf{U} = \mathbf{U}^T. \quad (4.22)$$

- \mathbf{V} and \mathbf{U} are positive definite,

$$\mathbf{x} \cdot \mathbf{V}\mathbf{x} \geq 0, \quad \mathbf{x} \cdot \mathbf{U}\mathbf{x} \geq 0, \quad \forall \mathbf{x} \in \mathbb{R}^3 \quad (4.23)$$

and they have the same eigenvalues.

This part of the deformation gradient corresponds to a pure strain; \mathbf{U} and \mathbf{V} are called the right and left stretch tensors, respectively.⁶ The denotation right and left implies that \mathbf{U} stands to the right and \mathbf{V} stands to the left of \mathbf{R} , no more!

- \mathbf{R} is proper orthogonal

$$\mathbf{R}\mathbf{R}^T = \mathbf{R}^T\mathbf{R} = \mathbf{I}, \quad \det \mathbf{R} = +1. \quad (4.24)$$

- The polar decomposition is unique.⁷ ■

⁶ Note that we use ‘stretch’ to denote deformation associated with ‘strain’ and ‘stretching’ to express ‘strain rate’.

⁷ The polar decomposition is unique for a tensor \mathbf{F} which is non-singular. For details see [15, Sect. 23], or any book on continuum mechanics, e.g. [8].

The above described polar decomposition enables us to interpret the deformation (Fig. 4.2) by stating that rotation follows stretch or stretch follows rotation. We now prove the polar decomposition theorem. Readers not interested in this proof may continue after formula (4.41).

Proof of the Polar Decomposition Theorem For the proof of this theorem, some basic knowledge of linear algebra is necessary, which is assumed to be known. The proof starts with the statement that $\mathbf{C} := \mathbf{F}^T \mathbf{F}$ and $\mathbf{B} := \mathbf{F} \mathbf{F}^T$ are symmetric and positive definite transformations. \mathbf{C} and \mathbf{B} are called right and left CAUCHY–GREEN deformation tensors, respectively. Based on this symmetry property these tensors must possess spectral representations

$$\mathbf{C} = \sum_{\alpha} \lambda_{\alpha}^{(C)} \mathbf{e}_{\alpha} \otimes \mathbf{e}_{\alpha}, \quad \mathbf{B} = \sum_i \lambda_i^{(B)} \mathbf{e}_i \otimes \mathbf{e}_i \quad (4.25)$$

with real *eigenvalues* $\lambda_{\alpha}^{(C)}$ and $\lambda_i^{(B)}$, which are positive since \mathbf{B} and \mathbf{C} are positive definite. The vectors \mathbf{e}_{α} and \mathbf{e}_i are the eigenvectors in the reference and present configurations, respectively; these can be directly interpreted as basis vectors of $\mathbb{R}_{\text{Ref}}^3$ and $\mathbb{R}_{\text{Pres}}^3$. On this ground, the right and left stretch tensors can be defined by

$$\begin{aligned} \mathbf{U} &:= \sum_{\alpha} \lambda_{\alpha}^{(U)} \mathbf{e}_{\alpha} \otimes \mathbf{e}_{\alpha}, & \lambda_{\alpha}^{(U)} &= \sqrt{\lambda_{\alpha}^{(C)}}, \\ \mathbf{V} &:= \sum_i \lambda_i^{(V)} \mathbf{e}_i \otimes \mathbf{e}_i, & \lambda_i^{(V)} &= \sqrt{\lambda_i^{(B)}}, \end{aligned} \quad (4.26)$$

where these are obviously symmetric and positive definite. This construction of the stretch tensors is unique and leads to $\mathbf{U}^2 = \mathbf{C}$ and $\mathbf{V}^2 = \mathbf{B}$. The existence of inverse tensors \mathbf{U}^{-1} , \mathbf{V}^{-1} is also guaranteed:

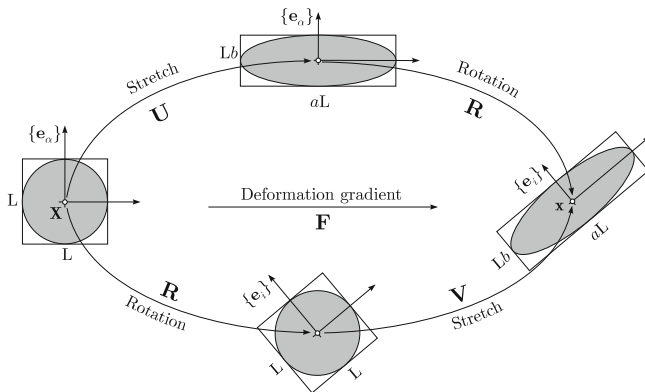


Fig. 4.2 Polar decomposition of the deformation gradient, interpreted as the compositional process of stretch followed by rotation or vice versa

$$\begin{aligned}
U^{-1} &= \sum_{\alpha} \left(\lambda_{\alpha}^{(U)} \right)^{-1} \mathbf{e}_{\alpha} \otimes \mathbf{e}_{\alpha}, \\
V^{-1} &= \sum_i \left(\lambda_i^{(V)} \right)^{-1} \mathbf{e}_i \otimes \mathbf{e}_i.
\end{aligned} \tag{4.27}$$

Thus, the first two points are verified.

With the right and left stretch tensors, we can now build orthogonal tensors $\mathbf{R} := \mathbf{F}U^{-1}$ and $\bar{\mathbf{R}} := V^{-1}\mathbf{F}$. The orthogonality follows from

$$\begin{aligned}
\mathbf{R}^T \mathbf{R} &= (\mathbf{F}U^{-1})^T (\mathbf{F}U^{-1}) = (U^{-T} \mathbf{F}^T) (\mathbf{F}U^{-1}) \\
&= U^{-T} (\mathbf{F}^T \mathbf{F}) U^{-1} = U^{-T} U^2 U^{-1} = \mathbf{I}, \\
\bar{\mathbf{R}} \bar{\mathbf{R}}^T &= (V^{-1} \mathbf{F}) (V^{-1} \mathbf{F})^T = (V^{-1} \mathbf{F}) (\mathbf{F}^T V^{-T}) \\
&= V^{-1} (\mathbf{F} \mathbf{F}^T) V^{-T} = V^{-1} V^2 V^{-T} = \mathbf{I}.
\end{aligned} \tag{4.28}$$

Therefore one has

$$\mathbf{F} = \mathbf{R}U = V\bar{\mathbf{R}}. \tag{4.29}$$

The uniqueness property of the polar decomposition follows from the fact that \mathbf{C} and \mathbf{B} are unique (via the spectral decomposition) according to their definition; thus, U and V are also uniquely defined. Since the deformation gradient \mathbf{F} is not singular, \mathbf{R} and $\bar{\mathbf{R}}$ are also unique.

In order to show $\mathbf{R} = \bar{\mathbf{R}}$, we use the orthogonality of \mathbf{R} and write

$$\begin{aligned}
\mathbf{F} &= \mathbf{R}U = \mathbf{R}U(\mathbf{R}^T \mathbf{R}) = (\mathbf{R}U\mathbf{R}^T) \mathbf{R} \\
&= \bar{\mathbf{V}} \mathbf{R} \\
&\stackrel{!}{=} V \bar{\mathbf{R}},
\end{aligned} \tag{4.30}$$

where $\bar{\mathbf{V}} := (\mathbf{R}U\mathbf{R}^T)$. As a result, one seemingly finds a further decomposition of \mathbf{F} for which $\mathbf{B} = V^2 = \bar{\mathbf{V}}^2$ is also valid. Because \mathbf{B} is unique so must also be V ; both these transformations must therefore be identical, i.e. $V = \bar{\mathbf{V}}$. Consequently, it immediately follows that $\mathbf{R} = \bar{\mathbf{R}}$.

We still need to corroborate the following statements:

- \mathbf{U} and \mathbf{V} have the same eigenvalues:

$$\lambda := \lambda^{(V)} = \lambda^{(U)} = \left(\lambda^{(B)} \right)^{\frac{1}{2}} = \left(\lambda^{(C)} \right)^{\frac{1}{2}} > 0. \quad (4.31)$$

Of these there are exactly three which may have different values.

- Eigenvectors $\mathbf{e}^{(V)}$ of \mathbf{V} and those of \mathbf{U} ($\mathbf{e}^{(U)}$) are related to each other through

$$\mathbf{e}^{(V)} = \mathbf{R} \mathbf{e}^{(U)}. \quad (4.32)$$

- The eigenvalue equation or *characteristic equation* of \mathbf{U} has the form

$$\lambda^3 - I_U \lambda^2 + II_U \lambda - III_U = 0, \quad (4.33)$$

where

$$I_U := \text{tr } \mathbf{U}, II_U := \frac{1}{2} (I_U^2 - I_{U^2}), III_U := \det \mathbf{U} \quad (4.34)$$

are the *principal invariants* of the tensor \mathbf{U} .

In order to prove the first expression, we start with the eigenvalue equation

$$(\mathbf{U} - \lambda^{(U)} \mathbf{I}) \mathbf{e}^{(U)} = \mathbf{0}, \quad (4.35)$$

which yields non-trivial solutions if $\det(\mathbf{U} - \lambda^{(U)} \mathbf{I}) = 0$. This is the *characteristic equation* of \mathbf{U} with which one can calculate the corresponding eigenvalues. If we further use the relation

$$\mathbf{U} = \mathbf{R}^T \mathbf{V} \mathbf{R}, \quad (4.36)$$

which follows directly from the polar decomposition, it reads

$$\begin{aligned} 0 &= \det(\mathbf{U} - \lambda^{(U)} \mathbf{I}) = \det(\mathbf{R}^T \mathbf{V} \mathbf{R} - \lambda^{(U)} \mathbf{I}) \\ &= \det(\mathbf{R}^T (\mathbf{V} - \lambda^{(U)} \mathbf{I}) \mathbf{R}) \\ &= \det \mathbf{R}^T \det(\mathbf{V} - \lambda^{(U)} \mathbf{I}) \det \mathbf{R} \\ \Rightarrow \quad \det(\mathbf{V} - \lambda^{(U)} \mathbf{I}) &= 0, \end{aligned} \quad (4.37)$$

since $\det \mathbf{R} = 1$. It follows from here that the eigenvalues of \mathbf{U} and \mathbf{V} are identical, $\lambda := \lambda^{(V)} = \lambda^{(U)}$. Because $\mathbf{U}^2 = \mathbf{C}$ and $\mathbf{V}^2 = \mathbf{B}$ and in view of their spectral decompositions, one also has $\lambda = (\lambda^{(C)})^{1/2} = (\lambda^{(B)})^{1/2}$. Thus the first point is proved.

Similarly, from the eigenvalue equation for \mathbf{U} one concludes

$$\begin{aligned}\mathbf{0} &= (\mathbf{U} - \lambda \mathbf{I}) \mathbf{e}^{(U)} = (\mathbf{R}^T \mathbf{V} \mathbf{R} - \lambda \mathbf{I}) \mathbf{e}^{(U)} \\ &= \mathbf{R}^T (\mathbf{V} - \lambda \mathbf{I}) \mathbf{R} \mathbf{e}^{(U)},\end{aligned}\quad (4.38)$$

or since \mathbf{R} is non-singular, after multiplication from left with \mathbf{R} ,

$$(\mathbf{V} - \lambda \mathbf{I}) \mathbf{R} \mathbf{e}^{(U)} = \mathbf{0}. \quad (4.39)$$

Thus, $\mathbf{R} \mathbf{e}^{(U)}$ is the eigenvector corresponding to the eigenvalue $\lambda = \lambda^{(V)}$; moreover, $\mathbf{e}^{(V)} = \mathbf{R} \mathbf{e}^{(U)}$, and thus the second point is likewise proved.

Finally, we can corroborate the characteristic equation (4.33) of a tensor \mathbf{U} , for example, by explicitly calculating $\det(\mathbf{U} - \lambda \mathbf{I}) = 0$. In case one chooses $\{\mathbf{e}^{(U)}\}$ as the basis, \mathbf{U} has diagonal form

$$\mathbf{U} = \begin{pmatrix} \lambda_1 & 0 & 0 \\ 0 & \lambda_2 & 0 \\ 0 & 0 & \lambda_3 \end{pmatrix}, \quad (4.40)$$

with the eigenvalues λ_α , $\alpha = 1, 2, 3$. From this we can immediately write the characteristic equation with *invariants* I_U , II_U and III_U , which are related to the eigenvalues as follows:

$$\begin{aligned}I_U &:= \text{tr } \mathbf{U} = \lambda_1 + \lambda_2 + \lambda_3, \\ II_U &:= \frac{1}{2} (I_U^2 - I_U^2) = \lambda_1 \lambda_2 + \lambda_2 \lambda_3 + \lambda_3 \lambda_1, \\ III_U &:= \det \mathbf{U} = \lambda_1 \lambda_2 \lambda_3, \text{ qed.}\end{aligned}\quad (4.41)$$

This completes the proof of the polar deposition theorem. ■

A geometric interpretation of the polar decomposition theorem follows from Fig. 4.2 and formula (4.18), which now takes the form

$$d\mathbf{x} = \mathbf{F} d\mathbf{X} = \mathbf{V} \mathbf{R} d\mathbf{X} = \mathbf{R} \mathbf{U} d\mathbf{X}. \quad (4.42)$$

Accordingly, a material line element $d\mathbf{X}$ may first be rotated by \mathbf{R} and subsequently stretched by \mathbf{V} , or it may first be stretched by \mathbf{U} and subsequently rotated by \mathbf{R} . Which of these mappings is first thought to be executed is not important, but it is physically obvious that the principal stretches on the one hand and the rotation on the other hand must be the same. This fact is expressed in the above proof by the fact that \mathbf{R} and $\bar{\mathbf{R}}$ are the same rotation matrices and the \mathbf{V} and \mathbf{U} possess the same eigenvalues.

This same property can also be stated in rate form. Indeed, differentiating (4.18) with respect to time, $d\dot{\mathbf{x}} = \dot{\mathbf{F}} d\mathbf{X}$, and using $\dot{\mathbf{F}} \mathbf{F}^{-1} = \mathbf{L}$ and $d\mathbf{X} = \mathbf{F}^{-1} d\mathbf{x}$ yields

$$d\dot{\mathbf{x}} = d\mathbf{v} = \mathbf{L} d\mathbf{x} = (\mathbf{D} + \mathbf{W}) d\mathbf{x}, \quad (4.43)$$

stating that the velocity increment at a point is composed of a stretching increment $\mathbf{D} \, d\mathbf{x}$ and a rotation increment $\mathbf{W} \, d\mathbf{x}$. It is interesting to observe that the product composition (4.42) valid for a finite deformation becomes an additive composition (4.43) when expressed in rate form.

The above results also give a direct interpretation for any vectorial physical quantity \mathbf{f} that obeys the equation

$$\frac{d\mathbf{f}}{dt} = \mathbf{L}\mathbf{f}, \quad \mathbf{f}(\mathbf{x}, t = 0) = \mathbf{f}_0. \quad (4.44)$$

It is easily shown that the solution of this initial value problem is given by

$$\mathbf{f} = \mathbf{F}\mathbf{f}_0 = \mathbf{R}\mathbf{U}\mathbf{f}_0. \quad (4.45)$$

Its interpretation is as follows: As time proceeds, the value of \mathbf{f} at time $t = 0$, \mathbf{f}_0 is stretched by \mathbf{U} and rotated by \mathbf{R} . We shall see that in a so-called barotropic fluid the specific vorticity $\boldsymbol{\omega}/\rho$ satisfies (4.44) and (4.45). Fluid dynamicists say that *vorticity is produced by vortex stretching and vortex tilting*.

Much more could be said about kinematics; however, with the above presentation a minimum amount of information is given that allows the deduction of the basic principles.

We close this subsection on kinematics by deriving a formula expressing the acceleration of a material point relative to two different bases, one at rest and assumed to be inertial, $\{\mathcal{O}, \hat{\mathbf{e}}_i\}$, and the other one moving, $\{\mathcal{O}^*, \hat{\mathbf{e}}_i^*\}$. Let \mathbf{r}_0 be the position vector of the origin of the moving base in the rest base $\overrightarrow{\mathcal{O}\mathcal{O}^*} = \mathbf{r}_0$, \mathbf{v}_0 its velocity and assume that the starred basis with origin \mathcal{O}^* rotates relative to the unstarred basis with angular velocity $\boldsymbol{\Omega}$, see Fig. 4.3. We shall refer to the unstarred and starred systems as the *absolute* and *relative* systems, respectively. If \mathbf{a} is a vector, then an absolute observer measures the time rate of change $d\mathbf{a}/dt$, while the relative observer sees this change of \mathbf{a} as $\delta\mathbf{a}/\delta t$; the two derivatives are related to one another by

$$\frac{d\mathbf{a}}{dt} = \frac{\delta\mathbf{a}}{\delta t} + \boldsymbol{\Omega} \times \mathbf{a}. \quad (4.46)$$

If \mathbf{a} is a vector that is fixed in the relative system, then $\delta\mathbf{a}/\delta t = \mathbf{0}$ and $d\mathbf{a}/dt = \boldsymbol{\Omega} \times \mathbf{a}$, which is immediately evident.⁸ Applying this rule to the position vector

$$\mathbf{x} = \mathbf{r}_0 + \mathbf{r} \quad (4.47)$$

⁸ For readers not familiar with kinematics this formula may still be difficult to grasp. However, if \mathbf{a} is fixed in the relative system and parallel to $\boldsymbol{\Omega}$, then $\boldsymbol{\Omega} \times \mathbf{a} = \mathbf{0}$. Indeed, in this case for an absolute observer, the vector \mathbf{a} changes only its position but not its orientation (Fig. 4.4a). On the other hand, if \mathbf{a} is perpendicular to $\boldsymbol{\Omega}$, then the absolute observer sees a change of \mathbf{a} in the plane perpendicular to $\boldsymbol{\Omega}$ and oriented perpendicular to \mathbf{a} (Fig. 4.4b), which is also geometrically obvious. The general case is shown in panel (c) of Fig. 4.4.

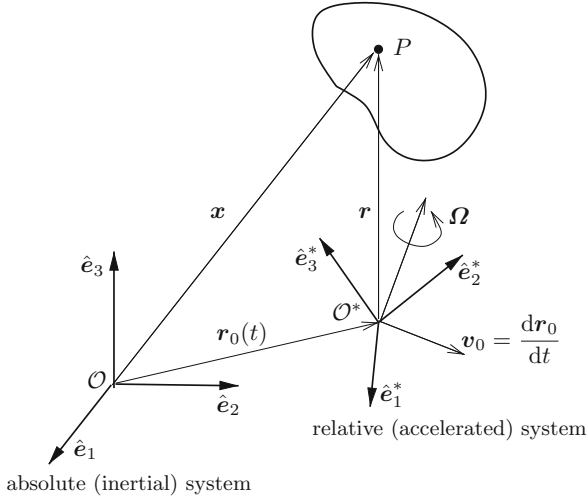


Fig. 4.3 Absolute (inertial) system $\{O, \hat{e}_i\}$ and, relative to it, relative (accelerated) system $\{O^*, \hat{e}_i^*\}$ with velocity dr_0/dt and angular velocity Ω

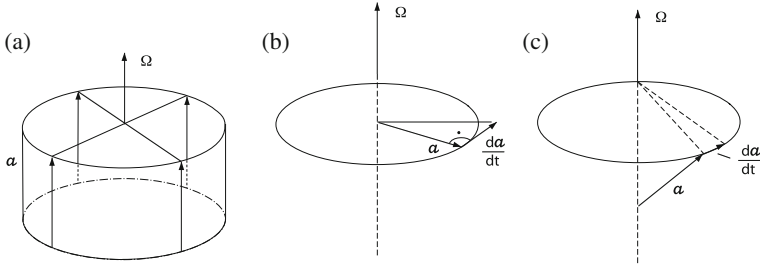


Fig. 4.4 To an absolute observer a vector a fixed in the relative system does not change if it is parallel to Ω (a), but rotates around the axis of Ω if it is not parallel to Ω (b) and (c)

yields

$$\frac{dx}{dt} = \frac{dr_0}{dt} + \Omega \times r + \frac{\delta r}{\delta t} \quad (4.48)$$

and

$$\begin{aligned} \frac{d^2x}{dt^2} &= \frac{d}{dt} \left(\frac{dr_0}{dt} + \Omega \times r + \frac{\delta r}{\delta t} \right) \\ &= \frac{d^2r_0}{dt^2} + \left(\frac{\delta}{\delta t} + \Omega \times \right) \left(\Omega \times r + \frac{\delta r}{\delta t} \right) \\ &= \frac{d^2r_0}{dt^2} + \frac{\delta^2 r}{\delta t^2} + 2\Omega \times \frac{\delta r}{\delta t} + \Omega \times (\Omega \times r) + \frac{\delta \Omega}{\delta t} \times r. \end{aligned} \quad (4.49)$$

This formula suggests the following definition:

Definition 4.5 *The various terms in (4.49) have the following denotations*

$\frac{d^2 \mathbf{x}}{dt^2}$	<i>absolute acceleration,</i>
$\frac{\delta^2 \mathbf{r}}{\delta t^2}$	<i>relative acceleration,</i>
$\frac{d^2 \mathbf{r}_0}{dt^2}$	<i>absolute acceleration of the origin \mathcal{O}^* of the moving system</i>
$2\boldsymbol{\Omega} \times \frac{\delta \mathbf{r}}{\delta t}$	<i>Coriolis acceleration, see Fig. 4.5</i>
$\boldsymbol{\Omega} \times (\boldsymbol{\Omega} \times \mathbf{r})$	<i>centripetal acceleration,</i>
$\frac{\delta \boldsymbol{\Omega}}{\delta t} \times \mathbf{r}$	<i>Euler acceleration,</i>
$\frac{\delta \mathbf{r}}{\delta t} = \mathbf{v}_r$	<i>relative velocity – velocity of a particle as recorded by the moving observer.</i>

■

In geophysical applications such as meteorology, physical oceanography and limnology, the absolute origin is identified by the centre of the Earth and the basis $\{\hat{\mathbf{e}}_i\}$ is given as a non-rotating system of axes in Fig. 2.3 denoted by 1, 2, 3. The relative system is fixed with the Earth with origin on the Earth surface and coordinate axes fixed with the Earth, usually the xy plane tangential to the Earth surface and the z -axis pointing towards the zenith. The Earth is approximated as a rigid sphere rotating with constant angular velocity $\boldsymbol{\Omega}$ about its axis connecting the south with the north pole. Thus, the absolute acceleration of the relative coordinate system equals $d^2 \mathbf{r}_0 / dt^2 = \boldsymbol{\Omega} \times (\boldsymbol{\Omega} \times \mathbf{r}_0)$ and the Euler acceleration vanishes. It follows that for the chosen Earth-fixed coordinate system the absolute acceleration takes the form

$$\frac{d^2 \mathbf{x}}{dt} = \frac{\delta^2 \mathbf{r}}{\delta t^2} + \boldsymbol{\Omega} \times (\boldsymbol{\Omega} \times (\mathbf{r}_0 + \mathbf{r})) + 2\boldsymbol{\Omega} \times \frac{\delta \mathbf{r}}{\delta t}. \quad (4.50)$$

Because in this book the observer consistently moves with the Earth, we shall denote

$$\begin{aligned} \frac{\delta \mathbf{r}}{\delta t} &= \mathbf{v}(\mathbf{x}, t), \\ \frac{\delta^2 \mathbf{r}}{\delta t^2} &= \frac{d\mathbf{v}(\mathbf{x}, t)}{dt} = \frac{\partial \mathbf{v}(\mathbf{x}, t)}{\partial t} + (\text{grad } \mathbf{v}(\mathbf{x}, t)) \mathbf{v}(\mathbf{x}, t) \end{aligned} \quad (4.51)$$

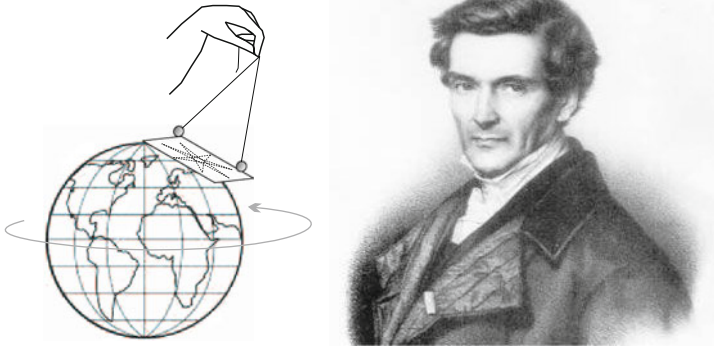


Fig. 4.5 Gaspard-Gustave de CORIOLIS (1792–1843), a French mathematician, mechanical engineer and scientist (photo from <http://en.wikipedia.org/>). A sketch of the FOUCAULT pendulum (left) is the most explicit demonstration of action of the CORIOLIS force

Gaspard-Gustave de CORIOLIS (21 May 1792 – 19 September 1843) was born in Paris. In 1816 he became a tutor at the École Polytechnique, in 1829 a professor of mechanics at the École Centrale des Arts et Manufactures. Upon the death of NAVIER in 1836, CORIOLIS succeeded him in the chair of applied mechanics at the École des Ponts and Chaussées and to NAVIER's place in the Académie des Sciences. In 1838 he succeeded DULONG as *Directeur des études* (director of studies) in the École Polytechnique. He died in 1843 at the age of 51 in Paris.

CORIOLIS is best known for his work on the supplementary forces that are detected in a rotating frame of reference, and one of those forces nowadays bears his name. In 1835, he published the paper that made his name famous, *Sur les équations du mouvement relatif des systèmes de corps* (*On the Equations of Relative Motion of a System of Bodies*). He showed that the laws of motion could be used in a rotating frame of reference if an extra term called the CORIOLIS acceleration is added to the equations of motion. It deals with the transfer of energy in rotating systems like waterwheels. CORIOLIS discussed the supplementary forces that are detected in a rotating frame of reference, and one of them would eventually bear his name. The term 'CORIOLIS force' was, however, not used until the beginning of the 20th century. Today, the name CORIOLIS has become strongly associated with geophysical fluid dynamics.

CORIOLIS was the first to coin the term 'work' for the transfer of energy by a force acting through a distance. In 1829 he published a textbook *Calcul de l'Effet des Machines* (*Calculation of the Effect of Machines*). In this period the correct expression for kinetic energy, $\frac{1}{2}v^2$, and its relation to mechanical work became established. CORIOLIS worked to extend the notion of kinetic energy and work to rotating systems. His first paper, *Sur le principe des forces vives dans les mouvements relatifs des machines* (*On the Principle of Kinetic Energy in the Relative Motion in Machines*), was read to the Académie des Sciences. In 1835 he published a mathematical memoir on collisions of spheres: *Théorie Mathématique des Effets du Jeu de Billard*, considered a classic on the subject.

The text is based on: <http://en.wikipedia.org/>

so that

$$\underbrace{\frac{d^2\mathbf{x}}{dt^2}}_{\text{absolute acceleration}} = \underbrace{\frac{d\mathbf{v}}{dt}}_{\text{relative acceleration}} + \underbrace{\boldsymbol{\Omega} \times (\boldsymbol{\Omega} \times (\mathbf{r}_0 + \mathbf{r}))}_{\text{centripetal acceleration}} + \underbrace{2\boldsymbol{\Omega} \times \mathbf{v}}_{\text{Coriolis acceleration}}. \quad (4.52)$$

Problem 4.2 *Show that for a frame fixed on the Earth*

- the centripetal acceleration is numerically larger than the Coriolis acceleration;⁹ in fact
 - centripetal acceleration $\sim 2.4 \times 10^{-2} \text{ (m s}^{-2}\text{)}$ for a location with the geographical latitude of 45° ,
 - Coriolis acceleration $\sim 1.5 \times 10^{-5} \text{ (m s}^{-2}\text{)}$ for a typical water velocity of 0.1 m s^{-1} in lakes;
- the centripetal acceleration is a vector directed at each point towards the axis of rotation with magnitude $|\boldsymbol{\Omega}|^2 r$ (see Fig. 4.6),
- the centripetal acceleration can be derived from a potential as follows:

$$\boldsymbol{\Omega} \times (\boldsymbol{\Omega} \times (\mathbf{r}_0 + \mathbf{r})) = -\text{grad } \Psi, \quad \Psi = \frac{|\boldsymbol{\Omega}|^2 r^2}{2}, \quad (4.53)$$

- it is customary to regard the centripetal acceleration as part of the gravity vector. Convince yourself that common gravimetric measurements indeed include this acceleration beyond the NEWTONian gravity force.¹⁰ So, instead of (4.52), geophysical fluid dynamicists often use

$$\frac{d^2 \mathbf{x}}{dt^2} = \frac{d\mathbf{v}}{dt} + 2\boldsymbol{\Omega} \times \mathbf{v} \quad (4.54)$$

as the expression of acceleration of material particles referred to an Earth-fixed coordinate system. \blacklozenge

⁹ In the rotating framework, the two acceleration terms can be interpreted as the results of the action of two forces – the centrifugal force and the CORIOLIS force. Although the former is the more palpable of the two, it plays no role in geophysical flows, however surprising this may be to the neophyte. The latter and less intuitive of the two turns out to be a crucial factor in geophysical motions.

¹⁰ In the absence of rotation, gravitational forces keep the matter together to form a spherical body. The outward pull caused by the centrifugal force distorts this spherical equilibrium, and the planet assumes a slightly flattened shape. The degree of flattening is precisely that necessary to keep the planet in equilibrium for its rotation rate. The centrifugal force is directed outwards, perpendicular to the axis of rotation, whereas the gravitational force points towards the planet's centre. The resulting force assumes an intermediate direction, and this direction is precisely the direction of the local vertical. Indeed, under this condition a loose particle has no tendency of its own to fly away from the planet. In other words, every particle at rest on the surface will remain at rest unless it is subjected to additional forces. The flattening of the Earth, as well as that of other celestial bodies in rotation, is important to neutralise the centrifugal force. But this is not to say that it greatly distorts the geometry. On the Earth, for example, the distortion is very slight, because gravity by far exceeds the centrifugal force; the terrestrial equatorial radius is 6378 km, slightly greater than its polar radius of 6357 km. The shape of the rotating oblate Earth is treated in detail by STOMMEL and MOORE [13]. For the sake of simplicity in all that follows, we will call the gravitational force the resultant force, aligned with the vertical and equal to the sum of the true gravitational force plus the centrifugal force.

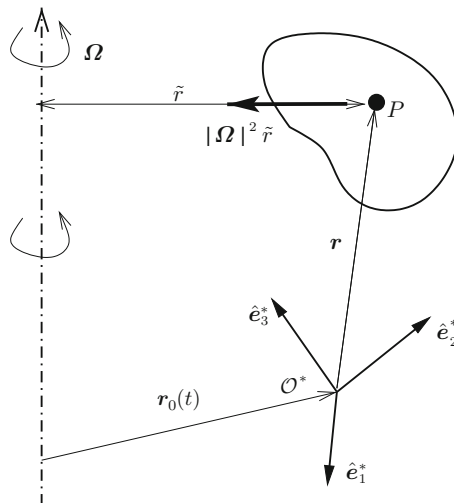


Fig. 4.6 Centripetal acceleration in a rotating coordinate system, directed at each point towards the axis of rotation with magnitude $|\Omega|^2 \tilde{r}$

4.2 Balance of Mass

As seen in Chap. 3, the mass of a material body is a conserved quantity, i.e. no mass within the body is produced nor does there any mass flow through the boundary of a material body. Let us think a body to be made of an infinite number of material volume elements $dV = dx_1 dx_2 dx_3$, and let us isolate such a volume element. If the actions of the surroundings of this element on it are duly accounted for, then we may treat the element as a body by itself and apply the dynamical equations (i.e. the mass, momentum and energy balances) to this element. This principle, expressing that *any part of a body is itself a body*, is so intuitive and appears to be so natural that most scientists apply it subconsciously and never mention it. However, one of its basis is the *continuity assumption of matter*, according to which mass is continuously distributed, and so it makes sense to define a *mass density*

$$\rho := \lim_{\Delta V \rightarrow 0} \frac{\Delta m}{\Delta V}, \quad (4.55)$$

which is the limit of the mass of a small volume element when its volume tends to zero. We all know that, strictly, this continuity assumption of matter does not hold, but the length scales over which it is violated are so small to be of no concern in geophysical applications¹¹ such as lake physics.

¹¹ An obvious manifestation where the continuity assumption is violated or its application overstretched is BROWNIAN motion. The shivering motion of the molecules is visible under the microscope. It is clearly the manifestation of the discrete structure of matter.

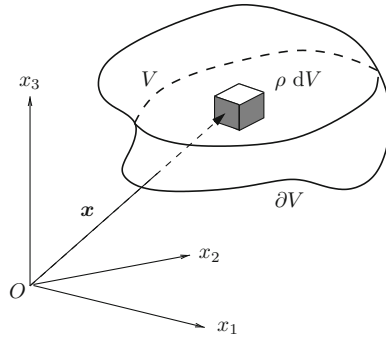


Fig. 4.7 Material body V with boundary ∂V . A volume element dV is isolated at position \mathbf{x}

With this continuity requirement one may write the mass of a body with volume V as the sum of the masses of the volume elements (see Fig. 4.7), viz.

$$\mathcal{M}_V = \iiint_V \rho(x_1, x_2, x_3, t) dx_1 dx_2 dx_3 \stackrel{(*)}{=} \int_V \rho dV. \quad (4.56)$$

Here, the summation is simply the volume integration of the function $\rho(x_1, x_2, x_3, t)$ over the three coordinates of the Cartesian coordinate system, and it is symbolically expressed as a triple integral. Since such a notation is heavy and actually not needed, if computations are not explicitly performed, the step $\stackrel{(*)}{=}$ indicates the abbreviated notation that is simple and uniquely understandable. Balance of mass for a material volume (3.2) states that

$$\dot{\mathcal{M}}_V = \frac{d\mathcal{M}_V}{dt} = \frac{d}{dt} \int_V \rho dV = 0, \quad (4.57)$$

where the volume V in (4.57) moves with the body as time proceeds.

There is *another way of formulating the law of conservation of mass* if instead of a material volume a *fixed* volume in three-dimensional space is considered. This is simply a spatial volume, and mass in this volume may grow according to (see Fig. 4.8)

$$\int_{V_{\text{fix}}} \frac{\partial \rho}{\partial t}(\mathbf{x}, t) dV. \quad (4.58)$$

Here we have identified the volume by the index $(\)_{\text{fix}}$ to emphasise that this volume always consists of the same spatial points. The growth of mass (4.58) within V_{fix} is due to the mass flux through the surface ∂V_{fix} . The flow through the surface element dA is given by $\rho(\mathbf{v} \cdot \mathbf{n})dA$, where \mathbf{v} is the EULERian velocity field and \mathbf{n} is the unit normal vector at the surface element pointing to the exterior of the body. Summing over the entire boundary surface yields

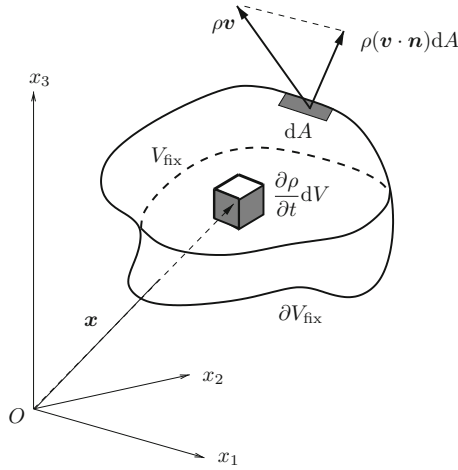


Fig. 4.8 Spatial volume V_{fix} with boundary ∂V_{fix} , indicating the growth of mass at an incremental volume element $(\partial \rho / \partial t) dV_{\text{fix}}$ as well as showing the flow of mass $\rho(\mathbf{v} \cdot \mathbf{n}) dA$ on a surface element dA with exterior unit normal vector \mathbf{n}

$$- \int_{\partial V_{\text{fix}}} \rho(\mathbf{v} \cdot \mathbf{n}) dA \quad (4.59)$$

as the total mass flux through the boundary ∂V_{fix} into the volume. Because for positive $\mathbf{v} \cdot \mathbf{n}$ this is a mass loss for the volume V_{fix} , the negative sign is inserted in (4.59). The alternative form of the mass balance (4.57) is therefore written as

$$\int_{V_{\text{fix}}} \frac{\partial \rho}{\partial t}(\mathbf{x}, t) dV = - \int_{\partial V_{\text{fix}}} \rho(\mathbf{v} \cdot \mathbf{n}) dA \quad (4.60)$$

or alternatively as

$$\dot{\mathcal{M}}_V = \int_{V_{\text{fix}}} \frac{\partial \rho}{\partial t} dV + \int_{\partial V_{\text{fix}}} \rho(\mathbf{v} \cdot \mathbf{n}) dA = 0. \quad (4.61)$$

Comparing (4.57) and (4.61) yields the formula

$$\frac{d}{dt} \int_V \rho dV = \int_{V_{\text{fix}}} \frac{\partial \rho}{\partial t} dV + \int_{\partial V_{\text{fix}}} \rho(\mathbf{v} \cdot \mathbf{n}) dA, \quad (4.62)$$

in which V is the material volume which momentarily occupies the same positions as V_{fix} so that actually $V = V_{\text{fix}}$.

The above formula (4.62) can be used to state a very important mathematical lemma, because it is valid for any function f . More precisely, it is no longer of relevance that the quantity ρ represents the mass density. It can in fact be any differentiable function $f(\mathbf{x}, t)$. So rewriting (4.62) in this form yields

$$\frac{d}{dt} \int_V f dV = \int_{V_{\text{fix}}} \frac{\partial f}{\partial t} dV + \int_{\partial V_{\text{fix}}} f(\mathbf{v} \cdot \mathbf{n}) dA. \quad (4.63)$$

This formula tells us how an integral over a material volume is differentiated with respect to time. The function f can be a scalar or any component of a vector so that (4.63) is valid also for a vector-valued function. In this form (4.63) is called REYNOLDS' *transport theorem*. It will be used later to derive local forms of the balances of momenta and energy.¹²

So far, and in Chap. 3, the concept of the balance law was formulated for a body as a whole. It was, however, already mentioned that any material part of a body cut out of it (in reality or imagination) is equally a body no matter how large or small it may be. More precisely, it is tacitly assumed or postulated that the physical laws, balances of mass, momenta, energy and entropy hold for any body part. If such a part is an infinitesimally small cube and the mathematical transformations are performed such that in the limit as the cube's volume tends to zero, the point form of the balance law emerges. This point form is also called *local balance law*. This will now be derived for the balance law of mass.¹³ So let us now use (4.60) for an infinitesimally small cube with side lengths dx_1, dx_2, dx_3 parallel to the coordinate axes, see Fig. 4.9a. The left-hand side of (4.60) is then simply given by

$$\int_{\text{cube}} \frac{\partial \rho}{\partial t} dV_{\text{cube}} = \frac{\partial \rho}{\partial t} dx_1 dx_2 dx_3, \quad (4.64)$$

in which \mathbf{x} is a point in the interior of the cube. Let us now concentrate on the right-hand side of (4.60). For an infinitesimal cube this surface integral constitutes the sum of corresponding expressions evaluated over the six surface elements bounding the cube. Consider first the two rectangular faces perpendicular to the x_1 -axis. The integrand function $\rho(\mathbf{v} \cdot \mathbf{n})$ is simply given here by $-(\rho v_1)(\bar{\mathbf{x}}, t)$, where $\bar{\mathbf{x}}$ is a point within the front surface element of Fig. 4.9b with area $dx_2 dx_3$, and the flow is into the cube for a positive v_1 component. On the opposite side of the cube, $\rho(\mathbf{v} \cdot \mathbf{n})$ is given by the same expression $(\rho v_1)(\bar{\mathbf{x}} + dx_1 \hat{\mathbf{e}}_1, t)$, but it is now evaluated for a point within its own surface. According to (2.34) an approximation of this is

¹² This is the first place where a physical law has led us to a mathematical lemma. We will encounter this situation again in this chapter when physical reasoning will allow us to come up with GAUSS' divergence theorem and a variant of it.

¹³ We apply in this chapter the balance laws of classical physics to *infinitesimal cubes* to derive their local form. This appears to be a bit primitive; especially since in Chap. 2 the formulation of the mathematical analysis was laid down to do this more elegantly. We do this because of didactic reasons and take the risk to be accused to be unnecessarily primitive. For less-trained students the 'volume element method' is easier to understand. More important for us is, however, the fact that the reader can openly follow how all quantities arising in the mass, momentum, energy and entropy balance laws are expressed in the 'volume element method'. We believe that the physics becomes this way particularly transparent, even though formulae evidently appear somewhat clumsy.

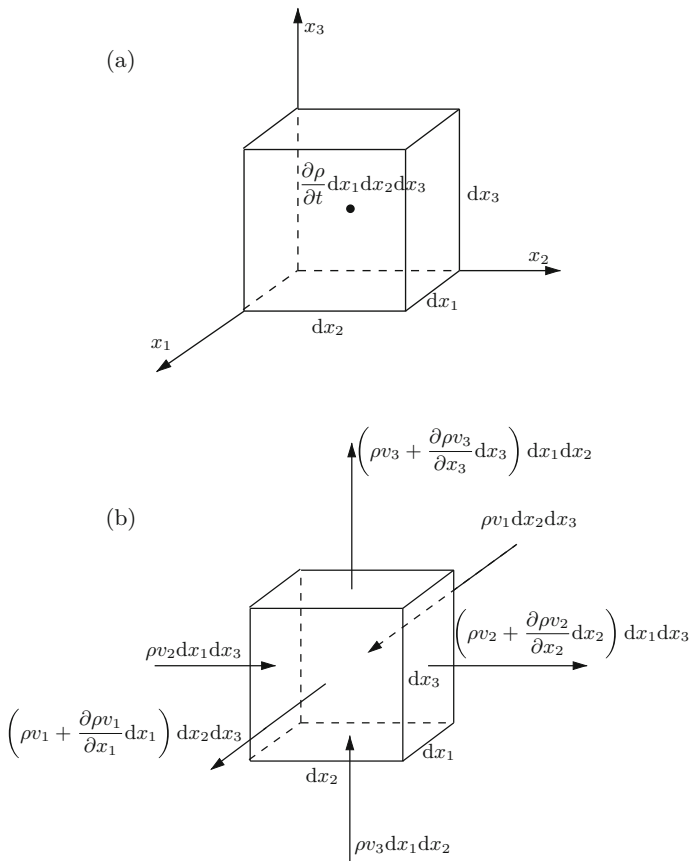


Fig. 4.9 (a) Infinitesimal cube fixed in space with side faces perpendicular to the (mutually orthogonal) coordinate axes x_1, x_2, x_3 , respectively, of a Cartesian coordinate system and side lengths dx_1, dx_2, dx_3 showing the growth of mass within it. (b) Mass flow through the surface elements of the same cube

$$(\rho v_1)(\bar{\mathbf{x}} + dx_1 \hat{\mathbf{e}}_1, t) \simeq (\rho v_1)(\bar{\mathbf{x}}, t) + \frac{\partial(\rho v_1)}{\partial x_1}(\bar{\mathbf{x}}, t) dx_1$$

so that $\rho \mathbf{v} \cdot \mathbf{n}$ in the three space directions is given by

$$\begin{aligned} -(\rho v_1)(\bar{\mathbf{x}}, t) + (\rho v_1)(\bar{\mathbf{x}} + dx_1 \hat{\mathbf{e}}_1, t) &= \frac{\partial(\rho v_1)}{\partial x_1}(\bar{\mathbf{x}}, t) dx_1, \\ -(\rho v_2)(\bar{\mathbf{x}}, t) + (\rho v_2)(\bar{\mathbf{x}} + dx_2 \hat{\mathbf{e}}_2, t) &= \frac{\partial(\rho v_2)}{\partial x_2}(\bar{\mathbf{x}}, t) dx_2, \\ -(\rho v_3)(\bar{\mathbf{x}}, t) + (\rho v_3)(\bar{\mathbf{x}} + dx_3 \hat{\mathbf{e}}_3, t) &= \frac{\partial(\rho v_3)}{\partial x_3}(\bar{\mathbf{x}}, t) dx_3, \end{aligned} \quad (4.65)$$

in which errors are $\mathcal{O}[(dx_1)^2, (dx_2)^2, (dx_3)^2]$. The mass flow through the cube's faces is obtained by multiplying the above expressions with the area increments $dx_2 dx_3$, $dx_3 dx_1$ and $dx_1 dx_2$, respectively, as shown in panel (b) of Fig. 4.9 so that

$$\begin{aligned} - \int_{\partial \text{cube}} \rho(\mathbf{v} \cdot \mathbf{n}) dA &= - \left\{ \frac{\partial \rho v_1}{\partial x_1} + \frac{\partial \rho v_2}{\partial x_2} + \frac{\partial \rho v_3}{\partial x_3} \right\} (dx_1 dx_2 dx_3)_{\text{cube}} \\ &= - \left\{ \frac{\partial \rho v_1}{\partial x_1} + \frac{\partial \rho v_2}{\partial x_2} + \frac{\partial \rho v_3}{\partial x_3} \right\} dV_{\text{cube}}. \end{aligned} \quad (4.66)$$

Thus, writing (4.60) down for the chosen infinitesimal cube yields, according to (4.64) and (4.66), after division by $dx_1 dx_2 dx_3$, the so-called *local balance law of mass*

$$\frac{\partial \rho}{\partial t} + \underbrace{\frac{\partial}{\partial x_1} (\rho v_1) + \frac{\partial}{\partial x_2} (\rho v_2) + \frac{\partial}{\partial x_3} (\rho v_3)}_{\text{div}(\rho \mathbf{v}) [\text{see (2.62)}]} = 0, \quad (4.67)$$

which symbolically may also be written as

$$\frac{d\rho}{dt} + \text{div}(\rho \mathbf{v}) = 0. \quad (4.68)$$

If in the last three expressions of (4.67) the product differentiation is explicitly executed, then one obtains

$$\underbrace{\frac{\partial \rho}{\partial t} + \frac{\partial \rho}{\partial x_1} v_1 + \frac{\partial \rho}{\partial x_2} v_2 + \frac{\partial \rho}{\partial x_3} v_3}_{\text{d}\rho/\text{d}t [\text{see (4.6)}]} + \rho \underbrace{\left\{ \frac{\partial v_1}{\partial x_1} + \frac{\partial v_2}{\partial x_2} + \frac{\partial v_3}{\partial x_3} \right\}}_{\text{div } \mathbf{v}} = 0. \quad (4.69)$$

In this equation we have indicated with braces how the various terms, which are written in their first line in Cartesian component form, can be expressed symbolically, and we have listed the reference equation number where the connection between symbolic and Cartesian notations has been introduced. Thus, the local form of the balance law of mass can also be written in the form

$$\frac{d\rho}{dt} + \rho \text{div } \mathbf{v} = 0. \quad (4.70)$$

We now have two different versions of the local balance law of mass, namely (4.68) and (4.70), and both allow significant inferences. They hold for arbitrary continuous bodies, be they compressible or not. Two different classes of processes are defined as follows:

Definition 4.6

- A process for which $\partial\rho/\partial t = 0$ for a non-vanishing time interval is said to have **steady density** during this time interval.
- A process for which $d\rho/dt = 0$ for a non-vanishing time interval is called a **density-preserving process**. ■

As seen from (4.68) and (4.70) this definition implies the following inferences:

- (1) For a steady process the specific mass flux or the specific momentum $\rho\mathbf{v}$ is *divergence free* or *solenoidal*

$$\operatorname{div}(\rho\mathbf{v}) = 0. \quad (4.71)$$

- (2) For a density-preserving process the velocity field is solenoidal

$$\operatorname{div} \mathbf{v} = 0. \quad (4.72)$$

This equation is often called the *continuity equation*.

There are a few subtleties which we wish to emphasise here, because sloppiness in the use of terminology has led and is still leading to confusion in this regard. The above definition speaks of *processes*. One may, alternatively, call a *material* to be density preserving, which would mean that the density of a material particle does not change with time. This then means that the density is only a function of the material particles, $\rho = \hat{\rho}(X)$, and once the particle is identified, its density remains constant as it is followed along its trajectory. Riding in imagination on this particle, no change in density is felt. The density-preserving property of a material is a constitutive assumption, and if it holds, the velocity field is necessarily solenoidal, i.e. divergence free [see (4.72)]. Now, tracing back the calculation which led from (4.60) to (4.68), it is seen that we have demonstrated that

$$\int_{\partial V_{\text{fix}}} \rho(\mathbf{v} \cdot \mathbf{n}) dA = \int_{V_{\text{fix}}} \operatorname{div}(\rho\mathbf{v}) dV. \quad (4.73)$$

This identity holds for any differentiable vector-valued function \mathbf{f} , not just $\rho\mathbf{v}$, and then corresponds to the divergence theorem.

Theorem 4.1 Divergence theorem (GAUSS theorem, for a biographical sketch, see Fig. 4.10) *Let \mathbf{f} be a differentiable vector-valued function. Then*

$$\int_{\partial V_{\text{fix}}} \mathbf{f} \cdot \mathbf{n} dA = \int_{V_{\text{fix}}} (\operatorname{div} \mathbf{f}) dV \quad (4.74)$$

where V_{fix} , ∂V_{fix} may also be replaced by V , ∂V . ⊗

This important theorem has been the basis of Chap. 2, Sect. 2.5 for the integral theorems of vector analysis. Here considerations of mass balance and assumptions

of differentiability of the integrand field have been sufficient to prove its validity. We think this is an elegant method of its derivation.

For a density-preserving fluid, ρ may be cancelled in (4.73) so that

$$\int_{\partial V_{\text{fix}}} \mathbf{v} \cdot \mathbf{n} \, dA = \int_{V_{\text{fix}}} \text{div } \mathbf{v} \, dV \stackrel{!}{=} 0, \quad (4.75)$$

which owing to (4.72) must vanish. However, this simply states that the flow of fluid volume into and out of the volume V_{fix} through the boundary is zero, or the volume does not change (Fig. 4.10).

Definition 4.7 *A material of which the volume does not change no matter how small or large the volume may be and how it may be deformed is called **volume preserving**.* ■

It follows: *A density-preserving process or a density-preserving material is at the same time volume preserving.* Another technical term for volume preserving is *isochoric*, so volume-preserving motions are also called *isochoric*.

The reader who is familiar with these concepts may have realised that the use of the term ‘incompressible’ was carefully avoided. The common literature employs in general the term incompressible when density preserving or volume preserving is meant. Here, we wish to reserve this term to a specialisation the explanation of which requires a somewhat lengthier introduction.

It is well known that the density of water varies with temperature, pressure, mineral composition (salinity) and possibly suspended material. Specialists have taken great care in measuring all these dependencies to great accuracy. So one may assume that functions of the form

$$\rho = \hat{\rho}(T, s, p, \dots) \quad (4.76)$$

are known; here T, s, p are temperature, salinity and pressure and the dots indicate other possible variables.

Definition 4.8 *An equation of the form (4.76) is called the **equation of state** or **thermal equation of state**. An equation of state of the form*

$$\hat{\rho}(T, s, p, \dots) = \text{constant}$$

defines a density-preserving material. ■

With the introduction of the equation of state, the property of incompressibility, how we use it, can now be defined.

Definition 4.9 *A material is called **incompressible** if the thermal equation of state does not depend on the pressure explicitly*



Fig. 4.10 *Left:* Augustin-Louis CAUCHY around 1840. Lithography of Zéphirin BELLIARD after a painting by Jean ROLLER. *Right:* GAUSS' portrait published in *Astronomische Nachrichten* 1828 (from <http://en.wikipedia.org/>)

Baron Augustin-Louis CAUCHY (21 August 1789 – 23 May 1857) was a French mathematician who was an early pioneer of analysis. He started the project of formulating and proving the theorems of infinitesimal calculus in a rigorous manner. He also gave several important theorems in complex analysis and initiated the study of permutation groups in abstract algebra. Among approximately 800 research articles and five complete textbooks, there are works on symmetric functions, symmetry groups and the theory of higher order algebraic equations, the proof of FERMAT's polygonal number theorem and papers on celestial mechanics. He invented the name for the determinant, systematised its study, gave definitions of limit, continuity and convergence and founded complex analysis by discovering the CAUCHY-RIEMANN equations. He presented a mathematical treatment of optics, hypothesised that ether had the mechanical properties of an elastic medium and published classical papers on wave propagation in liquids and isotropic and anisotropic elastic media. Between 1830 and 1839 CAUCHY published three versions of treatises in elasticity. He was a man of strong convictions and a devout Catholic.

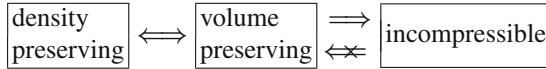
Johann Carl Friedrich GAUSS (30 April 1777 – 23 February 1855) was a German mathematician and scientist who contributed significantly to number theory, statistics, analysis, differential geometry, geodesy, geophysics, electrostatics, astronomy and optics. Gauss was a child prodigy and he made his first ground-breaking mathematical discoveries while still a teenager. He completed *Disquisitiones Arithmeticae*, his magnum opus, in 1798 at the age of 21. He discovered a construction of the heptadecagon and invented modular arithmetic, greatly simplifying manipulations in number theory. GAUSS proved the fundamental theorem of algebra which states that every non-constant single-variable polynomial over the complex numbers has at least one root. In 1831 GAUSS developed a fruitful collaboration with the physicist Wilhelm WEBER, leading to new knowledge in magnetism (including finding a representation for the unit of magnetism in terms of mass, length and time) and the discovery of KIRCHHOFF's circuit laws in electricity. He developed a method of measuring the horizontal intensity of the magnetic field which has been in use well into the second half of the 20th century and worked out the mathematical theory for separating the inner and outer sources of the Earth's magnetic field.

The text is partly based on <http://scienceworld.wolfram.com/> and <http://en.wikipedia.org/>

$$\frac{\partial \hat{\rho}}{\partial p}(T, s, p, \dots) = 0 \implies \rho = \hat{\rho}(T, s, \dots). \quad (4.77)$$

■

This definition makes a density- or a volume-preserving material automatically incompressible, but not vice versa:



Natural water is a material that is in general neither incompressible nor density preserving, but it is in most applications *nearly incompressible* and *nearly density preserving*. (In oceanography and limnology ρ varies seldom by more than 2%.) This is another reason why often confusion arises. In this context the definition of a *Boussinesq fluid* is helpful.

Definition 4.10 *A fluid is called a BOUSSINESQ fluid if the density is treated everywhere as a material constant except in the gravity force, where it is given by the equation of state.* ■

According to this definition the balance of mass (4.70) for a BOUSSINESQ fluid reduces to (4.72) so that the velocity field is requested to be solenoidal and the motion necessarily isochoric. This is an approximation that kinematically corresponds to density or volume preserving but accounts via the equation of state for variations of the density in the gravity (buoyancy) force. Within this BOUSSINESQ approximation the assumption of incompressibility can be incorporated by introducing an equation of state which does not depend on pressure, e.g. $\rho = \rho(T)$.

The BOUSSINESQ fluid is a very popular approximation and has therefore been thoroughly studied, including its rigorous mathematical derivation by an asymptotic analysis, see, e.g., [6]. It is applicable to all those situations for which acoustic wave phenomena can be ignored. Indeed, it is straightforward to prove that a BOUSSINESQ fluid does not permit longitudinal waves to be propagated, while the propagation of transverse waves is preserved.

Finally we mention that in most applications the pressure dependence of the equation of state is ignored. For very deep freshwater lakes such as Lake Baikal, this is not justified; so the BOUSSINESQ assumption cannot be maintained and the mass balance must in this case take the form (4.70).

Problem 4.3 *Consider a density-preserving or BOUSSINESQ fluid for which the velocity field $\mathbf{v}(\mathbf{x}, t)$ is solenoidal: $\operatorname{div} \mathbf{v} = 0$. Assume that $\mathbf{v} = \mathbf{V}_0 \exp[i(\mathbf{k} \cdot \mathbf{x} - \omega t)]$ is a plane harmonic wave with wavenumber \mathbf{k} and constant amplitude \mathbf{V}_0 . Show that such a harmonic wave propagates in the direction of \mathbf{k} and prove that \mathbf{V}_0 is necessarily perpendicular to \mathbf{k} : $\mathbf{V}_0 \cdot \mathbf{k} = 0$. Therefore the velocity field has vanishing component in the direction of \mathbf{k} – there are no longitudinal velocity components. The velocity field is necessarily transverse.* ♦

Remark: Acoustic waves are *longitudinal* waves. Therefore, sound waves can not be modelled with a BOUSSINESQ or a density-preserving fluid. Waves in a BOUSSINESQ fluid are necessarily *transverse* waves.

4.3 Balances of Momentum and Moment of Momentum, Concept of Stress, Hydrostatics

As seen in Chap. 3, the momentum equation applied to a body is a balance equation in which the time rate of change of the momentum of a body equals the sum of the forces acting on the body, see (3.3). If we think of the body to be made of an infinite number of material volume elements, as already done for the mass balance equation, then the momentum of the body may be written as the sum of all momenta of the mass elements with volume dV

$$\mathcal{P}_V = \iiint_V \rho(x_1, x_2, x_3) \mathbf{v}(x_1, x_2, x_3) dx_1 dx_2 dx_3 = \int_V \rho \mathbf{v} dV. \quad (4.78)$$

Similarly, the force \mathcal{K}_V acting on the body is the sum of all volume forces acting on the elements with volume dV . These volume forces are in almost all applications the gravity forces and written as

$$\mathcal{K}_V = \int_V \rho \mathbf{g} dV, \quad (4.79)$$

in which \mathbf{g} is the vector of the Earth's acceleration (and in the coordinate system of Fig. 2.3 given by $\mathbf{g} \hat{=} (0, 0, -g)$, where $g \simeq 9.81 \text{ m s}^{-2}$), see Fig. 4.11.

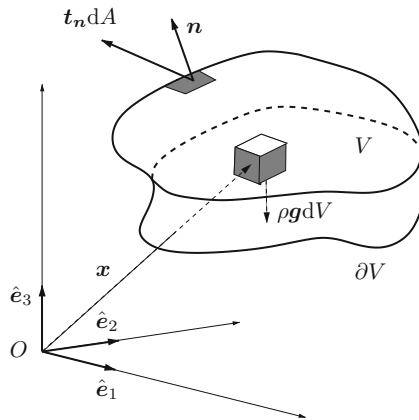


Fig. 4.11 Material volume V with boundary ∂V showing a volume element with its volume force $\rho \mathbf{g} dV$ and a surface force (traction) $\mathbf{t}_n dA$ on the surface element with exterior unit normal vector \mathbf{n}

The other types of forces that act on a body are its surface forces $\mathcal{K}_{\partial V}$. These forces can be understood if we recall the principle that any part of a body is itself a body. We cannot define a body in reality without isolating it in imagination from its surroundings. Indeed, if we speak of a lake, we isolate it from its neighbourhood by defining its free surface as part of the boundary with the atmosphere and the bottom surface as part of the boundary with the solid earth. River inlets and outlets may be other parts. The surface forces $\mathcal{K}_{\partial V}$ are the sum of all forces acting at the boundary ∂V ; at the free surface these are the atmospheric pressure and the wind stress, and at the bottom the normal pressure and the shear stresses due to the water motion.¹⁴ If the surface force per unit area of a surface increment with unit normal vector \mathbf{n} exterior to the body is denoted by \mathbf{t}_n , then

$$\mathcal{K}_{\partial V} = \int_{\partial V} \mathbf{t}_n \, dA \quad (4.80)$$

is the total surface force acting on the body.

Definition 4.11 *By definition, \mathbf{t}_n is a force per unit area, and since forces are vectors, \mathbf{t}_n is called **stress vector** at the surface element with unit normal vector \mathbf{n} or **traction vector**.* ■

The equation of motion (3.3) may now be written as follows:

$$\frac{d\mathcal{P}_V}{dt} = \mathcal{K}_{\partial V} + \mathcal{K}_V, \quad (4.81)$$

or

$$\frac{d}{dt} \int_V \rho \mathbf{v} \, dV = \int_{\partial V} \mathbf{t}_n \, dA + \int_V \rho \mathbf{g} \, dV. \quad (4.82)$$

Before exploiting this relation any further it seems adequate to explore the balance law of moment of momentum in an analogous fashion. To this end, the body is again divided into its cubic infinitesimal elements. Such an element has momentum $\rho \mathbf{v} \, dV$ as seen above and so its moment relative to the origin is $d\mathcal{L}_V^0 = \mathbf{x} \times \rho \mathbf{v} \, dV$, implying that the moment of momentum of all the elements of the body with volume V is given by

$$\mathcal{L}_V^0 = \int_V \mathbf{x} \times \rho \mathbf{v} \, dV, \quad (4.83)$$

i.e. the sum (= integral) of the moment of momentum of all elements.

¹⁴ The reader may feel somewhat uncomfortable, because he/she is here confronted with a concept that is not yet explained: pressure and shear stress. This is true; however, it is supposed that a vague understanding of these notions is present; it will in fact be one goal of this chapter to define these concepts rigorously.

The surface tractions per unit area with unit normal \mathbf{n} have also a moment relative to the origin, namely

$$d\mathcal{M}_{\partial V}^0 = \mathbf{x} \times \mathbf{t}_n dA \quad (4.84)$$

so that after integration over the boundary ∂V of the body V we have as contribution to the total moment

$$\mathcal{M}_{\partial V}^0 = \int_{\partial V} \mathbf{x} \times \mathbf{t}_n dA. \quad (4.85)$$

Similarly, the volume force $\rho \mathbf{g} dV$ of the volume element gives rise to the incremental moment

$$d\mathcal{M}_V^0 = \mathbf{x} \times \rho \mathbf{g} dV, \quad (4.86)$$

and after summation over the entire body

$$\mathcal{M}_V^0 = \int_V \mathbf{x} \times \rho \mathbf{g} dV. \quad (4.87)$$

The *balance law of moment of momentum* (3.4) expresses that the *time rate of change of the moment of momentum of a body with respect to an arbitrary fixed point equals the sum of all moments of external forces exerted on the body with respect to the same point*; thus

$$\frac{d\mathcal{L}_V^0}{dt} = \mathcal{M}_{\partial V}^0 + \mathcal{M}_V^0 \quad (4.88)$$

or according to (4.83), (4.85) and (4.87)

$$\frac{d}{dt} \int_V (\mathbf{x} \times \rho \mathbf{v}) dV = \int_{\partial V} (\mathbf{x} \times \mathbf{t}_n) dA + \int_V (\mathbf{x} \times \rho \mathbf{g}) dV. \quad (4.89)$$

The two important laws are now (4.82) and (4.89). In ensuing developments we will proceed from these.

Equation (4.89) and therefore the treatment of moment of momentum require additional remarks. We call the law (4.89) the *balance law of moment of momentum* and not the law of *angular momentum*. This is justified because each term in (4.89) is the moment of a corresponding momentum term. More generally, we could add terms as follows:

$$\frac{d}{dt} \int_V (\mathbf{x} \times \rho \mathbf{v} + \rho \mathbf{s}) dV = \int_{\partial V} (\mathbf{x} \times \mathbf{t}_n + \mathbf{m}_n) dA + \int_V (\mathbf{x} \times \rho \mathbf{g} + \rho \boldsymbol{\ell}) dV. \quad (4.90)$$

Here, s is the *spin* density, \mathbf{m}_n the *couple stress* traction and ℓ the *body couple* density. Statement (4.90) is the balance law of *angular* momentum of which the elements consist of moment of momentum plus spin contributions. Theories with the complexity (4.89) are sometimes referred to as BOLTZMANN continua and those based on (4.90) as COSSERAT or spin continua. Here, we shall only be concerned with (4.89).

4.3.1 Stress Tensor

Our intention will be eventually to write the balance laws of momentum (4.82) and moment of momentum (4.89) for an infinitesimal cubic element to obtain the *local* counterparts of these globally formulated laws. To this end, it is first necessary to introduce the concept of the *stress tensor*. In the above, the stress vector \mathbf{t}_n was introduced. It was said to form a vector on surface elements with unit normal vector \mathbf{n} , see Fig. 4.12a, and it was introduced on the boundary ∂V of a body V . Because (according to our basic assumption) any part of a body is again a body, we may apply the concept of a stress vector to the six surface elements of an infinitesimal cube; Fig. 4.12b is showing one surface element. Now, since at any point \mathbf{x} the value of \mathbf{t}_n will depend on the orientation of the surface element to which it applies, \mathbf{t}_n will, in general, be a function of \mathbf{x} and \mathbf{n} , $\mathbf{t}_n = \mathbf{f}(\mathbf{x}, \mathbf{n})$. This is why an index \mathbf{n} was used in the denotation of the stress vector. It shall be shown below that this dependence is linear, namely

$$\mathbf{t}_n = \mathbf{T}\mathbf{n}. \quad (4.91)$$

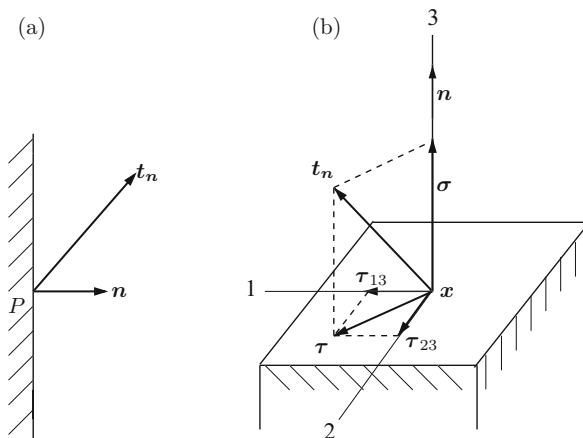


Fig. 4.12 (a) The stress vector \mathbf{t}_n at a point in a body depends on the direction of the surface \mathbf{n} . (b) The projection of the stress vector on the surface normal direction is called normal stress and denoted by σ ; the projection onto the surface element is called shear stress τ and it may be divided into two components within the plane

\mathbf{T} is called the CAUCHY *stress tensor* and the law (4.91) is called CAUCHY's *lemma*. If $\mathbf{t}_n \hat{=} (t_{n_1}, t_{n_2}, t_{n_3})$ and $\mathbf{n} \hat{=} (n_1, n_2, n_3)$, then

$$\mathbf{T} \hat{=} \begin{pmatrix} \sigma_1 & \tau_{12} & \tau_{13} \\ \tau_{21} & \sigma_2 & \tau_{23} \\ \tau_{31} & \tau_{32} & \sigma_3 \end{pmatrix}. \quad (4.92)$$

So, referred to a Cartesian basis, \mathbf{T} is equivalent to an array, called the *matrix* of the stress tensor, and the multiplication $\mathbf{T}\mathbf{n}$ in Cartesian component form has to be understood as a matrix–vector multiplication as follows:

$$\begin{pmatrix} t_{n_1} \\ t_{n_2} \\ t_{n_3} \end{pmatrix} = \begin{pmatrix} \sigma_1 & \tau_{12} & \tau_{13} \\ \tau_{21} & \sigma_2 & \tau_{23} \\ \tau_{31} & \tau_{32} & \sigma_3 \end{pmatrix} \begin{pmatrix} n_1 \\ n_2 \\ n_3 \end{pmatrix} = \begin{pmatrix} \sigma_1 n_1 + \tau_{12} n_2 + \tau_{13} n_3 \\ \tau_{21} n_1 + \sigma_2 n_2 + \tau_{23} n_3 \\ \tau_{31} n_1 + \tau_{32} n_2 + \sigma_3 n_3 \end{pmatrix}. \quad (4.93)$$

Here \mathbf{t}_n and \mathbf{n} are column vectors, i.e. the Cartesian components are arranged vertically as columns. The resulting three elements of the column vector \mathbf{t}_n are obtained as the sum of the products of the elements as indicated by the arrows.

It is also worth noting that the diagonal and off-diagonal elements of the matrix of \mathbf{T} are differently denoted by the letters σ : $\sigma_1, \sigma_2, \sigma_3$ and τ : $\tau_{12}, \tau_{13}, \tau_{21}, \tau_{23}, \tau_{31}, \tau_{32}$. This is so because these components belong to two different classes as follows:

Definition 4.12 *The diagonal elements of the matrix of the stress tensor are called **normal stress** components and designated by the letter σ (with components σ_i), while the off-diagonal elements are called **shear stress** components and designated by the letter τ (with components τ_{ij}).* ■

The interpretation is given in Figs. 4.12 and 4.13. The stress vector on the top element of the cube in Fig. 4.12b is projected onto the normal direction and onto the plane of the surface elements. It may have any arbitrary orientation in the plane it applies to. If a local coordinate system 1, 2, 3 is introduced as indicated in Fig. 4.12, then $\boldsymbol{\tau}$ has non-vanishing components in the x_1 - and x_2 -directions and these components are τ_{13} and τ_{23} , the second index indicating the surface normal direction.

For an infinitesimal cube cut out of a body, each of the six surface elements is subjected to a stress vector with components as indicated on the three front elements of Fig. 4.13. The corresponding components of the stress vector on the opposite sides of the cube, which are not shown in the figure, are (to zeroth order in the side

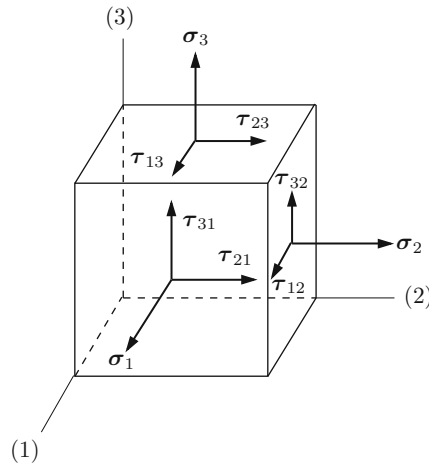


Fig. 4.13 Infinitesimal cube cut out of a body with faces perpendicular to the coordinate axes 1, 2, 3, respectively. Shown are the positively defined normal stress components $\sigma_1, \sigma_2, \sigma_3$ and the shear stress components $\tau_{23}, \tau_{31}, \dots$. The stress components not shown on the back faces are equal in magnitude and opposite in direction

length of the cube)¹⁵ equal and opposite in direction to those on the front faces. Thus the state of stress of the point P at the centre of the cube is given by the nine components shown in (4.92). In writing these components down, conventions are customary as follows:

Definition 4.13 *The normal stresses $\sigma_1, \sigma_2, \sigma_3$ carry the index of the direction into which they point, and they are positive when they represent tension and negative for pressure. The shear stress components are indexed as follows: The first index refers to the direction into which the stress component points, and the second index gives the normal direction of the surface. These shear stress components are counted positive if both the shear stress component and the surface normal point into a positive or a negative direction of the Cartesian basis. If one of the two is positive and the other negative, then the corresponding shear stress component is counted negative.* ■

The above computational rules tell us how the CAUCHY stress tensor looks like when written in Cartesian component form, but the proof of (4.91) and (4.93) must still be given. To this end, let us apply the balance law (4.82) to an infinitesimal tetrahedron with three planes parallel to the coordinate planes and one plane arbitrarily inclined as shown in Fig. 4.14. If a typical side length of this tetrahedron is Δh , then for continuous integrands the volume integrals in (4.82) are of order Δh^3 , while

¹⁵ What is meant here is that the value of the stress vector at the opposite cubic face is different in value by an amount that is proportional to the size of the side length (TAYLOR expansion!).

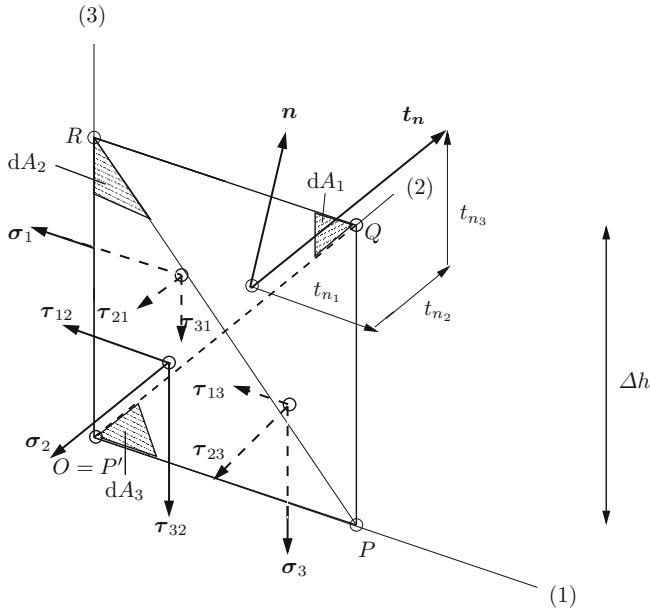


Fig. 4.14 Infinitesimal tetrahedron with three faces perpendicular to the coordinate lines 1, 2 and 3 and typical side length Δh . The stress components on the surface elements dA_1 , dA_2 and dA_3 are indicated as are those on the inclined element dA with surface normal \mathbf{n}

the surface integrals are of order Δh^2 . Letting the size of the tetrahedron shrink to zero such that its shape is preserved (which means $\Delta h \rightarrow 0$), it is obvious that the volume integral tends faster to zero than the surface integrals. Consequently, in this limit it is sufficient to request that

$$\lim_{\Delta h \rightarrow 0} \int_{\partial \text{tetrahedron}} \mathbf{t}_n dA = \mathbf{0}, \quad (4.94)$$

applied to the tetrahedron. Because the element is infinitesimal, the integral sign may be omitted, and (4.94) becomes

$$\sum_{i=1}^3 \mathbf{t}_{ni} dA_i + \mathbf{t}_n dA = \mathbf{0}, \quad (4.95)$$

where \mathbf{t}_{ni} are the stress vectors on the three coordinate surfaces with surface normals pointing in the i th coordinate direction. The respective components are indicated in Fig. 4.14. Analogously, dA_i is that infinitesimal triangular surface of the tetrahedron which is perpendicular to the i th coordinate direction. Writing down (4.95) in component form, i.e. summing all forces in the 1-direction and equating the result to zero yields

$$t_{n_1} dA - \sigma_1 dA_1 - \tau_{12} dA_2 - \tau_{13} dA_3 = 0. \quad (4.96)$$

The area of the surface element dA_i is the projection of the area of element dA onto the plane perpendicular to the i th direction; it is easily seen that this equals $dA_i = n_i dA$, where $\mathbf{n} \hat{=} (n_1, n_2, n_3)$. Substituting this into (4.96), the following result is obtained:

$$\begin{aligned} t_{n_1} &= \sigma_1 n_1 + \tau_{12} n_2 + \tau_{13} n_3, \\ t_{n_2} &= \tau_{21} n_1 + \sigma_2 n_2 + \tau_{23} n_3, \\ t_{n_3} &= \tau_{31} n_1 + \tau_{32} n_2 + \sigma_3 n_3, \end{aligned} \quad (4.97)$$

in which the second and third expressions have been obtained by writing the equations analogously to (4.96) in the x_2 - and x_3 -directions. This establishes the linear relation anticipated in (4.91). The result (4.97) is known in the literature as CAUCHY's *lemma*, as mentioned before.

The tetrahedral infinitesimal body sketched in Fig. 4.14 can also be used with slight modification to demonstrate that CAUCHY's lemma also generates NEWTON's third law, see Fig. 3.1. Indeed, if we move in imagination point P in this figure along the 1-axis towards point $O (= P')$, the tetrahedron degenerates to two parallel triangles OQR and $P'QR$. In this limit, (4.97) degenerates to

$$t_{n_1} = \sigma_1, \quad t_{n_2} = \tau_{21}, \quad t_{n_3} = \tau_{31}.$$

This states that the stress vector $(t_{n_1}, t_{n_2}, t_{n_3})$ acting on $P'QR$ equals the stress vector $(\sigma_1, \tau_{21}, \tau_{31})$ on OQR , which is exactly NEWTON's third law.

Whereas this lemma is a consequence of the balance of momentum applied to an infinitesimal tetrahedron, we now show that application of the balance law of moment of momentum to an infinitesimal cube shows that of the nine stress components of the CAUCHY stress tensor, only six are independent. To this end, application of (4.89) to an infinitesimal cube with typical side length Δh shows that for continuous integrands the volume integrals are of higher order small than the surface integrals so that angular momentum is satisfied in the limit as $\Delta h \rightarrow 0$ if

$$\lim_{\Delta h \rightarrow 0} \int_{\partial \text{cube}} \mathbf{x} \times \mathbf{t}_n dA = \mathbf{0}. \quad (4.98)$$

This equation says that the sum of the moments of all stress vectors acting on the surface of the infinitesimal cube must vanish. If we choose as origin of the coordinate system the centre of the cube, then summing all moments with respect to the x_3 -axis yields (see Fig. 4.15a)

$$(\tau_{21} dx_2 dx_3) dx_1 - (\tau_{12} dx_1 dx_3) dx_2 = 0 \implies \tau_{21} = \tau_{12} \quad (4.99)$$

and after cyclically extending this result for the other space directions

$$\tau_{12} = \tau_{21}, \quad \tau_{23} = \tau_{32}, \quad \tau_{31} = \tau_{13}. \quad (4.100)$$

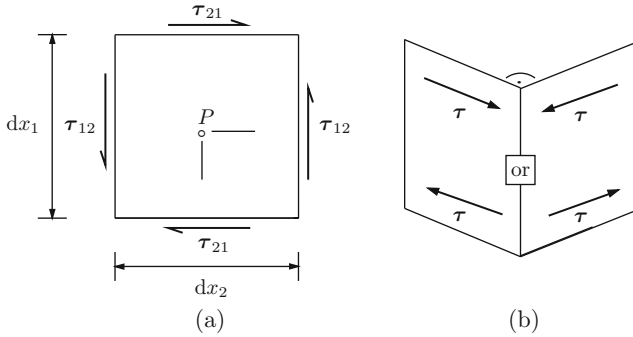


Fig. 4.15 (a) Projection onto the x_1x_2 -plane of an infinitesimal cubic element with those stress components indicated which cause a moment about the axis through P perpendicular to the drawing plane; (b) two material elements perpendicular to one another with shear stresses shown which are equal

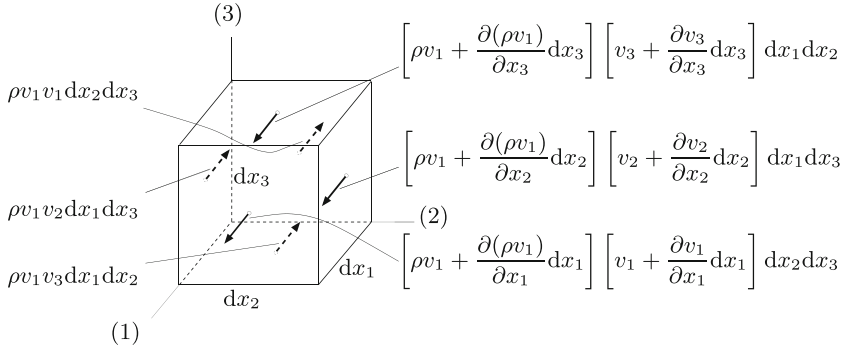


Fig. 4.16 Infinitesimal cubic element with the x_1 components of the terms $\rho \mathbf{v}(\mathbf{v} \cdot \mathbf{n}) dA$ shown on each surface element of the cube

Thus, the matrix (4.92) of the CAUCHY stress tensor is symmetric and possesses only six independent components. This result is valid for any orientation of the Cartesian basis. It follows that the shear stresses acting on material surface elements which are perpendicular to one another are equal in magnitude and either directed towards or away from the edge of the elements (see Fig. 4.15b).

4.3.2 Local Balance Law of Momentum or Newton's Second Law

After this somewhat lengthy presentation of the properties of the stress tensor, let us now apply the balance law of momentum, (4.82), for an infinitesimal cubic element

with side lengths dx_1, dx_2, dx_3 . If the REYNOLDS transport theorem (4.63) is used, then (4.82) takes the form

$$\begin{aligned} \int_{\text{cube}} \frac{\partial(\rho \mathbf{v})}{\partial t} dV + \int_{\partial \text{cube}} \rho \mathbf{v} (\mathbf{v} \cdot \mathbf{n}) dA \\ = \int_{\partial \text{cube}} \mathbf{T} \mathbf{n} dA + \int_{\text{cube}} \rho \mathbf{g} dV, \end{aligned} \quad (4.101)$$

where (4.91) has also been substituted. For the infinitesimal cubic element the volume integral does not have to be performed and the surface integral reduces to a summation over the six cubic faces; therefore, (4.101) becomes

$$\underbrace{\frac{\partial(\rho \mathbf{v})}{\partial t} dV}_{(1)} + \underbrace{\sum_{\alpha=1}^6 \rho \mathbf{v} (\mathbf{v} \cdot \mathbf{n}) dA_{\alpha}}_{(2)} = \underbrace{\sum_{\alpha=1}^6 \mathbf{T} \mathbf{n} dA_{\alpha}}_{(3)} + \underbrace{\rho \mathbf{g} dV}_{(4)}. \quad (4.102)$$

We shall exploit this equation in component form but shall explicitly demonstrate the calculation only for the x_1 -direction (Fig. 4.17). The volume terms then become

$$\begin{aligned} (1) &= \frac{\partial(\rho v_1)}{\partial t} dx_1 dx_2 dx_3, \\ (4) &= \rho g_1 dx_1 dx_2 dx_3 \quad (= 0 \text{ if the } x_1\text{-direction is horizontal}). \end{aligned} \quad (4.103)$$

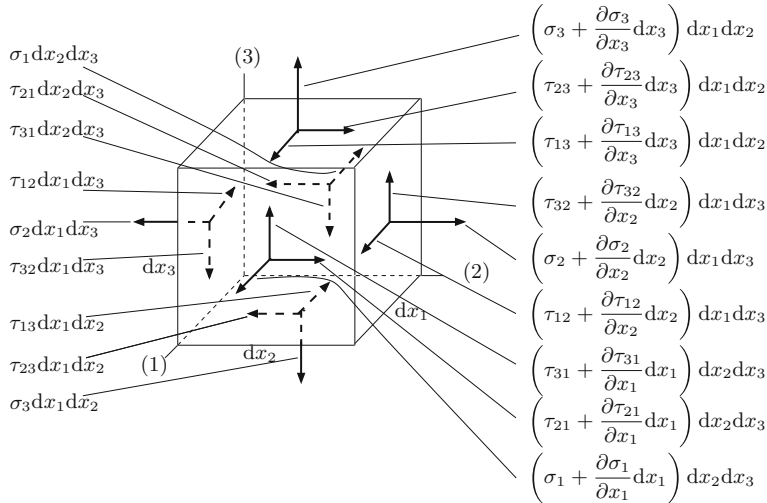


Fig. 4.17 Surface stress components at the six faces of the infinitesimal cubic element

More elaborate is the evaluation of the other two terms. As for the second one on the left-hand side of (4.102), contributions come from all six faces as indicated in Fig. 4.16. The contribution from the two faces perpendicular to the x_1 -direction is

$$\begin{aligned} (2)_1 &= -(\rho v_1) v_1 \, dx_2 \, dx_3 + \left[\rho v_1 + \frac{\partial(\rho v_1)}{\partial x_1} dx_1 \right] \left[v_1 + \frac{\partial v_1}{\partial x_1} dx_1 \right] dx_2 \, dx_3 \\ &\simeq \left[\frac{\partial(\rho v_1)}{\partial x_1} v_1 + \rho v_1 \frac{\partial v_1}{\partial x_1} \right] dx_1 \, dx_2 \, dx_3 = \frac{\partial(\rho v_1 v_1)}{\partial x_1} dx_1 \, dx_2 \, dx_3. \end{aligned}$$

Those from the faces perpendicular to the x_2 - and x_3 -directions are easily seen to be

$$(2)_2 \simeq \frac{\partial(\rho v_1 v_2)}{\partial x_2} dx_1 \, dx_2 \, dx_3, \quad (2)_3 \simeq \frac{\partial(\rho v_1 v_3)}{\partial x_3} dx_1 \, dx_2 \, dx_3.$$

Here the sign \simeq indicates that terms which are small of the fourth order in dx_i have been ignored. Thus

$$(2) = \left[\frac{\partial}{\partial x_1}(\rho v_1 v_1) + \frac{\partial}{\partial x_2}(\rho v_1 v_2) + \frac{\partial}{\partial x_3}(\rho v_1 v_3) \right] dx_1 \, dx_2 \, dx_3. \quad (4.104)$$

Finally, we must calculate the surface stress contribution (3). This is easily done by summing all contributions with stress components in the x_1 -direction yielding (see Fig. 4.17)

$$\begin{aligned} (3)_1 &= \left(\sigma_1 + \frac{\partial \sigma_1}{\partial x_1} dx_1 \right) dx_2 \, dx_3 - \sigma_1 \, dx_2 \, dx_3 \\ &\quad + \left(\tau_{12} + \frac{\partial \tau_{12}}{\partial x_2} dx_2 \right) dx_1 \, dx_3 - \tau_{12} \, dx_1 \, dx_3 \\ &\quad + \left(\tau_{13} + \frac{\partial \tau_{13}}{\partial x_3} dx_3 \right) dx_1 \, dx_2 - \tau_{13} \, dx_1 \, dx_2 \\ &= \left(\frac{\partial \sigma_1}{\partial x_1} + \frac{\partial \tau_{12}}{\partial x_2} + \frac{\partial \tau_{13}}{\partial x_3} \right) dx_1 \, dx_2 \, dx_3 \end{aligned} \quad (4.105)$$

with analogous expressions for $(3)_2$ and $(3)_3$.

Substituting the results (4.103), (4.104) and (4.105) into (4.102) leads to the following component form of the momentum equations

$$\begin{aligned}
\frac{\partial(\rho v_1)}{\partial t} + \frac{\partial}{\partial x_1}(\rho v_1 v_1) + \frac{\partial}{\partial x_2}(\rho v_1 v_2) + \frac{\partial}{\partial x_3}(\rho v_1 v_3) \\
&= \frac{\partial \sigma_1}{\partial x_1} + \frac{\partial \tau_{12}}{\partial x_2} + \frac{\partial \tau_{13}}{\partial x_3} + \rho g_1, \\
\frac{\partial(\rho v_2)}{\partial t} + \frac{\partial}{\partial x_1}(\rho v_2 v_1) + \frac{\partial}{\partial x_2}(\rho v_2 v_2) + \frac{\partial}{\partial x_3}(\rho v_2 v_3) \\
&= \frac{\partial \tau_{21}}{\partial x_1} + \frac{\partial \sigma_2}{\partial x_2} + \frac{\partial \tau_{23}}{\partial x_3} + \rho g_2, \\
\frac{\partial(\rho v_3)}{\partial t} + \frac{\partial}{\partial x_1}(\rho v_3 v_1) + \frac{\partial}{\partial x_2}(\rho v_3 v_2) + \frac{\partial}{\partial x_3}(\rho v_3 v_3) \\
&= \frac{\partial \tau_{31}}{\partial x_1} + \frac{\partial \tau_{32}}{\partial x_2} + \frac{\partial \sigma_3}{\partial x_3} + \rho g_3,
\end{aligned} \tag{4.106}$$

where the second and third equations are obtained by performing the analogous computations in the x_2 - and x_3 -directions. In these equations the symmetry of the CAUCHY stress tensor has not been made visible but can be easily accounted for by setting $\tau_{ji} = \tau_{ij}$ ($i, j = 1, 2, 3$). Moreover, the basis of the Cartesian coordinate system is usually so selected that the first two axes are horizontal and the third is vertical. For such a case, one then has $\mathbf{g} \hat{=}(0, 0, -g)$.

Definition 4.14 *Equations (4.106) are often called the **equations of motion**, and mathematicians call them to be in conservative form, because they are obtained from the conservation law of momentum without performing any simplification and have divergence form.* ■

An alternative form of the equations of motion is obtained if on the left-hand sides of (4.106) the product differentiations are executed. Indeed, one has

$$\begin{aligned}
\text{LHS(4.106)}_1 &= v_1 \underbrace{\left(\frac{\partial \rho}{\partial t} + \frac{\partial}{\partial x_1}(\rho v_1) + \frac{\partial}{\partial x_2}(\rho v_2) + \frac{\partial}{\partial x_3}(\rho v_3) \right)}_{=0, \text{ see mass balance (4.67)}} \\
&\quad + \rho \underbrace{\left(\frac{\partial v_1}{\partial t} + \frac{\partial v_1}{\partial x_1} v_1 + \frac{\partial v_1}{\partial x_2} v_2 + \frac{\partial v_1}{\partial x_3} v_3 \right)}_{dv_1/dt, \text{ see (4.6)}} = \rho \frac{dv_1}{dt},
\end{aligned}$$

and, similarly, one can show that

$$\text{LHS(4.106)}_2 = \rho \frac{dv_2}{dt}, \quad \text{LHS(4.106)}_3 = \rho \frac{dv_3}{dt}.$$

Therefore, the equations of motion can alternatively be written as

$$\begin{aligned}\rho \frac{dv_1}{dt} &= \frac{\partial \sigma_1}{\partial x_1} + \frac{\partial \tau_{12}}{\partial x_2} + \frac{\partial \tau_{13}}{\partial x_3} + \rho g_1, \\ \rho \frac{dv_2}{dt} &= \frac{\partial \tau_{21}}{\partial x_1} + \frac{\partial \sigma_2}{\partial x_2} + \frac{\partial \tau_{23}}{\partial x_3} + \rho g_2, \\ \rho \frac{dv_3}{dt} &= \frac{\partial \tau_{31}}{\partial x_1} + \frac{\partial \tau_{32}}{\partial x_2} + \frac{\partial \sigma_3}{\partial x_3} + \rho g_3.\end{aligned}\tag{4.107}$$

These equations are the component forms of the equations of motion that can also be written in symbolic vector form. Obviously

$$\rho \left(\frac{dv_1}{dt}, \frac{dv_2}{dt}, \frac{dv_3}{dt} \right) \hat{=} \rho \frac{d\mathbf{v}}{dt}, \quad \rho (g_1, g_2, g_3) \hat{=} \rho \mathbf{g},\tag{4.108}$$

and the remaining terms in (4.107) involving the Cartesian components of the CAUCHY stress tensor are defined to correspond to the divergence of the stress tensor

$$\operatorname{div} \mathbf{T} \hat{=} \begin{pmatrix} \frac{\partial T_{11}}{\partial x_1} + \frac{\partial T_{12}}{\partial x_2} + \frac{\partial T_{13}}{\partial x_3} \\ \frac{\partial T_{21}}{\partial x_1} + \frac{\partial T_{22}}{\partial x_2} + \frac{\partial T_{23}}{\partial x_3} \\ \frac{\partial T_{31}}{\partial x_1} + \frac{\partial T_{32}}{\partial x_2} + \frac{\partial T_{33}}{\partial x_3} \end{pmatrix} = \begin{pmatrix} \frac{\partial \sigma_1}{\partial x_1} + \frac{\partial \tau_{12}}{\partial x_2} + \frac{\partial \tau_{13}}{\partial x_3} \\ \frac{\partial \tau_{21}}{\partial x_1} + \frac{\partial \sigma_2}{\partial x_2} + \frac{\partial \tau_{23}}{\partial x_3} \\ \frac{\partial \tau_{31}}{\partial x_1} + \frac{\partial \tau_{32}}{\partial x_2} + \frac{\partial \sigma_3}{\partial x_3} \end{pmatrix}.\tag{4.109}$$

With this result (which can also rigorously be justified), (4.107) corresponds to

$$\rho \frac{d\mathbf{v}}{dt} = \operatorname{div} \mathbf{T} + \rho \mathbf{g},\tag{4.110}$$

in which $d\mathbf{v}/dt$ is the acceleration referred to an inertial system, i.e. the absolute acceleration. Similarly, by defining the dyadic product

$$\rho \mathbf{v} \otimes \mathbf{v} \hat{=} \rho \begin{pmatrix} v_1 v_1 & v_1 v_2 & v_1 v_3 \\ v_2 v_1 & v_2 v_2 & v_2 v_3 \\ v_3 v_1 & v_3 v_2 & v_3 v_3 \end{pmatrix}$$

the conservative form of the momentum equation (4.106) is given by

$$\frac{\partial \rho \mathbf{v}}{\partial t} + \operatorname{div} (\rho \mathbf{v} \otimes \mathbf{v}) = \operatorname{div} \mathbf{T} + \rho \mathbf{g},\tag{4.111}$$

from which (4.110) could be recovered by using product differentiation on the left-hand side of (4.111) and accounting for mass balance (4.70). With this equation, the derivation of the local form of the balance law of linear momentum is complete.

In summary, three different representations have been presented: (i) Equations (4.106), which are the three Cartesian components of the local balance of momentum as conservation laws, (ii) the analogous equations in which balance of momentum appears in the form ‘mass times acceleration equals the sum of the forces’, (4.107), and (iii) the corresponding symbolic representations, (4.110), (4.111).

In closing this presentation of the momentum equation, we mention that an analogous analysis could also be performed for the balance law of moment of momentum. We shall not perform these computations here, because, firstly, the result is simply the statement that the CAUCHY stress tensor is symmetric, which has already been proved, and secondly, because the computations performed with the mathematical prerequisites used here would be unwieldy. So, the statement $\mathbf{T} = \mathbf{T}^T$, in which the superscript $()^T$ denotes the transpose of \mathbf{T} , guarantees identical satisfaction of the law of moment of momentum.

4.3.3 Material Behaviour

So far, none of the mechanical principles allowed us to qualify the body, to which these principles were applied, as a *solid* or a *fluid body*. We now wish to make this distinction and *characterise a body as a fluid if it gives way to any non-vanishing shearing deformation*. Consider for instance the following idealised flow: A material placed between two parallel plates and subject to plane motion is set in motion by holding the bottom plate at rest while moving the upper plate with constant velocity U parallel to the plate, see Fig. 4.18a. If the material held between the plates

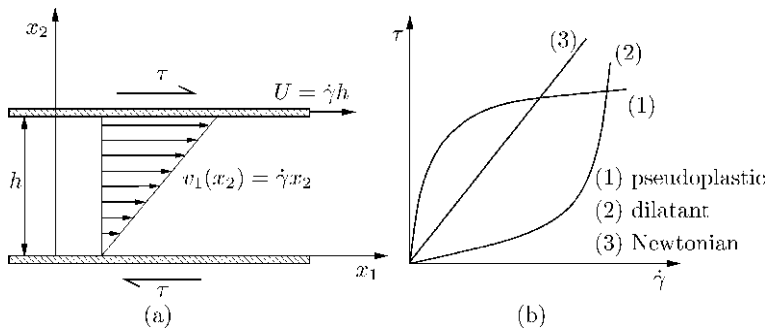


Fig. 4.18 (a) Steady shear flow between two parallel plates with an established linear velocity profile. (b) The functional relation $\tau = \tau(\dot{\gamma})$ is graphically represented; τ grows faster or slower than linearly with $\dot{\gamma}$ or is linear in $\dot{\gamma}$, denoted as dilatant, pseudoplastic and NEWTONian behaviour, respectively

offers some resistance to this motion, a velocity profile will be established which, in steady motion, is seen to be linearly distributed across the gap, $v_1 = v_1(x_2) = \dot{\gamma}x_2$. Of course, the motion of the upper plate relative to the lower plate can only be maintained if identical and opposite forces parallel to the plates are applied. This force per unit area is the shear traction τ , and experiments often show for steady state that

$$\dot{\gamma} = \frac{\tau}{\eta(|\tau|)}, \quad (4.112)$$

in which η is a phenomenological coefficient, called *dynamic shear viscosity*, which may be a constant or a function of the absolute value of the shear traction τ . Graphical representations of relation (4.112) (written inversely as $\tau = \tau(\dot{\gamma})$) are displayed in Fig. 4.18b. Functions with negative second-order derivative are called *pseudoplastic* – oil and polymeric fluids behave like this. Curves with positive second-order derivative characterise so-called *dilatant* fluids – honey and suspensions often behave like this. Finally, so-called *NEWTONian* fluids are characterised by a linear relationship between τ and $\dot{\gamma}$; water and air are such fluids. They are denoted after NEWTON, because NEWTON in his ‘Principia’¹⁶ [10] established such a relationship when he studied falling bodies in water or in air.

We shall restrict attention in the subsequent chapters exclusively to NEWTONian behaviour, because the media of concern here are water and – exceptionally – air. For these, the numerical values of the molecular dynamic shear viscosities¹⁷ are given by

$$\eta_{\text{water}} = 1.0 \times 10^{-3} \text{ (kg m}^{-1} \text{ s}^{-1}\text{)}, \quad \eta_{\text{air}} = 1.813 \times 10^{-5} \text{ (kg m}^{-1} \text{ s}^{-1}\text{)}. \quad (4.113)$$

In actual applications, it is not the dynamic viscosity that is used or referred to but rather the (molecular) *kinematic viscosity* defined by

$$\nu = \frac{\eta}{\rho} \quad (\text{m}^2 \text{ s}^{-1}), \quad (4.114)$$

and for water¹⁶ and air it takes the values

$$\nu_{\text{water}} = 1.0 \times 10^{-6} \text{ m}^2 \text{ s}^{-1}, \quad \nu_{\text{air}} = 1.48 \times 10^{-5} \text{ m}^2 \text{ s}^{-1}. \quad (4.115)$$

Physically, both kinematic and dynamic viscosities characterise the process of momentum exchange between material particles moving relative to one another with different speed. As long as this process is driven by molecular interactions, we observe a decrease of viscosity with increasing temperature because the interaction

¹⁶ In the first and second editions this topic is not treated; NEWTON included the linear case in the third edition (1726).

¹⁷ A more detailed description of the properties of water is given in Chap. 10.

between molecules becomes weaker when the molecules move faster. This dependence on temperature is rather strong. For instance, the viscosity of water drops by a factor of 2 if the temperature increases from 0 to 25°C. Likewise honey flows much more easily when being heated in a hot water bath. On the other hand, the dependence of the viscosities upon pressure is much weaker: As water is practically incompressible, a very high pressure needs to be applied if one wishes to change the distance between the molecules even only by a small amount. Under a pressure change of 100 atm (approximately 100 bars = 10^7 Pa) the viscosity of water changes only by approximately 0.6%.

Molecular interactions are significant for the momentum exchange only for small-scale, laminar flows. In geophysics, turbulent mixing is the driving mechanism for momentum exchange. In these processes the turbulent shear stress can be related to the mean shearing in the same formal way as for the laminar, small-scale processes, however with the molecular kinematic/dynamic viscosity replaced by the turbulent counterpart.¹⁸ Numerical values for the turbulent viscosities are much larger than those for the molecular counterparts, but their physical meaning is just the same; they describe the momentum exchange between the fluid particles, which are now not of molecular scale but of the scale of the flow structures, that are dictated both by the geometry of the domain in which the flow takes place and the resolution of the mean motion that one wishes to achieve. This sets in evidence that neither temperature nor pressure plays any significant role in the numerical determination of the viscosity in geophysical problems but rather the flow scales that are to be resolved. This fact points at one of the most difficult problems that lies at the basis of the physical description of flow properties in geophysical applications in meteorology, oceanography and limnology.

The simple shear experiment discussed above does not yet yield a materially constrained equation for the CAUCHY stress tensor, but only for a single component of it restricted to a very special state of flow. In order to completely describe the motion of a body, i.e. to obtain from the balance law of momentum a field equation that involves only the field variables ‘density’, ‘velocity’ and ‘temperature’, the CAUCHY stress tensor must be expressed in terms of such variables. To find such a representation, let us recall the statement that *a fluid body gives way to any shearing motion, however small*. Without loss of generality we may thus additively decompose the stress tensor \mathbf{T} into a contribution that does not suffer any shear stresses, \mathbf{T}_{eq} , and the remainder, which must possess the property that it is zero when the body is at rest, \mathbf{T}_{dyn} , so that

$$\mathbf{T} = \mathbf{T}_{\text{eq}} + \mathbf{T}_{\text{dyn}}. \quad (4.116)$$

The two contributions are called equilibrium and dynamical or non-equilibrium stress, respectively. The matrix of \mathbf{T}_{eq} can only possess diagonal elements, see

¹⁸ This relation has first been shown by PRANDTL (1925) [11]. Expositions of it are now contained in almost every book on (environmental and geophysical) fluid mechanics.

(4.92), and repeating the argument for an infinitesimal tetrahedron leading to (4.93) yields for the resultant forces on the triangular surface elements parallel to the coordinate axes

$$t_{n_1} = \sigma_1 n_1, \quad t_{n_2} = \sigma_2 n_2, \quad t_{n_3} = \sigma_3 n_3. \quad (4.117)$$

However, the traction on the inclined face must equally be in the direction of the unit normal \mathbf{n} (or opposite to it). Thus, necessarily

$$t_{n_1} = -pn_1, \quad t_{n_2} = -pn_2, \quad t_{n_3} = -pn_3. \quad (4.118)$$

The scalar p is a quantity called *pressure* or *hydrodynamic pressure*. Thermodynamics shows that for a density-preserving fluid p is an independent field variable determined by the field equations, while in a compressible fluid p is a function of density and temperature, $p = \hat{p}(\rho, T)$. If this dependence is being emphasised, p is also referred to as *thermodynamic pressure*, and the equation $p = \hat{p}(\rho, T)$ is called the (*thermal*) *equation of state*.

Equilibrating (4.117) and (4.118) thus leads to

$$\sigma_1 = \sigma_2 = \sigma_3 = -p, \quad (4.119)$$

and the matrix of the stress tensor \mathbf{T}_{eq} takes the form $\mathbf{T}_{\text{eq}} = -p\mathbf{1}$ or

$$\mathbf{T}_{\text{eq}} \hat{=} \begin{pmatrix} -p & 0 & 0 \\ 0 & -p & 0 \\ 0 & 0 & -p \end{pmatrix} = -p \begin{pmatrix} 1 & 0 & 0 \\ 0 & 1 & 0 \\ 0 & 0 & 1 \end{pmatrix}. \quad (4.120)$$

There remains the dynamical stress contribution \mathbf{T}_{dyn} . It should vanish for a state of rest (or more generally an uniform velocity field) and in the linear case be proportional to the spatial derivatives of the velocity field. Because \mathbf{T}_{dyn} is symmetric the gradient of the velocity field $\text{grad } \mathbf{v}$ cannot form the appropriate deformation rate, because $\text{grad } \mathbf{v}$ is not symmetric [see (4.9)]. However, the combination

$$\mathbf{D} := \frac{1}{2} (\text{grad } \mathbf{v} + (\text{grad } \mathbf{v})^T), \quad (4.121)$$

in which $(\text{grad } \mathbf{v})^T$ is the transpose of $\text{grad } \mathbf{v}$, is symmetric. \mathbf{D} is the *strain rate* or *stretching tensor* and, referred to a Cartesian basis, has the component form (4.15). It is customary to split \mathbf{D} into two parts, the first proportional to the unit tensor and the mean value of the sum of the diagonal elements of \mathbf{D} , $\mathbf{D}_{(1)} = \frac{1}{3}(\text{div } \mathbf{v})\mathbf{1}$ and the second, $\mathbf{D}_{(2)}$, the remainder, $\mathbf{D}_{(2)} = \mathbf{D} - \mathbf{D}_{(1)}$, called *strain rate deviator* or *stretching deviator*. It then follows that

$$\mathbf{T}_{\text{dyn}} = \zeta(\text{div } \mathbf{v})\mathbf{1} + 2\eta \left(\mathbf{D} - \frac{1}{3}(\text{div } \mathbf{v})\mathbf{1} \right), \quad (4.122)$$

is a possible linear relation between \mathbf{T}_{dyn} and \mathbf{D} ; ζ and η are two phenomenological coefficients, the *dynamic bulk* and *shear viscosities*. It is evident that for a density-preserving fluid (for which the velocity field is solenoidal) and for a BOUSSINESQ fluid (for which it is approximately solenoidal), (4.122) reduces to

$$\mathbf{T}_{\text{dyn}} = 2\eta \mathbf{D}, \quad (\text{div } \mathbf{v} = 0). \quad (4.123)$$

On the other hand, it is very difficult to determine for any fluid or gas the bulk viscosity ζ , one obvious reason being that it is small. This is motivation to request that $\zeta = 0$ so that (4.122) reduces in this case to

$$\mathbf{T}_{\text{dyn}} = 2\eta \left(\mathbf{D} - \frac{1}{3}(\text{div } \mathbf{v})\mathbf{1} \right). \quad (4.124)$$

We shall use these viscous stress relations only in the form (4.123) and then are led to the following component relation

$$\begin{pmatrix} \sigma_1 & \tau_{12} & \tau_{13} \\ \tau_{21} & \sigma_2 & \tau_{23} \\ \tau_{31} & \tau_{32} & \sigma_3 \end{pmatrix}_{\text{dyn}} = 2\eta \begin{pmatrix} \frac{\partial v_1}{\partial x_1} & \frac{1}{2} \left(\frac{\partial v_1}{\partial x_2} + \frac{\partial v_2}{\partial x_1} \right) & \frac{1}{2} \left(\frac{\partial v_1}{\partial x_3} + \frac{\partial v_3}{\partial x_1} \right) \\ & \frac{\partial v_2}{\partial x_2} & \frac{1}{2} \left(\frac{\partial v_2}{\partial x_3} + \frac{\partial v_3}{\partial x_2} \right) \\ \text{sym} & & \frac{\partial v_3}{\partial x_3} \end{pmatrix}. \quad (4.125)$$

In this form we tacitly assume that $\text{div } \mathbf{v} = 0$.

Problem 4.4 The phenomenological parameters ζ and η are called bulk and shear viscosities. Show that in a pure dilatant or contractant motion, in which the stretching \mathbf{D} is proportional to the unit tensor $\mathbf{1}$, ζ may indeed be interpreted as a viscosity of volume strain rate. Analogously, show that for simple shearing (4.124) reduces to the simple law $\tau = \eta \dot{\gamma}$ of the simple shear experiment introduced earlier, see Fig. 4.18. \blacklozenge

We close this subsection by specialising the equations of balance of momentum for two obvious special cases: (i) an *ideal fluid* and (ii) a *Newtonian Boussinesq fluid*. These are defined as follows:

Definition 4.15

- An **ideal fluid** is defined as an inviscid fluid; it cannot support any shear stresses. It may be compressible or volume–density preserving.
- A **Newtonian Boussinesq fluid** is defined by the constitutive relation for stress of the form

$$\mathbf{T} = -p(\rho, T)\mathbf{1} + 2\eta \mathbf{D}; \quad (4.126)$$

p is the thermodynamic pressure and η the dynamic viscosity. \blacksquare

The *momentum equation for an ideal fluid* is given by the equation

$$\rho \frac{d\mathbf{v}}{dt} = -\text{grad } p + \rho \mathbf{g}, \quad (4.127)$$

or in component form

$$\begin{aligned} \rho \frac{dv_1}{dt} &= -\frac{\partial p}{\partial x_1} + \rho g_1, \\ \rho \frac{dv_2}{dt} &= -\frac{\partial p}{\partial x_2} + \rho g_2, \\ \rho \frac{dv_3}{dt} &= -\frac{\partial p}{\partial x_3} + \rho g_3. \end{aligned} \quad (4.128)$$

This is so, because $\text{div } \mathbf{T} = -\text{grad } p$, as can easily be seen from (4.107) and (4.119). Equations (4.127) and (4.128) are also called the EULER equations, because it was Leonhard EULER who derived them for the first time.

The *momentum equations for a NEWTONian BOUSSINESQ fluid* are obtained by substituting (4.126) into (4.110). This yields

$$\rho \frac{d\mathbf{v}}{dt} = -\text{grad } p + \text{div } (2\eta \mathbf{D}) + \rho \mathbf{g}, \quad (4.129)$$

or for constant shear viscosity η , since $\text{div } \mathbf{v} = 0$,

$$\rho \frac{d\mathbf{v}}{dt} = -\text{grad } p + \eta \Delta \mathbf{v} + \rho \mathbf{g}, \quad (4.130)$$

in which Δ is the so-called LAPLACE operator; in component form

$$\begin{aligned} \rho \frac{dv_1}{dt} &= -\frac{\partial p}{\partial x_1} + \eta \left(\frac{\partial^2 v_1}{\partial x_1^2} + \frac{\partial^2 v_1}{\partial x_2^2} + \frac{\partial^2 v_1}{\partial x_3^2} \right) + \rho g_1, \\ \rho \frac{dv_2}{dt} &= -\frac{\partial p}{\partial x_2} + \eta \left(\frac{\partial^2 v_2}{\partial x_1^2} + \frac{\partial^2 v_2}{\partial x_2^2} + \frac{\partial^2 v_2}{\partial x_3^2} \right) + \rho g_2, \\ \rho \frac{dv_3}{dt} &= -\frac{\partial p}{\partial x_3} + \eta \left(\frac{\partial^2 v_3}{\partial x_1^2} + \frac{\partial^2 v_3}{\partial x_2^2} + \frac{\partial^2 v_3}{\partial x_3^2} \right) + \rho g_3. \end{aligned} \quad (4.131)$$

4.3.4 Hydrostatics

Because a fluid gives way to any shearing load, it can, when it is at rest, only support internal pressure but no shear stresses. It follows from (4.130) or (4.127) that in equilibrium for which the acceleration vanishes, the balance law of momentum reduces to a balance of forces. In a moving coordinate system the acceleration is given by [see (4.49)]

$$\mathbf{a}_{\text{abs}} = \frac{d\mathbf{v}}{dt} + \mathbf{a}_0 + \boldsymbol{\omega} \times (\boldsymbol{\omega} \times \mathbf{x}) + 2\boldsymbol{\omega} \times \mathbf{v} + \dot{\boldsymbol{\omega}} \times \mathbf{x}. \quad (4.132)$$

Here, $d\mathbf{v}/dt$ is the acceleration measured by an observer in the moving coordinate system, \mathbf{a}_0 is the translational acceleration of the origin of the moving coordinate system, $\boldsymbol{\omega}$ is its angular velocity relative to the inertial system which we think to be at rest and $\dot{\boldsymbol{\omega}}$ is its time rate of change. If the fluid is at rest in the moving system, then $\mathbf{v} = \mathbf{0}$, $d\mathbf{v}/dt = \mathbf{0}$ and the equation of motion reduces to

$$\rho (\mathbf{a}_0 + \boldsymbol{\omega} \times (\boldsymbol{\omega} \times \mathbf{x}) + \dot{\boldsymbol{\omega}} \times \mathbf{x}) = -\text{grad } p + \rho \mathbf{g}. \quad (4.133)$$

This is the hydrostatic equation, but in this generality it is usually not written down; it does neither possess meaningful solutions in this generality; for most applications $\dot{\boldsymbol{\omega}} = \mathbf{0}$ and often $\mathbf{a}_0 = \mathbf{0}$ or $\boldsymbol{\omega} \times (\boldsymbol{\omega} \times \mathbf{x}) = \mathbf{0}$ or both. We shall always restrict considerations to the case $\dot{\boldsymbol{\omega}} = \mathbf{0}$. This is so because the moving coordinate system in our case will be a system fixed on the globe and the angular velocity of the Earth is treated as a constant. Writing (4.133) for $\dot{\boldsymbol{\omega}} = \mathbf{0}$ as

$$\text{grad } p = \rho \mathbf{g} - \rho (\mathbf{a}_0 + \boldsymbol{\omega} \times (\boldsymbol{\omega} \times \mathbf{x})), \quad (4.134)$$

it is immediately seen that this equation can be fulfilled only if its right-hand side can be expressed as the gradient of a scalar quantity. Otherwise a hydrostatic equilibrium cannot exist.

We will now assume that

$$\rho \mathbf{g} - \rho (\mathbf{a}_0 + \boldsymbol{\omega} \times (\boldsymbol{\omega} \times \mathbf{x})) = -\text{grad } \Psi, \quad (4.135)$$

i.e. that such an equilibrium exists. Ψ is called the ‘force’ potential¹⁹ and the negative gradient of it delivers the force. With (4.135) we find from (4.134)

$$\text{grad } (p + \Psi) = 0. \quad (4.136)$$

This equation states that the sum $p + \Psi$ must have everywhere in the fluid the same value c so that the hydrostatic equation takes the integrated form

$$p + \Psi = c. \quad (4.137)$$

Definition 4.16

- *Surfaces of constant pressure are called **isobars** or **isobaric surfaces**.*
- *Surfaces of constant potential Ψ are called **equipotential surfaces**.* ■

¹⁹ For a frame of reference that is fixed with the rotating Globe, the gravity force possesses a potential, and so does the centrifugal force, see Problem 4.2 and Fig. 4.6. Moreover it is usually assumed that the motion of the Earth around the Sun is practically inertial for which $\mathbf{a}_0 = \mathbf{0}$.

It follows from (4.137) that the isobaric surfaces are identical to the equipotential surfaces. Let us illustrate the use of the hydrostatic equation by a few examples.

Example 4.1 Consider a density-preserving fluid confined to a container on a truck moving with constant acceleration a_0 along a horizontal street. Ignore the effects of the rotation of the Earth. Then in a Cartesian coordinate system in which the basis vectors \hat{e}_1, \hat{e}_2 are horizontal, while \hat{e}_3 is vertically upwards, (4.134) becomes

$$\text{grad } p = -\rho g \hat{e}_3 - \rho a_0 \hat{e}_1,$$

from which it follows that

$$p = -\rho g x_3 - \rho a_0 x_1 + p_0, \quad (4.138)$$

where p_0 is a reference pressure. Isobars are given by

$$x_3 = -\frac{a_0}{g} x_1 + \frac{p_0 - p_1}{\rho g} \quad (4.139)$$

with constant p_1 . This shows that isobars are planes which are inclined relative to the horizontal by an angle $|\alpha| = \arctan a_0/g$. These planes are also the equipotential surfaces for the potential

$$\Psi = -\rho g x_3 - \rho a_0 x_1 + \text{const.} \quad (4.140)$$

For a container at rest ($a_0 = 0$), isobaric and equipotential surfaces are horizontal, since

$$p = -\rho g x_3 + p_0. \quad (4.141)$$

•

This formula explains why the water in communicating vessels reaches the same level in the two vessels (Fig. 4.19). The free surface experiences the same outside atmospheric pressure, and since the density of the fluid is constant, the gravity potentials in the left and right vessels at the same height have the same value.

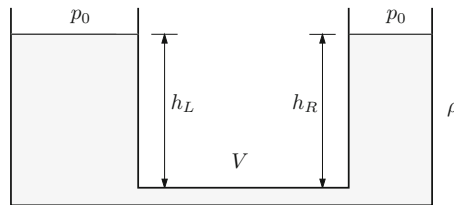


Fig. 4.19 Communicating vessels. If the density of the fluid of the two vessels is the same, the free surface levels h_L and h_R are also the same

Formula (4.141) also resolves the apparent *PASCAL paradoxon* according to which the force due to the pressure exerted on the bottom plate of two vessels filled with a fluid of constant density at equal levels is the same if the areas of the plates are the same irrespective of whether the total mass of the fluid confined in the vessels is the same or not (Fig. 4.20).

If the fluid or the gas at rest is not of constant density, then in an inertial frame the hydrostatic equation yields in the three coordinate directions

$$\frac{\partial p}{\partial x_1} = 0, \quad \frac{\partial p}{\partial x_2} = 0, \quad \frac{\partial p}{\partial x_3} = -\rho(x_3)g. \quad (4.142)$$

The first two equations imply that the pressure can only depend on the coordinate x_3 so that necessarily $\rho = \rho(x_3)$. Thus, according to (4.142)₃,

$$p = -g \int_{x_3^0}^{x_3} \rho(z) dz + p_0. \quad (4.143)$$

In limnology and oceanography x_3^0 is usually identified with the lake surface at rest, then p_0 may be identified with the atmospheric pressure. It is also common to write

$$\rho = \rho^*(1 + \sigma), \quad (4.144)$$

where ρ^* is a constant reference density, e.g. $\rho^* = \rho(T = 4^\circ\text{C})$, and σ is called the *specific density*, sometimes called *density anomaly*. Then (4.143) takes the form

$$p = \underbrace{p_0 + \rho^* g (x_3^0 - x_3)}_{\text{external pressure}} - \underbrace{\rho^* g \int_{x_3^0}^{x_3} \sigma(z) dz}_{\text{internal pressure}}, \quad (4.145)$$

in which the contribution due to the constant reference density is called *external pressure*, while the remainder is called the *internal pressure* due to density

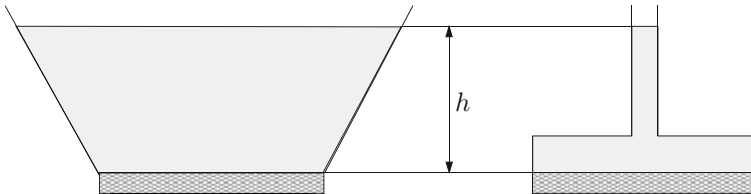


Fig. 4.20 PASCAL paradoxon: The force excited on the bottom plate by the fluid pressure is the same if the two plates have the same area, even though the total volume and therefore the weight of the fluid is not the same

variations.²⁰ A fluid at rest with density variations is called a *stratified fluid*. If such a fluid is subject to gravity forces alone, this stratification can occur in the form of horizontal layers only, i.e. the density must be constant at a certain depth below the free surface.

The hydrostatic equation can also be used to derive the formula for the ARCHIMEDEAN *buoyancy force*. To this end, consider a stratified fluid at rest – i.e. a fluid with variable density in the vertical direction – and imagine a body with volume V completely submerged, maintained also at rest²¹ (Fig. 4.21a). The vertical uplift on the body is referred to as a *buoyancy force*.

Actually, the formula for the ARCHIMEDEAN buoyancy force can be proved simply by the following Gedanken experiment. If the body with volume V is removed in imagination and the free volume is replaced by the surrounding fluid such that the layering due to stratification is preserved, Fig. 4.21b, then the replaced fluid will be in equilibrium with the surrounding fluid. This replaced fluid possesses the gravity force

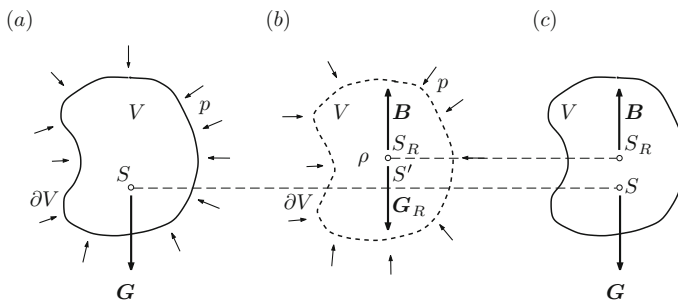


Fig. 4.21 Explaining the ARCHIMEDEAN principle. (a) In a (possibly stratified) fluid at rest a body with volume V is submerged. Its centre of gravity is S and it has the gravity force $\mathbf{G} = \int_V \rho_B \mathbf{g} dV$, where ρ_B is the density of the body. (b) Replacing in imagination the body by the fluid stratified as the surrounding fluid, this fluid is subjected to the gravity force $\mathbf{G}_R = \int_V \rho \mathbf{g} dV$ with centre of gravity S' and is evidently in equilibrium with the surrounding fluid. Obviously, the buoyancy force \mathbf{B} due to the pressure of the surrounding fluid onto the interface must be equal and opposite to \mathbf{G}_R with point of attack S_R vertically above or at S' . (c) The submerged body is thus subjected to \mathbf{G} and \mathbf{B} as indicated

²⁰ It is not clear to us why the denotations are like this. The first term may be called external pressure because, once ρ_* is selected, it is known when the external pressure p_0 and x_3^0 are known, thus quantities external to the lake. Alternatively, determination of the second term requires knowledge of σ , an internal variable. We will see later that barotropic (for external) and baroclinic (for internal) pressures, respectively, would be more adequate characterisations.

²¹ If the gravity force of the body and its buoyancy force are not in equilibrium, it is assumed that the body is supported or hung so that it is maintained at rest.

$$\mathbf{G}_R = \int_V \rho(x_3) \mathbf{g} \underbrace{dx_1 dx_2 dx_3}_{dV}, \quad (4.146)$$

and it has a centre of gravity²² S' that may be different from the centre of gravity of the body S that was removed. Since the gravity force of this replaced fluid is in equilibrium with the pressure distribution at the boundary, the buoyancy force must in absolute value be equal to G_R and opposite in direction, implying

$$\mathbf{B} = - \int_V \rho(x_3) \mathbf{g} dV. \quad (4.147)$$

This is the result proving the ARCHIMEDEAN principle.

Theorem 4.2 (ARCHIMEDEAN principle) *The buoyancy force of a submerged body in a still fluid is equal to the weight of the replaced fluid. Its centre of action is the centre of gravity of this replacement fluid.* \otimes

How is the buoyancy force computed? We present two different approaches of proof, one involving computations and the other using direct arguments. Its source is the pressure distribution exerted by the surrounding fluid on the boundary surface ∂V of the body. So, with the notation of Fig. 4.21a

$$\mathbf{B} = - \int_{\partial V} p \mathbf{n} dA, \quad (4.148)$$

where \mathbf{n} represents the exterior unit normal vector of the surface of the body. When the concept of integration is applied to the determination of the buoyancy force (4.148), rather complicated calculations are required for the evaluation of the integral because the direction \mathbf{n} of the curved surface changes from point to point. The problem can be greatly simplified by resolving the total force F of the fluid pressure on a submerged curved surface into its horizontal and vertical components F_H and F_V , respectively, as shown in Fig. 4.22a.

The curved line AB represents schematically the profile of a curved surface submerged in a fluid. The pressure may vary in any manner from p_A at A to p_B at B , but the pressure on any element of area dA is normal to dA . The differential force dF acting on dA is $p dA$, and the angle θ defines the slope of dA relative to the system of horizontal plane. The force dF can be resolved into its horizontal and vertical components

$$dF_H = p \sin \theta dA, \quad dF_V = p \cos \theta dA, \quad (4.149)$$

²² We use here the concept of centre of gravity. In general it differs from the centre of mass, but for a unidirectional gravity force field the two definitions ‘centre of mass’ and ‘centre of gravity’ coincide.

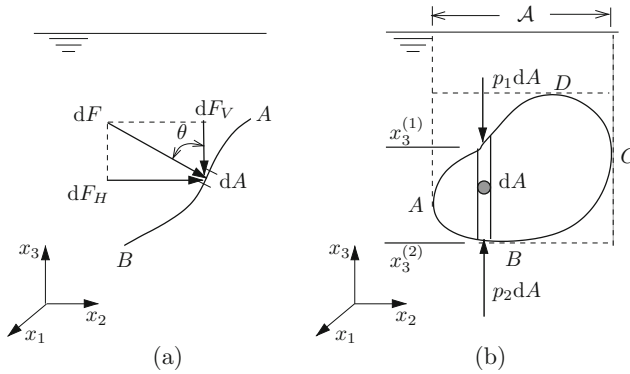


Fig. 4.22 (a) Surface segment AB with areal element dA at which a normal force $dF = p \, dA$ applies. This force is decomposed into dF_H and dF_V . θ measures the inclination of the surface element. (b) Body submerged in a still liquid. A and C mark the surface points farthest to the ‘left’ and ‘right’ and define the area \mathcal{A} , the projection of the body onto the (x_1, x_2) -plane. B and D mark the lowest and highest points in the x_3 -direction. The vertical column has horizontal cross-sectional area dA

and their sums (integrals) will be the components F_H and F_V of the resultant force on area AB ; thus

$$\begin{aligned} F_H &= \int^{AB} p \sin \theta \, dA = \int^{AB} p (dA)_V, \\ F_V &= \int^{AB} p \cos \theta \, dA = \int^{AB} p (dA)_H, \end{aligned} \quad (4.150)$$

where $(dA)_H$ and $(dA)_V$ are the projections of dA on the horizontal and vertical axes, respectively.

The method of calculating the force on a curved surface applies to all shapes of a surface and, therefore, to the surface of a totally submerged body $ABCD$ in Fig. 4.22b. The resultant horizontal pressure on the body at rest is equal to zero because the horizontal components of the pressure on the vertical projection from both sides are equal in magnitude and opposite in direction. On the two end surface elements of a vertical prism of horizontal cross section dA are two vertical pressure forces $p_1 \, dA$ and $p_2 \, dA$ as shown. The difference between the upward and downward pressure forces is the buoyant force dB on the vertical prism:

$$dB = p_2 \, dA - p_1 \, dA = (p_2 - p_1) dA. \quad (4.151)$$

Using the hydrostatic equation (4.142) or (4.143), it follows

$$p_2 - p_1 = g \int_{x_3^{(1)}}^{x_3^{(2)}} \rho(x_3) dx_3, \quad (4.152)$$

where $x_3^{(1)}$ and $x_3^{(2)}$ represent the vertical coordinates of the upper (ADC) and lower (ABC) surfaces of the immersed body.

The total buoyant force B on the entire submerged body $ABCD$ is obtained by summing over all columns, thus integrating over dB . Therefore, by substituting (4.152) into (4.151) and integrating over the horizontal area \mathcal{A} yields

$$B = \int_{\mathcal{A}} dB = \int_{\mathcal{A}} \int_{x_3^{(1)}}^{x_3^{(2)}} \rho(x_3) g \, dx_3 \, dA = \int_V \rho(x_3) g \, dV, \quad (4.153)$$

which is simply the gravity force acting on the fluid displaced by the submerged body. Thus, the law of the ARCHIMEDEAN buoyancy force is proved.

If the density of the fluid is constant $\rho(x_3) = \text{const}$, it follows from (4.153) or (4.147) that

$$B = \rho g V, \quad (4.154)$$

where V is the volume of the submerged body.

When a body floats on a surface separating two fluids of constant density ρ_1 and ρ_2 , respectively, as shown in Fig. 4.23a, (4.153) yields

$$B = \rho_1 g V_1 + \rho_2 g V_2, \quad (4.155)$$

in which V_1 and V_2 represent the volumes of the body parts submerged in the fluids of density ρ_1 and ρ_2 , respectively.

Furthermore, for a body floating at the free surface of a fluid of constant density ρ (Fig. 4.23b), if the air density is ρ_{air} , which is usually negligible, (4.155) becomes

$$B = \rho_{\text{air}} g V_1 + \rho g V_2 \simeq \rho g V_2, \quad (4.156)$$

where V_2 represents the submerged volume of the body in the fluid. The buoyant force is consequently equal to the weight of the displaced fluid. Since the floating

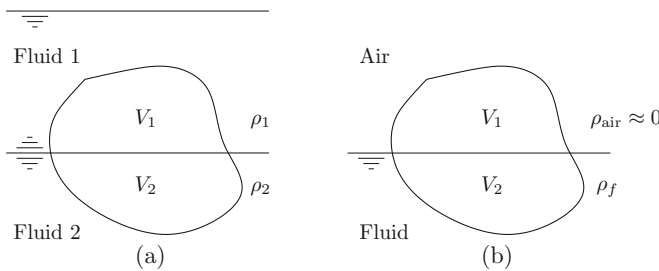


Fig. 4.23 Buoyant force of a body floating on a surface separating two fluids of constant density ρ_1 and ρ_2 (a) and at the free surface of a fluid (b)

body is statically in equilibrium, it follows that the buoyant force just balances the weight of the body.

By combining (4.147), (4.148) and (4.134) with $\mathbf{a}_0 = \mathbf{0}$ and $\boldsymbol{\omega} = \mathbf{0}$ the above proof of the ARCHIMEDEAN principle also leads to the following formula

$$\int_{\partial V} p \mathbf{n} \, dA = \int_V \text{grad } p \, dV \quad (4.157)$$

for any function p which is differentiable in V . This is a well-known formula in vector field theory and we think this proof of it is neat.²³

Problem 4.5 Consider a cylindrical glass of water on a rotating plate positioned such that the vertical rotation axis and the cylindrical axis of the glass coincide. Let the angular velocity $\boldsymbol{\omega}$ be constant and directed vertically upwards. Prove that the free surface is an axisymmetric paraboloid. ♦

4.4 Balance of Energy: First Law of Thermodynamics

The balance of energy or the first law of thermodynamics was already stated in Chaps. 2 and 3; it says that *the time rate of change of the kinetic plus internal energy of a body equals the power of working of the (external) surface and volume forces plus the heat supplied to the body by external agents within the body plus that flowing into the body through the boundary*, see, e.g., (3.5). If we consider the body, as before, being formed by infinitesimal elements, we have

$$\begin{aligned} \mathcal{E}_V^k &= \int_V \rho \frac{\mathbf{v} \cdot \mathbf{v}}{2} dV, & \mathcal{E}_V^i &= \int_V \rho \varepsilon dV, \\ \mathcal{L}_V &= \int_V \mathbf{v} \cdot \rho \mathbf{g} dV, & \mathcal{L}_{\partial V} &= \int_{\partial V} \mathbf{v} \cdot \mathbf{t}_n dA, \\ \mathcal{Q}_V &= \int_V \rho r dV, & \mathcal{Q}_{\partial V} &= - \int_{\partial V} \mathbf{q} \cdot \mathbf{n} dA. \end{aligned} \quad (4.158)$$

²³ The proof is not completely general as in (4.147), in which ρ is a function of x_3 only. Nevertheless, at two other situations we already had the occasion to prove theorems of mathematical analysis by tailoring the arguments to physical reasoning. For instance, by the balance of mass for a material volume and a volume fixed in space, but identical in size, the REYNOLDS theorem was derived [see (4.63)]; moreover using the same conservation law of mass the divergence theorem (GAUSS law) was obtained [see (4.73) and (4.75)]; and now the ARCHIMEDEAN principle was used to obtain (4.157), which is another form of GAUSS' law. This physical tailoring of mathematical facts is intentional here. The reader should be aware, however, of the fact that it does not replace a clean mathematical proof of the statements.

In these expressions

- $\frac{1}{2}\rho \mathbf{v} \cdot \mathbf{v}$ is the kinetic energy per unit volume,
- $\rho \varepsilon$ the specific internal energy per unit volume,
- $\rho \mathbf{g} \cdot \mathbf{v}$ the power of working of the volume forces per unit volume,
- $\mathbf{v} \cdot \mathbf{t}_n$ the power of working of the surface tractions,
- ρr the external energy supply or specific radiation to the volume element and
- $-\mathbf{q} \cdot \mathbf{n}$ the flow of heat through the boundary of the body.

Substituting (4.158) into (3.5) yields

$$\begin{aligned} \frac{\partial}{\partial t} \int_V \rho \left(\frac{\mathbf{v} \cdot \mathbf{v}}{2} + \varepsilon \right) dV &= \int_{\partial V} (\mathbf{v} \cdot \mathbf{t}_n - \mathbf{q} \cdot \mathbf{n}) dA \\ &+ \int_V (\mathbf{v} \cdot \rho \mathbf{g} + \rho r) dV \end{aligned} \quad (4.159)$$

or after using the REYNOLDS transport theorem (4.63)

$$\begin{aligned} &\underbrace{\int_{V_{\text{fix}}} \frac{\partial}{\partial t} \left(\rho \frac{\mathbf{v} \cdot \mathbf{v}}{2} + \rho \varepsilon \right) dV}_{(1)} + \underbrace{\int_{\partial V_{\text{fix}}} \rho \left(\frac{\mathbf{v} \cdot \mathbf{v}}{2} + \varepsilon \right) (\mathbf{v} \cdot \mathbf{n}) dA}_{(2)} \\ &= \underbrace{\int_{\partial V_{\text{fix}}} (\mathbf{v} \cdot \mathbf{t}_n - \mathbf{q} \cdot \mathbf{n}) dA}_{(3)} + \underbrace{\int_{V_{\text{fix}}} (\mathbf{v} \cdot \rho \mathbf{g} + \rho r) dV}_{(4)}. \end{aligned} \quad (4.160)$$

This form of the energy balance law will now be used for an infinitesimal cubic element with side lengths dx_1, dx_2, dx_3 . In much the same way as done before for the balances of mass and momentum, we may individually evaluate the four different terms of (4.160). The reader may verify that the indicated terms take the following forms:

$$(1) = \frac{\partial}{\partial t} \left(\rho \frac{\mathbf{v} \cdot \mathbf{v}}{2} + \rho \varepsilon \right) dV, \quad (4.161)$$

$$\begin{aligned} (2) &= \left\{ \frac{\partial}{\partial x_1} \left[\left(\rho \frac{\mathbf{v} \cdot \mathbf{v}}{2} + \rho \varepsilon \right) v_1 \right] + \frac{\partial}{\partial x_2} \left[\left(\rho \frac{\mathbf{v} \cdot \mathbf{v}}{2} + \rho \varepsilon \right) v_2 \right] \right. \\ &\quad \left. + \frac{\partial}{\partial x_3} \left[\left(\rho \frac{\mathbf{v} \cdot \mathbf{v}}{2} + \rho \varepsilon \right) v_3 \right] \right\} dV, \end{aligned} \quad (4.162)$$

$$\begin{aligned} (3) &= \left\{ \left[v_1 \left(\frac{\partial T_{11}}{\partial x_1} + \frac{\partial T_{12}}{\partial x_2} + \frac{\partial T_{13}}{\partial x_3} \right) - \frac{\partial q_1}{\partial x_1} \right] \right. \\ &\quad + v_2 \left(\frac{\partial T_{21}}{\partial x_1} + \frac{\partial T_{22}}{\partial x_2} + \frac{\partial T_{23}}{\partial x_3} \right) - \frac{\partial q_2}{\partial x_2} \\ &\quad \left. + v_3 \left(\frac{\partial T_{31}}{\partial x_1} + \frac{\partial T_{32}}{\partial x_2} + \frac{\partial T_{33}}{\partial x_3} \right) - \frac{\partial q_3}{\partial x_3} \right] \end{aligned}$$

$$\begin{aligned}
& + \left[\left(\frac{\partial v_1}{\partial x_1} T_{11} + \frac{\partial v_1}{\partial x_2} T_{12} + \frac{\partial v_1}{\partial x_3} T_{13} \right) + \left(\frac{\partial v_2}{\partial x_1} T_{21} + \frac{\partial v_2}{\partial x_2} T_{22} + \frac{\partial v_2}{\partial x_3} T_{23} \right) \right. \\
& \left. + \left(\frac{\partial v_3}{\partial x_1} T_{31} + \frac{\partial v_3}{\partial x_2} T_{32} + \frac{\partial v_3}{\partial x_3} T_{33} \right) \right] \} dV \\
& = \{[(3)_1] + [(3)_2]\} dV,
\end{aligned} \tag{4.163}$$

$$(4) = (\mathbf{v} \cdot \rho \mathbf{g} + \rho r) dV, \tag{4.164}$$

in which $\mathbf{t}_n = \mathbf{T} \mathbf{n}$ has been used, where \mathbf{T} is the Cauchy stress tensor with the components T_{ij} ($i, j = 1, 2, 3$). Forming the equation (1) + (2) = (3) + (4) and dropping the common factor dV then yields the local form of the balance law of energy. It is obvious that with the above notation the resulting equation looks unwieldy; not only a more compact notation will be more economical, but also the emerging equation will become more transparent. The reader can easily verify by recourse to the formulae (2.62) and (4.109) that

$$\begin{aligned}
(2) &= \operatorname{div} \left(\left(\rho \frac{\mathbf{v} \cdot \mathbf{v}}{2} + \rho \varepsilon \right) \mathbf{v} \right) dV, \\
(3) &= \{ \mathbf{v} \cdot \operatorname{div} \mathbf{T} - \operatorname{div} \mathbf{q} + [(3)_2] \} dV,
\end{aligned} \tag{4.165}$$

in which $[(3)_2]$ is the term in the second bracket of (4.163). To find a representation for this term, consider the Cartesian matrix representations

$$\operatorname{grad} \mathbf{v} \hat{=} \begin{pmatrix} \frac{\partial v_1}{\partial x_1} & \frac{\partial v_1}{\partial x_2} & \frac{\partial v_1}{\partial x_3} \\ \frac{\partial v_2}{\partial x_1} & \frac{\partial v_2}{\partial x_2} & \frac{\partial v_2}{\partial x_3} \\ \frac{\partial v_3}{\partial x_1} & \frac{\partial v_3}{\partial x_2} & \frac{\partial v_3}{\partial x_3} \end{pmatrix}, \quad \mathbf{T} \hat{=} \begin{pmatrix} T_{11} & T_{12} & T_{13} \\ T_{21} & T_{22} & T_{23} \\ T_{31} & T_{32} & T_{33} \end{pmatrix} \tag{4.166}$$

and form the product $(\operatorname{grad} \mathbf{v}) \mathbf{T}^T$, which corresponds to the matrix product of the matrices $(\operatorname{grad} \mathbf{v})$ and $(\mathbf{T})^T$. It is then straightforward to see that $[(3)_2]$ is the sum of the diagonal elements of this product matrix. With the Definition 2.18 of the trace we thus have

$$[(3)_2] = \operatorname{tr}((\operatorname{grad} \mathbf{v}) \mathbf{T}^T), \tag{4.167}$$

in which tr stands for ‘trace’. There is yet another way of writing (4.167), and it uses the property that the CAUCHY stress tensor is symmetric, $\mathbf{T} = \mathbf{T}^T$. To this end we split $(\operatorname{grad} \mathbf{v})$ into its symmetric and skew-symmetric contributions

$$\begin{aligned}
\mathbf{D} &:= \frac{1}{2} (\operatorname{grad} \mathbf{v} + (\operatorname{grad} \mathbf{v})^T), \quad \mathbf{D} = \mathbf{D}^T, \\
\mathbf{W} &:= \frac{1}{2} (\operatorname{grad} \mathbf{v} - (\operatorname{grad} \mathbf{v})^T), \quad \mathbf{W} = -\mathbf{W}^T,
\end{aligned} \tag{4.168}$$

already introduced in (4.13), (4.14), (4.15), (4.16), so that

$$\text{grad } \mathbf{v} = \mathbf{D} + \mathbf{W}. \quad (4.169)$$

\mathbf{D} and \mathbf{W} have the representations (4.15) and (4.16). Moreover, starting from [(3)₂] in (4.163) the reader may also demonstrate that

$$[(3)_2] = \text{tr}((\text{grad } \mathbf{v})\mathbf{T}^T) = \text{tr}(\mathbf{DT}), \quad (4.170)$$

while $\text{tr}(\mathbf{WT}) = 0$. Using (4.161), (4.164), (4.165) and (4.170) the local energy equation (1) + (2) – (3) – (4) = 0 takes the form

$$\begin{aligned} & \frac{\partial}{\partial t} \left(\rho \frac{\mathbf{v} \cdot \mathbf{v}}{2} + \rho \varepsilon \right) + \text{div} \left(\left(\rho \frac{\mathbf{v} \cdot \mathbf{v}}{2} + \rho \varepsilon \right) \mathbf{v} \right) \\ & + \text{div } \mathbf{q} - \mathbf{v} \cdot \text{div } \mathbf{T} - \text{tr}(\mathbf{DT}) - \mathbf{v} \cdot \rho \mathbf{g} - \rho r = 0. \end{aligned} \quad (4.171)$$

This equation is the *energy balance equation in conservative form*. It can be considerably simplified if the differentiations of the product terms in the first line are performed according to the product rule of differentiation. The reader may then show that (4.171) may also be written as follows:

$$\begin{aligned} & \left(\frac{\mathbf{v} \cdot \mathbf{v}}{2} + \varepsilon \right) \underbrace{\left\{ \frac{\partial \rho}{\partial t} + \text{div}(\rho \mathbf{v}) \right\}}_{=0, \text{ balance of mass (4.69)}} \\ & + \mathbf{v} \cdot \underbrace{\left\{ \rho \left(\frac{\partial \mathbf{v}}{\partial t} + (\text{grad } \mathbf{v})\mathbf{v} \right) - \text{div } \mathbf{T} - \rho \mathbf{g} \right\}}_{=0, \text{ balance of momentum (4.110)}} \\ & + \left\{ \rho \underbrace{\left(\frac{\partial \varepsilon}{\partial t} + (\text{grad } \varepsilon) \cdot \mathbf{v} \right)}_{d\varepsilon/dt} + \text{div } \mathbf{q} - \text{tr}(\mathbf{DT}) - \rho r \right\} \\ & = 0 \end{aligned}$$

or

$$\rho \frac{d\varepsilon}{dt} = -\text{div } \mathbf{q} + \text{tr}(\mathbf{DT}) + \rho r. \quad (4.172)$$

This is the *local balance law of internal energy*. It states that the time rate of change of the internal energy multiplied by the density is balanced by the heat flow, $-\text{div } \mathbf{q}$, the power of working expressed in terms of the CAUCHY stress tensor, $\text{tr}(\mathbf{DT})$, and the radiating sources, ρr . We emphasise that there is no global counterpart to the local balance law of internal energy, and this is the manifestation of the expression that the first law is a law for the mechanical and thermal energies together and not just one of the two.

The energy equation (4.172) is not yet in its most convenient form for application in heat transport processes taking place in lakes. To arrive at a physically more

transparent form, we split \mathbf{T} into equilibrium and dynamical stresses, $\mathbf{T} = \mathbf{T}_{\text{eq}} + \mathbf{T}_{\text{dyn}}$, explicitly as follows:

$$\mathbf{T} = \mathbf{T}_{\text{eq}} + \mathbf{T}_{\text{dyn}} = -p\mathbf{1} + 2\eta(\mathbf{E}), \quad \mathbf{E} = \mathbf{D} - \frac{1}{3}(\text{div } \mathbf{v})\mathbf{1}. \quad (4.173)$$

Here p is the thermodynamic pressure and $\mathbf{T}_{\text{dyn}} = 2\eta\mathbf{E}$ describes the *viscous contribution to the stress*, η being the *dynamic shear viscosity* and \mathbf{E} the *deviator of the stretching tensor*. The parameterization (4.173) ignores the bulk viscosity, but the fluid may still be compressible (for details, see Sect. 4.3.3). With the representation (4.173) one may easily show that

$$\begin{aligned} \text{tr}(\mathbf{DT}) &= \text{tr} \left[\left(\mathbf{E} + \frac{1}{3}(\text{div } \mathbf{v})\mathbf{1} \right) (-p\mathbf{1} + 2\eta\mathbf{E}) \right] \\ &= -p \underbrace{\text{tr } \mathbf{E}}_0 - \frac{1}{3}p(\text{div } \mathbf{v})\text{tr } \mathbf{1} + 2\eta \text{tr}(\mathbf{E}^2) + \frac{1}{3}(\text{div } \mathbf{v})2\eta \underbrace{\text{tr } \mathbf{E}}_0 \\ &= -p \text{div } \mathbf{v} + 2\eta \text{tr}(\mathbf{E}^2) = p \frac{1}{\rho} \frac{d\rho}{dt} + 2\eta \text{tr}(\mathbf{E}^2) \\ &= -\rho p \frac{d}{dt} \left(\frac{1}{\rho} \right) + 2\eta \text{tr}(\mathbf{E}^2). \end{aligned} \quad (4.174)$$

Notice that the first term on the right-hand side of the last line can be interpreted as the power of working of the pressure on the changes of the specific volume, while the second term is the power of working of the viscous stress components and may be justly called *dissipation*. Substituting (4.174) into (4.172) transforms the local balance law of internal energy into the equation

$$\rho \left(\frac{d\varepsilon}{dt} + p \frac{d}{dt} \left(\frac{1}{\rho} \right) \right) = -\text{div } \mathbf{q} + 2\eta \text{tr } \mathbf{E}^2 + \rho r. \quad (4.175)$$

At this point it is instructive to also write down a second form of the balance law of internal energy. With the *enthalpy function* h defined by $h = \varepsilon + p(1/\rho)$, (4.175) also takes the form

$$\rho \frac{dh}{dt} - \frac{dp}{dt} = -\text{div } \mathbf{q} + 2\eta \text{tr } \mathbf{E}^2 + \rho r. \quad (4.176)$$

Equations (4.175) and (4.176) are equivalent to one another. Moreover, in their derivation it was carefully observed that the fluid may experience volume or density changes, and we implemented a NEWTONian stress representation (4.173) with zero bulk viscosity. To transform (4.175) into an equation for the temperature, constitutive relations for the heat flux vector \mathbf{q} and the internal energy must be given. We choose

$$\mathbf{q} = -\kappa \text{grad } T, \quad \varepsilon = c_v(T - T^*), \quad h = c_p(T - T^*), \quad (4.177)$$

in which T is temperature (measured in centigrades), T^* is a reference temperature, κ is the *heat conductivity* and c_v , c_p are the *specific heats at constant volume* and *constant pressure*, respectively. In (4.177) the representations for the internal energy ε and the enthalpy h are a thermodynamic approximation as in these equations the major influence is assigned to temperature changes. With (4.177), (4.175) and (4.176) become

$$\rho \left(c_v \frac{dT}{dt} + p \frac{d}{dt} \left(\frac{1}{\rho} \right) \right) = \text{div} (\kappa \text{ grad } T) + 2\eta \text{ tr } \mathbf{E}^2 + \rho r. \quad (4.178)$$

$$\rho c_p \frac{dT}{dt} - \frac{dp}{dt} = \text{div} (\kappa \text{ grad } T) + 2\eta \text{ tr } \mathbf{E}^2 + \rho r. \quad (4.179)$$

For a BOUSSINESQ fluid, density variations are ignored everywhere except in the buoyancy force. In this case $\mathbf{E} \simeq \mathbf{D}$ and $pd(1/\rho)/dt$ may be ignored. Thus, for a BOUSSINESQ fluid

$$\rho c_v \frac{dT}{dt} = \text{div} (\kappa \text{ grad } T) + 2\eta \text{ tr } \mathbf{D}^2 + \rho r. \quad (4.180)$$

This is the heat conduction equation usually written down in oceanography and lake physics texts, but in most situations it is further simplified by ignoring the dissipation $2\eta \text{ tr } \mathbf{D}^2$.

It is claimed, WÜEST et al. [16], that for deep lakes such as Lake Baikal, the pressure term $pd(1/\rho)/dt$ should not be ignored when density variations are significant. Then the energy equation takes the form (4.178) or (4.179) with the dissipation usually being ignored. Such a formulation deviates from the common equations of a BOUSSINESQ fluid.

4.5 Diffusion of Suspended Substances

Imagine that the lake water contains a number of substances either in solution or in suspension and that the content of these substances varies in space and time. Such substances are, for instance, minerals, oxygen O_2 , carbon dioxide CO_2 , phosphate, nitrate and other chemical elements that are important for the ecological conditions of the lake. Yet other substances can be algae or phytoplankta, which are distributed in the water, however, now not in solution but in suspension. The typical characterisation of the presence of such substances is that they arise in proportions relative to the water which are small, i.e. *the mass per volume of the mixture* (of lake water and tracer substances) of each of these tracers *is small* in comparison with the mixture mass. We shall henceforth denote any such substance contained in the water a *tracer*, a *component* or a *constituent*. A certain component can perform chemical reactions with a number of other components. For instance, phytoplankta absorb

CO₂ by photosynthesis and the amount of CO₂ that is absorbed depends, among other things, on the CO₂ content of the water and the amount of light available through solar irradiation. Zooplankta prey on phytoplankta etc.

In this section we shall not go into any details of these biochemical processes but only wish to derive the governing equations by which the transport of tracers in a fluid is described. It is conceptually very easy and essentially only consists of a statement of mass balance and a constitutive equation for mass flux, as we shall now see.

Let ρ^α be the mass density of the tracer α ($\alpha = 1, 2, \dots, \nu$) per unit mixture volume and \mathbf{v}^α its velocity. Then, the balance of mass for an infinitesimal cube consists of the following terms:

- Growth of the mass of tracer α in the element with volume $dV = dx_1 dx_2 dx_3$

$$\frac{\partial \rho^\alpha}{\partial t} dV.$$

- Flux of mass of constituent α through the six surface elements of the cube

$$-\left[\frac{\partial}{\partial x_1} (\rho^\alpha v_1^\alpha) + \frac{\partial}{\partial x_2} (\rho^\alpha v_2^\alpha) + \frac{\partial}{\partial x_3} (\rho^\alpha v_3^\alpha) \right] dV = -\text{div} (\rho^\alpha \mathbf{v}^\alpha) dV.$$

- Production of mass of constituent α within the volume element due to biochemical reactions

$$\pi^\alpha dV.$$

The first of these must equal the remaining two contributions so that

$$\frac{\partial \rho^\alpha}{\partial t} dV = -\text{div} (\rho^\alpha \mathbf{v}^\alpha) dV + \pi^\alpha dV$$

or

$$\frac{\partial \rho^\alpha}{\partial t} + \text{div} (\rho^\alpha \mathbf{v}^\alpha) = \pi^\alpha, \quad (\alpha = 1, 2, \dots, \nu). \quad (4.181)$$

In this equation, π^α is the production per unit time and unit volume of the mass of constituent α . Here, it is assumed that a functional form for it is known and provided by the lake biochemist.

Equation (4.181) holds not only for all tracer masses ($\alpha = 1, 2, \dots, \nu$) but also for the fluid in which they are suspended ($\alpha = \nu + 1$). It is convenient to write down the mass balance for the mixture as a whole rather than for the fluid in which the tracers are ‘suspended’. Summing all constituent balance laws (4.181) from $\alpha = 1$ to $\alpha = \nu + 1$, we obtain

$$\frac{\partial \sum_{\alpha=1}^{v+1} \rho^\alpha}{\partial t} + \operatorname{div} \left(\sum_{\alpha=1}^{v+1} \rho^\alpha \mathbf{v}^\alpha \right) = \sum_{\alpha=1}^{v+1} \pi^\alpha, \quad (4.182)$$

in which the expression on the right-hand side is the specific mass production of the mixture. Since mass cannot be produced but only exchanged between the various components, we necessarily have

$$\sum_{\alpha=1}^{v+1} \pi^\alpha = 0. \quad (4.183)$$

Defining the mixture density ρ and the *barycentric* velocity \mathbf{v} by

$$\rho = \sum_{\alpha=1}^{v+1} \rho^\alpha, \quad \mathbf{v} = \frac{1}{\rho} \sum_{\alpha=1}^{v+1} \rho^\alpha \mathbf{v}^\alpha \quad (4.184)$$

(4.182) takes the form

$$\frac{\partial \rho}{\partial t} + \operatorname{div} (\rho \mathbf{v}) = 0. \quad (4.185)$$

Mathematical models describing the dispersion of tracer masses in a liquid commonly operate with the balance laws of mass, momenta and energy of the mixture as a whole plus v mass balances for the constituents. This implies that the barycentric velocity field, the mixture density and temperature as well as the constituent mass fractions are the basic field variables. The latter are introduced as follows:

Definition 4.17 *The mass fraction or the mass concentration of tracer α is defined by*

$$c^\alpha := \frac{\rho^\alpha}{\rho} \implies \rho^\alpha = \rho c^\alpha. \quad (4.186)$$

■

With this definition, (4.181) is now written as

$$\frac{\partial (\rho c^\alpha)}{\partial t} + \operatorname{div} (\rho^\alpha (\mathbf{v}^\alpha - \mathbf{v})) + \operatorname{div} (\rho c^\alpha \mathbf{v}) = \pi^\alpha,$$

which, after performing the product differentiation, yields

$$\begin{aligned} & \underbrace{c^\alpha \left(\frac{\partial \rho}{\partial t} + \operatorname{div} (\rho \mathbf{v}) \right)}_{=0, \text{ see (4.185)}} + \rho \underbrace{\left(\frac{\partial c^\alpha}{\partial t} + (\operatorname{grad} c^\alpha) \mathbf{v} \right)}_{\mathrm{d}c^\alpha/\mathrm{d}t} \\ &= -\operatorname{div} (\rho^\alpha (\mathbf{v}^\alpha - \mathbf{v})) + \pi^\alpha \end{aligned}$$

or

$$\rho \frac{dc^\alpha}{dt} = -\operatorname{div} \mathbf{j}^\alpha + \pi^\alpha. \quad (4.187)$$

Definition 4.18 *The vector*

$$\mathbf{j}^\alpha = \rho^\alpha (\mathbf{v}^\alpha - \mathbf{v}) \quad (4.188)$$

is called the diffusive mass flux of tracer α . ■

Equation (4.187) is called *Fick's second law* [4]. It equates the time rate of change of the mass of constituent α to the flux of this constituent through the body boundary plus the rate of its production per unit volume and could equally have been derived from the global law

$$\frac{d}{dt} \int_V \rho^\alpha dV = - \int_{\partial V} \mathbf{j}^\alpha \cdot \mathbf{n} dA + \int_V \pi^\alpha dV. \quad (4.189)$$

It is noted that the velocity used to evaluate the material derivative dc^α/dt is \mathbf{v} (not \mathbf{v}^α) and that \mathbf{v}^α arises only implicitly in the definition of the diffusive flux \mathbf{j}^α . In fact, it is the difference velocity $(\mathbf{v}^\alpha - \mathbf{v})$ by which the diffusive mass flux vector is defined; it is the excess of the velocity with which the tracer α moves relative to the mixture. It is not the purpose in diffusion theory to treat \mathbf{v}^α as an independent field. On the contrary, one regards the motion of the mixture with velocity \mathbf{v} as one of the basic variables. Of course, such a procedure is meaningful only if the magnitude of the difference velocity $|\mathbf{v}^\alpha - \mathbf{v}|$ is *small*: $|\mathbf{v}^\alpha - \mathbf{v}| \ll |\mathbf{v}|$. If a tracer particle is exactly moving with the mixture velocity, then this slip velocity is exactly zero, and (4.187) would take the form

$$\rho \frac{dc^\alpha}{dt} = \pi^\alpha, \quad (4.190)$$

valid without diffusion. In general, however, there is a small slip between a tracer α and the mixture so that a parameterisation of the diffusive mass flux vector is needed.

There is not much intuition needed to recognise that if ink is inserted into a container with still water, it will spread. It obviously flows from high concentration to lower concentration and will, after sufficient time, be uniformly distributed in the entire container. This observation may be a motivation to postulate a constitutive relation for the diffusive mass flux of a single constituent in the form

$$\mathbf{j} = -\rho D \operatorname{grad} c. \quad (4.191)$$

Geometrically, this equation says that the tracer at a point \mathbf{x} in space moves into the direction of steepest decent of the ‘topography $c(\mathbf{x}, t)$ ’ and the size of this speed is equal to the coefficient ρD , where ρ is the mixture density and D is called *diffusivity with dimension* $\text{m}^2 \text{s}^{-1}$. Equation (4.191) is called *Fick’s first law*²⁴ [4]. More generally, when there are several tracers present, a law such as (4.191) must be formulated for each constituent

$$\mathbf{j}^\alpha = - \sum_{\beta=1}^v \rho D^{\alpha\beta} \text{grad } c^\beta \quad (\alpha = 1, 2, \dots, v), \quad (4.192)$$

where $D^{\alpha\beta}$ ($\alpha, \beta = 1, 2, \dots, v$) are now diffusion coefficients and one generally supposes that $D^{\alpha\beta} = D^{\beta\alpha}$. Moreover, *it is a consequence of the second law of thermodynamics that $D^{\alpha\beta}$ is a non-negative definite $v \times v$ matrix*, a statement which we shall accept here without proof. Often, a diffusion process of a tracer α is not affected by a corresponding process of the tracer β . This suggests that the diffusive mass flux \mathbf{j}^α might in this case only be affected by the gradient of its own concentration c^α so that (4.192) reduces to

$$\mathbf{j}^\alpha = -\rho D^{\alpha\alpha} \text{grad } c^\alpha \quad (\text{no sum over } \alpha). \quad (4.193)$$

This is a simplification that is very often used in the parameterisation of diffusion processes.

Substitution of (4.192) into (4.187) yields

$$\rho \frac{dc^\alpha}{dt} = \sum_{\beta=1}^v \text{div} \{ \rho D^{\alpha\beta} \text{grad } c^\beta \} + \pi^\alpha \quad (\alpha = 1, 2, \dots, v). \quad (4.194)$$

These are v equations for the v concentrations c^α , in which the production terms are considered to be known. The material derivative of c^α

$$\frac{dc^\alpha}{dt} = \frac{\partial c^\alpha}{\partial t} + (\text{grad } c^\alpha) \mathbf{v} \quad (4.195)$$

involves the mixture (or barycentric) velocity \mathbf{v} which, together with the mixture density ρ , is described by the equations of motion and the mass balance equation of the fluid.

In a BOUSSINESQ *fluid* the density variations are very small²⁵ and are thus ignored in describing the diffusion problem so that (4.194) simplifies to

²⁴ For a fundamental paper on diffusion, see also [3].

²⁵ For lake and ocean water the relative density difference $\Delta\rho/\rho$ is generally between 10^{-2} and 10^{-3} and thus negligible. In the atmosphere, under usual conditions, $\Delta\rho/\rho$ seldom reaches values 10^{-1} or larger; this equally often justifies the application of the BOUSSINESQ assumption.

$$\frac{dc^\alpha}{dt} = \sum_{\beta=1}^v \operatorname{div} (D^{\alpha\beta} \operatorname{grad} c^\beta) + \bar{\pi}^\alpha \quad (\alpha = 1, 2, \dots, v), \quad (4.196)$$

in which $\bar{\pi}^\alpha = \pi^\alpha / \rho$ is the mass production of constituent α per unit time and unit mixture mass. If the reduced diffusive mass flux parameterisation (4.193) is used

$$\frac{dc^\alpha}{dt} = \operatorname{div} (D^{\alpha\alpha} \operatorname{grad} c^\alpha) + \bar{\pi}^\alpha \quad (\alpha = 1, 2, \dots, v), \quad (4.197)$$

This equation is formally the same as the energy equation (4.180), if in the latter dissipation is ignored. Equation (4.197) allows a coupling of the various tracers only through the production terms.

This completes the formal derivation of the basic equations generally used in lake physics. In subsequent chapters they will no longer be derived but only referred to.

4.6 Summary of Equations

Because the derivation of the preceding equations is rather long and it is difficult to isolate the significant statements, we shall now repeat the balance laws of mass, momentum energy and tracer mass in their local form at one place. This will be done in a form that is particularly useful for the applications which will follow in the subsequent chapters. These balance laws are

$$(4.70) \quad \frac{d\rho}{dt} + \rho \operatorname{div} \mathbf{v} = 0, \quad (4.198)$$

$$(4.110) \quad \rho \mathbf{a}_{\text{abs}} = \operatorname{div} \mathbf{T} + \rho \mathbf{g}, \quad (4.199)$$

$$(4.172) \quad \rho \frac{d\varepsilon}{dt} = -\operatorname{div} \mathbf{q} + \operatorname{tr}(\mathbf{T} \mathbf{D}) + \rho r, \quad (4.200)$$

$$(4.187) \quad \rho \frac{dc^\alpha}{dt} = -\operatorname{div} \mathbf{j}^\alpha + \pi^\alpha, \quad (4.201)$$

in which

$$(4.132) \quad \mathbf{a}_{\text{abs}} = \mathbf{a}_0 + \frac{d\mathbf{v}}{dt} + \boldsymbol{\omega} \times (\boldsymbol{\omega} \times \mathbf{x}) + \dot{\boldsymbol{\omega}} \times \mathbf{x} + 2\boldsymbol{\omega} \times \mathbf{v}. \quad (4.202)$$

The equation numbers on the left-hand side refer to where the respective equations have been stated in this form.

Equations (4.198), (4.199), (4.200), (4.201) and (4.202) shall be specialised for a moving frame that is fixed on the Earth with the x -axis pointing towards east, the y -axis pointing towards north and the z -axis pointing towards the zenith, Fig. 2.3. This is the standard frame used in meteorology and oceanography. The translational motion of this frame on the elliptical orbit of the Earth is ignored so that $\mathbf{a}_0 \approx \mathbf{0}$. Furthermore, the angular velocity of the Earth, from now on always denoted by $\boldsymbol{\Omega}$

(since ω will be reserved for frequency), is assumed to be constant so that $\dot{\boldsymbol{\Omega}} = \mathbf{0}$. Moreover, it is customary to absorb the centrifugal force into the gravity term, since

$$\boldsymbol{\Omega} \times (\boldsymbol{\Omega} \times \mathbf{x}) = -\text{grad} \left(\frac{\Omega^2(x^2 + y^2)}{2} \right). \quad (4.203)$$

All this implies that

$$\mathbf{a}_{\text{abs}} = \frac{d\mathbf{v}}{dt} + 2\boldsymbol{\Omega} \times \mathbf{v}, \quad \mathbf{g} - \boldsymbol{\Omega} \times (\boldsymbol{\Omega} \times \mathbf{x}) \rightarrow \mathbf{g}, \quad (4.204)$$

If we then also use (4.116) and (4.120) and write

$$\mathbf{T} = -p\mathbf{1} + \mathbf{T}_{\text{dyn}}, \quad (4.205)$$

the above equations (4.198), (4.199), (4.200) and (4.201) take the forms

$$\frac{d\rho}{dt} + \rho \operatorname{div} \mathbf{v} = 0, \quad (4.206)$$

$$\rho \left\{ \frac{d\mathbf{v}}{dt} + 2\boldsymbol{\Omega} \times \mathbf{v} \right\} = -\text{grad } p + \operatorname{div} \mathbf{T}_{\text{dyn}} + \rho \mathbf{g}, \quad (4.207)$$

$$\rho \left\{ \frac{d\varepsilon}{dt} + p \frac{d}{dt} \left(\frac{1}{\rho} \right) \right\} = -\operatorname{div} \mathbf{q} + \operatorname{tr} (\mathbf{T}_{\text{dyn}} \mathbf{D}) + \rho r, \quad (4.208)$$

$$\rho \frac{dc^\alpha}{dt} = -\operatorname{div} \mathbf{j}^\alpha + \pi^\alpha. \quad (4.209)$$

A number of approximations that are common in limnology and oceanography derive from these equations.

- In the **free convection approximation** use is made of the fact that $\rho = \rho_0(z) + \rho'(x, y, z, t)$, where $|\rho'| \ll |\rho_0(z)|$. Therefore the density is replaced by its static counterpart $\rho_0(z)$ everywhere except in the gravity force, and $d\rho/dt$ is ignored. This yields the system

$$\operatorname{div} \mathbf{v} = 0, \quad (4.210)$$

$$\rho_0(z) \left\{ \frac{d\mathbf{v}}{dt} + 2\boldsymbol{\Omega} \times \mathbf{v} \right\} = -\text{grad } p + \operatorname{div} \mathbf{T}_{\text{dyn}} + \rho \mathbf{g}, \quad (4.211)$$

$$\rho_0(z) \frac{d\varepsilon}{dt} = -\operatorname{div} \mathbf{q} + \operatorname{tr} (\mathbf{T}_{\text{dyn}} \mathbf{D}) + \rho_0(z)r, \quad (4.212)$$

$$\rho_0(z) \frac{dc^\alpha}{dt} = -\operatorname{div} \mathbf{j}^\alpha + \pi^\alpha. \quad (4.213)$$

- The **BOUSSINESQ approximation** goes one small step further in the approximation and replaces in (4.210), (4.211), (4.212) and (4.213) $\rho_0(z)$ everywhere by ρ^* , a constant reference value, viz.

$$\operatorname{div} \mathbf{v} = 0, \quad (4.214)$$

$$\rho^* \left\{ \frac{d\mathbf{v}}{dt} + 2\boldsymbol{\Omega} \times \mathbf{v} \right\} = -\operatorname{grad} p + \operatorname{div} \mathbf{T}_{\text{dyn}} + \rho \mathbf{g}, \quad (4.215)$$

$$\rho^* \frac{d\varepsilon}{dt} = -\operatorname{div} \mathbf{q} + \operatorname{tr}(\mathbf{T}_{\text{dyn}} \mathbf{D}) + \rho^* r, \quad (4.216)$$

$$\rho^* \frac{dc^\alpha}{dt} = -\operatorname{div} \mathbf{j}^\alpha + \pi^\alpha. \quad (4.217)$$

A fluid obeying these equations is often simply referred to as a *BOUSSINESQ fluid*.

- For wave studies the dissipative terms arising in the above equations are often ignored. Equations (4.210), (4.211), (4.212) and (4.213) then reduce to

$$\operatorname{div} \mathbf{v} = 0, \quad (4.218)$$

$$\rho_0(z) \left\{ \frac{d\mathbf{v}}{dt} + 2\boldsymbol{\Omega} \times \mathbf{v} \right\} = -\operatorname{grad} p + \rho \mathbf{g}, \quad (4.219)$$

$$\frac{d\varepsilon}{dt} = r, \quad (4.220)$$

$$\rho_0(z) \frac{dc^\alpha}{dt} = \pi^\alpha \quad (4.221)$$

and (4.214), (4.215), (4.216) and (4.217) become

$$\operatorname{div} \mathbf{v} = 0, \quad (4.222)$$

$$\rho^* \left\{ \frac{d\mathbf{v}}{dt} + 2\boldsymbol{\Omega} \times \mathbf{v} \right\} = -\operatorname{grad} p + \rho \mathbf{g}, \quad (4.223)$$

$$\frac{d\varepsilon}{dt} = r, \quad (4.224)$$

$$\rho^* \frac{dc^\alpha}{dt} = \pi^\alpha. \quad (4.225)$$

In the oceanographic literature this reduction is often referred to as the *adiabaticity assumption*,²⁶ but it is obvious to the reader versatile in thermodynamics, it has nothing in common with the classical adiabaticity assumption of thermodynamics.

- If the specific radiation and all tracer mass productions vanish,

$$r = 0, \quad \pi^\alpha = 0, \quad \text{for all } \alpha = 1, \dots, v, \quad (4.226)$$

²⁶ In this assumption not only the diffusive flux terms in the momentum, energy and tracer mass equations but also the power of working in the energy equation are omitted. Because of the omission of the diffusive terms the momentum, energy and tracer mass balance equations change their type from parabolic to hyperbolic.

and if $\varepsilon = \int_{T_0}^T c(\bar{T}) d\bar{T}$, then $\frac{d\varepsilon}{dt} = c(T) \frac{dT}{dt}$ so that the energy and tracer mass balance equations reduce to

$$\frac{dT}{dt} = 0, \quad \frac{dc^\alpha}{dt} = 0, \quad \text{for all } \alpha = 1, \dots, v. \quad (4.227)$$

The temperature and the tracer concentrations are materially constant in this case. With the thermal equation of state

$$\rho = \hat{\rho}(T, c^\alpha) \quad (4.228)$$

we may now deduce

$$\frac{d\rho}{dt} = \frac{\partial \hat{\rho}}{\partial T} \underbrace{\frac{dT}{dt}}_0 + \frac{\partial \hat{\rho}}{\partial c^\alpha} \underbrace{\frac{dc^\alpha}{dt}}_0 = 0, \quad (4.229)$$

implying that the density is also materially constant. The above equations thus take the forms

$$\operatorname{div} \mathbf{v} = 0, \quad (4.230)$$

$$\rho_0(z) \left\{ \frac{d\mathbf{v}}{dt} + 2\boldsymbol{\Omega} \times \mathbf{v} \right\} = -\operatorname{grad} p + \rho \mathbf{g}, \quad (4.231)$$

$$\frac{d\rho}{dt} = 0, \quad (4.232)$$

which constitute a drastic simplification as compared to (4.218), (4.219), (4.220) and (4.221). In a BOUSSINESQ fluid $\rho_0(z)$ is simply replaced by ρ^* . In the literature, (4.232) is sometimes claimed to be the result of the continuity equation, but as the derivation shows, it follows from a reduction of the energy and tracer mass balances and a special form of the thermal equation of state.

- The last transformation makes use of

$$\begin{aligned} p &= p_0(z) + p', & \rho &= \rho_0(z) + \rho', \\ p_0(z) &= \rho_0(z)g(z-h), \end{aligned} \quad (4.233)$$

where h is a constant. This implies

$$\frac{d\rho}{dt} = \frac{\partial \rho'}{\partial t} - \rho^* \frac{N^2}{g} w, \quad N^2(z) = -\frac{g}{\rho^*} \frac{d\rho_0(z)}{dz} \quad (4.234)$$

so that the BOUSSINESQ approximated equations (4.230), (4.231) and (4.232) take the forms

$$\operatorname{div} \mathbf{v} = 0, \quad (4.235)$$

$$\rho^* \left\{ \frac{d\mathbf{v}}{dt} + 2\boldsymbol{\Omega} \times \mathbf{v} \right\} = -\operatorname{grad} p' + \rho' \mathbf{g}, \quad (4.236)$$

$$\frac{\partial \rho'}{\partial t} - \rho^* \frac{N^2}{g} w = 0. \quad (4.237)$$

Note that for a particular ‘ground’ stratification the BRUNT–VÄISÄLÄ or buoyancy frequency $N(z)$ is a given prescribed function of z .

4.7 A First Look at the Boussinesq and Shallow-Water Equations

One of the prominent approximations which has fruitfully influenced the mathematical analysis of a large number of problems of geophysical fluid dynamics and led to considerable enlightenment of the physical understanding of flow problems in limnology, meteorology and oceanography is the so-called *shallow-water approximation*. It takes account of the fact that many processes of the dynamics of the atmosphere, the ocean and lakes have scales that are large in the horizontal and small in the vertical directions. For instance, typical wavelengths of atmospheric or water disturbances may be many kilometres, while the corresponding amplitudes are at most 100 m, and usually much less. Similarly, horizontal velocity components are generally large, while vertical velocity components are small. This suggests to introduce *aspect ratios*

$$\mathcal{A}_L := \frac{\text{typical vertical length scale}}{\text{typical horizontal length scale}},$$

$$\mathcal{A}_V := \frac{\text{typical vertical velocity scale}}{\text{typical horizontal velocity scale}},$$

to suppose that $\mathcal{A}_L \ll 1$, $\mathcal{A}_V \ll 1$ and to look at the governing equations in the limit as $\mathcal{A}_L \rightarrow 0$ and $\mathcal{A}_V \rightarrow 0$.

To compare the magnitudes of the various terms arising in the equations, e.g. (4.206), (4.207), (4.208) and (4.209), for the processes of interest, we transform them into dimensionless form by writing each physical quantity Ψ as $\Psi = [\Psi] \bar{\Psi}$. $[\Psi]$ is a typical value of the field Ψ for the processes under consideration, and $\bar{\Psi}$ is its dimensionless counterpart, of necessity of order unity, if $[\Psi]$ is appropriately chosen.

In the ensuing analysis, our intention will be to justify not only the shallow-water equations but equally also the BOUSSINESQ assumption. Thus we start with equations (4.206), (4.207), (4.208) and (4.209) in which all dissipation terms will be ignored²⁷ (adiabaticity!) and radiation and tracer mass productions will be neglected. The equations then read

²⁷ The more general case will be dealt with later.

$$\frac{\partial \rho}{\partial t} + \operatorname{div}(\rho \mathbf{v}) = 0, \quad (4.238)$$

$$\rho \left\{ \frac{\partial \mathbf{v}}{\partial t} + (\operatorname{grad} \mathbf{v}) \mathbf{v} + 2\boldsymbol{\Omega} \times \mathbf{v} \right\} = -\operatorname{grad} p + \rho \mathbf{g}, \quad (4.239)$$

$$\rho \left\{ \frac{\partial \varepsilon}{\partial t} + (\operatorname{grad} \varepsilon) \cdot \mathbf{v} - \frac{p}{\rho^2} \left[\frac{\partial \rho}{\partial t} + (\operatorname{grad} \rho) \cdot \mathbf{v} \right] \right\} = 0, \quad (4.240)$$

$$\rho \left\{ \frac{\partial c^\alpha}{\partial t} + (\operatorname{grad} c^\alpha) \cdot \mathbf{v} \right\} = 0, \quad \alpha = 1, \dots, \nu. \quad (4.241)$$

In the coordinate system of Fig. 2.3 the angular velocity of the Earth is represented by

$$\boldsymbol{\Omega} = \left(0, \frac{1}{2} \tilde{f}, \frac{1}{2} f \right), \quad f = 2\Omega \sin \phi, \quad \tilde{f} = 2\Omega \cos \phi, \quad (4.242)$$

in which f and \tilde{f} are the *first* and *second Coriolis parameters*, respectively, $\Omega = |\boldsymbol{\Omega}|$ and ϕ is the geographical latitude. Moreover, we shall choose

$$\varepsilon = c_v(T - T_0) \quad (4.243)$$

with constant c_v and constant T_0 . This implies that the energy equation is formulated in terms of internal energy rather than enthalpy. In oceanography, it seems to be the more popular approach.

We shall select the scales according to²⁸

$$\begin{aligned} (x, y, z) &= ([L]\bar{x}, [L]\bar{y}, [H]\bar{z}), \\ (u, v, w) &= \left([V]\bar{u}, [V]\bar{v}, [V]\frac{[H]}{[L]}\bar{w} \right), \\ (t, f, \tilde{f}) &= \left(\frac{1}{[f]}\bar{t}, [f]\bar{f}, [f]\bar{\tilde{f}} \right), \\ p &= \rho^* g z + \rho^* [f V L] \bar{p}, \\ \rho &= \rho^* (1 + [\sigma] \sigma), \\ T &= T_0 + [\Delta T] \theta, \\ c^\alpha &= [c^\alpha] \bar{c}^\alpha. \end{aligned} \quad (4.244)$$

It is seen that horizontal and vertical velocities are scaled differently and time is scaled with the CORIOLIS parameter. Furthermore, the scale for the vertical velocity

²⁸ Note that time is scaled here with a typical value of the CORIOLIS parameter. This automatically emphasises that processes are influenced by the rotation of the Earth. In problems where this is not important, time is scaled with $[H/V]$ or $[L/V]$. In those cases the choice $[H/V]$ leads to the shallow-water equations, while $[L/V]$ need to be chosen for avalanche equations and gravity currents, see [7, 12].

is such that $\mathcal{A}_L = [H]/[L] = \mathcal{A}_V = \mathcal{A}$. This choice guarantees that the divergence $\text{div } \mathbf{v}$ is preserved under non-dimensionalisation. Moreover, the pressure is decomposed into a hydrostatic part $\rho^* g z$ and a dynamic contribution $\rho^* [f V L] \bar{p}$. Of particular importance is how the density is scaled. It is assumed implicitly that density variations are small and for water $\rho^* \sim 1000 \text{ kg m}^{-3}$ and $[\sigma] \approx 10^{-3}$. Typical values for the scales are shown in Table 4.1.

Writing (4.238), (4.239), (4.240) and (4.241) in Cartesian component form and using (4.242), (4.243) and subsequently non-dimensionalising the emerging equations with the aid of (4.244), it can be shown that these non-dimensional equations take the following forms (the overbars are omitted):

$$\frac{[\sigma]}{\mathcal{R}_0} \frac{\partial \sigma}{\partial t} + \text{div } \mathbf{v} + [\sigma] \text{div } (\sigma \mathbf{v}) = 0, \quad (4.245)$$

$$(1 + [\sigma] \sigma) \left\{ \frac{\partial u}{\partial t} + \mathcal{R}_0 (\text{grad } u) \cdot \mathbf{v} + \mathcal{A} \tilde{f} w - f v \right\} = - \frac{\partial p}{\partial x}, \quad (4.246)$$

$$(1 + [\sigma] \sigma) \left\{ \frac{\partial v}{\partial t} + \mathcal{R}_0 (\text{grad } v) \cdot \mathbf{v} + f u \right\} = - \frac{\partial p}{\partial y}, \quad (4.247)$$

$$(1 + [\sigma] \sigma) \left\{ \mathcal{A}^2 \left[\frac{\partial w}{\partial t} + \mathcal{R}_0 (\text{grad } w) \cdot \mathbf{v} \right] - \mathcal{A} \tilde{f} u \right\} = - \frac{\partial p}{\partial z} - \mathcal{B} \sigma, \quad (4.248)$$

$$(1 + [\sigma] \sigma) \left\{ \left[\frac{\partial \theta}{\partial t} + \mathcal{R}_0 (\text{grad } \theta) \cdot \mathbf{v} \right] - \mathcal{C} \frac{\mathcal{B} z + [\sigma] p}{(1 + [\sigma] \sigma)^2} \left[\frac{\partial \sigma}{\partial t} + \mathcal{R}_0 (\text{grad } \sigma) \cdot \mathbf{v} \right] \right\} = 0, \quad (4.249)$$

$$(1 + [\sigma] \sigma) \left\{ \frac{\partial c^\alpha}{\partial t} + \mathcal{R}_0 (\text{grad } c^\alpha) \cdot \mathbf{v} \right\} = 0, \quad (\alpha = 1, 2, \dots, \nu). \quad (4.250)$$

All variables in these equations including the operators are dimensionless. The dimensionless calligraphic parameters are listed in Table 4.2 with their common nomenclature and orders of magnitude as obtained with the scales of Table 4.1.

Table 4.1 Physical parameters and typical orders of magnitude for the scales arising in (4.244)

$[f] \simeq 10^{-4} \text{ s}^{-1}$	Coriolis parameter
$\rho^* = 10^3 \text{ kg m}^{-3}$	Density
$[\sigma] \simeq 10^{-3}$	Density anomaly
$T_0 \simeq 10^\circ \text{C}$	Reference temperature
$[\Delta T] \simeq 10^\circ \text{C}$	Temperature range
$[L] \simeq 10^4 - 10^6 \text{ m}$	Horizontal length scale
$[H] \simeq 10 - 10^3 \text{ m}$	Vertical length scale
$[V] \simeq 10^{-2} - 10 \text{ m s}^{-1}$	Horizontal velocity scale
$c_p \simeq 4200 \text{ m}^2 \text{ s}^{-2} \text{ K}^{-1}$	Specific heat at constant pressure (10^5 Pa)
$c_v \simeq 4200 \text{ m}^2 \text{ s}^{-2} \text{ K}^{-1}$	Specific heat at constant volume
$[c^\alpha]$	Scale for mass fraction of constituents

Table 4.2 Dimensionless parameters

$\mathcal{A} = \frac{[H]}{[L]}$	$10^{-5} - 10^{-2}$	Aspect ratio
$\mathcal{R}_0 = \frac{[V]}{[f][L]}$	$10^{-4} - 10^0$	ROSSBY number
$[\sigma]$	10^{-3}	Density anomaly
$\mathcal{B} = \frac{g[\sigma][H]}{[f][V][L]}$	$\sim 10^{-1}$	Buoyancy parameter BOUSSINESQ number
$\mathcal{C} = \frac{[f][L][V]}{c_p[\Delta T]}$	$\sim 10^{-6} - 10^{-2}$	Pressure work parameter

Depending upon the orders of magnitude of the dimensionless parameters, various versions of the field equations emerge. Of particular interest for us are \mathcal{A} , $[\sigma]$ and \mathcal{C} . Their relative values suggest that approximations which will now formally be defined.

Definition 4.19 A BOUSSINESQ fluid is defined by (4.245), (4.246), (4.247), (4.248), (4.249) and (4.250), if the limit $[\sigma] \rightarrow 0$ is considered, while all other dimensionless parameters are held fixed. ■

Inspection of (4.245)–(4.250) shows that the mass balance equation reduces in this approximation to the continuity equation, $\operatorname{div} \mathbf{v} = 0$, since it is supposed that with $[\sigma] \rightarrow 0$, $[\sigma]/\mathcal{R}_0 \rightarrow 0$ also holds.²⁹ Furthermore, the factor $(1 + [\sigma]\sigma)$ on the left-hand sides of (4.246), (4.247), (4.248), (4.249) and (4.250) reduces to 1. This reduction is tantamount to assuming that the density is kept constant in all those terms of the physical balance laws which have the form $\rho d\Psi/dt = \dots$. However in (4.249) there is a further reduction, namely in the pressure work term that involves \mathcal{C} . This term is also usually missing in oceanographic and limnological applications.

Problem 4.6 Consider Lake Baikal and perform a scale analysis, i.e. substitute appropriate values for the scales and show that there are reasons for $\mathcal{B} \sim 1$ and $\mathcal{C} \sim 10^{-1}$ so that the pressure work term in the energy equation may not be ignored in this case. Show, equally, that the same also holds true for the deep ocean. ♦

For all ‘regular’ cases it is, however, justified to ignore the pressure work term. In this case the BOUSSINESQ approximated equations arise in their familiar form as stated in (4.222), (4.223), (4.224) and (4.225) (with non-vanishing radiation and tracer mass productions).

²⁹ Actually, it follows from Table (4.2) that $\mathcal{R}_0 \leq 10^{-3}$, $[\sigma]/\mathcal{R}_0$ is of order unity or larger. In such a case, the term involving $\partial\sigma/\partial t$ in (4.245) should not be dropped. This situation is studied, e.g., in BEREZIN and HUTTER [2].

Definition 4.20 *The shallow-water equations are those physical balance laws of mass, momentum, energy and tracer mass that emerge in the limit as the aspect ratio A becomes infinitely small, $A \rightarrow 0$, while all other dimensionless scale parameters are kept constant. This process is called the **shallow-water approximation**. ■*

Inspection shows that in (4.245), (4.246), (4.247), (4.248), (4.249) and (4.250) the aspect ratio arises at two significant places:³⁰ (i) linearly as a multiplier of the second Coriolis parameter and (ii) quadratically as a multiplier of dw/dt . Invoking the shallow-water approximation shows first that *the second Coriolis parameter disappears from all the equations*. Tracing this back to its origin, the assumption $\tilde{f} = 0$ means that of the angular velocity of the Earth, the component tangential to the Globe is ignored and only the component pointing towards the zenith is accounted for, see Fig. 2.3. A second consequence of the shallow-water assumption is that in the vertical momentum equation (4.248) the left-hand side vanishes, thus reducing the vertical momentum balance law to a force balance between the vertical component of the pressure gradient and the gravity (buoyancy) force; in physical-dimensional variables

$$-\frac{\partial p}{\partial z} - \rho g = 0. \quad (4.251)$$

Definition 4.21 *The reduction of the vertical momentum balance law to a balance between the vertical component of the pressure gradient and the gravity force is called the **hydrostatic pressure assumption**. ■*

It follows that *the shallow-water approximation implies the hydrostatic pressure assumption but not vice versa*. Indeed when invoking the hydrostatic pressure assumption the term $A\tilde{f}w$ in the x component (east!) of the momentum balance survives. *The two assumptions are equivalent only when the frame of reference is inertial*. Alternatively, in a perturbative improvement of the shallow-water equations the Coriolis effects involving \tilde{f} are more important than the vertical accelerations dw/dt .

Finally, (4.245), (4.246), (4.247), (4.248), (4.249) and (4.250) indicate when the convective terms may be ignored. Their neglect is justified when the ROSSBY number \mathcal{R}_0 is small. For long waves with small velocities, this is generally the case but is not justified when large amplitudes are considered.

³⁰ Equations (4.245), (4.246), (4.247), (4.248), (4.249) and (4.250) are already reduced by omitting all dissipative terms. Written in full length, the aspect ratio would also arise quadratically in those terms.

References

1. Batchelor, G.K.: *An Introduction to Fluid Mechanics*, Cambridge University Press, Cambridge (1967)
2. Berezin, Y.A. and Hutter, K.: On large scale vertical structures in incompressible fluids with thermal expansion. *Math. Models Methods Appl. Sci.* **7**, 113–123 (1997)
3. Einstein, A.: Über die von der molekularkinetischen Theorie der Wärme geforderte Bewegung von in ruhenden Flüssigkeiten suspendierten Teilchen. *Annalen der Physik* **17**, 549–560 (1905)
4. Fick, A.: Über Diffusion. *Poggendorff's Annalen der Physik* **94**, 59–86 (1855)
5. Gurtin, M.E.: *An Introduction to Continuum Mechanics*. Academic, New York, NY, 265 p. (1981)
6. Hutter, K.: Waves and oscillations in the ocean and in lakes. In: *Continuum Mechanics in Environmental Science and Geophysics*. (ed. Hutter, K.) Lecture Notes No. **337**, International Centre for Mechanical Sciences, Udine, Italy, Springer New York NY, 522 p. (1993)
7. Hutter, K.: Avalanche dynamics. In: *Hydrology of Disasters*. (ed. Singh, V.P.) Kluwer, Dordrecht, 317–394 (1996)
8. Hutter, K. and Jöhnk, K.: *Continuum Methods of Physical Modeling*. Springer, Berlin, 635 p. (2004)
9. Müller, I.: *Thermodynamics*. Pitman, 521 p. (1985)
10. Newton, I.: *Philosophiae naturalis pricipia mathematica*. London (1687) (1st edition); (1713) (2nd edition); (1726) (3rd edition)
11. Prandtl, L.: Bericht über Untersuchungen zur ausgebildeten Turbulenz. *Zeitschrift für angewandte Mathematik und Mechanik (ZAMM)*, **5** (2), 136–139 (1925)
12. Pudasaini, S.P. and Hutter, K.: *Avalanche Dynamics – Dynamics of rapid flows of dense granular avalanches*, Springer, Berlin, 602 p. (2007)
13. Stommel, H. and Moore, D.W.: *An Introduction to the Coriolis Force*. Columbia University Press, New York, NY (1989)
14. Truesdell, C.A.: *Rational Thermodynamics*. 2nd edition. Springer, Berlin, 578 p. (1984)
15. Truesdell, C.A. and Noll, W.: The non-linear field theories of mechanics In: *Encyclopedia of Physics*, Vol. **III/3** (ed. Flügge, S.) Springer, Berlin, 602 p. (1965)
16. Wüest, A., Ravens, T.M., Granin, N.G., Kocsis, O., Schurter, M. and Sturm, M.: Cold intrusions in Lake Baikal: Direct observational evidence for deep-water renewal. *Limnol. Oceanogr.* **50** (1), 184–196 (2005)

Chapter 5

Conservation of Angular Momentum–Vorticity

We have expressed the fundamental physical ideas – that mass, momentum and energy must be conserved – in the form of mathematical equations (balance laws) and demonstrated that the balance of moment of momentum in its local expression for a continuum requests that the (CAUCHY) stress tensor is symmetric, but beyond this does not produce any further local equation. So, it appears that the conservation law of moment of momentum is superfluous. This is not so; correct is that by requesting the CAUCHY stress to be symmetric and exploiting pointwise the balances of mass, momentum and energy then automatically also guarantee the balance law of angular momentum to be identically satisfied. However, since physically, linear momentum is associated with the *translational* motion and angular momentum with the *rotatory* motion, the rotational behavior can often better be identified if the law of balance of angular momentum is explicitly employed.

Up to now, we did not actually use the information contained in the law of conservation of angular momentum; however, lake, sea and ocean waters exhibit rotatory motions of all scales, from basin-wide gyres down to the smallest swirls and eddies (see Fig. 5.1). Conservation of moment of momentum imposes significant constraints on natural flows. Fluid mechanics possesses a number of intricate propositions related to the idea of conservation of rotatory motion to the water itself, but equally also to ‘water structures’ like gyres, gravity currents and large streams. In this chapter our intention is to analyse the phenomena ‘rotation’, ‘circulation’, ‘vorticity’ via a somewhat deeper approach and to use the inferences in the context of lake or ocean dynamics.

5.1 Circulation

Our focus will be mostly ideal (inviscid) fluids, but not exclusively. We begin with

Definition 5.1 *Let \mathcal{C} be a closed, smooth, simple, i.e. double-point free material line in \mathbb{R}^3 . The circulation of a flow field along \mathcal{C} is then defined as the line integral*

$$\Gamma := \oint_{\mathcal{C}} \mathbf{v}(\mathbf{x}, t) \cdot d\mathbf{x}, \quad (5.1)$$

Fig. 5.1 Various vortical motions visible due to phytoplankton bloom in the Baltic Sea on 02.08.1999 (satellite image from <http://visibleearth.nasa.gov/>)



where $\mathbf{v}(\mathbf{x}, t)$ is the velocity field, defined in a region encompassing \mathfrak{C} , and $d\mathbf{x}$ is the line increment tangential to the line, and the time is held fixed. ■

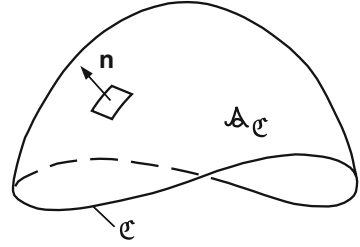
We emphasise that the closed curve \mathfrak{C} may be three dimensional. A direct implication of this definition is obtained, if the material time derivative of the circulation is evaluated. Indeed,

$$\begin{aligned}
 \dot{\Gamma} &= \frac{d}{dt} \oint_{\mathfrak{C}} \mathbf{v} \cdot d\mathbf{x} = \oint_{\mathfrak{C}} (\dot{\mathbf{v}} \cdot d\mathbf{x} + \mathbf{v} \cdot (d\mathbf{x})^*) \\
 &= \oint_{\mathfrak{C}} (\dot{\mathbf{v}} \cdot d\mathbf{x} + \mathbf{v} \cdot (\mathbf{L} d\mathbf{x})) = \oint_{\mathfrak{C}} (\dot{\mathbf{v}} + \mathbf{L}^T \mathbf{v}) \cdot d\mathbf{x} \\
 &= \oint_{\mathfrak{C}} \left(\dot{\mathbf{v}} + \text{grad} \left(\frac{v^2}{2} \right) \right) \cdot d\mathbf{x}.
 \end{aligned} \tag{5.2}$$

In this chain of transformations we have used the fact that $\mathbf{L} = \text{grad } \mathbf{v}$ and $\mathbf{L}^T \mathbf{v} = \text{grad } (v^2/2)$, $v^2 = \mathbf{v} \cdot \mathbf{v}$, which can easily be demonstrated in component form:

$$(\mathbf{L}^T \mathbf{v})_j \hat{=} L_{ij} v_i = \frac{\partial v_i}{\partial x_j} v_i = \frac{1}{2} \frac{\partial}{\partial x_j} (v_i v_i) \hat{=} \left(\text{grad} \frac{v^2}{2} \right)_j.$$

Fig. 5.2 Simple closed curve \mathcal{C} , spanning an area $\mathcal{A}_{\mathcal{C}}$. Note there are an infinity of surfaces spanned by \mathcal{C} in \mathbb{R}^3



In the next step of transformation we recall STOKES' integral theorem; according to it, one has (for a proof, see [Chap. 2](#))

$$\oint_{\mathcal{C}} \boldsymbol{\psi} \cdot d\mathbf{x} = \iint_{\mathcal{A}_{\mathcal{C}}} \text{curl } \boldsymbol{\psi} \cdot d\mathbf{A}, \quad (5.3)$$

in which $\boldsymbol{\psi}$ is any differentiable vector field in three dimensions and $\mathcal{A}_{\mathcal{C}}$ is any smooth surface spanned by the closed curve \mathcal{C} ; see [Fig. 5.2](#) with vectorial surface element $d\mathbf{A} = \mathbf{n} da$. If we apply STOKES' theorem to the vector field $\boldsymbol{\psi} = \text{grad}(v^2/2)$, we obtain

$$\oint_{\mathcal{C}} \text{grad} \left(\frac{v^2}{2} \right) \cdot d\mathbf{x} = \iint_{\mathcal{A}_{\mathcal{C}}} \underbrace{\text{curl grad} \left(\frac{v^2}{2} \right)}_{\mathbf{0}} \cdot d\mathbf{A} = 0. \quad (5.4)$$

This vanishes, because the curl of any gradient field is identically zero. Applying [\(5.4\)](#) to [\(5.2\)](#), we obtain

$$\dot{\Gamma} = \oint_{\mathcal{C}} \dot{\mathbf{v}} \cdot d\mathbf{x}. \quad (5.5)$$

This result holds for any differentiable vector field $\mathbf{v}(\mathbf{x}, t)$ along any closed simple smooth material curve \mathcal{C} that can be shrunk to zero without leaving the region where $\dot{\mathbf{v}}$ is continuously differentiable. The material need not be an ideal fluid, not even a fluid. The result is formally interesting, because the total time derivative 'outside' the integral simply carries over to the integrand function in [\(5.5\)](#).

Let us now specialise [\(5.5\)](#) for an EULER fluid, i.e. an inviscid fluid of which the momentum equation takes the form

$$\dot{\mathbf{v}} = -\frac{1}{\rho} \text{grad } p + \mathbf{f}. \quad (5.6)$$

If we substitute this into [\(5.5\)](#), then we have

$$\dot{\Gamma} = - \oint_{\mathcal{C}} \frac{1}{\rho} \underbrace{\text{grad } p \cdot d\mathbf{x}}_{dp} + \oint_{\mathcal{C}} \mathbf{f} \cdot d\mathbf{x}. \quad (5.7)$$

In the first integrand we have indicated that $\text{grad } p \cdot d\mathbf{x} = dp$ is simply the incremental change of p along \mathfrak{C} . In a *barotropic* ideal fluid p is a unique function of the density $p = p(\rho)$; thus dp/ρ can be viewed as the differential dP of a new function $P(\rho)$, the so-called *pressure function*; so,

$$\oint_{\mathfrak{C}} \frac{\text{grad } p \cdot d\mathbf{x}}{\rho} = \oint_{\mathfrak{C}} \frac{dp}{\rho} = \oint_{\mathfrak{C}} dP = 0, \quad (5.8)$$

of which the integral vanishes, because \mathfrak{C} is closed, so that the initial and end points of the integration are the same. Moreover, if we also assume that the body force possesses a unique *potential*, i.e. $\mathbf{f} = -\text{grad } U$, then with the same arguments we have

$$\oint_{\mathfrak{C}} \mathbf{f} \cdot d\mathbf{x} = - \oint_{\mathfrak{C}} \text{grad } U \cdot d\mathbf{x} = - \oint_{\mathfrak{C}} dU = 0. \quad (5.9)$$

With (5.8) and (5.9) the right-hand side of (5.7) vanishes. This result is summarised as

Theorem 5.1 (KELVIN's circulation theorem, after Lord KELVIN, 1824–1907) *In any flow field of an ideal, barotropic fluid with conservative body forces, the circulation, calculated for any material, closed, smooth curve, is temporally constant, symbolically,*

$$\frac{d\Gamma}{dt} = \frac{d}{dt} \oint_{\mathfrak{C}} \mathbf{v} \cdot d\mathbf{x} = \oint_{\mathfrak{C}} \dot{\mathbf{v}} \cdot d\mathbf{x} = 0 \iff \left\{ \begin{array}{l} \text{ideal, barotropic fluid} \\ \text{with conservative} \\ \text{body forces} \end{array} \right\}. \quad (5.10)$$

This theorem and its derivation allow us to formulate a number of intricate corollaries. To formulate these, we need the following definition:

Definition 5.2 *A differentiable vector field $\boldsymbol{\psi}$ in a region of \mathbb{R}^n , $n \leq 3$, is called **irrotational** or **vortex free**, if throughout this region*

$$\text{curl } \boldsymbol{\psi} = \nabla \times \boldsymbol{\psi} = \mathbf{0}. \quad (5.11)$$

*If the vector field $\boldsymbol{\psi}$ is the fluid velocity, then $\boldsymbol{w} = \text{curl } \mathbf{v}$ is called the **vorticity** of the flow field.*

With this definition, the corollaries of KELVIN's theorem now read as follows:

- (1) Consider an irrotational acceleration field, $\text{curl } \dot{\mathbf{v}} = \mathbf{0}$, in an ideal, barotropic fluid subject to a conservative body force. Then according to (5.8), (5.9), the

conditions of KELVIN's circulation theorem are satisfied. Therefore, Γ is constant along material lines, but may vary from trajectory to trajectory.

- (2) In a barotropic ideal fluid subject to a conservative body force the circulation is a conserved quantity, $\dot{\Gamma} = 0$. Hence according to the above item, $\dot{\Gamma} = 0$ implies $\text{curl } \dot{\mathbf{v}} = \mathbf{0}$. So, if $\text{curl } \mathbf{v} = \mathbf{0}$ in the entire flow field at the initial time, then $\text{curl } \mathbf{v} = \mathbf{0}$ at any later time. In words: *An irrotational flow field in a barotropic ideal fluid at an initial time remains irrotational for all time* as long as the velocity field remains differentiable, i.e. no discontinuities are formed.

We may interpret vorticity as the *tendency to form vortices*. In limnological and oceanographic applications the dominant large-scale flows are the water currents generated by wind, waves, density gradients, i.e. triggering mechanisms which, typically, generate horizontal water motions. The dominant component of the vorticity vector is then

$$\zeta := (\text{curl } \mathbf{v})_z = \hat{\mathbf{k}} \cdot \text{curl } \mathbf{v} = \frac{\partial v}{\partial x} - \frac{\partial u}{\partial y}, \quad (5.12)$$

where $\hat{\mathbf{k}}$ is the unit vector in the z -direction, (u, v) are the horizontal velocity components of the velocity field \mathbf{v} ; ζ is counted positive for counter-clockwise rotation when viewed from above. This is the same sense as the Earth's rotation in the northern hemisphere. The assumption that the flow is basically two-dimensional holds generally true, if the water flow in a lake or ocean extends over distances greater than a few kilometres.

For a rigid rotation around the origin O of the Oxy coordinate system, the velocity vector is tangential to circles, with linear speed $v_\varphi = r\omega$ (positive for counter-clockwise rotation), where ω is the angular velocity of this rigid-body motion around the origin O . With reference to Fig. 5.3 the velocity components are easily seen to be $(u, v) = \omega(-y, x)$, so that $\zeta = 2\omega$, according to (5.12). The angular momentum of a parcel with density ρ at a distance r from O with respect to O is given by $\rho r^2 \omega$.

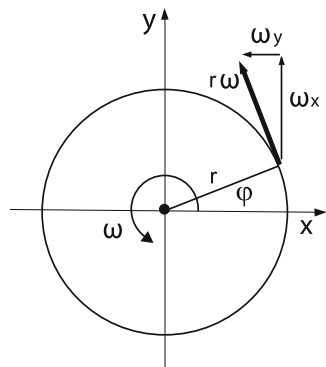


Fig. 5.3 Rigid rotation about the centre O with angular velocity ω , the Cartesian components being given by
 $u = -v_\varphi \sin \varphi = -\omega y$,
 $v = v_\varphi \cos \varphi = \omega x$

A direct application of this last example is the *planetary vorticity*, experienced by every body on the Earth. Everything on the Earth, including the oceans, the atmosphere and the water in lakes, rotates with the Earth. The *absolute velocity*, i.e. the velocity of an object on the Earth measured from an inertial frame, not participating in the rotation of the Earth, is composed of the *relative velocity* (measured by an observer on the Earth) and the *planetary velocity*, which is a rotation around the NS axis with angular velocity Ω . This planetary velocity for any particle on the Earth's surface is a rigid rotation with $v_\phi = (r \cos \phi)\Omega$ and vorticity vector $\omega_{\text{plane}} = 2\Omega \hat{k}$, with \hat{k} in the direction of the rotation axis. At the geographical latitude ϕ , this vector has a component tangential to the Earth surface, \tilde{f} , and a component pointing towards the zenith, f , viz.,

$$\begin{aligned}\omega_{\text{plane}} &= \tilde{f}\hat{e}_y + f\hat{e}_z, \\ \tilde{f} &:= 2\Omega \cos \phi, \quad f := 2\Omega \sin \phi,\end{aligned}\tag{5.13}$$

in which \hat{e}_y and \hat{e}_z are unit vectors tangential to the meridian and pointing towards north and directed towards the zenith, respectively, as indicated in Fig. 5.4. Moreover, f and \tilde{f} are the first and second CORIOLIS parameters. We have already seen that in the shallow water equations, \tilde{f} does not occur, so the first CORIOLIS parameter is more important, which is why oceanographers often identify the planetary vorticity just with f and write $\zeta_{\text{plane}} = f$. Its absolute value is zero at the equator and increases towards the poles.

As another informative idealised flow situation, consider uniform flow in the (x, y) plane along a step boundary as shown in Fig. 5.5. At the step a uniform velocity profile encounters a zero velocity field. In an ideal fluid this discontinuity will continue to the right of the step and form an idealised singular surface, called

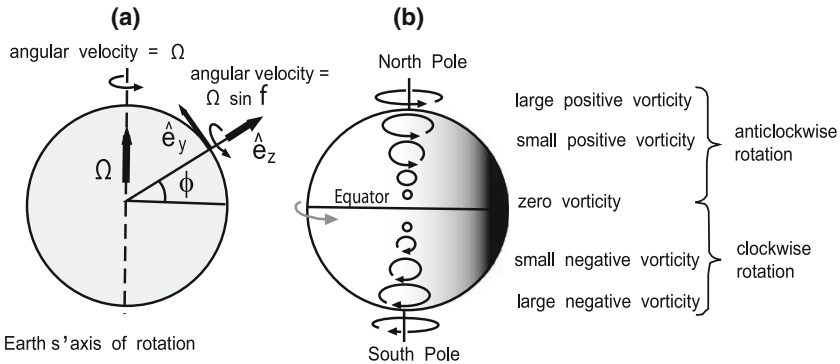


Fig. 5.4 (a) Diagram showing the derivation of the expression of the planetary vorticity of a fluid parcel on the surface of the Earth at latitude ϕ . (b) Schematic diagram illustrating the variations of the \hat{e}_z -component of the planetary vorticity with latitude; the *circular arrows* represent the value of f in the direction \hat{e}_z (viewed from above) at different latitudes, redrawn from [1]

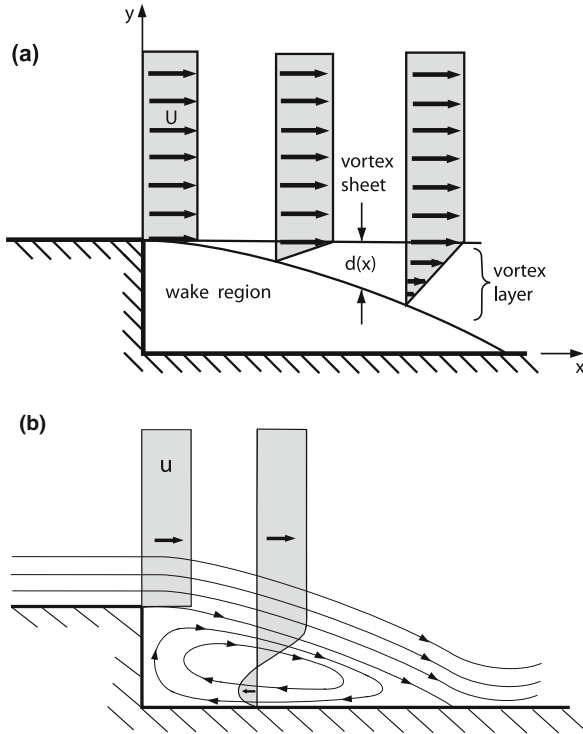


Fig. 5.5 (a) Parallel flow of a viscous fluid across an abrupt step. Formation of a vortex sheet and its transformation to a vortex layer, situation as established at an early time. (b) In steady state a recirculation flow is established in the wake region

a *vortex sheet*. In a real, viscous fluid the velocity will diffuse into the wake region with a velocity adjustment that gives rise to strong shearing, shown in idealised form in Fig. 5.5a as a linear velocity profile within the vortex sheet of thickness $d(x)$. In this layer with linear velocity profile, the vorticity vector is perpendicular to the flow plane and given by $\zeta = U/d(x)$. At the edge of the step, $\zeta = \infty$, since $d = 0$. Moreover, since $d(x)$ grows with increasing x , the value of the vorticity decreases with increasing x . In reality, because of the viscous effects a circulation flow will be established in the wake region as illustrated in panel (b) of Fig. 5.5. Near step-like boundary gyres may also occur, when the shoreline turns sharply to the sides and a gyre forms in the shadow region carrying away the vorticity of the shear flow.

Absolute vorticity is the sum of the relative and planetary vorticity,

$$\begin{aligned} \text{curl } \mathbf{v}_{\text{abs}} &= \text{curl } \mathbf{v}_{\text{rel}} + 2\boldsymbol{\Omega} \\ &= \left(\frac{\partial w}{\partial y} - \frac{\partial v}{\partial z} \right) \hat{\mathbf{e}}_x + \left(\frac{\partial u}{\partial z} - \frac{\partial w}{\partial x} + \tilde{f} \right) \hat{\mathbf{e}}_y + \left(\frac{\partial v}{\partial x} - \frac{\partial u}{\partial y} + f \right) \hat{\mathbf{e}}_z \end{aligned} \quad (5.14)$$

in which the expression on the second line is written in the basis $\{\hat{e}_x, \hat{e}_y, \hat{e}_z\}$ (see Fig. 5.4). For plane motion or conditions for which the shallow-water approximation is justified, the above relation reduces to

$$\zeta_{\text{abs}} = \zeta_{\text{rel}} + f, \quad \zeta_{\text{rel}} = \frac{\partial v}{\partial x} - \frac{\partial u}{\partial y}. \quad (5.15)$$

Relative vorticity ζ_{rel} is usually much smaller than f , and it is greatest at the edges of fast currents. To estimate orders of magnitudes for ζ_{rel} , consider the edge of some along-shore current in a large lake under strong wind action, where the velocity decreases by, roughly, $0.5(\text{m s}^{-1} \text{ km}^{-1}) = 5 \times 10^{-4} \text{ s}^{-1} = 0.43 \text{ cycles d}^{-1} \cong 0.5 \text{ cycle d}^{-1} \cong 1 \text{ cycle (2d)}^{-1}$. Even this large value for ζ_{rel} is roughly a factor of 2 smaller than f . Typical values for lakes are of the order of 1 cycle per week, making the neglect of the relative vorticity better justified.

All the above statements concern inviscid, barotropic fluids. An important question is, however, how the circulation changes with time, when the fluid is non-barotropic and viscous. In this case, expression (5.5) is still valid, but the acceleration via the balance of linear momentum and written in a non-inertial frame now takes the form¹

$$\dot{\mathbf{v}} = -\frac{1}{\rho} \text{grad } p + \frac{1}{\rho} \text{div } \mathbf{T}_v + \mathbf{f} - 2\boldsymbol{\Omega} \times \mathbf{v}, \quad (5.16)$$

where \mathbf{T}_v is the dissipative viscous stress. Thus, (5.5) may be written as

$$\dot{\Gamma} = - \int_{\mathcal{C}} \frac{1}{\rho} \text{grad } p \cdot d\mathbf{x} + \int_{\mathcal{C}} \frac{1}{\rho} (\text{div } \mathbf{T}_v) \cdot d\mathbf{x} + \underbrace{\int_{\mathcal{C}} \mathbf{f} \cdot d\mathbf{x}}_{\stackrel{(5.9)}{=} 0} - \int_{\mathcal{C}} 2(\boldsymbol{\Omega} \times \mathbf{v}) \cdot d\mathbf{x} \quad (5.17)$$

for a conservative body force. The pressure term in (5.17) can be transformed using STOKES' theorem (5.3) as follows:

$$\int_{\mathcal{C}} \frac{\text{grad } p}{\rho} \cdot d\mathbf{x} = \int_{\mathcal{A}_{\mathcal{C}}} \text{curl} \left(\frac{\text{grad } p}{\rho} \right) \cdot d\mathbf{a} = - \int_{\mathcal{A}_{\mathcal{C}}} \frac{\text{grad } \rho \times \text{grad } p}{\rho^2} \cdot d\mathbf{a}. \quad (5.18)$$

Therefore,

$$\dot{\Gamma} = - \int_{\mathcal{C}} 2\boldsymbol{\Omega} \times \mathbf{v} \cdot d\mathbf{x} + \int_{\mathcal{A}_{\mathcal{C}}} \frac{\text{grad } \rho \times \text{grad } p}{\rho^2} \cdot d\mathbf{a} + \int_{\mathcal{C}} \frac{1}{\rho} (\text{div } \mathbf{T}_v) \cdot d\mathbf{x}. \quad (5.19)$$

¹ Strictly, the contribution $\boldsymbol{\Omega} \times (\boldsymbol{\Omega} \times \mathbf{x})$ should be included on the right-hand side of (5.16). Instead, we regard the pressure to be reduced by $P_{\Omega} = -\frac{1}{2}\Omega^2 \mathbf{r}_{\perp}^2 \cdot \mathbf{r}_{\perp}^2$, where $\mathbf{r}_{\perp} = \mathbf{r} - (\mathbf{r} \cdot \hat{\mathbf{k}})\hat{\mathbf{k}}$.

Evidently, there are three mechanisms which are responsible for the time rate of change of the relative circulation: (1) the circulation due to the CORIOLIS force per unit mass; (2) that due to the pressure per unit mass; and (3) the circulation due to the viscous stresses per unit mass. The first term vanishes, if the frame of reference is inertial ($\mathbf{\Omega} = \mathbf{0}$), the second term is zero if $\rho = \rho(p)$ since then $\text{grad } \rho$ is parallel to $\text{grad } p$ and the third term vanishes in an inviscid fluid. Let us take a closer look:

- (1) Physically, the CORIOLIS effect can be better understood as follows (PEDLOSKY [9]). Note that

$$-(2\mathbf{\Omega} \times \mathbf{v}) \cdot d\mathbf{x} = -2\mathbf{\Omega} \cdot (\mathbf{v} \times d\mathbf{x}) = -2\mathbf{\Omega} \cdot \mathbf{n}_A v_\perp dx, \quad (5.20)$$

where \mathbf{n}_A is the unit vector parallel to $\mathbf{v} \times d\mathbf{x}$ and $v_\perp = \|\mathbf{v} \times \frac{d\mathbf{x}}{\|d\mathbf{x}\|}\|$ is the magnitude of the velocity component perpendicular to $d\mathbf{x}$; see Fig. 5.6. The rectangular area formed by \mathbf{v}_\perp and $d\mathbf{x}$ represents the incremental area $(\Delta A)^*$ per unit time swept out by the moving material line $\mathcal{C}(t)$ at the point P . So, we may write this as

$$(\Delta A)^* = \pm v_\perp dx, \quad (5.21)$$

where the (+)-sign ((-)-sign) applies when $(\Delta A)^*$ lies outside (inside) the loop \mathcal{C}^2 . Its projection perpendicular to $\mathbf{\Omega}$ is given by

$$(\Delta A_\Omega)^* = \mathbf{\Omega} \cdot \mathbf{n}_A v_\perp dx. \quad (5.22)$$

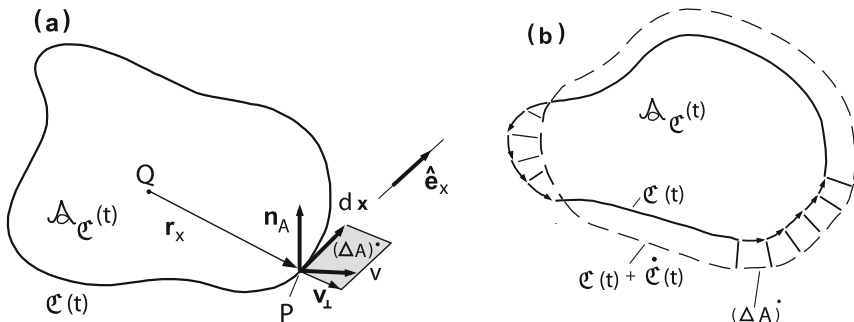
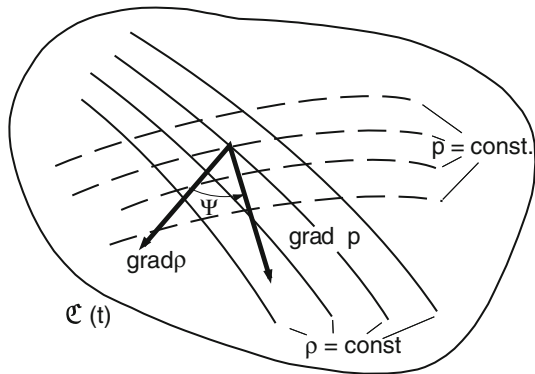


Fig. 5.6 (a) Circulation loop showing at a particular point P the velocity vector \mathbf{v} and the vectorial line increment, \mathbf{n}_A is the unit vector parallel to $\mathbf{v} \times d\mathbf{x}$ and $\hat{\mathbf{e}}_x$ is the unit vector tangential to \mathcal{C} at P . \mathbf{v}_\perp is the projection of \mathbf{v} perpendicular to $d\mathbf{x}$. Q is a point within $\mathcal{C}(t)$ lying on the surface $A_{\mathcal{C}(t)}$ spanned by $\mathcal{C}(t)$. (b) Material loop \mathcal{C} shown at time t (dashed) and $t + \Delta t$ (solid), $\Delta t = 1$, showing the growth of $A_{\mathcal{C}(t)}$ by the various $(\Delta A)^*$.

² To decide whether $(\Delta A)^*$ lies outside or inside $\mathcal{C}(t)$, we choose a point Q inside $\mathcal{C}(t)$ and define the vectors (see Fig. 5.6)

$$\mathbf{r}_x = \overrightarrow{QP}, \quad \mathbf{v}_\perp = \mathbf{v} - (\hat{\mathbf{e}}_x \cdot \mathbf{v})\hat{\mathbf{e}}_x.$$

Fig. 5.7 Lines of constant pressure and lines of constant density define the directions of $\text{grad } p$ and $\text{grad } \rho$. The angle ψ , if different from zero, gives a measure for baroclinicity



Therefore,

$$\begin{aligned} -2(\mathbf{\Omega} \times \mathbf{v}) \cdot d\mathbf{x} &= -2\mathbf{\Omega}(\Delta A_{\Omega})^* \\ \Rightarrow -\int_{\mathcal{C}} 2(\mathbf{\Omega} \times \mathbf{v}) \cdot d\mathbf{x} &= -2\mathbf{\Omega}(A_{\Omega})^*, \end{aligned} \quad (5.23)$$

where $(A_{\Omega})^*$ is the projection of the area swept out by the closed curve \mathcal{C} per unit time perpendicular to $\mathbf{\Omega}$. Thus, in the presence of planetary vorticity $\mathbf{\Omega}$ an increase of the area leads to a decrease of the circulation.

- (2) According to Fig. 5.7, $\text{grad } \rho \times \text{grad } p$ is positive, if the angle ψ between $\text{grad } \rho$ and $\text{grad } p$ is less than 180° . In this case the pressure term in (5.19) is positive, contributing to a growth of the circulation.
- (3) The contribution of the viscous stresses in (5.19) is evaluated here for a NEWTONIAN fluid without bulk viscosity. In this case

$$\text{div } \mathbf{T}_v = \mu(\text{div grad } \mathbf{v} - \frac{2}{3}\text{grad}(\text{div } \mathbf{v})),$$

so, if $\mu/\rho = \nu$ is treated as a constant

$$\begin{aligned} \int_{\mathcal{C}(t)} \frac{1}{\rho} (\text{div } \mathbf{T}_v) \cdot d\mathbf{x} &= \nu \int_{\mathcal{C}(t)} (\text{div grad } \mathbf{v} - \frac{2}{3}\text{grad}(\text{div } \mathbf{v})) \cdot d\mathbf{x} \\ &\approx \nu \int_{\mathcal{C}(t)} (\text{div grad } \mathbf{v}) \cdot d\mathbf{x}, \end{aligned} \quad (5.24)$$

Then,

$$(\Delta A)^* \text{ lies } \begin{cases} \text{outside of } \mathcal{C}(t) & \text{if } \mathbf{r}_x \cdot \mathbf{v}_\perp > 0. \\ \text{inside of } \mathcal{C}(t) & \text{if } \mathbf{r}_x \cdot \mathbf{v}_\perp < 0. \end{cases}$$

This definition works at least when $\mathcal{C}(t)$ lies in a plane and \mathbf{Q} is in this plane.

because $\text{div } \mathbf{v}$ is small. In this same approximation of near density preserving, since $\text{curl}(\text{curl } \mathbf{v}) = \text{grad div } \mathbf{v} - \text{div grad } \mathbf{v} \approx -\text{div grad } \mathbf{v}$ we have

$$\dot{\Gamma}_{\text{frict}} \approx -\nu \int_{\mathfrak{C}(t)} \text{curl}(\text{curl } \mathbf{v}) \cdot d\mathbf{x} = - \int_{\mathfrak{C}(t)} (\text{curl } \mathbf{w}) \cdot d\mathbf{x}. \quad (5.25)$$

For plane flow, for which the vorticity has a non-trivial contribution only in the z -direction, this becomes

$$\dot{\Gamma}_{\text{frict}} = \nu \int_{\mathfrak{C}(t)} \left(-\frac{\partial \zeta}{\partial y} dx + \frac{\partial \zeta}{\partial x} dy \right). \quad (5.26)$$

According to (5.25) the effect of the viscosity on the circulation is to reduce the circulation around Γ by an amount proportional to the strength of the curl of the vorticity.

5.2 Simple Vorticity Theorems

The ensuing analysis is facilitated, if we first define simple concepts connected with vorticity. The concepts are analogous to those when flow tubes and flow filaments are introduced.

Definition 5.3 A vortex line is an integral curve of the orientation field of the vorticity vector field $\mathbf{w} = \text{curl } \mathbf{v}$, i.e. it is the solution of the ordinary differential equation

$$\left. \begin{aligned} \frac{d\mathbf{x}}{d\sigma} &= \mathbf{w}(\mathbf{x}, t), \\ \sigma &= 0, \quad \mathbf{x} = \mathbf{x}_0, \end{aligned} \right\} \quad (5.27)$$

where σ parameterises the vortex line through the point $\mathbf{x} = \mathbf{x}_0$ and the time t is held fixed. ■

This definition allows us to form additional concepts. To this end, let \mathfrak{C} be a simple double-point free, closed material curve \mathfrak{C} in a flow field with non-vanishing circulation ($\Gamma \neq 0$). Consider now all those vortex lines which have their origin \mathbf{x}_0 on the (closed) curve \mathfrak{C} . The area spanned by \mathfrak{C} is called the cross-section of the tube. We are led then to the following.

Definition 5.4 (see Fig. 5.8)

- (1) All vortex lines through a closed double-point free curve \mathfrak{C} form a **vortex tube**.
- (2) A vortex tube with infinitesimal cross-section is called a **vortex filament**.

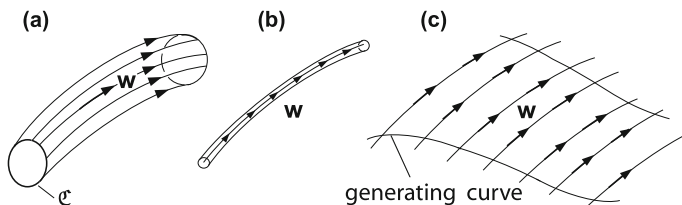


Fig. 5.8 (a) A simple closed double-point free curve having with each vortex line one point in common defines a *vortex tube*. (b) A vortex tube with infinitesimal cross-section is called a *vortex filament*. (c) All vortex lines having one point in common with a generating curve form a *vortex surface*

(3) All vortex lines having one common point with a generating (open or closed) curve form a **vortex surface**. ■

Let us now prove a number of simple lemmas. All these lemmas concern configurations on the mantle surface of vortex tubes. We summarise them in the following.

Theorem 5.2

- (i) The circulation of a flow field evaluated for a simply connected closed curve \mathcal{C}_1 that lies on the mantle surface of a vortex tube is zero; see Fig. 5.9a.
- (ii) For every closed curve that lies completely on the mantle surface of a vortex tube and encircles it, the circulation has the same value, i.e. the vortex tube is characterised by the value of its circulation; Fig. 5.9b.
- (iii) Vortex tubes in ideal barotropic fluids cannot end in the interior of a fluid. They must therefore be closed, i.e. torus-like, or they must end at boundaries of flow fields.
- (iv) Vortex tubes are material tubes. ■

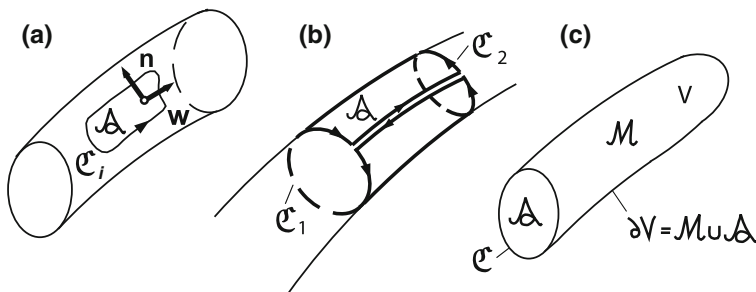


Fig. 5.9 (a) Circulation loop \mathcal{C}_1 completely situated on the mantle surface of a vortex tube, enclosing a simply connected region. (b) Two circulation loops encircling a vortex tube, complemented by a 'cut' along a boundary vortex line. The cut path is a circulation loop on the mantle surface of the vortex tube encircling a simply connected region; this explains that $\Gamma_{\mathcal{C}_1} = \Gamma_{\mathcal{C}_2}$. (c) A vortex tube assumed to end within the fluid. It has volume V and surface $\partial V = \mathcal{M} \cup \mathcal{A}$ where \mathcal{M} is the mantle surface and \mathcal{A} the tube cross-section spanned by the loop \mathcal{C}

Proof For statement (i), we evaluate the circulation around any closed double-point free curve \mathfrak{C}_i that lies on the mantle surface of a vortex tube and can be shrunk to a single point on this surface, as follows; see Fig. 5.9a,

$$\Gamma_{\mathfrak{C}_1} = \oint_{\mathfrak{C}_1} \mathbf{v} \cdot d\mathbf{x} = \iint_{\mathcal{A}_1} \underbrace{\mathbf{w} \cdot \mathbf{n}}_0 da = 0. \quad (5.28)$$

In this chain of equalities we have employed the STOKES theorem and then have used the fact that, on the mantle surface of a vortex tube, $\mathbf{w} = \text{curl } \mathbf{v}$ and \mathbf{n} are perpendicular to one another.

To prove statement (ii), consider Fig. 5.9b showing two closed curves, \mathfrak{C}_1 and \mathfrak{C}_2 , enclosing the same vortex tube. If these curves are, in imagination, connected with two neighboring vortex lines, then a closed line, completely on the mantle surface of the vortex tube, is formed, of which the circulation as indicated in the graph must vanish. Since the path along the two neighboring vortex lines is traversed in opposite directions, these contributions cancel out so that

$$\Gamma_{\mathfrak{C}_1} - \Gamma_{\mathfrak{C}_2} = 0 \quad \Rightarrow \quad \Gamma_{\mathfrak{C}_1} = \Gamma_{\mathfrak{C}_2}. \quad (5.29)$$

Since the choice of \mathfrak{C}_1 and \mathfrak{C}_2 is arbitrary, it follows that a vortex tube is characterised by the value of its circulation.

To prove item (iii) of the theorem, let us assume that the tube ends as shown in Fig. 5.9c. Then, the portion of the vortex tube from a selected cross-section to its end has finite volume V , and one may consider the divergence of the vorticity field, $\text{div } \mathbf{w} = \text{div } \text{curl } \mathbf{v} = 0$, which vanishes identically for any differentiable field \mathbf{v} . Then, we may deduce the following chain of identities:

$$0 = \int_V \text{div } \mathbf{w} dV \stackrel{(1)}{=} \int_{\partial V = \mathcal{M} \cup \mathcal{A}} \mathbf{w} \cdot \mathbf{n} dA \stackrel{(2)}{=} \int_{\mathcal{A}} \mathbf{w} \cdot \mathbf{n} dA \stackrel{(3)}{=} \oint_{\mathfrak{C}} \mathbf{v} \cdot d\mathbf{x} = \Gamma_{\mathfrak{C}}. \quad (5.30)$$

Here, \mathcal{M} is the mantle surface and \mathcal{A} the cross-section as shown in Fig. 5.9c. The volume integral of $\text{div } \mathbf{w}$ vanishes, since the integrand function vanishes. Step $\stackrel{(1)}{=}$, follows as a consequence of the divergence theorem. The integral over the mantle surface,

$$\int_{\mathcal{M}} \mathbf{w} \cdot \mathbf{n} dA = 0,$$

vanishes since \mathbf{w} and \mathbf{n} are perpendicular to one another on the mantle surface of a vortex tube. This explains step $\stackrel{(2)}{=}$. At $\stackrel{(3)}{=}$, STOKES' theorem is used for the cross-sectional area spanned by \mathfrak{C} . However, this integral is not allowed to vanish, since it is the circulation of the vortex tube.

It follows the assumption that the vortex tube ends within a barotropic ideal fluid is faulty. Vortex tubes are either closed, torus-like objects as best manifested in smoke rings, see Fig. 5.10, or they end at boundary walls.

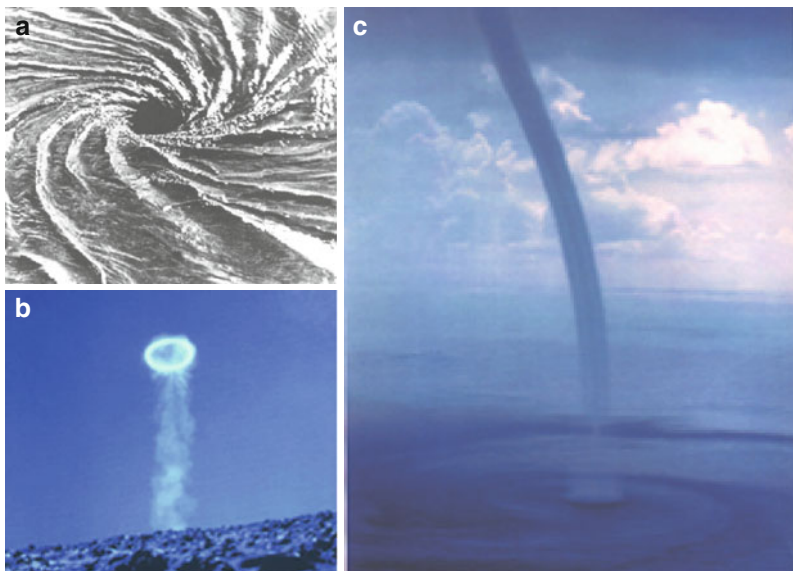


Fig. 5.10 Photographs of three well-known vortex phenomena. **(a)** Vortex at a turbine intake at Arapuni in New Zealand (from E.N. da C.Audrade. *New Scientist* (1963)); **(b)** in October 1969 an explosion of gas created this vortex ring on the snow-capped volcano Mount Actna in Sicily (copyright by Haroun Tazieff) (such rings are often created with cigarette smokes); **(c)** waterspout or tornado over water (from <http://www.srh.noaa.gov/>)

To prove statement *(iv)* that vortex tubes are material tubes, we consider a circulation loop on the mantle of a vortex tube as shown Fig. 5.9a. For this loop, $\Gamma_{\mathcal{C}_i} = 0$. Since in a barotropic ideal fluid KELVIN's theorem also holds, we also have $\dot{\Gamma}_{\mathcal{C}_i} = 0$. These two facts together prove the statement. They say that the value of $\Gamma_{\mathcal{C}_i}$ is carried with the material as the time proceeds, expressing exactly the fact that vortex tubes are material tubes, if the fluid is barotropic and ideal. ■

One additional implication is that all differentiable flows of ideal and barotropic fluids [these are the conditions that KELVIN's theorem holds] which start from rest are irrotational, since they are trivially irrotational, when they are at rest. This makes also clear that this cannot hold in a flow involving shock discontinuities, since across the shock differentiability is violated.

There are other theorems, e.g. about BERNOULLI surfaces, they are of lesser significance here and will not further be touched upon.

5.3 Helmholtz Vorticity Theorem

A very important result that can directly be deduced from a transformation of the momentum equation of an ideal fluid is the vorticity theorem due to HELMHOLTZ (1821–1894). To derive it, we consider the EULER equations (valid for an ideal fluid)

$$\frac{\partial \mathbf{v}}{\partial t} - \mathbf{v} \times \mathbf{w} + \text{grad} \left(\frac{v^2}{2} \right) = -\frac{1}{\rho} \text{grad } p + \mathbf{f}$$

and apply to it the curl operator; this yields

$$\frac{\partial \mathbf{w}}{\partial t} - \text{curl}(\mathbf{v} \times \mathbf{w}) = -\text{curl} \left(\frac{1}{\rho} \text{grad } p \right) + \text{curl } \mathbf{f}, \quad (5.31)$$

in which $\mathbf{w} = \text{curl } \mathbf{v}$, as before. This equation is called the *vorticity equation*. We also used the fact that $\text{curl grad } (\cdot) = \mathbf{0}$. Recalling the vector identities

$$\begin{aligned} \text{curl}(\mathbf{a} \times \mathbf{b}) &= (\text{grad } \mathbf{a})\mathbf{b} - (\text{grad } \mathbf{b})\mathbf{a} - \mathbf{a} \text{div } \mathbf{b} - \mathbf{b} \text{div } \mathbf{a}, \\ \text{curl}(\lambda \mathbf{b}) &= (\text{grad } \lambda) \times \mathbf{b} - \lambda \text{curl } \mathbf{b} \end{aligned} \quad (5.32)$$

(these can best be proved by using Cartesian index notation), using the first in $\mathbf{v} \times \mathbf{w}$ and the second in $\text{grad } p/\rho$, viz.,

$$\begin{aligned} \text{curl}(\mathbf{v} \times \mathbf{w}) &= (\text{grad } \mathbf{v})\mathbf{w} - (\text{grad } \mathbf{w})\mathbf{v} - \mathbf{w} \text{div } \mathbf{v}, \\ \text{curl} \left(\frac{1}{\rho} \text{grad } p \right) &= \text{grad} \left(\frac{1}{\rho} \right) \times \text{grad } p = -\frac{1}{\rho^2} \text{grad } \rho \times \text{grad } p \end{aligned} \quad (5.33)$$

(here we used the fact that $\text{div } \mathbf{w} = 0$ and $\text{curl grad } p = \mathbf{0}$), then (5.31) may, alternatively, be written as

$$\begin{aligned} &\underbrace{\frac{\partial \mathbf{w}}{\partial t} + (\text{grad } \mathbf{w})\mathbf{v}}_{\frac{d\mathbf{w}}{dt}} + \underbrace{\mathbf{w} \text{div } \mathbf{v}}_{-\frac{\mathbf{w}}{\rho} \frac{d\rho}{dt}} \\ &= (\text{grad } \mathbf{v})\mathbf{w} + \frac{1}{\rho^2} (\text{grad } \rho) \times (\text{grad } p) + \text{curl } \mathbf{f}. \end{aligned} \quad (5.34)$$

Note that the first two terms on the left-hand side of this equation are equal to $d\mathbf{w}/dt$ and the last term can be transformed with the aid of the mass balance to $-\mathbf{w} \frac{1}{\rho} \frac{d\rho}{dt}$. All three terms together are also expressible as $\rho \frac{d}{dt}(\mathbf{w} / \rho)$. Thus, (5.34) also takes the alternative form

$$\frac{d}{dt} \left(\frac{\mathbf{w}}{\rho} \right) = (\text{grad } \mathbf{v}) \frac{\mathbf{w}}{\rho} + \frac{1}{\rho^3} \text{grad } \rho \times \text{grad } p + \frac{1}{\rho} \text{curl } \mathbf{f}. \quad (5.35)$$

This is the first form of the HELMHOLTZ equation. It is often simply referred to as the *vorticity equation* and holds in this form for an ideal, *inviscid* fluid. For a barotropic fluid $p = p(\rho)$ and $\text{grad } p = (dp/d\rho)\text{grad } \rho$, the term with the cross-product on the right-hand side of (5.35) vanishes since $\text{grad } \rho$ is parallel to $\text{grad } p$. Moreover, if the specific volume force is conservative, $\mathbf{f} = -\text{grad } U$, then the HELMHOLTZ theorem may be summarised as follows:



Fig. 5.11 Left: Hermann Ludwig Ferdinand von HELMHOLTZ (<http://en.wikipedia.org/>). Right: Hans ERTEL, a pioneer in geophysical sciences, meteorology and hydrodynamics (<http://verplant.org/history-geophysics/>)

Hermann Ludwig Ferdinand von HELMHOLTZ (31 August 1821 to 8 September 1894) was a German physician and physicist who made significant contributions to many areas of modern science. In physiology and psychology, he is known for his mathematical description of the eye, theories of vision, ideas on the visual perception of space, color vision research, and on the sensation of tone, perception of sound and empiricism. In physics, he is known for his theories on the conservation of energy, work in electrodynamics, chemical thermodynamics and on a mechanical foundation of thermodynamics. In analysis, he is known for the theorem that a differentiable vector field can be split into irrotational and solenoidal parts, a theorem of significance in mathematical physics. As a philosopher, HELMHOLTZ is known for his philosophy of science, ideas on the relation between the laws of perception and the laws of nature, the science of aesthetics and ideas on the civilising power of science. A large German association of research institution, the HELMHOLTZ Gesellschaft (Association), is named after him.

Hans ERTEL (24 March 1904 to 2 July 1971) was a German natural scientist and a pioneer in geophysics, meteorology and hydrodynamics. He developed into a capable theoretical physicist early on and was capable to publish research results or theoretical approaches in this subject already as a young man. ERTEL's famous potential vorticity theorem of 1941–1943 belongs today to the basic work of modern geo- and astrophysics. The main areas of emphasis in his research were physical hydrography (more than 60 works), theoretical hydrodynamics, special hydrodynamics of the northern German seas and coasts, hydraulic nomography, hydrographic cartography, the history of European weather and theoretical fluid mechanics. As a member of the *Deutsche Akademie der Wissenschaften zu Berlin, East Germany* (DAW, German Academy of Sciences Berlin), ERTEL founded and led the Institute for Physical Hydrography of this academy. In 1949, he was elected to be a full member of the DAW and was its vice president from 1951 to 1961. The research on geo-ecology, which began under his leadership, is considered to be pioneering work today.

The text is partly based on <http://verplant.org/history-geophysics/> and <http://en.wikipedia.org/>.

Theorem 5.3 (Helmholtz' vorticity theorem)³ Consider an ideal, barotropic, compressible or density-preserving fluid exposed to a conservative force field. Let $\mathbf{v}(\mathbf{x}, t)$ be its differentiable velocity field, $\mathbf{w}(\mathbf{x}, t)$ its vorticity field and $\rho(\mathbf{x}, t)$ the density field. Then,

³ For a biographical sketch see Fig. 5.11.

$$\frac{d}{dt} \left(\frac{\mathbf{w}}{\rho} \right) = (\text{grad } \mathbf{v}) \frac{\mathbf{w}}{\rho}, \quad (5.36)$$

or, if we introduce the **vorticity per unit mass** $\boldsymbol{\omega}$ by $\mathbf{w} = \rho \boldsymbol{\omega}$,

$$\frac{d}{dt} (\boldsymbol{\omega}) = (\text{grad } \mathbf{v}) \boldsymbol{\omega}. \quad (5.37)$$

■

The proof is immediate from (5.35). This theorem can easily be explored with results that have important theoretical implications.

As a first application, consider *plane flow* in the (x, y) -plane. Then,

$$\text{grad } \mathbf{v} = \begin{pmatrix} \frac{\partial u}{\partial x} & \frac{\partial u}{\partial y} & 0 \\ \frac{\partial v}{\partial x} & \frac{\partial v}{\partial y} & 0 \\ 0 & 0 & 0 \end{pmatrix} \quad \text{and} \quad \mathbf{w} = \begin{pmatrix} 0 \\ 0 \\ \frac{\partial v}{\partial x} - \frac{\partial u}{\partial y} \end{pmatrix}, \quad (5.38)$$

so that $(\text{grad } \mathbf{v}) \mathbf{w} = \mathbf{0}$. In this case, (5.37) reduces to

$$\frac{d\boldsymbol{\omega}}{dt} = \mathbf{0} \quad \Rightarrow \quad \boldsymbol{\omega} = \text{const on particle trajectories} \quad (5.39)$$

or since for plane flow $\boldsymbol{\omega} = (\zeta/\rho) \hat{\mathbf{k}}$,

$$\frac{d}{dt} \left(\frac{\zeta}{\rho} \right) = 0 \quad \Rightarrow \quad \frac{\zeta}{\rho} = \text{const on particle trajectories}. \quad (5.40)$$

The vorticity per unit mass is a conserved quantity, a vector perpendicular to the plane of motion that is carried along with the fluid particle.

The behavior is quite different in *three-dimensional flow*. In this case, the right-hand side of (5.35) or (5.37) does not necessarily vanish. More specifically, (5.37) can easily be integrated, the result being

$$\boldsymbol{\omega}(t) = \mathbf{F}(t) \boldsymbol{\omega}(\tau) = \mathbf{F}(t) \boldsymbol{\omega}_0, \quad (5.41)$$

where t is the present time, while τ is the initial time for which $\mathbf{F} = \mathbf{1}$, and \mathbf{F} is the deformation gradient

$$\mathbf{F} = \frac{\partial \boldsymbol{\chi}(\mathbf{X}, t)}{\partial \mathbf{X}}. \quad (5.42)$$

To corroborate result (5.41), we take

$$\begin{aligned} \dot{\boldsymbol{\omega}} &= \dot{\mathbf{F}} \boldsymbol{\omega}(\tau) = \frac{\partial \dot{\mathbf{x}}}{\partial \mathbf{X}} \boldsymbol{\omega}(\tau) = \frac{\partial \mathbf{v}}{\partial \mathbf{x}} \frac{\partial \boldsymbol{\chi}}{\partial \mathbf{X}} \boldsymbol{\omega}(\tau) \\ &= (\text{grad } \mathbf{v}) \mathbf{F}(t) \boldsymbol{\omega}(\tau) = (\text{grad } \mathbf{v}) \boldsymbol{\omega}(t), \end{aligned}$$

which is (5.37), as expected.

To interpret result (5.41) recall that for a continuous motion $\mathbf{x} = \chi(\mathbf{X}, t)$ the material line increment $d\mathbf{x}$ at time t is related to the corresponding vectorial line increment at the initial time, $d\mathbf{X}$, according to

$$d\mathbf{x} = \mathbf{F}d\mathbf{X}. \quad (5.43)$$

This agrees formally with (5.41) and implies the following: *The vorticity vectors per unit mass, $\boldsymbol{\omega}$, change with time exactly as vectorial material line elements do.* For constant density, i.e. density-preserving fluids, this can also be expressed as follows: *When vortex filaments are stretched the specific vorticity increases, when they are squeezed it decreases.*

A further property can directly be obtained from (5.37) or (5.41) by decomposing the deformation into strain (rate) and rotation (rate). Recall that the velocity gradient,

$$\begin{aligned} \text{grad } \mathbf{v} &= \mathbf{D} + \mathbf{W}, \\ \mathbf{D} &:= \text{sym}(\text{grad } \mathbf{v}), \mathbf{W} = \text{skw}(\text{grad } \mathbf{v}) \end{aligned} \quad (5.44)$$

can be additively decomposed into its symmetric and skew-symmetric parts, and that the symmetric part, \mathbf{D} , called *strain rate tensor* or *stretching tensor* describes the rate of strain at a point, while \mathbf{W} is the *vorticity tensor* that describes the local rotation and is related to the vorticity vector according to

$$\mathbf{W}\mathbf{a} = \boldsymbol{\omega} \times \mathbf{a} \quad \text{for all } \mathbf{a} \neq \mathbf{0}. \quad (5.45)$$

With decomposition (5.44), (5.37) reads

$$\dot{\boldsymbol{\omega}} = \mathbf{D}\boldsymbol{\omega} + \mathbf{W}\boldsymbol{\omega}. \quad (5.46)$$

According to this formula, vortex lines change per unit time by the amount $\mathbf{D}\boldsymbol{\omega}$ through stretching and by the amount $\mathbf{W}\boldsymbol{\omega}$ through rotation.

The same conclusion, now integrated in time, can also be drawn from (5.41). To this end, recall the theorem of polar decomposition of \mathbf{F} (see the polar decomposition theorem in chapter 4). According to this theorem the (non-singular) deformation gradient \mathbf{F} can be decomposed as follows (note, this is a product decomposition):

$$\mathbf{F} = \mathbf{R}\mathbf{U} = \mathbf{V}\mathbf{R}. \quad (5.47)$$

Here, \mathbf{U} and \mathbf{V} are called right and left stretch tensors and \mathbf{R} is an orthogonal transformation, $\mathbf{R}\mathbf{R}^T = \mathbf{1}$; moreover, $\mathbf{U}^2 = \mathbf{F}^T\mathbf{F}$ and $\mathbf{V}^2 = \mathbf{F}\mathbf{F}^T$. It is shown in kinematics of continuous motions that \mathbf{U} and \mathbf{V} describe the strain that has

accumulated since the onset of the motion, while \mathbf{R} describes the accumulated rotation. So, according to (5.41) and (5.47)

$$\boldsymbol{\omega} = \mathbf{R} \mathbf{U} \boldsymbol{\omega}_0 = \mathbf{V} \mathbf{R} \boldsymbol{\omega}_0. \quad (5.48)$$

In the first representation the total change of a vortex filament is represented as a stretch followed by a rotation; in the second this order is reversed (see Fig. 4.2). In short one says: Vortex filaments in three-dimensional motions are deformed by *stretching* and *tilting*.

The HELMHOLTZ vorticity theorem must also be applied to ideal fluids referred to a permanently rotating frame of reference with constant angular velocity $\boldsymbol{\Omega}$. In this case the EULER equations of a barotropic fluid subject to a conservative body force take the form⁴

$$\frac{\partial \mathbf{v}}{\partial t} - \mathbf{v} \times \boldsymbol{\omega} = -\text{grad} \left(P(\rho) + \frac{v^2}{2} + U - \frac{|\boldsymbol{\Omega}|^2 \hat{r}^2}{2} \right) - 2\boldsymbol{\Omega} \times \mathbf{v}. \quad (5.49)$$

Here P is the pressure function of the barotropic fluid, U is the potential of the specific body force, $\boldsymbol{\Omega}^2 \hat{r}^2 / 2$ is the potential due to the rotation of the frame of reference due to $(\boldsymbol{\Omega} \times \mathbf{x}) \times \mathbf{x}$, see (5.27), (5.72), (5.73), and the last term on the right-hand side is the CORIOLIS force. For $\boldsymbol{\Omega} = \text{constant}$ equation (5.49) can also be rewritten as

$$\frac{\partial \mathbf{v}}{\partial t} - \mathbf{v} \times (\boldsymbol{\omega} + 2\boldsymbol{\Omega}) = -\text{grad} \left(P(\rho) + \frac{v^2}{2} + U - \frac{\boldsymbol{\Omega}^2 \hat{r}^2}{2} \right), \quad (5.50)$$

and if we take its curl, the term on the right-hand side vanishes and the left-hand side becomes

$$\frac{\partial (\boldsymbol{\omega} + 2\boldsymbol{\Omega})}{\partial t} - \text{curl} (\mathbf{v} \times (\boldsymbol{\omega} + 2\boldsymbol{\Omega})) = \mathbf{0}, \quad (5.51)$$

in which we have added $\partial(2\boldsymbol{\Omega})/\partial t = \mathbf{0}$.

The remainder of the computations now parallels that from (5.31) to (5.35) and will not be repeated here. The result is

Theorem 5.4 (Helmholtz' vorticity theorem in a permanently rotating frame)

Consider an ideal, barotropic, compressible or density-preserving fluid. Let $\mathbf{v}(\mathbf{x}, t)$ be its differentiable velocity field, $\boldsymbol{\omega}(\mathbf{x}, t)$ its vorticity field, $\boldsymbol{\Omega}$ the angular velocity of the frame and $\rho(\mathbf{x}, t)$ the density field. Then

$$\frac{d}{dt} \left(\frac{\boldsymbol{\omega} + 2\boldsymbol{\Omega}}{\rho} \right) = (\text{grad } \mathbf{v}) \left(\frac{\boldsymbol{\omega} + 2\boldsymbol{\Omega}}{\rho} \right). \quad (5.52)$$

⁴ Note, \hat{r} is the radial distance of the point in question from the axis of rotation.

The sum $\mathbf{w} + 2\mathbf{\Omega}$ is called the **absolute vorticity**. ■

The solution of equation (5.52) is, of course, again given by

$$\left(\frac{\mathbf{w} + 2\mathbf{\Omega}}{\rho}\right)(\mathbf{x}, t) = \mathbf{F}(\mathbf{x}, t) \left(\frac{\mathbf{w} + 2\mathbf{\Omega}}{\rho}\right)_0 \quad (5.53)$$

and interpretations of vortex stretching and vortex tilting are the same as before, now applied to the absolute vorticity.

Let us now apply (5.52) to *plane flow* or flows for which the shallow-water assumption is justified. Then $\hat{f} = 0$, $\boldsymbol{\omega}_{\text{abs}} = (\zeta + f)\hat{\mathbf{k}}$ and the right-hand side of (5.52) vanishes. So,

$$\frac{d}{dt} \left(\frac{\zeta + f}{\rho} \right) = \frac{1}{\rho} \frac{d\zeta_{\text{abs}}}{dt} - \frac{1}{\rho^2} \frac{d\rho}{dt} \zeta_{\text{abs}} \stackrel{!}{=} 0, \quad (5.54)$$

which, on using the mass balance equation $\dot{\rho} = -\rho(\frac{\partial u}{\partial x} + \frac{\partial v}{\partial y})$ takes the form

$$\frac{d\zeta_{\text{abs}}}{dt} + \zeta_{\text{abs}} \left(\frac{\partial u}{\partial x} + \frac{\partial v}{\partial y} \right) = 0$$

or

$$\frac{d(\zeta + f)}{dt} + (\zeta + f) \left(\frac{\partial u}{\partial x} + \frac{\partial v}{\partial y} \right) = 0. \quad (5.55)$$

This equation can also be derived by different methods. The derivation from (5.52), however, shows particularly clearly that (5.55) does neither contain any vortex stretching nor vortex tilting since the right-hand side of (5.52) vanishes for the derivation of (5.55). It is also clear where the second term on the left-hand side comes from: It is due to density variations.

A further consequence of Theorem 5.4 is

Theorem 5.5 (Taylor–Proudman theorem) *A steady slow flow of a density-preserving fluid in a rotating system is (essentially) plane. The flow takes place in a plane perpendicular to the axis of rotation.* ■

For the *proof* we note that $\mathbf{\Omega}$ is constant; so, of the left-hand side of (5.52) only the quadratic term $(\text{grad } \mathbf{w})\mathbf{v}/\rho$ survives, which is of higher order small. The right-hand side reduces in first order to $(\text{grad } \mathbf{v})(2\mathbf{\Omega}/\rho)$; so,

$$(\text{grad } \mathbf{v})\mathbf{\Omega} + \mathcal{O}(2) = \mathbf{0}, \quad (5.56)$$

where $\mathcal{O}(2)$ are terms of second order small. If we choose a Cartesian coordinate system such that its z -axis is in the direction of $\mathbf{\Omega}$, then this equation can be interpreted as $\partial \mathbf{v} / \partial z \cong 0$, i.e. the velocity field remains unchanged in the direction

of $\boldsymbol{\Omega}$. Changes or variations in the velocity field only occur in planes perpendicular to $\boldsymbol{\Omega}$. The velocity field is essentially plane and perpendicular to $\boldsymbol{\Omega}$. ■

5.4 Potential Vorticity Theorem

Another theorem that is important in rotating fluids and has found applications in meteorology and oceanography is the vorticity theorem due to ERTEL. It is known as the *Theorem of conservation of potential vorticity*.⁵ To derive it, we start from (5.52), HELMHOLTZ' vorticity theorem for a barotropic ideal fluid referred to a rotating frame. Moreover, we assume that a differentiable scalar function $\lambda(\mathbf{x}, t)$ is given for which the evolution equation

$$\frac{d\lambda(\mathbf{x}, t)}{dt} = \psi_\lambda(\mathbf{x}, t) \quad (5.57)$$

holds, where $\psi_\lambda(\mathbf{x}, t)$ is a prescribed differentiable function. We now take (5.52) and multiply both sides scalarly with $\text{grad } \lambda$. This yields

$$\frac{d}{dt} \left(\frac{\mathbf{w} + 2\boldsymbol{\Omega}}{\rho} \right) \cdot (\text{grad } \lambda) = (\text{grad } \mathbf{v}) \left(\frac{\mathbf{w} + 2\boldsymbol{\Omega}}{\rho} \right) \cdot (\text{grad } \lambda). \quad (5.58)$$

Alternatively, we may prove the vector identity

$$\begin{aligned} \left(\frac{\mathbf{w} + 2\boldsymbol{\Omega}}{\rho} \right) \cdot \frac{d}{dt} (\text{grad } \lambda) &= \left(\frac{\mathbf{w} + 2\boldsymbol{\Omega}}{\rho} \right) \cdot \text{grad} \left(\frac{d\lambda}{dt} \right) \\ &\quad - (\text{grad } \lambda) \cdot \left(\text{grad } \mathbf{v} \left(\frac{\mathbf{w} + 2\boldsymbol{\Omega}}{\rho} \right) \right). \end{aligned} \quad (5.59)$$

It may most easily be proved using Cartesian index notation. When equations (5.58) and (5.59) are added together, the two terms on the left-hand side can be combined to yield

$$\frac{d}{dt} \left(\frac{1}{\rho} (\mathbf{w} + 2\boldsymbol{\Omega}) \cdot \text{grad } \lambda \right), \quad (5.60)$$

while the right-hand side becomes

$$\frac{1}{\rho} (\mathbf{w} + 2\boldsymbol{\Omega}) \text{grad} \left(\frac{d\lambda}{dt} \right) = \left(\frac{\mathbf{w} + 2\boldsymbol{\Omega}}{\rho} \right) \cdot \text{grad } \psi_\lambda, \quad (5.61)$$

where (5.57) has been used. We now introduce

⁵ ERTEL, Hans (1904–1971) (see Fig. 5.11) published his potential vorticity theorem in 1942 [3] with follow-up papers in the same year [4–6], but his work remained, relatively unknown until TRUESDELL [12] proved that ERTEL's vorticity theorem holds in average for any medium suffering no tangential acceleration on any boundary and summarised the work in a survey in the *Handbuch der Physik* [13]. HIDE [7] published a magnetic analogue of his potential vorticity theorem and KATZ [8] and TREDER [11] applied it to relativity. A selection of papers is given by SCHRÖDER and TREDER [10].

Definition 5.5 Let $\mathbf{w} = \text{curl } \mathbf{v}$ be the vorticity field of the velocity field of an ideal barotropic fluid and $\lambda(\mathbf{x}, t)$ a differentiable scalar field. Let, moreover, $\boldsymbol{\Omega}$ be the constant angular velocity of the frame of reference. Then

$$\pi_\lambda := \frac{1}{\rho}(\mathbf{w} + 2\boldsymbol{\Omega}) \cdot \text{grad } \lambda \quad (5.62)$$

is called the **potential vorticity associated with λ** . ■

Equating (5.60) and (5.61) yields the following.

Theorem 5.6 (Potential vorticity theorem, Ertel's vorticity theorem) Let \mathbf{v} be the velocity field of an ideal, barotropic compressible or density-preserving fluid and $\mathbf{w} + 2\boldsymbol{\Omega}$ its absolute vorticity. Let, moreover, $\lambda(\mathbf{x}, t)$ and $\psi_\lambda(\mathbf{x}, t)$ be two differentiable scalar fields which satisfy the evolution equation (5.57). Let, furthermore, the potential vorticity π_λ associated with λ be defined as in Definition 5.5. Then, this potential vorticity obeys the evolution equation

$$\frac{d\pi_\lambda}{dt} = \left(\frac{\mathbf{w} + 2\boldsymbol{\Omega}}{\rho} \right) \cdot \text{grad } \psi_\lambda. \quad (5.63)$$

■

Note there is not only one single potential vorticity equation, but there are many; each λ and ψ_λ , satisfying (5.57), gives rise to its own potential vorticity equation.

If ψ_λ is not a function of \mathbf{x} , $\psi = \psi(t)$, with $\text{grad } \psi_\lambda = 0$, then (5.63) implies the following.

Theorem 5.7 (Potential vorticity corollary) Assume that the conditions of Theorem 5.6 are fulfilled, but that, specially, ψ_λ is at most a function of the time. Then, the potential vorticity is conserved along particle trajectories, in formulae

$$\frac{d\lambda}{dt} = \psi_\lambda(t) \quad \Rightarrow \quad \frac{d\pi_\lambda}{dt} = 0. \quad (5.64)$$

■

Obviously, for $\psi_\lambda = 0$ the same conclusion holds.

Let us give a number of examples:

- (1) Consider flow of an ideal fluid parallel to the (x, y) -plane which itself is rotating with angular velocity $\boldsymbol{\Omega} = \Omega \hat{\mathbf{e}}_z$. Select

$$\lambda = z, \quad \text{grad } \lambda = \hat{\mathbf{e}}_z, \quad \psi_\lambda = 0, \quad \text{grad } \psi_\lambda = 0. \quad (5.65)$$

Then, according to (5.62)

$$\pi_{\lambda=z} = \frac{\zeta + 2\Omega}{\rho}. \quad (5.66)$$

This potential vorticity agrees with the absolute vorticity per unit mass. With (5.65) and (5.66), the conservation law of potential vorticity is the same as the HELMHOLTZ vorticity theorem. Indeed, forming $d\pi_{\lambda=z}/dt = 0$ yields

$$\frac{d}{dt}(\zeta + 2\Omega) - \frac{\dot{\rho}}{\rho}(\zeta + 2\Omega) = 0 \quad (5.67)$$

or when using the mass balance equation $\dot{\rho}/\rho = -(\partial u/\partial x + \partial v/\partial y)$,

$$\frac{d}{dt}(\zeta + 2\Omega) + (\zeta + 2\Omega) \left(\frac{\partial u}{\partial x} + \frac{\partial v}{\partial y} \right) = 0, \quad (5.68)$$

which is the same as (5.55), if we set $2\Omega = f$.

- (2) Consider now a barotropic, density-preserving fluid in the shallow water approximation for which $\tilde{f} = 0$. Let

$$z = b(x, y, t) \quad \text{and} \quad z = b(x, y, t) + H(x, y) + \xi(x, y, t) \quad (5.69)$$

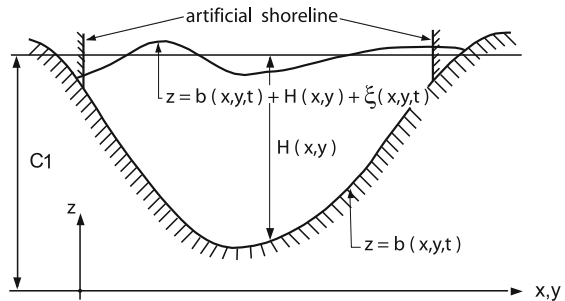
be the basal and free surfaces, respectively, see Fig. 5.12, and choose λ and ψ_λ as in (5.65) of example (1). Then, dropping the constant density in (5.66), the potential vorticity equation (5.64)₂ takes the form

$$\frac{d}{dt}(\zeta + f) = 0. \quad (5.70)$$

It is known that in a barotropic fluid the horizontal velocity components (u, v) are independent of z . This implies that also $\zeta + f$ is independent of z . So, we wish to average (integrate) (5.70) over depth,

$$\int_b^{b+H+\xi} \frac{d}{dt}(\zeta + f) dz = 0, \quad (5.71)$$

Fig. 5.12 Vertical cut through a lake or ocean, indicating the free and bottom surfaces. Note, ξ is the surface elevation



where ξ is the free surface deflection. Interchanging integration and differentiation and using LEIBNIZ' rule transform (5.71) into

$$\frac{d}{dt} \int_b^{b+H+\xi} (\zeta + f) dz - (\zeta + f)|_{b+H+\xi} \left(\frac{db}{dt} + \frac{d(H+\xi)}{dt} \right) + (\zeta + f)_b \frac{db}{dt} = 0. \quad (5.72)$$

With the z -independence of $(\zeta + f)$, (5.72) simplifies to

$$\frac{d}{dt} ((\zeta + f)(b + H + \xi)) - (\zeta + f) \frac{d}{dt} (H + \xi) = 0 \quad (5.73)$$

or, after a simple transformation, if b does not depend on time,

$$\frac{d}{dt} \left(\frac{\zeta + f}{H + \xi} \right) = \frac{d}{dt} \langle \pi \rangle_{bt} = 0. \quad (5.74)$$

The function

$$\langle \pi \rangle_{bt} := \frac{\zeta + f}{H + \xi} \quad (5.75)$$

is called the barotropic (depth-averaged) potential vorticity. It is constant along horizontal projections of the particle trajectories. Note that in the derivation of (5.74) from (5.73) a division by $(H + \xi)$ is used; this implies that $(H + \xi)$ should never become zero and requires that vertical shorelines are introduced such that $H_{\text{shore}} > \max_{\text{along shore}} (|\xi|)$, as indicated in Fig. 5.12. In lakes $H \gg |\xi|$, over most part of the lake domain (except shallow shore regions). Ignoring the latter, one may make use of the rigid lid assumption and drop in (5.75) ξ in comparison to H . In that case the barotropic potential vorticity is

$$\langle \pi \rangle_{bt}^{\text{rigid lid}} = \frac{\zeta + f}{H}. \quad (5.76)$$

There is a second, alternative way of deriving (5.75), using a different potential vorticity, which equally leads to (5.74), (5.75). To see this, write (5.69) as

$$\begin{aligned} F_b &:= b(x, y, t) - z \equiv 0, \\ F_s &:= H(x, y) + b(x, y, t) + \xi(x, y, t) - z \equiv 0 \end{aligned} \quad (5.77)$$

and observe that $H(x, y) + z = c_1 = \text{const}$. Then choose

$$\lambda_\varepsilon := \frac{H + z}{F_s - F_b + \varepsilon} = \frac{H + z}{H + \xi + \varepsilon} = \frac{c_1}{\varepsilon}, \quad (5.78)$$

where $\varepsilon > 0$ is a small positive constant, which is needed to make λ_ε bounded in the entire lake domain. (We formally keep ε in all formulae and take the limit $\varepsilon \rightarrow 0$ in the final formulae.) With (5.78) we may define for a density-preserving fluid ($\rho = \text{const}$)

$$\pi_H^\varepsilon = (\mathbf{w} + 2\mathbf{\Omega}) \cdot \text{grad } \lambda_\varepsilon = (\mathbf{w} + 2\mathbf{\Omega}) \cdot \text{grad} \left(\frac{H + z}{H + \xi + \varepsilon} \right)$$

and obtain with $\psi_{\lambda_\varepsilon} = 0$, the result $d\pi_{\text{bt}}/dt = 0$. In the shallow water approximation this reduces to

$$\pi_{\text{bt}}^\varepsilon = \frac{(\zeta + f)}{H + \xi + \varepsilon} \xrightarrow{\varepsilon \rightarrow 0} \frac{\zeta + f}{H + \xi} \xrightarrow{\xi \rightarrow 0} \frac{\zeta + f}{H}, \quad (5.79)$$

which is the same as (5.76). In (5.79) we have regularised the problem by choosing an adequate value for ε , while in (5.76) vertical shorelines were used to regularise the formula.

As an example, consider a column of homogeneous water in a current encompassing the entire depth of a real basin. Assume that the column is spinning (see Fig. 5.13) about its own axis, in the anticlockwise direction on the northern hemisphere, i.e. it has positive relative vorticity. What will happen if the rotating column moves into a region of greater depth? It will become longer and thinner, the water will spin faster, i.e. its relative vorticity will increase (i.e. become more positive). Looked at this from the point of view of angular momentum, the angular momentum of each particle of the water is $mr^2\omega$. When the column stretches, the average radius r decreases and so, for angular momentum to be conserved, the speed of rotation ω must increase. Because of the effect of changes of the length H of the water column, the property that is actually conserved is therefore not $(f + \zeta)$, the absolute vorticity, but $(f + \zeta)/H$, the potential vorticity.

The above argument ignores f and is therefore unrealistic for water bodies of greater extent. For large-scale motions in the ocean, away from coastal

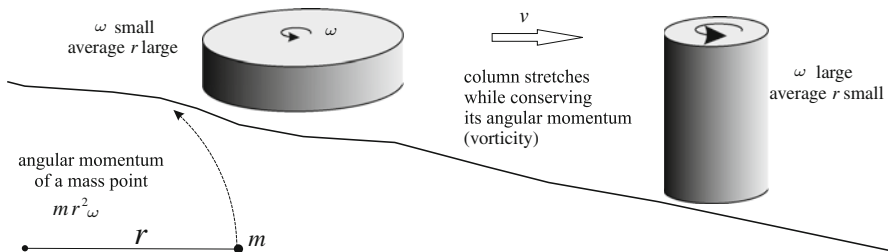


Fig. 5.13 Production of relative vorticity by the changes in the height of a fluid column. As the vertical fluid column moves from left to right, vertical stretching reduces the moment of inertia of the column, causing it to spin faster. The angular momentum of a particle of mass m moving with angular velocity ω in a circle of radius r is given by $mr^2\omega$ (after [1], with changes)

boundaries and other regions of large current shear, f is very much greater than ζ . This means that $(f + \zeta)/H$ is approximately equal to f/H , and it is f that must change in response to changes in H , and as f is simply a function of latitude, it can only be changed by the water changing its latitude. The fact that conservation of f/H causes currents to swing equatorwards and polewards over topographic highs and lows, respectively, is sometimes referred to as *topographic steering*; see Fig. 5.14. Lines of constant f/H are called *isotrophs*.

In studies of potential vorticity in the real ocean, H , the ‘depth of the water column’, need not be the total depth to the sea floor. It may be the thickness of the *body of water* under consideration, and so it could, for example, be the depth from the bottom of the permanent thermocline to the sea floor. Thus, the conservation of potential vorticity in fact couples changes in depth, relative vorticity and changes in latitude. All three interact and (i) changes in the depth H of the flow alter its relative vorticity ζ (see Fig. 5.13), while (ii) changes in latitude require a corresponding change in ζ . As a column of water moves equatorward, f decreases and ζ must increase.

The concept of conservation of potential vorticity may be used to derive inferences of far-reaching consequences. For instance, in large basins of ocean scale, the flow tends to be zonal if the water depth is constant or it follows the isotrophs $f/H = \text{constant}$; this constant is equal to π_{bt} when the rigid lid assumption and $|\zeta| \ll f$ are imposed. Small deviations of the flow from the isotrophs, e.g. due to wind, cause small changes in ζ , leading to a small meridional component to the flow. If the depth is changing (say, a barotropic flow encounters a subsurface ridge, Fig. 5.14a), the (meso-scale) flow tends to keep the isobath. At larger scale, if the depth decreases, $\zeta + f$ must also decrease, which requires that f decreases; as a result, the flow tends to turn towards the equator. If the change in depth is sufficiently large, so that no change in latitude could conserve

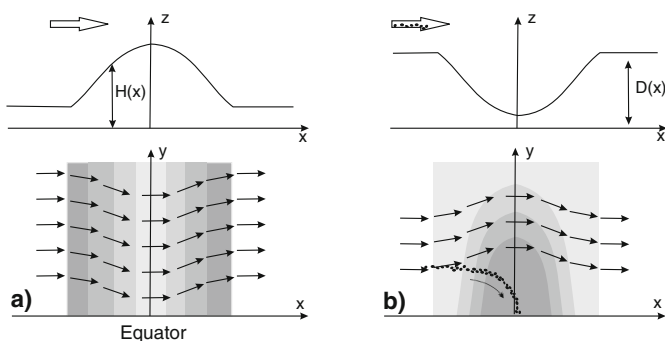


Fig. 5.14 (a) Barotropic flow over a subsurface ridge is turned equatorward to conserve potential vorticity. *Top view* of water flow parallel to the equator (redrawn, initially from DIETRICH et al. [2]). (b) Turbidity flow, crossing a submarine canyon, divides into the sediment-rich heaviest part, which rushes down-slope due to gravity, and the remainder of the flow, which keeps on moving along the same isobath and even up-slope to conserve the vorticity of the initial flow

potential vorticity, the flow will be unable to cross the ridge. This situation is called *topographic blocking*.

Dynamics of a turbidity flow, crossing a submarine canyon, provides another example of the influence of vorticity (Fig. 5.14b). Such flows usually have large relative vorticity and carry lots of sediments. Having approached the canyon, the flow divides into two currents: the sediment-rich heaviest part rushes down-slope, while the remainder of the flow keeps on moving along the same isobath, i.e. upwards in the canyon; see ZATSEPIN [14].

- (3) This is an example for a flow state under baroclinic conditions. If we let

$$\begin{aligned}\lambda &= \rho, \quad \frac{d\lambda}{dt} = \frac{d\rho}{dt} = -\rho \operatorname{div} \mathbf{v} = \psi_\lambda, \\ \operatorname{grad} \psi_\lambda &= \operatorname{grad} \left(\frac{d\rho}{dt} \right) = -\operatorname{grad} (\rho \operatorname{div} \mathbf{v}).\end{aligned}\tag{5.80}$$

The *baroclinic potential vorticity* may then be defined as

$$\pi_{bc} = \pi_{\lambda=\rho} = \left(\frac{\mathbf{w} + 2\boldsymbol{\Omega}}{\rho} \right) \cdot \operatorname{grad} \rho,\tag{5.81}$$

and the balance law of potential vorticity, (5.63), becomes

$$\frac{d}{dt} \left[\left(\frac{\mathbf{w} + 2\boldsymbol{\Omega}}{\rho} \right) \cdot \operatorname{grad} \rho \right] = \left(\frac{\mathbf{w} + 2\boldsymbol{\Omega}}{\rho} \right) \cdot \operatorname{grad} \left(\frac{d\rho}{dt} \right).\tag{5.82}$$

So, in this case λ is strictly not conserved along particle trajectories, and neither is the baroclinic potential vorticity.

In the ocean or a lake under summer stratification, the density can be decomposed as

$$\rho(x, y, z, t) = \rho_0(z) + \rho'(x, y, z, t).\tag{5.83}$$

In the metalimnion, i.e. the vicinity of the thermocline we have $\rho_0 \gg \rho'$. Moreover, $\operatorname{grad} (d\rho/dt) = \operatorname{grad} (d\rho'/dt)$ can be expected to be very small. So, approximately in the shallow water approximation, for which $\tilde{f} = 0$, the baroclinic potential vorticity reduces to

$$\pi_{bc}^{\text{app}} \approx \frac{\zeta + f}{\rho_0} \frac{d\rho_0}{dz} \approx f \frac{1}{\rho_0} \frac{d\rho_0}{dz},\tag{5.84}$$

where the further approximation on the far right follows from the inequality $|\zeta| \ll f$. So, the potential vorticity π_{bc}^{app} is approximately conserved.

Formula (5.84) is useful, because its far right approximation allows the potential vorticity of various layers of a lake – epilimnion, metalimnion and hypolimnion – to be determined directly from hydrographic data without knowledge of the velocity field.

References

1. Bearman, G. (ed.): *Ocean Circulation*. The Open University. Butterworth-Heinemann. Oxford, Boston, MA, 238 p. (1998)
2. Dietrich G., Kalle, K., Krauss, W. and Siedler, G.: *General Oceanography*. 2nd Edition Translated by Susanne and Hans Ulrich Roll. Wiley (Wiley-Interscience) New York, NY (1980)
3. Ertel, H.: Ein neuer hydrodynamischer Erhaltungssatz. *Die Naturwissenschaften* **30**. Jg. Heft 36, 543–544 (1942)
4. Ertel, H.: Ein neuer hydrodynamischer Wirbelsatz. *Meteorologische Zeitschrift* **59**. Jg. Heft 9, 277–281 (1942)
5. Ertel, H.: Über hydrodynamische Wirbelsätze. *Physik. Z. (Leipzig)* **59**. Jg. Heft, 526–529 (1942)
6. Ertel, H.: Über das Verhältnis des neuen hydrodynamischen Wirbelsatzes zum Zirkulationssatz von V. Bjerknes. *Meteorologische Zeitschrift* **59** Jg. Heft 12, 161–168, (1942)
7. Hide, R.: The magnetic analogue of Ertel's potential vorticity theorem. *Ann. Geophysicae* **1**(1), 59–60 (1983)
8. Katz, J.: Relativistic potential vorticity. *Proc. R. Soc. London A* **391**, 415–418 (1984)
9. Pedlosky, J.: *Geophysical Fluid Dynamics*. Springer, Berlin (1982)
10. Schröder, W. and Treder, H.-J.: Theoretical concepts and observational implications in meteorology and geophysics (Selected papers from the IAGA symposium to commemorate the 50th anniversary of Ertel's potential vorticity). Interdivisional commission on history of the International Association of Geomagnetism and Aeronomy. ISSN: 179-5658.
11. Treder, H.-J.: Zur allgemeinen relativistischen und kovarianten Integralformen der Ertelschen Wirbeltheoreme. *Gerlands Beitr. Geophys.* **79**, 1 (1970)
12. Truesdell, C.A.: On Ertel's vorticity theorem. *Zeitschrift für Angew. Math. & Phys. (ZAMP)* **2**, 109–114 (1951)
13. Truesdell, C.A. and Toupin, R.C.: *The Classical Field Theories of Mechanics*: In Handbuch der Physik (ed. S. Flügge) Bd. III/1. Prinzipien der klassischen Mechanik und Feldtheorie, Springer, Berlin (1960)
14. Zatsepin, A.G., Gritsenko, V.A., Kremenetsky, V.V., Poyarkov, S.G. and Stroganov, O.Yu.: Laboratory and numerical investigation of process of propagation of density currents along bottom slope. *Oceanology* **45**(1), 5–15 (2005)

Chapter 6

Turbulence Modelling

6.1 A Primer on Turbulent Motions

The first basic thoughts and experiments on turbulence are due to REYNOLDS [20] who studied the flow of a fluid through pipes with circular cross-sections. He recognised (by adding dye through a pipette to the fluid) that, basically, two flow regimes exist. In one case, the so-called *laminar* flow, the dye forms a coherent thin filament; in the second case, known as *turbulent* flow, the dye filament is torn very quickly after it left the nozzle of the pipette and is spread over the entire cross-section of the pipe; Fig. 6.1. If one slowly increases the discharge in the pipe, starting from laminar conditions, one observes a sudden change from laminar to turbulent flow. The critical quantity that characterises this change is the REYNOLDS number

$$\mathcal{R}_e = \frac{VD}{\nu}, \quad \text{if } \mathcal{R}_e > 2000 \text{ then the flow is turbulent,}$$

where V , D , ν are the mean axial velocity, the inner pipe diameter and the kinematic viscosity of the fluid. The velocity profiles, averaged over a time interval (which eliminates rapid fluctuations), look like as shown in Fig. 6.1b. The transition from the laminar to the turbulent regime takes place between $\mathcal{R}_e = 500$ and 2000. Unless precursory measures are taken, the flow is always turbulent when $\mathcal{R}_e > 2000$.

6.1.1 Averages and Fluctuations

In Fig. 6.1b the velocity profile for the turbulent flow was drawn for the temporally *mean* velocity, because the actual velocity profile is fraught with strong fluctuations, which appear to be random. Such fluctuations are seen in turbulent flows in time series of the velocity at a fixed point (see, e.g. Fig. 6.2) as well as spatial variations at fixed time. The time and space scales of these pulsations are for most applications not relevant; one is rather interested in some average behaviour, for which space and time scales extend over many typical ‘periods’ of the turbulent fluctuations. This

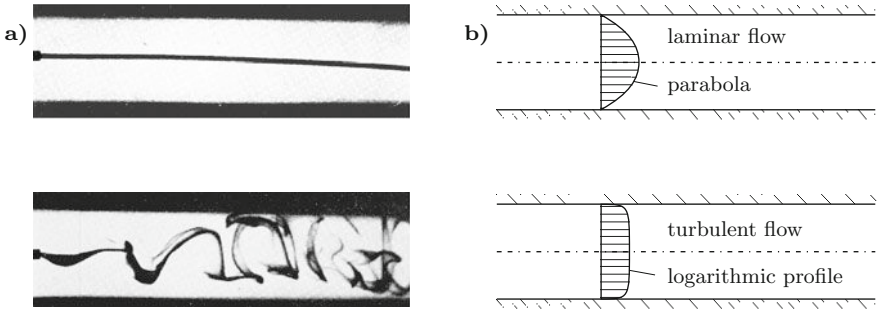


Fig. 6.1 (a) Laminar and turbulent flow in a cylindrical pipe. To visualise the flow dye is added to the water through a capillary pipette. The nozzle of this pipette is visible at the left end of the photographs on the left (courtesy Royal Soc. London [20]). (b) Mean velocity profiles in a circular pipe under steady laminar and turbulent conditions, respectively

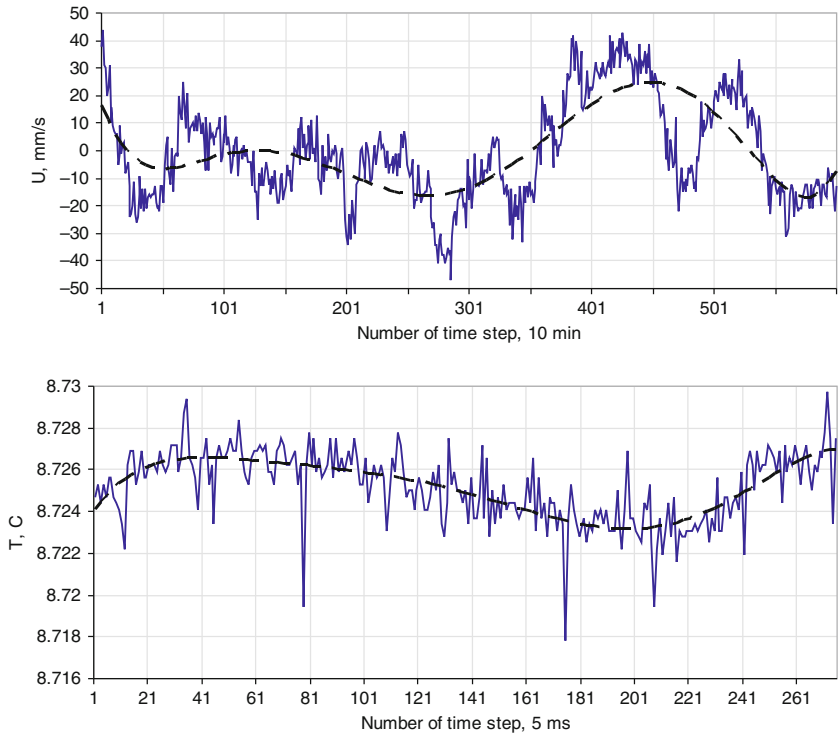


Fig. 6.2 Typical example of a measured signal. *Upper panel:* Time variations of the northward component of current speed during the period of 100 h measured by ADCP in the middle of Lake Constance at a depth of 2 m on 24–28 October 2001 (courtesy of Andreas Lorke, data delivered to [2]). *Lower panel:* Water temperature in laboratory flume, measured with the time step of 5 ms

suggests to additively decomposing the velocity into two contributions, the mean value¹ $\langle \mathbf{v} \rangle$ and the fluctuations \mathbf{v}' ,

$$\mathbf{v} = \langle \mathbf{v} \rangle + \mathbf{v}'. \quad (6.1)$$

If the mean value $\langle \mathbf{v} \rangle$ is taken as a temporal average, defined by

$$\langle \mathbf{v} \rangle_T(\mathbf{x}, t) := \frac{1}{T} \int_{t-T/2}^{t+T/2} \mathbf{v}(\mathbf{x}, \tau) d\tau, \quad (6.2)$$

then this value depends on the large-scale time interval of averaging, T , and so does the ‘subscale’ fluctuation velocity \mathbf{v}' . It is also fairly obvious that the method of splitting an oscillating variable into a mean value and a fluctuating quantity depends on the exact mathematical properties of the averaging operator, often called *filter*.

6.1.2 Filters

The first filter used in describing the turbulent fluid behavior is essentially due to REYNOLDS. For a biographical sketch, see Fig. 6.3. It is based on the assumption that, on a local scale, the pulsations have the properties of a *stationary random process*. If $u(\mathbf{x}, t)$ is the variable in question, it assumes a certain value with a given probability. If \wp is this probability, then $u(\mathbf{x}, t, \wp)$ denotes the probability density with which the function $u(\mathbf{x}, t)$ assumes the value assigned to \wp . The statistically most probable value of $u(\mathbf{x}, t)$ is obtained by integration over all probabilities, namely,

$$\langle u \rangle_S(\mathbf{x}, t) := \int_0^\infty u(\mathbf{x}, t, \wp) d\wp, \quad (6.3)$$

where

$$\int_0^\infty d\wp = 1. \quad (6.4)$$

This filter satisfies the following properties

¹ The choice, how large these time and space scales are, is problem dependent. For problems of geophysical fluid dynamics, meteorology, oceanography and limnology, they may be kilometers and hours or days, in a technical application of aerodynamics or machine hydrodynamics, they may be millimeters and milliseconds. So, the choice of mean values is always connected with some subjective reasoning.

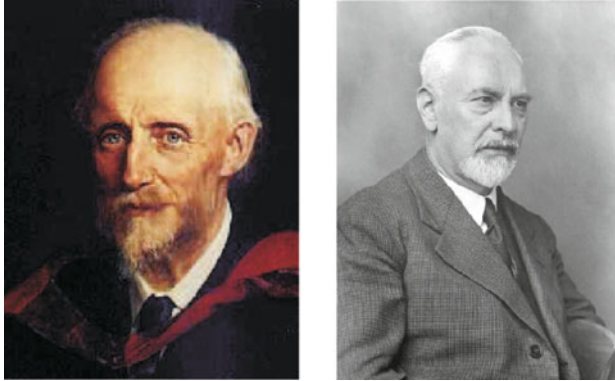


Fig. 6.3 *Left:* Osborne Reynolds in 1903. *Right:* Ludwig Prandtl (<http://en.wikipedia.org/>)

Osborne REYNOLDS (23 August 1842 to 21 February 1912) was a mathematician with degree from Cambridge University (1867) and prominent innovator in the understanding of fluid dynamics. He was appointed professor of engineering at Owens College in Manchester, the first professor in UK university history to hold the title of ‘Professor of Engineering’. REYNOLDS most famously studied the conditions in which the flow of fluid in pipes transitioned from laminar flow to turbulent flow. His studies of condensation and heat transfer between solids and fluids brought radical revision in boiler and condenser technology. He also proposed a mathematical procedure which is now known as REYNOLDS averaging of turbulent flows. This led to the ‘bulk’ description of turbulent flow as expressed in the REYNOLDS-averaged NAVIER–STOKES equations. His final theoretical model, published in the mid-1890s, is still the standard mathematical framework used today. Another subject which REYNOLDS studied in the 1880s was the mechanical behaviour of granular materials.

Ludwig PRANDTL (4 February 1875 to 15 August 1953) was a German engineer, a pioneer in the development of rigorous systematic mathematical analyses which he used to underlay the science of aerodynamics. In the 1920s he developed the mathematical basis for subsonic aerodynamics including transonic velocities. His studies identified the boundary layer, thin airfoils and lifting-line theories. In 1901 PRANDTL became a professor of fluid mechanics at the *Technische Hochschule Hannover*, where he developed many of his most important theories. In 1904, now professes at the University in Göttingen, he delivered a groundbreaking paper, *Fluid Flow with Very Little Friction*, in which he described the boundary layer, its importance for drag and streamlining and the flow separation as a result of the boundary layer, clearly explaining the concept of stall for the first time. In 1918–1919, he published the LANCHESTER–PRANDTL wing theory. Considerable work was included on the nature of induced drag and wingtip vortices and turbulence. Other works examined the problem of compressibility at high subsonic speeds, known as the PRANDTL–GLAUERT correction. He also worked on meteorology, turbulence, plasticity and structural mechanics.

The text is based on <http://en.wikipedia.org/>.

6.1.2.1 Properties of the Statistical Filter

- (i) *Linearity*: Let u, w be two quantities of a turbulent field and a a real number. Then,

$$\langle u + aw \rangle = \langle u \rangle + a \langle w \rangle. \quad (6.5)$$

- (ii) *Commutability with differentiations*: The filter operation must commute with any temporal or spatial differentiation

$$\langle \partial u \rangle = \partial \langle u \rangle, \quad \text{where} \quad \partial \in \left\{ \frac{\partial}{\partial x}, \frac{\partial}{\partial y}, \frac{\partial}{\partial z}, \frac{\partial}{\partial t} \right\}. \quad (6.6)$$

- (iii) *Invariance under multifold averaging*

$$\langle \langle u \rangle \rangle = \langle u \rangle$$

or more generally

$$\langle \langle \dots \langle u \rangle \dots \rangle \rangle = \langle u \rangle. \quad (6.7)$$

The reader may easily show that the statistical filter (6.3) satisfies all these three properties. On the other hand, the reader can easily show that the temporal average (6.2) does not satisfy property (iii).

In the following we *shall now assume that the chosen filter satisfies all three conditions*. This hypothesis is called the *ergodic hypothesis*. It is often used in experiments, when results are being exploited, even when no conditions of statistical and homogeneous turbulence prevail. It is also convenient to verify and memorise the following rules:

Computational rules of the statistical filter:

$$\begin{aligned} \langle \langle u \rangle \rangle &= \langle u \rangle, \\ \langle u' \rangle &= \langle u' \rangle' = 0, \\ \langle \langle u \rangle v \rangle &= \langle u \rangle \langle v \rangle, \\ \langle \langle u \rangle v' \rangle &= 0, \\ \langle uv \rangle &= \langle u \rangle \langle v \rangle + \langle u' v' \rangle. \end{aligned} \quad (6.8)$$

In modern turbulence theory, models are being developed, which request the invariance of the multifold filtering as well as those which negate it. *Reynolds-Averaged Navier–Stokes (RANS)* models satisfy the conditions of the statistical filter; models for which $\langle u' \rangle \neq 0 \longleftrightarrow \langle \langle u \rangle \rangle \neq \langle u \rangle$ do not. These models are summarised under the name *Large Eddy Simulation (LES)* models.

6.1.3 Isotropic Turbulence

Consider a fluid flow with a pulsating velocity field $\mathbf{v}(\mathbf{x}, t)$. Assume that at a fixed spatial point we measure the pulsating components of the velocity $\mathbf{v} = (v_1, v_2, v_3)$, $\mathbf{v}' = (v'_1, v'_2, v'_3)$. Products of the fluctuating velocity components are $v'_i v'_j$ ($i, j = 1, 2, 3$) and their averages $\langle v'_i v'_j \rangle$ are called *correlations* of the velocity components. Symbolically we write

$$\mathbf{Q}_2 := \langle \mathbf{v}'(\mathbf{x}, t) \otimes \mathbf{v}'(\mathbf{x}, t) \rangle \quad (6.9)$$

and call \mathbf{Q}_2 the second statistical moment of the velocity field at \mathbf{x} , if $\langle \cdot \rangle$ is the statistical filter. If \mathbf{Q}_2 has the property that

$$\begin{aligned} v'_i v'_j &= 0 \quad \text{if } i \neq j \quad (i, j = 1, 2, 3), \\ \langle (v'_1)^2 \rangle &= \langle (v'_2)^2 \rangle = \langle (v'_3)^2 \rangle = \langle (u')^2 \rangle \end{aligned} \quad (6.10)$$

for any orthogonal triad, then \mathbf{Q}_2 is called *isotropic*. More formally expressed we say that \mathbf{Q}_2 is invariant under any rotation or inversion of the coordinates. Taking any n th-order statistical moment

$$\mathbf{Q}_n := \underbrace{\langle \mathbf{v}'(\mathbf{x}, t) \otimes \dots \otimes \mathbf{v}'(\mathbf{x}, t) \rangle}_{n\text{-fold}}, \quad (6.11)$$

we may now define isotropic turbulence as follows:

Definition 6.1 A turbulent velocity field \mathbf{v} is called isotropic, if all its statistical moments \mathbf{Q}_n are invariant under any rotation and inversion² of the three-dimensional coordinate system. ■

In practice only a finite number of moments arises. One then says that a turbulent field is isotropic, if all arising statistical moments are invariant under arbitrary rotations.

One variable which is of special interest in turbulence is the so-called *turbulent kinetic energy*. We introduce it via

Definition 6.2 The turbulent kinetic energy k is defined as

$$k := \frac{1}{2} \langle \mathbf{v}' \cdot \mathbf{v}' \rangle = \frac{1}{2} \sum_{i=1}^3 \langle v_i'^2 \rangle \stackrel{(6.10)^2}{=} \frac{3}{2} \langle (u')^2 \rangle. \quad (6.12)$$

The quantity $\langle (u')^2 \rangle^{1/2}$ is called the **turbulent kinetic intensity**. ■

² Henceforth, we shall no longer explicitly mention inversions, but when speaking of arbitrary rotations we mean that inversions are included.

Problem 6.1 *To gain some experience with the above concepts, the reader is asked to verify the following properties:*

$$\begin{aligned}
 (1) \quad \mathbf{Q}_2 &= \frac{2}{3}k\mathbf{I}, \\
 (2) \quad \mathbf{Q}_{2n+1} &= \mathbf{0}, \\
 (3) \quad (\mathbf{Q}_4)_{ijkl} &= \langle u'^2 v'^2 \rangle \delta_{ijkl} + \frac{1}{2} (\langle u'^4 \rangle - \langle u'^2 v'^2 \rangle) (\delta_{ik} \delta_{jl} + \delta_{il} \delta_{jk})
 \end{aligned} \tag{6.13}$$



We prove the first two statements:

- (1) Let us denote the components of the Cartesian coordinates and velocity vectors in the rotated coordinate system by x_i^* and v_i^* , respectively. The invariance of \mathbf{Q}_2 under any rotation implies

$$\langle v_i^* v_j^* \rangle \stackrel{!}{=} \langle v'_i v'_j \rangle \text{ for } (i, j = 1, 2, 3). \tag{6.14}$$

If we consider as an example a rotation about the x_3 -axis by an angle $\pi/2$, then the new and old coordinates are related by

$$x_1^* = x_2, \quad x_2^* = -x_1, \quad x_3^* = x_3, \tag{6.15}$$

and the new and old velocity components are connected by

$$v_1^* = v'_2, \quad v_2^* = -v'_1, \quad v_3^* = v'_3. \tag{6.16}$$

Substitution into (6.14) yields

$$\begin{aligned}
 \langle v_1^* v_1^* \rangle &= \langle v'_2 v'_2 \rangle \stackrel{(6.14)}{=} \langle v'_1 v'_1 \rangle, \\
 \langle v_2^* v_2^* \rangle &= \langle (-v'_1)(-v'_1) \rangle = \langle v'_1 v'_1 \rangle, \\
 \langle v_1^* v_2^* \rangle &= \langle v'_2(-v'_1) \rangle = -\langle v'_1 v'_2 \rangle, \quad \longrightarrow \langle v'_1 v'_2 \rangle = 0.
 \end{aligned} \tag{6.17}$$

A similar choice, viz.,

$$\begin{aligned}
 x_1^* &= x_3, & x_2^* &= x_2, & x_3^* &= -x_1, \\
 v_1^* &= v'_3, & v_2^* &= v'_2, & v_3^* &= -v'_1,
 \end{aligned} \tag{6.18}$$

now yields

$$\begin{aligned}
 \langle v_1^* v_1^* \rangle &= \langle v'_3 v'_3 \rangle \stackrel{(6.14)}{=} \langle v'_1 v'_1 \rangle, \\
 \langle v_3^* v_3^* \rangle &\stackrel{(6.14)}{=} \langle v'_3 v'_3 \rangle, \\
 \langle v_1^* v_3^* \rangle &= \langle v'_3(-v'_1) \rangle = -\langle v'_1 v'_3 \rangle \stackrel{(6.14)}{=} \langle v'_1 v'_3 \rangle \quad \longrightarrow \langle v'_1 v'_3 \rangle = 0, \\
 \langle v_2^* v_3^* \rangle &= \langle v'_2(-v'_1) \rangle = -\langle v'_1 v'_2 \rangle \stackrel{(6.17)}{=} 0.
 \end{aligned} \tag{6.19}$$

Summary of results (6.17) and (6.19) corroborates the correctness of statement (6.10).

(2) We take the mirror operation

$$x_1^* = -x_1, \quad x_2^* = -x_2, \quad x_3^* = -x_3$$

yielding $\mathbf{v}^* = -\mathbf{v}$. So, according to (6.11) we have

$$\mathcal{Q}_{2n+1}^* = (-1)^{2n+1} \underbrace{\langle \mathbf{v}'(\mathbf{x}, t) \otimes \cdots \otimes \mathbf{v}'(\mathbf{x}, t) \rangle}_{(2n+1)\text{-fold}},$$

so that $\mathcal{Q}_{2n+1}^* = \mathcal{Q}_{2n+1}$ implies also $\mathcal{Q}_{2n+1}^* = (-1) \mathcal{Q}_{2n+1}$, proving statement (6.13)₂.

(3) We leave the proof of (6.13)₃ to the reader. \diamond

Isotropic turbulence is an adequate description in the ocean and in lakes only in special situations and at very small spatial scales. On length scales of metres to kilometres, the horizontal and vertical velocity fluctuations have generally distinct characteristics such that $\mathcal{Q}_2 \neq \frac{2}{3}k\mathbf{I}$. In a homogeneous water mass this is so, because the depth scales and the horizontal extents of the lake basins are different by one to two orders of magnitude. In a stratified lake, buoyancy is responsible that the depth scale of characteristic turbulent eddies is even more constrained than under homogeneous conditions.

6.1.4 REYNOLDS Versus FAVRE Averages

The above calculations have all been done in preparation of the derivation of averaged field equations. In this regard, the conservation law of mass points at a subtlety, which we shall explain now. Therefore, consider the mass balance equation

$$\frac{\partial \rho}{\partial t} + \operatorname{div}(\rho \mathbf{v}) = 0, \quad (6.20)$$

which, when averaged, takes the form

$$\left\langle \frac{\partial \rho}{\partial t} \right\rangle + \langle \operatorname{div}(\rho \mathbf{v}) \rangle = 0 \quad (6.21)$$

or, in view of properties (6.6) and (6.8)₅,

$$\frac{\partial \langle \rho \rangle}{\partial t} + \operatorname{div}(\langle \rho \rangle \langle \mathbf{v} \rangle) + \operatorname{div}(\langle \rho' \mathbf{v}' \rangle) = 0. \quad (6.22)$$

Here, besides the mean fields $\langle \rho \rangle$ and $\langle \mathbf{v} \rangle$, there appears an additional second moment, $\langle \rho' \mathbf{v}' \rangle$; its negative value, $-\langle \rho' \mathbf{v}' \rangle$, has the meaning of a surface mass flux. One wishes to avoid this mass flux in order to assign to the averaged body boundaries some notion of ‘averaged material surfaces’. There are generally two situations, which are typical.

Case (1): Consider a density-preserving or a BOUSSINESQ fluid for which the variation of ρ is only accounted for in the buoyancy force. In this situation $\langle \rho \rangle = \rho = \text{constant}$, $\rho' = 0$ and (6.22) reduces to

$$\text{div} \langle \mathbf{v} \rangle = 0. \quad (6.23)$$

There is automatically no turbulent mass flux.

Case (2): For a compressible fluid, (6.22) stays as it is. However, by introducing a density-weighted average of the velocity vector, a ‘virtual’ mass flux can be avoided. To prove this, we need

Definition 6.3 *The density-weighted average $\{f\}$ of a field quantity f is defined as*

$$\{f\} := \frac{\langle \rho f \rangle}{\langle \rho \rangle}, \quad (6.24)$$

so that

$$f = \{f\} + f'' \quad (6.25)$$

is decomposed into the so-called FAVRE average $\{f\}$ and the fluctuating deviation f'' from it. ■

Applying (6.24) to the velocity, the FAVRE average of the velocity may be interpreted as a *barycentric velocity*. Moreover, f'' is not the fluctuation $(f')'$. The double dash is simply a notation to distinguish f' from f'' . It is easy to show that

$$\{f\} = \langle f \rangle + \frac{\langle \rho' f' \rangle}{\langle \rho \rangle}, \quad f'' = f' - \frac{\langle \rho' f' \rangle}{\langle \rho \rangle}. \quad (6.26)$$

Putting in (6.26)₂ $f = \mathbf{v}$, solving the emerging equation for $\langle \rho' \mathbf{v}' \rangle$ and substituting the resulting expression into the last term in (6.22) yields

$$\frac{\partial \langle \rho \rangle}{\partial t} + \text{div}(\langle \rho \rangle \{ \mathbf{v} \}) = 0, \quad (6.27)$$

which is free of a mass flux term. It is obviously valid for compressible and density-preserving fluids, since for $\rho = \text{constant}$, (6.27) simply reduces to $\text{div} \mathbf{v} = 0$.

6.2 Balance Equations for the Averaged Fields

6.2.1 Motivation

The purpose in geophysical fluid mechanics in studying turbulent motions in the atmosphere, the ocean and lakes is to determine the distribution of the field variables such as velocity, pressure, temperature, tracer concentration. These fields are certain averages of the true fields, which, in turbulent flows, are fluctuating. Turbulent motion manifests itself often as a cascade of vortical structures, of which the sizes are restricted by the extent of the domains where the motion takes place. In a lake, bounded by its shores, the largest gyre that can occur is of the horizontal extent of the lake basin. By fluid flow instabilities these gyres break into smaller ones of cascading dimension to very small eddies. So, the sizes of these vortical structures are from approximately 1 mm to several kilometres (in the ocean up to thousands of kilometres). In a theoretical description the motion can only be resolved to a certain length, usually twice the grid size by which the governing equations are discretised in a numerical solution scheme. It is one of the fundamental facts of hydrodynamics of water or air that on the smallest time scale (≈ 1 s) and on the smallest space scale (≈ 1 mm) (below which dissipation turns into heat), the NAVIER–STOKES equations are the adequate description of the fluid motion by which the turbulent eddies from the smallest size through all sizes can be well reproduced. Comparison of turbulent velocity fields with results from such *Direct Numerical Simulations (DNS)* has corroborated this over and over again. It is, however, impossible in general to resolve the dynamical processes to such small length and time scales. Averaging the NAVIER–STOKES equations will filter out the pulsations on the small time and space scales, but the loss of information is partly counteracted by the correlation terms which must be parameterised in a way similar to material constitutive closure relations.

We shall demonstrate this procedure for a BOUSSINESQ fluid or a fluid satisfying the free convection assumption of which the governing equations are as follows:

- Continuity equation

$$\operatorname{div} \mathbf{v} = 0,$$

- Momentum equation

$$\frac{\partial \mathbf{v}}{\partial t} + \operatorname{div}(\mathbf{v} \otimes \mathbf{v}) + 2\boldsymbol{\Omega} \times \mathbf{v} = -\frac{1}{\rho} \operatorname{grad} p + \nu \operatorname{div} \operatorname{grad} \theta + \frac{\rho}{\rho_0} \mathbf{g},$$

- Heat equation

$$\frac{\partial \theta}{\partial t} + \operatorname{div}(\theta \mathbf{v}) = \chi^{(\theta)} \operatorname{div} \operatorname{grad} \theta + \frac{\varphi}{\rho c_v} + \frac{r}{c_v}, \quad (6.28)$$

- Thermal equation of state

$$\rho = \hat{\rho}(\theta) \quad \text{or} \quad \rho = \hat{\rho}(\theta, p) \quad \text{or} \quad \rho = \hat{\rho}(\theta, p, s),$$

- Tracer mass balance

$$\frac{\partial c}{\partial t} + \text{div}(c\mathbf{v}) = \chi^{(c)} \text{div grad} c + \phi^{(c)}.$$

In these equations $\{\mathbf{v}, \theta, \rho, c\}$ are the velocity, temperature, density and concentration fields; $\rho_0(z)$ is the reference density for the lake at rest, often taken to be $\rho_* = \rho(4^\circ\text{C})$, the density of pure water at 4°C ; furthermore, $\{\nu, \chi^{(\theta)}, \chi^{(c)}, c_v\}$ are the (molecular) viscosity, the thermal and species diffusivities and the specific heat at constant volume, while $\{\boldsymbol{\Omega}, \varphi, r, \phi^{(c)}\}$ are the angular velocity of the Earth, the dissipation rate density, the radiation density and the production rate density of species c . Besides the CORIOLIS acceleration the momentum equation contains here a buoyancy term. Moreover, the density is a field variable, which is determined via the thermal equation of state for the density, which for not too deep lakes is approximately given by a quadratic function of the temperature. For deep lakes as, e.g. Lake Baikal or Lake Tanganyika, the pressure dependence of the density must also be accounted for, and in lagoons and strongly mineralised lakes an additional dependence is that on the salinity s , for which a diffusion equation must hold. In all these cases the reference density ρ_0 may be position dependent. It is assumed, however, that $\{\nu, \chi^{(\theta)}, \chi^{(c)}, c_v, \rho c_v\}$ are all constant.

6.2.2 Averaging Procedure

Equations (6.28) are now subject to the statistical filter operation as this was done for the balance of mass, (6.20), (6.21), and (6.22). In a first attempt this will be done for a REYNOLDS averaging procedure. Treating $\{\mathbf{v}, p, \theta, c\}$ as independent variables, we choose³

$$\mathbf{v} = \langle \mathbf{v} \rangle + \mathbf{v}', \quad p = \langle p \rangle + p', \quad \theta = \langle \theta \rangle + \theta', \quad c = \langle c \rangle + c'. \quad (6.29)$$

If these decompositions are substituted into (6.28) and the resulting equations are averaged, the results of the problem stated below are obtained.

Problem 6.2 *Show that by averaging equations (6.28), the following averaged field equations are obtained:*

³ If mass balance says that the velocity field is solenoidal, then REYNOLDS averaging for \mathbf{v} does not have to be replaced by FAVRE averaging.

- *Continuity equation*

$$\operatorname{div}\langle \mathbf{v} \rangle = 0,$$

- *Momentum equation*

$$\begin{aligned} \frac{\partial \langle \mathbf{v} \rangle}{\partial t} + \operatorname{div}(\langle \mathbf{v} \rangle \otimes \langle \mathbf{v} \rangle) + 2\boldsymbol{\Omega} \times \langle \mathbf{v} \rangle \\ = -\frac{1}{\rho_0} \operatorname{grad}\langle p \rangle + \nu \operatorname{div} \operatorname{grad}\langle \mathbf{v} \rangle + \frac{\langle \rho \rangle}{\underline{\underline{\rho_0}}} g - \underline{\underline{\operatorname{div}(\langle \mathbf{v}' \otimes \mathbf{v}' \rangle)}}, \end{aligned} \quad (6.30)$$

- *Energy equation*

$$\frac{\partial \theta}{\partial t} + \operatorname{div}(\langle \theta \rangle \langle \mathbf{v} \rangle) = \chi^{(\theta)} \operatorname{div} \operatorname{grad}\langle \theta \rangle + \frac{1}{\rho c_v} \frac{\langle \varphi \rangle}{\underline{\underline{\rho c_v}}} + \frac{r}{c_v} - \underline{\underline{\operatorname{div}\langle \mathbf{v}' \theta' \rangle}},$$

- *Tracer mass balance*

$$\frac{\partial \langle c \rangle}{\partial t} + \operatorname{div}(\langle c \rangle \langle \mathbf{v} \rangle) = \chi^c \operatorname{div} \operatorname{grad}\langle c \rangle + \langle \phi^{(c)} \rangle - \underline{\underline{\operatorname{div}\langle \mathbf{v}' c' \rangle}}.$$

◆

In these equations the singly underlined terms are the correlation products, which can be identified with flux terms of momentum, energy and tracer mass, respectively. It is customary to associate these with special names.

Definition 6.4

(i) *The quantity*

$$\mathbf{R} := -\rho \langle \mathbf{v}' \otimes \mathbf{v}' \rangle \quad (6.31)$$

is called **Reynolds stress tensor**; it was first introduced by REYNOLDS in 1894 [21].

(ii) *The flux of energy*

$$\mathbf{q}_t := \rho c_v \langle \mathbf{v}' \theta' \rangle \quad (6.32)$$

is called the **turbulent heat flux vector**.

(iii) *The flux vector*

$$\mathbf{j}_t := \langle \mathbf{v}' c' \rangle \quad (6.33)$$

is called the **turbulent species mass flux vector** or simply the **turbulent mass flux vector**. ■

Quantities (6.31), (6.32) and (6.33) must be parameterised in terms of the averaged fields. Examples for these will be given below.

Equations (6.30) also contain two other averaged fields, $\langle \rho \rangle$ and $\langle \phi \rangle$, which must equally be expressed in terms of the independent averaged fields. We shall now address the parameterisations of all these quantities in due order.

6.2.3 Averaged Density Field $\langle \rho \rangle$

We start with the equation of state in its simplest form $\rho = \hat{\rho}(\theta)$. If we substitute $\theta = \langle \theta \rangle + \theta'$, assume that $|\theta'| \ll |\langle \theta \rangle|$ and employ TAYLOR series expansion, we obtain

$$\rho(\langle \theta \rangle + \theta') = \rho(\langle \theta \rangle) + \left. \frac{d\rho}{d\theta} \right|_{\langle \theta \rangle} \theta' + \frac{1}{2} \left. \frac{d^2\rho}{d\theta^2} \right|_{\langle \theta \rangle} \langle (\theta')^2 \rangle + \dots, \quad (6.34)$$

so that after averaging

$$\langle \rho(\langle \theta \rangle + \theta') \rangle = \langle \rho(\langle \theta \rangle) \rangle + \left\langle \frac{1}{2} \left. \frac{d^2\rho}{d\theta^2} \right|_{\langle \theta \rangle} \right\rangle \langle (\theta')^2 \rangle + \dots, \quad (6.35)$$

in which $\langle \rho(\langle \theta \rangle) \rangle \equiv \rho(\langle \theta \rangle)$. This result is interesting: to lowest order $\langle \rho(\theta) \rangle$ is simply $\rho(\langle \theta \rangle)$, but when temperature fluctuations are not small, then the second term on the right-hand side of (6.35) with the autocorrelation $\langle (\theta')^2 \rangle$ is also important. This contribution may be written as

$$\frac{1}{2} \kappa \langle (\theta')^2 \rangle, \quad \kappa := \left. \frac{d^2\rho}{d\theta^2} \right|_{\langle \theta \rangle}, \quad (6.36)$$

where κ is the curvature of the density as a function of temperature (which for a quadratic equation of state $\rho(\theta)$, $0 \leq \rho \leq 30^\circ\text{C}$ can be taken as constant). If this second-order term is not negligible, it must be expressed in terms of the original independent fields. We conclude that the higher order approximation of the density function has led to a new temperature correlation for which an additional closure condition is needed.

It is now pretty clear, how $\langle \rho \rangle$ can be evaluated when $\rho = \rho(\theta, a)$ where a is either p or s . The reader is asked to show this in the following problem:

Problem 6.3 Assume that the thermal equation of state is given as $\rho = \rho(\theta, a)$, where $a = p$ (Lake Baikal) and $a = s$ (lagoons). Show that in this case

$$\langle \rho(\theta, a) \rangle = \rho(\langle \theta \rangle, \langle a \rangle) + \frac{1}{2} \kappa_\theta \langle (\theta')^2 \rangle + \kappa_{\theta a} \langle a' \theta' \rangle + \frac{1}{2} \kappa_a \langle (a')^2 \rangle + \dots \quad (6.37)$$

with

$$\kappa_\theta := \frac{\partial^2 \rho}{\partial \theta^2} \Big|_{\langle \theta \rangle \langle a \rangle}, \quad \kappa_{\theta a} = \frac{\partial^2 \rho}{\partial \theta \partial a} \Big|_{\langle \theta \rangle \langle a \rangle}, \quad \kappa_a = \frac{\partial^2 \rho}{\partial a^2} \Big|_{\langle \theta \rangle \langle a \rangle}. \quad (6.38)$$

Depending upon the numerical values for κ_θ , $\kappa_{\theta a}$, κ_a some of the higher order terms may be ignored. \blacklozenge

6.2.4 Dissipation Rate Density $\langle \phi \rangle$

The dissipation rate density per unit mass for a density-preserving NAVIER–STOKES fluid is given by

$$\begin{aligned} \frac{1}{\rho} \langle \phi \rangle &= \left\langle \frac{1}{\rho} (\mathbf{t}' \cdot \mathbf{D}) \right\rangle = \left\langle \frac{1}{\rho} (2\eta \mathbf{D} \cdot \mathbf{D}) \right\rangle = 2\nu \langle \mathbf{D} \cdot \mathbf{D} \rangle \\ &= 2\nu \langle \mathbf{D} \rangle \cdot \langle \mathbf{D} \rangle + 2\nu \langle \mathbf{D}' \cdot \mathbf{D}' \rangle \\ &= \underbrace{4\nu II_{\langle \mathbf{D} \rangle}}_{\text{dissipation rate due to the mean velocity}} + \underbrace{4\nu \langle II_{\mathbf{D}'} \rangle}_{\text{turbulent dissipation rate}}, \end{aligned} \quad (6.39)$$

in which $II_A = \frac{1}{2} \text{tr} A^2$. As before, when evaluating $\langle \rho \rangle$ the dissipation rate density consists of two contributions, the dissipation rate due to the mean velocity field plus the turbulent dissipation rate. This latter term is again a correlation quantity and is a very important variable in modern higher order turbulent closure conditions.

So far, we have encountered two scalar quantities. Because of their importance in turbulence modeling we state them explicitly in

Definition 6.5

(1) The **turbulent kinetic energy (density)** k is defined as

$$k := \frac{1}{2} \langle \mathbf{v}' \cdot \mathbf{v}' \rangle, \quad (6.40)$$

(2) The **turbulent dissipation rate (density)** is defined as

$$\varepsilon := 4\nu \langle II_{\mathbf{D}'} \rangle. \quad (6.41)$$

They are both correlations of the velocity fluctuations. \blacksquare

6.2.5 Reynolds Stress Hypothesis

A very important concept of turbulence theory is the REYNOLDS hypothesis and the introduction of the *eddy viscosity*. It may be determined from the idea that the

state of turbulence of the velocity field is connected with the mean field through its gradient; the larger the gradient of the mean velocity field, the larger will be the generated turbulent activity. The fundamental idea goes back to BOUSSINESQ [3], who in the situation of a simple shear flow wrote in analogy to the corresponding laminar flow

$$\tau_t = \rho \nu_t \frac{\partial \langle v_1 \rangle}{\partial x_2}, \quad (6.42)$$

in which τ_t is the turbulent (REYNOLDS) shear stress, v_1 the x_1 -parallel turbulent-averaged velocity and ν_t , sometimes written as ϵ_t , is a *turbulent kinematic viscosity*, also called *turbulent exchange coefficient*. This second denotation is due to PRANDTL [18] who interprets the turbulent stress as an exchange of momentum due to the pulsating velocity.⁴

It transpires from relation (6.42) that its generalisation into three dimensions could be $\mathbf{R} = \hat{\mathbf{R}}(\langle \mathbf{D} \rangle)$, e.g. $\mathbf{R} = \rho 2\nu_t \langle \mathbf{D} \rangle$ (it satisfies (6.42) under conditions of simple shear).⁵ However, in view of definition (6.31) we have $\text{tr} \mathbf{R} = -\rho \langle \mathbf{v}' \cdot \mathbf{v}' \rangle \stackrel{(6.12)}{=} -2\rho k$. On the other hand, for a BOUSSINESQ fluid $\text{tr}(\langle \mathbf{D} \rangle) = 0$. It follows that one must request that

$$-\langle \mathbf{v}' \otimes \mathbf{v}' \rangle = \frac{\mathbf{R}}{\rho} = -\frac{2}{3}k\mathbf{I} + 2\nu_t \langle \mathbf{D} \rangle$$

or

$$\mathbf{R} = -\frac{2}{3}\rho k\mathbf{I} + 2\rho \nu_t \langle \mathbf{D} \rangle. \quad (6.43)$$

This parameterisation of the REYNOLDS stress tensor contains two modeling parameters of turbulence, the turbulent kinetic energy, k plus the turbulent kinematic viscosity, ν_t .

6.2.5.1 Turbulent Heat Flux q_t and Turbulent Species Mass Flux j_t

Here we may postulate that these vectors orient themselves on the gradients of the mean temperature and mean concentration fields, respectively. This then suggests

⁴ Reading PRANDTL's paper is highly recommended. A translation into the English language of the significant paragraphs along with the German original is given on pages 466–468 in [7].

⁵ Note that for simple shear

$$\langle \mathbf{D} \rangle = \begin{pmatrix} 0 & \frac{1}{2} \frac{\partial \langle v_1 \rangle}{\partial x_2} & 0 \\ \frac{1}{2} \frac{\partial \langle v_1 \rangle}{\partial x_2} & 0 & 0 \\ 0 & 0 & 0 \end{pmatrix} \quad \text{and} \quad \mathbf{R} = \begin{pmatrix} 0 & \tau_{12} & 0 \\ \tau_{12} & 0 & 0 \\ 0 & 0 & 0 \end{pmatrix}.$$

closure conditions analogous to FOURIER's law of heat conduction and FICK's first law of mass flux as follows:

$$\frac{1}{\rho c_v} \mathbf{q}_t := \langle \mathbf{v}' \theta' \rangle = -\chi_t^{(\theta)} \text{grad} \langle \theta \rangle, \quad (6.44)$$

$$\mathbf{j}_t := \langle \mathbf{v}' c' \rangle = -\chi_t^{(c)} \text{grad} \langle c \rangle. \quad (6.45)$$

The newly introduced scalar quantities $\chi_t^{(\theta)}$ and $\chi_t^{(c)}$ are called *eddy diffusivities* of heat and mass, respectively.

The above averaging procedure of the NAVIER–STOKES equations has brought into evidence a number of new turbulent quantities, which can be grouped as

$$\text{Group 1 : } \{k, \varepsilon, \nu_t, \chi_t^{(\theta)}, \chi_t^{(c)}\} \quad (6.46)$$

$$\text{Group 2 : } \{\langle (\theta')^2 \rangle, \langle (a')^2 \rangle, \langle \theta' a' \rangle\} \quad (6.47)$$

where $a = s$ or $a = p$. Those in group 1 are scalar coefficients of which numerical values need to be prescribed, whereas the variables in the second group arose when the density function $\rho(\theta, a)$ was averaged to second order; see (6.32). In the lowest order approximation, in which $\langle \rho(\theta, a) \rangle \approx \rho(\langle \theta \rangle, \langle a \rangle)$, these variables are of no relevance.⁶ If we consider this case, there remain, however, still the five quantities of the first group. They may, in general, be functions of $\langle \theta \rangle, \langle c \rangle$ and all invariants of $\langle \mathbf{D} \rangle, \text{grad} \langle \theta \rangle$ and $\text{grad} \langle c \rangle$, but it is customary in turbulence theory to assume $\{\nu_t, \chi_t^{(\theta)}, \chi_t^{(c)}\}$ to be functions of $\{k, \varepsilon, \langle \theta \rangle, \langle c \rangle\}$, and in heterogeneous turbulence also of the spatial coordinates; hence,

$$\{\nu_t, \chi_t^{(\theta)}, \chi_t^{(c)}\} = f_{cts}(k, \varepsilon, \langle \theta \rangle, \langle c \rangle, \mathbf{x}). \quad (6.48)$$

Moreover, it is also customary to introduce the ratios between the eddy viscosity and the turbulent diffusivities of heat and mass

$$\sigma_\theta := \frac{\nu_t}{\chi_t^{(\theta)}}, \quad \sigma_c := \frac{\nu_t}{\chi_t^{(c)}} \quad (6.49)$$

and to call σ_θ *turbulent PRANDTL number* and σ_c *turbulent SCHMIDT number*. The turbulent heat and mass fluxes can then be written as

$$\langle \mathbf{v}' \theta' \rangle = -\frac{\nu_t}{\sigma_\theta} \text{grad} \langle \theta \rangle, \quad \langle \mathbf{v}' c' \rangle = -\frac{\nu_t}{\sigma_c} \text{grad} \langle c \rangle. \quad (6.50)$$

⁶ What is meant here is that no new turbulent closure must be given if the equation of state is prescribed.

As long as one chooses for $\{\nu_t, \sigma_\theta, \sigma_c\}$ independent functional representations of $\{k, \varepsilon, \langle\theta\rangle, \langle c\rangle\}$, (6.50) is equivalent to (6.48). If, however, σ_θ and σ_c are assumed to be constant, then the functional dependencies of $\chi_t^{(\theta)}$ and $\chi_t^{(c)}$ are affine to that of ν_t . This is a kind of similarity rule, sometimes not being experimentally corroborated, but often employed. In this simple case, one then only needs to find a relation for

$$\nu_t = \hat{\nu}_t(k, \varepsilon, \langle\theta\rangle, \langle c\rangle, \mathbf{x}). \quad (6.51)$$

If ν_t neither depends on $\langle\theta\rangle$ nor on $\langle c\rangle$, then, apart from a dependence on \mathbf{x} , (6.51) reduces to

$$\nu_t = \hat{\nu}_t(k, \varepsilon, \cdot), \quad \text{or, even simpler} \quad \nu_t = \hat{\nu}_t(k, \cdot), \quad (6.52)$$

where the dot stands for a possible \mathbf{x} -dependence. If the parameterisations of ν_t on k, ε (and \mathbf{x}) or on k (and \mathbf{x}) are known, one then only needs additional algebraic or differential equations for k or k and ε to fix the turbulent viscosity. Depending upon, which case prevails, one then speaks of *one- or two-equation models*. In early turbulence modeling the turbulent viscosity was often assumed to be at most a function of position.

6.2.6 One- and Two-Equation Models

The derivation of the REYNOLDS-averaged evolution equations (6.30) has naturally led to two new quantities characterising the subgrid⁷ behaviour for the averaged fields, the turbulent kinetic energy k and the turbulent dissipation rate ε . These two quantities were then taken to determine the actual values of the turbulent viscosity ν_t and diffusivities $\chi_t^{(\theta)}$ and $\chi_t^{(c)}$. PRANDTL in his seminal papers [18, 19] describes the eddy viscosity as a function of the mean velocity gradient and a mixing length, $\nu_t = \ell^2 |\partial \langle v_1 \rangle / \partial x_2|$, for simple shearing which in three-dimensional flows may be extrapolated to have the form

$$\nu_t = 2\ell^2 \sqrt{\Pi_{(D)}}, \quad (6.53)$$

(which was *not* proposed in this form by PRANDTL). This formula is dimensionally correct, but it requires parameterisation of the mixing length ℓ . This was done by PRANDTL himself in his paper of 1933 [19], by postulating a balance law of the form

$$\frac{\partial \ell}{\partial t} + \text{div}(\ell \langle \mathbf{v} \rangle) + 2\ell \sqrt{\Pi_{(D)}} + \dots = 0 \quad (6.54)$$

⁷ The small-scale behavior on time scales, which are typical of the filtered variables, is also called *subgrid* behaviour. This denotation is motivated by numerics, in which the choice of the mesh or grid size delimits the reproduction of processes whose length and time scales are at least twice the grid size. Processes with smaller scales are then operating on scales of subgrid size.

for the mixing length. PRANDTL's proposal is an example of a one-equation model. If ℓ is determined by (6.54), the turbulent viscosity and diffusivities are known via the equations

$$\nu_t = 2\ell^2 \sqrt{\Pi_{(D)}}, \quad \chi_t^{(\theta)} = \frac{\nu_t}{\sigma_\theta}, \quad \chi_t^{(c)} = \frac{\nu_t}{\sigma_c} \quad (6.55)$$

and, since dimensionally, $[k] = [\nu_t^2/\ell^2]$, one may also set

$$k = c_k 4\ell^2 \Pi_{(D)}. \quad (6.56)$$

In (6.55) and (6.56), σ_θ , σ_c and c_k are fitting constants.

On the other hand, if one dispenses with the postulation of (6.53), then an additional scalar turbulent quantity remains undetermined, e.g. k and ℓ or another variable that can be related to k , ε and ℓ . One is then forced to propose an evolution equation for an additional quantity, which characterises the turbulent intensity. Such quantities are, for instance, the

- turbulent dissipation rate, ε ,
- turbulent kinetic energy, k ,
- turbulent vorticity, ω ,

where these and the turbulent length scale are dimensionally related by

$$[\varepsilon] = \frac{[k^{3/2}]}{[\ell]}, \quad [\omega] = \frac{[k]}{[\ell^2]}. \quad (6.57)$$

Two-equation models have been proposed for the turbulent variable scales

$$(k, \ell), \quad (k, \varepsilon), \quad (k, \omega).$$

They are called $(k - \ell)$ -model, $(k - \varepsilon)$ -model and $(k - \omega)$ -model, respectively. For each of these, balance law-type evolution equations have been proposed. The most popular one is the $(k - \varepsilon)$ -model, [8, 9], and it has extensively been tested against experiments. However, the $(k - \omega)$ -model has also gained popularity in geophysical applications, [32, 33].

For all these models a direct connection with the turbulent viscosity must still be established. This is obtained with the aid of dimensional analysis by appropriately constructing the physical dimension of the quantity under question. For instance, it can easily be shown that

$$[\nu_t] = \frac{[k^2]}{[\varepsilon]} = [k^{1/2}][\ell] = \frac{[k]}{[\omega^{1/2}]}$$

from which we may postulate the parameterisations

$$\nu_t = c_\mu \frac{k^2}{\varepsilon} = c'_\mu k^{1/2} \ell = c''_\mu k \omega^{-1/2}, \quad (6.58)$$

in which the various c_μ 's are constants adjusted by experiment.⁸

6.3 k - ε Model for Density-Preserving and Boussinesq Fluids

In this section the most popular first-order turbulence model will be presented for use in later chapters of the third volume of this treatise, the $(k - \varepsilon)$ -model. This model uses evolution equations for the specific turbulent kinetic energy, k , and the specific turbulent dissipation rate, ε . The model will not be derived, but presented and motivated. Basic for the model is relation, (6.58)₁, or

$$\nu_t = c_\mu \frac{k^2}{\varepsilon}. \quad (6.59)$$

Since dimensionally $[\nu_t] = [k]^2/[\varepsilon]$, it follows that c_μ is a dimensionless scalar, which in the $(k - \varepsilon)$ -model is taken to be a constant. For k and ε , evolution (partial differential) equations of balance type are derived. These will also contain scalar parameters and must equally be determined numerically by validating the model.

Historically, the $(k - \varepsilon)$ -model has originally been developed in the 1970's by HANSALIC and LAUNDER [5], JONES and LAUNDER [8] and LAUNDER and SPALDING [9]. It has, in the last decades, attracted great attention in the engineering and the geophysical modeling community. RODI [22, 23] describes its applicability in geophysics and the hydraulic engineering community, and WEIS [31] and UMLAUF [29] put it into the proper perspective with other two-equation models. A derivation using continuum mechanical principles is given in HUTTER and JÖHNK [7]. For its derivation the reader is asked to consult the specialised literature.

6.3.1 The Balance Equations

The REYNOLDS-averaged forms of the balance laws of mass, momentum, energy and tracer mass are stated in (6.30). In the $(k - \varepsilon)$ -closure scheme these are, however, complemented by balance laws for the turbulent kinetic energy, k , and its dissipation rate, ε . These equations have the form

⁸ Even though values for the c_μ 's have been obtained by experiment, these constants exhibit some notion of universality, i.e. their numerical values are assumed to hold for (nearly) all turbulent processes.

$$\begin{aligned}\frac{\partial k}{\partial t} + \operatorname{div}(k\langle \mathbf{v} \rangle) &= -\operatorname{div}(\boldsymbol{\phi}^k) + \pi^k, \\ \frac{\partial \varepsilon}{\partial t} + \operatorname{div}(\varepsilon\langle \mathbf{v} \rangle) &= -\operatorname{div}(\boldsymbol{\phi}^\varepsilon) + \pi^\varepsilon,\end{aligned}\tag{6.60}$$

in which $\boldsymbol{\phi}^k$ and $\boldsymbol{\phi}^\varepsilon$ are flux and π^k and π^ε are production terms. These equations are the local forms of the global statements.

$$\begin{aligned}\frac{d}{dt} \int_{\omega} k \, dv &= - \int_{\partial\omega} \boldsymbol{\phi}^k \cdot \mathbf{n} \, da + \int_{\omega} \pi^k \, dv, \\ \frac{d}{dt} \int_{\omega} \varepsilon \, dv &= - \int_{\partial\omega} \boldsymbol{\phi}^\varepsilon \cdot \mathbf{n} \, da + \int_{\omega} \pi^\varepsilon \, dv,\end{aligned}\tag{6.61}$$

two forms, which are more convenient when numerical solutions are sought.

The essence of the $(k - \varepsilon)$ -model, which makes it an improved description of the turbulent dynamic parameterisation over the zeroth-order closure schemes, lies in the postulation of these variables plus corresponding variables in (6.30) (the underlined terms).

6.3.2 Closure Relations

The flux terms in the $(k - \varepsilon)$ -model, (6.30), are parameterised as stated in (6.43), (6.44) and (6.45), viz.,

$$\begin{aligned}\frac{\mathbf{R}}{\rho} &= -\langle \mathbf{v}' \otimes \mathbf{v}' \rangle = -\frac{2}{3} \rho k \mathbf{I} + 2\nu_t \langle \mathbf{D} \rangle, \\ \frac{\mathbf{q}_t}{\rho c_v} &= \langle \mathbf{v}' \theta' \rangle = -\frac{\nu_t}{\sigma_\theta} \operatorname{grad} \langle \theta \rangle, \\ \mathbf{j}_t &= \langle \mathbf{v}' c' \rangle = -\frac{\nu_t}{\sigma_c} \operatorname{grad} \langle c \rangle,\end{aligned}\tag{6.62}$$

in which (6.49), (6.50) have also been used to relate the turbulent thermal and species diffusivities via the PRANDTL and SCHMIDT numbers to the kinematic turbulent viscosity, ν_t , which is given in the form as stated in (6.59). With this choice, the turbulent viscosity evolves now in time according to as k and ε evolve in space and time according to their balance laws (6.60).

The flux terms in (6.60) are analogously parameterised, namely as

$$\boldsymbol{\phi}^k = -\frac{\nu_t}{\sigma_k} \operatorname{grad} k, \quad \boldsymbol{\phi}^\varepsilon = -\frac{\nu_t}{\sigma_\varepsilon} \operatorname{grad} \varepsilon\tag{6.63}$$

with two new PRANDTL numbers, σ_k and σ_ε , to be numerically determined.

The judicious selection of the production rate densities π^k and π^ε is the heart of the construction of the $(k - \varepsilon)$ -model and goes beyond the goals of this book. We shall only state the results and ask the reader to consult the specialised literature, see, e.g. [7, 22, 23]. For a BOUSSINESQ fluid one gets

$$\pi^k = \operatorname{div}(v \operatorname{grad} k) + 4v_t II_{\langle \mathbf{D} \rangle} - \varepsilon + \frac{\langle \rho \rangle \langle \alpha_\theta \rangle}{\rho^*} \frac{v_t}{\sigma_\theta} \mathbf{g} \cdot \operatorname{grad} \langle \theta \rangle, \quad (6.64)$$

$$\pi^\varepsilon = \operatorname{div}(v \operatorname{grad} \varepsilon) + 4c_1 k II_{\langle \mathbf{D} \rangle} - c_2 \frac{\varepsilon^2}{k} + c_3 \frac{\langle \rho \rangle \langle \alpha_\theta \rangle}{\rho^*} \frac{c_\mu}{\sigma_\theta} k \mathbf{g} \cdot \operatorname{grad} \langle \theta \rangle, \quad (6.65)$$

in which

$$\langle \alpha_\theta \rangle = - \frac{1}{\hat{\rho} \langle \theta \rangle} \frac{\partial \rho(\theta)}{\partial \theta} \Big|_{\langle \theta \rangle} \quad (6.66)$$

is the coefficient of thermal expansion and

$$II_{\langle \mathbf{D} \rangle} = \frac{1}{2} \langle \mathbf{D} \rangle \cdot \langle \mathbf{D} \rangle. \quad (6.67)$$

In (6.64), (6.65) the divergence terms can be combined with the turbulent flux terms (6.63). The second and third terms on the right-hand side of (6.64), (6.65) are the classical production terms of the $(k - \varepsilon)$ -model of density-preserving fluids, while the last terms are due to the buoyancy effects of the BOUSSINESQ fluid.

For the postulation of the dissipation rate density $\langle \phi \rangle$, we choose (6.39). Moreover, the radiation is taken as $\rho r = \operatorname{div} \mathbf{I}$, where \mathbf{I} is the POINTING vector. This choice has the geophysical application in mind, where the radiation is essentially due to solar irradiation. With the z -coordinate perpendicular to the Earth's surface, the dominant variation of the POINTING vector is vertical, so that with sufficient accuracy we may set

$$\rho r = \operatorname{div} \mathbf{I} \approx \frac{\partial I_z}{\partial z}, \quad (6.68)$$

in which

$$I_z = I_0 \exp \left\{ \int_0^z (k_w + \dots) dz \right\}, \quad (6.69)$$

where $z < 0$, I_0 is the value of the POINTING vector for $z = 0$ and $k_w \approx 0.3$ is the *extinction coefficient* of clear water which, in lakes and the ocean, varies from position to position; furthermore, the dots indicate additional possible influences by a phytoplankton population, etc.

6.3.3 Summary of $(k - \varepsilon)$ -Equations

Upon substitution of the above representations into the balance laws (6.30) and (6.60) the following field equations for turbulent motions in a BOUSSINESQ fluid are obtained:

- Balance of mass

$$\operatorname{div}\langle \mathbf{v} \rangle = 0.$$

- Balance of momentum

$$\begin{aligned} & \frac{\partial \langle \mathbf{v} \rangle}{\partial t} + \operatorname{div}(\langle \mathbf{v} \rangle \otimes \langle \mathbf{v} \rangle) + 2\boldsymbol{\Omega} \times \langle \mathbf{v} \rangle \\ &= -\frac{1}{\rho^*} \operatorname{grad} \langle p \rangle + \operatorname{div} (2(\nu + \nu_t) \langle \mathbf{D} \rangle) + \frac{\langle \rho \rangle}{\rho^*} \mathbf{g}. \end{aligned}$$

- Balance of energy

$$\begin{aligned} & \frac{\partial \langle \theta \rangle}{\partial t} + \operatorname{div}(\langle \mathbf{v} \rangle \langle \theta \rangle) \\ &= \operatorname{div} \left(\left(\chi^{(\theta)} + \frac{\nu_t}{\sigma_\theta} \right) \operatorname{grad} \langle \theta \rangle \right) + \frac{4\nu}{c_v} II_{\langle \mathbf{D} \rangle} + \frac{\varepsilon}{c_v} + \frac{1}{\rho^* c_v} \operatorname{div} \mathbf{I}. \end{aligned}$$

- Balance of species mass (we write c for any c_α)

$$\frac{\partial \langle c \rangle}{\partial t} + \operatorname{div}(\langle \mathbf{v} \rangle \langle c \rangle) = \operatorname{div} \left(\left(\chi^{(c)} + \frac{\nu_t}{\sigma_c} \right) \operatorname{grad} \langle c \rangle \right) + \langle \Phi^c \rangle. \quad (6.70)$$

- Balance of turbulent kinetic energy

$$\begin{aligned} & \frac{\partial k}{\partial t} + \operatorname{div}(\langle \mathbf{v} \rangle k) \\ &= \operatorname{div} \left(\left(\nu + \frac{\nu_t}{\sigma_k} \right) \operatorname{grad} k \right) + 4\nu_t II_{\langle \mathbf{D} \rangle} - \varepsilon + \frac{\langle \rho \rangle \langle \alpha_\theta \rangle}{\rho^*} \frac{\nu_t}{\sigma_\theta} \mathbf{g} \cdot \operatorname{grad} \langle \theta \rangle. \end{aligned}$$

- Balance of turbulent dissipation rate

$$\begin{aligned} & \frac{\partial \varepsilon}{\partial t} + \operatorname{div}(\langle \mathbf{v} \rangle \varepsilon) \\ &= \operatorname{div} \left(\left(\nu + \frac{\nu_t}{\sigma_\varepsilon} \right) \operatorname{grad} \varepsilon \right) + 4c_1 k II_{\langle \mathbf{D} \rangle} - c_2 \frac{\varepsilon^2}{k} + \frac{\langle \rho \rangle \langle \alpha_\theta \rangle}{\rho^*} \frac{c_3 c_\mu}{\sigma_\theta} \mathbf{g} \cdot \operatorname{grad} \langle \theta \rangle. \end{aligned}$$

In these equations no expression has been proposed for the production rate density $\langle \Phi^c \rangle$ of species c . Its postulation depends on the particular problem at hand, which is the reason why it remains unspecified. For salinity we, however, have $\langle \Phi^{(s)} \rangle = 0$.

Table 6.1 Numerical values for the closure constants of the $(k - \varepsilon)$ -model

$c_\mu = 0.09$	$c_1 = 0.126$	$c_2 = 1.92$
$c_3 \approx 0$	$\sigma_k = 1.4$	$\sigma_\varepsilon = 1.3$

Moreover, it should also be mentioned that the buoyancy-related terms in the balance relations of turbulent kinetic energy and dissipation rate have formally been derived for an equation of state $\rho = \hat{\rho}(\theta)$. A contribution due to salinity has been ignored.

To the many empirical constants which arise in the above equations, numerical values must be assigned. These are collected in Table 6.1. The values for the constants c_μ , c_1 , c_2 , c_3 and σ_k , σ_ε have been obtained by simple model calculations (for details, see [23]). Values for $c_3 \approx 0$ are very small, but not certain, which is why the corresponding term in the ε -equation is usually ignored.

6.3.4 Boundary Conditions

The field equations (6.70) form a set of $7 + n$ (' n ' for n species mass balances) equations for the unknown fields \mathbf{v} (3), p (1), θ (1), c_α ($\alpha = 1, \dots, n$), k (1), ε (1) unknowns. They constitute a system of non-linear partial differential equations for which boundary and initial conditions must be prescribed. The equations are of parabolic type (they are of first order in the time variable and of second order in the space variables (via the flux parameterisation)). Therefore, boundary conditions must be formulated at the solid bottom and at the free surface for all diffusive-type equations.

(α) *Boundary conditions for momentum:* The bottom surface is generally treated as rigid and material; only for extremely shallow lakes with small depths [less than ≈ 10 m, e.g. lagoons: Vistula (Poland–Russia), Kuronian lagoons (Russia–Lithuania), Neusiedler See (Austria–Hungary), Lake Wuxi (China), Lake Chad (Africa), see also Table 1.1], strong winds will cause sediment transport at the bottom. Excluding these cases, the fixed *bottom surface* may allow a certain discharge of water, Q_\perp^{ground} , into the ground and the velocity tangential to the bed may be either zero (no-slip condition) or related to the basal shear traction. Let us introduce the notation

$$\begin{aligned}
 v_\perp^s &:= \mathbf{v}^s \cdot \mathbf{n}, \\
 \mathbf{v}_\parallel^s &:= \mathbf{v}^s - (\mathbf{v}^s \cdot \mathbf{n})\mathbf{n} = \mathbf{v}^s - v_\perp^s \mathbf{n}, \\
 p_\perp^s &:= -\mathbf{n} \cdot \mathbf{t}^s \mathbf{n}, \\
 \mathbf{t}_\parallel^s &:= \mathbf{t}^s \mathbf{n} - (\mathbf{n} \cdot \mathbf{t}^s \mathbf{n})\mathbf{n} = \mathbf{t}^s \mathbf{n} + p_\perp^s \mathbf{n},
 \end{aligned} \tag{6.71}$$

in which s is a label for a surface ($s = b$ for the bottom surface) and \mathbf{n} is the unit normal vector perpendicular to the surface and exterior to the lake domain. v_\perp^s , \mathbf{v}_\parallel^s , p_\perp^s and \mathbf{t}_\parallel^s are, in turn, the water velocity normal and parallel to the surface, and the

surface normal pressure and the traction parallel to it. With notation (6.71), the *basal boundary conditions* read (the superscript s = b stands for ‘bottom surface’)

$$\begin{aligned}\langle v_{\perp}^b \rangle &= Q_{\perp}^{\text{ground}}, \\ \mathbf{t}_{\parallel}^b &= -\rho^* c_D^b |\langle \mathbf{v}_{\parallel}^b \rangle| \langle \mathbf{v}_{\parallel}^b \rangle.\end{aligned}\tag{6.72}$$

For $Q_{\perp}^{\text{ground}} = 0$ the bottom surface is impermeable for the water; this is the usual case. Should groundwater accretion be substantial, then $Q_{\perp}^{\text{ground}} \neq 0$ follows from a groundwater model. ρ^* is the water density at 4°C and $c_D^b \approx 1.5 \times 10^{-3}$ is the basal drag coefficient; $c_D^b \rightarrow \infty$ corresponds to the no-slip condition, $\langle \mathbf{v}_{\parallel}^b \rangle = \mathbf{0}$ (this must be so in order to have \mathbf{t}_{\parallel}^b bounded in this limit) and $c_D^b = 0$ yields frictionless sliding for which $\mathbf{t}_{\parallel}^b = \mathbf{0}$.

At the *free surface*, momentum is transferred by wind and atmospheric pressure. Such traction boundary conditions are usually prescribed as follows:

$$\begin{aligned}\mathbf{t}_{\parallel}^s &= \rho_a c_D^s |\mathbf{W}_{\parallel}| \mathbf{W}_{\parallel}(\mathbf{x}^s, t), \\ p_{\perp}^s &= p^{\text{atm}}(\mathbf{x}, t),\end{aligned}\tag{6.73}$$

in which $\rho_a \approx 1.4 \text{ kg m}^{-3}$ is the density of air at atmospheric pressure, $c_D^s \approx 1.2 \times 10^{-3}$ is the drag coefficient and \mathbf{W}_{\parallel} the wind velocity parallel to the water surface, ordinarily 10 m above the water surface. Wind velocities measured at different heights above the water surface affect differently the value of c_D^s ; adjustments are then necessary. A dependence of the atmospheric pressure on the spatial coordinate and time can often be ignored for lakes; in such cases the prescription of $p^{\text{atm}}(\mathbf{x}, t)$ can be dispensed with (since for a constant atmospheric pressure its effect in the momentum equation is zero). Only in storm surge situations $\text{grad } p^{\text{atm}}(\mathbf{x}, t)$ is $\neq 0$ and must be accounted for.

(β) *Boundary conditions for the temperature:* At the bottom surface one usually requests that the surface temperature is prescribed, viz.,

$$\langle \theta(\mathbf{x}^b, t) \rangle = [\theta(z^b, t)]^{\text{static}},\tag{6.74}$$

where $\theta(z^b, t)$ is the static temperature distribution for a certain stratification, prescribed and held constant. The time dependence on the right-hand side of (6.74) expresses a slow seasonal variation of the temperature due to stratification. Alternatively to (6.74), one may also prescribe continuity of the heat flow across the bottom surface

$$\mathbf{q}^b \cdot \mathbf{n} = Q_{\perp}^{\text{geoth}},\tag{6.75}$$

where (6.75) is to be preferred over (6.74) in regions with strong volcanic activity (e.g. in Iceland). When the thermal regime of the lake is coupled to the thermal

regime of the ground, then continuity of both the temperature and the heat flow across the basal surface is required⁹:

$$[[\langle \theta(\mathbf{x}^b, t) \rangle]] = 0, \quad [[\mathbf{q}^b \cdot \mathbf{n}]] = 0 \quad (6.76)$$

in which $[[f]] := f^+ - f^-$ is the difference of the values of f on the side of the ground (f^+) and of the water (f^-).

This situation is, however, exceptional. It requires the solution of the heat equation in a layer of solid ground, say 2–5 km thick, where the boundary condition at the lower soil level would be a prescription of the geothermal heat.

The boundary condition at the lake or ocean-free surface is a radiation balance, which is expressed as

$$\langle \mathbf{q} \rangle^s \cdot \mathbf{n} = Q_{\text{ir}}^a - Q_{\text{ir}}^w + Q_\ell + Q_s. \quad (6.77)$$

Here, Q_{ir}^a and Q_{ir}^w are the (black body) radiation of air above the surface and water, while Q_ℓ and Q_s are the latent and sensible heat fluxes between water and air. For their explicit parameterisations, see the specialised literature, e.g. [7, pp. 582–584].

(γ) *Boundary conditions for species concentration*: Boundary conditions for tracer substances depend on the kind of biochemical–physical processes to which these substances are subjected and whether biochemical interaction processes take place. We therefore simply state here that, at the basal boundary and the free surface, either the concentration or its normal derivative or a combination of these is generally prescribed at the lake boundaries.

(δ) *Boundary conditions for k and ε* : These are rather difficult to postulate, because the peculiar conditions of turbulence near boundaries are not physically transparent. Commonly one wishes to prescribe numerical values for k and ε or their fluxes (derivatives of k and ε perpendicular to the surface). Such values or formulae can often only be obtained by consideration of the dynamics of the boundary layer.

At the *bottom surface*, where the flow is at most weakly turbulent, one may assume that turbulence has died out, so that one may require

$$k = 0, \quad \varepsilon = 0 \quad \text{at the bottom.} \quad (6.78)$$

However, close to solid walls the $(k - \varepsilon)$ -model requires the introduction of wall functions to properly describe the turbulent boundary layer. This means that (6.78) is approximate and should be taken as a gross simplification of the correct behaviour.

At the *free surface* a physically appropriate postulation of the boundary conditions is more complicated and also more critical. A fairly simple and also physically rather transparent assumption is to request that there is no conductive

⁹ Strictly, (6.75) and (6.76) require that there is no water discharge into the ground and that dissipative heat due to viscous sliding can be ignored.

loss of turbulent kinetic energy and turbulent energy dissipation through the free surface. With the gradient-type relations (6.63) this says

$$\frac{\partial k}{\partial \mathbf{n}} = \mathbf{0}, \quad \frac{\partial \varepsilon}{\partial \mathbf{n}} = \mathbf{0} \quad \text{at the free surface.} \quad (6.79)$$

SVENSSON [26] alternatively establishes formulae which relate k and ε with the surface wind shear stress and heat flow and the atmospheric boundary layer thickness.

6.4 Final Remarks

In the previous sections some elements of the formulation of turbulence theory were laid down. Even though our attempt to the subject was to present these elements with a certain rigour, it has been restricted and certainly does not do justice to the available present knowledge. The existing literature is vast, and various aspects, both mathematical and physical, are treated.¹⁰ Here in this last section we limit attention to only a few remarks concerning (i) higher order turbulence models, (ii) large eddy simulations (**LES**) and direct numerical simulations (**DNS**) and (iii) anisotropic turbulence closure conditions as employed by the early modellers in physical oceanography and limnology.

6.4.1 Higher Order RANS Models

One limitation of the $(k - \varepsilon)$ -model or any other two-variable turbulence closure model is the gradient-type closure ‘philosophy’ expressed by (6.62), (6.63). If the PRANDTL numbers arising in these relations are constant, it only allows an adjustment of the turbulent viscosity, expressed as $\nu_t = c_\mu k^2 / \varepsilon$. With this procedure the flux representations (6.62), (6.63) are so-called isotropic tensor and vector relations, which do not allow the modelling of anisotropic turbulent flow states. Anisotropy is, however, reality in most geophysical flows in the atmosphere, the ocean and lakes, particularly when these are stratified.

An obvious generalisation could be to employ a second (or even higher order) closure scheme, i.e. to formulate a transport equation for the REYNOLDS stress tensor (deviator), but such schemes require six (five) additional transport equations for the REYNOLDS stresses (deviators) and three equations for the turbulent heat flux vector and additional three ones for each tracer substance, and possibly an additional

¹⁰ Let us suggest to the reader a selection of books exclusively or partly devoted to turbulence in alphabetical order: BATCHELOR [1], FRISCH [4], HINZE [6], HUTTER and JÖHNK [7], LESIEUR [10], LUMLEY [11, 12], MCCOMB [13], MONIN and YAGLOM [14, 15], PIQUET [17], ROTTA [24], TENNEKES and LUMLEY [27], TOWNSEND [28]. We offer apologies for the omission of certainly many others.

equation for $\langle(\theta')^2\rangle$. These equations also involve higher order closure relations and must then be numerically solved together with the other field equations. This is computationally expensive. More economical are so-called *non-linear* or *algebraic* REYNOLDS *stress models* and corresponding models for the heat flux, the tracer fluxes and $\langle(\theta')^2\rangle$. Such models establish a closure condition for

$$\mathbf{R}^D = \mathbf{R} + \frac{2}{3}\rho k \mathbf{I} \quad \text{or} \quad \mathbf{A} = \mathbf{R}^D - 2\rho v_t \langle \mathbf{D} \rangle, \quad (6.80)$$

in which \mathbf{R}^D or \mathbf{A} must now depend not only on $\langle \mathbf{D} \rangle$ but also on other variables, e.g. $\langle \mathbf{W} \rangle = \text{skw grad} \langle \mathbf{v} \rangle = \frac{1}{2}(\text{grad} \langle \mathbf{v} \rangle - (\text{grad} \langle \mathbf{v} \rangle)^T)$, $\langle \mathbf{D} \rangle$ and others. $\langle \mathbf{W} \rangle$ is the vorticity tensor and $\langle \mathbf{D} \rangle$ the total time derivative of $\langle \mathbf{D} \rangle$. These serve only as examples. A judicious determination of objective functional relations of the form

$$\mathbf{A} = \mathbf{A}(\langle \mathbf{D} \rangle, \langle \mathbf{D} \rangle', \langle \mathbf{W} \rangle, \langle \theta \rangle, \langle \text{grad} \theta \rangle, \dots) \quad (6.81)$$

requires techniques, which are analogous to thermodynamic constitutive procedures employed in continuum mechanics.¹¹ Apart from the references already mentioned above, summarising overviews are given by HUTTER and JÖHNK (Chap. 12) [7] and, from a different viewpoint, by SANDER [25].

Notice that for $\mathbf{A} = \mathbf{0}$, the REYNOLDS stress tensor is given by (6.62)₁. Because with this choice the functional form of the REYNOLDS stress tensor is affine (or collinear or parallel) to $\langle \mathbf{D} \rangle$, a non-vanishing tensor \mathbf{A} is sometimes called the ‘*anisotropy tensor*’. However, as we shall see below, the classical approach to anisotropic turbulence has taken a different route, which is also theoretically somewhat questionable. Future attempts to anisotropic turbulence will have to follow the modern approach, which has just been briefly touched here.

6.4.2 Large Eddy Simulation and Direct Numerical Simulation

It was shown in this chapter how the REYNOLDS-averaged field equations could be derived from the full balance laws of physics by applying to them a filter operation $\langle(\cdot)\rangle$. Depending upon the mathematical properties of the filter operations, different balance laws of the averaged physical laws can be obtained, but explicitly only one such set, the REYNOLDS-averaged equation set (**RANS**), was presented. Recall that these equations are founded on the supposition that repeated averages do not lead to new results.¹² This is the so-called *ergodic* property; it is an assumption,

¹¹ We would like to warn the reader that questions of invariance under EUCLIDEAN transformations forbid a direct use of $\langle \mathbf{D} \rangle$ and $\langle \mathbf{W} \rangle$ in relations such as (6.81). ‘Objective’ derivatives of $\langle \mathbf{D} \rangle$ and, similarly, ‘objective’ vorticity measures must be used in closure proposals for \mathbf{A} ; see [7].

¹² In mathematical terms this means that $\langle \langle f \rangle \rangle = \langle f \rangle$, which implies that $\langle f' \rangle = 0$. An operator P on f with the property $PPf = Pf$ is also called a *projection*. So, REYNOLDS averaging is a projection filter. If this projection property does not hold, then $\langle f' \rangle \neq 0$, in general.

which is in general not satisfied in dynamic turbulent processes. Modern turbulent theories, in which discrepancies with experiments are visible when RANS are used, also employ a different filter operation, which does not fulfill ergodicity. Such an approach is known under the ‘label’ *Large Eddy Simulation (LES)*. It is still dictated by the formulation of averaging the small-scale turbulent equations by employing a filter operation to them, which does not obey ergodicity. The NAVIER–STOKES–FOURIER–FICK equations as such remain untouched; they are believed to describe *all* hydrodynamic phenomena, which for some processes can be formulated in terms of these equations at all; this is today’s firm conviction. The problem lies in the fact that different physical processes must be viewed simultaneously at different length scales: e.g. large-scale motions which generate small-scale eddies at an obstruction. The range of length scales generally extend in geophysical fluid mechanics over many orders of magnitude, from several kilometers down to millimetres. When attempting to solve a problem numerically, the selected mesh size defines the length scales of the eddies, which are not resolved by the mesh size. These eddies must be parameterised and the turbulent stress tensor, which describes the subgrid eddy momentum exchange, often takes the form of an algebraic REYNOLDS stress parameterisation. From what has just been said, it is, however, no surprise that the grid length of the mesh generally enters these tensor relations as a parameter. For further details, the reader is asked to consult the specialised (mentioned) literature.

Since the NAVIER–STOKES–FOURIER–FICK equations are indeed believed to describe all fluid flows correctly, their solutions will generate physically realisable processes, provided the grid size of the mesh is smaller or at least not larger than the so-called KOLMOGOROV length, below which the remaining turbulent energy is dissipated into heat; this length is in lakes and the ocean of the order of 1 mm. Such computations, known as *Direct Numerical Simulations (DNS)* are, of course, uneconomical for realistic scenarios; they should, however, neither be underestimated, because they can in simple test scenarios be used to judge whether other simple LES or RANS formulations lead to similar results for a given problem, for which corroborating measurements are available.

6.4.3 *Early Anisotropic Closure Schemes*

The pioneers in modelling dynamic processes in physical oceanography took a pragmatic approach to anisotropic turbulence. This approach is still very much in use today – we demonstrate its application in the EKMAN problem and its extensions – however, the approach is in fact conceptually faulty (for details, see Appendix A in WANG [30]), despite its apparent success, e.g. in the determination of wind-induced currents. Because electronic computations were non-existent at those times or in their early developments, considerations were restricted to the purely mechanical equations of a BOUSSINESQ fluid, which is homogeneous or at most vertically stratified. For this situation the governing equations of mass and linear momentum are

$$\begin{aligned} \operatorname{div}\langle \mathbf{v} \rangle &= 0, \\ \rho^* \frac{d\langle \mathbf{v} \rangle}{dt} + 2\boldsymbol{\Omega} \times \langle \mathbf{v} \rangle &= -\operatorname{grad}\langle p \rangle + \operatorname{div}\rho \mathbf{R} + \rho \mathbf{g}, \end{aligned} \quad (6.82)$$

in which the viscous term $\nu \nabla^2 \langle \mathbf{v} \rangle$ has been ignored and

$$\rho \mathbf{R} := -\rho \langle \mathbf{v}' \times \mathbf{v}' \rangle \quad (6.83)$$

is the REYNOLDS stress tensor. For this tensor, let us now choose the simplest possible parameterisation, which takes into account the experimentally observed anisotropy in the horizontal and vertical directions. It has been proposed in the form

$$\rho \mathbf{R} := \begin{pmatrix} t_{xx} & t_{xy} & t_{xz} \\ t_{yx} & t_{yy} & t_{yz} \\ t_{zx} & t_{zy} & t_{zz} \end{pmatrix} = \rho \begin{pmatrix} \nu_H \frac{\partial u}{\partial x} & \nu_H \frac{\partial u}{\partial y} & \nu_V \frac{\partial u}{\partial z} \\ \nu_H \frac{\partial v}{\partial x} & \nu_H \frac{\partial v}{\partial y} & \nu_V \frac{\partial v}{\partial z} \\ \nu_H \frac{\partial w}{\partial x} & \nu_H \frac{\partial w}{\partial y} & \nu_V \frac{\partial w}{\partial z} \end{pmatrix} \quad (6.84)$$

and was introduced in this form by MUNK [16]. So, the following expression enters the momentum equation (6.82):

$$\operatorname{div}(\rho \mathbf{R}) = \begin{pmatrix} \frac{\partial}{\partial x} \left(\rho \nu_H \frac{\partial u}{\partial x} \right) + \frac{\partial}{\partial y} \left(\rho \nu_H \frac{\partial u}{\partial y} \right) + \frac{\partial}{\partial z} \left(\rho \nu_V \frac{\partial u}{\partial z} \right) \\ \frac{\partial}{\partial x} \left(\rho \nu_H \frac{\partial v}{\partial x} \right) + \frac{\partial}{\partial y} \left(\rho \nu_H \frac{\partial v}{\partial y} \right) + \frac{\partial}{\partial z} \left(\rho \nu_V \frac{\partial v}{\partial z} \right) \\ \frac{\partial}{\partial x} \left(\rho \nu_H \frac{\partial w}{\partial x} \right) + \frac{\partial}{\partial y} \left(\rho \nu_H \frac{\partial w}{\partial y} \right) + \frac{\partial}{\partial z} \left(\rho \nu_V \frac{\partial w}{\partial z} \right) \end{pmatrix}, \quad (6.85)$$

with different horizontal and vertical exchange coefficients ν_H and ν_V . In the above equations we have used the notation $\langle \mathbf{v} \rangle = (u, v, w)$ to denote the Cartesian components of the averaged velocity vector $\langle \mathbf{v} \rangle$. At the early times (the 1930s – 1950s of the last century) it was generally assumed that turbulent isotropy prevails in the horizontal planes, while in the vertical direction turbulent processes work differently, implying $\nu_H \neq \nu_V$. With such a choice, the vertical coordinate axis is distinguished and must be one of the axes of the possible Cartesian axes.

The parameterisation of the REYNOLDS stress tensor according to (6.84) is actually conceptually faulty for at least two reasons. First, $\mathbf{R} = -\langle \mathbf{v}' \otimes \mathbf{v}' \rangle$ is symmetric, $\mathbf{R} = \mathbf{R}^T$, by definition, but representation (6.84) is *not* symmetric. Second, and more subtle: If a gradient-type relation is postulated, then one may write

$$\mathbf{R} = \hat{\mathbf{R}}(\langle D \rangle), \quad (6.86)$$

where $\langle \mathbf{D} \rangle = \text{sym grad} \langle \mathbf{v} \rangle$. Now, under an arbitrary rotation \mathbf{Q} of the coordinate system, \mathbf{R} and $\langle \mathbf{D} \rangle$ change as¹³

$$\mathbf{R}^* = \mathbf{Q} \mathbf{R} \mathbf{Q}^T, \quad \langle \mathbf{D} \rangle^* = \mathbf{Q} \langle \mathbf{D} \rangle \mathbf{Q}^T, \quad (6.87)$$

in which \mathbf{Q} is an orthogonal transformation, $\mathbf{Q} \mathbf{Q}^{-1} = \mathbf{Q} \mathbf{Q}^T = \mathbf{1}$, and \mathbf{Q}^T is the transpose of \mathbf{Q} . Therefore, a parameterisation (6.86) must also satisfy

$$\mathbf{Q} \hat{\mathbf{R}}(\langle \mathbf{D} \rangle) \mathbf{Q}^T = \hat{\mathbf{R}}^*(\mathbf{Q} \langle \mathbf{D} \rangle \mathbf{Q}^T). \quad (6.88)$$

It is one of the fundamental assumptions that the functional representation $\hat{\mathbf{R}}^*(\cdot)$ does not depend on the orientation of the coordinates. This assumption reads

$$\hat{\mathbf{R}}^*(\mathbf{Q} \langle \mathbf{D} \rangle \mathbf{Q}^T) = \hat{\mathbf{R}}(\mathbf{Q} \langle \mathbf{D} \rangle \mathbf{Q}^T). \quad (6.89)$$

This assumption may be called the *assumption of turbulent objectivity*. With it, (6.88) takes the form

$$\mathbf{Q} \hat{\mathbf{R}}(\langle \mathbf{D} \rangle) \mathbf{Q}^T = \hat{\mathbf{R}}(\mathbf{Q} \langle \mathbf{D} \rangle \mathbf{Q}^T) \quad (6.90)$$

and must hold true for all orthogonal transformations \mathbf{Q} .

Functions, which satisfy (6.90) are so-called *isotropic tensor functions of tensors of second rank*. It can be shown, see, e.g. [7], that the most general form of the solution of (6.90) is

$$\mathbf{R} = \alpha_0 \mathbf{1} + \alpha_1 \langle \mathbf{D} \rangle + \alpha_2 \langle \mathbf{D} \rangle^2 \quad (6.91)$$

with scalar coefficients $\alpha_j = \hat{\alpha}_j(II_{\langle \mathbf{D} \rangle}, III_{\langle \mathbf{D} \rangle})$, where $II_{\langle \mathbf{D} \rangle}$ and $III_{\langle \mathbf{D} \rangle}$ are the principal invariants of the deviator $\langle \mathbf{D} \rangle$. Equation (6.84) is of the form (6.86), but it is *not* expressible as (6.91). What does this mean? Well, it means that an anisotropic representation of (6.86) violates the general transformation property (6.90), which such a functional relation must obey. However, (6.88) still holds. Thus, MUNK's expression may just violate the assumption of turbulent objectivity. So, we shall now *reject the assumption of turbulent objectivity*.

With the intention to come close to MUNK's REYNOLDS stress proposal (6.84), we shall now assume that \mathbf{R} is given by (6.86) and derivable from a potential as follows:

$$\rho \mathbf{R} = \rho \frac{\partial \Phi(\langle \mathbf{D} \rangle)}{\partial \langle \mathbf{D} \rangle}, \quad (6.92)$$

¹³ These transformations are the expression of the fact that for two observers, who are moving relative to one another according to a rigid-body motion $\mathbf{x}^*(t) = \mathbf{Q}(t)\mathbf{x} + \mathbf{b}(t)$, the REYNOLDS stress and the mean strain rate tensors \mathbf{R} , $\langle \mathbf{D} \rangle$ and \mathbf{R}^* , $\langle \mathbf{D} \rangle^*$, respectively, transform as (6.87) for any rotation \mathbf{Q} .

with the following potential

$$\Phi = \frac{1}{2} \eta_{ijkl} \langle D_{ij} \rangle \langle D_{kl} \rangle. \quad (6.93)$$

Therefore, $\rho \mathbf{R}$ is linearly related to $\langle \mathbf{D} \rangle$ according to

$$\rho \mathbf{R} = \mathcal{M} \langle \mathbf{D} \rangle, \quad \rho \mathcal{R}_{ij} = \eta_{ijkl} \langle D_{kl} \rangle. \quad (6.94)$$

The coefficient ‘matrix’ $\mathcal{M} = [\eta_{ijkl}]$ consists of $3 \times 3 \times 3 \times 3 = 81$ entries. Not all of them are independent. Their number can considerably be reduced by symmetry requirements. First, since Φ is a scalar and $\langle \mathbf{D} \rangle$ a symmetric second-order tensor, $\langle \mathbf{D} \rangle$ may be identified by a six-dimensional vector $\dot{\mathbf{e}}$. Furthermore, $\rho \mathbf{R}$ is also symmetric and is equivalent to the six-dimensional vector $\rho \mathbf{R}$:

$$\begin{aligned} \dot{\mathbf{e}} &= (\langle D_{11} \rangle, \langle D_{22} \rangle, \langle D_{33} \rangle, \langle D_{23} \rangle, \langle D_{31} \rangle, \langle D_{12} \rangle), \\ \mathbf{R} &= (R_{11}, R_{22}, R_{33}, R_{23}, R_{31}, R_{12}). \end{aligned} \quad (6.95)$$

So, (6.93) and (6.94) read

$$\Phi = \frac{1}{2} \dot{\mathbf{e}} \cdot [\mathbf{M}] \dot{\mathbf{e}}, \quad \mathbf{R} = [\mathbf{M}] \dot{\mathbf{e}}, \quad (6.96)$$

in which $[\mathbf{M}]$ is a 6×6 matrix with 36 entries. It follows that at most 36 entries of \mathbf{M} are independent. Moreover, because of the potential property (6.92), it is easy to show that the matrix $[\mathbf{M}]$ is symmetric, so that at most 21 entries of $[\mathbf{M}]$ are independent. In view of the transverse isotropy of the ocean or lake turbulence, which we are now going to postulate, this number can still be reduced considerably. Transverse isotropy means here that the turbulence behavior in the horizontal is independent of any rotation of the coordinates about the vertical axis. Moreover, if any of the coordinate axes are rotated by 180° , invariance against this transformation expresses that transverse isotropy includes orthotropy. If Φ^* is the representation which obtains when (6.93) is written in the rotated coordinates, then symmetry relative to the coordinate transformation \mathbf{Q} yields

$$\frac{1}{2} \eta_{ijkl} \langle D \rangle_{ij} \langle D \rangle_{kl} = \Phi \stackrel{!}{=} \Phi^* = \frac{1}{2} \eta_{ijkl} Q_{im} Q_{jn} Q_{kp} Q_{lq} \langle D \rangle_{mn} \langle D \rangle_{pq}. \quad (6.97)$$

For the choices

$$\mathbf{Q}_1 = \begin{pmatrix} -1 & 0 & 0 \\ 0 & -1 & 0 \\ 0 & 0 & 1 \end{pmatrix} \quad \text{and} \quad \mathbf{Q}_2 = \begin{pmatrix} -1 & 0 & 0 \\ 0 & 1 & 0 \\ 0 & 0 & -1 \end{pmatrix} \quad (6.98)$$

which correspond to rotations of the coordinate axes around the z - and y -axes by 180° , (6.97) yields for these two rotations

$$\begin{aligned}\eta_{1123} = \eta_{2223} = \eta_{3323} = \eta_{1113} = \eta_{2213} = \eta_{3313} = \eta_{2312} = \eta_{1312} = 0, \\ \eta_{1123} = \eta_{2223} = \eta_{3323} = \eta_{2313} = \eta_{1112} = \eta_{2212} = \eta_{3312} = \eta_{1312} = 0.\end{aligned}$$

A rotation about the x -axis by 180° does not yield additional new results. Thus, for orthotropic turbulence, the matrix $[\mathbf{M}]$

$$[\mathbf{M}]^{\text{orth}} = \begin{pmatrix} \eta_{1111} & \eta_{1122} & \eta_{1133} & 0 & 0 & 0 \\ & \eta_{2222} & \eta_{2233} & 0 & 0 & 0 \\ & & \eta_{3333} & 0 & 0 & 0 \\ & & & \eta_{2323} & 0 & 0 \\ & & & & \eta_{1313} & 0 \\ \text{sym} & & & & & \eta_{1212} \end{pmatrix} \quad (6.99)$$

has only nine independent exchange coefficients. If we apply

$$\mathbf{Q} = \begin{pmatrix} \cos \phi & \sin \phi & 0 \\ -\sin \phi & \cos \phi & 0 \\ 0 & 0 & 1 \end{pmatrix} \quad (6.100)$$

to (6.97) (with $[\mathbf{M}]$ given by $[\mathbf{M}]^{\text{orth}}$) for an infinitesimal angle ϕ , corresponding to $\cos \phi \approx 1$, $\sin \phi \approx \varepsilon$, it is easily shown that

$$\begin{aligned}\eta_{1313} = \eta_{2323}, \quad \eta_{1133} = \eta_{2233}, \quad \eta_{1111} = \eta_{2222}, \\ \eta_{1212} = \frac{1}{2}(\eta_{1111} - \eta_{1122}),\end{aligned} \quad (6.101)$$

so that

$$[\mathbf{M}]_{\text{isotropic}}^{\text{transverse}} = \begin{pmatrix} \eta_{1111} & \eta_{1122} & \eta_{1133} & 0 & 0 & 0 \\ & \eta_{1111} & \eta_{1133} & 0 & 0 & 0 \\ & & \eta_{3333} & 0 & 0 & 0 \\ & & & \eta_{2323} & 0 & 0 \\ & & & & \eta_{2323} & 0 \\ \text{sym} & & & & & \frac{1}{2}(\eta_{1111} - \eta_{1122}) \end{pmatrix} \quad (6.102)$$

or with the notation

$$a = \eta_{1111}, \quad b = \eta_{3333}, \quad c = 2\eta_{2323}, \quad d = \eta_{1122}, \quad e = \eta_{1133}, \quad (6.103)$$

$$[\mathbf{M}]_{\text{isotropic}}^{\text{transverse}} = \begin{pmatrix} a & d & e & 0 & 0 & 0 \\ & a & e & 0 & 0 & 0 \\ & & b & 0 & 0 & 0 \\ & & & c & 0 & 0 \\ & & & & c & 0 \\ \text{sym.} & & & & & a - d \end{pmatrix}. \quad (6.104)$$

Accordingly, transverse isotropic turbulence is in the context of (6.96) described by five turbulent exchange coefficients. However, this number can still be reduced by requesting that \mathbf{R} is a deviator,

$$\text{tr} \mathbf{R} = 0 \quad (6.105)$$

implying

$$a + d + e = 0, \quad 2e + d = 0. \quad (6.106)$$

The assumption $\text{tr} \mathbf{R} = 0$ is sometimes known as STOKES assumption. We conclude as follows: *If the REYNOLDS stress tensor \mathbf{R} obeys transverse isotropy in a Cartesian system with horizontal–vertical coordinate axes, it is described by three independent exchange coefficients.* In particular, with the abbreviations

$$a - d = 2\nu_H, \quad c = 2\nu_V \quad (6.107)$$

the tensor \mathbf{R} possesses the representation

$$\begin{aligned} R_{11} &= 2\nu_H \langle D_{11} \rangle + (4\nu_H - 3a) \langle D_{33} \rangle, \\ R_{22} &= 2\nu_H \langle D_{22} \rangle + (4\nu_H - 3a) \langle D_{33} \rangle, \\ R_{33} &= -6(\nu_H - a) \langle D_{33} \rangle, \\ R_{23} &= 2\nu_V \langle D_{23} \rangle, \\ R_{31} &= 2\nu_V \langle D_{31} \rangle, \\ R_{12} &= 2\nu_V \langle D_{12} \rangle, \end{aligned} \quad (6.108)$$

in which we also used that $\text{tr} \langle \mathbf{D} \rangle = 0$. From this, it easily follows that

$$\begin{aligned} \text{div} R_x &:= \frac{\partial R_{11}}{\partial x} + \frac{\partial R_{12}}{\partial y} + \frac{\partial R_{13}}{\partial z} \\ &= \frac{\partial}{\partial x} \left(\nu_H \frac{\partial u}{\partial x} \right) + \frac{\partial}{\partial y} \left(\nu_H \frac{\partial u}{\partial y} \right) + \frac{\partial}{\partial z} \left(\nu_V \frac{\partial u}{\partial z} \right) \\ &\quad + \frac{\partial}{\partial x} \left[(3(\nu_H - a) + \nu_V) \frac{\partial w}{\partial z} \right] \\ &\quad + \frac{\partial \nu_H}{\partial y} \frac{\partial v}{\partial x} - \frac{\partial \nu_H}{\partial x} \frac{\partial v}{\partial y} + \frac{\partial \nu_V}{\partial z} \frac{\partial w}{\partial x} - \frac{\partial \nu_V}{\partial x} \frac{\partial w}{\partial z}, \end{aligned} \quad (6.109)$$

$$\begin{aligned}
\operatorname{div} R_y &:= \frac{\partial R_{12}}{\partial x} + \frac{\partial R_{22}}{\partial y} + \frac{\partial R_{23}}{\partial z} \\
&= \frac{\partial}{\partial x} \left(\nu_H \frac{\partial v}{\partial x} \right) + \frac{\partial}{\partial y} \left(\nu_H \frac{\partial v}{\partial y} \right) + \frac{\partial}{\partial z} \left(\nu_V \frac{\partial v}{\partial z} \right) \\
&\quad + \frac{\partial}{\partial y} \left[(3(\nu_H - a) + \nu_V) \frac{\partial w}{\partial z} \right] \\
&\quad + \frac{\partial \nu_H}{\partial x} \frac{\partial u}{\partial y} - \frac{\partial \nu_H}{\partial y} \frac{\partial u}{\partial x} + \frac{\partial \nu_V}{\partial z} \frac{\partial w}{\partial y} - \frac{\partial \nu_V}{\partial y} \frac{\partial w}{\partial z},
\end{aligned} \tag{6.110}$$

$$\begin{aligned}
\operatorname{div} R_z &:= \frac{\partial R_{13}}{\partial x} + \frac{\partial R_{23}}{\partial y} + \frac{\partial R_{33}}{\partial z} \\
&= \frac{\partial}{\partial x} \left(\nu_V \frac{\partial w}{\partial x} \right) + \frac{\partial}{\partial y} \left(\nu_V \frac{\partial w}{\partial y} \right) \\
&\quad + \frac{\partial}{\partial z} \left[6(a - \nu_H) - \nu_V \right] \frac{\partial w}{\partial z} \\
&\quad + \frac{\partial \nu_V}{\partial x} \frac{\partial u}{\partial z} - \frac{\partial \nu_V}{\partial z} \frac{\partial u}{\partial x} + \frac{\partial \nu_V}{\partial y} \frac{\partial v}{\partial z} - \frac{\partial \nu_V}{\partial z} \frac{\partial v}{\partial y}.
\end{aligned} \tag{6.111}$$

These relations do not reduce to MUNK's expressions (6.85), not even when the horizontal exchange coefficient is assumed to be constant.

However, when the momentum equations are subject to the shallow-water scaling, it can be shown that, see [30],

$$\begin{aligned}
\operatorname{div} R_x &= \frac{\partial}{\partial x} \left(\nu_H \frac{\partial u}{\partial x} \right) + \frac{\partial}{\partial y} \left(\nu_H \frac{\partial u}{\partial y} \right) + \frac{\partial}{\partial z} \left(\nu_V \frac{\partial u}{\partial z} \right) \\
&\quad + \frac{\partial}{\partial x} \left[(3(\nu_H - a)) \frac{\partial w}{\partial z} \right] \\
\operatorname{div} R_y &= \frac{\partial}{\partial x} \left(\nu_H \frac{\partial v}{\partial x} \right) + \frac{\partial}{\partial y} \left(\nu_H \frac{\partial v}{\partial y} \right) + \frac{\partial}{\partial z} \left(\nu_V \frac{\partial v}{\partial z} \right) \\
&\quad + \frac{\partial}{\partial y} \left[(3(\nu_H - a)) \frac{\partial w}{\partial z} \right] \\
\operatorname{div} R_z &= 0.
\end{aligned} \tag{6.112}$$

In the derivation of (6.112) the assumption $\nu_H = \text{const}$ has been used. Relations (6.112) can neither be reduced to MUNK's turbulence parameterisation in the shallow-water approximation unless

$$\frac{\partial}{\partial x} \left[(3(\nu_H - a)) \frac{\partial w}{\partial z} \right] = 0, \quad \frac{\partial}{\partial y} \left[(3(\nu_H - a)) \frac{\partial w}{\partial z} \right] = 0. \tag{6.113}$$

Therefore, *only when the vertical gradient of the vertical velocity component can be ignored or when $v_H = a$, MUNK's assumption agrees with the transverse isotropic turbulence without contradiction.*

Let us close this section with a few remarks:

- Evidently, we have not been able to derive the anisotropic closure relation (6.85) without contradiction from general invariance principles of physics. Postulate (6.84) for the REYNOLDS stress tensor violates both the symmetry requirement for $\rho \mathbf{R}$ and the general transformation properties. Equations (6.87) and (6.88), however, have extensively been used in interpretations of wind-induced ocean and circulation dynamics, obviously with reasonable success.
- Even if we accept the anisotropic REYNOLDS stress parameterisation (6.108) or its simplification (6.112), it still violates the transformation property (6.87)₁ for all those orthogonal transformations, which go beyond those of transverse isotropy, i.e. restrict the anisotropy even further. The transformations are valid for all orthogonal transformations, and a linear relation of the form $\mathbf{R} = \mathcal{M}(\mathbf{D})$, which obeys (6.87) for all \mathbf{Q} 's, has necessarily the form $\mathbf{R} = 2\nu_T \langle \mathbf{D} \rangle$ which is isotropic.
- A correct anisotropic REYNOLDS stress relation must therefore be of the class $\mathbf{R} = \hat{\mathbf{R}}(\langle \mathbf{D} \rangle, A_j, \dots)$, in which A_j , $j = 1, 2, \dots$, are anisotropy measures. The simplest form of these are the algebraic REYNOLDS stress models, which were briefly mentioned earlier.

References

1. Batchelor, G.K.: *The Theory of Homogeneous Turbulence*. Cambridge University Press, Cambridge, 197 p. (1953)
2. Bäuerle, E., Chubarenko, B., Chubarenko, I., Halder, J., Hutter, K. and Wang, Y.: Autumn Physical Limnological Experimental Campaign in the Mainau Island Littoral Zone of Lake Constance (Constance Data Band) 12 October – 19 November 2001. *Report of the 'Sonderforschungsbereich 454 Bodenseelittoral'*, 85 p. (2002)
3. Boussinesq, J.: *Essay sur la théorie des eaux courantes. Mémoires présentés par div. Savants à l'Académie des Sciences de l'institut de France. Tome 23* (avec supp. in *Tome 24*), (1877)
4. Frisch, U.: *Turbulence, the Legacy of A.N. Kolmogorov*. Cambridge University Press, Cambridge, 296 p. (1995)
5. Hansalic, K. and Launder, B.E.: A Reynolds stress model of turbulence and its application to thin shear flows. *J. Fluid Mech.* **52**, 609–638 (1972)
6. Hinze, J.O.: *Turbulence*. McGraw Hill, New York NY, 790 p. (1975)
7. Hutter, K. and Jöhnk, K.: *Continuum Methods of Physical Modeling*. Springer, Berlin, 635 p. (2004)
8. Jones, W.P. and Launder, B.E.: The prediction of laminarisation with a two-equation model of turbulence. *J. Heat Mass Transf.* **15**, 301–314 (1972)
9. Launder, B.E. and Spalding, D.B.: The numerical computation of turbulent flow. *Comp. Meth. Appl. Mech. Eng.* **3**, 269–288 (1974)
10. Lesieur, M.: *Turbulence in Fluids*. Kluwer, Dordrecht, 411 p. (1990)
11. Lumley, J.L.: *Stochastic Tools in Turbulence*. Academic, New York NY, 194 p. (1978)
12. Lumley, J.L.: Computational modeling of turbulence flows. *Adv. Appl. Mech.* **18**, 123–17 (1983)

13. McComb, W.D.: *The Physical of Fluid Turbulence*. Clarendon, Oxford, 572 p. (1990)
14. Monin, A.S. and Yaglom, A.M.: *Statistical Fluid Mechanics*, Vol. 1 (ed. Lumley, J.) MIT, Cambridge, MA, 769 p. (1971)
15. Monin, A.S. and Yaglom, A.M.: *Statistical Fluid Mechanics*, Vol. 2 (ed. Lumley, J.) MIT, Cambridge, MA, 874 p. (1975)
16. Munk, W.H.: On the wind-driven ocean circulation. *J. Metereol.* **7**, 79 (1950)
17. Piquet, J.: *Turbulence Flows, Models and Physics*. Springer, Berlin, 761 p. (1999)
18. Prandtl, L.: Bericht über Untersuchungen zur ausgebildeten Turbulenz. *Zeitschrift für angewandte Mathematik und Mechanik (ZAMM)* **5**(2), 136–39 (1925)
19. Prandtl, L.: Neuere Ergebnisse der Turbulenzforschung. *Zeitschr. VDI* **77**, 105–113 (1933)
20. Reynolds, O.: An experimental investigation of circumstances which determine whether the motion of water shall be direct or sinuous, and of the law of resistance in parallel channels. *Phil. Trans. R. Soc. Lond.* **A-174**, 935–982 (1883)
21. Reynolds, O.: On the dynamical theory of turbulent incompressible viscous fluids and the determination of the criterion. *Phil. Trans. R. Soc. Lond.* **A 186**, 123–164 (1894)
22. Rodi, W.: Examples of calculation methods for flow and mixing in stratified fluids. *J. Geophys. Res. (C5)*, **92**, 5305–5328 (1987)
23. Rodi, W.: *Turbulence Models and Their Application in Hydraulics*. IAHR Monograph Series, A.A. Balkema, Rotterdam/Brookfield (1993)
24. Rotta, J.C.: *Turbulente Strömungen, eine Einführung in die Theorie und ihre Anwendungen*. Teubner, Stuttgart, 267 p. (1972)
25. Sander, J.: Dynamical equations and turbulent closures in geophysics. *Continuum Mech. Thermodyn.* **10**, 1–28 (1998)
26. Svensson, U.: *A mathematical model for the seasonal variation of the thermocline*. Report 1002, Department of Water Resources Engineering, University of Lund, Sweden, 187 p. (1978)
27. Tennekes, H.J.L. and Lumley, J.L.: *A First Course in Turbulence*. MIT, Cambridge, MA, 300 p. (1972)
28. Townsend, A.A.: *The Structure of Turbulent Shear Flow*. Cambridge University Press, Cambridge, 429 p. (1976)
29. Umlauf, L.: *Turbulence Parameterization in Hydro-Biological Models for Natural Waters*. Ph. D. Dissertation, Department of Mechanics, Darmstadt University of Technology, Darmstadt, Germany, 231 p. (2001)
30. Wang, Y.: *Windgetriebene Strömungen in einem Rechteckbecken und im Bodensee*. PhD thesis, Darmstadt University of Technology, Shaker Verlag, Aachen. ISBN 3-8265-1381-9, 432 p. (1996)
31. Weis, J.: *Ein Algebraisches Reynolds-Spannungs-Modell*. Ph. D. Dissertation, Department of Mechanics, Darmstadt University of Technology, Darmstadt, Germany, 111 p. (2001)
32. Wilcox, D.C.: Reassessment of the scale-determining equation for advanced turbulence models. *AIAA J.* **26**(11), 1299–1310 (1988)
33. Wilcox, D.C.: *Turbulence Modeling for CFD*. DCW Industries, Inc., La Cañada, California, 2nd Edition (1998)

Chapter 7

Introduction to Linear Waves

Waves in open waters, such as the ocean, lakes, channels, arise in a variety of forms and types and have various physical reasons for their formation. We will have the occasion in a number of subsequent chapters (in volume 2) to investigate the important types of waves in the geophysical context as they apply to lakes, the ocean and, to limited extent, also to the atmosphere. Here, in this chapter, our intention is to lay the foundations of the mathematical description and physical implications which one may deduce from them.

At the heart such an analysis is the answer to the simple question, *What is a wave?* An immediate and perhaps unbiased answer might be the transfer of information from a point A in space to point B. The process of this transmission may then be called ‘wave’. A beautiful statement, attributed to EINSTEIN, that expresses the essentials of what is meant by waves is as follows¹:

Irgend ein Klatsch, der, sagen wir, in Washington aufgebracht wird, gelangt sehr rasch nach New York, wenn auch nicht eine einzige von den an der Weitergabe beteiligten Personen tatsächlich von der einen Stadt in die andere reist. Wir haben es vielmehr gewissermaßen mit zwei ganz verschiedenen Bewegungen zu tun, der des Gerüchtes selbst, das von Washington nach New York dringt, und der jener Personen, die das Gerücht verbreiten.

So, for a wave the transmission of the information is important and this motion may be entirely different from the motion of the carrier medium. There may be a connection between the two, there may be none; in fact there are physical situations (e.g. electromagnetic waves in vacuo) for which a carrier medium does not even exist. For acoustic waves and for surface water waves, however, the medium through which the wave propagates is important, but the motion of the water or gas is distinct from that of the wave itself. An evident example is certainly known to the reader:

¹ ‘Any gossip which, say, is spread in Washington arrives very quickly in New York, even though not a single person who participates in the spreading of the rumor really travels from one city to the other. Rather, we are dealt here with two entirely different motions, that of the rumor itself, which propagates from Washington to New York, and that of the people who are spreading the gossip.’

We have seen the German quotation at an exhibition ‘TECHNORAMA’ in Winterthur, Switzerland, but were not able to trace the exact source of the quotation.

When fishing with a fish rod at the shore of a lake or pond, it sometimes happens that a surface wave from a boat approaches the shore. The crest of this wave when passing the fishline does not catch the line and carry it along; rather, the line with its buoy performs a more or less violent oscillation induced by the passing wave that is localised to the neighbourhood of where the line was before the wave passed and that dies out rather quickly.

In the ensuing analysis we shall derive the classical wave equation and then reduce it to its simplest form for which solutions will be constructed. Their properties will then give us the possibility to discuss key features that are typical of all waves and whose knowledge is indispensable when water waves in the ocean or in lakes are discussed.

7.1 The Linear Wave Equation and Its Properties

The literature on waves is abundant and due justice cannot be done by referencing some books in a brief note. Almost every college physics book contains one to several chapters on waves. Many books on fluid mechanics also have chapters on fluid waves. We give here a selection of books which are likely held at many university libraries: in alphabetical order: BATCHELOR [1], FEYNMAN et al. [2], LAMB [3], LANDAU and LIFSHITZ [4], LAUTRUP [5], PHILLIPS [13], WALKER [16].

Books exclusively devoted to waves in general, water waves or ocean waves, are, e.g. LEIBOVICH and SEEBASS [7], LIDTHILL [8], LEBLOND and MYSAK [6], MEI [10], MASSEL [9], STOKER [14], WHITHAM [18].

VAN DYKE [15] published a picture book on scientific photographs with many snapshots of water (and other) waves. The Encyclopedia Britannica Educational Corporation, 425 North Michigan Avenue, Chicago, 60611, distributes an educational film on *Waves in Fluids*, a 16 mm B&W sound film, 33 min in length with film notes by A. E. BRYSON.

We will introduce the concept of a wave by looking at *acoustic waves* in a liquid or in a gas. Physically, this wave type cannot be described in a BOUSSINESQ fluid; but of course, sound propagates in water, which everybody may have experienced when diving in a lake or the ocean and hearing within the water the sound of motors from boats which may hardly be visible because they are too far away.

To derive the acoustic wave equation, consider a homogeneous infinite medium. Assume it to be compressible and at rest with density ρ_0 , velocity $\mathbf{v}_0 = \mathbf{0}$ and pressure p_0 such that $\text{grad } p_0 = \rho_0 \mathbf{g}$. Consider perturbations of these fields, so that

$$\rho = \rho_0 + \rho', \quad \mathbf{v} = \mathbf{v}_0 + \mathbf{v}' = \mathbf{v}', \quad p = -\rho g z + p'. \quad (7.1)$$

The balance laws of mass and linear momentum (ignoring dissipative terms)

$$\begin{aligned} \frac{\partial \rho}{\partial t} + (\text{grad } \rho) \mathbf{v} + \rho \text{div } \mathbf{v} &= 0, \\ \frac{\partial \mathbf{v}}{\partial t} + (\text{grad } \mathbf{v}) \mathbf{v} &= -\frac{1}{\rho} \text{grad } p + \mathbf{g} \end{aligned} \quad (7.2)$$

may then be written down in terms of the primed perturbation fields. When this is done and all product terms of primed quantities are omitted – this corresponds to the linear approximation – then (7.2), now expressed in terms of the perturbation fields, takes the form:

$$\frac{\partial \rho}{\partial t} + \rho_0 \operatorname{div} \mathbf{v} = 0, \quad \frac{\partial \mathbf{v}}{\partial t} = -\frac{1}{\rho_0} \operatorname{grad} p, \quad (7.3)$$

in which, for simplicity, the primes have been omitted. Equation (7.3)₂ can be differently expressed, if the thermal equation of state is used. We assume for the simple situation dealt with here that $p = p(\rho)$; this is the thermal equation of state of a so-called *barotropic* or *elastic fluid* first treated by EULER, Fig. 7.1. With this law we have

$$\operatorname{grad} p = \left. \frac{dp}{d\rho} \right|_0 \operatorname{grad} \rho = c_0^2 \operatorname{grad} \rho. \quad (7.4)$$

Definition 7.1 *The quantity c_0 , defined by*

$$c_0^2 := \left. \frac{dp}{d\rho} \right|_0 \quad [\text{m}^2 \text{s}^{-2}], \quad (7.5)$$

is the speed of sound of a linear barotropic fluid. ■

For water at 20°C and normal pressure it is approximately 1450 m s^{-1} . Differentiating (7.3)₁ with respect to time and substituting (7.3)₂ and (7.4) leads to

$$\frac{\partial^2 \rho}{\partial t^2} = c_0^2 \operatorname{div} \operatorname{grad} \rho. \quad (7.6)$$

The operator $\operatorname{div} \operatorname{grad}$ is the *Laplacean operator*, denoted by Δ or ∇^2 . In Cartesian coordinates it takes the form

$$\nabla^2 \rho = \frac{\partial^2 \rho}{\partial x^2} + \frac{\partial^2 \rho}{\partial y^2} + \frac{\partial^2 \rho}{\partial z^2}, \quad (7.7)$$

as can be easily checked by the reader. One may write (7.6) in terms of the pressure rather than density. Using $\rho = \rho(p)$, the reader may easily prove that (7.6) then becomes

$$\frac{\partial^2 p}{\partial t^2} = c_0^2 \nabla^2 p, \quad (7.8)$$

and it can equally, though not so easily, be shown that also the velocity \mathbf{v} or its potential ϕ , if $\mathbf{v} = \operatorname{grad} \phi$, satisfies this same equation. Equation (7.6) or (7.8) is called the *classical linear wave equation*. Thus we have shown the following.

Proposition 7.1 *Linear acoustic waves in a homogeneous fluid medium are described by the wave equation*

$$\frac{\partial^2 \Phi}{\partial t^2} = c_0^2 \nabla^2 \Phi, \quad c_0^2 := \left. \frac{dp}{d\rho} \right|_0, \quad (7.9)$$

where Φ stands for the density ρ , the pressure p , the velocity \mathbf{v} or the velocity potential ϕ . c_0 is the speed of sound for a fluid at rest. ■

Remark: In the above, no use was made of the balance law of energy, which may be written as demonstrated in (4.175). If in that equation dissipation and heat conduction are ignored – in an EULER fluid these terms vanish by definition – and if no radiation arises, then (4.175) (multiplied with the non-zero factor $1/(\rho T)$, where T is the absolute temperature) may be written as

$$\frac{d\eta}{dt} := \frac{1}{T} \left(\frac{d\varepsilon}{dt} + p \frac{d}{dt} \left(\frac{1}{\rho} \right) \right) = 0.$$

In thermodynamics this is shown to be the material time derivative of the specific entropy. It follows that in an acoustic wave of an EULER fluid the entropy for material particles does not change. In this connection the following definition is useful:

Definition 7.2

- *Processes in which heat exchange between material particles and the environment is absent are called **adiabatic**. They are characterised by a vanishing heat flux vector.*
- *Processes for which the entropy does not change along particle trajectories are called **isentropic**. If the entropy is constant throughout the region, the processes are called **homentropic**.* ■

It follows from this definition that in an ideal fluid adiabatic processes are also isentropic and vice versa. Moreover, in a viscous fluid in which dissipation and heat conduction are ignored and in which no radiation is operating, the entropy remains materially constant. If at time t_0 the value of the entropy is the same for all material particles, the speed of sound c_0 as defined in (7.5) is then that evaluated for this value of the entropy. This is the reason why one speaks in those circumstances of the *adiabatic speed of sound*.

It is not difficult to see from the above derivation why acoustic waves cannot be described in a BOUSSINESQ fluid. In such a fluid, the time derivative $\partial\rho/\partial t$ is ignored in (7.3)₁ (since $\text{div } \mathbf{v} = 0$) implying that an equation of the form (7.9) can never be derived.

Closer scrutiny is now required to see that (7.9) indeed describes waves. *Plane waves* are obtained if all variables depend only upon a single variable of a Cartesian frame, say x . This is the direction of wave propagation. Equation (7.9) then takes the form

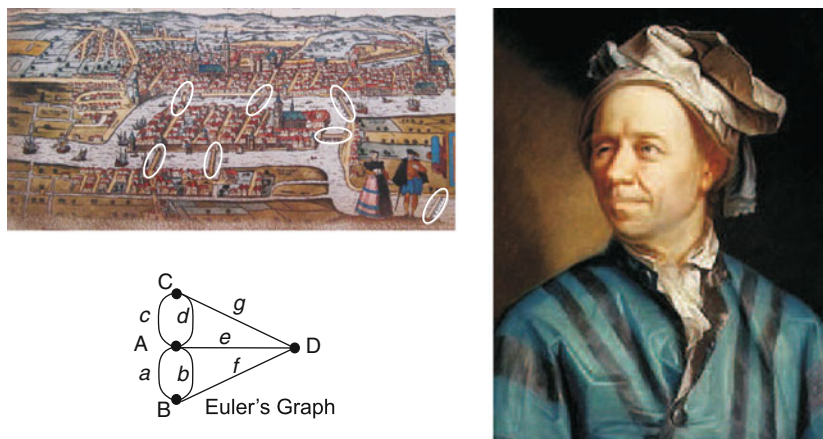


Fig. 7.1 *Right:* Leonhard EULER. Portrait by Emanuel HANDMANN 1753 (<http://en.wikipedia.org/>). *Left:* The graph theory originates with Leonard EULER's 1736 paper 'The Seven Bridges of Königsberg'. Map of Königsberg in EULER's time showing the actual layout of the seven bridges, highlighted by ovals

Leonhard EULER (15 April 1707 to 18 September 1783) was a pioneering Swiss mathematician and physicist who spent most of his life in Russia and Germany. EULER's early formal education started in Basel. At the age of 13 he enrolled at the University of Basel and, in 1723, received his Master of Philosophy with a dissertation that compared the philosophies of DESCARTES and NEWTON. In May 1727 EULER arrived in St. Petersburg, took a position in the mathematics department of the Russian Academy of Sciences, just established by Peter the Great, and settled into life in St. Petersburg. EULER swiftly rose through the ranks in the academy and was made professor of physics in 1731 and head of the mathematics department. Concerned about the continuing turmoil in Russia, EULER left St. Petersburg in 1741 to take a post at the Berlin Academy. He lived for 25 years in Berlin, where he wrote over 380 articles. In 1766, exposed to conditions of negligence by the emperor Friedrich the Great, EULER accepted an invitation of Catherine the Great to return to the St. Petersburg Academy where he spent the rest of his life.

EULER made important discoveries in fields as diverse as infinitesimal calculus and graph theory. He also introduced much of the modern mathematical terminology and notation, particularly for mathematical analysis. He is also renowned for his work in mechanics. For instance, he complemented NEWTON's second law by the balance of angular momentum, the second pillar of classical continuum physics. EULER worked in almost all areas of mathematics: geometry, infinitesimal calculus, trigonometry, algebra and number theory, as well as continuum physics, lunar theory and other areas of physics. He has been exceptionally productive; if printed, his works, many of which are of fundamental interest, would occupy between 60 and 80 quarto volumes.

Some of EULER's greatest successes were in solving real-world problems analytically and in describing numerous applications of the BERNOULLI numbers, VENN diagrams, EULER numbers, the constants e and π , continued fractions and integrals. He demonstrated equivalence of LEIBNIZ's differential calculus and NEWTON's method of fluxions and developed tools that made it easier to apply calculus to physical problems. In the context of this book his work is apparent through the EULER equations, the equations of motion of inviscid fluids.

The text is based on <http://en.wikipedia.org/>

$$\frac{\partial^2 \Phi}{\partial t^2} = c^2 \frac{\partial^2 \Phi}{\partial x^2}, \quad -\infty < x < \infty, \quad (7.10)$$

where Φ stands for ρ , p , ϕ , and the speed of sound $c = c_0$ is a constant. The solution of (7.10) will now be sought on the whole real line subject to the initial conditions

$$\Phi(x, 0) = \chi(x), \quad \frac{\partial \Phi}{\partial t}(x, 0) = \Psi(x). \quad (7.11)$$

A general solution of the wave equation due to D'ALEMBERT is representable in the form

$$\Phi(x, t) = f(x - ct) + g(x + ct) \quad (7.12)$$

with differentiable f and g . Indeed, the reader may check by substitution of (7.12) into (7.10) that both f and g satisfy the differential equation identically. These two functions can be determined from initial conditions (7.11), namely

$$\begin{aligned} f(x) + g(x) &= \chi(x), \\ c[-f(x) + g(x)]' &= \Psi(x), \end{aligned} \quad (7.13)$$

in which primes denote differentiation with respect to x . $\chi(x)$ and $\Psi(x)$ are functions which vanish sufficiently fast when $x \rightarrow \pm\infty$. Integrating (7.13)₂ yields

$$\begin{aligned} \int_{-\infty}^x [-f(\zeta) + g(\zeta)]' d\zeta &= \frac{1}{c} \int_{-\infty}^x \Psi(\zeta) d\zeta =: \psi(x), \\ \implies -f(x) + g(x) &= \psi(x). \end{aligned} \quad (7.14)$$

In the last step, $f(-\infty) = g(-\infty) = 0$ has been used, which is justified by the assumed localisation of the initial conditions. From (7.13)₁ and (7.14), we may now deduce

$$\begin{aligned} f(x) &= \frac{1}{2} [\chi(x) - \psi(x)], \\ g(x) &= \frac{1}{2} [\chi(x) + \psi(x)], \end{aligned} \quad (7.15)$$

so that

$$\begin{aligned} f(x - ct) &= \frac{1}{2} \chi(x - ct) - \frac{1}{2c} \int_{-\infty}^{x-ct} \Psi(\zeta) d\zeta, \\ g(x + ct) &= \frac{1}{2} \chi(x + ct) + \frac{1}{2c} \int_{-\infty}^{x+ct} \Psi(\zeta) d\zeta. \end{aligned} \quad (7.16)$$

If these results are now substituted into (7.12) the final form of D'ALEMBERT'S (1717–1783) general solution of the wave equation (7.10) subject to the initial conditions (7.11) is obtained in the form

$$\Phi(x, t) = \frac{1}{2} [\chi(x - ct) + \chi(x + ct)] + \frac{1}{2c} \int_{x-ct}^{x+ct} \Psi(\zeta) d\zeta. \quad (7.17)$$

An interpretation of this equation disclosing the wave character is obtained as follows: for constant argument $\zeta_+ = x - ct$, i.e. for an observer moving with the speed of sound in the positive x -direction, the value of $f(\zeta_+)$ remains constant; $f(x - ct)$ is therefore a wave propagating with the speed of sound in the positive x -direction. Analogously, for a constant argument $\zeta_- = x + ct$ the value of $g(\zeta_-)$ remains constant; $g(x + ct)$ must therefore be a wave that propagates into the negative x -direction. Generally, wave solution (7.12) or (7.17) consists of two waves propagating without change of shape with velocity c in opposite directions along the x -axis.

Example 7.1 Consider a motion from an initial state of rest. Then $\Psi(x) = 0$, so that the last integral term in (7.17) vanishes. Consequently, a given initial perturbation $\chi(x)$ propagates with half the initial amplitude both to the right and to the left, respectively, whereby, for a fixed time, the triangular signals cut in halves and correspondingly shifted add up to form the total signal. Figure 7.2 shows how the two left and right propagating waves develop from the initial triangular profile. Once the perturbations have left the region of mutual interaction, they propagate independently as triangles with half the initial height towards left and right. •

Problem 7.1 Consider the half line $x > 0$ and a wave that starts from rest from infinity and approaches the wall at $x = 0$. Show that the solution of the wave equation is again given by

$$\Phi(x, t) = \frac{1}{2} [\chi(x - ct) + \chi(x + ct)], \quad (7.18)$$

but that the reflection condition $\Phi(0, t) = 0$ at $x = 0$ requires now

$$\chi(ct) = -\chi(-ct) \implies \chi(x) = -\chi(-x). \quad (7.19)$$

The perturbation $\chi(x)$ for $x > 0$ must therefore be anti-symmetrically extended to the half line $x < 0$. Show graphically how a triangular disturbance is reflected at the wall. ♦

There is a second and more common way of solving the wave equation (7.10) subject to initial conditions (7.11). It explicitly uses the fact that the initial value problem (7.10), (7.11) is linear. Let θ be given by

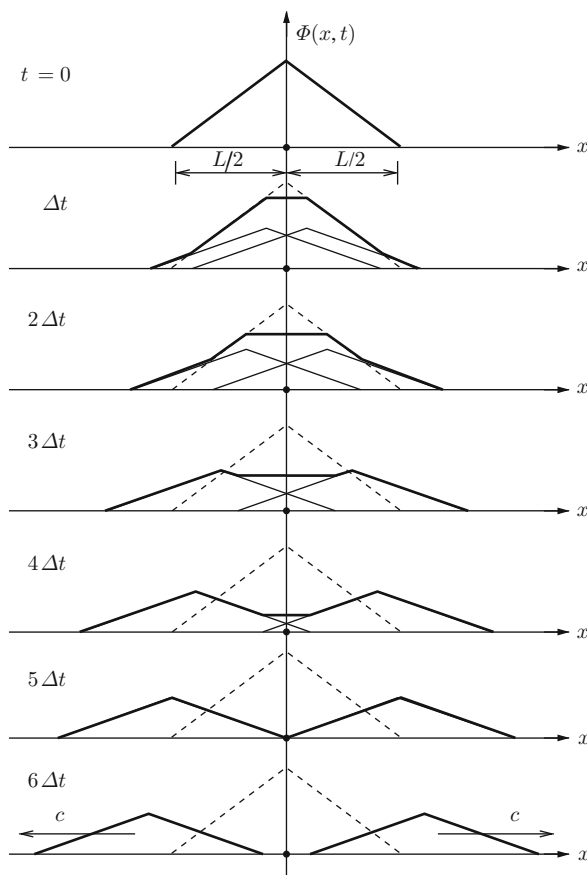
$$\theta = kx - \omega t. \quad (7.20)$$

Definition 7.3 $\theta = kx - \omega t$, in which k and ω are constants, is called the **phase**, k the **wavenumber** and ω the (circular) **frequency**. ■

It follows that $\sin \theta$ and $\cos \theta$ are solutions of (7.10), provided that

$$\omega^2 = k^2 c^2 \rightarrow c = \frac{\omega}{k}. \quad (7.21)$$

Fig. 7.2 Construction of the D'ALEMBERT solution of the wave equation. A triangular perturbation $\Phi(x, 0)$, released from rest, propagates towards left and right with an amplitude that is half the initial amplitude



Definition 7.4 A relation of the form

$$\omega = W(k) \quad (7.22)$$

is called **dispersion relation** and

$$c := \frac{\omega}{k} = \frac{W(k)}{k} \quad (7.23)$$

is called **phase speed**. ■

Now, because of the relation

$$\exp(i\theta) = \cos \theta + i \sin \theta, \quad (7.24)$$

also the exponential function $e^{i\theta}$ is a solution of (7.10), it is simply complex valued. Solutions that are physically meaningful must be real valued, and so we

conclude that the physical solutions which can be extracted from the expression $\Phi = \Phi_0 \exp(i\theta)$ with possibly complex valued Φ_0 are simply

$$\mathcal{R}e[\Phi_0 e^{i\theta}] \quad \text{and} \quad \mathcal{I}m[\Phi_0 e^{i\theta}].$$

It is mathematically more convenient to perform the computations with the complex-valued exponential functions rather than the trigonometric functions and to isolate the real and imaginary parts at the very end.

The frequency and wavenumber must be related by the dispersion relation. It follows that the expressions

$$\Phi = \sum_{m=1}^{\infty} A_m \exp(i\theta_m), \quad \theta_m = k_m x - \omega_m t \quad (7.25)$$

or

$$\Phi = \int A(\omega) \exp(i\theta) d\omega, \quad \theta = kx - \omega t, \quad (7.26)$$

in which A_m are complex constants and $A(\omega)$ is a complex-valued continuous (square-integrable) function, are equally solutions of (7.10) as long as the phases θ_m or θ satisfy the dispersion relation (7.21). Proceeding for the moment with (7.25), exploration of the initial conditions (7.11) yields

$$\begin{aligned} \Phi(x, 0) &= \sum_{m=1}^{\infty} A_m \exp(ik_m x) = \chi(x), \\ \frac{\partial \Phi}{\partial t}(x, 0) &= - \sum_{m=1}^{\infty} A_m i\omega_m \exp(ik_m x) = \Psi(x). \end{aligned} \quad (7.27)$$

Alternatively, integral representation (7.26) leads to

$$\begin{aligned} \Phi(x, 0) &= \int_{-\infty}^{\infty} A(\omega) \exp(ikx) d\omega = \chi(x), \\ \frac{\partial \Phi}{\partial t}(x, 0) &= - \int_{-\infty}^{\infty} A(\omega) i\omega \exp(ikx) d\omega = \Psi(x). \end{aligned} \quad (7.28)$$

Thus, (7.25) together with (7.27), or (7.26) with (7.28), also construct the solution to the initial value problem (7.10), (7.11) for given functions $\chi(x)$ and $\Psi(x)$.

Representations (7.27) are the famous *Fourier expansions* of the functions $\chi(x)$ and $\Psi(x)$, and for given $\chi(x)$ and $\Psi(x)$ the coefficients A_m can be determined. The two functions are then expressed in terms of the so-called *Fourier series*. Analogously, (7.26) is a *Fourier-integral* representation of the solution which is complete if (7.28) are inverted for $A(\omega)$. It is not the purpose here to construct

these inversions – we are satisfied to have made plausible that they can be found in principle. As a result, however, we will henceforth, when encountering linear wave equations, seek solutions by superposing exponential functions with phases whose wavenumber and frequency satisfy the dispersion relation.

Returning to the three-dimensional case in Cartesian coordinates, i.e. according to (7.7) and (7.9),

$$\frac{\partial^2 \Phi}{\partial t^2} = c^2 \left(\frac{\partial^2 \Phi}{\partial x^2} + \frac{\partial^2 \Phi}{\partial y^2} + \frac{\partial^2 \Phi}{\partial z^2} \right), \quad (7.29)$$

we now seek solutions to (7.29) of the form

$$\Phi(x, y, z, t) = \Phi_0 \exp(i\theta) = \Phi_0 \exp(i(\mathbf{k} \cdot \mathbf{x} - \omega t)), \quad (7.30)$$

in which Φ_0 is an amplitude of which the value is arbitrary for the homogeneous equation (7.29). \mathbf{k} is the *wavenumber vector* and ω the *frequency* and $\theta = (\mathbf{k} \cdot \mathbf{x} - \omega t)$ is the *phase*, as before. It possesses the following properties.

Problem 7.2 *Prove that the surfaces of constant phases $\theta = \text{constant}$ represent planes in \mathbb{R}^3 (when $t = \text{constant}$). The wavenumber vector is perpendicular to these planes and points in the direction to which the planes move with increasing time; see Fig. 7.3. Moreover, the phase will be constant for an observer who moves with the velocity*

$$\frac{d\mathbf{x}}{dt} = \mathbf{c} = \frac{\omega}{|\mathbf{k}|} \frac{\mathbf{k}}{|\mathbf{k}|}. \quad (7.31)$$



Because of the properties stated in Problem 7.2 the solutions of the form (7.30) are called *plane waves* and \mathbf{c} in (7.31) is called the *phase velocity*. This velocity measures the velocity of an individual crest or trough or node of harmonic excitation (7.30). Note also that

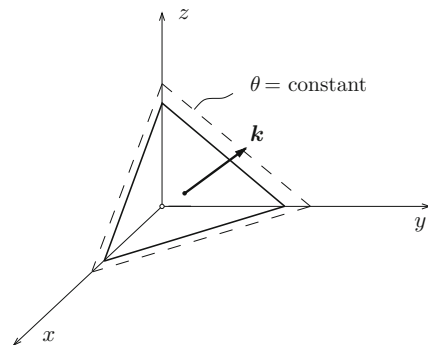


Fig. 7.3 Planes of constant phase are perpendicular to the wavenumber vector and move for increasing time into the direction of \mathbf{k}

$$\frac{d\theta}{dt} = \frac{\partial\theta}{\partial t} + \frac{d\mathbf{x}}{dt} \cdot \frac{\partial\theta}{\partial\mathbf{x}} = 0, \quad (7.32)$$

if \mathbf{c} is given by (7.31). This means that the phase is constant for an observer moving with the phase speed. Now, (7.30) implies the relations

$$\begin{aligned} \text{grad } \Phi &= (i\mathbf{k}) \Phi, & \text{div grad } \Phi &= -(\mathbf{k} \cdot \mathbf{k}) \Phi = -|\mathbf{k}|^2 \Phi, \\ \frac{\partial \Phi}{\partial t} &= (-i\omega) \Phi, & \frac{\partial^2 \Phi}{\partial t^2} &= -\omega^2 \Phi, \end{aligned} \quad (7.33)$$

so, upon substitution into (7.29), again the dispersion relation

$$\omega = W(|\mathbf{k}|) = c|\mathbf{k}| = ck \quad (7.34)$$

emerges, or when solved for c

$$c(k) = \frac{\omega}{k} = \frac{1}{k} W(k), \quad (7.35)$$

so that, in general, the phase speed is a function of the modulus of the wavenumber vector. In the present case of the classical wave equation the phase speed is constant and thus independent of the wavenumber (or of the frequency). There are, however, cases for which the phase speed does depend on the wavenumber. Such a case will be encountered in Chap. 8. Indeed, consider (8.68),

$$\mathcal{L}^2 \left[\frac{\partial^2 w}{\partial z^2} \right] + N^2 \nabla_H^2 w = 0, \quad (7.36)$$

with

$$\mathcal{L} = \frac{\partial^2}{\partial t^2} + f^2, \quad N = -\frac{1}{\rho_*} \frac{d\rho_0}{dz} g, \quad \nabla_H^2 = \frac{\partial^2}{\partial x^2} + \frac{\partial^2}{\partial y^2},$$

and solve it for the vertical velocity component w by the method of separation of variables. Writing

$$w(x, y, z, t) = Z_n(z) w_n(x, y, t), \quad (7.37)$$

the following equation for w_n is obtained:

$$\mathcal{L} w_n - gh_n \nabla_H^2 w_n = 0, \quad (7.38)$$

where gh_n are the eigenvalues of the vertical mode analysis (see (8.72)). Equation (7.38) is also a linear wave equation and can be solved by the plane-wave representation (7.30), leading to the dispersion relation

$$(\omega^2 - f^2) = gh_n |\mathbf{k}|^2 \rightarrow \omega = \sqrt{gh_n k^2 + f^2},$$

so

$$W(k) = \sqrt{gh_n k^2 + f^2} \quad (7.39)$$

and

$$c(k) = \frac{\omega}{k} = \frac{1}{k} \sqrt{gh_n k^2 + f^2}. \quad (7.40)$$

The phase speed is here an explicit function of k . This leads us to the following definition:

Definition 7.5 *If the phase velocity is not a function of the wavenumber, the wave propagation is termed **non-dispersive**. Then $W(k) = ck$, where c is constant. If the phase velocity is a function of the wavenumber, then the wave propagation is termed **dispersive** and $c(k) = k^{-1} W(k)$.* ■

Dispersion has to do with *spreading*. So dispersive waves propagate with different phase speeds at different wavenumbers. A signal comprising different FOURIER components will therefore spread in time since to each frequency and wavenumber there belongs its own phase speed.

A concept of great physical importance that is intimately connected with dispersion is the derivative of $W(k)$, $c_{\text{gr}} = W'(k)$.

Definition 7.6 *The derivative of the frequency as a function of the wavenumber, $\omega = W(k)$,*

$$c_{\text{gr}} := \frac{dW}{dk} \quad [\text{m s}^{-1}] \quad (7.41)$$

*has the dimension of a velocity and is called **group velocity**.* ■

It is evident from the above definitions that for a non-dispersive wave the phase and group velocities have the same values, $c = c_{\text{gr}}$. Alternatively, they differ from one another when the waves are dispersive. For instance, for (7.39)

$$c_{\text{gr}} = \frac{gh_n k}{\sqrt{gh_n k^2 + f^2}} \neq \frac{1}{k} \sqrt{gh_n k^2 + f^2} = c.$$

The group velocity is an important concept, because it is the velocity with which a group of waves having distinct but nearly the same wavenumbers travels. Furthermore, it can be shown that *the energy of a wave travels with the group velocity*.

To elucidate these facts, consider a particular value of k and the corresponding value of $\omega = W(k)$ as reference values and perturb these slightly. Then, to $k + \Delta k$ there belongs

$$\begin{aligned}\omega + \Delta \omega &= W(k + \Delta k) = W(k) + c_{\text{gr}}|_k \Delta k + \mathcal{O}(\Delta k^2) \\ &\simeq W(k) + c_{\text{gr}} \Delta k.\end{aligned}$$

The phase to this perturbed wavenumber is

$$\theta^+ = (k + \Delta k)x - (\omega + \Delta \omega)t = \theta + \Delta k(x - \bar{c}_{\text{gr}}t), \quad (7.42)$$

where θ is the unperturbed phase and $\bar{c}_{\text{gr}} = \Delta \omega / \Delta k$. Similarly, we can perturb θ to a smaller wavenumber, $k - \Delta k$, and obtain analogously

$$\theta^- = (k - \Delta k)x - (\omega - \Delta \omega)t = \theta - \Delta k(x - \bar{c}_{\text{gr}}t). \quad (7.43)$$

If we consider the two solutions

$$\Phi^+ = \Phi_0 \exp(i\theta^+), \quad \Phi^- = \Phi_0 \exp(i\theta^-), \quad (7.44)$$

add these together and substitute (7.42) and (7.43), then we obtain the combined solution

$$\Phi = \Phi^+ + \Phi^- = 2\Phi_0 \cos(\Delta k(x - \bar{c}_{\text{gr}}t)) \exp(i\theta). \quad (7.45)$$

This solution may be considered as one at the reference wavenumber k and reference frequency ω with its amplitude modulated by the cosine function $\cos(\Delta k(x - \bar{c}_{\text{gr}}t))$. A snapshot of this solution is shown in Fig. 7.4. The unperturbed wave

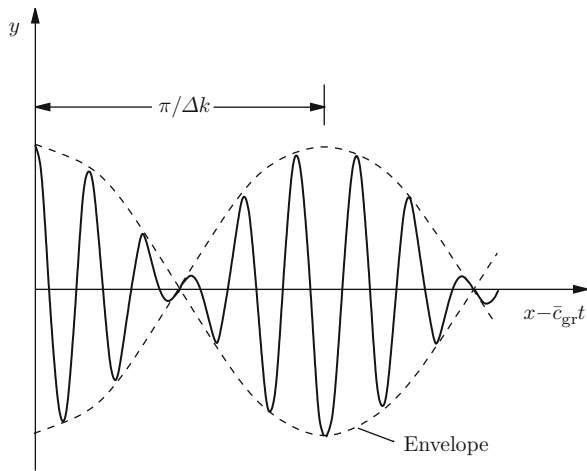


Fig. 7.4 Snapshot of wave solution (7.45) with beats. The unperturbed wave travels with the phase velocity, the modulated amplitude with the group velocity

$\exp(i\theta)$ propagates with the phase velocity, but the solution has *beats*, corresponding to the changes in amplitude. The envelope travels with the group velocity. Each lobe of the envelope may be interpreted as a group of waves and the velocity \bar{c}_{gr} may be interpreted as the velocity of the group. Obviously, in the limit as $\Delta k \rightarrow 0$, $\bar{c}_{\text{gr}} \rightarrow c_{\text{gr}}$.

7.2 Surface Gravity Waves Without Rotation

Having laid the foundations of linear wave analysis in the last section, we shall in this section be concerned with an introductory account of linear surface waves in homogeneous water. Rotation of the coordinate system will be ignored in a first step as our intention is to elucidate how waves travel in such a fluid system without rotation of the frame of reference. We will see that water waves are in principle *dispersive*, but there is a *non-dispersive* limit, which is limnologically significant. This is the long-wave approximation, called *shallow water approximation (SWA)*. However, we first treat the more general case which applies to all wavelengths.

Consider a layer of an ideal incompressible fluid referred to an inertial frame in two-dimensional plane motion with free surface $z = \zeta(x, t)$; Fig. 7.5. In the absence of the rotation of the frame of reference the linearised continuity and momentum equations take the forms

$$\text{div } \mathbf{v} = 0 \quad \text{and} \quad \rho \frac{\partial \mathbf{v}}{\partial t} = -\text{grad } p', \quad (7.46)$$

in which p' is the perturbation pressure such that the total pressure p equals

$$p = -\rho g z + p'. \quad (7.47)$$

By taking the divergence of the momentum equation (7.46)₂ and substituting (7.46)₁, it is seen that

$$\text{div grad } p' = \Delta p' = 0. \quad (7.48)$$

Thus, the perturbation pressure must satisfy the LAPLACE equation. This is an interesting result, because the LAPLACE equation is *not* a wave equation. Where do water

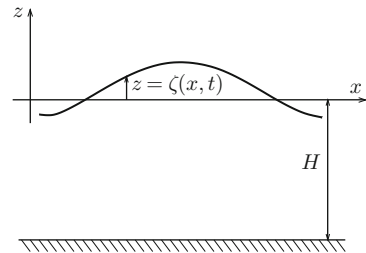


Fig. 7.5 Plane surface wave in a layer of ideal incompressible fluid

waves in a homogeneous fluid body then come from? It is the motion of the surface – the boundary – that induces the waves as we shall soon see.

So, the boundary conditions are physically the crucial element. Let us begin at the *basal surface*, which in Fig. 7.5 we chose to be located at $z = -H$, where H is constant. Here the fluid velocity must be tangential to the surface, $\mathbf{v} \cdot \mathbf{n} = 0$, where \mathbf{n} is the unit exterior normal, here $-\mathbf{e}_z$. Thus $\mathbf{v} \cdot \mathbf{e}_z = 0$ or

$$w = 0, \quad \text{at } z = -H. \quad (7.49)$$

At the *free surface* $z = \zeta(x, t)$ we assume vanishing surface traction; this means that an outside (atmospheric) pressure and shear traction are assumed to be small or absent. The traction on a surface with exterior unit normal \mathbf{n} is given by $\mathbf{t} \mathbf{n}$. So the traction-free condition reads $\mathbf{t} \mathbf{n} = \mathbf{0}$. The stress tensor \mathbf{t} and the unit normal vector \mathbf{n} in two dimensions are given by

$$\mathbf{t} \hat{=} \begin{pmatrix} -p & \tau \\ \tau & -p \end{pmatrix}, \quad \mathbf{n} \hat{=} \frac{\begin{pmatrix} -\frac{\partial \zeta}{\partial x}, 1 \end{pmatrix}^T}{\sqrt{1 + \left(\frac{\partial \zeta}{\partial x}\right)^2}}, \quad (7.50)$$

respectively, so that the stress boundary condition becomes

$$\left. \begin{aligned} p \frac{\partial \zeta}{\partial x} + \tau &= 0, \\ -\tau \frac{\partial \zeta}{\partial x} - p &= 0, \end{aligned} \right\} \implies \begin{cases} p = 0, \\ \tau = 0, \end{cases} \quad \text{at } z = \zeta(x, t). \quad (7.51)$$

Because field equation (7.48) involves only the pressure, the second condition will not be needed. This is, in general, not so and is here due to the assumption that the fluid is inviscid. The difficulty with the simple boundary condition (7.51)₁ is that the argument variable z is an unknown function of x and t , $p = p(x, z = \zeta(x, t))$, because the geometry of the free surface is an unknown that is part of the solution of the problem. To linear approximation, a TAYLOR series expansion yields

$$p(x, z = \zeta(x, t)) = p(x, 0) + \frac{\partial p}{\partial z}(x, 0)\zeta + \mathcal{O}(\zeta^2) = 0, \quad (7.52)$$

which implies, in view of $p = p_0 + p'$ and $p_0 = -\rho g z$,

$$\underbrace{p_0(x, 0)}_0 + \underbrace{\frac{\partial p_0}{\partial z}(x, 0) \zeta}_{-\rho g \zeta(x, t)} + \underbrace{\frac{\partial p'}{\partial z}(x, 0) \zeta + \mathcal{O}(\zeta^2)}_{\mathcal{O}(\zeta p')} = 0,$$

so that

$$p'(x, 0) = \rho g \zeta(x, t) + \text{higher order terms}. \quad (7.53)$$

Thus, we have now expressed the original boundary condition (7.51), valid at the unknown position of the free surface in terms of a new expression, (7.53), now valid at the undeformed free surface, $z = 0$, and involving the free surface displacement function $\zeta(x, t)$ explicitly. This transformation has, however, only been achieved by linearising the statement and, therefore, restricting these displacements to small values.

There is a further condition which must hold on a free boundary; this is the *kinematic equation of motion* of the surface. To derive it, we start from the equation describing the free surface,

$$F_s(x, z, t) \equiv \zeta(x, t) - z = 0 \quad (7.54)$$

and state that this equation holds for all time. So dF_s/dt , which is the time rate of change of F_s following the surface, must equally vanish,

$$\frac{dF_s}{dt} = 0, \quad \implies \quad \frac{\partial \zeta}{\partial t} + \frac{\partial \zeta}{\partial x} \frac{dx}{dt} - \frac{dz}{dt} = 0, \quad (7.55)$$

in which $dx/dt = u$ and $dz/dt = w$ are the x - and z -components of the surface velocity. Thus, we have the final equation

$$\frac{\partial \zeta}{\partial t} + \frac{\partial \zeta}{\partial x} u - w = 0, \quad \text{at } z = \zeta(x, t). \quad (7.56)$$

This equation is exact, but it has two complications: first, it is explicitly non-linear through its middle term, second, it is also implicitly non-linear because the argument $z = \zeta(x, t)$ is unknown. If we linearise it by employing a TAYLOR series expansion in each term and then drop the terms which are of higher order small (i.e. products of perturbation terms), we obtain

$$\frac{\partial \zeta}{\partial t}(x, t) - w(x, 0, t) = 0, \quad \text{at } z = 0. \quad (7.57)$$

The above somewhat lengthy analysis completes the formulation of the boundary value problem; it comprises (7.48), (7.49), (7.53) and (7.57), which will now be repeated at one place:

$$\left. \begin{aligned} \Delta p' &= 0, & z &\in (0, -H), \\ \frac{\partial \zeta}{\partial t} - w &= 0, \\ p' &= \rho g \zeta, \\ w &= 0, & z &= -H, \end{aligned} \right\} z = 0, \quad \left. \vphantom{\begin{aligned} \Delta p' &= 0, \\ \frac{\partial \zeta}{\partial t} - w &= 0, \\ p' &= \rho g \zeta, \\ w &= 0, \end{aligned}} \right\} -\infty < x < \infty. \quad (7.58)$$

This (linearised) boundary value problem is formulated in those variables that are physically the most direct ones. In this sense all the variables are the most natural

ones. Mathematically, it is more convenient to express every statement of (7.58) in terms of the perturbation pressure. This can be achieved by writing down the vertical component of the (linearised) momentum equation (7.46)₂,

$$\frac{\partial w}{\partial t} = -\frac{1}{\rho} \frac{\partial p'}{\partial z}. \quad (7.59)$$

Using this in (7.58) whereby the boundary conditions involving w are differentiated once with respect to time yields the final form of the boundary value problem

$$\left. \begin{aligned} \Delta p' &= \frac{\partial^2 p'}{\partial x^2} + \frac{\partial^2 p'}{\partial z^2} = 0, & z \in (0, -H), \\ \left. \begin{aligned} \frac{\partial^2 \zeta}{\partial t^2} &= -\frac{1}{\rho} \frac{\partial p'}{\partial z}, \\ p' &= \rho g \zeta, \end{aligned} \right\} & z = 0, \\ \frac{\partial p'}{\partial z} &= 0, & z = -H, \end{aligned} \right\} \quad -\infty < x < \infty, \quad (7.60)$$

which describes surface waves in a layer of constant depth of a density-preserving fluid. The derivation was presented at this place, because it will in a similar fashion be employed at several places later in this text.

Consider a plane-wave solution

$$(p', \zeta) = (p_0(z), \zeta_0) e^{i(kx - \omega t)}, \quad (7.61)$$

in which $p_0(z)$ and ζ_0 are amplitudes, the former being obviously z -dependent; k is the wavenumber and ω the frequency. Substituting expressions (7.61) into (7.60)₁ shows that $p_0(z)$ must satisfy the differential equation

$$\frac{d^2 p_0}{dz^2} - k^2 p_0 = 0$$

with the general solution²

$$p_0(z) = A \cosh[k(z + H)] + B \sinh[k(z + H)]. \quad (7.62)$$

Imposing boundary conditions (7.60)_{3,4} yields

² Definitions of the hyperbolic functions:

$$\sinh x = \frac{e^x - e^{-x}}{2}, \quad \cosh x = \frac{e^x + e^{-x}}{2}, \quad \tanh x = \frac{\sinh x}{\cosh x} = \frac{e^x - e^{-x}}{e^x + e^{-x}}.$$

$$A = \frac{\rho g \zeta_0}{\cosh(kH)}, \quad B = 0 \quad (7.63)$$

and (7.60)₂ determines a relation between the frequency ω and the wavenumber k , viz.

$$\omega^2 = gk \tanh(kH). \quad (7.64)$$

This is the *dispersion relation* of the linearised surface gravity waves on a liquid layer of constant depth. It follows that *surface gravity waves are generally dispersive*, since the *phase velocity* $c_{\text{ph}} = (\omega/k^2)k$ and the *group velocity* $c_{\text{gr}} = d\omega/dk$,

$$\begin{aligned} c_{\text{ph}} &= \sqrt{\frac{g}{k} \tanh(kH)} \frac{k}{k}, \\ c_{\text{gr}} &= \frac{1}{2} \left\{ \sqrt{\frac{g \tanh(kH)}{k}} + \sqrt{\frac{gk}{\tanh(kH)}} \frac{H}{\cosh^2(kH)} \right\} \frac{k}{k} \end{aligned} \quad (7.65)$$

differ from one another. Dimensionless representations of these speeds, valid for all H , are

$$\begin{aligned} \frac{c_{\text{ph}}}{\sqrt{gH}} &= \sqrt{\frac{\tanh(kH)}{kH}} \quad \text{or} \quad \frac{\omega}{\sqrt{g/H}} = \sqrt{kH \tanh(kH)}, \\ \frac{c_{\text{gr}}}{\sqrt{gH}} &= \frac{1}{2} \left\{ \sqrt{\frac{\tanh(kH)}{kH}} + \frac{\sqrt{kH}}{\cosh^2(kH) \sqrt{\tanh(kH)}} \right\}, \end{aligned} \quad (7.66)$$

and these are graphically displayed in Fig. 7.6. Approximate expressions for the phase and group speeds are obtained if these formulae are evaluated in the limit as $k \rightarrow \infty$. (Note: the wavelength l and wavenumber k are related by $l = 2\pi/k$.) Since $\tanh(kH) \rightarrow 1$ and $\cosh(kH) \rightarrow \infty$ as $k \rightarrow \infty$, this limit yields

$$\left. \begin{aligned} \lim_{k \rightarrow \infty} \frac{c_{\text{ph}}}{\sqrt{gH}} &= \frac{1}{\sqrt{kH}}, \\ \lim_{k \rightarrow \infty} \frac{c_{\text{gr}}}{\sqrt{gH}} &= \frac{1}{2} \frac{1}{\sqrt{kH}}, \\ \lim_{k \rightarrow \infty} \frac{\omega}{\sqrt{g/H}} &= \sqrt{kH}, \end{aligned} \right\} \begin{array}{l} \text{short-wave approximation,} \\ \text{valid for } kH \geq 2. \end{array} \quad (7.67)$$

The *short-wave* group velocity is thus half the short-wave phase velocity and both decay like $1/\sqrt{kH}$ as $k \rightarrow \infty$. These limits are shown as dashed lines in Fig. 7.6. The graphs indicate that for $kH \geq 2$ the short-wave approximation (7.67) is a valid approximation. *In a layer of depth H , waves with wavelengths $l \lesssim H/2$ may, with sufficient accuracy, be considered as short.*

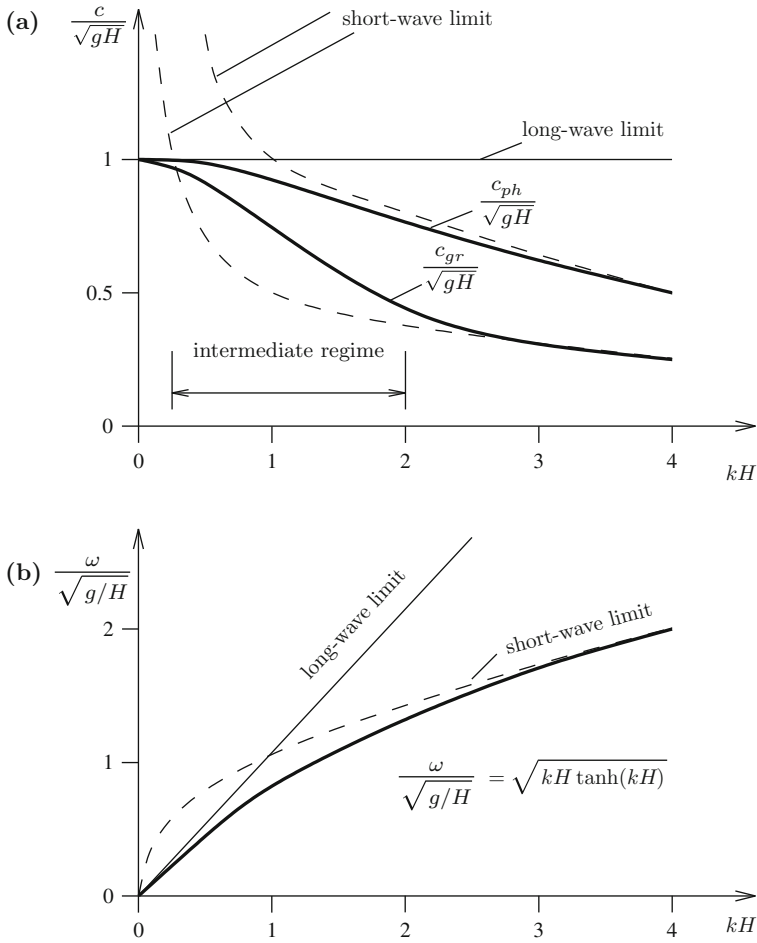


Fig. 7.6 (a) Dimensionless phase and group speeds plotted against dimensionless wavenumber kH . (b) Dimensionless frequency $\omega/\sqrt{g/H}$ plotted against dimensionless wavenumber kH . In both graphs long-wave and short-wave limits are also indicated

The other limit of *long waves* is obtained, if the limit $k \rightarrow 0$ is considered. Because $\tanh(kH) \rightarrow kH$ and $\cosh(kH) \rightarrow 1$ as $k \rightarrow 0$, this limit is given by the formulae

$$\left. \begin{aligned} \lim_{k \rightarrow 0} \frac{c_{ph}}{\sqrt{gH}} &= 1, \\ \lim_{k \rightarrow 0} \frac{c_{gr}}{\sqrt{gH}} &= 1, \\ \lim_{k \rightarrow 0} \frac{\omega}{\sqrt{g/H}} &= kH \end{aligned} \right\} \begin{aligned} &\text{long-wave approximation,} \\ &\text{valid for } kH \leq 0.1\pi. \end{aligned} \quad (7.68)$$

The long-wave group velocity equals the long-wave phase velocity and both are constant and equal to

$$c_{\text{ph}} = c_{\text{gr}} = \sqrt{gH}, \quad \omega = \sqrt{gH}k. \quad (7.69)$$

This limiting behaviour is shown in Fig. 7.6 as thin solid lines. As implied by the graphs this long-wave behaviour is sufficiently accurately described by (7.68) as long as $kH \leq \pi/10$, or $l \geq 20H$. A surface wave with wavelength larger than approximately 20 water depths may with sufficient accuracy be treated with the equations of the long wavelength approximation. These results merit special mentioning in a rule.

Rule:

- In a homogeneous water layer of depth H waves with wavelengths shorter than $H/2$ may mathematically be treated as short waves. For such waves the layer behaves as if it were infinitely deep.
- Alternatively, waves with wavelengths larger than approximately 20 times the water depth may mathematically be treated with the equations of the long-wave approximation.
- Waves with wavelengths in the interval $H/2 < l < 20H$ are intermediate and suggest no approximation.

The long-wave approximation leads to equations which are known as *shallow-water equations*. These will be dealt with to great extent in subsequent chapters, because they describe with sufficient accuracy the most important problems in lake hydrodynamics.

Let us now return to the general case of which the solution for the perturbation pressure is given in (7.61), (7.62) and (7.63). Horizontal and vertical velocity components, u , w and surface elevation ζ can be computed from the pressure by back substitution into the original equations, e.g. (7.46)₁, (7.58)₃, (7.59). What obtains reads as follows:

$$\begin{aligned} p' &= \rho g \zeta_0 \frac{\cosh(k(z+H))}{\cosh(kH)} e^{i(kx-\omega t)}, \\ \zeta &= \zeta_0 e^{i(kx-\omega t)}, \\ u &= \frac{kg}{\omega} \zeta_0 \frac{\cosh(k(z+H))}{\cosh(kH)} e^{i(kx-\omega t)}, \\ w &= \frac{kg}{\omega} \zeta_0 \frac{\sinh(k(z+H))}{\cosh(kH)} e^{i(kx-\omega t)-i\pi/2}. \end{aligned} \quad (7.70)$$

It is seen that the vertical velocity component lags behind the other three variables by a quarter period. Short- and long-wave approximations will be discussed below.

Interesting physical insight is gained from evaluating the *trajectories of the fluid particles*. These can be determined from the equations

$$\frac{dx}{dt} = \mathcal{R}e(u(x, z, t)) \quad \frac{dz}{dt} = \mathcal{R}e(w(x, z, t)), \quad (7.71)$$

where u and w are given in (7.70)_{3,4}, subject to the initial conditions

$$x(t = 0) = x_0, \quad z(t = 0) = z_0. \quad (7.72)$$

Equations (7.71) and (7.72) form a system of two first-order ordinary differential equations (ODE). They constitute an initial value problem that can easily numerically be solved using software of ODE integrators. This is not what we are here aiming for. Our goal is an (approximate) analytic solution of these equations. To this end, we suppose that the particles do not move far away from their position at rest (recall the discussion involving a wave passing a fish rope at the beginning of this chapter!). We may then, for the integration of (7.71), treat x and z on the right-hand sides as constants. Thus, we replace x and z by x_0 and z_0 to identify this fact and then obtain

$$\frac{dx}{dt} = \mathcal{R}e(u(x_0, z_0, t)), \quad \frac{dz}{dt} = \mathcal{R}e(w(x_0, z_0, t)) \quad (7.73)$$

and after integration

$$\begin{aligned} x - x_0 &= \int_0^t \mathcal{R}e(u(x_0, z_0, \tau)) d\tau = f(x_0, z_0, t), \\ z - z_0 &= \int_0^t \mathcal{R}e(w(x_0, z_0, \tau)) d\tau = g(x_0, z_0, t). \end{aligned} \quad (7.74)$$

Equations (7.74) constitute the parameter representation of the trajectory through the point (x_0, z_0) . By eliminating the time between the two equations an explicit form, $I(x, z) = 0$, of the trajectory through the point (x_0, z_0) can be obtained.

With (7.70)_{3,4} the specific forms of (7.73) for our example are

$$\frac{dx}{d\tau} = U_0(z_0) \mathcal{R}e(e^{-i\omega\tau}), \quad \frac{dz}{d\tau} = -iU_0(z_0) \tanh(k(z_0 + H)) \mathcal{R}e(e^{-i\omega\tau}), \quad (7.75)$$

in which

$$\tau = -\frac{x_0}{c_{ph}} + t, \quad U_0(z_0) = \frac{kg}{\omega} \zeta_0 \frac{\cosh(k(z_0 + H))}{\cosh(kH)}. \quad (7.76)$$

Straightforward integration of (7.75) yields

$$\begin{aligned} x - x_0 &= \mathcal{R}e \left\{ i \frac{U_0}{\omega} e^{-i\omega\tau} \right\} = \frac{U_0}{\omega} \sin \omega \tau, \\ z - z_0 &= \mathcal{R}e \left\{ \frac{U_0}{\omega} \tanh(k(z_0 + H)) e^{-i\omega\tau} \right\} = \frac{U_0}{\omega} \tanh(k(z_0 + H)) \cos \omega \tau, \end{aligned} \quad (7.77)$$

in which (x_0, z_0) is a fixed point in (x, z) -space and \mathcal{Re} denotes ‘real part’. By eliminating time from (7.77) and using the dispersion relation (7.64), the trajectories of the particles are obtained as follows:

$$\frac{(x - x_0)^2}{\left(\frac{\zeta_0 \cosh(k(z_0 + H))}{\sinh(kH)}\right)^2} + \frac{(z - z_0)^2}{\left(\frac{\zeta_0 \sinh(k(z_0 + H))}{\sinh(kH)}\right)^2} = 1. \quad (7.78)$$

Equations (7.77) and (7.78) are the two forms of the trajectory representations through (x_0, z_0) ; they disclose the following properties, some of which are also graphically displayed in Fig. 7.7:

- Trajectories are ellipses with ratio of the vertical (b) and horizontal (a) principal semi-axes

$$\left(\frac{b}{a}\right)^2 = \tanh^2(k(z_0 + H)) \leq 1. \quad (7.79)$$

*These ellipses are traversed in the clockwise direction, when the wave propagates from left to right.*³

- For $z_0 = 0$ their aspect ratio is largest, namely $\tanh(kH)$, for $z_0 = -H$ it is zero, i.e. ellipses collapse to a double line (a single line traversed twice).
- The size of the ellipses is described by $U_0(z)/\omega$, indicating a decrease with increasing depth:

$$\frac{a(z = -H)}{a(z = 0)} = \frac{1}{\cosh(kH)}. \quad (7.80)$$

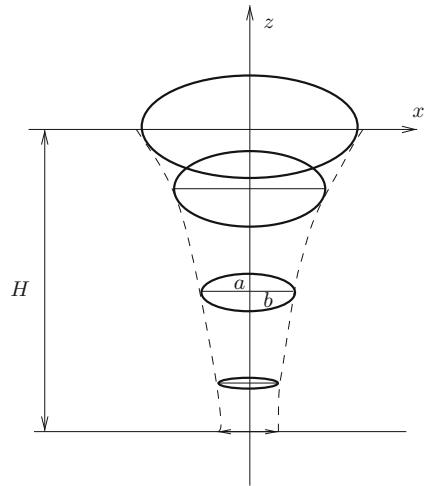


Fig. 7.7 Particle trajectories for fluid particles at various depths as determined by (7.78)

³ This can be inferred from (7.77).

- In the limit as $H \rightarrow \infty$ the ellipses become circles whose radius decays exponentially with depth:

$$\lim_{H \rightarrow \infty} a = \lim_{H \rightarrow \infty} b = \zeta_0 e^{kz_0}. \quad (7.81)$$

Thus, the particle motion is effectively restricted to a ‘boundary layer of thickness’ $1/k$.

Another characterisation of the flow is provided by the *streamlines*; these are defined as the integral curves of the tangential field to the velocity at a fixed time, viz.

$$\frac{dx}{d\sigma} = \operatorname{Re}[u(x, z, t)], \quad \frac{dz}{d\sigma} = \operatorname{Re}[w(x, z, t)], \quad (7.82)$$

where σ is the curve parameter. With relations (7.70)_{3,4} this yields

$$\begin{aligned} \frac{dz}{dx} &= \frac{\operatorname{Re}[w(x, z, t)]}{\operatorname{Re}[u(x, z, t)]} = \frac{\sinh(k(z+H)) \sin(kx - \omega t)}{\cosh(k(z+H)) \cos(kx - \omega t)} \\ &= \tanh(k(z+H)) \tan(kx - \omega t). \end{aligned} \quad (7.83)$$

It follows from this formula that $dz/dx \rightarrow \infty$ where $u = 0$ and that $dz/dx = 0$ where $w = 0$. So, for a given motion, streamlines are horizontal where the surface inclination is largest, and they are vertical at positions of wave crests and wave troughs.

Particle trajectories and streamlines can be made visible in an experiment, e.g. by adding small buoyant particles to a fluid that are visible but still sufficiently small to be dragged by the fluid without any slip. If such conditions prevail, photographs with long exposure time will trace the particles along their ‘journey’ and thus record portions of the trajectories. If, on the other hand, the exposure time is short, the particles will traverse a very short distance during this time. Their traces will be essentially straight and tangential to the instantaneous velocity field. So such photographs will indicate the streamline pattern.

Photographs with long exposure time have been taken by WALLET and RUELLAN [17] at the Laboratoire Dauphinois d’Hydraulique, Grenoble, and are reproduced here in Fig. 7.8. Relevant at this moment is only the top figure on the left, which shows the trajectories of buoyant particles during one period for a purely harmonic wave coming from the left. It is seen that the trajectories are practically ellipses, nearly circular at the free surface but thin close to the bottom. Some open loops indicate a slow drift to the right near the surface and to the left near the bottom. These results corroborate beautifully the property expressed earlier that the motion of the wave itself and that of the particles may be vastly distinct from one another. Here the wave moves with the phase velocity from left to right, while the particles perform bounded motions along closed trajectories. The fact that the trajectories are closed is, however, not a property of the physical system; it is here due to both the

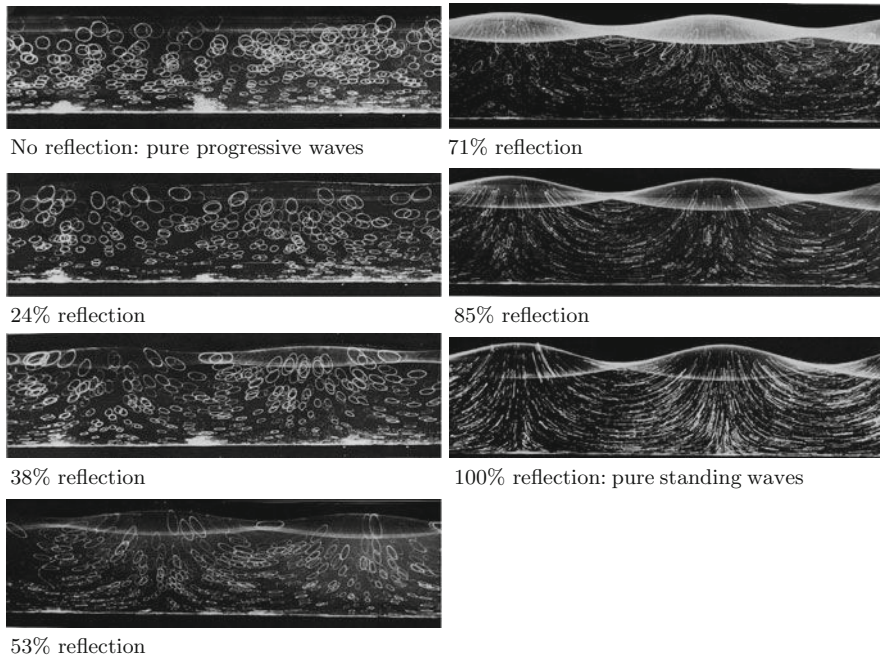
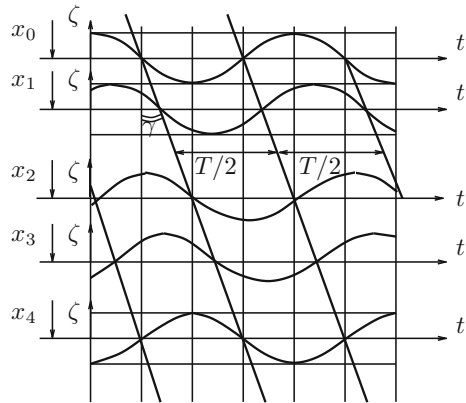


Fig. 7.8 Particle trajectories in plane periodic water waves. Two wave trains of the same frequency travelling in opposite directions are produced by a progressive wave coming from the left that is reflected by a partially absorbent barrier. The *top photograph on the left* shows the pure progressive wave with no reflection. Its amplitude is 4% of the wavelength and the water depth is 22%. White particles suspended in the water are photographed during one period. Their trajectories are practically ellipses traversed clockwise, nearly circular at the free surface and flattened towards the bottom. As the reflection is increased, the orbits become increasingly flattened and inclined. Complete reflection gives a pure standing wave in the last photograph, where the trajectories are along streamlines. There, the upper and lower envelopes of the water surface show that the vertical motion does not vanish at the nodes, where the horizontal velocity is nil, from VAN DYKE [15], originally photographed by WALLET and RUELLAN [17] © Houille Blanche

linearisation of the boundary value problem as expressed by (7.60) and the second linearisation of the differential equations (7.71) determining the trajectories of the fluid particles. If, for instance, this second linearisation is not implemented (x_0, z_0 on the right-hand side are replaced by x, z) and (7.75) are solved exactly, then the trajectories are no longer ellipses and neither are they closed. However, the photographs demonstrate that the error due to these simplifications is rather small.

Problem 7.3 By using an available software of ODE integrations or by employing his own program the reader may integrate (7.71) with u and w given in (7.70)_{3,4} exactly and demonstrate that for a harmonic wave from left to right, there is an average drift of the particles, at the surface to the right and at the base to the left. This drift can be made visible by plotting the trajectories for a number of selected particles for a number of periods $T = 2\pi/\omega$. ■

Fig. 7.9 Time series (7.84) plotted for five different positions x . The distances $x_j - x_{j-1}$ ($j = 1, 2, 3, 4$) are plotted with the same ratio as in field observations. Then the angle γ is a measure of the phase speed: $\cotan \gamma = c_{ph}$



Finally, we end this analysis by illustrating the propagating wave by a graph that is popular in physical limnology when analysing data taken from thermistor chains, current metres or limnigraphs. Imagine for the present situation that a harmonic wave of the surface elevation is observed along a channel at the positions x_0, x_1, x_2, x_3, x_4 and that these data can be represented as

$$\begin{aligned} \zeta &= \zeta_0 \operatorname{Re} [\exp (i(k(x-x_0)-\omega t))] \\ &= \zeta_0 [\cos (k(x-x_0)) \cos \omega t + \sin (k(x-x_0)) \sin \omega t], \end{aligned} \quad (7.84)$$

where for x the above positions of the limnigraphs must be substituted. If we now plot a chart of the five time series (7.84) at the positions x_0, x_1, x_2, x_3, x_4 , one below the other such that the distances between consecutive time series are $x_j - x_{j-1}$, $j = 1, 2, 3, 4$, then the plot of Fig. 7.9 is obtained. Connecting in this graph the corresponding zeros between the individual time series yields the inclined straight lines at a distance of $T/2$, where T is the period of the wave from which the circular frequency $\omega = 2\pi/T$ can be deduced. The angle γ between the inclined lines and the vertical in these plots is then a measure of the phase speed. Indeed, in the units of time and distance of the graph, $\cotan \gamma = c_{ph}$. The figure therefore provides an explicit representation of the propagating wave.

7.2.1 Short-Wave Approximation

We have seen that the length scale, which appears in dispersion relation (7.64) and typifies the character of the waves, is the fluid depth H . For short waves, relations (7.67) give the asymptotic expressions for the dispersion relation

$$\omega^2 = gk \quad (\text{short waves}) \quad (7.85)$$

and the phase and group velocities valid for $kH \gg 1$ (actually, it requires only $kH \geq 2$ as shown in Fig. 7.6). Since in this limit the cosh and sinh functions may be replaced by $\frac{1}{2}$ exp-functions, relations (7.70) take the forms

$$\begin{aligned} p' &= \rho g \zeta_0 e^{kz} e^{i(kx - \omega t)}, \\ \zeta &= \zeta_0 e^{i(kx - \omega t)}, \\ u &= \frac{kg}{\omega} \zeta_0 e^{kz} e^{i(kx - \omega t)}, \\ w &= \frac{kg}{\omega} \zeta_0 e^{kz} e^{i(kx - \omega t) - i\pi/2}. \end{aligned} \quad (7.86)$$

These are the perturbation pressure, surface displacement and velocities of the so-called *deep-water waves* because $H \gg k^{-1}$. From the exponential z -dependence of the pressure and the velocity field it is seen that these quantities are confined to a distance (in z) on the order of k^{-1} from the surface, so propagation is unaffected by the bottom, if the water depth is approximately three times the wavelength or more. This may be used as a definition.

Definition 7.7 *Water waves in a homogeneous water layer are called **deep-water waves**, if their wavelength is less than about one-half to one-third of the water depth. These waves are dispersive and their dispersion relation is given by (7.85).* ■

As an application, consider the following example:

Example 7.2 *The dominant waves which one sees on the ocean surface have periods $2\pi\omega^{-1}$ of order 10 s. By (7.85) a deep-water wave has a wavelength shorter than $2\pi k^{-1} = 2\pi g/\omega^2 \sim 160$ m, its e-folding depth is $k^{-1} \simeq 25$ m and its phase speed is 15 m s^{-1} ! The deep-water approximation is therefore reasonable for such waves when the depth is greater than 50 m. When such a wave approaches a shallow shore region its frequency remains constant, but owing to the finite-depth-dispersion relation the wave will become shorter and the phase speed decreases. It follows that deductions about wavelength and phase speed made by observing waves on a beach can lead to erroneous conclusions about their properties in deep water.* ●

7.2.2 Long-Wave Approximation

This approximation is obtained if $k^{-1} \gg H$, i.e. if the wavelength is much larger than the water depth, and the dispersion relation was found in this limit to be

$$\omega = \sqrt{gH}k \quad (\text{long waves}), \quad (7.87)$$

with equal phase and group velocities; see (7.68). The waves obeying this limiting dispersion relation are called *shallow-water waves* because wavelengths are much

larger than H ; they are *non-dispersive* because the phase speed is independent of the wavenumber. This speed depends on g and the water depth and is given as follows:

depth [m]	:	100	500	1000	5000
speed [m s ⁻¹]	:	30	70	100	200

Such waves travel forth and back in Lake Zürich (30 km long) in 45 min, Lake Constance (60 km long) in 70 min and could cross the Atlantic ocean in 7 h. The corresponding approximation to (7.70) is

$$\begin{aligned}
 p' &= \rho g \zeta_0 e^{i(kx - \omega t)}, \\
 \zeta &= \zeta_0 e^{i(kx - \omega t)}, \\
 u &= \sqrt{\frac{g}{H}} \zeta_0 e^{i(kx - \omega t)}, \\
 w &= \sqrt{\frac{g}{H}} \zeta_0 k(z + H) e^{i(kx - \omega t) - i\pi/2},
 \end{aligned} \tag{7.88}$$

i.e. the pressure perturbation and the horizontal velocity are independent of depth. Since the density perturbation is zero, this is precisely the result which would be obtained if the pressure were calculated from the hydrostatic equation. Thus, we have explicitly demonstrated that *in this linear wave approximation the long-wave, shallow-water and hydrostatic pressure assumptions are equivalent*. We also see from (7.88)₄ that the vertical velocity increases linearly with z from zero at the bottom to $\partial \zeta / \partial t$ at the surface.

We summarise (on this basis and in view of the rule stated on p. 240) as follows:

Definition 7.8 *In a homogeneous water layer waves are called **shallow-water waves**, if their wavelength is larger than about 20 times the water depth. These waves are non-dispersive and their dispersion relation of the linearised theory is given by (7.87).* ■

Comparison of the pressure formulae for general, deep and shallow-water waves, (7.70)₁, (7.86)₁ and (7.88)₁, respectively, shows that pressure perturbations are attenuated with depth except in the shallow-water approximation. It follows that data from a pressure gauge positioned at the bottom of a lake must be used with care to interpret corresponding surface fluctuations. Such measurements will filter out all short surface waves and, if not properly corrected, will give erroneous results for intermediate wavelengths.

7.2.3 Standing Waves – Reflection

Consider two surface water waves that propagate in opposite directions. We assume first that the two waves have equal frequencies and amplitudes. In the linear

approximation, (7.70) still apply but must be written down for the forward as well as the backward moving wave with $\exp(i(kx - \omega t))$ being replaced by $\exp(i(kx + \omega t))$. Written down for the surface displacement ζ this yields

$$\zeta_{\text{forward}} = \zeta_0 e^{i(kx - \omega t)}, \quad \zeta_{\text{backward}} = \zeta_0 e^{i(kx + \omega t)}, \quad (7.89)$$

so that their sum is given by

$$\begin{aligned} \zeta &= \zeta_{\text{forward}} + \zeta_{\text{backward}} = \zeta_0 e^{ikx} (e^{i\omega t} + e^{-i\omega t}) \\ &= 2 \zeta_0 e^{ikx} \cos \omega t. \end{aligned} \quad (7.90)$$

Applying this procedure to all variables of (7.70) and restricting the formulae to the real parts show that the perturbation pressure, surface elevation and velocity components are given by

$$\begin{aligned} p' &= 2\rho g \zeta_0 \frac{\cosh(k(z + H))}{\cosh(kH)} \cos kx \cos \omega t, \\ \zeta &= 2\zeta_0 \cos kx \cos \omega t, \\ u &= 2 \frac{kg}{\omega} \zeta_0 \frac{\cosh(k(z + H))}{\cosh(kH)} \sin kx \sin \omega t, \\ w &= -2 \frac{kg}{\omega} \zeta_0 \frac{\sinh(k(z + H))}{\cosh(kH)} \cos kx \sin \omega t. \end{aligned} \quad (7.91)$$

This is a *standing wave*, a notion we shall now define.

Definition 7.9 A wave is called **standing**, if within its domain of existence there are finite dimensional sub-domains with time-independent boundaries at which at least one of the field variables remains constant for all time. ■

If the domain is one dimensional then the sub-domains are separated by *points*; in two and three dimensions they are *lines* and *areas*, respectively. A single point in two or three dimensions, at which some field variable has a constant value, does, however, not define a standing wave. In such a situation one sometimes calls such waves as *quasi-standing*. We shall encounter them when analysing waves in non-inertial frames.

Solution (7.91) is a standing wave since p' , ζ and w vanish for $kx = (2n+1)\pi/2$, so that the velocity field is purely horizontal at these points. Alternatively, when $kx = n\pi$ then p' , ζ and w go through maxima and minima (i.e. their amplitudes are largest), but u is zero. In this case of one spatial dimension for the surface elevation ζ the locations of vanishing wave field are points. Alternatively, for the variables p' , u , w the domain is two dimensional and the locations of vanishing wave fields p' , u , w are (vertical) lines. When solution (7.91) is interpreted as a wave field in a channel, in which the field variables do not show a dependence on the cross-channel coordinate y , then the points of zero value of the surface elevation

are lines across the channel. They are called *nodal lines* for the variable ζ . To the left and right of these lines the surface elevation has opposite signs; they are called to be in *counter-phase*.⁴ Figure 7.10 shows a graphical representation of standing wave solution (7.91). It displays the sinusoidal variation of the surface deflection at a fixed time as it varies along the channel. The wave height does not vary across the channel so that nodal lines and, more generally, the lines of constant wave height are straight lines across the channel. Projected onto the horizontal plane are arrows, which indicate how the horizontal velocity component varies with position and in conformity with the surface elevation (actually the double arrows (\leftrightarrow) are indicative of the size of the velocity amplitude). As is seen, the horizontal velocity vanishes in cross-sections where wave crests and wave troughs occur, and it goes through maxima at nodal lines of the surface elevation. To contrast these locations from those of the nodal lines, they are often denoted as *anti-nodal lines*. The division of the (infinite) channel into sub-domains can be executed in this case in two different ways. On the one hand, the rectangular boxes between two consecutive nodal lines (NN) separate the regions where surface elevations move consecutively in counter-phase. The horizontal velocities vary from a maximum (minimum) at

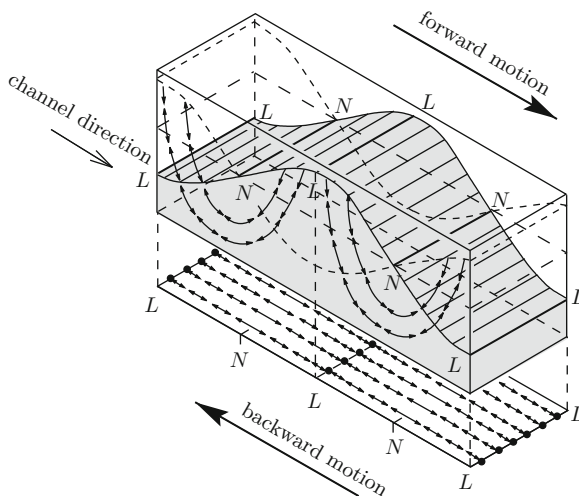


Fig. 7.10 A standing wave without rotation in a uniform depth model (according to MORTIMER [11, 12]). The figure shows the surface elevation (*solid lines*) and in counter-phase (*dashed*). Indicated are the nodal (NN) and anti-nodal (LL) lines. The lower, partly covered *rectangle* shows the horizontal velocities as *double arrows* indicating their magnitudes. Vanishing longitudinal velocities (*points*) correspond to positions of anti-nodes for the surface elevations. Redrawn from C.H. MORTIMER [11] with changes

⁴ It is often customary to call two periodic motions which are in counter-phase to be *out of phase*. This is not precise, because any two motions, which are not in phase, are out of phase. However, only a phase angle of $180^\circ (= \pi)$ characterises counter-phase behaviour.

one nodal line to a minimum (maximum) at the neighbouring nodal line. On the other hand, the sub-domains may be defined as the boxes between cross-sections at anti-nodes (LL). Physically, this choice here is more appealing, because there is never a mass exchange between these boxes.

To determine the particle trajectories for standing waves (7.91) the ordinary differential equations (7.71) must be solved. If these equations are again linearised as indicated in (7.73) integration is straightforward and yields

$$\begin{aligned} x - x_0 &= -\frac{2gk\zeta_0}{\omega^2} \sin(kx_0) \cos \omega t \frac{\cosh(k(z_0 + H))}{\cosh(kH)}, \\ z - z_0 &= \frac{2gk\zeta_0}{\omega^2} \cos(kx_0) \cos \omega t \frac{\sinh(k(z_0 + H))}{\cosh(kH)}. \end{aligned} \quad (7.92)$$

It is easily seen from these relations that particle trajectories are straight segments with inclination

$$\tan(\alpha) = \frac{z - z_0}{x - x_0} = -\cotan(kx_0) \tanh(k(z_0 + H)). \quad (7.93)$$

The last panel in Fig. 7.8 shows a photograph of particle trajectories of a standing wave and corroborates that these trajectories are straight segments which, in a period, are traversed by the particles forth and back. This motion is also indicated in Fig. 7.10 at the frontal vertical plane of the channel.

The streamlines for the standing wave solution (7.91) follow from the integration of the differential equation

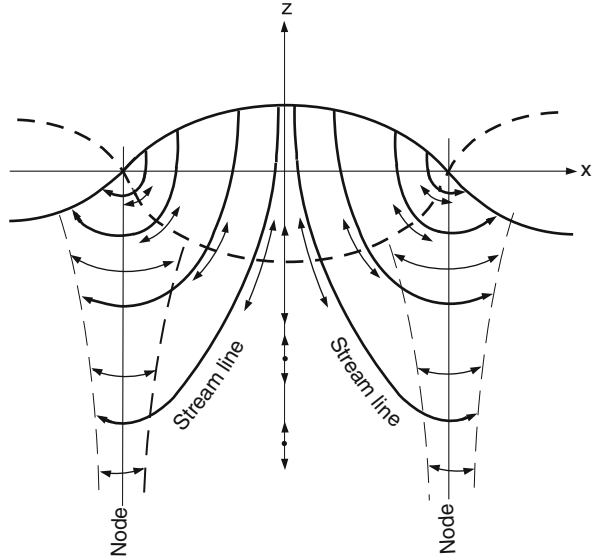
$$\frac{dz}{dx} = \frac{w}{u} = -\cotan(kx) \tanh(k(z + H)). \quad (7.94)$$

The right-hand side is here the same as the right-hand side in (7.93). So, in this linear case the streamlines are (very nearly) the integral curves of the particle trajectory segments. They are shown in Figs. 7.10 and 7.11 and indicate very clearly that the particle velocity is vertical at wave crests and troughs but horizontal at nodal lines.

The standing wave solution (7.91) was obtained as a result of the superposition of a forward-moving wave plus a backward-moving wave with the same frequency and amplitude. At the positions $kx_n = n\pi$, the velocity component u vanishes for all cross-channel positions and all times, and so we may in imagination insert a wall across the channel at these positions without affecting the motion. Thus, the standing wave may equally be interpreted as a reflection of a forward-moving wave at a wall, where the backward-moving wave is persistently created to accommodate the zero-horizontal-velocity condition at the position of the wall.

This complete reflection is an ideal situation that may not be realised, but its effects are large; particle trajectories have changed from ellipses for propagating waves to straight lines for standing waves. Partial reflection is achieved by walls that absorb part of the energy of the incoming wave or, equivalently, which only reflect a wave with smaller amplitude. This case may be described by the solution

Fig. 7.11 Streamlines in a standing gravity wave. Particle trajectories are straight line segments tangential to the streamlines



$$\begin{aligned}
 p' &= \rho g \zeta_0 \frac{\cosh(k(z+H))}{\cosh(kH)} [e^{i(kx-\omega t)} + \lambda e^{i(kx+\omega t)}], \\
 \zeta &= \zeta_0 [e^{i(kx-\omega t)} + \lambda e^{i(kx+\omega t)}], \\
 u &= \frac{kg}{\omega} \zeta_0 \frac{\cosh(k(z+H))}{\cosh(kH)} [e^{i(kx-\omega t)} + \lambda e^{i(kx+\omega t)}], \\
 w &= \frac{kg}{\omega} \zeta_0 \frac{\sinh(k(z+H))}{\cosh(kH)} [e^{i(kx-\omega t)-i\pi/2} + \lambda e^{i(kx+\omega t)-i\pi/2}].
 \end{aligned} \tag{7.95}$$

We shall not dwell upon the details of this solution which now depends on the parameter $\lambda \in [0, 1]$. The result is that particle trajectories are still ellipses which become thinner as λ moves from 0 to 1 for which the standing wave solution is obtained. Experiments with partial reflection have also been conducted. Figure 7.8 shows the traces of the particle trajectories from pure propagation (top panel) to standing wave (bottom panel) with increasing degree of reflection from top to bottom.

It is a property of the standing wave solution (7.91) that walls can be inserted at all positions $kx_n = n\pi$, $n = 0, \pm 1, \pm 2, \dots, \pm\infty$, without affecting the motion. In this way the solutions of the unidirectional surface wave motion in rectangular basins can be constructed. Figure 7.10 can be interpreted in this way. Walls are thought to be erected here such that two modes, each with wavelength $l = 2\pi/k$, fill the rectangle. Of course any countable number of modes can fit a channel of a given length L if only $k_n = n\pi/L$.

This brings us in the next section to the study of oscillations in rectangular basins of constant depth when effects of the rotation of the Earth are absent.

7.3 Free Linear Oscillations in Rectangular Basins of Constant Depth

Consider a rectangular basin filled to depth H with a density-preserving fluid. Let a Cartesian coordinate system be chosen such that its origin and axes are oriented as shown in Fig. 7.12.

The governing equations of the free linear oscillations of a layer of water with uniform density are given by (7.58), in which, however, the horizontal variables x and y vary according to $0 < x < L$, $0 < y < B$.

Thus, the boundary value problem, analogous to (7.60), now reads

$$\left. \begin{aligned} \Delta p' &= \frac{\partial^2 p'}{\partial x^2} + \frac{\partial^2 p'}{\partial y^2} + \frac{\partial^2 p'}{\partial z^2} = 0, & z \in (0, -H), \\ \frac{\partial^2 \zeta}{\partial t^2} &= -\frac{1}{\rho} \frac{\partial p'}{\partial z}, \\ p' &= \rho g \zeta, \\ \frac{\partial p'}{\partial z} &= 0, \end{aligned} \right\} \begin{aligned} & z = 0, \\ & z = -H, \end{aligned} \left\{ \begin{aligned} 0 < x < L, \\ 0 < y < B. \end{aligned} \right. \quad (7.96)$$

This constitutes a linear free initial boundary value problem – ‘free’, because there is no external driving. A harmonic solution may be determined by choosing

$$\begin{aligned} p'(x, y, z, t) &= \bar{p}(x, y, z) e^{i\omega t}, \\ \zeta(x, y, t) &= \bar{\zeta}(x, y) e^{i\omega t}, \end{aligned} \quad (7.97)$$

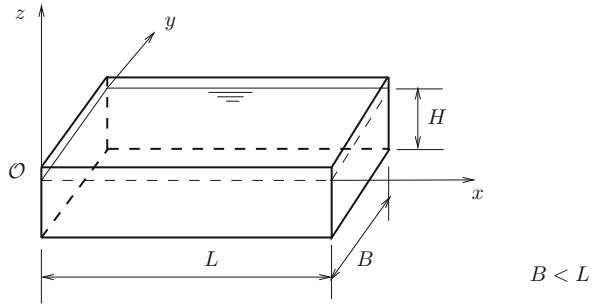
yielding the following time-independent boundary value problem

$$\left. \begin{aligned} \Delta \bar{p} &= \frac{\partial^2 \bar{p}}{\partial x^2} + \frac{\partial^2 \bar{p}}{\partial y^2} + \frac{\partial^2 \bar{p}}{\partial z^2} = 0, & z \in (0, -H), \\ -\omega^2 \bar{\zeta} &= -\frac{1}{\rho} \frac{\partial \bar{p}}{\partial z}, \\ \bar{p} &= \rho g \bar{\zeta}, \\ \frac{\partial \bar{p}}{\partial z} &= 0, \end{aligned} \right\} \begin{aligned} & z = 0, \\ & z = -H, \end{aligned} \left\{ \begin{aligned} 0 < x < L, \\ 0 < y < B. \end{aligned} \right. \quad (7.98)$$

This is a free boundary value problem involving a parameter ω , which is unknown and must be determined in the course of the construction of its solution.

Definition 7.10 A free boundary value problem involving a parameter is called an **eigenvalue problem** or a **proper value problem**. The free parameter is called the **eigenvalue** or **proper value** and the solution functions are called **eigenfunctions** or **eigenmodes**. ■

Fig. 7.12 Rectangular basin with length L , width B and constant water depth H . The Cartesian coordinate system is chosen with the origin O at the corner and on the undisturbed water level; x - and y -axes are in the plane of the still undeformed water surface and z is vertically upward



An eigenvalue problem only possesses solutions if the eigenvalue assumes certain distinct values. As one could surmise from the construction of the standing wave solutions, the length, L , and the width, B , will fix the wavenumbers k_x and k_y of wave solutions of the form $\exp [i(\pm k_x x \pm k_y y \mp \omega t)]$ and the dispersion relation (which relates ω and k_x, k_y) will then determine to each admissible pair (k_x, k_y) the consistent frequency. In this connection, one may see the solution of an eigenvalue problem as the *quantised* satisfaction of the dispersion relation.

Solutions to eigenvalue problem (7.98) have already been determined in the last section. Indeed, formulae (7.91) may be regarded as standing wave solutions in the rectangle of Fig. 7.12, if the wavenumber is chosen as $k_{xn} = \frac{n\pi}{L}$, $k_y = 0$ where $n = \pm 1, \pm 2, \dots, \pm \infty$. Thus,

$$\begin{aligned}
 p'(x, y, z, t) &= 2 P_0^n(z) \cos \left(\frac{n\pi x}{L} \right) \cos \omega_n t, \\
 \zeta(x, y, t) &= 2 \zeta_0^n \cos \left(\frac{n\pi x}{L} \right) \cos \omega_n t, \\
 u(x, y, z, t) &= 2 U_0^n(z) \sin \left(\frac{n\pi x}{L} \right) \sin \omega_n t, \\
 v(x, y, z, t) &= 0, \\
 w(x, y, z, t) &= -2 W_0^n(z) \cos \left(\frac{n\pi x}{L} \right) \sin \omega_n t,
 \end{aligned} \tag{7.99}$$

in which

$$\begin{aligned}
 P_0^n(z) &= \rho g \zeta_0^n \frac{\cosh(k_n(z + H))}{\cosh(k_n H)}, \\
 U_0^n(z) &= \frac{k_n}{\rho \omega_n} P_0^n(z), \\
 W_0^n(z) &= \tanh(k_n(z + H)) U_0^n(z)
 \end{aligned} \tag{7.100}$$

and $n = 1, 2, \dots, \infty$ are solutions of the surface water waves. All variables are independent of y , i.e. the transversal direction of the rectangle. For each n solution (7.99)

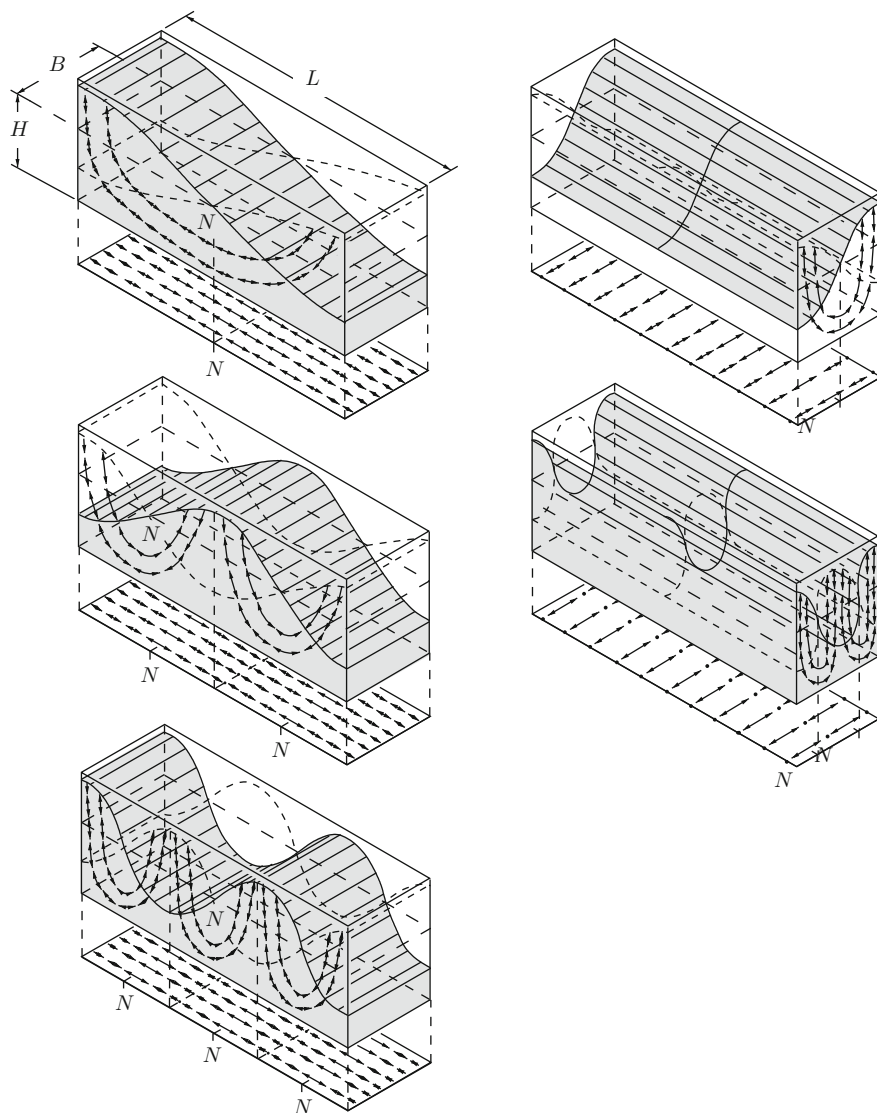


Fig. 7.13 Rectangular basin with length L , width B and constant water depth H . The *left column* shows longitudinal eigenmode solutions for $n = 1, 2, 3$ while the *right column* shows analogous transverse eigenmode solutions for $m = 1, 2$ (after MORTIMER with changes and additions [11, 12])

is called a *longitudinal (eigen)mode* of the water motion in rectangle. Often one calls the mode belonging to the mode number n the *n th longitudinal mode*. Figure 7.13 shows the spatial distribution of the first three modes.

Just as there are longitudinal oscillations in a rectangle, there may also be purely *transversal modes*, which are given by

$$\begin{aligned}
p'(x, y, z, t) &= 2 P_0^m(z) \cos\left(\frac{m\pi y}{B}\right) \cos \omega_m t, \\
\zeta(x, y, t) &= 2 \zeta_0^m \cos\left(\frac{m\pi y}{B}\right) \cos \omega_m t, \\
u(x, y, z, t) &= 0, \\
v(x, y, z, t) &= 2 V_0^m(z) \sin\left(\frac{m\pi y}{B}\right) \sin \omega_m t, \\
w(x, y, z, t) &= -2 W_0^m(z) \cos\left(\frac{m\pi y}{B}\right) \sin \omega_m t,
\end{aligned} \tag{7.101}$$

in which

$$\begin{aligned}
P_0^m(z) &= \rho g \zeta_0^m \frac{\cosh(k_m(z+H))}{\cosh(k_m H)}, \\
V_0^m(z) &= \frac{k_m}{\rho \omega_m} P_0^m(z), \\
W_0^m(z) &= \tanh(k_m(z+H)) V_0^m(z)
\end{aligned} \tag{7.102}$$

are the same functions as (7.100) but with indices m rather than n , and $m = 1, 2, \dots, \infty$. In the above equations the dispersion relations, similar to (7.64),

$$\begin{aligned}
\omega_n^2 &= g k_n \tanh(k_n H), & k_n &= \frac{n\pi}{L}, & n &= 1, 2, \dots, \infty, \\
\omega_m^2 &= g k_m \tanh(k_m H), & k_m &= \frac{m\pi}{B}, & m &= 1, 2, \dots, \infty
\end{aligned} \tag{7.103}$$

allow only quantised solutions between the wavenumbers and frequencies. Examples of transverse mode solutions are also shown in Fig. 7.13.

We have discussed the above solutions not only because they are particularly interesting but also because later when the rotation of the Earth is added as a further complexity, they will be seen to be the non-rotational analogues of what then will turn out to be the so-called KELVIN and POINCARÉ waves.

There are yet further eigenmode solutions for the rectangle in which the pressure, surface elevation and velocity components vary in all space directions. In view of the above longitudinal and transversal solutions it is not difficult to guess that a possible solution for the pressure may be of the form

$$\begin{aligned}
p'(x, y, z, t) &= \left\{ P_1(z) \sin\left(\frac{n\pi x}{L}\right) \sin\left(\frac{m\pi y}{B}\right) \right. \\
&\quad + P_2(z) \sin\left(\frac{n\pi x}{L}\right) \cos\left(\frac{m\pi y}{B}\right) \\
&\quad + P_3(z) \cos\left(\frac{n\pi x}{L}\right) \sin\left(\frac{m\pi y}{B}\right) \\
&\quad \left. + P_4(z) \cos\left(\frac{n\pi x}{L}\right) \cos\left(\frac{m\pi y}{B}\right) \right\} \cos \omega t.
\end{aligned} \tag{7.104}$$

Problem 7.4 Using the linearised momentum equation $\rho \partial \mathbf{v} / \partial t = -\text{grad } p'$, construct the expressions for the u - and v -velocity components that are in conformity with (7.104). Show, moreover, that the boundary conditions

$$\begin{aligned} u(0, y, z, t) &= 0, & u(L, y, z, t) &= 0, \\ v(x, 0, z, t) &= 0, & v(x, B, z, t) &= 0 \end{aligned} \quad (7.105)$$

imply $P_1(z) = P_2(z) = P_3(z) = 0$. In summary, thus,

$$\begin{aligned} p' &= P_4(z) \cos\left(\frac{n\pi x}{L}\right) \cos\left(\frac{m\pi y}{B}\right) \cos \omega t, \\ u &= \frac{P_4(z)}{\rho} \frac{n\pi}{L} \frac{1}{\omega} \sin\left(\frac{n\pi x}{L}\right) \cos\left(\frac{m\pi y}{B}\right) \sin \omega t, \\ v &= \frac{P_4(z)}{\rho} \frac{m\pi}{B} \frac{1}{\omega} \cos\left(\frac{n\pi x}{L}\right) \sin\left(\frac{m\pi y}{B}\right) \sin \omega t \end{aligned} \quad (7.106)$$

are the only admissible representations for p' , u and v . ◆

As p' satisfies Laplace's equation (7.96)₁, $\Delta p' = 0$, it is easy to see that P_4 obeys the equation

$$\frac{d^2 P_4}{dz^2} - \underbrace{\left(\frac{n^2 \pi^2}{L^2} + \frac{m^2 \pi^2}{B^2} \right)}_{k_{n,m}^2} P_4(z) = 0, \quad (7.107)$$

with the solution

$$P_4(z) = \alpha^{n,m} \cosh(k_{n,m}(z + H)) + \beta^{n,m} \sinh(k_{n,m}(z + H)). \quad (7.108)$$

Boundary conditions (7.98)_{2,3,4} imply $\beta^{n,m} = 0$ and

$$\omega_{n,m}^2 = g k_{n,m} \tanh(k_{n,m} H), \quad k_{n,m}^2 = \frac{n^2 \pi^2}{L^2} + \frac{m^2 \pi^2}{B^2}, \quad (7.109)$$

$$\zeta = \frac{\alpha^{n,m}}{\rho g} \cosh(k_{n,m} H) \cos\left(\frac{n\pi x}{L}\right) \cos\left(\frac{m\pi y}{B}\right) \cos \omega t. \quad (7.110)$$

If we substitute all these relations back, then (7.106) and (7.110) take the following forms:

$$\begin{aligned}
p^{n,m} &= P_0^{n,m}(z) \cos\left(\frac{n\pi x}{L}\right) \cos\left(\frac{m\pi y}{B}\right) \cos \omega_{n,m} t, \\
\zeta^{n,m} &= \zeta_0^{n,m} \cos\left(\frac{n\pi x}{L}\right) \cos\left(\frac{m\pi y}{B}\right) \cos \omega_{n,m} t, \\
u^{n,m} &= \frac{n\pi}{L} \frac{1}{\rho \omega_{n,m}} P_0^{n,m}(z) \sin\left(\frac{n\pi x}{L}\right) \cos\left(\frac{m\pi y}{B}\right) \sin \omega_{n,m} t, \\
v^{n,m} &= \frac{m\pi}{B} \frac{1}{\rho \omega_{n,m}} P_0^{n,m}(z) \cos\left(\frac{n\pi x}{L}\right) \sin\left(\frac{m\pi y}{B}\right) \sin \omega_{n,m} t,
\end{aligned} \tag{7.111}$$

in which

$$P_0^{n,m}(z) = \rho g \zeta_0^{n,m} \frac{\cosh(k_{n,m}(z+H))}{\cosh(kH)}, \tag{7.112}$$

$$\zeta_0^{n,m} = \frac{\alpha^{n,m}}{\rho g} \cosh(k_{n,m} H) \tag{7.113}$$

and $\omega_{n,m}$ satisfies the quantised dispersion relation (7.109). In (7.111) we have on the left-hand side attached to p' , etc. the superscript n, m , $p^{n,m}$ etc., because the solution only belongs to the mode (n, m) . Finally, using continuity equation (7.46)₁

$$\frac{\partial w}{\partial z} = -\frac{\partial u}{\partial x} - \frac{\partial v}{\partial y},$$

the vertical velocity component can be computed. We leave it to the reader to prove that

$$w^{n,m} = W_0^{n,m}(z) \cos\left(\frac{n\pi x}{L}\right) \cos\left(\frac{m\pi y}{B}\right) \sin \omega_{n,m} t, \tag{7.114}$$

in which

$$W_0^{n,m}(z) = -\frac{k_{n,m}}{\rho \omega_{n,m}} \tanh(k_{n,m}(z+H)) P_0^{n,m}(z). \tag{7.115}$$

Alternatively, (7.114) and (7.115) can also be obtained by using the vertical component of the linearised momentum equation (7.46)₂,

$$\rho \frac{\partial w}{\partial t} = -\frac{\partial p'}{\partial z}.$$

Expressions (7.111), (7.112), (7.113), (7.114) and (7.115), together with the quantised dispersion relation (7.109), define the true two-dimensional eigenoscillations of the surface gravity waves in a rectangle of constant depth. The integers n and m thereby characterise the longitudinal and transversal mode orders

and are referred to as longitudinal and transversal mode numbers. Notice that the formulae also incorporate the purely longitudinal and transversal modes as follows:

$$\begin{aligned} n \neq 0, \quad m = 0 &\implies n\text{th order pure longitudinal mode,} \\ n = 0, \quad m \neq 0 &\implies m\text{th order pure transversal mode.} \end{aligned}$$

The reader can easily check this property by comparing formulae (7.109), (7.111), (7.112), (7.113), (7.114) and (7.115) with the earlier representations (7.99), (7.100), (7.101), (7.102) and (7.103), respectively.

Formulae (7.111) and (7.114) imply that the shapes of the spatial distributions of the variables p' , ζ , u , v , w do not vary with time, but are fixed once and for all when the geometry of the basin is fixed. The sinusoidal variation in time changes the scale and direction according to the variation of the sin- and cos-functions with time. This is a property of standing waves: *the spatial distribution of the shape of the eigenfunctions is fixed and time independent*. It will later be seen that this property is not maintained when the rotation of the Earth is taken into account. Figures 7.14 and 7.15 show the distribution of the surface elevation and horizontal velocity for the modes with $(n, m) = (1, 0; 0, 1; 2, 0; 0, 2; 1, 1; 2, 2; 2, 1; 1, 2; 3, 1; 1, 3; 3, 2; 2, 3)$.

Finally, the most general free wave solution in a rectangle of constant depth is a linear combination over all modes with positive, entire m, n , such that $m + n \geq 1$. Thus,

$$\{p', \zeta, u, v, w\} = \sum_{\substack{n>0, m>0 \\ n+m \geq 1}}^{\infty} \{p^{n,m}, \zeta^{n,m}, u^{n,m}, v^{n,m}, w^{n,m}\}$$

defines this most general solution, along which the variables on the right-hand side are given by (7.111), (7.112), (7.113), (7.114) and (7.115). The quantities $\zeta_0^{n,m}$ can be viewed as the free amplitudes that are in a forced problem related to the forcing.

7.4 Concluding Remarks

In this chapter an introductory outline to linear waves, in general, and to water waves, in particular, was given. The subject was introduced with the example of acoustic waves, which are the longitudinal waves in a compressible liquid. Spatially one-dimensional waves were constructed with the method of D'ALEMBERT and then by an exponential – harmonic – representation. This latter solution technique led to the notions of phase, wavenumber, frequency, dispersion relation, as well as phase speed and group velocity and showed itself as *the* powerful plane-wave solution technique for linear waves in general.

On this basis of the governing equations for a fluid in the BOUSSINESQ and shallow-water approximations, surface gravity waves in a non-rotating frame were studied, first in one spatial dimension and later in two. It was recognised that linear surface water waves are dispersive – their group velocity depends on frequency; only

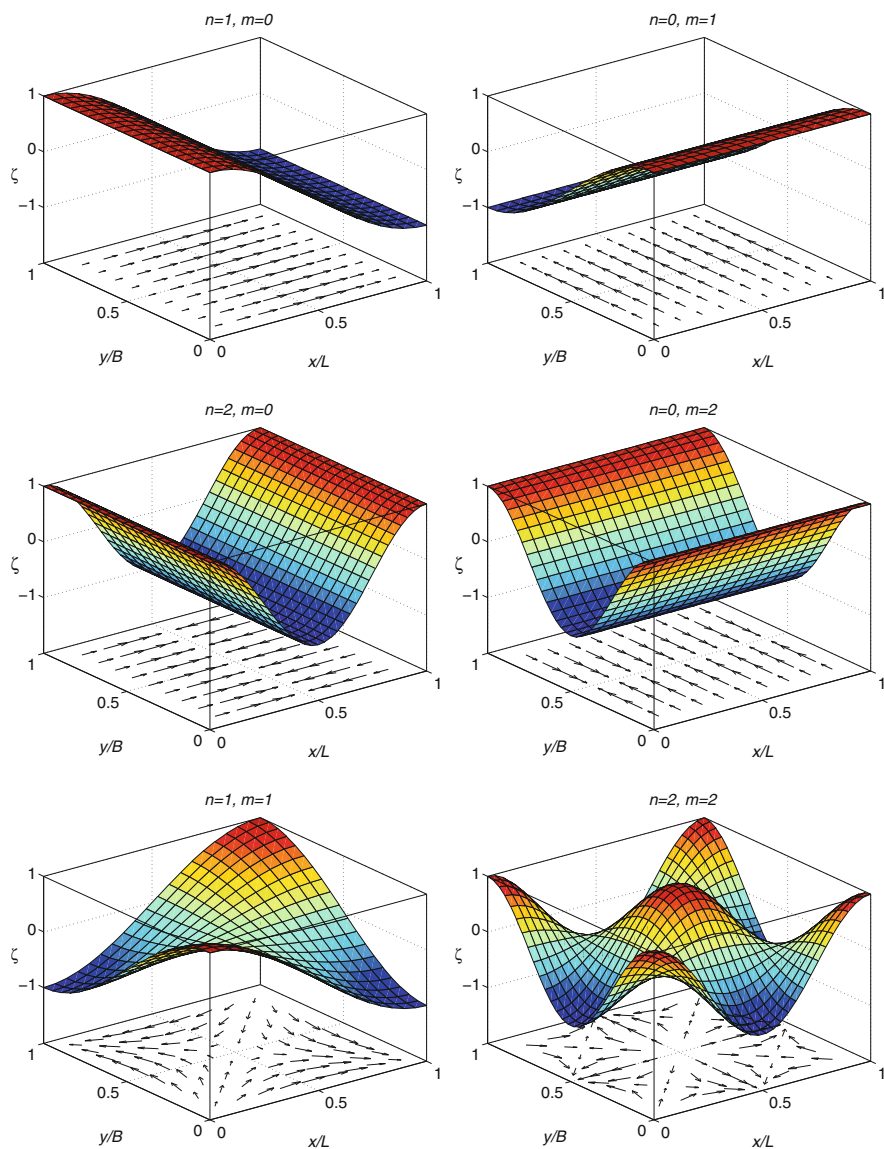


Fig. 7.14 Distributions of the surface elevations and horizontal velocities for the different modes. The first four panels repeat the longitudinal, $(n, m) = (1, 0), (2, 0)$ and transversal, $(n, m) = (0, 1), (0, 2)$ modes already displayed in Fig. 7.13. The two panels in the bottom show the most simple two-dimensional waveforms for $(n, m) = (1, 1)$ and $(n, m) = (2, 2)$

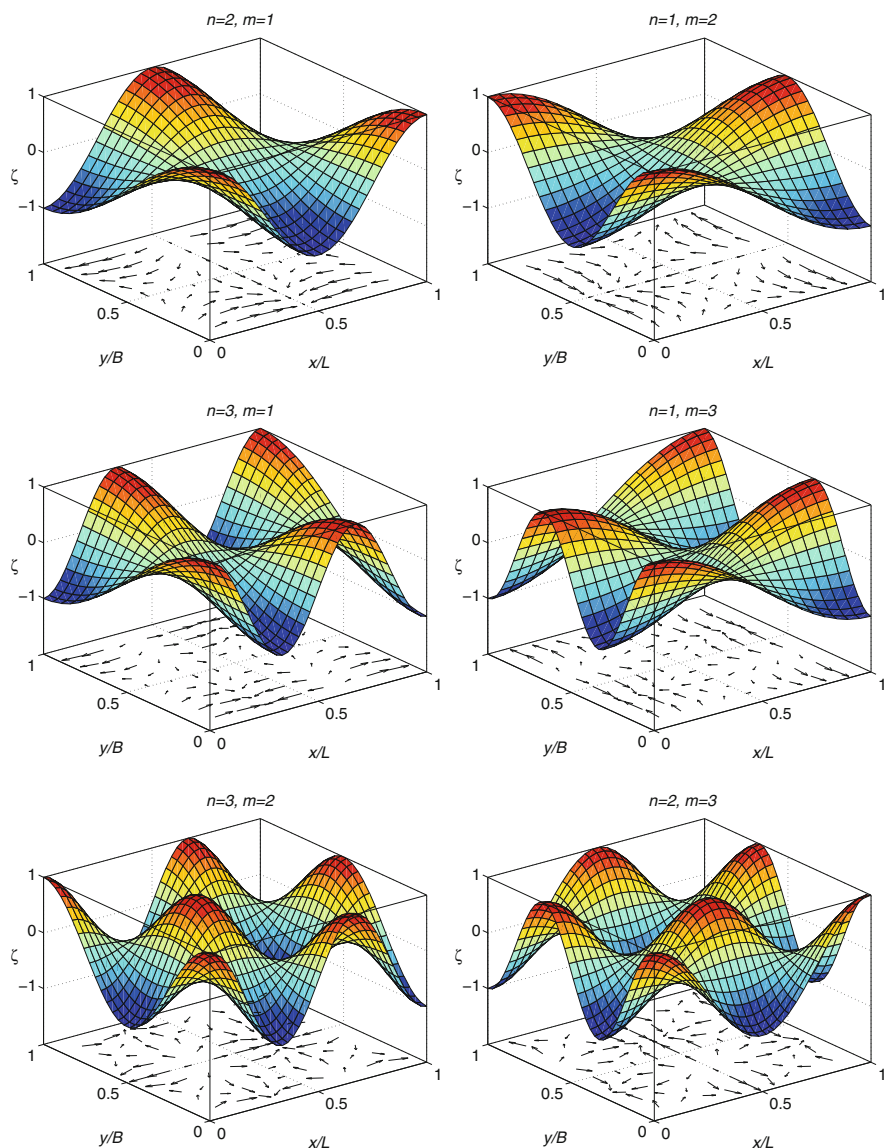


Fig. 7.15 Distributions of the surface elevations and horizontal velocities for the modes with (n, m) as indicated. All modes are truly two dimensional

in their limiting form as long waves they are non-dispersive, while the dispersive nature remains in tact in the deep-water wave limit.

Material particles in unidirectional harmonic linear water waves move in elliptical orbits; they are nearly circular close to the free surface of a water layer and have decreasing amplitude and increasing aspect ratio from the free to the bottom surface.

With reflection of such a wave from a wall, the elliptical eccentricity increases with increasing degree of reflection. In a standing wave, where forward- and backward-moving harmonic waves have the same strength, the orbits are linear (see Fig. 7.8). This picture is only slightly altered by non-linearity, giving rise to the so-called STOKES drift, but such cases were not treated in this chapter.

Linear water waves on a non-rotating frame become standing waves with quantised frequencies, if the domain of their existence is fully bounded. Solutions were constructed in a rectangular basin of constant depth. Frequencies and modes of the water movements are in this case determined from a linear eigenvalue problem. The standing character is given by the fact that these solutions may possess lines other than boundary lines in the solution domain, along which the free surface elevation function or a horizontal velocity component, vanish for all time. The existence of these steady lines is typical for surface gravity waves in non-rotating frames.

On the Earth, which is a rotating non-inertial system, rotation will change this behaviour. In fact the conditions will be delineated for which the assumption of a non-rotating frame may lead to acceptable approximate behaviour.

References

1. Batchelor, G.K.: *An Introduction to Fluid Mechanics*. Cambridge University Press, Cambridge, 615 p. (1970)
2. Feynman, R.P., Leighton, R.B. and Sands, M.: *The Feynman Lectures on Physics*. Vol. 1. Addison Wesley, Reading, MA (1963)
3. Lamb, H., Sir: *Hydrodynamics*, (reproduced from the 6th edition). Dover, New York, NY, 738 p. (1945)
4. Landau, L.D. and Lifshitz, E.M.: *Fluid Mechanics*. Pergamon, Oxford, 536 p. (1982)
5. Lautrup, B.: *Physics of Continuous Matter, Exotic and Everyday Phenomena in the Macroscopic World*. IoP: Institute of Physics Publishing, Philadelphia, PA, 608 p. (2005)
6. LeBlond, P.H. and Mysak, L.A.: *Waves in the Ocean*. Elsevier, Amsterdam, 602 p. (1978)
7. Leibovich, S. and Seebass, A.R.: *Nonlinear Waves*. Cornell University Press, London, 331 p. (1974)
8. Lighthill, J.: *Waves in Fluids*. Cambridge University Press, Cambridge, 504 p. (1978)
9. Massel, S.R.: *Ocean Surface Waves: Their Physics and Prediction*. World Scientific, Singapore, 491 p. (1996)
10. Mei, C.-C.: *The Applied Dynamics of Ocean Surface Waves*. 2nd Edition. Wiley-Interscience, New York, NY, 740 p. (1989)
11. Mortimer, C.H.: Lake hydrodynamics. *Mitt. Int. Ver. Theor. Angew. Limnol.* **20**, 124–197 (1974)
12. Mortimer, C.H.: *Lake Michigan in Motion*. The University of Wisconsin Press, Milwaukee, WI, 310 p. (2004)
13. Phillips, O.M.: *The Dynamics of the Upper Ocean*. Cambridge University Press, Cambridge, 261 p. (1966)
14. Stoker, J.J.: *Water Waves*. Interscience, New York, NY, 543 p. (1957)
15. Van Dyke, M.: *An Album of Fluid Motion*. Parabolic, Stanford, CA (1976)
16. Walker, J.: *Fundamentals of Physics*. John Wiley & Sons (Asia) Pte Ltd, International Student Edition, 1300 p. (2008), 8th Edition. www.wiley.com/college/halliday
17. Wallet, A. and Ruellan, F.: Trajectoires internes dans un clapotis partiel (Trajectories of particles within a partial clapotis). *Houille Blanche* **5**, 483–489 (1950)
18. Whitham, G.B.: *Linear and Nonlinear Waves*. Wiley, New York, NY, 636 p. (1974)

Chapter 8

The Role of the Distribution of Mass Within Water Bodies on Earth

8.1 Motivation

Chapter 4 was devoted to the derivation and presentation of the governing equations of fluid mechanics and thermodynamics as they apply to fluid bodies under motion. The intention was to build a basic understanding of the mathematical description of the physical laws of balances of mass, momenta and energy in a form sufficiently general to all situations which one could possibly encounter in applications of physical limnology needed for this book.

The purpose of this chapter is different. It is assumed that the readers have acquired a basic understanding of the physical laws, so that they can now be employed. This will be done under very simple circumstances to isolate and highlight the limnological implications as far as possible. Gravity, wind and radiation, how do they reign the hydrodynamic processes in the ocean and in lakes? Radiation by the Sun heats up the near surface water layers and so stratifies the water. Wind, through the action of shear at the surface, destabilises this layer by turbulent mixing and advective transport. The two processes establish a density field giving rise to a spatially and temporally varying mass distribution. Consequently, the gravity force as one of the driving elements is equally space and time dependent. So, while wind and radiation are the *primae causae* of the density distribution, it is the latter that causes a gravity force variation that is so critical in establishing the rich dynamic response of the Earth's water bodies. It is the purpose of this chapter to demonstrate with easy but typical examples that the mass distribution within a water body plays a significant role in establishing the dynamics of the physical processes in lakes (and the ocean). Density variations are its manifestation as they are the cause for the inhomogeneous distribution of the water masses. This is not to say that the motions established in a homogeneous water mass are not important; these motions are different in their structure from the motions arising in a stratified fluid. For this reason different nomenclatures have been introduced to characterise motions under the two situations: one commonly calls processes arising in homogeneous water *barotropic processes*, while those due to the very small variations of the water density are called *baroclinic processes*. A justification for these denotations will be given later.

The ‘weather and climate’ in a lake is established by the input of momentum and energy provided by outside sources. One of these sources is due to the rotation of the Earth and manifests itself in the momentum balance as the CORIOLIS acceleration – or with negative sign and multiplied by ρ – the CORIOLIS force. This additional force is the cause that the water in large reservoirs on Earth does not stay motionless: the state of rest is not present among steady-state solutions on the rotating planet.¹ The most common steady-state motions arise when the CORIOLIS force balances the pressure gradient; they are called *geostrophic*, and their significance for the general water circulation depends on the scale: from a leading role in the ocean to significant modifications in lakes. Important is that these forces prescribe the structure of the current field in all water bodies of the Earth (except perhaps small ponds). Momentum is also transferred from the atmosphere to the lake by the wind via the shear traction exerted at the water surface. This shear traction drives the water motion, primarily close to the water surface, however through diffusion of momentum by viscous and turbulent shear, it is also transported to depth. Persistent wind action causes *circulation* of the water masses, different for homogeneous and stratified water bodies; gusty winds, or the fluctuating components of the wind field, are responsible for the *oscillating response*. This separation in circulation and oscillation is adequate for both homogeneous and stratified water bodies. In the former the largest wave activities arise *at the water surface* and surface elevation amplitudes are relatively small (when measured in water-depth scales), in the latter the wave activity primarily arises *inside the water body*, is largest where the vertical density gradients are large – i.e. in the *metalimnion close to the thermocline* – and persists for long times with, generally, small attenuation. Because of the response of the water masses for the two different situations at the free surface and within the water body, barotropic processes are also referred to as *external*, and baroclinic processes are called *internal*. There is another typical feature by which the two can be characterised. Barotropic wave processes are considered to be fast, whereas on timescales of these baroclinic ones they are slow. We shall analyse this difference in later chapters at greater depth; here it may suffice to mention that the ratio of the wave velocity of a barotropic wave signal to that of a baroclinic wave under common summer stratification takes values of about 30–100.

Whereas the wind action brought into a lake by advective transport and turbulence intensity is responsible for the destruction of a given stratification, integrated heat flux through the water surface is generally responsible for its build-up. The main heat fluxes at the water surface arise due to incoming solar energy, backward infrared irradiation of the water body into the outer space, turbulent heat exchange with the atmosphere and change of phase at the water surface. The solar irradiation during daylight heats the near-surface water, supplying spectrally distributed energy. Infrared radiation, which is proportional to the water temperature to the fourth power, takes this energy away day and night. Turbulent heat exchange with

¹ More specifically, CORIOLIS and centripetal accelerations together prevent such a rest state. When centripetal accelerations are omitted, rest states are admissible.

warmer or colder air (called also *sensible heat flux*) can be both positive and negative, depending on the relative temperature difference and on wind speed. Heat flux at the surface, also arising due to possible phase change processes, called *latent heat flux*, is the most difficult to quantify; commonly, only evaporation is taken into account via various parameterisations. In summer, on average, the integral heat input during daytime is larger than its loss during night; the upper layer water masses are heated. Turbulence activity and advection transport this heat to larger depths, establishing a mixing process between the warmer water at the higher levels and the colder water at the lower ones. Since this turbulent mixing is dissipative, turbulent energy is attenuated with increasing depth, so that mixing of the warmer upper level water with the colder water below eventually ceases. This level is about at the thermocline, but not exactly, so that the level of *evanescent turbulent activity* is sometimes called the *turbocline* (e.g. [9]).

Conversely, integrated heat loss at the free surface in winter is, on average, larger than the heat input through solar irradiation, implying that the lake water near the surface cools in winter. Turbulence will again contribute to the mixing. As the net balance of heat added to, and subtracted from, the lake varies with time, the lake's thermal regime will equally vary through the annual seasons, a process that is sometimes referred to as the *seasonal variation of the thermocline*. Figure 8.1 shows the temperature profiles at monthly time slices through the year 1962/1963 for the

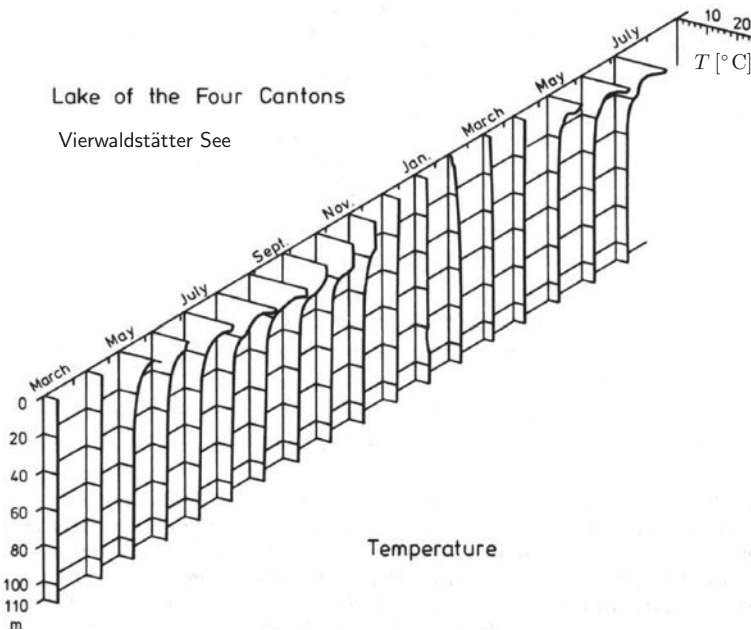


Fig. 8.1 Vertical temperature variations in the Vierwaldstätter See (Lake of the Four Cantons, Switzerland) from March 1962 to July 1963, (from an internal report of the Laboratory of Hydraulics, Hydrology and Glaciology at ETH Zurich)

Vierwaldstätter Sea (in Central Switzerland). Obviously, every lake is subject to its own wind and radiation scenario throughout the year. In the example of Fig. 8.1 conditions are such that the turbulence activity is strong enough that the entire water column is mixed twice a year – in spring and in autumn (so-called *dimictic* lake²). Such conditions are often referred to as spring/fall homothermy or overturn. This is the case for many large lakes (e.g. Great Lakes of America, European lakes such as Geneva, Constance, Ladoga, Onega) and it is ‘fortunate’ because the entire lake is ventilated with O₂ this way twice a year and thus naturally preserved from *anoxia*. In the deepest lake in the world (1636 m), Lake Baikal, this seasonal overturn directly mixes in spring and autumn the uppermost 250–300 m, and triggers forced convection in deeper layers, which finally ensures high concentration of oxygen (not less than 9.5–10 mg l⁻¹) in the deep layers [34]. As a result, there are few lakes in the world to compete with this cold lake in biotic diversity.

There are lakes – they are rather deep and often located at low latitudes – in which the turbulent mixing never reaches the bottom. These lakes are called *meromictic* (*mero*, partly). In these cases, there exists generally no alternative mechanism that would provide a ventilation of the deeper parts of the lake. Such lakes are then usually *oxygen depleted* at depth and hostile to any oxygen-based life. An example of this sort is tropical Lake Tanganyika – the second largest of the African lakes, the second deepest (1470 m; next to Lake Baikal) and the longest (670 km) freshwater lake of the world. It is meromictic, permanently temperature-stratified with strong vertical oxygen concentration gradients. This warm lake, with water temperature of about 23–25°C throughout the year, is anoxic below a depth of 100–200 m, and it contains the largest volume of anoxic freshwater in the world. Since there are virtually no temperature changes in Lake Tanganyika, there are no driving forces for vertical mixing and water exchange with the surface, and so at depth the lake is oxygen depleted [5].

Alternatively, in shallow lakes which are exposed to strong winds the turbulent mixing may reach the bottom several times through the seasons; they are generally very well ventilated and offer a friendly environment to the living organisms. It is seen that lake physics exerts here a dominant effect on the biological conditions that may exist in a lake.

The above discussion suggests, but does not prove yet, that heating of a lake through solar irradiation establishes a water body with warm and light water at the top and cold and heavy water below it. If this structure is so for any two neighbouring infinitesimally small layers, i.e. if an infinitesimally thin horizontal layer of fluid is underlain by a heavier infinitesimally small layer of fluid throughout the depth, then this water mass is called *stably stratified*. This situation simply prevails if the density is monotonously increasing with depth. If, however, the density profile is not strictly monotonous, then there are sublayers where heavy water would lie above light water, which cannot be: immediate local mixing will arise until a new monotonous density profile is established. The water body is then called *unstably*

² For detailed classification of lakes due to their mixing regime, see Chap. 1, Fig. 1.9, or books of HUTTER and JÖHNK [19], HUTCHINSON [16].

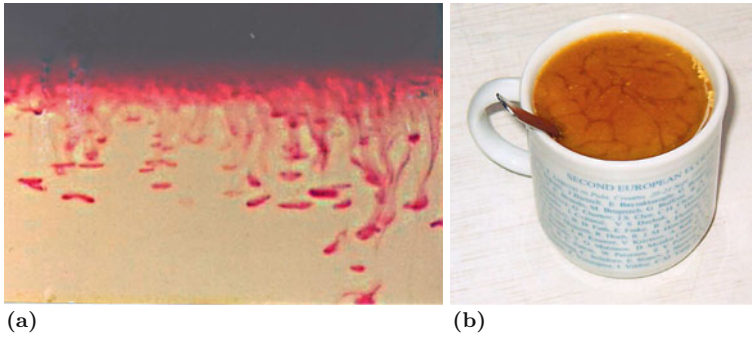


Fig. 8.2 Fingering: heavy lobes intruding in the lighter water below, accompanied with turbulence: **(a)** visualisation from a laboratory experiment (photo from <http://www.math.ualberta.ca/>, the experiment performed by J. CHOBOTER), **(b)** coffee cup experiment as described in the main text

stratified. The mixing manifests itself locally by heavy lobes intruding the lighter water below it. The process is called ‘fingering’, and individual vortices separate with time and are incorporated in the lighter fluid below (see, e.g., [9, 37]). Turbulence generally accelerates this process, see Fig. 8.2. A kitchen experiment visualising this can be made with a cup of hot coffee that is spoiled with sour milk. Once the coffee has sufficiently cooled at the surface (it takes about 1–2 min only) the effect of the downward convection is seen in the formation of cells, of which the darker boundaries mark the locations of downward motion and convergence of horizontal currents at the surface by the lobes whereas the paler cell interiors suffer an upward convection and a horizontal divergence to maintain continuity.

In closing this introduction, we collect the various new terms in the following definition.

Definition 8.1

- **Barotropic or external** processes in the ocean or in lakes and reservoirs with free surfaces are those motions that are taking place under conditions of uniform (constant) density distributions. Such motions are primarily generated by external (atmospheric) forcing and manifest themselves with motion activity throughout the depth of the water.
- **Baroclinic or internal** processes are those motions in a fluid body that are due to inhomogeneous density distribution. They are primarily due to these variations – which are internal – and for their existence the water surface need not be free, i.e. they even persist when the free surface would be covered by a rigid lid. Amplitudes of variations of physical parameters are generally largest where density gradients are biggest.
- **Geostrophic motion** is the motion that is generated by the balance between the CORIOLIS force and the pressure gradients.
- A fluid mass at rest in a vessel with free surface and subject to gravity forces is called **stably stratified**, if the density varies only with depth and is monotonously

increasing with depth. Such a fluid mass is **unstably stratified**, if the density varies with depth and possesses segments in which the density decreases with depth. Such a fluid mass is **neutrally stable** if its density is constant.

- The **turbocline** is that depth in the ocean or a lake below which the surface-induced turbulent activity vanishes. ■

8.2 Processes of Surface Water Penetration to Depth

Observations reveal *three general mechanisms* of surface water penetration into deeper layers of a lake:

1. Wind mixing and thermal convection *from the surface*.
2. Gravity currents *along the bottom slope*.
3. Converging currents in *frontal zones*.

(1) At the surface, *wind mixing* exists permanently at varied strength, and it homogenises the upper centimetres to metres of a lake body. Mechanisms of mixing are LANGMUIR circulation cells of various scales (see, e.g., [24]; [8]; [7]) and turbulence generated by *surface wave breaking*. The processes of the seasonal upper-layer lake cooling are *thermal convection* as shown in Fig. 8.2b and *turbulent mixing*. Both processes homogenise the water in the upper layer, below which an abrupt temperature change arises, Fig. 8.3a. As time proceeds the turbulent eddies continue to erode the thermocline. This process enlarges the upper layer depth, lowers its temperature and continues as long as wind and convection supply energy for turbulent mixing.

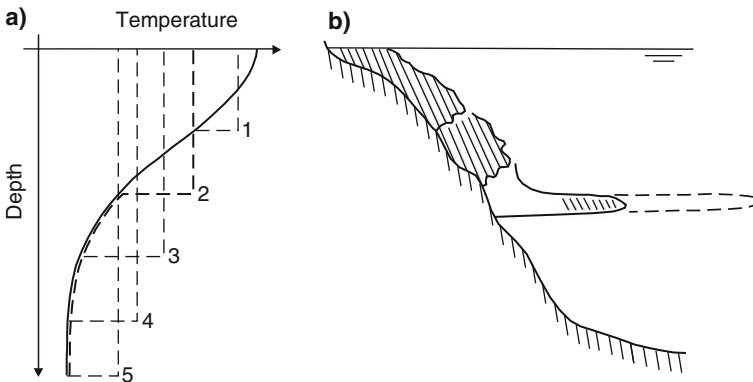


Fig. 8.3 (a) Temperature–depth profile and its development with time (shown *dashed*) as a consequence of thermocline erosion by wind-induced and convective mixing. The *solid* sigmoidal curve shows the temperature profile at the beginning. The labels 1, . . . , 5 mark thermocline positions at consecutive time slices. The *heavy dashed* line shows the intermediate stage 2 with the well-mixed layer above the thermocline and the smooth profile below it. (b) Motion of a gravity current down the lake slope until the density of the current reaches the ambient density where it is layering and spreading

During the winter time this surface convection can penetrate several hundred metres. One should understand, however, that the picture of vertical mixing is not uniform in the horizontal direction. First, generation of various local winds over surrounding topography and its natural spatial inhomogeneity and temporal variability predetermine a stochastic component of the development of the mixing process in a lake. At the same time, convective overturning intrinsically has a structure, dependent on the spatial scale and intensity of the external forcing; this adds a certain regular structure, manifested in formation of convective cells, rolls, thermals, chimneys, etc. Fascinating is the similarity of the process at different space scales: convective cells in a cup in the laboratory (see Fig. 8.2) are about 1 cm in diameter, the very regions of descending flow (*thermals*) – only a few millimetres. In Lake Geneva, FER et al. [11] report about ‘... “plumes” of relatively cold water, typically 5 m wide and 20 m apart, ... found in the near-surface convective mixed layer when air temperatures are 7°C below the surface water temperature’. At larger scale, in the Mediterranean Sea, there is a classical example of mixing in Gulf of Lions under cold and dry ‘mistral’ wind: ‘violent mixing’ occurs within the region of 30–50 km in diameter, extending to depth of 2000 m (e.g. [30]). In the ocean, such narrow regions of intense vertical mixing down to great depths, called *convective chimneys*, are also observed in the Weddel Sea [12], the Ross Sea [21] and the Labrador Sea [25]. They are typically 5–15 km in diameter, reach 1500–2000–4000 m depth and persist for several days [22], becoming unstable under the influence of the Earths rotation. Figure 8.4, taken from SEND and MARSHALL [33], illustrates various stages of this convection process, termed the *deep ocean convection*. Recently, chimney-like structures were also reported in Lake Baikal (SHIMARAEV, personal communication).

(2) Along-the-slope gravity currents arise when denser waters originate for some reason over sloping lake boundaries. Causes may be cold or turbid river inflow; turbidity currents due to surface or internal wave breaking; more rapid autumn cooling of the water in the near-shore zone than in the main lake body. Gravity currents move along the bottom slope down to the level of the corresponding density, separate from the slope and penetrate along the isopycnic surface very far into the lake; they are usually very turbulent and dynamically separated from the surrounding layers (Fig. 8.3b).

In this regard, river-induced density currents are important since they exist *permanently*. The way the incoming river water spreads in the lake does not only depend on the initial momentum and the relative difference of the respective densities of the river and the lake waters, which sometimes strongly vary with depth (since observations typically show strong sedimentation of fluvial material in the close vicinity of the river mouth [1]. It is also dependent on the pre-existing circulation in the lake near the river mouth: wind-driven currents, buoyancy processes, and internal oscillations all play a substantial role in the spreading of water entering the lake. As an example, we mention here an observation near the mouth of the river Rhine in Lake Constance: during the flood in June 1991, the incoming water plunged down to 60 m [2].

Thermally induced down-slope gravity currents are considered at present as a very effective mechanism of water exchange between the shallow and deep parts of

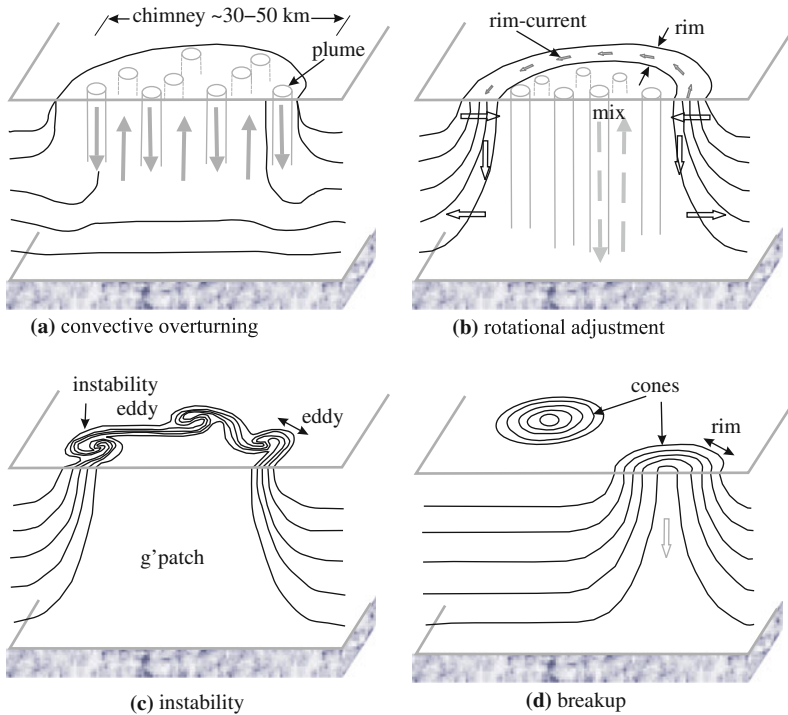
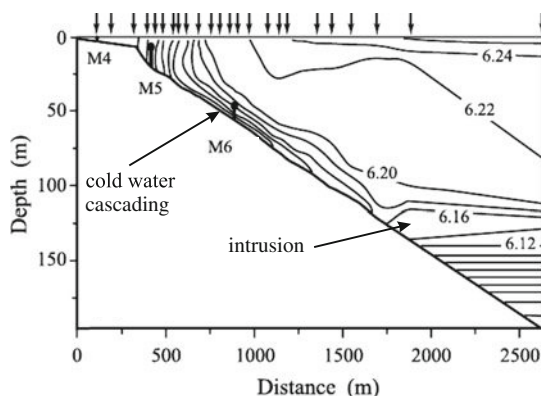


Fig. 8.4 Deep convection in the ocean. Stages of the development of a convective chimney: **(a)** initial state of intense convective overturning within limited volume; **(b)** subsequent geostrophic adjustment of the chimney via the formation of the rim current; **(c)** instability of the rim current, its meandering and formation of eddies; **(d)** recession of the eddies and slumping of the dense cone down to the level of their neutral buoyancy. Redrawn from SEND and MARSHALL [33], with changes. © American Meteorological Society, reprinted with permission

natural basins. During periods in winter favouring convection, a relatively uniform heat loss from the water surface results in a spatial temperature variation where the temperature of the shallow well-mixed waters at the edges of deep lakes or that of continental shelves surrounding the oceans falls more rapidly than that of deeper waters overlying the thermocline. As a consequence, water over shallow regions becomes relatively dense and descends along the neighbouring slope as a gravity current or *cascade*. COOPER and VAUX [4], who invented the term, had observed the phenomenon of cascading water from the UK Celtic Sea shelf in the winter of 1913/1914. Nowadays, winter cascading is widely reported in the ocean (see IVANOV et al. [20] for a review), large seas (e.g. in Mediterranean, LEAMAN and SCHOTT [26]) and lakes (e.g. [11]). In open waters far from shore, denser surface water detaches from the slope below the upper mixed layer, forming either convective plumes, or large isopycnal intrusions, or experiencing shearing into many thinner layers. Figure 8.5 presents an observation of cascading cold water from the near-shore zone and underwater slope of Lake Geneva made in January 2000 [11].

Fig. 8.5 Isotherms derived from CTD profilings conducted between 12:00 and 15:00 (local time), 20 January 2000, in near-shore zone of Lake Geneva. The contours are in degree CELSIUS. The profiling stations are indicated by arrows. Vertical moorings deployed during the experiments are shown as M4, M5, M6. From FER et al. [11], with changes



The very process of the cascading formation is quite difficult to describe: on the one hand, it can be considered as a gravity current with very large entrainment (e.g. in [11]), on the other hand it results from temperature differences along the horizontal boundary, and thus is a sort of horizontal convective exchange flow (see, e.g., [32, 35]). For the present discussion, thermally induced autumn gravity currents are of special interest because of the *deeper and deeper penetration of the surface water* when littoral water becomes colder and colder.³

(3) A *hydrologic front* in a lake, sea or the ocean is a region, where spatial gradients of the main thermo-dynamical characteristics are much larger (one order of magnitude at least) than those for a mean smooth distribution, typical for the given area [10]. Many physical reasons can lie behind their formation in a lake: topographic effects, wind-induced transport, river inflow, coastal upwelling, and many others. For all of them, however, one feature remains unchanged: every front is associated with a zone of convergence of surface currents, and thus – by continuity – water must descend there. Among other kinds of fronts, investigated by oceanographers in all natural basins, there is one of particular importance and interest for limnology: the *thermal bar*, arising in every lake in which the water in its seasonal cycle reaches the temperature of its maximum density, T_* . For pure water under atmospheric pressure this temperature is 3.98°C (sometimes simply stated as 4.0°C), at the depth of about 900 m it is 2.13°C. This shows that for deep lakes the pressure dependence in the thermal equation of state should not be omitted. In large lakes, thermal bars are formed during the spring and autumn periods of transition when the thermal *structure* of the lake water body changes from a wintry-homogenised to a summery-stratified regime, and vice versa; for this reason, the thermal bar is sometimes called a *structural front*. To better understand its nature and dynamics, let us lay down the reasoning in three steps.

³ From a point of view of direct application, it is obvious that determination of the directions of steepest descent, orthogonal to the bathymetric lines will provide a first information about the likely routes which such heavy littoral water might take when it dives to larger depths.

First step: The dependence of water density on temperature. Physical reason for the formation of this front is the *non-linearity* of the equation of state for water. The coefficient of thermal expansion, α changes its sign at 3.98°C . This means that, when water is heated, say, from 2 to 6°C , its density first increases, then it decreases; when the same process is performed backwards, i.e. water is cooled from 6 to 2°C , the effect on density is exactly the same.

Second step: Mixing regime in the vertical water column. If now the vertical water column is subjected to these direct and inverse processes, in both cases it first will be convectively mixed (irrespective of whether by cooling or heating) and afterwards density stratified.

Third step: Influence of the sloping boundary. Let us imagine now how this process develops in a basin with sloping bottom. During the spring and fall periods of transition, the temperature of the off-shore water body does not change as fast as that of the near land water masses. So, say, *during autumn cooling*, water in the deep off-shore lake areas (where the water temperature is larger than 4°C) is homogenised by vertical convective mixing, while the littoral zone (with a water temperature less than 4°C) under the same cooling conditions is (inversely) stratified. In spring, the situation is repeated in the same very order: now *under spring heating conditions*, the thermoinertial main-lake water body (with a temperature below 4°C) is again convectively mixing, while the shallow waters (above 4°C) acquire (direct) summer stratification. In both cases, under *the same conditions at the surface all over the lake* (heating in spring or cooling in autumn) there are two regions in the basin with principally different mixing regimes: in the deeper part the water is vertically convectively mixing, while in the shallow part it is stably stratified. The interface between these regions in the water body is a surface with the temperature of maximum density.

The thermal bar front develops in a lake in two phases, called the *slow* and *fast* stages of the development. In the *slow* stage, *cabbeling*⁴ plays the main role in the formation of the front: the lake water surface has a variable temperature, say, smaller than 4°C on-shore and larger than 4°C off-shore, and there exists a line in between with the 4°C temperature of maximum density, Fig. 8.6a. Consequently, in the absence of other motions, the water near this line will sink down along the 4°C surface, forming a convergence zone at the surface and a typical frontal division in the lake body. In the *fast* stage, large-scale horizontal differences in the hydrostatic pressure between deep and shallow parts become important; they drive basin-scale horizontal exchange flows, Fig. 8.6b. At this stage, the frontal division is no longer vertical, and the very front is associated with a leading edge of a subsurface jet,

⁴ Cabbeling, generally, is a physical process that is caused by the nonlinear terms in the expression of the density as a function of salinity and temperature measured at constant pressure. In physical oceanography, more specifically, cabbeling is a phenomenon that occurs when two water masses with identical densities but different temperatures and salinities mix to form a third water mass with a greater density than either of its constituents. This densification upon mixing is thought to cause the mixed fluid to flow downwards, away from the zone of mixing, and so will allow new source fluids to come in contact. For further reading, see, e.g. [29].

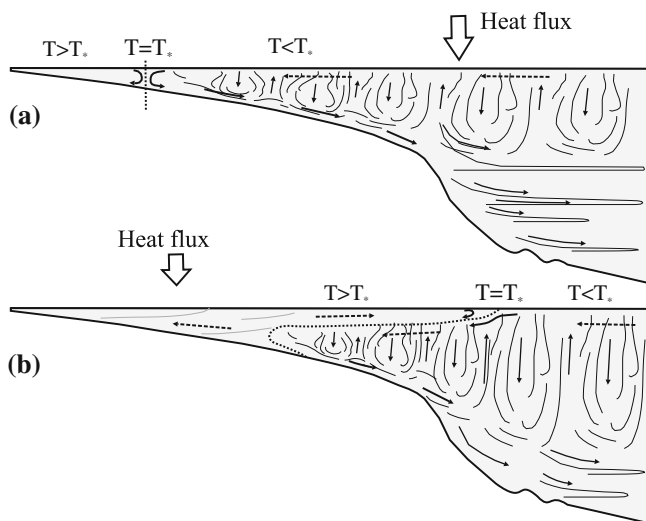


Fig. 8.6 Stages of the development of the thermal bar under spring heating conditions: **(a)** *slow* stage: when the process of cabbeling causes a converging flow region on the surface, the front within the water body is close to the vertical and denser water cascades are developed along the underwater slopes; **(b)** later *fast* stage: when horizontal pressure differences within the water body become important, the front is S-shaped and cascading still goes on in deeper parts, where the water temperature is still below T_*

transporting lighter littoral waters off-shore, above denser open-lake water masses [3, 34, 36].

Thus, the thermal bar separates the lake body dynamically into the deep and littoral parts, which have their own circulations and thermal structures. Observations show (e.g. [36]) that, typically, a cyclonic circulation (counterclockwise rotating on the northern hemisphere) is generally observed in the littoral belt, while anticyclonic (clockwise rotating) motion prevails in the interior part. Important for the present discussion is that the presence of the thermal bar in lakes indicates that there are favourable conditions for surface water penetration to depth – by both cabbeling at the front and denser water cascading along the slopes in the vertically mixing deep part of a lake. Field observations show that this mixing is very effective in lake water ventilation: all the dimictic lakes are well ventilated.

The above-described cascading and cabbeling mechanisms work only in upper water layers, influenced by seasonal heat fluxes. A number of investigations on the dynamics of the water motion in the deepest Lake Baikal revealed an additional mixing mechanism, related to the water density anomaly, which supplies the lake waters by oxygen, keeping them at no less than 75% saturation [13]. Free convection from the surface can reach in Lake Baikal depths of 150–250 m only, and deeper layers are permanently weakly stably stratified, being always above the temperature of maximum density. Most remarkably, it was found by biochemical analyses that near-bottom waters (at about 900 m!) are significantly ‘younger’ than those at

intermediate depth [14, 23, 38]. Recently, WÜEST et al. [39] reported about direct observational evidence for deep-water renewal of the near-bottom layer in the deepest part (1461 m) by cold-water (about 3.2°) intrusions, appearing most often in June, when the thermal bar is observed in the lake. In this situation, the *thermobaric effect*⁵ is important. The temperature of maximum density decreases with the pressure (i.e. with the depth), so that denser water, cascading from slopes during spring heating (with a temperature below T_* at the surface), should pass some potential barrier at the level where the ambient water temperature equals $\sim T_*$ – and flow into the stably stratified deep region with $T > T_*$, being now *colder and denser* than the surrounding water.

The above discussion makes it clear that general ‘mixing’ of waters in lakes may be implemented via various mixing mechanisms. They are sometimes subdivided into ‘mixing’ and ‘stirring’ processes: the former act to smooth spatial gradients, the latter to enhance them. This way, turbulent mixing, induced by any external or internal source, always homogenises the water body, while wind action may either homogenise it (via shear-flow instabilities or surface wave breaking) or enhance spatial gradients when pushing large water masses with distinct characteristics into another area. The same happens with solar radiation and heat exchange through the lake surface: they may cause both convection and stratification in vertical water columns, depending on the water temperature relative to the temperature of maximum density, the sign of the heat flux or peculiarities of absorption of solar radiation in the water. In the presence of sloping boundaries (which is always the case in lakes!), vertical mixing becomes immediately linked with horizontal water exchange, generating stirring processes (down-slope gravity currents, denser water cascades, intrusions), which in turn may either homogenise or stratify vertical water columns in open-lake areas. It is clear that mixing of a stably stratified water body will make it less stable, until neutral conditions are reached.

8.3 Homogenisation of Water Masses Requires Energy

It is intuitively clear that homogenisation of the water in a stably stratified lake requires energy. The centre of gravity of a *stably* stratified water column lies below the centre of gravity when the water column is mixed and has uniform density. Qualitatively this is obvious, because in a stably stratified water column the heavy fluid lies below the light fluid. So, homogenisation requires to lift the centre of gravity of the stratified column to that of the homogenised body (which is at half the depth of the column) [32]. This corresponds to an increase in the potential gravitational energy of the water mass.

This description assigns the change in the position of the centre of mass solely to the mixing of water of different densities that is established when the water is homogenised. It is the sole process when, e.g. salt water at different salt

⁵ Thermobaric effect – influence of the pressure on the coefficient of thermal expansion of water.

concentrations (and constant temperature) is mixed. When pure water or water at constant salt concentration but non-uniform temperature is homogenised, the temperature changes with the mixing. Because of the thermal expansion which above 4°C is accompanied with a temperature rise, the centre of mass of a water column also changes its position as a consequence of the thermal expansion of the water. Both effects are significant in a lake and, depending upon the situation, may amplify or counteract each other. We shall analyse the two effects separately.

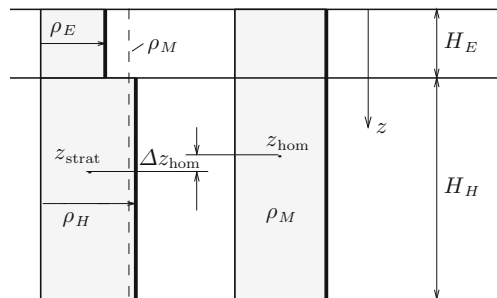
8.3.1 Constant Density Layers

To quantify the change in potential energy due to homogenisation by mixing, i.e. to give an order of magnitude involved in it, consider a rectangular basin $15 \times 60 \text{ km}^2$ (about the size of Lake Constance) with constant depth.⁶ Let the fluid mass be divided into two layers of constant density and sharp interface, as shown in Fig. 8.7. This corresponds to an idealised division of the water column into epi- and hypolimnion. As already mentioned above, the ensuing analysis will also be performed under the assumption that the density variation is not caused by temperature variations but by variations in salt concentration instead. This allows us in a first step to ignore the thermal expansion of the water that is subject to temperature variations. The influence of the thermal expansion will be dealt with in a second step.

With these prerequisites and with reference to Fig. 8.7 the homogenised density ρ_M follows from the equation of mass conservation:

$$\rho_M(H_E + H_H) = \rho_E H_E + \rho_H H_H \implies \rho_M = \frac{\rho_E H_E + \rho_H H_H}{H_E + H_H} \quad (8.1)$$

Fig. 8.7 Two-layer model having a light epilimnion with density ρ_E and layer depth H_E and heavy hypolimnion with density $\rho_H > \rho_E$ and depth H_H . After homogenisation the density is ρ_M



⁶ We select here a rectangular basin with constant depth to have the same horizontal area of the lake at all depths. This allows in the ensuing analysis to work with water columns only and to omit the influence of the variable lake area with depth. The more complicated case may be treated as an exercise.

and the centre of mass lies at

$$z_{\text{hom}} = \frac{H_E + H_H}{2}. \quad (8.2)$$

The corresponding centre of mass of the layered configuration follows from a condition of the static moment of the layered water masses with respect to the free surface

$$\rho_E H_E \frac{H_E}{2} + \rho_H H_H \left(\frac{1}{2} H_H + H_E \right) = z_{\text{strat}} \rho_M (H_E + H_H) \quad (8.3)$$

and setting this equal to the static moment of the homogenised water masses as done in (8.3) on the right-hand side. This yields, when solved for z_{strat} ,

$$z_{\text{strat}} = \frac{\frac{1}{2} \rho_E H_E^2 + \frac{1}{2} \rho_H H_H^2 + \rho_H H_E H_H}{\rho_E H_E + \rho_H H_H}. \quad (8.4)$$

The centre of mass of the two-layer fluid is lifted by homogenisation by the amount

$$\Delta z_{\text{hom}} = z_{\text{strat}} - z_{\text{hom}} = \frac{(\rho_H - \rho_E) H_E H_H}{2(\rho_E H_E + \rho_H H_H)}, \quad (8.5)$$

which is indeed positive when $\rho_H > \rho_E$. For $H_E = 10$ m, $H_H = 100$ m and $(\rho_H - \rho_E)/\rho_H = 10^{-3}$, (8.5) implies $\Delta z_{\text{hom}} \sim 4.5$ mm. It follows that *homogenising the water masses of a typical alpine lake with a typical summer stratification requires that its centre of gravity rises by a few millimetres.*

The change in gravitational potential energy of the water mass of the column (per unit area) is given by

$$\begin{aligned} \Delta \pi_{\text{hom}} &= \rho_M (H_E + H_H) g \Delta z_{\text{hom}} \stackrel{(8.1)}{=} (\rho_E H_E + \rho_H H_H) g \Delta z_{\text{hom}} \\ &= \frac{1}{2} (\rho_H - \rho_E) g H_E H_H. \end{aligned} \quad (8.6)$$

If we assume for simplicity that the epilimnion depth is constant but the hypolimnion depth varies with position in the xy -plane, then the total change in gravitational energy becomes

$$\Delta \Pi_{\text{hom}} = \int_A \Delta \pi_{\text{hom}}(x, y) dx dy = \frac{1}{2} (\rho_H - \rho_E) g H_E \underbrace{\int_A H_H(x, y) dx dy}_{V_H}.$$

Hence

$$\Delta \Pi_{\text{hom}} = \frac{1}{2} (\rho_H - \rho_E) g H_E V_H, \quad (8.7)$$

in which A is the lake area and V_H is the lower (hypolimnion) layer volume.

Let us evaluate this change in potential energy for a lake reminiscent of Lake Constance, i.e. a cube with dimensions $(15 \times 10^3, 60 \times 10^3, 10 + 100)$ m, corresponding to 15 km width, 60 km length, 10 m epilimnion depth and 100 m hypolimnion depth. A weak summer stratification amounts to a difference of the water densities in the hypolimnion and epilimnion of 1 kg m^{-3} ; a strong stratification would be about three times larger. Thus,

$$\begin{aligned}\Delta \Pi_{\text{hom}} &= \frac{1}{2} \times 1 \times 10 \times 10 \times (15 \times 10^3 \times 60 \times 10^3 \times 100) \\ &= 4.5 \times 10^{12} [\text{kg m}^2 \text{s}^{-2}] = 4.5 \times 10^{12} \text{ J}.\end{aligned}$$

Here we have used $g = 10 \text{ m s}^{-2}$ for simplicity.⁷ The reader may vary the numbers somewhat. The change in potential energy due to homogenisation for a lake of the size of Lake Constance is thus of the order of 10^{12} – 10^{13} [J].

This energy is now compared with a typical magnitude of the power of working of the wind input on the surface of a lake. The shear traction (stress) exerted on a horizontal surface element is usually parameterised by the wind speed as follows:

$$\tau_{\text{air}} = \rho_{\text{air}} c u_{\text{wind}}^2, \quad (8.8)$$

in which $\rho_{\text{air}} = 1.4 \text{ kg m}^{-3}$ is the density of the air under normal conditions ($p = 10^5 \text{ Pa}$, $T = 20^\circ\text{C}$; we ignore variations), c is the dimensionless drag coefficient and u_{wind} the wind speed, measured usually 10 m above the water surface. Values for c depend upon where, i.e. at which level above the water surface, the wind speed is measured, and, to some extent, also upon the state of the water surface (i.e. its waves) and the fetch both of which are correlated to the wind speed; here we are only interested in a rough estimate. Then we may simply take $c = 10^{-3}$, since values lie around $(0.7\text{--}2.0) \times 10^{-3}$.

The power of working of the shear traction expended by the water motion is given by

$$P = \tau_{\text{air}} u_{\text{water}} = \rho_{\text{air}} c u_{\text{wind}}^2 u_{\text{water}}. \quad (8.9)$$

This is a local quantity evaluated via the local wind speed u_{wind} and the local water surface velocity u_{water} . To evaluate the power exerted on the entire lake surface the distributions of the wind speed and surface water velocity fields must be known, but this is never the case; so we shall assume an idealised, perhaps somewhat unrealistic situation in which u_{wind} and u_{water} are uniformly distributed, and choose $u_{\text{water}} \simeq 0.05 u_{\text{wind}}$. Then an order of magnitude of the total power of working is

$$P \simeq 0.05 \rho_{\text{air}} c u_{\text{wind}}^3 A, \quad (8.10)$$

⁷ Whenever estimates are made, we shall set g equal to 10 m s^{-2} rather than 9.81 m s^{-2} . This will henceforth no longer be mentioned.

Table 8.1 Shear stress power P evaluated for three different wind speeds using formula (8.10) and the time required for homogenisation $t_{\text{hom}} = \Delta\Pi_{\text{hom}}/P$, where $\Delta\Pi_{\text{hom}} = 5 \times 10^{12}$ J

u_{wind} [m s ⁻¹]	u_{wind}^3 [m ³ s ⁻³]	A [m ²]	P [W]	t_{hom} [d]
2	8	9×10^8	5.04×10^5	115
5	125		7.88×10^6	7.34
10	1000		6.30×10^7	0.92

in which A is the area of the lake surface. Table 8.1 gives values of P for various wind speeds. A wind speed of 2 m s^{-1} is not exceptional, 5 m s^{-1} is a strong wind and 10 m s^{-1} is a wind speed of an exceptional storm.⁸ The numbers of Table 8.1 show that the power of working exerted by the wind is respectable (recall that power plants generate a few hundred megawatts (10^6 W)). So, the wind in strong storms attacks a lake of the size of Lake Constance with a total power comparable to the power generated by one common unit of a power plant.

A further computation provides equally interesting information. Suppose that all power due to the wind action at the lake surface is used without loss for rising the centre of gravity by homogenisation. How long would a wind have to blow to achieve this? If we take for $\Delta\Pi_{\text{hom}} = 5 \times 10^{12}$ J, and for the powers the values in column 4 of Table 8.1, then the values in the last column of Table 8.1 are obtained.⁹ A wind with speed 2 m s^{-1} would have to last persistently for 115 days to homogenise the water in the two-layer stratified water column, while a strong wind would need only a day to achieve this. Irrespective of how realistic these numbers are in any particular case – realistic times for homogenisation are certainly longer, because of the dissipation and the transfer to wave activity and not to mixing – the numerical values for t_{hom} teach us the following: *Storms are very efficient in changing the water mass distribution.* They accelerate the mixing processes tremendously simply because the power of working of the shear tractions at the free surface grows approximately with the third power of the wind speed.

Yet a further example of useful information is as follows: Compare the energy needed to lift the centre of mass of a water column due to homogenisation with

⁸ Whether a storm is strong or exceptional depends on the regional meteorological conditions and the number of recurrences. An objective scale is the BEAUFORT's scale, according to which wind speeds define the following conditions:

$5 - 8 \text{ m s}^{-1}$,	moderate wind,
$10 - 20 \text{ m s}^{-1}$,	strong wind,
$20 - 30 \text{ m s}^{-1}$,	storm,
$> 30 \text{ m s}^{-1}$,	hurricane.

With this scale, a lake in a mountainous region would seldom be subject to a storm.

⁹ The times t_{hom} can be calculated according to $t_{\text{hom}} = \Delta\Pi_{\text{hom}}/P$, however here the results are the same if $\Delta\pi_{\text{hom}}/P$ is evaluated instead. This is so because we assumed uniform wind and uniform surface water velocity.

the heat loss due to seasonal cooling. We use the same exemplary rectangular basin located at mid-latitudes.

During the summer months the air temperature immediately above the water surface is above that of the epilimnion water at the water surface. In autumn, and through the winter months, this is reverse. This reversal of the temperature difference between air and surface water begins for Lake Constance, for example, about in August. The flux of heat is then on average from the relatively warmer epilimnion water to the cooler air. The water becomes denser in this process, autumn convection starts which eventually leads to the homogenisation of the water body. In Lake Constance, e.g., this usually happens in January–February at a water temperature of approximately 4–5°. Table 8.2 shows some climatic data (averages taken at Friedrichshafen over 50 years). Plotting the temperature difference ΔT between air and surface against time shows a growing tendency from mid-August to mid-January but not uniformly. Thus, the following estimates are made with $\Delta T_{\text{mean}} = 4.7^\circ\text{C}$.

The heat transfer per unit time from the water to the atmosphere can be parameterised according to NEWTON's law as

$$q = \alpha(T_{\text{water}} - T_{\text{air}}), \quad (8.11)$$

where α is the heat transfer coefficient, and the amount of heat that is available at mid-August for this transfer is

$$Q = c_w m (T_{\text{summer}} - 4^\circ\text{C}), \quad m = \rho A h_{\text{th}}, \quad (8.12)$$

in which c_w is the specific heat of water, A is the area of the lake and h_{th} is the thermocline depth. For a lake with $L = 60$ km, $B = 15$ km, $h_{\text{th}} = 10$ m, $c_w \simeq 4.2 \times 10^3 \text{ J kg}^{-1} \text{ K}^{-1}$ and $T_{\text{summer}} = 22^\circ\text{C}$ this yields $Q \simeq 6.8 \times 10^{17} \text{ J}$, which is about 10,000–100,000 times larger than the change in potential energy due to homogenisation.

Alternatively, based on the mean value of ΔT , Q may be calculated as

$$Q = \int_{\text{Aug}}^{\text{Jan}} q A \, dt \simeq A \alpha \Delta T_{\text{mean}} \Delta t_c, \quad (8.13)$$

Table 8.2 Monthly mean temperatures of the air and surface water for Lake Constance taken from the 'World Lakes Database' (<http://www.ilec.or.jp>)

	T_{air}	T_{water}	$\Delta T = T_{\text{water}} - T_{\text{air}}$
August	17.6	22.0	4.4
September	14.3	16.5	2.2
October	8.9	13.4	4.5
November	4.2	9.2	5.0
December	0.5	7.4	6.9
January	−1.0	4.3	5.3
Mean			4.7

where Δt_c is the 5-month period from mid-August to mid-January, and ΔT_{mean} is the mean temperature difference in the same period, $\Delta T_{\text{mean}} = 4.7^\circ\text{C}$. Thus,

$$\alpha = \frac{Q}{A \Delta T_{\text{mean}} \Delta t_c} \simeq 12.4 [\text{J K}^{-1} \text{m}^{-2} \text{s}^{-1}]. \quad (8.14)$$

So, slightly more than 10 J of heat is transferred from the water to the air per square metre and per second when the difference of the water–air temperature is 1°K .

Finally, let us estimate how long it would take with the above value of α to transfer the same amount of heat that corresponds to the change in potential energy by homogenisation, $\Delta \Pi_{\text{hom}}$ as given in (8.7). This time, we obtain the following equation:

$$\Delta \Pi_{\text{hom}} = \int_0^{\Delta t} q A \, dt \simeq \alpha A \Delta T_{\text{mean}} \Delta t,$$

from which $\Delta t = \Delta \Pi_{\text{hom}} / (\alpha A \Delta T_{\text{mean}}) \simeq 86 \text{ s}$ is obtained, thus slightly more than a minute.

8.3.2 Continuous Density Variation

The analysis, performed for a water column stratified in two layers of constant density, can also be performed for a continuously stratified fluid as shown in Fig. 8.8. The mean density and the centre of gravity (or mass) are now derived by applying the zeroth and first moments of the density function $\rho(z)$ with respect to the free surface, viz.

$$\rho_M H = \int_0^H \rho(z) \, dz, \quad \rho_M H z_{\text{strat}} = \int_0^H \rho(z) z \, dz,$$

from which we deduce

$$\rho_M = \frac{1}{H} \int_0^H \rho(z) \, dz, \quad z_{\text{strat}} = \int_0^H \rho(z) z \, dz \Big/ \int_0^H \rho(z) \, dz, \quad (8.15)$$

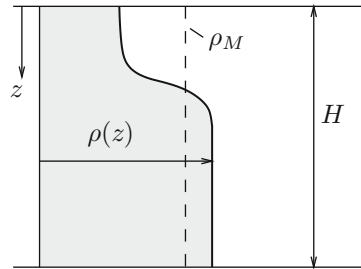


Fig. 8.8 Water column of extent H with continuous density distribution $\rho(z)$

as well as

$$\Delta z_{\text{hom}} = (z_{\text{strat}} - \frac{1}{2}H). \quad (8.16)$$

These formulae can be simplified by introducing the density offset $\Delta\rho(z)$ from the mean density ρ_M according to

$$\rho(z) = \rho_M + \Delta\rho(z). \quad (8.17)$$

Substituting this into (8.15) shows that

$$\int_0^H \Delta\rho(z) dz = 0, \quad z_{\text{strat}} \int_0^H \rho(z) dz = \rho_M \frac{H^2}{2} + \int_0^H \Delta\rho(z) z dz,$$

implying that the lifting of the centre of gravity is given by

$$\Delta z_{\text{hom}} = \frac{1}{H} \int_0^H \frac{\Delta\rho(z)}{\rho_M} z dz. \quad (8.18)$$

With this result the change in potential energy can be written as

$$\begin{aligned} \Delta\pi_{\text{hom}} &= \rho_M g H \Delta z_{\text{hom}} = \int_0^H \Delta\rho(z) g z dz, \\ \Delta\Pi_{\text{hom}} &= \int_A \left(\int_0^H \Delta\rho(z) g z dz \right) dx dy, \end{aligned} \quad (8.19)$$

for a water column of unit cross area and the entire lake, respectively. The reader may easily check that application of the two-layer stratification reproduces the formulae (8.5), (8.6) and (8.7).

Problem 8.1 Repeat the above analysis for a lake with variable bathymetry. Let $S(z)$ be the horizontal area bounded by the lake bottom at depth z . Derive alternative formulae to (8.18) and (8.19) that account for this topographic variation.

Consider a basin with power-law depth variation of S , see Fig. 8.9, for which $S(z) = S_0(1 - z/H_0)^n$, $n > 1$, and estimate its influence on Δz_{hom} , $\Delta\pi_{\text{hom}}$ and $\Delta\Pi_{\text{hom}}$, respectively, for various values of n . ♦

Problem 8.2 The two-layer approximation with sharp interface is a relatively rough representation of the stratification of a real lake. The piecewise linear

Fig. 8.9 Variation of S/S_0 as a function of $(1 - z/H_0)$ for different values of n

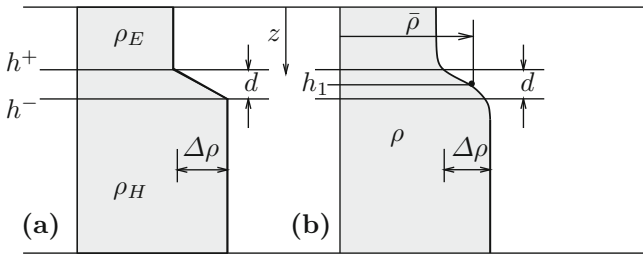
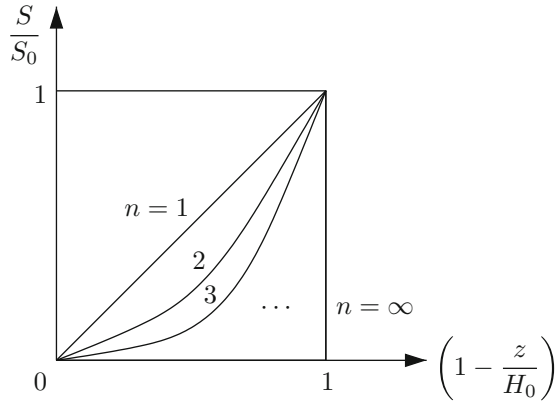


Fig. 8.10 (a) Three-layer density distribution with a constant-density upper layer and a constant-density bottom layer, with linear connection over a transition layer of thickness d . (b) Sigmoidal density profile connecting essentially constant-density epi- and hypolimnia with a smooth curve in the metalimnia. $\bar{\rho}$ is the density at the point of inflection of the profile, $\Delta\rho$ and d are the density differences between the epi- and hypolimnion and the thickness of the metalimnion, respectively

(3 layer) density profile of Fig. 8.10a and the so-called sigmoidal density profile of Fig. 8.10b are more accurate. They are given by the following density functions:

(i)

$$\rho(z) = \begin{cases} \rho_E, & 0 \leq z \leq h^+, \\ \rho_E + \frac{\Delta\rho}{d}(z - h^+), & h^+ \leq z \leq h^-, \\ \rho_H, & h^- \leq z \leq H, \end{cases} \quad \Delta\rho = \rho_H - \rho_E, \quad (8.20)$$

(ii)

$$\rho(z) = \bar{\rho} \exp\left(\frac{\Delta\rho}{2\bar{\rho}} \tanh\left(\frac{2}{d}(z - h_1)\right)\right), \quad (8.21)$$

where $\bar{\rho}$, $\Delta\rho$, d , h^+ , h^- , h_1 are defined in the figure. Use an algebraic computer software (e.g. MATHEMATICA or MAPLE) to determine Δz_{strat} , $\Delta\pi_{\text{hom}}$ and $\Delta\Pi_{\text{hom}}$. \blacklozenge

8.3.3 Influence of the Thermal Expansion

Let us now estimate the influence of the effect of thermal expansion to the position of the centre of mass in a water column due to homogenisation. We consider again the situation of Fig. 8.7 with two layers of constant density and assume that the temperature is everywhere above 4°C. Homogenisation increases the density in the epilimnion and thus decreases the epilimnion temperature and thickness by ΔH_E , but lowers the density in the hypolimnion and correspondingly increases the hypolimnion temperature and thickness by ΔH_H . Figure 8.11 illustrates this new situation. The position of the centre of mass of the two-layer column is still given by formula (8.4), but according to Fig. 8.11 the corresponding position of the homogenised column is given by¹⁰

$$z_{\text{hom}} = \frac{1}{2} (H_E + H_H - \Delta H_E - \Delta H_H). \quad (8.22)$$

Because homogenisation results in the epilimnion in a temperature drop the ‘homogenised epilimnion thickness’ is smaller than in the stratified situation ($\Delta H_E < 0$). Similarly, the ‘homogenised hypolimnion thickness’ is larger than in

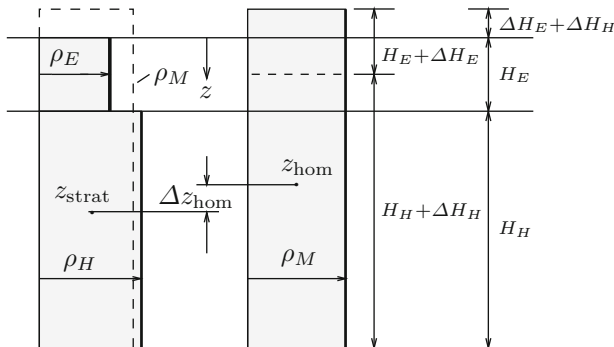


Fig. 8.11 Two-layer model as in Fig. 8.7. However, the thermal expansion in the homogenisation process is now accounted for, expressed by ΔH_E and ΔH_H , respectively

¹⁰ Formula (8.22) treats ΔH_E and ΔH_H analogously as if both were positive even though for (summer) stratification mixing leads to a temperature drop in the epilimnion for which a thermal contraction is expected. This is the case provided the epilimnion temperature is above $T_* = 4^\circ\text{C}$. The sign of ΔH_E will decide whether under given conditions a thermal expansion (positive) or contraction (negative) will arise.

the stratified situation ($\Delta H_H > 0$), since homogenisation yields a small temperature increase. With (8.4) and (8.22) the centre of mass of the two-layer fluid is lifted in homogenisation by the amount

$$\begin{aligned} \Delta z_{\text{hom}} &= z_{\text{strat}} - \frac{1}{2} (H_E + H_H) + \frac{1}{2} (\Delta H_H + \Delta H_E) \\ &\stackrel{(8.5)}{=} \frac{(\rho_H - \rho_E)H_E H_H}{2(\rho_E H_E + \rho_H H_H)} + \frac{1}{2} (\Delta H_E + \Delta H_H). \end{aligned} \quad (8.23)$$

The first term on the right-hand side is the same as (8.5) and represents the effect of mixing alone, the second bracketed term is due to thermal expansion and may be positive or negative, depending upon the thermal stratification and thicknesses of the epilimnion and hypolimnion layers.

To evaluate ΔH_E and ΔH_H , we use a parabolic parameterisation of the density

$$\rho = \rho_* \left(1 - \varepsilon(T - T_*)^2\right), \quad \varepsilon = 6.8 \times 10^{-6} [^\circ\text{C}^{-2}], \quad (8.24)$$

where ρ_* and T_* are the density and temperature of water at maximum density (i.e. 10^3 kg m^{-3} and 4°C , respectively). Now, since the total epilimnion and hypolimnion masses are conserved, one has

$$\rho_M(H_E + \Delta H_E) = \rho_E H_E, \quad \rho_M(H_H + \Delta H_H) = \rho_H H_H, \quad (8.25)$$

or, after substitution of (8.24)

$$\begin{aligned} \Delta H_E &= \varepsilon \frac{(T_M - T_*)^2 - (T_E - T_*)^2}{1 - \varepsilon(T_M - T_*)^2} H_E (< 0), \\ \Delta H_H &= \varepsilon \frac{(T_M - T_*)^2 - (T_H - T_*)^2}{1 - \varepsilon(T_M - T_*)^2} H_H (> 0), \end{aligned} \quad (8.26)$$

in which the terms in parentheses hold true provided $T_j > T_{\text{freeze}}$ ($j = E, H, M$). In these equations T_M is still not known. The equation from which it can be deduced is the heat balance during mixing. It is assumed that no heat is lost during mixing. This yields

$$c_w \rho_H H_H T_H + c_w \rho_E H_E T_E = c_w \rho_M (H_H + H_E + \Delta H_H + \Delta H_E) T_M, \quad (8.27)$$

which can be approximated to

$$H_H T_H + H_E T_E \simeq (H_H + H_E) T_M \implies T_M = \frac{H_H T_H + H_E T_E}{H_H + H_E}. \quad (8.28)$$

For $H_E = 10 \text{ m}$, $H_H = 100 \text{ m}$ and $T_E = 12^\circ\text{C}$, $T_H = 4^\circ\text{C}$ corresponding to $(\rho_H - \rho_E)/\rho_H \simeq 10^{-3}$, (8.26) together with (8.28) implies $\Delta H_E = -4.32 \text{ mm}$, $\Delta H_H = 0.36 \text{ mm}$ and thus $\Delta H_E + \Delta H_H \simeq -4 \text{ mm}$. This is of the same order of

magnitude – but different sign – as the elevation of the centre of mass is due to the effect of mixing alone, as given in (8.5) or due to the first term on the right-hand side of (8.23), namely 4.5 mm. Thus, considering the effect of the thermal expansion will substantially reduce the change of the potential energy by homogenisation: In summary, this result implies that in freshwater lakes levitation of the centre of gravity by homogenisation is influenced by both mixing and thermal expansion. In the situation treated above the two effects nearly neutralise each other. In a lagoon or the ocean where salt concentration plays a role, the two effects compete differently and the shift of the centre of gravity of a water mass may likely be more due to mixing than thermal expansion.

8.4 Motion of Buoyant Bodies in a Stratified Still Lake

In this section we shall substantiate some statements concerning the stability and instability, respectively, expressed in the introductory paragraphs of this chapter.¹¹ To this end, we envisage a quiescent fluid mass stratified with a continuous density profile $\rho(z)$ as, e.g., sketched in Fig. 8.8. Moreover, we focus on a small body (a particle, a plankton) or simply a certain volume of water that we think in imagination is separated from the water in its vicinity by a massless skin just like a balloon. This body – we shall call it henceforth simply particle – is, at a given depth, supposed to be in equilibrium with its surrounding liquid. We choose this level as the origin of a vertical coordinate ζ . If the particle is now displaced from its position $\zeta = 0$ to an arbitrary position above it, then the particle in its new position will no longer be in equilibrium. As a result a motion will set in. The question is how the equation of motion for this particle looks like. This, we will now attack.

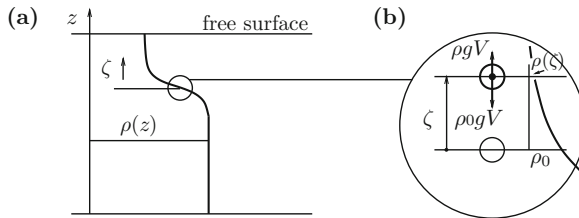


Fig. 8.12 (a) Density profile $\rho(z)$. The z -axis is vertical with origin on the still free surface. The ζ -axis is equally vertical with $\zeta = 0$ at the position where the isolated particle, shown as a circle, is in equilibrium with the surrounding fluid. (b) Close-up of the position of the particle showing the particle in its equilibrium position $\zeta = 0$ and displaced by ζ . The forces that are indicated are its gravity force and the buoyancy force

¹¹ This topic is a fashionable subject in elementary physics courses of College Physics, see, e.g., [18] or in courses on Environmental Fluid Mechanics, Meteorology, etc. The influence of friction, expressed in a hydrodynamic drag is, however, generally not treated.

Figure 8.12 shows the particle with volume V in its rest position $\zeta = 0$. It possesses the gravity force $\rho_0 g V$, since it is in equilibrium with the surrounding fluid with density ρ_0 . (We imagine the extent of the particle to be so small that density variations in the vertical over the particle length can be ignored.) When the particle is displaced to the general position ζ its gravity force is still the same, even if it is not wrapped in a massless skin, because during its motion the fluid inside this hull has no time to adjust its temperature (and salinity) to those of the surrounding fluid. At the position ζ the buoyancy force is, however, given by the pressure of the surrounding fluid which has density $\rho(\zeta)$. Thus according to the ARCHIMEDIAN principle explained in Chap. 4 the buoyancy force is $\rho g V$ and is pointing upwards.

Writing down NEWTON's second law 'mass times acceleration equals the sum of all external forces acting on the particle' leads, when written down for the vertical direction, to the equation

$$\underbrace{\rho_0 V}_{\text{mass}} \underbrace{\frac{d^2 \zeta}{dt^2}}_{\text{acc}} = \underbrace{\rho g V}_{\text{buoyancy force}} - \underbrace{\rho_0 g V}_{\text{gravity force}}. \quad (8.29)$$

Here friction is ignored and the mass is given using ρ_0 to evaluate its gravity force, but the buoyancy force is built with ρ . If we suppose ζ to be small – small on the length scale over which the density changes appreciably – the density $\rho(\zeta)$ may be expressed in terms of its TAYLOR series expansion about $\zeta = 0$ yielding

$$\rho(\zeta) = \rho_0 - \left(-\frac{d\rho}{dz} \right)_0 \zeta + \text{higher order terms}, \quad (8.30)$$

where we have written

$$\left(\frac{d\rho}{dz} \right)_0 = - \left(-\frac{d\rho}{dz} \right)_0,$$

because $(d\rho(z)/dz)$ is negative for a stably stratified fluid mass. Here we have identified the density gradient by the index $(\bullet)_0$ to express that it is evaluated in the position $\zeta = 0$. Substituting (8.30) into (8.29) and simplifying the resulting equation yields

$$\frac{d^2 \zeta}{dt^2} + N^2 \zeta = 0, \quad N^2 := \frac{1}{\rho_0} \left(-\frac{d\rho}{dz} \right)_0 g. \quad (8.31)$$

Definition 8.2 N , having the dimension of a frequency, and given by

$$N^2 := \frac{1}{\rho_0} \left(-\frac{d\rho}{dz} \right)_0 g, \quad [\text{s}^{-2}], \quad (8.32)$$

is called **buoyancy frequency** or **Brunt-Väisälä frequency** after British and Finnish oceanographers¹² (Fig. 8.13). ■

Substituting typical values of the vertical density gradient $|d\rho/dz| \sim 10^{-3} - 10^{-1} \text{ kg m}^{-4}$ yields $N = 10^{-3} - 10^{-2} \text{ s}^{-1}$. It is also obvious that N^2 characterises *stability* of vertical stratification at a given location and

$$N^2 > 0, \quad \text{if } \left(\frac{d\rho}{dz} \right) < 0, \quad N^2 < 0, \quad \text{if } \left(\frac{d\rho}{dz} \right) > 0. \quad (8.33)$$

The former typifies a stable stratification, the latter an unstable stratification, as will soon become more explicitly apparent.

For a linear stratification equation (8.31) is a second-order ordinary differential equation with a constant coefficient N^2 , of which the solution we are now going to construct:

Case I: For constant $N^2 > 0$ (8.31) is the differential equation of the harmonic oscillator, of which the general solution is given by

$$\zeta = A \sin(Nt) + B \cos(Nt), \quad (8.34)$$

where A and B are constants of integration. A and B are determined by fulfilling the initial conditions

$$\zeta(t=0) = \zeta_0, \quad \frac{d\zeta}{dt}(t=0) = V_0 \quad (8.35)$$

implying $B = \zeta_0$ and $A = V_0/N$, so that

$$\zeta = \frac{V_0}{N} \sin(Nt) + \zeta_0 \cos(Nt). \quad (8.36)$$

This solution can also be rewritten as

$$\zeta = A_0 \sin(Nt + \varphi_0), \quad (8.37)$$

where

$$A_0 = \sqrt{(V_0/N)^2 + \zeta_0^2}, \quad \varphi_0 = \arctan\left(\frac{\zeta_0}{V_0/N}\right). \quad (8.38)$$

¹² Accounting also for the compressibility, the buoyancy frequency is

$$N^2 = \frac{g}{\rho} \left(-\frac{d\rho}{dz} + \frac{g^2}{c^2} \right),$$

where c is the speed of sound. This expression is useful for estimation of stability of the stratification in homogeneous layers in a lake interior.

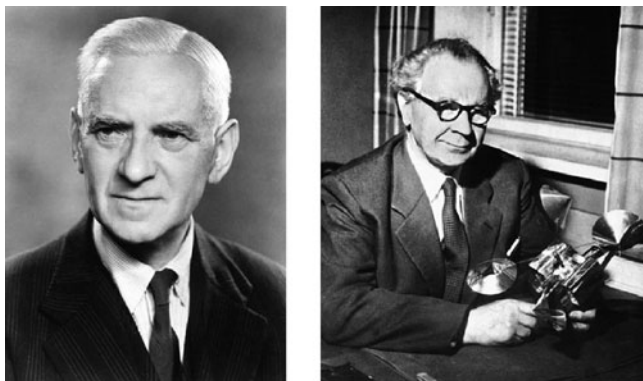


Fig. 8.13 *Left:* Sir David BRUNT, father of meteorology, 1945 (<http://www.scienceandsociety.co.uk>). *Right:* Vilho VÄISÄLÄ (<http://www.ths.fi>)

Sir David BRUNT (17 June 1886–5 February 1965) was a trained mathematician from Aberystwith (Wales) and Cambridge (England), where he held the Isaac NEWTON studentship, and, after a brief spell in astronomy, primarily worked in meteorology. In 1916 he entered the Meteorological Office (MO) of the United Kingdom where he was involved in the analysis of variance of time series which led to his book *The Combination of Observations* 1917. His research and part time teaching for many years at Imperial College (IC), London, led him to the classic *Physical and Dynamical Meteorology* (1934). In 1934 he also left the MO to assume the chair of meteorology at IC. He became physical secretary of the Royal Society of London in which capacity he supervised the British expedition to the Halley Bay (Antarctica) during the International Geophysical Year 1956–1957. BRUNT's research began with periodogram analyses in the 1920; subsequently, he moved to dynamic meteorology of the troposphere by careful collecting data on pressure, temperature, wind and their analysis. He also did research on atmospheric radiation and, later, the reaction of men to his atmospheric environment. BRUNT served as president of the Royal Meteorological Society and the Physical Society. He independently discovered the buoyancy frequency now named after him and VÄISÄLÄ. In Antarctica, as a tribute to his merits as a supervisor of the British expedition there, the BRUNT Ice Shelf was named after him.

Vilho VÄISÄLÄ (28 September 1889–12 August 1969) was a Finnish meteorologist. He was inventor of meteorological instruments and an esteemed scientist in his field. After graduation in mathematics in 1912 from the University of Helsinki, VÄISÄLÄ began his 36 years of employment at the Finnish Meteorological Institute in aerological measurements, specialising in the research of the higher troposphere. Measurements were conducted by attaching a thermograph to a kite. In 1917, he published his dissertation in mathematics *The single-valuedness of the inverse function of the elliptic integral of the first kind*. His dissertation was the first and is still said to be the only mathematical doctoral thesis written in the Finnish language. VÄISÄLÄ participated in the development of radiosonde, a device attached to a balloon and launched to measure air in the higher atmosphere. VÄISÄLÄ authored and co-authored over 100 scientific papers and a total of 10 patented inventions. In 1936 he started his own company, manufacturing radiosondes and – later – other meteorological instruments. The formula for the buoyancy frequency carries his name. In 1948 he became professor of meteorology in the University of Helsinki.

The text is based on <http://www.scienceandsociety.co.uk>, the *Obituary Notes* of P. A. SHEPARD of the Royal Astronomical Society, <http://www.vaisala.com> and <http://en.wikipedia.org/>.

Thus, the particle oscillates about its equilibrium position with amplitude A_0 persistently in time. Because $|\sin(Nt + \varphi_0)| \leq 1$ the oscillatory motion is bounded: $-A_0 \leq \zeta \leq A_0$. The fluid is stably stratified in the vicinity of $\zeta = 0$ because the particle simply oscillates about its equilibrium position with a period $T_b = 2\pi/N$.

Case II: For constant $N^2 < 0$ the differential equation (8.31) may be written as

$$\frac{d^2\zeta}{dt^2} - |N^2|\zeta = 0 \quad (8.39)$$

and possesses the solution

$$\zeta = A \exp(|N|t) + B \exp(-|N|t). \quad (8.40)$$

Subject to the initial conditions (8.35), it may be written as

$$\zeta = \frac{1}{2|N|}(V_0 + |N|\zeta_0) \exp(|N|t) - \frac{1}{2|N|}(V_0 - |N|\zeta_0) \exp(-|N|t). \quad (8.41)$$

Evidently as $t \rightarrow \infty$ the first term on the right-hand side of (8.41) becomes unbounded, whereas the second term is vanishingly small. Therefore, unless the initial conditions are such that $\zeta_0 = 0$ and $V_0 = 0$, the particle will move arbitrarily far away from its initial position. This obviously corresponds to an unstable equilibrium.

We thus have reached the following result:

Result 8.1 *The sign of N^2 is an indication of whether a fluid mass in the neighbourhood of $\zeta = 0$ is stably or unstably stratified, where N^2 is evaluated according to (8.32). Conversely, if a water mass is stably stratified then $N^2 > 0$. A fluid particle displaced in a stratified fluid from its equilibrium position and left free will oscillate, if $N^2 > 0$ with a period*

$$T_b = \frac{2\pi}{N} = 2\pi \left/ \sqrt{\frac{1}{\rho_0} \left(-\frac{d\rho_0}{dz} \right) g} \right., \quad (8.42)$$

called buoyancy period. If $N^2 < 0$, the particle will never return to its original position once it is displaced from its equilibrium position and so the initial unstable stratification will be destroyed. \otimes

Typical values of the buoyancy period obviously depend on the values of the specific density gradients. Table 8.3 provides some values. It is seen that the buoyancy periods for realistic stratifications are a few minutes or longer, and evidently the period grows with decreasing stratification, approaching infinity when $d\rho/dz \rightarrow 0$. Thus: *The weaker the stratification the smaller the BRUNT-VÄISÄLÄ frequency and the larger the buoyancy period.*

Table 8.3 Some values of the specific density gradient $1/\rho(-d\rho/dz)$, the BRUNT-VÄISÄLÄ frequency N and the buoyancy period $T_b = 2\pi/N$

$\frac{1}{\rho}(-\frac{d\rho}{dz})$	[m ⁻¹]	10 ⁻⁶	10 ⁻⁵	10 ⁻⁴	10 ⁻³	10 ⁻²
N	[s ⁻¹]	3.16×10^{-3}	10 ⁻²	3.16×10^{-2}	10 ⁻¹	3.16×10^{-1}
$T_b <$	[s]	1987	628	198.7	62.8	19.9
	[min]	33	10.4	3.3	1.04	0.33
		Realistic stratification	←	•	→	Very strong stratification

Problem 8.3 Assume a thermal equation of state of the form $\rho = \rho(T)$; express the BRUNT-VÄISÄLÄ frequency in terms of the temperature and temperature gradient $(-dT/dz)$ and make a graph displaying the buoyancy period in terms of $(-dT/dz)$. ♦

8.4.1 Influence of Friction

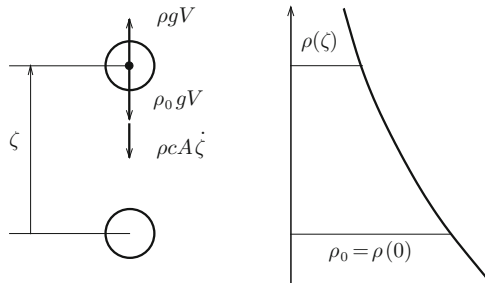
The above analysis ignores friction. This is why an oscillation of such a buoyant particle about its equilibrium position persists forever, once the motion has been initialised. Let us ask the question of how friction will change the findings, in particular with regard to the buoyancy period and the motion of a particle when it is being displaced out of its equilibrium position.

Returning to Fig. 8.12 we only need to complement the forces exerted on the particle by a frictional force, see Fig. 8.14. We postulate that this frictional force opposes the motion and is proportional to the particle velocity as follows:

$$F_{\text{fric}} = -\rho_0 c A \frac{d\zeta}{dt}, \quad (8.43)$$

in which c is the *drag coefficient* and A a typical cross-section of the particle perpendicular to the motion (for a spherical particle with diameter D , $A = D^2\pi/4$). Thus, NEWTON's second law for the particle, written for the vertical direction, with the forces shown in Fig. 8.14 now takes the form

Fig. 8.14 Fluid particle in its equilibrium position $\zeta = 0$ and in an arbitrary position ζ with acting forces, gravity and friction opposing its motion and buoyancy force in the direction of the motion. Shown is also the density profile $\rho(\zeta)$ of the ambient fluid



$$\underbrace{\rho_0 V \frac{d^2 \zeta}{dt^2}}_{\text{mass} \times \text{acc}} = \underbrace{\rho g V}_{\text{buoyancy force}} - \underbrace{\rho_0 g V}_{\text{gravity force}} - \underbrace{\rho_0 c A \frac{d\zeta}{dt}}_{\text{frictional force}}, \quad (8.44)$$

or when using (8.30) as before

$$\frac{d^2 \zeta}{dt^2} + 2\gamma \frac{d\zeta}{dt} + N^2 \zeta = 0, \quad (8.45)$$

where

$$\gamma := \frac{1}{2} c \frac{A}{V}, \quad [\gamma] = [\text{s}^{-1}] \quad (8.46)$$

is the friction coefficient. It depends on the drag coefficient, the cross-section of the particle perpendicular to the direction of the motion and the volume of the particle, and it has the dimension of a frequency and is, for a given particle and a given fluid, as the buoyancy frequency, a constant.¹³ Detailed analyses of solutions of equations (8.45) can be found in almost any elementary physics book which treats linear oscillations of solids or fluids, e.g. [31].

The linear ordinary differential equation with constant coefficients (8.45) has solutions of the form $\zeta = Ae^{\lambda t}$; substituting this representation into (8.45) leads to the characteristic equation

$$\lambda^2 + 2\gamma\lambda + N^2 = 0$$

with the solutions

$$\lambda_{1,2} = -\gamma \pm \sqrt{\gamma^2 - N^2}. \quad (8.47)$$

It follows that the most general solution of (8.45) has the form

$$\zeta = A_1 e^{\lambda_1 t} + A_2 e^{\lambda_2 t}, \quad (8.48)$$

in which A_1, A_2 are constants of integration which are determined by satisfying the initial conditions

$$\zeta(0) = \zeta_0, \quad \frac{d\zeta}{dt}(0) = V_0, \quad (8.49)$$

implying

$$A_1 = -\frac{\lambda_2 \zeta_0 - V_0}{\lambda_1 - \lambda_2}, \quad A_2 = \frac{\lambda_1 \zeta_0 - V_0}{\lambda_1 - \lambda_2}. \quad (8.50)$$

¹³ Note however, through the ratio A/V this constant depends on the geometry of the particle.

The qualitative behaviour of the solution (8.48) depends on the relative magnitudes of γ^2 and N^2 , which will now be discussed in due order.

Case I: $N^2 > 0$ and $\gamma^2 > N^2$. This is the case of strong friction in a stably stratified fluid for which $\lambda_{1,2} < 0$, as can easily be inferred from (8.47). Hence both exponential functions in (8.48) have negative exponents, implying that the solution is exponentially decaying as t increases. The particle does not oscillate and simply returns to equilibrium as shown in Fig. 8.15a.

Case II: $N^2 > 0$ and $\gamma^2 < N^2$. Case I is physically not realistic for natural water because the friction is far too large. For the situation of case II, λ_1 and λ_2 are conjugate complex

$$\lambda_{1,2} = -\gamma \pm i\sqrt{N^2 - \gamma^2}, \quad (8.51)$$

in which $i = \sqrt{-1}$ is the imaginary unit. Thus (8.48) may now be written as

$$\begin{aligned} \zeta &= A_1 \exp \left[\left(-\gamma + i\sqrt{N^2 - \gamma^2} \right) t \right] + A_2 \exp \left[\left(-\gamma - i\sqrt{N^2 - \gamma^2} \right) t \right] \\ &= e^{-\gamma t} \left\{ A_1 \exp \left(i\sqrt{N^2 - \gamma^2} t \right) + A_2 \exp \left(-i\sqrt{N^2 - \gamma^2} t \right) \right\}, \end{aligned} \quad (8.52)$$

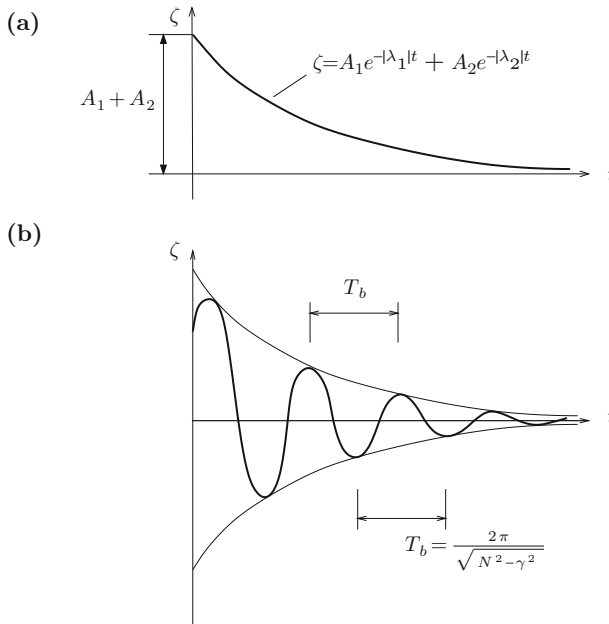


Fig. 8.15 (a) Solution of $\zeta(t)$ as given in (8.48) when λ_1 and λ_2 are both negative and damping is above critical. (b) Corresponding solution (8.53) when damping is small

which, on using EULER's formula,¹⁴ can also be written as

$$\begin{aligned}\zeta &= e^{-\gamma t} \left\{ c_1 \sin \left(\sqrt{N^2 - \gamma^2} t \right) + c_2 \cos \left(\sqrt{N^2 - \gamma^2} t \right) \right\}, \\ c_1 &= i(A_1 - A_2), \quad c_2 = (A_1 + A_2).\end{aligned}\quad (8.53)$$

This solution is an exponentially damped oscillation and looks like the graph shown in Fig. 8.15b. The periodic part of the solution has a circular frequency given by $\sqrt{N^2 - \gamma^2}$ and the buoyancy period of the damped oscillation is given by

$$\begin{aligned}T_b &= \frac{2\pi}{\sqrt{N^2 - \gamma^2}} = \frac{2\pi}{N} \frac{1}{\sqrt{1 - \frac{\gamma^2}{N^2}}} \\ &\simeq \frac{2\pi}{N} \left(1 + \frac{1}{2} \frac{\gamma^2}{N^2} \right) + \text{higher order terms.}\end{aligned}\quad (8.54)$$

The approximate value is appropriate if $\gamma^2 \ll N^2$. A typical value for γ^2 may be $\Gamma^2 N^2$ with $\Gamma^2 \ll 0.001$, so that

$$T_b \simeq \frac{2\pi}{N} \left(1 + \frac{1}{2} \Gamma^2 \right). \quad (8.55)$$

It follows that the buoyancy period can be computed without making a considerable error by neglecting the viscous damping.

How long does it take until the oscillating particle has essentially come to rest? This rest state is theoretically never exactly reached, because the exponential function $e^{-\gamma t}$ arising in (8.53) never reaches the zero value except at $t = \infty$. A typical quantity characterising the persistent attenuation of ζ with time is the so-called *e-folding time*: This is the time it takes until the amplitude of oscillation becomes e times smaller, i.e. the amplitude function $e^{-\gamma t}$ in (8.53) reaches the value $e^{-1} = 0.367$. This requires

$$e^{-\gamma T_{\text{fold}}} = e^{-1} \implies T_{\text{fold}} = \frac{1}{\gamma} = \frac{1}{\Gamma N}. \quad (8.56)$$

For $\Gamma^2 = 10^{-4}$ (a large value!) and $N = 10^{-3}$, this yields $T_{\text{fold}} = 10^5 \text{ s} = 27.8 \text{ h}$. It follows that *the oscillations of buoyant particles in a stably stratified still ambient fluid persist for a very long time. The lifetime of such motions is of the order of several days.*

Case III: $N^2 < 0$. Since also $\gamma^2 > 0$, both values for λ in (8.47) are real, and $\lambda_1 > 0$ while $\lambda_2 < 0$. It follows that ζ in (8.48) takes now the form

$$\zeta = A_1 \exp \underbrace{[(-\gamma + \sqrt{\gamma^2 - N^2})t]}_{>0} + A_2 \exp \underbrace{[(-\gamma - \sqrt{\gamma^2 - N^2})t]}_{<0}.$$

¹⁴ $e^{i\theta} = \cos \theta + i \sin \theta$.

Because the first exponent in this expression is positive, ζ will grow indefinitely as t increases. This corresponds to instability. We have thus learned that friction has not altered the fact that N alone describes the stability of the stratification. $N^2 > 0$ characterises a stable and $N^2 < 0$ an unstable stratification of the fluid. This instability may be only local, i.e. $N^2 < 0$ may hold true only within a sublayer of the water column. So, within this layer, mixing will occur until $N^2 > 0$ is re-established. In this connection one sometimes speaks of *locally* unstable stratification.

8.5 Internal Oscillations – The Dynamical Imprint of the Density Structure

In the last section we have seen that a buoyant particle in an otherwise still, stably stratified liquid will, when being displaced out of its equilibrium position, oscillate with the buoyancy period. Much richer motions of similar nature appear in the entire stratified water body if its equilibrium is disturbed by some external influence. As we have seen in the beginning of Chap. 7, this disturbance, propagating through space and time by transference of energy and without motion of the medium as a whole is called a *wave*. The subject treated in this section gives a first account of *internal waves* in a stratified layer, a subject that is treated by many others in great detail.¹⁵ In this section, our intention is to demonstrate that the stratified fluid itself will perform internal oscillations after excitement, e.g. by wind; the vertical displacements of the fluid particles in such motions depend on how the density varies over depth. In fact, these vertical displacements (or the vertical velocities if the latter are not determined) are directly coupled to the density distribution which is conveniently expressed in terms of the BRUNT–VÄISÄLÄ frequency. In Fig. 8.16 the squared buoyancy frequency N^2 for an episode in Lake Zürich in 1978 is shown as a function of depth; the insert shows a typical distribution of N^2 . In Fig. 8.17 we have sketched idealised as well as realistic density distributions together with the corresponding profiles of the BRUNT–VÄISÄLÄ frequency. We will see that the amplitudes of the vertical oscillations are large, where the buoyancy frequency is large, and they are very small at the water surface.

Our analysis will not be complete and will oversimplify the exact facts here and there. The principal objective is to build a fundamental physical understanding; a more complete analysis will follow in Volume II of this book series.

It is in principle very easy to see by direct observation that the interior of a stratified lake is subject to permanent oscillations. One only needs to moor a thermistor chain at a midlake position, say, such that its 11 thermistors¹⁶ lie primarily in the

¹⁵ A biased short list is LIGHTHILL [28], LEBLOND and MYSAK [27], HUTTER [17], [18].

¹⁶ Thermistor chains are usually 10, 20 or 50 m long and have 11 thermistors which are 1, 2 or 5 m apart.

Fig. 8.16 Squared BRUNT-VÄISÄLÄ frequency N^2 as determined from measurement at a midlake position in Lake Zürich, taken on 15 September 1978. The insert map shows its schematic distribution. For the selected ω -value waves can only exist in the indicated band, called waveguide

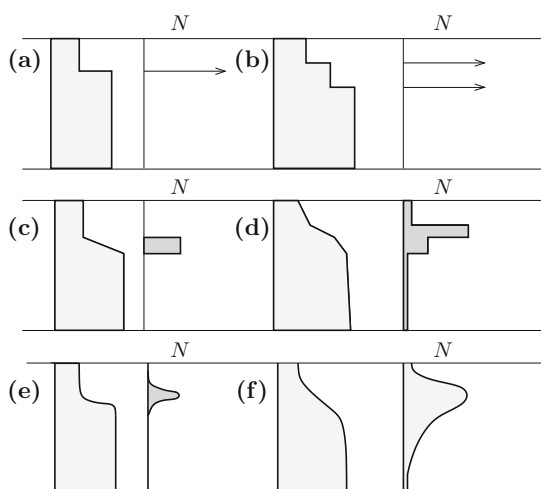
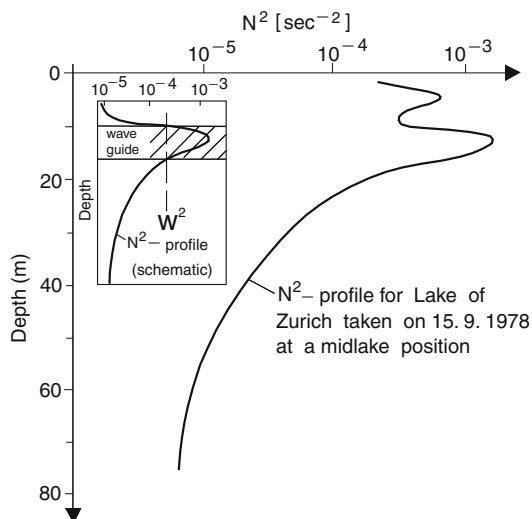


Fig. 8.17 Profiles of density, $\rho(z)$, and buoyancy frequency, $N(z)$, for typical idealised and realistic stratifications. (a) Two layers with constant density; N is a DIRAC pulse. (b) Three layers with constant density; N consists of two DIRAC pulses. (c) Three layers with constant-linear-constant density distribution; N is constant where the density profile is linear. (d) Piecewise linear density profile generates a piecewise constant N -profile. (e) A so-called sigmoidal density profile connects two constant density profiles with a smooth curve. The N -profile consists of a 'hump' where the density varies appreciably. (f) Typical realistic density profile with corresponding N -profile. The N -profile reaches a maximum at the thermocline location

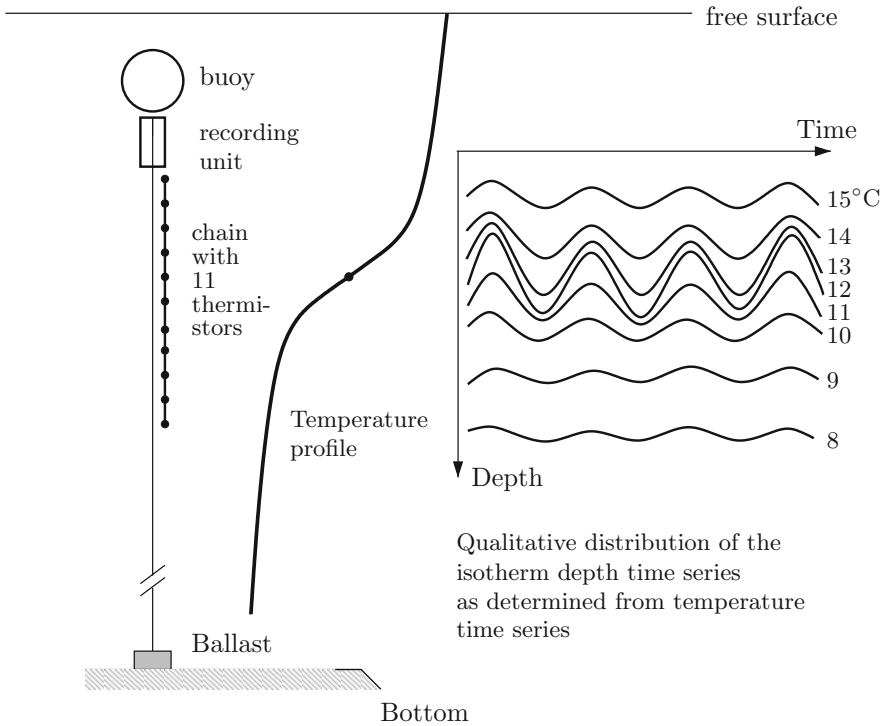


Fig. 8.18 Sketch of a mooring consisting of a ballast weight, a metallic cord and a buoy holding the arrangement tight in the vertical. Within this cord a thermistor chain and its electronic recording unit are mounted at a selected depth, which preferably extends over the metalimnion and somewhat more. The time series on the right show how the isotherm-depth amplitudes vary in conformity with the vertical temperature gradient. Amplitudes grow with growing temperature gradient

metalimnion and also record the temperature at the lower part of the epilimnion and the upper part of the hypolimnion; such a situation is sketched in Fig. 8.18. Each thermistor will record the temperature as a function of time, and from these time series it is, in principle, an easy matter to construct *isotherm–depth–time series*. These curves indicate at which depth at a certain time the water with a prescribed temperature can be found. Because the water in a column moves up and down and the individual water particles maintain their temperature, if thermal diffusion is ignored, the isotherm–depth–time series is reminiscent of the vertical displacement of the water at the mooring position.

Because for lakes the chemical composition of the water does not, in general, affect the density, the thermal equation of state is $\rho = \hat{\rho}(T)$, implying that surfaces of constant temperature are also the surfaces of constant density, called the *isopycnal surfaces*. So, *isopycnal–depth–time series* and *isotherm–depth–time series* are in lakes often the same curves. This is not so when salt affects the density as is always

the case for the ocean, and may also be important for largely contaminated lakes such as reservoirs formed from strip mining excavations.¹⁷

Figure 8.18 shows a principal sketch of how isotherm–depth–time series looks like, and Fig. 8.19 gives an example deduced from records in Lake Zürich. It is evident that the oscillations are conspicuous in the metalimnion with largest amplitudes at the thermocline level, that they are attenuated as one moves into the epi- and hypolimnion. There are two aspects associated with these fluctuations. *First*, one may ask how the period may be explained. From Fig. 8.19 we infer without even performing a FOURIER transformation that these periods are on the order of hours (perhaps from 1 to 50 h). The answer to this question will not be addressed in this section. We only note here that the buoyancy frequency at the thermocline (which is about 10^{-3} s^{-1} , corresponding to a period of about 15 min in this example) gives an upper limit to the internal wave frequencies. What we are concerned with here is the *second* question, namely how the amplitudes of such oscillations are distributed with depth. In fact we wish to prove and to quantify that, *if the lake is stratified*, the metalimnion is the region of dynamic activity. For vanishing buoyancy frequency this internal activity is simply null.

8.5.1 Fundamental Equations

The basic equations that govern the motion in a stratified lake have been derived in Chap. 4 and will be written down here under the following restrictive and simplifying assumptions:

- Linearisation: all convective terms in the momentum equation are ignored, and in the energy equation only the contribution from the vertical convection is accounted for. This means that all variables are considered to have small deviations from their equilibrium values.
- Viscous stresses, heat conduction and dissipation are ignored.
- The vertical momentum equation reduces to the *hydrostatic force balance*.
- Non-inertial effects (CORIOLIS accelerations) are ignored.
- The fluid is vertically stratified.

The equilibrium state is considered here as a state of rest with vanishing velocity $\mathbf{v}_{\text{eq}} = \mathbf{0}$, stable density distribution, $\rho_{\text{eq}} = \rho_0(z)$, and pressure distribution $p_{\text{eq}} = -\int_0^z \rho_0(\bar{z})g \, d\bar{z}$, where z is measured upwards from the mean (still) water surface. Denoting perturbations by a prime (except for u, v , since their equilibrium values

¹⁷ The dynamically important quantity is in fact the density distribution and therefore the distribution of the isopycnal surfaces rather than the isotherm–depth–time series. In a situation in which the thermal equation of state has the form $\rho = \hat{\rho}(T, s)$, where s is salinity, measurements of temperature and salinity–time series will yield the density–time series from which the isopycnal time series can be constructed.

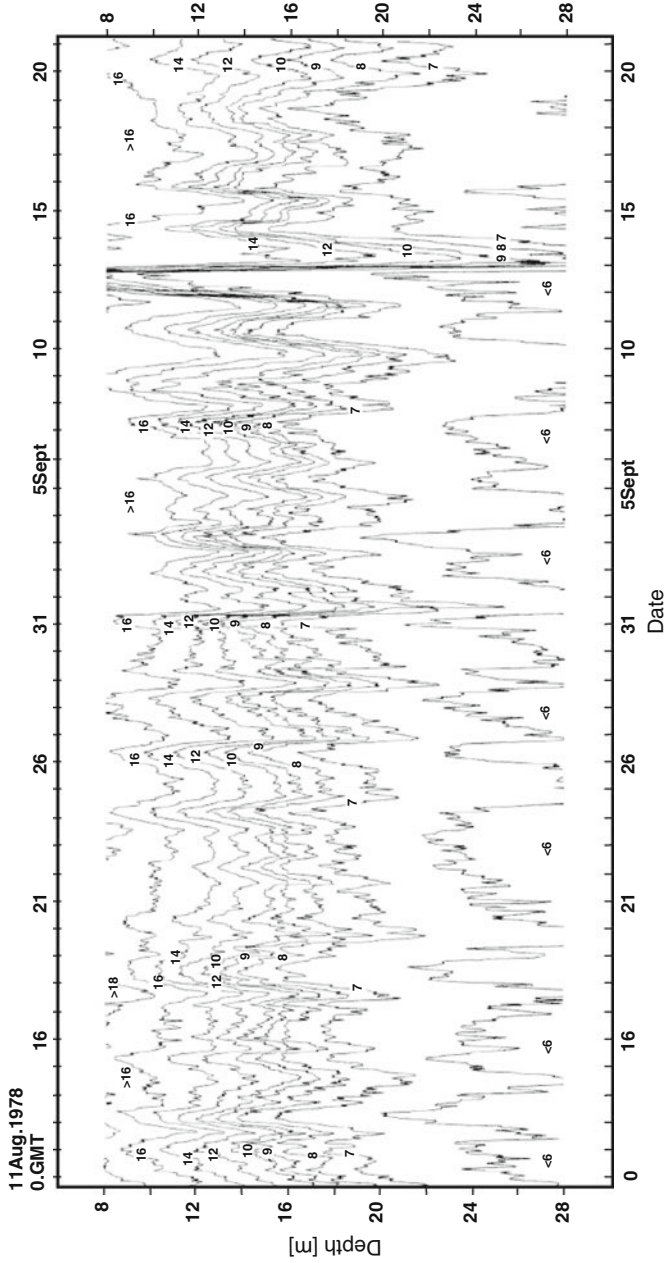


Fig. 8.19 Hourly averaged isotherm–depth–time series within the depth range of 8–28 m and plotted for temperatures from 6 to 16°C. (Lake Zürich field campaign, 1978) [15], © Laboratory of Hydraulics, Hydrology and Glaciology at ETH Zürich

are zero), the balance laws of mass, momentum and energy take the forms (see Chap. 4, (4.235), (4.236), (4.237))

$$\frac{\partial u}{\partial x} + \frac{\partial v}{\partial y} + \frac{\partial w}{\partial z} = 0, \quad (8.57)$$

$$\frac{\partial u}{\partial t} - f v = -\frac{1}{\rho_*} \frac{\partial p'}{\partial x}, \quad (8.58)$$

$$\frac{\partial v}{\partial t} + f u = -\frac{1}{\rho_*} \frac{\partial p'}{\partial y}, \quad (8.59)$$

$$0 = -\frac{\partial p'}{\partial z} - \rho' g, \quad (8.60)$$

$$\frac{\partial \rho'}{\partial t} - \rho_* \frac{N^2}{g} w = 0. \quad (8.61)$$

The first of these equations is the continuity equation expressing the conservation of volume (or mass since our model equations are those of a BOUSSINESQ fluid). Equations (8.58), (8.59) and (8.60) are the balances of momentum in the x -, y - and z -directions; ρ_* is a constant reference density (e.g. at the water temperature 4°C). The acceleration is ignored in (8.60). Under such circumstances it actually reads

$$\frac{\partial p}{\partial z} = -\rho g \implies \frac{\partial p_{\text{eq}}}{\partial z} + \frac{\partial p'}{\partial z} = -\rho_0(z)g - \rho' g,$$

explaining (8.60) and also justifying

$$\frac{\partial p}{\partial x} = \frac{\partial p'}{\partial x}, \quad \frac{\partial p}{\partial y} = \frac{\partial p'}{\partial y}, \quad \frac{\partial p}{\partial z} = -\rho' g.$$

Most difficult to understand in the above equations is probably (8.61); it follows from the energy equation under the above-mentioned simplifying assumptions of vanishingly small thermal diffusion, dissipation and radiation. The energy equation then takes the form $\rho_* c_v dT/dt = 0$; since for pure water¹⁸ $\rho = \rho(T)$, this is equivalent to $d\rho/dt = 0$, or in view of $\rho = \rho_0(z) + \rho'$ and ignoring higher order nonlinear terms,

$$\frac{d\rho}{dt} = \frac{\partial \rho'}{\partial t} - \left(-\frac{d\rho_0}{dz}\right)w = \frac{\partial \rho'}{\partial t} - \frac{\rho_*}{g} \underbrace{\frac{1}{\rho_*} \left(-\frac{d\rho_0}{dz} g\right)}_{N^2} w = 0,$$

which explains (8.61). We emphasise that N is only a function of z .

¹⁸ This is an exact statement for an incompressible material for which ρ cannot depend on pressure. However, water is only nearly incompressible. So, (8.61) is an approximation for the case that the thermal equation of state does not depend on pressure.

Equations (8.57), (8.58), (8.59), (8.60), (8.61) constitute five linear partial differential equations for the five unknowns u , v , w , p' and ρ' . They do not in this form provide easy access to extract a physical understanding from them. This access is better achieved if a single equation is deduced for one of the five variables. We shall choose the vertical component of the velocity vector, w , because it will directly answer the initial question concerning the amplitude distribution of the oscillations through the water column.

In what follows we shall now demonstrate the reduction of (8.57), (8.58), (8.59), (8.60), (8.61) to a single equation for w . In a first step we differentiate (8.58) with respect to time and substitute (8.59); analogously we do the same with the roles for (8.58) and (8.59) interchanged. This yields

$$\mathcal{L}[u] = -\frac{1}{\rho_*} \frac{\partial^2 p'}{\partial x \partial t} - \frac{f}{\rho_*} \frac{\partial p'}{\partial y}, \quad \mathcal{L}[v] = -\frac{1}{\rho_*} \frac{\partial^2 p'}{\partial y \partial t} + \frac{f}{\rho_*} \frac{\partial p'}{\partial x}, \quad (8.62)$$

in which

$$\mathcal{L}[\cdot] := \left(\frac{\partial^2}{\partial t^2} + f^2 \right) [\cdot]. \quad (8.63)$$

Second, from the continuity equation (8.57) we may deduce

$$\begin{aligned} \mathcal{L} \left[\frac{\partial^2 w}{\partial z^2} \right] &= -\frac{\partial}{\partial z} \left(\mathcal{L} \left[\frac{\partial u}{\partial x} \right] + \mathcal{L} \left[\frac{\partial v}{\partial y} \right] \right) \\ &\stackrel{(8.62)}{=} \frac{1}{\rho_*} \left(\frac{\partial^2}{\partial x^2} \left(\frac{\partial^2 p'}{\partial z \partial t} \right) + \frac{\partial^2}{\partial y^2} \left(\frac{\partial^2 p'}{\partial z \partial t} \right) \right). \end{aligned} \quad (8.64)$$

Third, (8.60) and (8.61) may be combined to eliminate the density perturbations, yielding,

$$\frac{\partial^2 p'}{\partial z \partial t} = -g \frac{\partial \rho'}{\partial t} = -\rho_* N^2 w. \quad (8.65)$$

Substituting (8.65) into (8.64) reveals the desired result, namely

$$\mathcal{L} \left[\frac{\partial^2 w}{\partial z^2} \right] + N^2 \left(\frac{\partial^2 w}{\partial x^2} + \frac{\partial^2 w}{\partial y^2} \right) = 0. \quad (8.66)$$

By introducing the two-dimensional *Laplace operator*

$$\nabla_H^2[w] = \frac{\partial^2 w}{\partial x^2} + \frac{\partial^2 w}{\partial y^2}, \quad (8.67)$$

an alternative form to write (8.66) is therefore also

$$\mathcal{L} \left[\frac{\partial^2 w}{\partial z^2} \right] + N^2 \nabla_H^2[w] = 0. \quad (8.68)$$

This is a partial differential equation for w which is of second order in the space and time variables (it involves only second-order spatial and temporal derivatives). We wish to solve it subject to certain initial conditions and boundary conditions at the lake surface and its bottom, which will be specified below only as far as needed to quantify the vertical distribution of w .

8.5.2 Eigenvalue Problem for the Vertical Mode Structure in Constant Depth Basins

Equation (8.68) involves as independent variables three space coordinates, x , y , z and the time. If x , y are horizontal and z is vertical, then the z -coordinate is parallel to the dominant direction of stratification. So, we may ask the question whether (8.68) permits solutions $w(x, y, z, t)$ for which the z -dependence separates from the other variables in the form

$$w(x, y, z, t) = Z_n(z)w_n(x, y, t). \quad (8.69)$$

Here we have introduced an index n for reasons that will shortly become apparent; it also allows us to differentiate between the functions w and w_n . Substituting (8.69) into (8.68) yields, on recognising that Z_n does not depend on x , y and t , while w_n does not depend on z ,

$$Z_n''(z)\mathcal{L}[w_n(x, y, t)] = -N^2(z)Z_n(z)\nabla_H^2 w_n(x, y, t) \quad (8.70)$$

or upon division by $Z_n\mathcal{L}[w_n]$ and $N^2(z)$,

$$\underbrace{\frac{1}{N^2(z)} \frac{Z_n''(z)}{Z_n(z)}}_{f(z)} = - \underbrace{\frac{\nabla_H^2[w_n(x, y, t)]}{\mathcal{L}[w_n(x, y, t)]}}_{g(x, y, t)}, \quad (8.71)$$

in which the prime denotes differentiation with respect to z . In (8.71), the left-hand side is only a function of z , while the right-hand side is a function of x , y , t . Two such functions can only be the same when they do not depend at all upon their independent variables, i.e. are the same constant. We shall choose

$$f(z) = g(x, y, t) = -\frac{1}{gh_n} (= \text{const}). \quad (8.72)$$

This implies, on the one hand, that

$$\mathcal{L}[w_n(x, y, t)] - gh_n \nabla_H^2[w_n(x, y, t)] = 0 \quad (8.73)$$

and, on the other hand, that

$$Z_n''(z) + \frac{N^2(z)}{gh_n} Z_n(z) = 0. \quad (8.74)$$

Thus, we have derived via the *separation of variables technique* (8.69) from (8.68) (that describes the motion of the vertical velocity component w) two equations describing, on the one hand, its horizontal and temporal variability, and, on the other hand, the vertical variability. This is a separation of one high-dimensional problem into two problems of lower dimension (either three (x, y, t) or one dimension (z)). This reduction has been bought at the expense of the introduction of a yet unknown separation constant gh_n , which must be determined along with the solution of the problem.

In the ensuing analysis we shall set the construction of the solution of the horizontal and temporal problem (8.73) aside and shall only deal with (8.74). This is a second-order linear ordinary differential equation with variable coefficient which can be solved provided boundary conditions at $z = 0$ (water surface) and at $z = -H$ (bottom) are prescribed. We shall for simplicity assume that the free surface is immobile to vertical motions so that $w(x, y, z = 0, t) = 0$, implying $Z_n(z = 0) = 0$. This assumption is obviously not exact – there are nontrivial and small displacements and thus velocities at the free surface – but in view of the discussion in connection with Fig. 8.19 this approximation seems to be tolerable. Physically, this means that the amplitudes of the surface displacements are negligibly small in comparison to corresponding amplitudes of vertical displacements of internal fluid particles in the metalimnion. This assumption is called the *rigid lid assumption*. At a flat bottom the impermeability requirement simply demands that $w(x, y, z = -H, t) = 0$ implying $Z_n(z = -H) = 0$. Thus, we have to solve the following *boundary value problem*:

$$\begin{aligned} Z_n''(z) + \frac{N^2(z)}{gh_n} Z_n(z) &= 0, \quad 0 > z > -H, \\ Z_n &= 0, \quad z = 0, \\ Z_n &= 0, \quad z = -H. \end{aligned} \quad (8.75)$$

This problem is a so-called *Sturm–Liouville eigenvalue problem* for the eigenvalues gh_n and the corresponding eigenfunctions. The attribute ‘STURM–LIOUVILLE’ tells the mathematicians certain properties which can rigorously be proved:

Theorem 8.1 (Properties of Sturm–Liouville problems)

- *There is a countably infinite number of positive eigenvalues gh_n which can be ordered according to their size.* This now explains the introduction of the index n . It can be used as counting index for the different eigenvalues gh_0, gh_1, \dots, gh_n .

- *The eigenfunctions belonging to different eigenvalues are orthonormal to one another in the sense that*

$$\int_{-H}^0 N^2(z) Z_n(z) Z_m(z) dz = \begin{cases} 1, & n = m, \\ 0, & n \neq m. \end{cases} \quad (8.76)$$

For $n = m$ the chosen value on the right-hand side is to a certain extent arbitrary. It corresponds to a particular normalisation of the eigenfunctions.

- *The set of eigenfunctions is complete, i.e. any (quadratically integrable) function $f(z)$, $0 \geq z \geq -H$ can be expanded in terms of these functions.* \otimes

We shall not prove the first and third of these statements,¹⁹ but the second is easily corroborated as follows: We multiply (8.75)₁, on both sides with $Z_m(z)$ and integrate the resulting equation from $z = -H$ to $z = 0$. This yields

$$\int_{-H}^0 Z_n''(z) Z_m(z) dz + \int_{-H}^0 \frac{N^2(z)}{gh_n} Z_n(z) Z_m(z) dz = 0.$$

Writing this equation down again with indices m and n interchanged,

$$\int_{-H}^0 Z_m''(z) Z_n(z) dz + \int_{-H}^0 \frac{N^2(z)}{gh_m} Z_m(z) Z_n(z) dz = 0$$

and subtracting the two equations yields

$$\int_{-H}^0 (Z_m'' Z_n - Z_n'' Z_m) dz + \int_{-H}^0 \left(\frac{1}{gh_m} - \frac{1}{gh_n} \right) N^2 Z_m Z_n dz = 0.$$

Performing next an integration by parts of the first integral, viz.

$$\int_{-H}^0 (Z_m'' Z_n - Z_n'' Z_m) dz = [Z_m' Z_n - Z_n' Z_m]_{-H}^0 - \int_{-H}^0 \underbrace{(Z_m' Z_n' - Z_n' Z_m')}_0 dz \stackrel{!}{=} 0$$

and using the boundary conditions (8.75)_{2,3} shows this term to be zero. Thus, since for $m \neq n$ the eigenvalues are numerically different, we have that

$$\int_{-H}^0 N^2(z) Z_m(z) Z_n(z) dz = 0 \quad \text{for } m \neq n$$

¹⁹ A proof of the theorem can be found in many books on linear algebra – inner product spaces – or in books on mathematical physics, e.g. [6].

proving the second of (8.76). As for $m = n$, we are free to choose the numerical value of the integral, because its integrand is positive. We choose (8.76)₁ and thus fix the numerical value of $\max_{-H \leq z < 0} [Z_n(z)]$, qed.

It is advantageous to write the eigenvalue problem in non-dimensional form. So we write

$$\zeta = -\frac{z}{H}, \quad Z_n(z) = W Z_n(\zeta). \quad (8.77)$$

Then, (8.75) becomes

$$\begin{aligned} \frac{d^2 Z_n}{d\zeta^2} + \lambda_n^2 Z_n &= 0, \quad \lambda_n^2 := \frac{H^2 N^2}{gh_n}, \\ Z(0) &= 0, \quad Z(1) = 0. \end{aligned} \quad (8.78)$$

In this case, the orthonormal relation of the eigenfunctions (8.76) becomes

$$W^2 H \int_0^1 N^2(\zeta) Z_n(\zeta) Z_m(\zeta) d\zeta = \begin{cases} 1, & n = m, \\ 0, & n \neq m. \end{cases} \quad (8.79)$$

8.5.2.1 Example a: Linear Stratification

This corresponds to $N^2 = \text{const}$ or $\rho(z) = Az + B$. Such a stratification is not realistic for lakes but it enjoys the property that differential equation (8.78)₁ has constant coefficients, analytical solutions can easily be constructed and the implications of the eigenvalue problem (8.78) be discussed qualitatively.

For $N^2 = \text{const}$ or $\lambda_n^2 = \text{const}$, the differential equation (8.78) possesses the general solution

$$Z_n = A_n \cos(\lambda_n \zeta) + B_n \sin(\lambda_n \zeta), \quad (8.80)$$

and the first boundary condition implies $A_n = 0$, while the second yields

$$0 = B_n \sin(\lambda_n) \implies \lambda_n = n\pi, \quad n = 1, 2, \dots,$$

so that

$$Z_n = B_n \sin(n\pi \zeta), \quad gh_n = \frac{H^2 N^2}{n^2 \pi^2}. \quad (8.81)$$

We have thus indeed found a countably infinite number of eigenvalues gh_n , which can be ordered; increasing n in integer steps decreases gh_n quadratically. The

dimensionless eigenfunctions belonging to gh_n are the trigonometric sin functions and these are obviously orthogonal. Indeed, (8.79) becomes

$$\begin{aligned} W^2 H N^2 \int_0^1 \mathcal{Z}_n(\zeta) \mathcal{Z}_m(\zeta) d\zeta &= B_m B_n N^2 W^2 H \int_0^1 \sin(n\pi\zeta) \sin(m\pi\zeta) d\zeta \\ &= \begin{cases} \frac{1}{2} B_n^2 N^2 W^2 H, & n = m, \\ 0, & n \neq m, \end{cases} \end{aligned} \quad (8.82)$$

from which the normalised amplitudes could be computed. The values of the amplitudes B_n are, however, not uniquely determinable and neither is it important, because we have, in the original problem formulation, not specified the driving forces of the motion. So, (8.81) determines the *shape* of the vertical velocity distribution. For each integer $n = 1, 2, 3, \dots$, it is different as shown in Fig. 8.20a. Each of the solutions is called a *mode* and because the equations are linear the most general solution is a linear combination of all these modes:

$$\mathcal{Z}(\zeta) = \sum_{n=1}^{\infty} \mathcal{Z}_n(\zeta) = \sum_{n=1}^{\infty} B_n \sin(n\pi\zeta). \quad (8.83)$$

In this expansion the coefficients B_n are related to the driving forces (which we have not specified here).

It is evident from the graphs in Fig. 8.20a that the oscillating activity of the vertical velocity component lies inside the fluid layer, since all amplitude maxima are

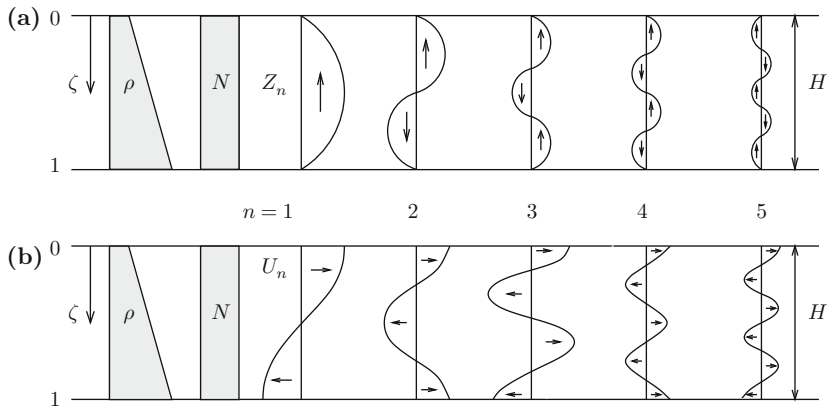


Fig. 8.20 The five lowest order internal or baroclinic modes for a linearly stratified fluid layer of depth H . The two left profiles in both graphs show the density and buoyancy frequency profiles. (a) Vertical distribution of the *vertical velocity component* for the first five modes; the profiles are the sinusoidal functions $\sin(n\pi\zeta)$. Arrows indicate the direction of motion modulo its sign. (b) Same as (a) but showing the five lowest modes of the *horizontal velocity component*. Arrows again indicate the direction (modulo its sign) of the flow

arising within this layer. However, the trigonometric functions are not restricted in this figure to a typical metalimnion, because a linear stratification encompassing the entire layer depth was chosen. This latter quality will change when a more realistic distribution of the BRUNT–VÄISÄLÄ frequency is chosen. That this is important can convincingly be seen when $N = 0$ is selected, corresponding to no stratification. Then, the boundary value problem (8.75) admits only the zero solution. This demonstrates that (8.75) describes the baroclinic internal motion and not the barotropic external counterpart.

An interesting and important question is what kind of horizontal motion is associated with these vertical velocity profiles. It is not our intention here to describe this horizontal velocity distribution in all its details. A simple analysis, however, allows us at least to determine its vertical mode structure. To this end it suffices to consider the continuity equation (8.57) which may be written as

$$\nabla_H \cdot \mathbf{v}_H = \frac{\partial u}{\partial x} + \frac{\partial v}{\partial y} = -\frac{\partial w}{\partial z} = -w_n(x, y, t) \frac{dZ_n(z)}{dz}, \quad (8.84)$$

where, on the right-hand side, the separation of variable representation (8.69) has been substituted, and restriction to the n th mode has been implemented. The left-hand side of (8.84) describes the horizontal divergence of the horizontal velocity components. The divergence operator involves no differentiations with respect to the z -variable. Therefore, the function dZ_n/dz describes the vertical variation of the horizontal velocity components. So, if we write

$$u(x, y, z, t) = U_n(z)u_n(x, t), \quad v(x, y, z, t) = 0, \quad (8.85)$$

and thus assume that the motion is in the x -direction only, then (8.84) and (8.85) imply

$$\frac{\partial u_n(x, t)}{\partial x} U_n(z) = -w_n(x, t) \frac{dZ_n(z)}{dz}, \quad (8.86)$$

so that

$$U_n(z) \propto \frac{dZ_n}{dz} \propto \frac{dZ_n}{d\zeta} \propto \cos(n\pi\zeta), \quad (8.87)$$

where we have left the amplitude unspecified. *The vertical distribution of the horizontal velocity is proportional to the z -derivative of the vertical distribution of the (negative) vertical velocity.*

Problem 8.4 Prove that the conclusion (8.87) can also be derived when the motion is three-dimensional, i.e. when

$$u(x, y, z, t) = U_n(z)u_n(x, y, t), \quad v(x, y, z, t) = V_n(z)v_n(x, y, t),$$

then

$$U_n(z) \propto V_n(z) \propto \frac{dZ_n}{dz}(z). \quad \blacklozenge$$

For the five lowest order baroclinic modes these distributions are shown in Fig. 8.20b. It is seen that each mode divides the water column into a number of sublayers. This number equals $(n+1)$, which is the number of zeros of the $U_n(\zeta)$ -profile plus 1. The direction of the velocity in each of these sublayers changes whenever a zero of the U_n -profile function is crossed. This is indicated in Fig. 8.20b by the arrows. For $n = 1$ this division yields an upper and a lower layer in which the motion is to-and-fro, respectively, reminiscent of a forward motion in the epilimnion and a return motion in the hypolimnion and vice versa. In the first higher baroclinic mode ($n = 2$) there are three layers with horizontal velocities that are ‘to-fro-to’ as one reaches larger depths, etc. The general motion is a linear combination of all these modes with an anticipated decrease of the significance of the higher order modes. In fact, in real measurements, the fundamental baroclinic mode ($n = 1$) is generally dominantly excited and clearly observed, the higher order baroclinic modes are present usually with much lesser energy (and amplitude). Indeed, one may, in field measurements, observe the lowest ($n = 1$) and first higher baroclinic mode ($n = 2$), but has so far not been able to clearly identify any of the higher ones ($n > 3$).

A further interesting property can be read off from Fig. 8.20b. For each mode the volume flux, i.e. the integral of the horizontal velocity over depth is zero. So, *there is no net transport of fluid in the horizontal direction*. This result is seen here to be the property of the trigonometric function $\cos(n\pi\zeta)$. *The volume flux to the right adds up to the same value as the volume flux to the left*. However this is so even for stratifications different from that of Fig. 8.20; it simply follows from the assumptions of plane motion, volume preserving and rigid lid. And it is equally independent of the fact whether a baroclinic wave is the compound of a number of modes.

There still remains an interpretation of the eigenvalues, given in (8.81)₂. They have the physical dimension of a squared velocity, and h_n is a length whereby the notation h_n suggests a depth. So $gh_n = c_n^2$ is the n th mode-shallow-water velocity (as we shall prove later on). Table 8.4 gives numerical values of $\sqrt{gh_n}$ for $N = 10^{-2} \text{ s}^{-1}$ and $H = 100 \text{ m}$ (appropriate for, e.g. Lake Constance). The corresponding speeds $c_n = \sqrt{gh_n}$ are of the order of 30 cm s^{-1} and less. Important is that with increasing mode numbers the value of the velocity decreases proportionally to $1/n$. Later, we will learn that the velocities c_n are the phase velocities of the corresponding modes. It follows that *the higher the baroclinic mode number is,*

Table 8.4 Values for $\sqrt{gh_n}$ and h_n according to (8.81) for $H = 100 \text{ m}$ and $N = 10^{-2} \text{ s}^{-1}$

n	1	2	3	4	5
$\sqrt{gh_n}$ [cm s ⁻¹]	32	16	10.6	8.0	6.4

the slower will be the propagation of the corresponding wave. This fact suggests a reason why higher order baroclinicity is principally difficult or virtually impossible to observe. In reality these waves are damped by viscous effects. For equal distances travelled by two waves of different baroclinic mode numbers, $n_2 > n_1$, the higher baroclinic wave (n_2) goes through a larger number of cycles than the lower baroclinic wave (n_1) when travelling this distance and will therefore be subject to more dissipation than the lower baroclinic wave. It is therefore likely that an internal wave with an initially rich vertical structure consisting of many modes, each with appreciable energy, will be quickly modified in which low-order baroclinic modes survive, while the higher modes have essentially died out.

8.5.2.2 Example b: Constant Density Epi- and Hypolimnion, Linear Stratification in the Metalimnion

A more realistic density profile that mimics the summer stratification is a profile in which the epilimnion and hypolimnion have constant densities, ρ_E and ρ_H , respectively, with $\rho_E < \rho_H$, which are connected in the metalimnion as shown in Fig. 8.21. This yields zero buoyancy frequency in the epi- and hypolimnion and constant buoyancy frequency in the metalimnion. The differential equation (8.78) must in this case separately be solved for the epi-, meta- and hypolimnion (denoted for brevity as regions I, II and III) with zero boundary conditions at the free surface (rigid lid assumption) and at the base; the three solutions are then smoothly connected at the interfaces between epi- and metalimnion and meta- and hypolimnion, respectively.

Region I ($0 \geq z \geq -h^+$ or $0 \leq \zeta \leq \zeta^+$):

Because of the vanishing buoyancy frequency the differential equation (8.78)₁ is simply $\mathcal{Z}_n^I{}''(\zeta) = 0$ of which the solution is a linear function $\mathcal{Z}_n^I = A + B\zeta$, which, in view of the rigid lid assumption, at $\zeta = 0$, becomes

$$\mathcal{Z}_n^I(\zeta) = B_n \zeta, \quad 0 \leq \zeta \leq \zeta^+ \quad (8.88)$$

with still undetermined constant B_n .

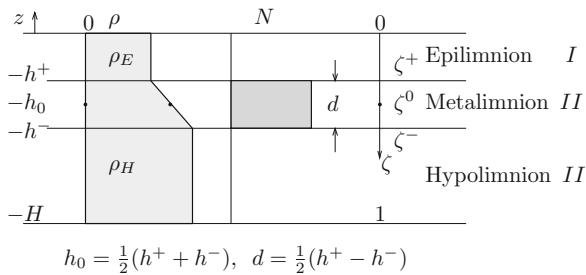


Fig. 8.21 Constant epilimnion and hypolimnion densities, linearly connected in the metalimnion of thickness d . The corresponding buoyancy frequency is piecewise constant with zeros in the epi- and hypolimnion

Region II ($-h^+ \geq z \geq -h^-$ or $\zeta^+ \leq \zeta \leq \zeta^-$):

In this region N is constant, (8.78)₁ is a differential equation with constant coefficients and possesses the solution

$$\mathcal{Z}_n^{\text{II}}(\zeta) = C_n \sin(\lambda_n \zeta) + D_n \cos(\lambda_n \zeta), \quad \zeta^+ \leq \zeta \leq \zeta^- \quad (8.89)$$

with two constants of integration, C_n and D_n .

Region III ($-h^- \geq z \geq -H$ or $\zeta^- \leq \zeta \leq 1$):

The conditions are here the same as in region I; thus, $\mathcal{Z}_n^{\text{III}}$ is linearly distributed in ζ (or z) and must vanish at $\zeta = 1$ (or $z = -H$) implying

$$\mathcal{Z}_n^{\text{III}}(\zeta) = F_n(\zeta - 1), \quad \zeta^- \leq \zeta \leq 1. \quad (8.90)$$

The solutions (8.88), (8.89) (8.90) contain four still unknown constants which will be deduced by requiring continuity of \mathcal{Z}_n and \mathcal{Z}'_n at $\zeta = \zeta^+$ (or $z = -h^+$) and $\zeta = \zeta^-$ (or $z = -h^-$), respectively. These conditions imply the following four equations:

$$\begin{aligned} B_n h^+ &= C_n \sin(\lambda_n \zeta^+) + D_n \cos(\lambda_n \zeta^+), \\ B_n &= \lambda_n C_n \cos(\lambda_n \zeta^+) - \lambda_n D_n \sin(\lambda_n \zeta^+), \\ F_n(h^- - H) &= C_n \sin(\lambda_n \zeta^-) + D_n \cos(\lambda_n \zeta^-), \\ F_n &= \lambda_n C_n \cos(\lambda_n \zeta^-) - \lambda_n D_n \sin(\lambda_n \zeta^-). \end{aligned} \quad (8.91)$$

By eliminating B_n and F_n two homogeneous equations emerge for C_n and D_n which allow a non-trivial solution only provided that the determinant of this system vanishes. This yields the eigenvalue equation

$$\frac{\tan(\lambda_n \zeta^+) - \lambda_n \zeta^+}{1 + \lambda_n \zeta^+ \tan(\lambda_n \zeta^+)} = \frac{\tan(\lambda_n \zeta^-) - (\zeta^- - 1)\lambda_n}{1 + \lambda_n (\zeta^- - 1) \tan(\lambda_n \zeta^-)} \quad (8.92)$$

for the eigenvalue λ_n . It possesses a countably infinite number of solutions which can be ordered according to the counting index n . Once (8.92) is satisfied, B_n , C_n and F_n can be expressed in terms of D_n as follows:

$$\begin{aligned} B_n &= -\lambda_n D_n \{A_n(\lambda_n) \cos(\lambda_n \zeta^+) + \sin(\lambda_n \zeta^+)\}, \\ C_n &= -D_n A_n(\lambda_n), \\ F_n &= -\lambda_n D_n \{A_n(\lambda_n) \cos(\lambda_n \zeta^-) + \sin(\lambda_n \zeta^-)\} \end{aligned} \quad (8.93)$$

with

$$A_n(\lambda_n) := \frac{1 + \lambda_n \zeta^+ \tan(\lambda_n \zeta^+)}{\tan(\lambda_n \zeta^+) - \lambda_n \zeta^+}. \quad (8.94)$$

Before we discuss this solution it is worth checking whether the result has any chance to be correct. If we set $h^+ = 0$ ($\zeta^+ = 0$) and $h^- = H$ ($\zeta^- = 1$) then the linear stratification extends over the entire water column. The eigenvalue equation (8.92) reduces in this case to $\tan(\lambda_n) = 0$ or $\lambda_n = n\pi$. Furthermore, $\Lambda_n = \infty$, and therefore $D_n = 0$ (in order to have finite C_n). So the solution reduces to that of the previous example, which we expected. For the general case, we, however, have

$$\mathcal{Z}_n(\zeta) = \begin{cases} B_n(\lambda_n)\zeta, & 0 \leq \zeta \leq \zeta^+, \\ C_n(\lambda_n) \sin(\lambda_n \zeta), & \zeta^+ \leq \zeta \leq \zeta^-, \\ F_n(\lambda_n)(\zeta - 1), & \zeta^- \leq \zeta \leq 1 \end{cases} \quad (8.95)$$

with λ_n evaluated from (8.92) and the constants of integration given by (8.93) and (8.94).

Problem 8.5 Write a program that determines the solution of (8.92), (8.93), (8.94), (8.95) and generates graphs for the profiles (8.95). ♦

If the function (8.95) and its z -derivative are graphically displayed, then the profiles of vertical and horizontal velocity, $\mathcal{Z}_n(\zeta)$ and $U_n(\zeta)$, of Fig. 8.22 are obtained.

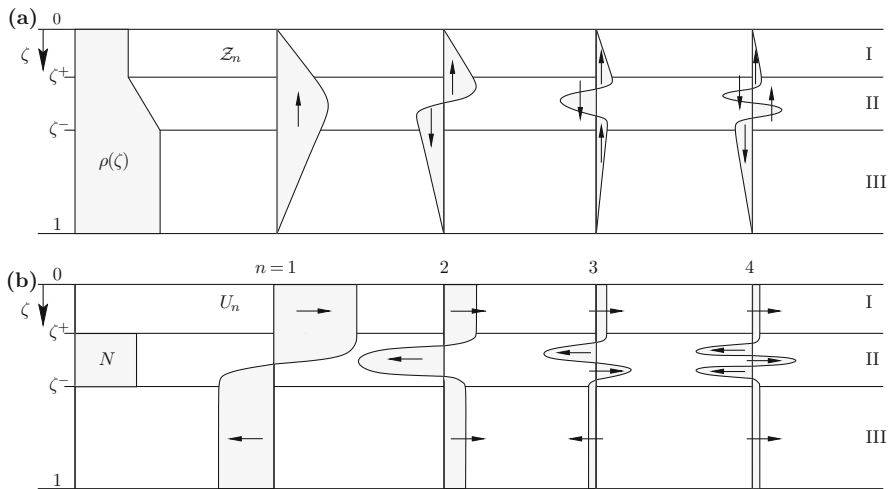


Fig. 8.22 The four lowest order internal modes for a stratification that has constant density in the epilimnion (I) and hypolimnion (III) with linear connection of these two values in the metalimnion (II). (a) shows the density distribution and the four lowest order modes of the vertical velocity distribution. (b) shows the corresponding buoyancy frequency and the four lowest order modes for the horizontal velocity. The arrows indicate the direction of the flow (modulo its sign). Figure is only a sketch

Qualitatively, the same results are obtained as shown in Fig. 8.20, but with quantitative differences which are important. The figure displays in the top panel the density profile and the four first modes of the vertical velocity component. In the bottom part of the figure, the corresponding buoyancy frequency and the profiles of the four lowest order modes of the horizontal velocity are shown. Evidently, the horizontal velocity in the respective sublayers that are separated by the zeros of the function $dZ_n/d\zeta$ changes its direction. The lowest order baroclinic mode consists of two layers in which the horizontal velocity is to-and-fro with relatively large values of the velocity both in the epi- and hypolimnion. Recall that the volume flux in the upper layer (from the zero of the U_1 -function to the free surface) has the same amount as the return flux in the lower layer. This implies that, roughly, the ratio of the epilimnion velocity to the hypolimnion velocity is equal to the inverse ratio of their depths. It is further evident that for the higher order baroclinic modes the horizontal velocity is constant with depth in the top and bottom layers (since $N = 0$ there) and that conspicuous oscillations with velocities forth and back, etc. arise where $N \neq 0$. Because for each mode ($n \geq 2$) the total volume flux must vanish, the amplitudes of these harmonic oscillations in region II are large in comparison to the values of the ‘tails’ in regions I and III. When trying to identify the baroclinic modes from measurements via isotherm–depth–time series and/or velocity measurements it is compelling that such instruments are moored in the metalimnion and not in the epi- and hypolimnion. Instruments deployed in the epi- and hypolimnion are not likely to reveal reliable information for $n \geq 2$ or $n \geq 3$.

This analysis has shown that the dominant activity of the internal oscillations is seen in the metalimnion where the value of the buoyancy frequency is large. Relatively strong currents in the epi- and hypolimnion may arise for the lowest modes ($n = 1, 2$ and perhaps 3). They become rapidly small as n increases and are then only large and possibly measurable in the metalimnion. It follows that *thermistor chains should, whenever possible, be moored in the metalimnion. Current metres may, however, also be positioned in the epi- and hypolimnion.*

8.5.2.3 Example c: The Constant Density Layer Approximation

As one could easily infer from the above discussion, the dominant mode is the fundamental mode, and so, one may in anticipation of reproducing only the main features of baroclinicity restrict the analysis to a model which only produces this mode. Mathematically, this behaviour can be extracted from the model of Fig. 8.21 by letting the metalimnion thickness shrink to zero, $d \rightarrow 0$, while maintaining the strength of the stratification, $N^2 d$, within it. The eigenvalue problem is still given by (8.75) with $N = 0$ or its nondimensional form (8.78) with $\lambda_n = 0$ in regions I and III, but in region II we now write

$$\frac{N^2}{gh_n} d = \frac{1}{\rho_*} \left(\frac{\rho_H - \rho_E}{d} g \right) \frac{1}{gh_n} d = \frac{1}{\rho_*} \frac{\rho_H - \rho_E}{h_n},$$

which is kept constant in the limit as $d \rightarrow 0$. In fact, we can write this limit in the form

$$\lim_{d \rightarrow 0} \left\{ \frac{N^2}{gh_n} \right\} = \frac{1}{\rho_*} \frac{\rho_H - \rho_E}{h_n} \delta(z + h_E), \quad (8.96)$$

where $h_E = h^+ = h^-$ and $\delta(\cdot)$ is the DIRAC delta function

$$\delta(x) = \begin{cases} \infty, & x = 0, \\ 0, & x \neq 0, \end{cases} \quad \int_{-\infty}^{\infty} \delta(x) dx = 1. \quad (8.97)$$

Then, expression (8.96) ensures that, for a stratification with an infinitely thin metalimnion at $z = -h_E$, the buoyancy frequency tends to infinity within the metalimnion, but elsewhere is equal to zero, and the strength of the stratification remains unchanged

$$\int_{-H}^0 \left\{ \frac{N^2}{gh_n} \right\} dz = \frac{1}{\rho_*} \frac{\rho_H - \rho_E}{h_n}. \quad (8.98)$$

The solutions for the vertical profile of the vertical velocity component in regions I and III are still given by (8.88) and (8.90), or²⁰

$$\begin{aligned} Z^{\text{I}}(z) &= Bz, \\ Z^{\text{III}}(z) &= F(z + H), \end{aligned} \quad (8.99)$$

which have to be continuously connected at $z = h_E$, yielding

$$Bh_E = F(h_E - H) \rightarrow F = B \frac{h_E}{h_E - H}. \quad (8.100)$$

Alternatively in the infinitely thin region II the differential equation (8.75) can formally be written as

$$Z''(z) + \frac{1}{\rho_*} \frac{\rho_H - \rho_E}{h_n} \delta(z + h_E) Z(z) = 0, \quad (8.101)$$

which when integrated from $-(h_E + 0)$ to $-(h_E - 0)$ implies

$$\int_{-(h_E+0)}^{-(h_E-0)} Z''(z) dz + \frac{1}{\rho_*} \frac{\rho_H - \rho_E}{h_n} \int_{-(h_E+0)}^{-(h_E-0)} \delta(z + h_E) Z(z) dz = 0$$

²⁰ We omit the index n , because only a single mode does exist in this case, as will be demonstrated shortly. Furthermore, here we prefer to use the dimensional forms of the equations.

or

$$\underbrace{Z'(-h_E - 0))}_{Z'(-h_E)} - \underbrace{Z'(-h_E + 0))}_{Z'''(-h_E)} + \frac{\rho_H - \rho_E}{\rho_* h_n} \underbrace{Z(-h_E)}_{Z^I(-h_E)} = 0. \quad (8.102)$$

Substituting (8.99) and (8.100) transforms this equation into

$$B \left[\frac{h_E}{h_E - H} - 1 \right] = \frac{\rho_H - \rho_E}{\rho_* h_n} B h_E,$$

from which the eigenvalue

$$h_n = \frac{\rho_H - \rho_E}{\rho_*} \frac{h_E(H - h_E)}{H} = \frac{\Delta\rho}{\rho_*} \frac{h_E h_H}{h_E + h_H} \quad (8.103)$$

is determined. This corroborates that the index n can be dropped, also in $h_n = h_i$. It is called the *equivalent depth* and is given by the product of the normed density difference between the hypolimnion and epilimnion and a depth which is the product of the epilimnion and hypolimnion thicknesses divided by the depth of the total water column. Thus, all oscillations within the metalimnion are lost when its thickness becomes vanishingly small, and there remains only a mode that corresponds to the fundamental mode before. Correspondingly, the horizontal velocities in the upper and lower layers, given by Z' , are uniformly distributed over the respective depths as follows:

$$U^I = B, \quad U^{III} = -\frac{h_E}{H - h_E} B, \quad (8.104)$$

and these obviously satisfy the equal flux condition

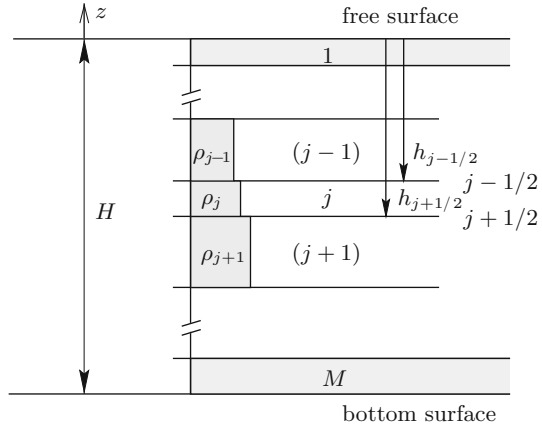
$$U^I h_E = -U^{III}(H - h_E). \quad (8.105)$$

The constant-density-two-layer approximation is a very popular reduction of the full model, because it is able to capture the essential ingredients of the internal wave dynamics that can be observed in lakes. As we have already pointed out, higher order baroclinic modes of a continuous stratification are difficult to identify by measurements because they have appreciable signals only in the metalimnion which for higher order modes have the tendency to die out quickly.

The computation can easily be formalised for an arbitrary number of layers, say M , see Fig. 8.23. Denote the layers from top to bottom by $j = 1, 2, \dots, M$. Let the layer densities ρ_j be constant and assume stable stratification for which $\rho_{j+1} > \rho_j$ for all j . Denote the interfaces between the layers $j - 1$ and j by $j - 1/2$ and the corresponding distance from the free surface by $h_{j-1/2}$. With these definitions the vertical variation of the vertical velocity component in the layers $j - 1$ and j is then given by linear functions as follows:

$$\begin{aligned} Z_{j-1} &= A_{j-1}H + B_{j-1}z, \\ Z_j &= A_jH + B_jz, \end{aligned} \quad (8.106)$$

Fig. 8.23 Water column of depth H is divided into M layers of constant density with density jumps at the interfaces between the layers. The layers are enumerated from $j = 1$ to $j = M$ and the interfaces have half integer identifiers



where A_{j-1} , A_j and B_{j-1} , B_j are constants to be determined. (We have multiplied the constants A_j with H to make A_j , B_j to have the same dimension.) At the interface between the layer $j - 1$ and the layer j the function Z is continuous,

$$Z_{j-1}(-h_{j-1/2}) = Z_j(-h_{j-1/2}) \quad (8.107)$$

and the derivative Z' must satisfy a jump condition analogous to (8.102), namely

$$Z'_{j-1}(-h_{j-1/2}) - Z'_j(-h_{j-1/2}) = -\frac{\rho_j - \rho_{j-1}}{\rho_* h_n} Z_{j-1}(-h_{j-1/2}). \quad (8.108)$$

If the representations (8.106) are substituted into (8.107) and (8.108), two equations emerge involving A_{j-1} , A_j , B_{j-1} , and B_j which, after some simple transformations, can be written in the form

$$\begin{pmatrix} A_j \\ B_j \end{pmatrix} = \begin{bmatrix} 1 + \frac{\Delta\rho_{j-1/2}}{\rho_*} \frac{\zeta_{j-1/2}}{\zeta_n} & -\frac{\Delta\rho_{j-1/2}}{\rho_*} \frac{\zeta_{j-1/2}^2}{\zeta_n} \\ \frac{\Delta\rho_{j-1/2}}{\rho_*} \frac{1}{\zeta_n} & 1 - \frac{\Delta\rho_{j-1/2}}{\rho_*} \frac{\zeta_{j-1/2}}{\zeta_n} \end{bmatrix} \begin{pmatrix} A_{j-1} \\ B_{j-1} \end{pmatrix}, \quad (8.109)$$

where

$$\Delta\rho_{j-1/2} = \rho_j - \rho_{j-1}, \quad \zeta_{j-1/2} = \frac{h_{j-1/2}}{H}, \quad \zeta_n = \frac{h_n}{H}. \quad (8.110)$$

The matrix is called *transfer matrix* and will be denoted by T_{j-1} . Then

$$\begin{pmatrix} A_j \\ B_j \end{pmatrix} = T_{j-1} \begin{pmatrix} A_{j-1} \\ B_{j-1} \end{pmatrix}, \quad (8.111)$$

and repeated application yields

$$\begin{pmatrix} A_j \\ B_j \end{pmatrix} = T_{j-1} T_{j-2} \cdots T_1 \begin{pmatrix} A_1 \\ B_1 \end{pmatrix} \quad (8.112)$$

as well as

$$\begin{pmatrix} A_M \\ B_M \end{pmatrix} = T_{M-1} T_{M-2} \cdots T_1 \begin{pmatrix} A_1 \\ B_1 \end{pmatrix} = T_{\text{total}} \begin{pmatrix} A_1 \\ B_1 \end{pmatrix}. \quad (8.113)$$

Thus, we have been able to relate the final vector $(A_M, B_M)^T$ to the initial vector $(A_1, B_1)^T$.

Next we wish to impose the boundary conditions. At the free surface the rigid lid assumption requires $A_1 = 0$ and at the base the vanishing of the vertical velocity component at $z = -H$ implies $A_M - B_M = 0$. Thus

$$(T_{\text{total}})_{12} - (T_{\text{total}})_{22} = 0. \quad (8.114)$$

This is an $(M - 1)$ -order polynomial equation for the eigenvalue ζ_n . It possesses $(M - 1)$ solutions which can be ordered according to their magnitude. Once these eigenvalues are computed, $(A_j, B_j)^T$ can be determined from (8.112) by starting from $(A_1, B_1)^T = (0, B_1)^T$, which in turn, fixes the solution (8.106) for all $j = 1, 2, \dots, N$.

Problem 8.6 Apply (8.114) to the two-layer model and reproduce with the use of the transfer matrix listed in (8.109) the result (8.103). ♦

Problem 8.7 Consider a three-layer model with constant densities in each layer and derive the eigenvalue equation for the eigenvalues ζ_n . Show in particular that there are two eigenvalues, ζ_1 and ζ_2 , with two eigenmodes. ♦

8.6 Closure

The attempt in this chapter was to demonstrate to the reader that the distribution of mass – i.e. the variation of the water density – within a water body on Earth chiefly dictates how such water bodies behave and react to external forces. The chapter was begun with a verbal description how gravity, wind and solar irradiation may affect the response of a lake to these external sources. The non-linear dependence of the mass density as a function of temperature exerts a dominant effect on how water mass is distributed in a lake. The mere existence of density variations dynamically gives rise to two different types of modes of motion: barotropic or ‘external’ processes, which are essentially imprinted to the lake domain by driving processes at the boundaries, the free surface (wind, atmospheric pressure variation);

and baroclinic or 'internal' processes, which owe their existence to the variation of the buoyancy forces.

Solar irradiation and loss of heat at the surface, of course, also affect the density distribution of the water; the non-linear behaviour of the thermal equation of state with its density maximum at 4°C (for pure water at normal pressure) gives rise to induced convective flow and related possible local mixing of unstably stratified fluid layers and ventilation of the hypolimnion with oxygen-rich surface water. Because the point of maximum density is also pressure and salinity dependent and may even be lost at large salinity and pressure, shallow and deep lakes show different responses to radiative heat input and free surface heat loss. Formation of the thermal bar depends on it as does LANGMUIR circulation.

Homogenisation of a stratified fluid mass in a basin requires energy, since the centre of gravity of the homogenised body lies some millimetres above the centre of gravity of the stably stratified fluid body with the same geometry. The energy needed for this lift is gigantic, but the energy transfer by wind alone is by far larger than the energy that is needed. Mixing, and therefore generation, of conditions of unstable stratification is a prerequisite for its inception. These mechanisms are vital for the so-called overturning process of the water masses of a lake and the associated enrichment of the benthic boundary layer by oxygen.

The motion of the internal water masses in a lake was explained by looking at an isolated small body confined by a virtual skin and in equilibrium with the surrounding water. When experiencing a small displacement out of the equilibrium position, this 'balloon' either oscillates with the buoyancy or BRUNT-VIÄSÄLÄ period if the surrounding water is stably stratified or leaves its unstable equilibrium level with no return.

This gedanken experiment then leads naturally to the analysis of internal oscillations and their characterisation by the existing density structure which, on timescales of the internal oscillations is thought to be frozen into the water performing the oscillations. The linearised shallow water equations of a BOUSSINESQ fluid in a *constant depth fluid layer* with vertical stratification and rigid lid boundary conditions at the undeformed free and bottom surface define the linearised boundary value problem for such waves. A separation of variables technique allowed decomposition of the horizontal and vertical processes with a separation constant serving as eigenvalue for the vertical problem. The emerging STURM-LIOUVILLE eigenvalue problem determined a countable infinite ordered set of eigenvalues and associated eigenfunctions, which depend on the vertical density variation. Solutions were constructed for an n -layer ($n \geq 2$) model with constant densities and a three-layer model with linear stratification in each layer. The characteristic mathematical feature of these solutions is that the vertical eigenvalue problem is uncoupled from the horizontal wave problem, which can be attacked once the vertical problem has been solved. Physically, the distinctive feature is that the amplitudes of the vertical displacements of water particles are proportional to the vertical density gradients, thus generally largest in the metalimnion at the thermocline position.

References

1. Bäuerle, E. and Hollan, E.: Seenphysikalische und limnologische Dokumentation zur Vorstreckung des Alpenrheins in den Bodensee. Eine Literaturstudie. *Ber. IGKB* **42**, 122p. (1993)
2. Bäuerle, E., Ollinger, D. and Ilmberger, J.: Some meteorological, hydrological, and hydrodynamical aspects of Upper Lake Constance. In: *Adv. Limnol.* **53**. Lake Constance. Characterisation of an ecosystem in transition. E.Schweizerbart'sche Verlagsbuchhandlung (Nägele u. Obermiller), Stuttgart (1998)
3. Chubarenko, I.P. and Demchenko, N.Yu.: Laboratory modeling of a thermal bar structure and related circulation in a basin with a sloping bottom. *Oceanology* **48**(3), 356–370 (2008)
4. Cooper, L.H.N. and Vaux, D.: Cascading over the continental slope of water from the Celtic Sea. *J. Mar. Biol. Assoc. UK* **28**, 719–750 (1949)
5. Coulter, G.W.: Low apparent oxygen requirements of deep-water fishes in Lake Tanganyika. *Nature* **215**, 317–318 (1967)
6. Courant, R. and Hilbert D.: *Methods of Mathematical Physics*. Interscience, New York NY. Vol.1, 561p. (1953), Vol.2, 830p. (1962)
7. Cox, S.M. and Leibovich, S.: Langmuir circulations in a surface layer bounded by a strong thermocline. *J. Phys.Oceanogr.* **23**, 1330–1345 (1993)
8. Craik, A.D.D. and Leibovich, S.: A rational model for Langmuir circulations. *J. Fluid Mech.* **73**, 401–426 (1976)
9. Fedorov, K.N.: *Fine Thermohaline Structure of Ocean Water Masses*. Hydrometeoizdat, Leningrad, 184 p. (1976) (in Russian)
10. Fedorov, K.N.: *Physical Nature and Structure of the Oceanic Fronts*. Leningrad, Hydrometeoizdat, 296 p. (1983) (in Russian)
11. Fer, I., Lemmin, U. and Thorpe, S.A.: Observations of mixing near the sides of a deep lake in winter. *Limnol. Oceanogr.* **47**(2), 535–544 (2002)
12. Foster, T.D. and Carmack, E.C.: Frontal zone mixing and Antarctic Bottom Water formation in the Southern Weddel Sea. *Deep-Sea Res.* **23**, 301–317 (1976)
13. Grachev, M.: Slow renewal of deep waters. *Nature* **349**, 654–655 (1991)
14. Hohmann, R., Hofer, M., Kipfer, R., Peeters, F., Imboden, D.M. and Shimaraev, M.N.: Distribution of helium and tritium in Lake Baikal. *J. Geophys. Res.* **103**(12), 823–838 (1998)
15. Horn, W.: *Zürichsee 1978: Physikalisch-limnologisches Messprogramm und Datensammlung*. Interner Bericht Versuchsanstalt für Wasserbau, Hydrologie und Glaziologie an der ETH, Zürich (1981)
16. Hutchinson, G.E.: *A treatise on limnology*. Geography, Phys. And Chemistry, New York NY, 1016 p. (1957)
17. Hutter, K.: Linear gravity waves, Kelvin waves, Poincaré waves, Theoretical modelling and observations. In: *Hydrodynamics of Lakes*. (ed. Hutter, K.) Springer, New York, NY, 39–80 (1984)
18. Hutter, K.: Waves and oscillations in the ocean and in lakes. In: *Continuum Mechanics in Environmental Sciences and Geophysics*. (ed. Hutter, K.) Springer, New York, NY 79–240 (1993)
19. Hutter, K. and Jöhnk, K.: *Continuum Methods of Physical Modeling*. Springer Berlin, 635 p. (2004)
20. Ivanov, V.V., Shapiro, G.I., Huthnance, J.M., Aleynik, D.L. and Golovin, P.N.: Cascades of dense water around the world ocean. *Prog. Oceanog.*, **60**(1), 47–98 (2004)
21. Jacobs, S.S., Amos, A.F. and Bruchhauser, P.M.: Ross Sea oceanography and Antarctic Bottom Water formation. *Deep-Sea Res.* **17**, 935–962 (1970)
22. Killworth, P.D.: On 'chimney' formation in the ocean. *J.Phys.Oceanogr.* **9**, 531–554 (1979)
23. Kodonev, G.G.: Deep-water renewal in Lake Baikal. *Geol. Geofiz.* **42**, 1127–1136 (2001)
24. Langmuir, I.: Surface motion of water induced by wind. *Science* **87**, 119–123 (1938)
25. Lazier, J.R.N.: The renewal of Labrador Sea water. *Deep-Sea Res.* **20** 341–353 (1973)

26. Leaman, K.D. and Schott, F.A.: Hydrographic structure of the convection regime in the Gulf of Lions: winter 1987. *J. Phys. Oceanogr.* **21**, 575–598 (1991)
27. LeBlond, P.H. and Mysak, L.A.: *Waves in the Ocean*. Elsevier, Amsterdam, 602 p. (1978)
28. Lighthill, J.: *Waves in Fluids*. Cambridge University Press, Cambridge, 504 p. (1978)
29. McDougall, T.J.: Thermobaricity, cabbeling and water mass conversion. *J. Geophys. Res.* **92** (C5), 5448–5464 (1987)
30. MEDOC Group: Observation of formation of deep water in the Mediterranean Sea. *Nature* **227**, 1037–1040 (1970)
31. Meirowich, L.: *Analytical Methods of Vibration*. MacMillan, London, 555 p. (1969)
32. Rossby, H.T.: On thermal convection driven by non-uniform heating from below: an experimental study. *Deep-Sea Res.* **12**, 9–16 (1965)
33. Send, U. and Marshall, J.: Integral effect of deep convection. *J. Phys. Oceanogr.* **25**, 855–872 (1975)
34. Shimaraev, M.N., Verbolov, V.I., Granin, N.G. and Sherstyankin, P.P.: *Physical Limnology of Lake Baikal: a Review*. Baikal International Center for Ecological Research, Irkutsk-Okayama, 81 p. (1994)
35. Sturman, J.J., Oldham, C.E. and Ivey, G.N.: Steady convective exchange flow down slopes. *Aquat. Sci.* **61**, 260–278 (1999)
36. Tikhomirov, A.I.: *Thermics of Large Lakes*. Leningrad, Nauka, 232 p. (1982) (in Russian)
37. Turner, J.S.: *Buoyancy Effects in Fluids*. Cambridge University Press, Cambridge, MA 432 p (1973)
38. Weiss, R.F., Carmack, E.C. and Koropalov, V.M.: Deepwater renewal and biological production in Lake Baikal. *Nature* **349**, 665–669 (1991)
39. Wüest, A., Ravens, T., Granin, N., Kocsis, O., Schurter, M. and Sturm, M.: Cold intrusions in Lake Baikal: Direct observational evidence for deep-water renewal. *Limnol. Oceanogr.* **50**(1), 184–196 (2005)

Chapter 9

Vertical Structure of Wind-Induced Currents in Homogeneous and Stratified Waters

9.1 Preview and Scope of This Chapter

In this chapter the intention is to describe the vertical and (eventually) also horizontal structure of the horizontal current in lakes which are subjected to external wind forces. The water will be assumed to be homogeneous or stratified in two layers, and the internal friction and the effects of the rotation of the Earth will play an important role in the establishment of the current distribution.

The focus will be, first, on steady applied wind input into narrow one- and two-layer fluid systems of finite horizontal extent and finite or infinite vertical extent for which the effects of the rotation of the Earth can be ignored. The hydrodynamic equations are formulated in a simplified form in which conditions of linearity are fulfilled with sufficient accuracy, and it will be assumed that among all viscous stresses only the vertical shear stress components are of significance, and these can be parameterised by a linear NEWTONian rheology. Simple solutions are developed for water movements in a narrow rectangular basin subjected to steady wind directed along its length. Vertical structures of current are derived for one- and two-layered systems. These solutions are constructed for constant vertical eddy viscosity; this assumption allows analytical construction of solutions and therefore leads to a direct physical understanding of the circulation pattern that is developed in one- and two-layered fluid systems.

While the finite horizontal extent of the fluid system is an important prerequisite for the establishment of the circulation pattern in one- and two-layered systems, the structure of the vertical distribution of the horizontal current in a homogeneous layer of fluid subject to steady uniform wind when both the internal friction and the rotation of the Earth are taken into account is best seen when the horizontal extent is infinite. The formulation of this problem for constant vertical eddy viscosity is known as the EKMAN [12] theory (1905), and the vertical structure of the horizontal current is established in the form of the so-called EKMAN spiral. A typical parameter of the governing equations of this problem is the so-called EKMAN depth $D = \pi \sqrt{2\nu/f}$, where ν is the constant vertical eddy viscosity and f the CORIOLIS parameter. If a fluid layer is infinitely deep, then the horizontal current due to steady, uniform wind rotates anticyclonically with increasing depth and decreases exponentially such that at a depth equal to D the angle of rotation is 180° relative to the surface current and

its magnitude is reduced by a factor $\exp(-\pi) = 0.0432$. Moreover, the horizontal current at the free surface is rotated *cum sole*¹ by an amount of 45° . On the other hand, if the fluid layer is of finite depth H , then this EKMAN solution is modified according to the H/D ratio. For $H/D \gg 1$ (effectively $H/D > 1.5$) the solution is very close to the classical EKMAN solution. For $H/D < 1$ the rotation of the horizontal current with depth is less conspicuous and decreases with decreasing value of H/D . Furthermore, the angle of deviation of the direction of the surface water current from the direction of the wind is less than 45° , for $H/D < 0.1$ it is smaller than 10° . A similar effect is also exerted by a non-constant vertical distribution of the vertical eddy viscosity, implying that appropriate consideration to the numerical values of the viscosity and its spatial distribution is practically very important.

One key feature of the EKMAN problem in a fluid layer of infinite horizontal extent is the fact that for uniform atmospheric pressure the absence of side boundaries prevents the free surface from any deformation. So, a first step to guarantee solutions in regions of finite extent is to add in the horizontal momentum equation a horizontal pressure gradient due to the weight of the non-uniformly displaced fluid and to pretend that this surface displacement is known as a function of the horizontal coordinates. The steady EKMAN problem can also be constructed for this case, and the additional currents due to this pressure gradient are called *gradient currents*. The next step is then the postulation that the vertical distribution of the horizontal current thus constructed is adequate also in a finite lake domain with variable bathymetry. The only missing link is then the complementation of these equations with the depth-integrated continuity equation. What results is an elliptical differential equation for the depth-integrated volume transport stream function. The method has been applied to real lakes despite the fact that it is very difficult in practice to find wind scenarios which are close to steady state. Results are presented for Lake Erie as applied by GEDNEY and LICK [20], and comparison of the limited results with observation is surprisingly good.

A last application of the 'EKMAN solution procedure' is its extension to time-dependent wind input and therefore time-dependent lake response. Here, an approach of solution due to PLATZMAN is presented. This approach is approximate (as are all others). The gist of the approach is in this case to vertically integrate the horizontal momentum equations. This generates a term τ_b/ρ , where τ_b is the shear stress at the basal surface, which must be parameterised to transform the vertically integrated continuity and horizontal momentum equations into an integrable system of evolution equations. The various methods differ by the approach how the closure for τ_b/ρ is achieved. The first proposal has been given by WELANDER in 1957 [52]; we present here in detail PLATZMAN's [43] (1963) solution, who has applied his method to a storm surge analysis of Lake Erie, of which an excerpt is presented. Observed and measured surface elevation time series (set-up) at six limnigraph stations around Lake Erie show very good agreement (Fig. 9.1).

¹ Cum sole [Latin: 'with the sun'] – ancient expression of the rotation in the same direction as the Sun moves during a day, i.e. clockwise in the Northern Hemisphere, anticlockwise in the Southern. Convenient and still often used in geophysics since it shows how a moving body is turned by the Coriolis force in both hemispheres. Opposite direction is 'contra solem' [Latin: 'against the sun'].



Fig. 9.1 *Left:* George W. PLATZMAN (<http://news.uchicago.edu/>). *Right:* Vagn Walfrid EKMAN (<http://en.wikipedia.org/>)

Vagn Walfrid EKMAN (3 May 1874 – 9 March 1954) was a Swedish oceanographer. He became committed to oceanography at the University of Uppsala on hearing Vilhelm BJERKNES lecture on fluid dynamics. During the expedition of the *Fram*, Fridtjof NANSEN had observed that icebergs tend to drift not in the direction of the prevailing wind but at an angle of $20 - 40^\circ$ to the right. BJERKNES invited EKMAN, still a student, to investigate the problem and, in 1905, EKMAN published his theory of the EKMAN spiral which explains the phenomenon in terms of the balance between frictional effects in the ocean and the CORIOLIS force, which arises from planetary rotation. On completing his doctorate in Uppsala in 1902, EKMAN joined the International Laboratory for Oceanographic Research, Oslo, where he worked for 7 years, not only extending his theoretical work but also developing experimental techniques and instruments, e.g. the EKMAN current metre and EKMAN water bottle. From 1910 to 1939 he continued his theoretical and experimental work at the University of Lund, where he was professor of mechanics and mathematical physics. He was elected a member of the Royal Swedish Academy of Sciences in 1935. A gifted amateur bass singer, pianist, and composer, he continued working right up to his death.

George W. PLATZMAN (19 April 1920 – 02 August 2008), meteorologist, who earned his bachelor's and master's degrees in mathematics and physics from the Universities Chicago and Arizona in 1940 and 1941, respectively, and a Ph.D. in meteorology from the University of Chicago in 1947, joined the faculty of the University's Meteorology Department in 1948. He remained there when he retired as Professor Emeritus. PLATZMAN, one of the founders of modern meteorology, transformed weather forecasting from qualitative guesswork to quantitative science. He specialised in dynamic meteorology and oceanography, including numerical weather prediction and storm surges, which are caused by wind and in the Great Lakes' area due to Hurricanes. He has pioneered weather forecast by computer, laid down the theory of storm surges and participated in the development of advanced computer software to model and forecast variations of surface elevation fields in the ocean and in lakes. He summarised his research in seminal papers, e.g. articles on the ocean tides and the storm surge theory and a comprehensive review of the ROSSBY wave. PLATZMAN's personal interests included collecting early printed editions of musical compositions by Frédéric CHOPIN. He established the Rose K. PLATZMAN Memorial Collection at the University of Chicago Library in honour of his mother.

The text is based on <http://en.wikipedia.org/> and <http://news.uchicago.edu/>

9.2 Hydrodynamic Equations Applied to a Narrow Lake Under Steady Wind

In this section the linear viscous hydrodynamic equations are used to develop simple solutions for water movements in a narrow rectangular basin subjected to steady wind directed along its length. Vertical structures of the current are derived for one- and two-layer systems, representing, respectively, a lake during conditions of winter homogeneity and summer stratification. Simplicity is intended so that analytical solutions of the governing equations are achieved by linearisation, the use of constant coefficients of the momentum viscosity, later somewhat relaxed, and the neglect of the CORIOLIS force. The solutions illustrate some important facts about the dynamics of wind-driven flows in a long narrow lake of constant depth.² The solutions provide insight into the current behaviour and may be guiding elements for circulations in more complicated basins for which solutions must be sought by numerical means.

9.2.1 Wind-Induced Steady Circulation in a Narrow Homogeneous Lake of Constant Depth

Consider a rectangular basin of length ℓ and depth h , subjected to a steady longitudinal wind stress τ_s of prescribed distribution along the length of the basin. Atmospheric pressure p_a is assumed to be uniform and constant over the water surface and time. We take the axes $Oxyz$ with O in the undisturbed lake surface (at one end); Ox is directed along the length and Oz vertically downwards as shown in Fig. 9.2. The y -axis is towards the reader, but since motions are assumed to be plane, the Oy direction is under the stated assumptions not relevant.

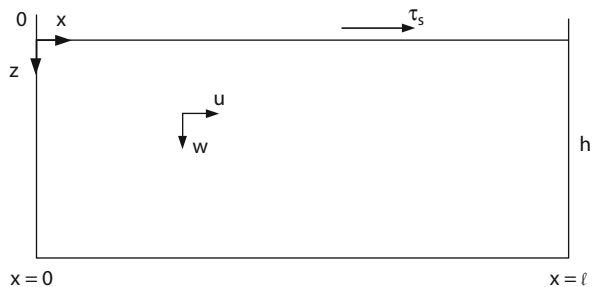


Fig. 9.2 Rectangular basin. Definition of wind shear stress, velocity components, u , w and Cartesian coordinates x , y , z

² The qualification of the basin to be 'narrow' is necessary since only under such a restriction the Coriolis force can be ignored.

Problem 9.1 Assuming that the motion is two-dimensional in the vertical xz -plane, ignoring CORIOLIS and non-linear convective acceleration, retaining only vertical shears and ignoring the other NEWTONian viscous stresses show that the dynamical equations take the forms

$$\begin{aligned} -\frac{\partial p}{\partial x} + \frac{\partial \tau_{zx}}{\partial z} &= 0, & \frac{\partial u}{\partial x} + \frac{\partial w}{\partial z} &= 0, \\ \frac{\partial p}{\partial z} &= \rho g, & \frac{\partial}{\partial x} \int_0^h u \, dz &= 0. \end{aligned} \quad (9.1)$$

The equations on the left are what remains of the horizontal and vertical momentum equations – they reduce to a force balance; the equations on the right are the continuity equation and the zero flux condition through any vertical cross-section due to the incompressibility and steady flow conditions. Moreover,

$$\tau_{zx} = \rho \nu \left(\frac{\partial u}{\partial z} + \frac{\partial w}{\partial x} \right) \simeq \rho \nu \frac{\partial u}{\partial z}, \quad (9.2)$$

in which ν is the kinematic viscosity (here of the turbulent motion).³ ◆

For homogeneous water, $\rho = \text{constant}$ and, therefore, by satisfying the surface condition

$$p = p_a \quad \text{at } z = -\zeta, \quad (9.3)$$

where p_a is assumed to be a constant, (9.1)₃ may be integrated to give

$$p = p_a + \rho g(z + \zeta), \quad (9.4)$$

so that

$$\frac{\partial p}{\partial x} = \rho g \frac{\partial \zeta}{\partial x}. \quad (9.5)$$

Hence, from (9.1)₁ we deduce

$$\frac{\partial \tau_{zx}}{\partial z} = \rho g \frac{\partial \zeta}{\partial x},$$

³ In turbulent motions (9.2) generally takes the form

$$\tau_{zx} = \rho \nu_V \frac{\partial u}{\partial z} + \rho \nu_H \frac{\partial w}{\partial x}$$

and it is concluded that $|\nu_V \partial u / \partial z| \gg |\nu_H \partial w / \partial x|$. For a detailed explanation of turbulence, see Chap. 6.

which may be integrated to yield

$$\tau_{zx} = \rho g \frac{\partial \zeta}{\partial x} z + A = \rho v \frac{\partial u}{\partial z}, \quad (9.6)$$

from which for constant v it follows that

$$\rho v u = \frac{1}{2} \rho g \frac{\partial \zeta}{\partial x} z^2 + Az + B. \quad (9.7)$$

The two constants of integration, A and B , may be determined by satisfying, first, the bottom no-slip condition

$$u = 0 \quad \text{at } z = h, \quad (9.8)$$

which gives

$$0 = \frac{1}{2} \rho g \frac{\partial \zeta}{\partial x} h^2 + Ah + B. \quad (9.9)$$

Using this equation to eliminate B in (9.7) yields

$$\rho v u = \underbrace{\frac{1}{2} \rho g \frac{\partial \zeta}{\partial x} (z^2 - h^2)}_{\text{'set up current'}} + \underbrace{A (z - h)}_{\text{'slope' or 'gradient' current}}. \quad (9.10)$$

Second, to find A , note that (9.1)₄ implies that the longitudinal velocity obeys $\int_0^h u dz = \text{constant}$, which owing to

$$u = 0 \quad \text{at } x = 0, x = \ell \quad (9.11)$$

implies

$$\int_0^h u dz = 0. \quad (9.12)$$

Equations (9.10) and (9.12) yield

$$A = -\frac{2}{3} \rho g h \frac{\partial \zeta}{\partial x}. \quad (9.13)$$

Therefore, from (9.6),

$$\tau_{zx} = \frac{1}{3} \rho g \frac{\partial \zeta}{\partial x} (3z - 2h), \quad (9.14)$$

and from (9.10)

$$u = \frac{g}{6\nu} \frac{\partial \zeta}{\partial x} (h - z)(h - 3z). \quad (9.15)$$

The last two formulae show that the vertical shear stresses and the longitudinal velocities have been found; however, they are expressed in terms of the set-up $\partial \zeta / \partial x$, which still must be determined. To find $\partial \zeta / \partial x$, the surface condition

$$\tau_{zx} = -\tau_s \quad \text{at } z = 0 \quad (9.16)$$

(note for a wind in the positive x -direction the surface shear stress is negative in the chosen coordinate system) is inserted in (9.14) to give

$$\tau_s = \frac{2}{3} \rho g h \frac{\partial \zeta}{\partial x} \quad \rightarrow \quad \frac{\partial \zeta}{\partial x} = \frac{3\tau_s}{2\rho g h}. \quad (9.17)$$

Substituting this result into (9.14) and (9.15) generates the further results

$$\tau_{zx} = -\frac{\tau_s}{2h} (2h - 3z), \quad u = \frac{\tau_s}{4\rho \nu h} (h - z)(h - 3z). \quad (9.18)$$

Next, the vertical velocity component is found from the continuity equation by integration; this yields

$$w = - \int_h^z \frac{\partial u}{\partial x} dz \quad (+ w(z = h) = 0), \quad (9.19)$$

where the term in parentheses expresses the no-flux condition through the bottom boundary. Inserting (9.18)₂ into (9.19) allows evaluation of the integral. The result is

$$w = -\frac{\tau'_s}{4\rho \nu h} z(z - h)^2, \quad \tau'_s := \frac{d\tau_s}{dx}. \quad (9.20)$$

With the velocity components u and w determined, the streamlines of the fluid particles can be computed by integrating the equation

$$\frac{dz}{dx} = \frac{w}{u} = -\frac{\tau'_s}{\tau_s} \frac{z(h - z)}{h - 3z}, \quad (9.21)$$

from which we deduce

$$- \int \frac{3z - h}{z(z - h)} dz = \int \frac{\tau'_s}{\tau_s} dx,$$

whence

$$-\ln(z(z-h)^2) = \ln \frac{\tau_s}{C},$$

and therefore

$$z(z-h)^2 \tau_s = C. \quad (9.22)$$

The choice of the value for the constant of integration, C , parameterizes the streamlines.

Notice that the above solution, expressed by (9.18)_{1,2}, (9.20) and (9.22), satisfies the requirement that the vertically integrated flow at any cross-section between $x = 0$ and $x = \ell$ vanishes; but it still does not automatically satisfy the boundary conditions (9.11) locally for all depths. To satisfy completely the no-flow conditions at each end, we need to define τ_s such that

$$\tau_s = 0 \quad \text{at } x = 0 \text{ and } x = \ell. \quad (9.23)$$

Practically, these conditions are no severe limitation of the wind stress τ_s since, except for (9.23), the distribution of τ_s along the length of the basin is still arbitrary. Finally, integrating (9.17)₂ and satisfying the volume-preserving condition

$$\int_0^\ell \zeta dx = 0$$

yields the elevation of the water surface in the form

$$\begin{aligned} \zeta &= \frac{3}{2\rho gh} \left\{ \int_0^x \tau_s(x') dx' - \frac{1}{\ell} \int_0^\ell dx \int_0^x \tau_s(x') dx' \right\} \\ &= \frac{3}{2\rho gh} \left\{ \int_0^x \tau_s(x') dx' - \frac{1}{\ell} \int_0^\ell (\ell - x) \tau_s(x) dx \right\}, \end{aligned} \quad (9.24)$$

where the expression in the second line has been obtained by employing integration by parts in the double integral. When τ_s is uniformly distributed over x , then $\tau_s(x) = \text{constant} = \tau_0$, and (9.24) reduces to

$$\zeta = \frac{3\tau_0}{4\rho gh} (2x - \ell). \quad (9.25)$$

Summarizing, the non-dimensional forms of the stress, current, streamline and elevation formulae take the forms

$$\begin{aligned}
\hat{\tau} &:= \frac{\tau_{zx}}{(-\tau_s)} = 1 - \frac{3}{2}\mathfrak{z}, \\
\hat{u} &:= \frac{u}{\left(\frac{h\tau_s}{4\rho\nu}\right)} = (1 - \mathfrak{z})(1 - 3\mathfrak{z}), \\
\hat{w} &:= \frac{w}{\left(\frac{h^2\tau'_s}{4\rho\nu}\right)} = -\mathfrak{z}(1 - \mathfrak{z})^2, \\
3(1 - \mathfrak{z})^2 &= \hat{C} := \frac{C}{\tau_s h^2}, \\
\hat{\zeta} &:= \frac{\zeta}{h} = \frac{3(\tau_s)_{\max}}{2\rho gh} \left(\frac{\ell}{h}\right) \left\{ \int_0^{\mathfrak{x}} \frac{\tau_s}{(\tau_s)_{\max}}(\mathfrak{x}') d\mathfrak{x}' - \int_0^1 (1 - \mathfrak{x}') \frac{\tau_s}{(\tau_s)_{\max}} d\mathfrak{x}' \right\},
\end{aligned} \tag{9.26}$$

in which $\mathfrak{x} := x/\ell$ and $\mathfrak{z} := z/h$ are the dimensionless length and depth coordinates $\hat{\tau}$, \hat{u} , \hat{w} , and the streamlines are plotted in Fig. 9.3a, b as solid lines. Note, the wind-driven flow near the surface and the counter-current at greater depths are formed by two competing effects, which are best set in evidence by the formulae (9.10) and (9.13). The first term on the right-hand side of (9.10) may be called the ‘set-up current’ and is negative, i.e. against the wind. The second term is positive (note, A is negative for positive set-up) and generally denoted ‘slope’, ‘gradient’ or ‘wind drift’ current and varies linearly with depth.

The vertical shear stress is linearly distributed with depth and assumes at the bottom half the value of the wind stress, but is oppositely directed. Furthermore, the longitudinal return current assumes its maximum value $(1/3)u_{\text{surface}} = (1/3)u_{\text{sc}}$ at $(2/3)h$, and the maximum vertical velocity is the $4/27$ part of the scale velocity $w_{\text{sc}} = (h^2\tau'_s/(4\rho\nu))$ and is reached at the depth of $(1/3)h$. Moreover, \hat{u} and \hat{w} are independent of the length coordinate since the scale velocities

$$u_{\text{sc}} = \frac{h\tau_s}{4\rho\nu}, \quad w_{\text{sc}} = \frac{h^2\tau'_s}{4\rho\nu} \tag{9.27}$$

contain this dependence via τ_s and τ'_s , respectively. The formulae indicate that the absolute values of u and w are determined by u_{sc} and w_{sc} . This implies that for prescribed τ_s , ρ and ν , the velocity components u and w grow linearly and quadratically with h . This is certainly unrealistic. So, the (turbulent) viscosity ν should vary with depth and grow at least in proportion to h^2 for u and w , to remain bounded as h becomes large. This is consistent with the fact that the magnitudes of the coefficients of eddy viscosity usually increase with the size of the region considered ([46], p. 104). The general character of the streamlines in the vertical xz -plane is sketched in panel (b) of Fig. 9.3. They form closed loops, symmetric here relative to the position $\mathfrak{x} = 1/2$ and are sketched in the figure for a symmetric wind stress distribution, which reaches a maximum midway between the basin ends. ‘Alternating’

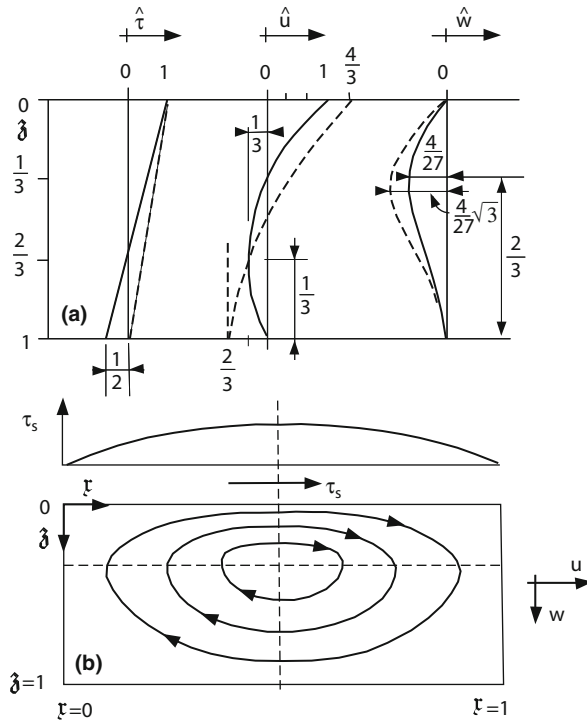


Fig. 9.3 (a) Vertical structure of the vertical shear $\hat{\tau}_{xz}$ and current components \hat{u} and \hat{w} for no slip at the bottom ($\delta = 0$, solid lines) and perfect sliding at the bottom ($\delta = 1/2$, dashed lines) according to (9.26). (b) Streamlines as obtained with $\delta = 0$ and the corresponding wind stress distribution. The basin is narrow perpendicular to the plane of the figure and CORIOLIS forces are ignored in the construction of the solution, adapted from HEAPS [23]

circulation cells which are counter-rotated would form if the wind shear stress $\tau_s(x)$ would alter its sign in $x \in [0, \ell]$.

This derivation follows HEAPS [23]. An alternative derivation has also been carried out by BYE [4], using, however, a formulation for ν based on the PRANDTL mixing length.

9.2.2 Influence of Bottom Slip on the Wind-Induced Circulation

The preceding solution for circulation in a homogeneous narrow lake assumes zero slip at the bottom, see (9.8). Alternatively, a slip condition may be used in which the shear stress at the bottom is expressed as

$$\tau_{xz} = k\rho u \quad \text{at } z = h, \quad (9.28)$$

in which k is the friction (drag) coefficient. For $k = 0$ the basal shear stress vanishes and ideal slip conditions prevail; for $k \rightarrow \infty$ the basal shear stress remains only bounded if $u \rightarrow 0$ at the base, which corresponds to the no-slip condition treated in the last subsection.

The sliding friction law (9.28) is subject to criticism as it is well known that measurements suggest $k = c|u|$, where c is now a dimensionless parameter. However, c is neither a constant under realistic conditions of turbulence. So, we take (9.28) with constant k with dimension m s^{-1} as a first approximation for which an analytical solution can be constructed. Improvements of the parameterisation of the sliding law will be dealt with later on in this chapter.

Problem 9.2 Repeat the analysis of Sect. 9.2.1 if basal friction is prescribed by (9.28) and show that formulae (9.26) for the dimensionless shear stress $\hat{\tau}$, velocity components \hat{u} , \hat{w} and surface set-up $\hat{\xi}$ can be written as

$$\begin{aligned}\hat{\tau} &= \frac{(1 + \delta) - \frac{3}{2}\mathfrak{z}}{(1 + \delta)}, \\ \hat{u} &= \frac{(1 - \mathfrak{z})(1 - 3\mathfrak{z} + 4\delta) - 2\delta}{(1 + \delta)}, \\ \hat{w} &= -\frac{\mathfrak{z}(1 - \mathfrak{z})(1 - \mathfrak{z} + 2\delta)}{(1 + \delta)}, \\ \hat{\xi} &= \frac{3(\tau_s)_{\max}}{2\rho gh(1 + \delta)} \left(\frac{\ell}{h} \right) \left\{ \int_0^{\mathfrak{r}} \frac{\tau_s}{(\tau_s)_{\max}}(\mathfrak{r}') d\mathfrak{r}' - \int_0^1 (1 - \mathfrak{r}') \frac{\tau_s}{(\tau_s)_{\max}} d\mathfrak{r}' \right\},\end{aligned}\tag{9.29}$$

where

$$\delta = \frac{1}{\beta + 2}, \quad \beta = \frac{kh}{\nu}\tag{9.30}$$

are non-dimensional parameters. ◆

The results (9.29) reduce for $\delta = 0$ (or $\beta \rightarrow \infty$) to the earlier results and embrace for

$$0 \leq k < \infty, \quad 0 \leq \beta < \infty, \quad \frac{1}{2} \geq \delta > 0\tag{9.31}$$

all basal conditions from no slip ($\beta \rightarrow \infty$, $\delta = 0$) to perfect sliding ($\beta = 0$, $\delta = 1/2$). The vertical profiles of the shear stresses and velocity components for perfect sliding at the bottom are displayed in Fig. 9.3a as dashed lines. We observe

- For perfect slip the shear stresses $\hat{\tau}$ do not change sign with depth and vanish at the bottom. For viscous sliding the profiles lie between the solid and dashed lines.

- The horizontal current \hat{u} increases at the free surface by $1/3$ to the value $4/3$ and reaches the value $-2/3$ at the bottom with slope zero (vertical tangent). For viscous sliding the position of the relative maximum of the return current lies at $\mathfrak{z} = (2/3)(1 + \delta)$ (for $\delta = 1/2$ this yields $\mathfrak{z} = 1$) and has a value between 0 and $-2/3$.
- The absolute value of the vertical current between the surface and the bottom becomes larger but the profile remains the same. In this case the maximum of the absolute value of \hat{w} occurs at

$$\mathfrak{z}_{\max} = \frac{2}{3}(1 + \delta) \pm \sqrt{\frac{4}{9}(1 + \delta)^2 - \frac{1}{3}(1 + 2\delta)}. \quad (9.32)$$

For no-bottom slip, $\delta = 0$, these maxima occur at $\mathfrak{z}_{\max} = 1/3$ and $\mathfrak{z}_{\max} = 1$, implying that $\hat{w}|_{\mathfrak{z}=1} = 0$ and $d\hat{w}/d\mathfrak{z}|_{\mathfrak{z}=1} = 0$, while $\hat{w}|_{\mathfrak{z}=1/3} = 4/27$. On the other hand, for perfect basal sliding $\hat{w}|_{\mathfrak{z}=1}$ has a non-zero upward vertical gradient (the second relative maximum is outside the fluid region $\mathfrak{z}_{\max} > 1$). The absolute maximum of \hat{w} inside the rectangular basin arises at $\mathfrak{z}_{\max} = 1 - \sqrt{1/3}$ and takes the value $\hat{w}|_{\mathfrak{z}=1-\sqrt{1/3}} = \hat{w}|_{\mathfrak{z}=0.426} = 4\sqrt{3}/27$. This value is a factor $\sqrt{3}$ larger than when the no-slip condition is applied at the bottom, and it lies below the relative maximum of \hat{w} in the no-slip case.

From the above description and Fig. 9.3a it is quite easy to qualitatively guess the distributions of $\hat{\tau}$, \hat{u} and \hat{w} for values of δ in the interior of the interval $\delta \in (0, 1/2)$.

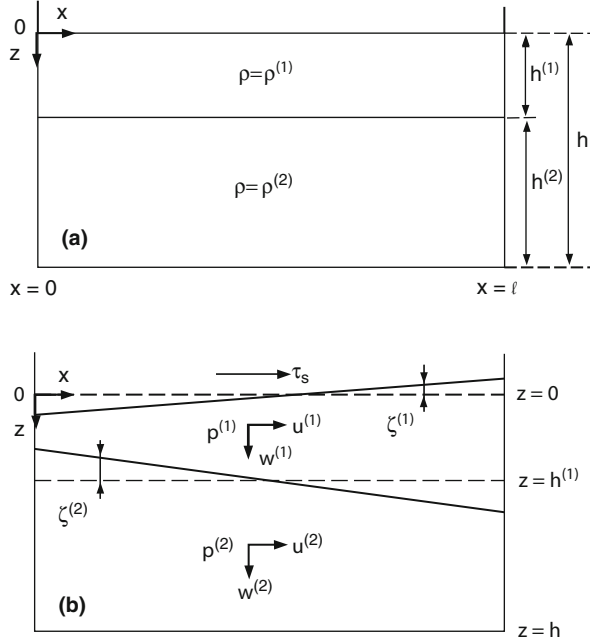
9.2.3 Wind-Induced Steady Circulation in a Narrow Lake Stratified in Two Layers

As one would expect, the circulation pattern induced in a layered fluid is quite different from that of a homogeneous fluid. Consider a narrow rectangular basin with constant ρ_1, h_1 (epilimnion) and constant $\rho_2 > \rho_1, h_2$ (hypolimnion) and assume the interface between the two layers to be impermeable. We interpret this interface as the thermocline and suppose it to be sharp, i.e. without thickness. (Remarks concerning a diffuse interface will be given later in the book.) Notation and sketches of the geometry in a configuration at rest and in motion are given in Fig. 9.4.

Problem 9.3 *When considerations are restricted to plane flow in the xz -plane, CORIOLIS forces and convective accelerations are neglected, and only vertical shear stresses of the viscous stresses are retained, show that the balance laws of mass and momentum in the two layers can be written as*

$$\begin{aligned} -\frac{\partial p^{(i)}}{\partial x} + \frac{\partial \tau_{zx}^{(i)}}{\partial z} &= 0, & \frac{\partial u^{(i)}}{\partial x} + \frac{\partial w^{(i)}}{\partial z} &= 0, \\ \frac{\partial p^{(i)}}{\partial z} &= \rho^{(i)} g, & (i &= 1, 2). \end{aligned} \quad (9.33)$$

Fig. 9.4 Two-layered basin. (a) Definition of the geometry of the two-layer basin, coordinates and notation. (b) The two layers are shown with deformed surfaces (*solid*) and notation of the wind shear stress, τ_s , displacements $\zeta^{(1)}$, $\zeta^{(2)}$ and velocities $u^{(i)}$, $w^{(i)}$ ($i = 1, 2$)



Moreover, volume preserving under steady conditions implies for each layer and all $x \in [0, \ell]$

$$\int_0^{h_1} u^{(1)} dz = 0, \quad \int_{h_1}^h u^{(2)} dz = 0. \quad (9.34)$$

Equations (9.33)_{1,3} give the horizontal and vertical momentum balance laws when acceleration terms are ignored, and (9.33)₂ expresses local volume preserving in both layers. \blacklozenge

If we also assume constant vertical (eddy) viscosities $\nu^{(i)}$ ($i = 1, 2$) in the upper and lower layers, respectively, we have for linear (NEWTONian) behaviour

$$\tau_{zx}^{(i)} = \rho^{(i)} \nu^{(i)} \frac{\partial u^{(i)}}{\partial z}, \quad (i = 1, 2), \quad (9.35)$$

in which contributions $\rho^{(i)} \nu^{(i)} [\partial w^{(i)} / \partial x]$ have been ignored as in (9.2). Equations (9.33), (9.34) and (9.35) must be complemented by boundary and transition

conditions at the free surface, the interface and the bottom surface. Because we are restricting considerations to a linear theory, these are formulated at the undeformed surfaces and read

(i) At the free surface

$$\left. \begin{aligned} p^{(1)} &= \text{constant} (= p_a), & \text{at } z = -\zeta_1, \\ \tau_{zx}^{(1)} &= -\tau_s(x), & \text{at } z = 0, \end{aligned} \right\} \quad (9.36)$$

expressing constant atmospheric pressure and prescribed steady wind shear stress, a function of x .

(ii) At the interface between the upper and the lower layers we have

$$\left. \begin{aligned} p^{(1)} &= p^{(2)}, & \text{at } z = h_1 - \zeta_2, \\ \tau_{zx}^{(1)} &= -\tau_{zx}^{(2)}, & \text{at } z = h_1, \end{aligned} \right\} \quad (9.37)$$

and this requests continuity of pressure and vertical shear stresses.⁴ We also assume the two layers not to intermix at the interface but to slide on one another according to the sliding law

$$\tau_{zx}^{(1)} = k^{(1)} \rho^{(1)} (u^{(2)} - u^{(1)}), \quad \text{at } z = h_1, \quad (9.38)$$

where $k^{(1)}$ is a constant drag coefficient. For free slip between the fluids at the interface we have $k^{(1)} = 0$, implying vanishing shear stress $\tau_{zx}^{(1)}$ for no relative slip ($k^{(1)} \rightarrow \infty$), implying $u^{(1)} = u^{(2)}$.

(iii) At the basal surface we impose a viscous linear sliding condition

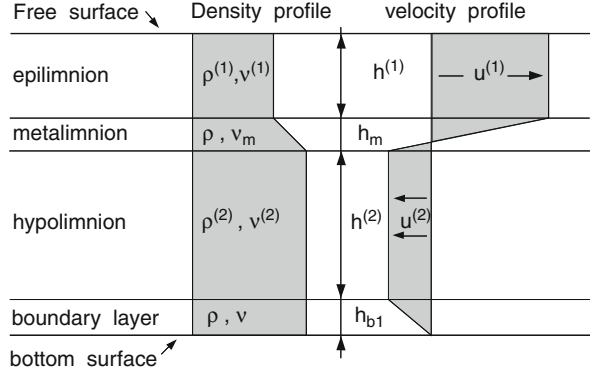
$$\tau_{zx}^{(2)} = k^{(2)} \rho^{(2)} u^{(2)}, \quad (9.39)$$

where $k^{(2)}$ is a constant, and $k^{(2)} = 0$ and $k^{(2)} \rightarrow \infty$ correspond to perfect slip and no slip, respectively.

The parameterisations (9.38) and (9.39) need further explanations. They are limiting approximations for a diffuse metalimnion and a bottom boundary layer as sketched in Fig. 9.5. Within the metalimnion of thickness h_m the vertical shear stress is approximately given by

⁴ Notice that the continuity requirement in (9.36) and (9.37) for pressure is requested to be satisfied at the actual interface position, while that for the shear stresses is applied at the undeformed interface. Scrutiny of the solution of the formulated problem with both continuity statements (9.36) and (9.37) applied at the deformed surface shows that non-linearities are avoided when the shear stress continuity is requested to be fulfilled at the undeformed interface.

Fig. 9.5 Constant depth water mass with epilimnion, metalimnion, hypolimnion and bottom boundary layer, all of constant depth. In the layers the densities ρ and kinematic viscosities ν and the horizontal velocities are constant or linearly distributed as sketched. The layer depths $h^{(1)}$, h_m , $h^{(2)}$ and h_{bl} are assumed constant



$$\tau_{zx} = \rho \nu \frac{\partial u}{\partial z} = \rho \nu \frac{u^{(2)} - u^{(1)}}{h_m} \quad (9.40)$$

for a linear velocity profile. At the edge of the metalimnion this yields

$$\tau_{zx}^{(1)} = k^{(1)} \rho^{(1)} (u^{(2)} - u^{(1)}), \quad k^{(1)} := \frac{\nu^{(1)}}{h_m}, \quad \text{at } z = h_1. \quad (9.41)$$

Direct measurements suggest that $\nu^{(1)}$ grows with increasing local velocity gradient $\partial u / \partial z$. For a metalimnion whose thickness becomes very small, one may estimate that $\nu^{(1)}$ is of the order h_m . So, $k^{(1)}$ may be interpreted as the boundary limit

$$k^{(1)} = \lim_{h_m \rightarrow 0} \frac{\nu^{(1)}}{h_m}. \quad (9.42)$$

Similarly, in the bottom boundary layer

$$\tau_{zx} = \rho \nu \frac{\partial u}{\partial z} \simeq \rho \nu \frac{u^{(2)}}{h_{bl}}, \quad (9.43)$$

where in the far right, a linear velocity profile has been assumed. At the upper edge of the bottom boundary layer (Fig. 9.5), we have

$$\tau_{zx}^{(2)} = \rho^{(2)} k^{(2)} u^{(2)}, \quad k^{(2)} := \frac{\nu^{(2)}}{h_{bl}}, \quad (9.44)$$

and we may again identify the drag coefficient with the limit

$$k^{(2)} = \lim_{h_{bl} \rightarrow 0} \frac{\nu^{(2)}}{h_{bl}}, \quad (9.45)$$

of a boundary layer with vanishingly small thickness. Of course, this interpretation of the sliding law is rough, but it has a physical basis for its justification.

If we integrate the pressure equations (9.33)₃ in both layers subject to the boundary conditions (9.36)₁ and (9.37)₁ at the free and interface surfaces, we find

$$\begin{aligned} p^{(1)} &= p_a + \rho^{(1)} g \left(z + \zeta^{(1)} \right), \\ p^{(2)} &= p_a + \rho^{(1)} g \left(h^{(1)} + \zeta^{(1)} - \zeta^{(2)} \right) + \rho^{(2)} g \left(z - h^{(1)} + \zeta^{(2)} \right), \end{aligned} \quad (9.46)$$

and consequently from (9.33)₁ in both layers

$$\begin{aligned} \frac{\partial \tau_{zx}^{(1)}}{\partial z} &= \rho^{(1)} g \frac{\partial \zeta^{(1)}}{\partial x}, \\ \frac{\partial \tau_{zx}^{(2)}}{\partial z} &= \rho^{(1)} g \frac{\partial \zeta^{(1)}}{\partial x} + \left(\rho^{(2)} - \rho^{(1)} \right) g \frac{\partial \zeta^{(2)}}{\partial x}. \end{aligned} \quad (9.47)$$

Integrating these two equations with respect to z in the respective layers, using (9.35), enforcing the volume-preserving conditions (9.34), ensuring the shear stress condition (9.37)₂ and enforcing the slip condition (9.39) at the bottom surface, yields the following expressions:

- for the shear stresses in the layers

$$\begin{aligned} \tau_{zx}^{(1)} &= - \left\{ g \rho^{(1)} h^{(1)} \left(1 - \mathfrak{z}^{(1)} \right) G^{(1)} + \frac{2}{3} \left(1 + \delta^{(2)} \right) g \rho^{(1)} h^{(2)} G^{(2)} \right\}, \\ \tau_{zx}^{(2)} &= - g \rho^{(1)} h^{(2)} \left[\frac{2}{3} \left(1 + \delta^{(2)} \right) - \mathfrak{z}^{(2)} \right] G^{(2)}, \end{aligned} \quad (9.48)$$

- for the horizontal velocities in the layers

$$\begin{aligned} u^{(1)} &= \frac{g (h^{(1)})^2}{6\nu^{(1)}} \left[3 \left(\mathfrak{z}^{(1)} \right)^2 - 6\mathfrak{z}^{(1)} + 2 \right] G^{(1)} \\ &\quad + \frac{g h^{(1)} h^{(2)}}{3\nu^{(1)}} \left(1 + \delta^{(2)} \right) \left(1 - 2\mathfrak{z}^{(1)} \right) G^{(2)}, \\ u^{(2)} &= \frac{g (h^{(2)})^2}{6\nu^{(2)}} \left(\frac{\rho^{(1)}}{\rho^{(2)}} \right) \left[3 \left(\mathfrak{z}^{(2)} \right)^2 - 4 \left(1 + \delta^{(2)} \right) \mathfrak{z}^{(2)} + 1 + 2\delta^{(2)} \right] G^{(2)}, \end{aligned} \quad (9.49)$$

in which

$$\begin{aligned} G^{(1)} &= \frac{\partial \zeta^{(1)}}{\partial x}, \quad G^{(2)} = \frac{\partial \zeta^{(1)}}{\partial x} + \frac{\rho^{(2)} - \rho^{(1)}}{\rho^{(1)}} \frac{\partial \zeta^{(2)}}{\partial x}, \\ \delta^{(2)} &= \frac{1}{\beta^{(2)} + 2}, \quad \beta^{(2)} = \frac{k^{(2)} h^{(2)}}{v^{(2)}}, \\ \mathfrak{z}^{(1)} &= \frac{z}{h^{(1)}}, \quad \mathfrak{z}^{(2)} = \frac{z - h^{(1)}}{h^{(2)}}. \end{aligned} \quad (9.50)$$

The variables $\mathfrak{z}^{(1)}$ and $\mathfrak{z}^{(2)}$ are the non-dimensional variables in the upper and lower layers, respectively, which both have the ranges $\mathfrak{z}^{(i)} \in [0, 1]$ ($i = 1, 2$), respectively.

In the expressions (9.48), (9.49) and (9.50) all boundary and transition conditions are incorporated except the wind shear stress condition (9.36)₂ and the slip condition (9.38); these are now used to determine $G^{(i)}$ and $\partial \zeta^{(i)} / \partial x$ ($i = 1, 2$). The results are as follows:

$$G^{(1)} = \frac{\tau_s}{g \rho^{(1)} h^{(1)}} \left(1 + \frac{2}{3} \left(1 + \delta^{(2)} \right) \lambda \right), \quad G^{(2)} = -\frac{\lambda \tau_s}{g \rho^{(1)} h^{(2)}}, \quad (9.51)$$

where

$$\lambda = \beta^{(1)} \left\{ \frac{4}{3} \left(1 + \delta^{(2)} \right) \left(3 + \beta^{(1)} \right) + \left(1 + 2\delta^{(2)} \right) \alpha \beta^{(1)} \right\}^{-1}, \quad (9.52)$$

$$\alpha = \frac{\rho^{(1)} v^{(1)} h^{(2)}}{\rho^{(2)} v^{(2)} h^{(1)}}, \quad \beta^{(1)} = \frac{k^{(1)} h^{(1)}}{v^{(2)}}. \quad (9.53)$$

Combination of (9.50) and (9.51) yields the following expressions for the surface and interface displacement gradients

$$\begin{aligned} \frac{\partial \zeta^{(1)}}{\partial x} &= \frac{\tau_s}{g \rho^{(1)} h^{(1)}} \left[1 + \frac{2}{3} \left(1 + \delta^{(2)} \right) \lambda \right], \\ \frac{\partial \zeta^{(2)}}{\partial x} &= -\frac{\tau_s}{g \rho^{(1)} h^{(2)}} \left[\lambda - \frac{h^{(2)}}{h^{(1)}} \left(1 + \frac{2}{3} \left(1 + \delta^{(2)} \right) \lambda \right) \right] \frac{\rho^{(1)}}{\rho^{(2)} - \rho^{(1)}}. \end{aligned} \quad (9.54)$$

These show that the surface slope grows with the wind, whereas the interface slope is inclined against the wind, see Fig. 9.4b. Moreover, when $\lambda = 0$ ($\beta^{(1)} = 0$, $k^{(1)} = 0$), i.e. when the interface slip is ideal with vanishing shear, one has

$$\left| \frac{\partial \zeta^{(2)} / \partial x}{\partial \zeta^{(1)} / \partial x} \right| = \frac{\rho^{(1)}}{\rho^{(2)} - \rho^{(1)}}. \quad (9.55)$$

By integration, this ratio also carries over to $|\zeta^{(2)} / \zeta^{(1)}|$; so, with $(\rho^{(2)} - \rho^{(1)}) / \rho^{(2)} = \mathcal{O}(10^{-3}) - \mathcal{O}(10^{-2})$ we have

$$\left| \frac{\zeta^{(2)}}{\zeta^{(1)}} \right| = \mathcal{O}(10^3) - \mathcal{O}(10^2) \quad (9.56)$$

for typical summer stratification. When the surface elevation is in the millimetres, the interface (thermocline) displacement may reach metres and the thermocline may cut the free surface at the downwind end of the lake. Such a case is, however, not covered by this linear theory.

If the expressions $G^{(1)}$ and $G^{(2)}$ as obtained in (9.51) are substituted into (9.48) and (9.49), the vertical structures of the vertical shear stresses and horizontal currents, in non-dimensional form, are obtained as follows:

$$\begin{aligned} \hat{\tau}_{zx}^{(1)} &= \frac{\tau_{zx}^{(1)}}{(-\tau_s)} = 1 - \mathfrak{z}^{(1)} - \frac{2}{3}\lambda \left(1 + \delta^{(2)}\right) \mathfrak{z}^{(1)}, \\ \hat{\tau}_{zx}^{(2)} &= \frac{\tau_{zx}^{(2)}}{(-\tau_s)} = \lambda \left(\mathfrak{z}^{(2)} - \frac{2}{3} \left(1 + \delta^{(2)}\right) \right), \end{aligned} \quad (9.57)$$

$$\begin{aligned} \hat{u}^{(1)} &= \frac{u^{(1)}}{\left(\frac{h^{(1)}\tau_s}{6\rho^{(1)}\nu^{(1)}}\right)} = 3 \left(\mathfrak{z}^{(1)}\right)^2 - 6\mathfrak{z}^{(1)} + 2 + \frac{2}{3}\lambda \left(1 + \delta^{(2)}\right) \left(3 \left(\mathfrak{z}^{(1)}\right)^2 - 1\right), \\ \hat{u}^{(2)} &= \frac{u^{(2)}}{\left(\frac{h^{(2)}\tau_s}{6\rho^{(2)}\nu^{(2)}}\right)} = -\lambda \left(3 \left(\mathfrak{z}^{(2)}\right)^2 - 4 \left(1 + \delta^{(2)}\right) \mathfrak{z}^{(2)} + 1 + 2\delta^{(2)}\right). \end{aligned} \quad (9.58)$$

In these expressions, the only x -dependence is exhibited in $\tau_s(x)$. The dimensional counterparts of (9.58) can now be used in the continuity equation (9.33)₂ to obtain the vertical currents by integration with respect to z . In this process the interfacial and basal boundary conditions

$$\begin{aligned} w_1 &= w_2 & \text{at } z &= h_1, \\ w_2 &= 0 & \text{at } z &= h = h_1 + h_2 \end{aligned} \quad (9.59)$$

must be used. The result of this integration can, in non-dimensional form, be written as

$$\begin{aligned} \hat{w}^{(1)} &= \frac{w^{(1)}}{\left(\frac{(h^{(1)})^2 \tau'_s}{6\rho^{(1)}\nu^{(1)}}\right)} = \mathfrak{z}^{(1)} \left(1 - \mathfrak{z}^{(1)}\right) \left(\mathfrak{z}^{(1)} - 2 + \frac{2}{3}\lambda \left(1 + \delta^{(2)}\right) \left(\mathfrak{z}^{(1)} + 1\right)\right), \\ \hat{w}^{(2)} &= \frac{w^{(2)}}{\left(\frac{(h^{(2)})^2 \tau'_s}{6\rho^{(2)}\nu^{(2)}}\right)} = \lambda \mathfrak{z}^{(2)} \left(\left(\mathfrak{z}^{(2)}\right)^2 - 2 \left(1 + \delta^{(2)}\right) \mathfrak{z}^{(2)} + 1 + 2\delta^{(2)}\right). \end{aligned} \quad (9.60)$$

The formulae (9.54), (9.57), (9.58) and (9.60) indicate that for a frictionless interface ($k^{(1)} = 0 \rightarrow \beta^{(1)} = 0 \rightarrow \lambda = 0$) one has $\tau_{zx}^{(2)} = 0$, $u^{(2)} = 0$, $w^{(2)} = 0$, indicating no motion in the lower layer, but non-vanishing interface slope with larger absolute value than for $\lambda \neq 0$. It follows that λ is an important non-dimensional parameter, which controls the degree to which horizontal momentum is transmitted across the interface from the upper to the lower layer.

Having determined the velocity components in the two layers, expressed in (9.58) and (9.60), the streamlines may be determined by solving the ordinary differential equations

$$\begin{aligned}\frac{d\mathfrak{z}^{(1)}}{dx} &= \frac{1}{h^{(1)}} \frac{w^{(1)}}{u^{(1)}} = \frac{\tau'_s(x)}{\tau_s(x)} \left(N^{(1)}(\mathfrak{z}^{(1)}) \right)^{-1}, \\ \frac{d\mathfrak{z}^{(2)}}{dx} &= \frac{1}{h^{(2)}} \frac{w^{(2)}}{u^{(2)}} = \frac{\tau'_s(x)}{\tau_s(x)} \left(N^{(2)}(\mathfrak{z}^{(2)}) \right)^{-1},\end{aligned}\tag{9.61}$$

$$\begin{aligned}N^{(1)}(\mathfrak{z}^{(1)}) &= \frac{3(\mathfrak{z}^{(1)})^2 - 6\mathfrak{z}^{(1)} + 2 + \frac{2}{3}\lambda(1 + \delta^{(2)})(3(\mathfrak{z}^{(1)})^2 - 1)}{\mathfrak{z}^{(1)}(1 - \mathfrak{z}^{(1)}) \left[\mathfrak{z}^{(1)} - 2 + \frac{2}{3}\lambda(1 + \delta^{(2)})(\mathfrak{z}^{(1)} + 1) \right]}, \\ N^{(2)}(\mathfrak{z}^{(2)}) &= \frac{-\lambda \left[3(\mathfrak{z}^{(2)})^2 - 4(1 + \delta^{(2)})\mathfrak{z}^{(2)} + 1 + 2\delta^{(2)} \right]}{\lambda \mathfrak{z}^{(2)} \left[(\mathfrak{z}^{(2)})^2 - 2(1 + \delta^{(2)})\mathfrak{z}^{(2)} + 1 + 2\delta^{(2)} \right]},\end{aligned}$$

in which $\tau'_s(x) = d\tau_s/dx$. These differential equations are separable and possess the solutions

$$\begin{aligned}\tau_s(x) \exp \left\{ - \int_0^{\mathfrak{z}^{(1)}} N^{(1)}(\xi) d\xi \right\} &= C_1, \\ \tau_s(x) \exp \left\{ - \int_0^{\mathfrak{z}^{(2)}} N^{(2)}(\xi) d\xi \right\} &= C_2,\end{aligned}\tag{9.62}$$

where C_1 and C_2 are constants of integration.

Figure 9.6 displays the structure of the flow for the case of free slip⁵ at the bottom ($k^{(2)} = \beta^{(2)} = 0$, $\delta^{(2)} = 1/2$). Panels (a) and (b) are schematic but panels (c) and (d) are plotted for $\lambda = 0.3$ (this value is possible since $0 < \lambda < 3/(4(1 + \delta^{(2)}))$) as β and α are varied from 0 to ∞). Figure 9.6a shows for a symmetric wind stress the induced circulation cells in the epi- and hypolimnia. The free surface current goes with the wind stress and leads to a circulation with return current above the interface. This counter-current induces a current in the same direction just below the interface, which forms a loop in the hypolimnion with return flow at the bottom that goes with the wind. The two circulation loops are traversed with opposite rotations.

⁵ By free slip or ideal slip we mean frictionless slip for which $\tau_b \equiv 0$.

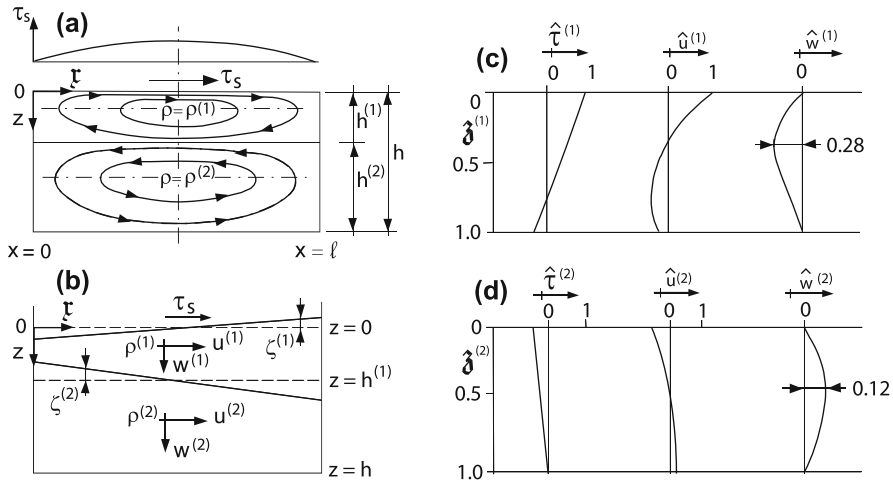


Fig. 9.6 Wind-induced steady flow in a narrow rectangular basin on a non-rotating frame: (a) streamlines in the two layers for a steady symmetric longitudinal wind τ_s . The two gyres rotate in opposite directions; (b) free and interface surface gradients (schematic); (c) upper layer dimensionless vertical shear stress $\hat{\tau}_{zx}^{(1)}$ and velocities $\hat{u}^{(1)}$, $\hat{w}^{(1)}$ plotted against normalised depth $z/h^{(1)} =: \hat{z}^{(1)} \in [0, 1]$. (d) Same as (c), but for the lower layer and plotted against normalised depth $(z - h^{(1)})/h^{(2)} =: \hat{z}^{(2)} \in [0, 1]$, adapted from HEAPS [23]

Note, moreover, that the current in the hypolimnion does not exist, if the interface is frictionless ($k^{(1)} = 0$, see (9.41)). Figure 9.6b sketches the positions of the free and interface surface displacements. The slope of the free surface is with the wind, with surface high and low at the downwind and upwind ends of the basin, respectively. The corresponding pressure increase due to the weight of the displaced water is counter-balanced by a downstroke of the interface and corresponding epilimnion down-welling of the water at the downwind end of the basin. A pressure balance of the displaced water masses reproduces (9.55) as the slope ratio of the two surfaces.

Panels (c) and (d) of Fig. 9.6 show the vertical structure of the shear stress and current components for free slip at the bottom. The shear stresses are linearly distributed over depth with opposite signs in the two layers and (for free slip at the bottom) reaching the value zero at the bottom. The vertical structure of the horizontal current is parabolic of second order with sign changes within the layers in accordance with the loop structure in panel (a). The vertical current is also polynomial of third order and with no sign change within each layer, but in opposite directions in the two layers, also in accordance with the loops of panel (a).

The preceding analysis transpires that the transfer of motion from the epilimnion to the hypolimnion depends chiefly upon the frictional behaviour of the shear layer spanning the thermocline. In the mathematical formulae this is expressed by the sliding law (9.38) in which the interface shear stress is proportional to the difference of the velocities in the hypo- and epilimnion close to the interface with constant $k^{(1)}$. A simple linear model made clear that an order of magnitude for $k^{(1)}$ is given by $k^{(1)} = \nu_m / h_m$, where ν_m is the kinematic viscosity in the metalimnion and h_m a measure for its thickness.

Shear instability in the thermocline, which must influence the values of v_m and h_m (and hence $k^{(1)}$), has, e.g. been discussed by MORTIMER (1961) [38], (1974) [39]. It is known that turbulence and therefore active mixing will either increase or subside at the thermocline level, and the dimensionless characteristic number, which is a measure for this transition is the RICHARDSON number, defined by

$$\mathbb{R}_i = \frac{g \frac{\partial \rho}{\partial z}}{\rho \left(\frac{\partial u}{\partial z} \right)^2}. \quad (9.63)$$

MILES (1967) [37] has shown for a linearly stratified fluid layer that a parallel simple shear flow with velocity $u(z)$ is stable as long as $\mathbb{R}_i > 1/4$, but will become unstable as soon as $\mathbb{R}_i < 1/4$. Even though the flow in a lake is locally only approximately simple shear flow, experience has shown that $\mathbb{R}_i = 1/4$ marks approximately the transition to instability. For the present model we may assume (see (9.42))

$$k^{(1)} = k^{(1)}(\mathbb{R}_i), \quad \text{where} \quad \mathbb{R}_i = \frac{gh_m (\rho^{(2)} - \rho^{(1)})}{\rho^{(1)} (u^{(2)} - u^{(1)})^2}. \quad (9.64)$$

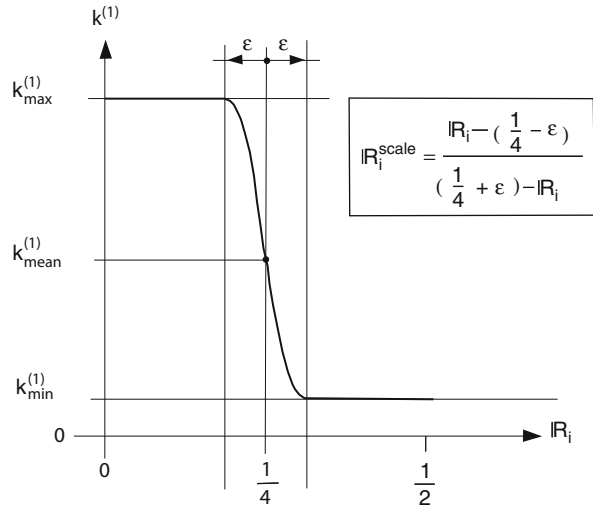
An acceptable parameterisation for $k^{(1)}$ may be

$$\begin{aligned} k^{(1)}(\mathbb{R}_i) &= \left(k_{\max}^{(1)} - k_{\min}^{(1)} \right) f \left(\mathbb{R}_i^{\text{scale}} \right) + k_{\min}^{(1)}, \\ \mathbb{R}_i^{\text{scale}} &= \frac{\mathbb{R}_i - \left(\frac{1}{4} - \varepsilon \right)}{\left(\frac{1}{4} + \varepsilon \right) - \mathbb{R}_i}, \\ f &= \begin{cases} 1, & 0 \leq \mathbb{R}_i \leq \frac{1}{4} - \varepsilon, \\ \exp \left\{ - \left(\frac{\mathbb{R}_i^{\text{scale}}}{\sigma^{\text{scale}}} \right)^2 \right\}, & \frac{1}{4} - \varepsilon < \mathbb{R}_i \leq \frac{1}{4} + \varepsilon, \\ 0, & \mathbb{R}_i > \frac{1}{4} + \varepsilon. \end{cases} \end{aligned} \quad (9.65)$$

This parameterisation assigns to $k^{(1)}$ the value $k_{\min}^{(1)}$ when the RICHARDSON number \mathbb{R}_i exceeds the value 0.25 by the amount ε ; the value $k_{\max}^{(1)}$ is assumed, when the RICHARDSON number lies between zero and a value smaller than 0.25 by the amount ε and it connects these two values with a Gaussian curve having variance σ^{scale} . The graph of $k^{(1)}$ according to (9.65) is displayed in Fig. 9.7; it has four parameters $k_{\max}^{(1)}$, $k_{\min}^{(1)}$, ε and σ^{scale} . The first two are relatively easy to determine: ε is a measure for the bandwidth of the transition from $k_{\min}^{(1)}$ to $k_{\max}^{(1)}$ and σ^{scale} is a measure of the skewness of the sigmoidal curve segment.

At $\mathbb{R}_i = 1/4$, $\mathbb{R}_i^{\text{scale}} = 1$; if we call that value of the function (9.65) f_{crit} , then (9.65) implies

Fig. 9.7 Drag coefficient $k^{(1)}$ as a function of the RICHARDSON number according to the parameterisation (9.65)



$$f_{\text{crit}} = \exp \left(- \left(\frac{1}{\sigma^{\text{scale}}} \right)^2 \right) \rightarrow \sigma^{\text{scale}} = \left(\frac{-1}{\ln(f_{\text{crit}})} \right)^{1/2},$$

$$k_{\text{crit}}^{(1)} = k_{\max}^{(1)} + k_{\min}^{(1)} (1 - f_{\text{crit}}), \quad (9.66)$$

a relation, which may help in the determination of the parameters.

MUNK and ANDERSON [40] gave an expression for the dependence of ν_m on $|R_i|$. The assumption employed in the above analysis, namely that the interface is impermeable, is unrealistic when mixing occurs, since water is then exchanged between the two layers. Such an exchange will increase h_m , and there will be a return to stable shear flows when $|R_i|$ subsequently exceeds the value one-fourth, for details see [6].

9.3 Ekman Theory and Some of Its Extensions

In the last section the simplest flow of a homogeneous fluid in a narrow rectangular basin of negligible width and of constant depth due to a steady wind shear stress applied at its surface was analysed when the effect of the rotation of the Earth was ignored. Consideration is now given to the vertical structure of wind-induced motion in infinitely large lakes or oceans, taking the rotation of the Earth into account. The water is assumed to be homogeneous. EKMAN's [12] basic solution for wind-induced currents – called drift currents – in the open sea is presented. Subsequently, the generalisation of that theory to account for steady and time-dependent motions

in real basins is described. This generalisation basically concerns alterations of the theory when the vertical eddy viscosity (assumed constant in EKMAN's theory) varies with depth, when finite depth and finite extensions of the basin are considered.

9.3.1 Ekman Spiral

9.3.1.1 Spiral Below Water Surface

Consider the currents produced in an ocean or lake of infinite extent, which are generated under the following restricting assumptions:

- the water is homogeneous, $\rho = \text{constant}$;
- the horizontal pressure gradient vanishes

$$\nabla_H p = 0, \quad \frac{\partial p}{\partial x} = \frac{\partial p}{\partial y} = 0;$$

- the vertical velocity is zero, $w = 0$;
- the horizontal components of the extra stress tensor vanish

$$\sigma_{xx}^E = \sigma_{yy}^E = \tau_{xy}^E = 0;$$

- the vertical momentum balance reduces to the hydrostatic pressure equation;
- the vertical viscosity coefficient is constant, $\nu = \text{constant}$;
- processes are steady: $\partial(\cdot)/\partial t = 0$.

With these assumptions, the horizontal momentum equations reduce to

$$\frac{1}{\rho} \frac{\partial \tau_{zx}}{\partial z} = -fv, \quad \frac{1}{\rho} \frac{\partial \tau_{zy}}{\partial z} = fu, \quad (9.67)$$

and the closure relations for the shear stresses take the forms

$$\tau_{zx} = \rho\nu \frac{\partial u}{\partial z}, \quad \tau_{zy} = \rho\nu \frac{\partial v}{\partial z}. \quad (9.68)$$

Substituting these relations into (9.67) and observing that ρ and ν are constant yields

$$\frac{\partial^2 u}{\partial z^2} = -\frac{f}{\nu}v, \quad \frac{\partial^2 v}{\partial z^2} = \frac{f}{\nu}u. \quad (9.69)$$

These two second-order differential equations of the real-valued variables u and v can be written as a single second-order equation of the complex variable

$$\mathbf{w} = u + iv, \quad (9.70)$$

where $i = \sqrt{-1}$. Indeed, adding $i \times (9.69)_2$ to $(9.69)_1$ yields

$$\frac{d^2 \mathbf{w}}{dz^2} = \frac{if}{\nu} \mathbf{w} = \frac{2if}{2\nu} \mathbf{w} = \frac{(i+1)^2 f}{2\nu} \mathbf{w}, \quad (9.71)$$

or

$$\frac{d^2 \mathbf{w}}{dz^2} = \frac{(i+1)^2 \pi^2}{D^2} \mathbf{w}, \quad (9.72)$$

where

$$D := \pi \sqrt{\frac{2\nu}{f}} \quad (9.73)$$

has the dimension of a length and is called the *Ekman depth*. Solutions of (9.72) are only functions of z and have the form

$$\mathbf{w}(z) = A \exp \left\{ \frac{(1+i)\pi}{D} z \right\} + B \exp \left\{ -\frac{(1+i)\pi}{D} z \right\} \quad (9.74)$$

with two constants of integration, A and B .

Infinite Depth

These constants follow from the boundary conditions

$$\begin{aligned} \tau_{zx} + i\tau_{zy} &= \rho\nu \frac{\partial \mathbf{w}}{\partial z} = -i\tau_s \quad \text{at } z = 0, \\ \mathbf{w} &= 0 \quad \text{at } z = h. \end{aligned} \quad (9.75)$$

The first states that the constant wind shear stress τ_s acts in the y -direction and is uniformly distributed over the entire free surface, the latter states that the bottom surface is impenetrable. EKMAN looked at an infinitely deep ocean, $h \rightarrow \infty$. For this case, $(9.75)_2$ implies $A = 0$, and $(9.75)_1$ yields

$$\mathbf{w}(z) = (1+i) \frac{D\tau_s}{2\pi\nu\rho} \exp \left\{ -\frac{(1+i)\pi}{D} z \right\}, \quad (9.76)$$

which may, alternatively, be written as

$$\mathbf{w}(z) = \frac{\sqrt{2}\pi\tau_s}{\rho f D} \exp \left\{ -\pi \frac{z}{D} \right\} \exp \left\{ i \left(\frac{\pi}{4} - \pi \frac{z}{D} \right) \right\}. \quad (9.77)$$

To derive this, we have used the identity $(1 + i) = \sqrt{2}\exp(i\pi/4)$. At the surface $z = 0$ this yields

$$\mathbf{w}(z = 0) = \mathbf{w}_s = \frac{\sqrt{2}\pi\tau_s}{\rho f D} \exp\left\{\frac{i\pi}{4}\right\}, \quad (9.78)$$

or using EULER's formula $e^{i\varphi} = (\cos \varphi + i \sin \varphi)$,

$$\mathbf{w}_s = (u + iv) = W_s (\cos \pi/4 + i \sin \pi/4), \quad (9.79)$$

$$W_s = \frac{\sqrt{2}\pi\tau_s}{\rho f D}. \quad (9.80)$$

Here, W_s is the strength of the surface current in terms of the wind shear stress. Since the wind has been assumed to blow in the positive y -direction, the current at the free surface is at 45° to the right of the wind (to the left on the Southern Hemisphere). Moreover, it follows from (9.77) that the horizontal current decreases exponentially with depth (as $\exp(-\pi z/D)$), and its angle of deflection to the right of the wind is given by $\pi/2 - (\pi/4 - \pi z/D) = \pi/4 + \pi z/D$. This angle increases with depth. So, with increasing depth the current at a fixed xy -position rotates cum sole around the vertical line at that position. Its modulus (absolute value) is given by

$$|\mathbf{w}| = W_s \exp\left(-\pi \frac{z}{D}\right), \quad (9.81)$$

and its angle to the right of the wind is given by

$$\theta(z) = \left(\pi \frac{z}{D} + \frac{\pi}{4}\right). \quad (9.82)$$

This current system is called the **EKMAN spiral** after **EKMAN** [12] who first described it, see Fig. 9.1. Figure 9.8 displays in panel (a) this current system. At the **EKMAN** depth, $z = D$, the modulus of the current relative to the current at the surface takes the value

$$\frac{|\mathbf{w}|_{z=D}}{W_s} = e^{-\pi} \sim \frac{1}{23} = 0.043, \quad (9.83)$$

and its direction is opposite to the surface current. At the depth of twice the **EKMAN** depth, $z = 2D$, the direction of the current is the same as that on the water surface, and its modulus is

$$\frac{|\mathbf{w}|_{z=2D}}{W_s} = e^{-2\pi} \sim \frac{1}{535} = 0.0019. \quad (9.84)$$

If the velocities at increasing depth are projected onto the xy -plane (panel (b) of Fig. 9.8) the tips of the current vectors trace a logarithmic spiral, which coils

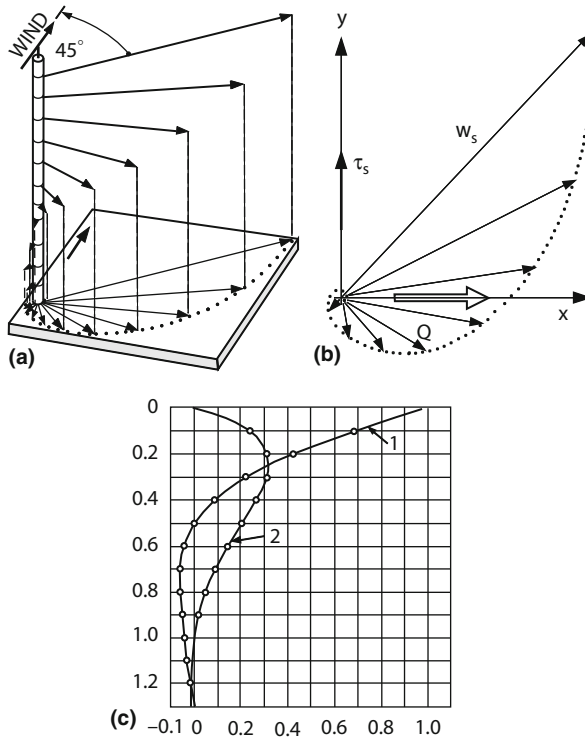


Fig. 9.8 EKMAN spiral (a) plotted in perspective view, (b) shown in the projection into the hodo-graph plane, tracing a logarithmic spiral, (c) plotted as components in the direction of the surface current, (1), and perpendicular to it, (2). Shown as *double arrow* in (b) is also the vertically integrated total volume (mass) flux Q , which is 90° to the right of the wind shear stress, constructed from figures by Laska [35], © Laboratory of Hydraulics, Hydrology and Glaciology at ETH Zurich

indefinitely around the origin of the xy -coordinate system. If the components of the horizontal current in the direction of the surface current and perpendicular to it are plotted against z , then the two curves in Fig. 9.8c are obtained.

The vertically integrated volume flux may be written as

$$\begin{aligned}
 Q &= Q_x + iQ_y = \int_{-\infty}^0 w dz \\
 &= \frac{\sqrt{2}\pi\tau_s}{\rho f D} \int_0^\infty \exp \left\{ -\frac{\pi}{D} z(1+i) + i\frac{\pi}{4} \right\} dz \\
 &= \frac{\tau_s}{\rho f}.
 \end{aligned} \tag{9.85}$$

This is also called the total transport; it is directed perpendicular to the wind stress and to the right of it.

At this point it should be asked what can be extracted from the EKMAN solution from an applied point of view. Can the current rotation with depth and the decay of the current modulus with depth be observed in measurements? Attempts towards an answer of this question have been undertaken by many of the early physical oceanographers, and below we follow the description of HEAPS [23] who has briefly summarised it. HEAPS writes

Expressing the wind stress in terms of the square of the wind speed

$$\tau_s = \rho_A C_D W^2, \quad (9.86)$$

where W denotes the wind speed, ρ_A the density of air and C_D a drag coefficient, it follows from (9.78) that

$$|w_s| = \frac{\sqrt{2}\pi\rho_A C_D}{\rho} \frac{W^2}{fD} = \frac{\pi\rho_A C_D}{\sqrt{2}\Omega\rho} \frac{W^2}{D \sin \phi}, \quad (9.87)$$

where Ω is the angular frequency of the rotation of the Earth and ϕ the geographical latitude. Therefore, the ratio of the surface current to the wind speed, the so-called wind factor (α' , say), is

$$\alpha' = \frac{|w_s|}{W} = \frac{\pi\rho_A C_D}{\sqrt{2}\Omega\rho} \frac{W}{D \sin \phi}. \quad (9.88)$$

On the basis of observations in various seas and oceans prior to 1939, EKMAN derived the empirical relation

$$\alpha' = \frac{0.0127}{\sqrt{\sin \phi}}. \quad (9.89)$$

Comparing (9.88) and (9.89) yields

$$D = \frac{A_0 W}{\sqrt{\sin \phi}} \quad \left(A_0 = \frac{\pi\rho_A C_D}{0.0127 \times \sqrt{2}\Omega\rho} \right). \quad (9.90)$$

The value of A_0 depends critically on the choice of the drag factor C_D . Thus, measuring W in m s^{-1} and D in m, it transpires that $A_0 = 7.6$ from SVERDRUP, JOHNSON and FLEMING [50], p. 494 and DEFANT [10], p. 422, whereas $A_0 = 4.3$ from POND and PICKARD [44], p. 88. Knowing τ_s and D in terms of the wind speed from (9.86) and (9.90), the vertical structure of the current may be determined from (9.77). POND and PICKARD [44], p. 89 give the illuminating Table 9.1 of values, based on (9.89) and (9.90).

Table 9.1 EKMAN depth as function of wind speed and geographical latitude according to POND and PICKARD [44]

	$\phi = 10^\circ$ $\alpha' = 0.030$	45° 0.015	80° 0.013
$W = 10 \text{ m s}^{-1}$	$D = 100$	50	45 m
$W = 20 \text{ m s}^{-1}$	$D = 200$	100	90 m

Combining (9.73) and (9.90) gives a formula for the eddy viscosity in the EKMAN spiral in terms of the wind speed as follows:

$$\nu = \frac{\Omega A_0^2}{\pi^2} W^2. \quad (9.91)$$

According to DEFANT [10], pp. 422–423, this formula with W in m s^{-1} holds for $W > 6 \text{ m s}^{-1}$ with $\rho \Omega A_0^2 / \pi^2 = 4.3$, while ν is proportional to W^3 for $W < 6 \text{ m s}^{-1}$. It follows from (9.86) and (9.91) that ν is directly proportional to τ_s .

Observations of the angle of deflection of the surface current from the wind direction have shown considerable deviations from the classical 45° result. The EKMAN spiral is not a clearly observed distribution of current. The reasons may have to do with the highly idealised nature of the EKMAN theory outlined above, specifically in its assumption of

- (i) no land boundaries,
- (ii) infinitely deep water,
- (iii) eddy viscosity uniform through the vertical,
- (iv) steady-state motion,
- (v) homogeneous water.

This much for HEAPS' text. In what follows we shall, step-by-step, relax the underlying assumptions of the EKMAN problem, loosely following the above itemisation.

Finite Depth

Let us start by assuming a layer of a homogeneous fluid of infinite extent and constant finite depth h that is subjected to a steady uniform wind. In this case, the steady complex-valued drift current can also be determined by (9.74), but it is now advantageous to write the general solution in the form

$$w(z) = A \sinh \left\{ \frac{(1+i)\pi}{D} (z-h) \right\} + B \cosh \left\{ \frac{(1+i)\pi}{D} (z-h) \right\}, \quad (9.92)$$

which is simply another linear combination of the fundamental solution of (9.72). A and B are constants of integration to be determined by the boundary conditions

$$\begin{aligned} \rho\nu \frac{\partial \mathbf{w}}{\partial z}(0) &= -i\tau_s \quad (\text{prescribed shear in the } y \text{ direction}), \\ \mathbf{w}(h) &= 0 \quad (\text{no slip}). \end{aligned} \quad (9.93)$$

The second of these implies $B = 0$ and the first yields A such that

$$\mathbf{w}(z) = (1+i) \frac{D\tau_s}{2\pi\rho\nu} \frac{\sinh\{(1+i)a(1-\mathfrak{z})\}}{\cosh\{(1+i)a\}}, \quad (9.94)$$

where

$$a = \frac{\pi h}{D}, \quad \mathfrak{z} = \frac{z}{h}. \quad (9.95)$$

Vertical structures of the current from (9.94) are illustrated in Fig. 9.9 for various values of h/D . The spiral for $h/D = 1.25$ is very close to the EKMAN spiral for the infinitely deep ocean $h/D \rightarrow \infty$. The graph shows the important influence of

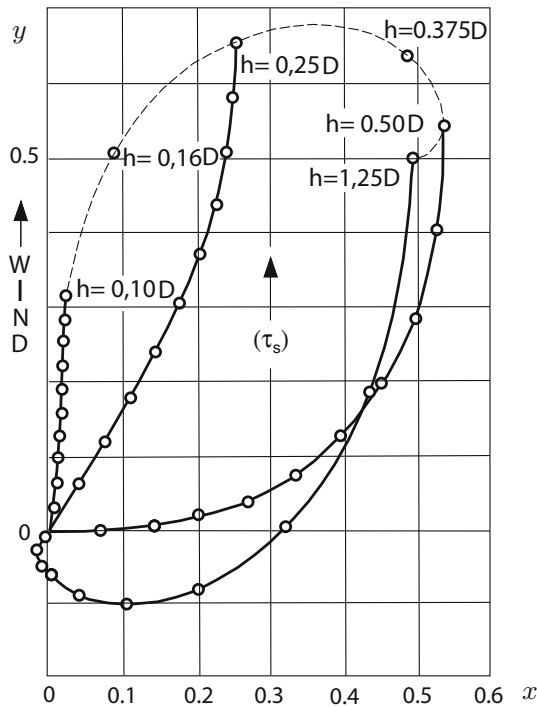


Fig. 9.9 Vertical structure of the wind-induced current for the EKMAN problem in a basin of finite depth h for $h/D = 0.1, 0.25, 0.5, 1.25$ marked in steps of $0.1h$ from the surface down to the bottom. The thin dashed line connects the velocities at the free surface for $h/D \in [0.1, 1.25]$. For $h/D > 0.5$, the rotation of the current through the EKMAN layer is nearly 45° ; for $h/D < 0.5$ this angle of deviation is smaller, for $h/D < 0.1$ practically 0° , adapted from HEAPS [23]

bottom friction in a fluid layer whose depth is smaller than the EKMAN depth D . As h decreases, the angle of deflection of the current from the wind direction decreases and the effect of the Earth's rotation becomes smaller. For very small values of a , TAYLOR series expansions transform (9.94) into

$$\mathbf{w}(z) = \frac{ih\tau_s}{\nu\rho}(1 - \mathfrak{z}) \quad \left(\frac{\pi h}{D} \ll 1 \right). \quad (9.96)$$

This says that the currents are in the direction of the wind independent of the rotation of the Earth and they decay linearly with depth.

The thin dashed line in Fig. 9.9 connects the surface points of the spirals for particular values of h/D . As the curve is traced, the angle between the Oy -axis and the straight line connecting the origin O with one of its points defines the angle between the direction of the wind and the surface current for that value of h/D . This deflection angle can be shown to be given by

$$\alpha = \frac{\pi}{4} - \arctan \left\{ \frac{\sin(2a)}{\sinh(2a)} \right\}, \quad (9.97)$$

and is given in Table 9.2 for a selection of h/D values. This table shows that for $h/D > 0.5$ the deflection angle is practically 45° ; it only takes smaller values for $h/D < 0.5$.

Finally, the total volume transport is given by

$$\begin{aligned} Q &= \int_0^h \mathbf{w}(z) dz = \frac{(1+i)D\tau_s}{2\rho\nu h} \frac{1}{\cosh\{(1+i)a\}} \int_0^1 \sinh\{(1+i)a(1-\mathfrak{z})\} d\mathfrak{z} \\ &= \frac{\tau_s}{\rho f} \left\{ 1 - \frac{1}{\cosh\{a(1+i)\}} \right\}. \end{aligned} \quad (9.98)$$

Clearly, as $h \rightarrow \infty$ ($a \rightarrow \infty$), we have $\alpha \rightarrow \pi/4$ and $Q_x \rightarrow \tau_s/(\rho f)$, $Q_y \rightarrow 0$, as expected.

The physical understanding of this finite depth EKMAN problem also profits from the following, alternative interpretation of the current structure. Under a steady current, friction at the fluid bed generates an EKMAN spiral also above the bottom surface. As the current decreases towards the bottom from the main stream flow, it rotates counterclockwise, in the opposite sense to the wind-driven near-surface EKMAN spiral. Problem 9.4 formulates the equations for this bottom spiral and the reader is asked to verify its solution.

Table 9.2 Deflection angle of the surface current velocity from the direction of the wind for the EKMAN problem in a finite depth basin

h/D	0.1	0.25	0.5	0.75	1.0	1.5
α	5°	21.5°	45°	45.5°	45°	45°

9.3.1.2 Spiral Above Bottom Surface

Problem 9.4 *Let us focus at the lower part of an ocean or lake, say the hypolimnion, and assume that there is an appreciable current at depth, which is sufficiently above the bottom surface. Such an upper hypolimnion current might be generated by pressure gradients, e.g. it may be considered to be induced by the set-up of a steady wind and the accompanied inclination of the thermocline. In such a situation the steady pressure gradient is primarily responding to the CORIOLIS acceleration via the geostrophic balance*

$$f(\mathbf{k} \times \mathbf{v}) = -\text{grad } p.$$

According to this equation the so-called geostrophic current is along the isobars with the pressure highs (lows) to the right (to the left) on the Northern Hemisphere. So, we may think that the upper hypolimnion is subject to a geostrophic current induced by the steady, uniform pressure distribution. How does this current change with depth, in particular as the bottom surface is approached when the no-slip condition applies? ♦

We approximate this problem by considering a half space $[(x, y, z) \in \mathbb{R} \times \mathbb{R} \times \mathbb{R}^+]$ of constant density ρ . Assume that the fluid is subjected to a constant pressure gradient in the y -direction, $\partial p / \partial y = -\rho v G$ (the coordinate system can be chosen such that the x -axis is locally parallel to the isobar and the horizontal pressure gradient is perpendicular to it). The problem is to find the horizontal velocity distribution for $z > 0$ that is induced by this constant pressure gradient.

Assume the velocity field to be given as

$$u = u(z), \quad v = v(z), \quad w \equiv 0. \quad (9.99)$$

Prove that with this choice the continuity equation is identically satisfied and the incompressible NAVIER–STOKES equations reduce to

$$\begin{aligned} \frac{d^2 u}{dz^2} + \frac{f}{v} v &= 0, \\ \frac{d^2 v}{dz^2} - \frac{f}{v} u + G &= 0, \end{aligned} \quad (9.100)$$

where $\partial p / \partial y = -\rho v G$. Let $U = (v/f)G$ be the geostrophic current induced by G and assume that (9.100) are to be solved subject to the boundary conditions

$$\begin{aligned} u = v &= 0, & \text{at } z &= 0, \\ u &= U, & \text{at } z &\rightarrow \infty, \end{aligned} \quad (9.101)$$

i.e. $z = 0$ agrees with the horizontal bottom surface where the no-slip condition is imposed, and the z -axis points upwards with the geostrophic current applied at $z \rightarrow \infty$.

Introduce the complex-valued velocity

$$\mathcal{W} = (u - U) + iv \quad (9.102)$$

and show that (9.100) and (9.101) are equivalent to the complex-valued two-point boundary value problem

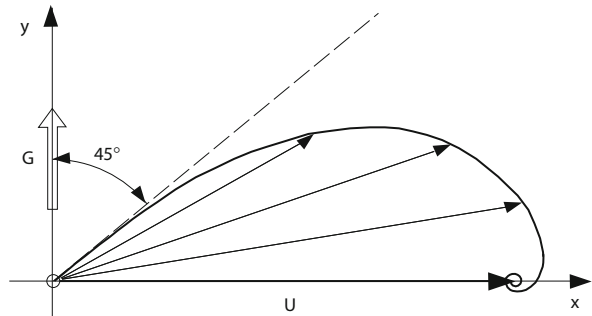
$$\begin{aligned} \frac{d^2 \mathcal{W}}{dz^2} + \frac{if}{\nu} \mathcal{W} &= 0, & 0 < z < \infty, \\ \mathcal{W} &= -U, & \text{at } z = 0, \\ \mathcal{W} &= 0, & \text{at } z \rightarrow \infty. \end{aligned} \quad (9.103)$$

Show that the solution of (9.103) is given by

$$\begin{aligned} \mathcal{W}(z) &= -U \exp \left\{ -(1+i) \frac{\pi z}{D} \right\}, \quad D := \pi \sqrt{\frac{2\nu}{f}}, \\ \text{or } u(z) &= U \left\{ 1 - \exp \left(-\frac{\pi z}{D} \right) \cos \left(\frac{\pi z}{D} \right) \right\}, \\ v(z) &= U \exp \left(-\frac{\pi z}{D} \right) \sin \left(\frac{\pi z}{D} \right). \end{aligned} \quad (9.104)$$

The EKMAN spiral to this solution is displayed in Fig. 9.10. Accordingly, for small z , close to the bottom surface the current is small and approaches the zero value at the bottom surface 45° to the left of the geostrophic current U , which is perpendicular to the pressure gradient G . Moreover, as one moves from large values of z towards the

Fig. 9.10 Vertical structure of the steady bottom boundary layer current for $z > 0$ for the EKMAN problem when a constant uniform geostrophic current U is prescribed in the x -direction at large z ($\rightarrow \infty$), adapted from LACOMB [32]



bottom at $z = 0$ the velocity vector decreases and rotates contra solem clockwise) until it approaches the bottom with zero value and rotated by 45° .

The vertical structure of the current in a deep lake – deeper than the EKMAN depth – therefore has an EKMAN layer near the surface with frictional depth D say, and one near the bottom of frictional depth D' say. When the total depth is small and the layers overlap ($h < D + D'$) the respective spirals tend to cancel each other.

9.3.1.3 Non-constant Vertical Eddy Viscosity

The assumption of a constant viscosity is not realistic for the vertical distribution of the horizontal wind-induced current in the free surface EKMAN layer. This layer is almost always subjected to turbulence, i.e. fluctuating horizontal velocities which give rise to turbulent shear stresses, in particular surface parallel shear stresses. These are measurable in terms of fluctuations of horizontal velocity components and the density. Alternatively, these stresses can also be expressed in terms of the strain rate tensor \mathbf{D} of the *mean* motion⁶ in the form $\boldsymbol{\tau} = \rho \nu_t \mathbf{D}$, where ν_t is the turbulent viscosity, often called *eddy viscosity*, to express its presence as a result of the meso-scale turbulent eddies. Measurements show that in the ocean or in a lake ν_t varies with depth with a near-zero value at the free surface, growing with depth, reaching a maximum value at some depth, say at $0.2 \times H$ and beyond this level rapidly decreasing. On the other hand, the simplifications which led to EKMAN's equation remain valid; the only change is a different postulate for the vertical distribution of the eddy viscosity.

EKMAN's problem of wind-induced flow has been solved by MADSEN [36] by assuming that the eddy viscosity increases linearly with depth from a value of zero at the free surface, $z = 0$. The law of increase follows PRANDTL's theory of turbulent boundary layer [45], in which

$$v = \kappa u_* z, \quad u_* := \sqrt{\tau_s / \rho}, \quad (9.105)$$

where $\kappa = 0.41$ is VON KÁRMÁN's constant and u_* is the friction velocity. Substituting (9.105) into (9.68) and the resulting expression into (9.67) yields

$$\frac{d}{dz} \left(z \frac{d\mathbf{w}}{dz} \right) = \frac{if}{\kappa u_*} \mathbf{w}, \quad \mathbf{w} = u + iv, \quad z \in (0, \infty). \quad (9.106)$$

In an infinitely deep ocean this equation must be solved subject to the boundary conditions

⁶ We write here \mathbf{D} rather than $\langle \mathbf{D} \rangle$, which was used to denote the strain rate tensor of the mean velocity field. We do this for simplicity of notation.

$$\begin{aligned} -\rho\kappa u_* z \frac{dw}{dz} &= \tau_s = \tau_{sx} + i\tau_{sy}, \quad z \rightarrow 0, \\ w &= \text{bounded}, \quad z \rightarrow \infty. \end{aligned} \quad (9.107)$$

The first relates the vertical shear stress to the wind shear stress at the surface; the second requires finiteness of the current at infinity. Note also that (9.107)₁ requires dw/dz to behave as $\sim z^{-1}$ when $z \rightarrow 0$ approaches the free surface to make a non-vanishing shear stress possible; this is equivalent to a logarithmic singularity of w as $z \rightarrow 0$.

Let

$$\xi = \frac{if}{\kappa u_*} z \rightarrow \frac{d}{dz} = \frac{if}{\kappa u_*} \frac{d}{d\xi}. \quad (9.108)$$

Then (9.106) and (9.107) take the forms

$$\begin{aligned} \frac{d}{d\xi} \left(\xi \frac{dw}{d\xi} \right) &= w, \quad \xi \in (0, \infty), \\ -\rho\kappa u_* \xi \frac{dw}{d\xi} &= \tau_s, \quad \xi \rightarrow 0, \\ w &= \text{bounded}, \quad \xi \rightarrow \infty. \end{aligned} \quad (9.109)$$

Equation (9.109)₁ can be put into the standard form of BESSEL's differential equation of zeroth order. It possesses the general solution

$$w = AI_0(2\sqrt{\xi}) + BK_0(2\sqrt{\xi}), \quad (9.110)$$

where A, B are arbitrary constants of integration and I_0, K_0 are the *modified* BESSEL functions of zeroth order [1]. Since I_0 exhibits an exponential growth as $\xi \rightarrow \infty$, we have $A = 0$. The second constant, B , then follows from (9.109)₂,

$$-\kappa u_* \xi \frac{dw}{d\xi} \Big|_{\xi \rightarrow 0} = \kappa u_* \sqrt{\xi} BK_1(2\sqrt{\xi}) = \frac{\tau_s}{\rho} \quad \text{as } \xi \rightarrow 0, \quad (9.111)$$

in which K_1 is the first-order-modified BESSEL function of the second kind. Substituting for K_1 its asymptotic expansion for small ξ [1], we obtain $B = 2\tau_s/(\rho\kappa u_*)$ or

$$w = \frac{2}{\rho\kappa u_*} K_0 \left(2\sqrt{\xi} \right) \tau_s. \quad (9.112)$$

For uniform wind shear stress in the y -direction of the form $\tau_s = i\tau_{s,y}$ and with $\tau_{s,y} = \rho u_*^2$ and $\bar{\xi} = -i\xi = fz/(\kappa u_*)$, (9.112) can be shown [36] to be expressible as

$$\begin{aligned}
 w &= i \frac{2u_*}{\kappa} K_0 \left(2\sqrt{\bar{\xi}} e^{i\frac{\pi}{4}} \right) \\
 &= i \frac{2u_*}{\kappa} \left\{ \ker \left(2\sqrt{\bar{\xi}} \right) + i \operatorname{kei} \left(2\sqrt{\bar{\xi}} \right) \right\}
 \end{aligned} \tag{9.113}$$

(see [1]), which possesses the asymptotic representation

$$w = \frac{u_*}{\kappa} \left\{ \frac{\pi}{2} + \bar{\xi} \ln \bar{\xi} + i(-2\gamma - \ln \gamma) \right\} \quad \text{as } \bar{\xi} \rightarrow 0, \tag{9.114}$$

in which $\gamma = 0.577\dots$ is EULER's constant. Representation (9.113) agrees with ELLISON's [13] solution for the atmospheric boundary layer.

To examine the variation of the steady drift current with depth the solution given by (9.113) is plotted in Fig. 9.11. The velocity vector is indicated at increments of $\sqrt{\bar{\xi}} = 0.1$, with the surface current given by

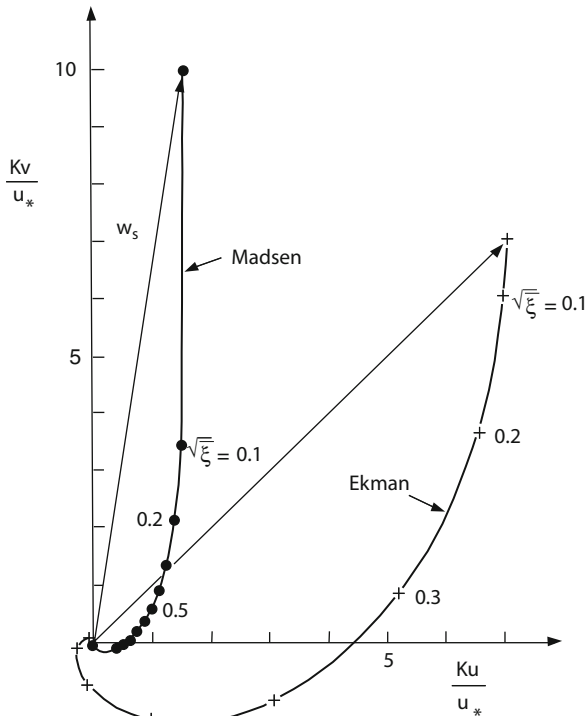


Fig. 9.11 Vertical velocity structure of a pure drift current in an infinitely deep homogeneous sea of finite lateral extent, comparing the spiral based on $v = \kappa u_* z$, (•) and the classical EKMAN spiral, (+), from MADSEN [36], ©American Meteorological Society, reprinted with permission

$$\mathbf{w}_s = \frac{u_*}{\kappa} \left\{ \frac{\pi}{2} + i \left(-1.15 + \ln \left(30 \frac{\kappa u_*}{k_s f} \right) \right) \right\} \quad (9.115)$$

from (9.114), and $k_s = 5$ cm as roughness length, to avoid the singularity at $\bar{\xi} = 0$. Note the extremely rapid decrease and rotation of the drift current with depth, a consequence of the logarithmic velocity deficit near the surface. Note, moreover, that according to (9.115), the deflection angle θ_s between the surface shear stress and the steady surface drift current is given by

$$\tan \theta_s = \frac{\pi/2}{-1.15 + \ln \left(30 \frac{\kappa u_*}{k_s f} \right)}, \quad (9.116)$$

where the deflection is to the right in the Northern Hemisphere. As can be inferred from this and Fig. 9.11, θ_s is $\sim 10^\circ$ and the velocity at $\sqrt{\bar{\xi}} = 0.1$ is approximately one-third of its value at the surface with a deflection angle of $\theta = 25^\circ$ as compared to $\theta_s = 9^\circ$. It is also evident from this figure that there is practically no motion at the depth corresponding to $\bar{\xi} = 1$; so,

$$z = \frac{\kappa u_*}{f} \quad (9.117)$$

can indeed be regarded as a measure of the extent of the frictional influence.

Interestingly, despite the considerable differences between the details of the velocity structure predicted by the EKMAN solution with constant vertical viscosity and this one, the two solutions share a common feature. The total mass transport predicted by (9.113) is found to be

$$\begin{aligned} Q &= Q_x + iQ_y = \frac{2u_*}{\kappa} \int_0^\infty \left\{ -\text{kei} \left(2\sqrt{\bar{\xi}} \right) + i \text{ker} \left(2\sqrt{\bar{\xi}} \right) \right\} d\bar{\xi} \\ &= \frac{u_*^2}{f} \int_0^\infty \{ -\beta \text{kei} \beta + i \beta \text{ker} \beta \} d\beta = \frac{u_*^2}{f}, \end{aligned} \quad (9.118)$$

which is identical to the result obtained from EKMAN's theory as it should be since the result is independent of ν .

The above solution of the complex-valued differential equation (9.106) exhibits a logarithmic singularity at $z = 0$. To avoid it, a coordinate shift

$$\bar{z} = z + z_0, \quad \text{where } z_0 > 0 \quad (9.119)$$

is applied. The two-point boundary value problem now becomes

$$\left. \begin{aligned} ((\bar{z} + z_0)\mathbf{w}')' &= \frac{if}{\kappa u_*} \mathbf{w} & 0 < \bar{z} < \infty, \\ \rho \kappa u_* (\bar{z} + z_0) &= -i\tau_s & \text{at } \bar{z} = 0, \\ \mathbf{w} &= 0 & \text{at } \bar{z} \rightarrow \infty. \end{aligned} \right\} \quad (9.120)$$

Now, the singularity is avoided since $\bar{z} = 0$ is never attained. $z_0 > 0$ is a *roughness length* and of the order of millimetres, e.g. $z_0 = 1.5$ mm.

HEAPS [23] writes ‘The results obtained by MADSEN, compared with those by EKMAN’s theory show a more rapid decrease and rotation of the current vector with depth: due to a steep logarithmic fall of the velocity component in the wind direction, near to the surface and downwards from it. For a range of wind speeds, MADSEN’s model gives an angle of deflection of the surface current to the right of the wind stress about 10° and a wind factor of approximately 0.03. These values agree with deductions made from surface drift experiments and observations of oil spill trajectories (PEARCE and COOPER, [42], figure 1) [. . .]. MADSEN’s model shows that the depth of the wind-induced motion (down to a level of practically no current) is approximately $0.41u_*/f$, a length which corresponds to D in the Ekman theory. Setting $D = 0.41u_*/f$ [. . .] [and using the definition (9.73) of the frictional depth] yields an expression for the corresponding constant eddy viscosity in the EKMAN theory:

$$\nu = 0.008 \frac{u_*^2}{f}. \quad (9.121)$$

(from HEAPS [23]).’

A linear increase of the eddy viscosity with depth cannot be realistic, since turbulent intensity decreases with depth and may die out completely at large depth. HEAPS continues that ‘SVENSSON [49] employed a turbulence model (using $k - \varepsilon$ closure condition⁷) to determine the vertical structure of current in the surface EKMAN layer. A vertical eddy viscosity distribution of the form shown in Fig. 9.12b was obtained, showing a linear increase in viscosity near the sea surface as in MADSEN’s model, turning, however, into a decrease lower down. The depth of penetration of the motion was found to be approximately $1.0u_*/f$. The use of a constant eddy viscosity

⁷ In the $k - \varepsilon$ model the kinematic viscosity ν is parameterised according to

$$\nu = c_\mu \frac{k^2}{\varepsilon}$$

where $c_\mu = 0.09$ is a dimensionless constant, k is the specific turbulent kinetic energy with dimension $\text{m}^2 \text{s}^{-2}$ and ε the specific dissipation rate of turbulent kinetic energy with dimension $\text{m}^2 \text{s}^{-3}$. The model is complemented by postulating evolution equations for k and ε , so that the kinematic viscosity can vary with time and position. For the presentation of the $k - \varepsilon$ model, see Chap. 6.

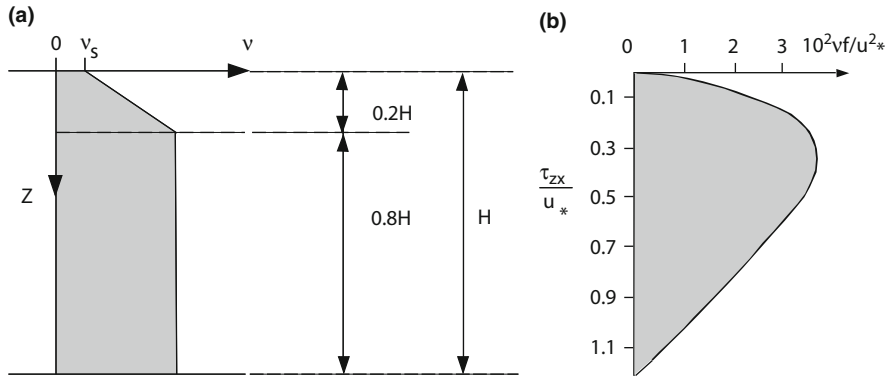


Fig. 9.12 (a) Eddy viscosity distribution with a surface wall layer. (b) Eddy viscosity distribution from SVENSSON's turbulence model, using $k - \varepsilon$ closure condition

$$\nu = 0.026u_*^2 \quad (9.122)$$

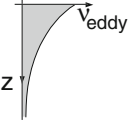
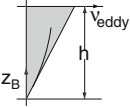
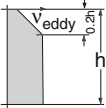
was found to give velocity and shear stress distributions in good agreement with those obtained from the turbulence model [. . .]. An eddy viscosity decaying with depth reflects the expected condition of diminishing turbulence intensity as distance below the surface increases', [23]. Theories prescribing different vertical variations of the eddy viscosity and treating the EKMAN problem in a homogeneous fluid of infinite or finite depth are summarised in Table 9.3. Accordingly, the eddy viscosity either increases or decreases as the free surface is approached from below. HEAPS [23] writes 'While a decrease seems most likely on the weight of evidence so far available, there appears to be little or no observational evidence to confirm this for the full range of wind speeds. According to work performed by CSANADY between 1976 and 1982 (see Table 9.3) the surface EKMAN layer can be considered to consist of a relatively thin layer at the free surface through which the eddy viscosity varies linearly with depth from a small surface value ν_s and an outer layer through which the eddy viscosity remains constant. Thus,

$$\nu = \begin{cases} \kappa u_* z + \nu_s, & 0 \leq z < \frac{h}{\kappa \mathbb{R}_e}, \\ \frac{u_* h}{\mathbb{R}_e} + \nu_s, & \frac{h}{\kappa \mathbb{R}_e} \leq z \leq h, \end{cases} \quad (9.123)$$

where h is the depth of the EKMAN layer and \mathbb{R}_e a REYNOLDS number lying between 12 and 20', implying that $h/(\kappa \mathbb{R}_e) \in [0.125, 0.208]$. Then, with $h = 0.4u_*/f$ say, the eddy viscosity in the outer layer takes the value

$$\nu = (0.02 - 0.033) \frac{u_*^2}{f} + \nu_s. \quad (9.124)$$

Table 9.3 Vertical distributions of eddy viscosity used by various authors for the solution of the EKMAN problem in an infinite homogeneous fluid layer

Exponential decay with depth ($h \rightarrow \infty$)	DOMBROKLONSKIY (1969) [11] LAI & RAO (1976) [33] WITTEN & THOMAS (1976) [54]
	
Proportional to the height z_B above the bottom surface	THOMAS (1975) [51]
	
Proportional to $z_B^{4/3}$	FJELDSTAD (1930) [15]
Linearly distributed to a certain depth ($0.2h$) from the surface, then constant	CSANADY (1976)–(1982) [5–9] PEARCE & COOPER (1981) [42] BOWDEN et al. (1959) [3] HEAPS & JONES (1984) [24]
	

According to HEAPS [23], ‘PEARCE and COOPER [42] have used (9.123) for computations of wind-induced flows in shallow water of depth h (Fig. 9.12a) employing a slip condition at the sea bed. BOWDEN et al. [3] proposed a similar distribution of vertical eddy viscosity to account for the presence of the wall layer adjacent to the sea bed in tidal flow; the corresponding theory was worked out by HEAPS and JONES [24]. Generally, the profile of eddy viscosity is modified by a wall layer at the sea surface and a wall layer at the sea bed. These layers have distinct length and velocity scales when the corresponding EKMAN layers do not overlap. At the bottom, the stress, and hence u_* , depends on the motion of the water.’

Practically, the construction of the current is determined by a patching together of a near-surface PRANDTL layer in which, because of its thinness, the CORIOLIS effects due to the rotation of the Earth are ignored and an EKMAN solution below this viscous PRANDTL layer. The stress is assumed to remain constant through the PRANDTL layer, but the eddy viscosity is taken as linearly increasing through this layer. Consequently, if the uniform wind stress τ_s points in the positive y -direction, the momentum equations in this layer take the forms

$$\begin{aligned} -\rho(\kappa u_* z) \frac{\partial u}{\partial z} &= 0, \\ -\rho(\kappa u_* z) \frac{\partial v}{\partial z} &= \tau_s = \rho u_*^2, \end{aligned} \tag{9.125}$$

whence

$$\begin{aligned} \frac{\partial u}{\partial z} &= 0 & \rightarrow & u = u_s, \\ \frac{\partial v}{\partial z} &= -\frac{u_*}{\kappa z} & \rightarrow & v = v_s - \frac{u_*}{\kappa} \ln \left(\frac{z}{z_0} \right). \end{aligned} \quad (9.126)$$

Thus, the velocity profile through the PRANDTL layer is logarithmic and parallel to the wind shear stress; u_s and v_s denote the components of the current at the free surface (the top of the PRANDTL layer) taken at $z = z_0 > 0$ to avoid the logarithmic singularity. At the bottom of this PRANDTL layer, at $z = z_1$, the velocity components u_1 and v_1 are given by what is obtained as surface current of the EKMAN problem (of finite or infinite) depth, e.g. (9.78) for the infinite depth case. This is so, because the wind stress is transmitted through the PRANDTL layer without change. Therefore, from (9.126),

$$u_s = u_1, \quad v_s = v_1 + \frac{u_*}{\kappa} \ln \left(\frac{z_1}{z_0} \right). \quad (9.127)$$

HEAPS remarks that this says that the surface current obtained with a PRANDTL layer may be obtained from the surface current derived from the pure EKMAN theory by adding a logarithmic contribution in the direction of the wind. Such an addition increases the magnitude of the surface current and reduces its angle of deflection from the wind direction.

CSANADY [9] proposed instead of (9.127)

$$u_s = u_1, \quad v_s = v_1 + \frac{u_*}{\kappa} \ln \left(\frac{z_1}{z_0} \right) + 8.5u_*, \quad (9.128)$$

but gives no justification for the last term of (9.128).

9.3.2 Steady Wind-Induced Circulation in a Homogeneous Lake on the Rotating Earth

The steady wind-driven currents analysed so far have been characterised by increasing complexity of the original EKMAN problem. The infinite extent of the fluid basin prevented horizontal pressure gradients from being formed because of the absence of boundaries. Complexities were added by (i) replacing infinitely deep-water domains by finite depth basins and (ii) replacing constant eddy viscosities by functional relations accounting for their vertical variations. So-called *gradient currents* are established if the horizontal pressure gradient does not vanish, $\text{grad}_H p \neq 0$. In the present approximation

$$p = p_a + \rho g(z + \zeta) \quad (9.129)$$

with constant atmospheric pressure p_a but variable free surface elevation, this implies $\text{grad}_H \zeta \neq 0$. In steady state and with simplifications analogous to those of the previous sections, the governing equations take the forms

$$\begin{aligned} -fv &= -g \frac{\partial \zeta}{\partial x} + \frac{\partial}{\partial z} \left(\nu \frac{\partial u}{\partial z} \right), \\ fu &= -g \frac{\partial \zeta}{\partial y} + \frac{\partial}{\partial z} \left(\nu \frac{\partial v}{\partial z} \right), \\ \frac{\partial u}{\partial x} + \frac{\partial v}{\partial y} + \frac{\partial w}{\partial z} &= 0, \end{aligned} \quad (9.130)$$

where (9.129) has been substituted. Equations (9.130)_{1,2} are the steady linearised horizontal momentum equations, in which only the horizontal shear stresses are accounted for and a NEWTONian viscous closure has been applied, and (9.130)₃ is the continuity equation which is the only field equation in which the vertical velocity component arises.

With

$$\mathbf{w} = u + iv, \quad \frac{\partial \zeta}{\partial n} = \frac{\partial \zeta}{\partial x} + i \frac{\partial \zeta}{\partial y}, \quad \tau_s = \tau_{sx} + i \tau_{sy} \quad (9.131)$$

equations (9.130)_{1,2} take the forms

$$if\mathbf{w} = -g \frac{\partial \zeta}{\partial n} + \frac{\partial}{\partial z} \left(\nu \frac{\partial \mathbf{w}}{\partial z} \right), \quad (9.132)$$

subject to the boundary conditions

$$\left. \begin{aligned} -\rho \nu \frac{\partial \mathbf{w}}{\partial z} &= \tau_s, & \text{at } z = 0, \\ \mathbf{w} &= 0, & \text{at } z = h. \end{aligned} \right\} \quad (9.133)$$

Here, τ_s is the prescribed surface wind stress, and $\mathbf{w} = 0$ expresses the basal no-slip condition. The boundary value problem (9.132) and (9.133) is linear and τ_s as well as $\partial \zeta / \partial n$ can be treated as externally prescribed quantities, at least momentarily. Therefore, its solution is a linear combination of the external terms, viz.,

$$\mathbf{w} = P(z)\tau_s + Q(z)\frac{\partial \zeta}{\partial n}. \quad (9.134)$$

In this representation the functions P and Q only depend on the depth variable z , but τ_s and $\partial \zeta / \partial n$ can have x, y -dependences. So, $\mathbf{w} = \mathbf{w}(x, y, z)$.

Problem 9.5 Prove by solving the two-point boundary value problem (9.132), (9.133) that

$$\begin{aligned}
 Q(z) &= i \frac{g}{f} \left\{ \frac{\cosh \left((1+i) \frac{\pi z}{D} \right)}{\cosh \left((1+i) \frac{\pi h}{D} \right)} - 1 \right\}, \\
 P(z) &= \frac{(1-i)D}{2\pi\rho\nu} \left\{ \frac{\sinh \left((1+i) \frac{\pi}{D} (z-h) \right)}{\sinh \left((1+i) \frac{\pi h}{D} \right)} \right\},
 \end{aligned} \tag{9.135}$$

where $D = \pi \sqrt{2\nu/f}$.

Hint: Because of the linearity of the problem, it is advantageous to solve two problems: and (i) $\tau_s = 0$, $\partial\zeta/\partial n \neq 0$ and (ii) $\tau_s \neq 0$, $\partial\zeta/\partial n = 0$. ♦

As is evident from (9.134) and (9.135), the functions P and Q describe the vertical distribution of the horizontal current due to the wind shear stress and the surface gradient, respectively.

For $\tau_s = \tau_{sx}$ the function P has already been discussed in connection with Fig. 9.8; for a surface gradient in the y -direction, $\partial\zeta/\partial x = 0 \rightarrow \partial\zeta/\partial n = i\partial\zeta/\partial y$ and with $\tau_s = 0$ the distribution of the horizontal current is shown in Fig. 9.13. The fluid region is bounded along a line parallel to (but here identical with) the x -axis. The figure shows the projection of the gradient current at all z -levels into the hodograph plane. For a layer depth smaller than D , the surface current tends towards the direction of the gradient $\partial\zeta/\partial n$, expressing the influence of the bottom friction. The deflection angle between the current and the gradient direction decreases as the basin becomes shallower. On the other hand, for depths larger than the EKMAN depth, the surface current is practically equal to that obtained by a geostrophic balance.

With the representations (9.134) and (9.135) we are now in the possession of all ingredients to describe analytically the steady wind-induced currents in an enclosed

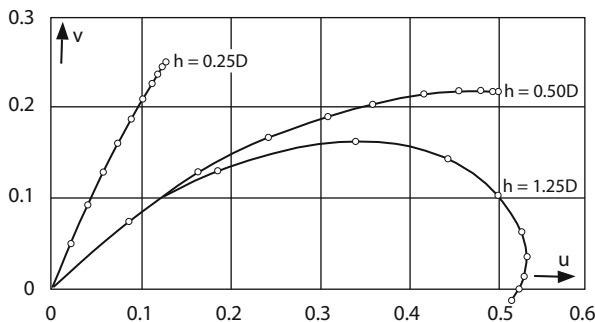


Fig. 9.13 Vertical structure of the gradient currents in a basin of depth h nearly equal to or smaller than the EKMAN depth D , according to LACOMB [32]

lake or ocean basin. To this end, note that $w(z)$ can be integrated over depth; this yields

$$W = \int_0^h w dz = \frac{A}{\rho f} \tau_s + \frac{gh}{f} B \frac{\partial \zeta}{\partial n}, \quad (9.136)$$

where A and B are depth integrals of P and Q and as such functions of h/D , or when separating real and imaginary parts

$$\begin{aligned} U &= \frac{1}{\rho f} (A_1 \tau_{sx} - A_2 \tau_{sy}) + \frac{gh}{f} \left(B_1 \frac{\partial \zeta}{\partial x} - B_2 \frac{\partial \zeta}{\partial y} \right), \\ V &= \frac{1}{\rho f} (A_2 \tau_{sx} + A_1 \tau_{sy}) + \frac{gh}{f} \left(B_2 \frac{\partial \zeta}{\partial x} + B_1 \frac{\partial \zeta}{\partial y} \right), \end{aligned} \quad (9.137)$$

with

$$U = \int_0^h u dz, \quad V = \int_0^h v dz. \quad (9.138)$$

(U, V) , (A_1, A_2) and (B_1, B_2) are the real and imaginary parts of W , A , B , respectively. Moreover, integrating the continuity equation over depth yields

$$\frac{\partial \zeta}{\partial t} + \frac{\partial U}{\partial x} + \frac{\partial V}{\partial y} = 0 \quad \xrightarrow{\text{steady flow}} \quad \frac{\partial U}{\partial x} + \frac{\partial V}{\partial y} = 0. \quad (9.139)$$

Thus, the depth-integrated volume (and because of density preserving when multiplied with ρ , mass) transport is solenoidal. Equation (9.139)₂ suggests the introduction of the *transport stream function*

$$U = \frac{\partial \psi}{\partial y}, \quad V = -\frac{\partial \psi}{\partial x}. \quad (9.140)$$

Substituting these on the left-hand sides of (9.137) and solving the emerging equations for $\partial \zeta / \partial x$ and $\partial \zeta / \partial y$ gives

$$\begin{aligned} \frac{\partial \zeta}{\partial x} &= \frac{f}{g} \left(\beta_1 \frac{\partial \psi}{\partial y} - \beta_2 \frac{\partial \psi}{\partial x} \right) - \frac{1}{\rho g} (\beta_3 \tau_{sx} + \beta_4 \tau_{sy}), \\ \frac{\partial \zeta}{\partial y} &= -\frac{f}{g} \left(\beta_1 \frac{\partial \psi}{\partial x} + \beta_2 \frac{\partial \psi}{\partial y} \right) + \frac{1}{\rho g} (\beta_4 \tau_{sx} - \beta_3 \tau_{sy}), \end{aligned} \quad (9.141)$$

where

$$\begin{aligned} \beta_1 &= B_1 / ((B_1^2 + B_2^2)h), \quad \beta_2 = B_2 / ((B_1^2 + B_2^2)h), \\ \beta_3 &= \beta_1 A_1 + \beta_2 A_2, \quad \beta_4 = \beta_2 A_1 - \beta_1 A_2. \end{aligned} \quad (9.142)$$

Differentiating (9.141)₁ with respect to y and (9.141)₂ with respect to x and subtracting the two emerging relations lead to the equations

$$E[\psi] := \nabla^2 \psi + \gamma_1 \frac{\partial \psi}{\partial x} + \gamma_2 \frac{\partial \psi}{\partial y} = \gamma_3, \quad (9.143)$$

in which

$$\begin{aligned} \gamma_1 &= \frac{1}{\beta_1} \left(\frac{\partial \beta_1}{\partial x} - \frac{\partial \beta_2}{\partial y} \right), & \gamma_2 &= \frac{1}{\beta_1} \left(\frac{\partial \beta_1}{\partial y} + \frac{\partial \beta_2}{\partial x} \right), \\ \gamma_3 &= \frac{1}{\rho f \beta_1} \left[\beta_3 \left(\frac{\partial \tau_{sx}}{\partial y} - \frac{\partial \tau_{sy}}{\partial x} \right) + \beta_4 \left(\frac{\partial \tau_{sx}}{\partial x} + \frac{\partial \tau_{sy}}{\partial y} \right) \right. \\ &\quad \left. + \left(\frac{\partial \beta_4}{\partial x} + \frac{\partial \beta_3}{\partial y} \right) \tau_{sx} + \left(\frac{\partial \beta_4}{\partial y} - \frac{\partial \beta_3}{\partial x} \right) \tau_{sy} \right]. \end{aligned} \quad (9.144)$$

The derivation of (9.143) and (9.144), in slightly different form, is also given by GEDNEY and LICK (1972) [20] and the coefficient functions can be found in GEDNEY's Ph.D. dissertation [19].

Equation (9.143) is a second-order partial differential equation for the volume transport stream function ψ for applied wind shear stress. The coefficient functions γ_1 and γ_2 depend only on h/D and horizontal derivatives of it and are known for any lake since they can be derived from A and B , the depth integrals of $P(z)$ and $Q(z)$. The term on the right-hand side of (9.143), γ_3 is a linear combination of the horizontal wind shear stress components and their x - and y -derivatives with pre-factors which are again functions deducible from A and B . Therefore, for a given basin, the left-hand side (9.143) is independent of the wind shear stress. This only enters its right-hand side.

The elliptic equation (9.143) is solved subject to the boundary conditions along the shore of the basin. For a lake for which the current due to river inflows and river outflow is negligible in terms of the induced currents, one may assume that the shoreline is impermeable. With the flow normal to the circumscribing lateral boundary given by

$$\psi = \int_0^s \left(U \frac{dy}{ds} - V \frac{dx}{ds} \right) ds, \quad (9.145)$$

where s is the arc length measured along the boundary from some fixed position on it, and U , V are the transport components along the shore, vanishing flow normal to the shore periphery then implies

$$\psi = 0. \quad (9.146)$$

Equations (9.143) and (9.146) describe the boundary value problem

$$\begin{aligned} E[\psi(x, y)] &= \gamma_3(\tau_s), & (x, y) \in D \subset \mathbb{R}^2, \\ \psi &= 0, & (x, y) \in \partial D, \end{aligned} \quad (9.147)$$

which must be solved for a particular lake for given prescribed surface shear stress distribution. Once $\psi(x, y)$ is known, the surface displacement gradient can be determined from (9.141) and the horizontal transport components from (9.140). The horizontal current w then follows from (9.134) and subsequently the vertical velocity from the continuity equation (9.130)₃

$$w = \frac{\partial}{\partial x} \int_z^h u dz + \frac{\partial}{\partial y} \int_z^h v dz. \quad (9.148)$$

This completes the solution. The method, however, calls for a number of remarks:

- HEAPS [23], whom the derivation follows, states: ‘The above method, first proposed by WELANDER [52], has been used to study wind-driven currents in Lake Ontario [2] and Lake Erie [20]. Consistent with the developments described above, the eddy viscosity was assumed to be a constant. However, the use of the method when vertical eddy viscosity varies linearly from zero at the bottom to a maximum $\kappa u_* h$ at the surface has been investigated by THOMAS [51]. The case in which vertical eddy viscosity decreases exponentially with depth from a prescribed constant maximum at the surface has been investigated by WITTEN and THOMAS’ [54].
- The method can also be applied to more flexible conditions, e.g. by changing the bottom boundary condition to general slip and/or the use of an eddy viscosity which may vary with depth. This will alter the functions $P(z)$ and $Q(z)$ and, consequently A , B and the subsequent coefficient functions β_i , ($i = 1, \dots, 4$) and γ_i ($i = 1, 2, 3$), which depend on A and B . The conceptual procedure as such would not change.
- The method is approximate not only by the mentioned simplifications but indirectly and somewhat hidden by the fact that the functions $P(z)$ and $Q(z)$ in (9.135) (or alternative variants of them) are constructed on the assumption of a basin of infinite horizontal extent and constant depth. Their use in the construction of the elliptic boundary value problem is, therefore, strictly, not justified. Moreover, the use of these functions in a lake domain with variable depth is, strictly, neither permissible, but the method makes use of this assumption via the coefficients β_i ($i = 1, \dots, 4$) and γ_i ($i = 1, 2, 3$) and their x - and y -derivatives. For weak variations of the bathymetry, the results might be acceptable if one restricts attention to sub-regions of the lake, which are distant from shore. However, no studies have been found by which errors would have been identified.

9.3.3 Wind-Driven Steady Currents in Lake Erie

In their application of the above solution technique to the steady distribution of the vertical structure of the horizontal currents in Lake Erie, GEDNEY and LICK [20] were confronted with the problem of solving the partial differential equation (9.143) in a lake domain with N islands. This means that boundary conditions must be fulfilled at exterior and interior boundaries. The solution procedure is strictly based on the linearity of the problem and uses the fact that the surface gradient $\partial\zeta/\partial n$ is known from (9.136) once W is determined. So

$$\frac{\partial\zeta}{\partial s} = \cos\alpha \frac{\partial\zeta}{\partial x} + \sin\alpha \frac{\partial\zeta}{\partial y}, \quad (9.149)$$

in which α is the angle between the x - and s -directions, is equally determined at any point in the lake domain. Consider now the integral $\oint_C (\partial\zeta/\partial s)ds$ along any closed double-point free curve in the lake domain. Then, it is clear that after a complete revolution around a closed curve C , the surface elevation ζ must reach the same value, implying that

$$\oint_C \frac{\partial\zeta}{\partial s} ds = 0, \quad (9.150)$$

for otherwise ζ could experience a jump. This condition must, in particular, hold for a closed path along the boundary of an island along which the transport stream function is constant. If this constant is inappropriately chosen, then condition (9.150) will be violated.

To solve (9.147), the values of the stream function on each island boundary and on the outer shore are selected by a composition from N linearly independent stream functions

$$\psi = \psi_0 + \sum_{\alpha=1}^N d_{\alpha} \psi^{\alpha}, \quad (9.151)$$

where for $N = 3$ the stream function boundary and wind conditions are shown in Table 9.4. In this table $\psi_r(s)$ is the value of the stream function on the external

Table 9.4 Stream function boundary conditions

ψ^i boundary condition					
ψ^i solution	External shore	Island 1	Island 2	Island 3	Wind cond.
ψ^0	$\psi_r(s)$	1^a	1^a	1^a	τ_{sx}, τ_{sy}
ψ^1	0	1	0	0	0
ψ^2	0	0	1	0	0
ψ^3	0	0	0	1	0

^aNote, the stream function values for ψ_0 at the island boundary can be any constant, the same for all islands (here equal to 1) since the total stream function is determined up to a constant value

boundary and specified by the river inflow and outflow (having value zero at impermeable segments of the shore and a value equal to the unit-width discharge at inflow or outflow segments with appropriate sign). The constants d_α ($\alpha = 1, 2, \dots, N$) are determined such that (9.150) is satisfied along each boundary encircling the island.

GEDNEY and LICK [20] solved (9.143) for the four different boundary conditions by finite difference methods whose detailed implementation will not be repeated here. Lake Erie was partitioned into two regions: (i) an island region with 0.802 km square meshes and (ii) the remainder with 3.22 km square meshes, using second-order symmetric finite difference schemes and non-symmetric schemes at boundary grid points, see Fig. 9.14 which also shows the bathymetry and the island region in relation to the entire lake. The entire discretised domain was occupied with 5050 grid points.

Numerical solutions for the stream function and velocities in Lake Erie were constructed for a constant kinematic viscosity, $\nu = 0.0038 \text{ m}^2 \text{ s}^{-1}$ and for a uniform wind from W 50°S (in standard notation SSW (220°) of 10.1 m s^{-1} speed. This speed was measured at 6 m above the lake surface and it led to a wind shear stress magnitude

$$\tau = 2.73 \times 10^{-3} \rho_a W_a^2,$$

where ρ_a and W_a are the density of air and the 6 m wind speed, respectively, in which the drag coefficient was determined from independent measurements [53].

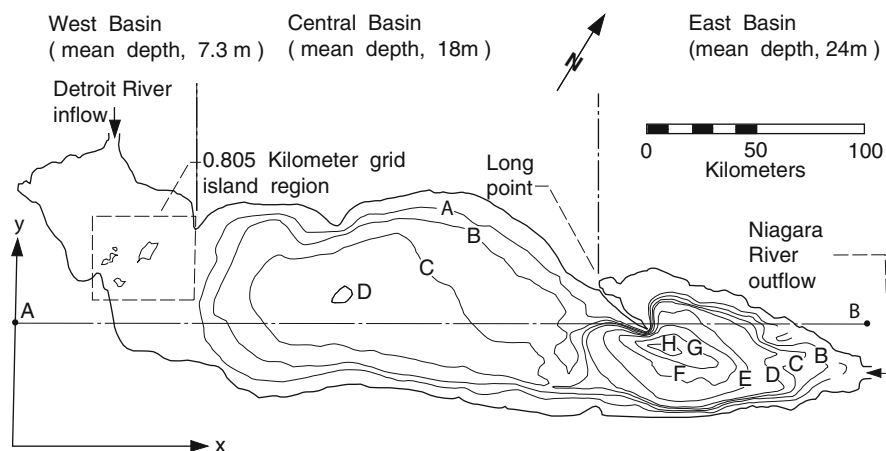


Fig. 9.14 Lake Erie bathymetry with depth levels in metres as follows: A: 15.2 m; B: 18.3 m; C: 21.6 m; D: 24.4 m; E: 33.5 m; F: 42.7 m; G: 51.6 m and H: 58.0 m. Morphologically, the lake is divided into the West basin with mean depth 7.3 m, central basin with mean depth 18 m and East basin with mean depth 24 m. The *dashed rectangle* outlines the island region enclosing two islands plus three additional smaller islands collapsed numerically to one. Inflow and outflow river locations with $5380 \text{ m}^3 \text{ s}^{-1}$ discharge are also indicated, from GEDNEY and LICK [20]

Figure 9.15 shows isolines of the stream function for the above wind conditions. In the Northern and Southern portion of the central basin it shows a clockwise and counterclockwise rotating volume transport gyre, respectively. In the Eastern basin, the gyre structure is analogous, whereby the gyre in the North is ‘squeezed’ because of the narrowing between the two basins. These gyres are evidently generated by the bathymetric slopes along the shores, as it is well known that a constant bottom slope causes a single gyre that intensifies the flow close to the boundary (Fig. 9.16). The asymmetry of the gyres is evidently due to the different intensities of $\partial h/\partial y)/h$ along the Northern and Southern shores.

Figure 9.17 displays lake velocity plots for the W 50°S wind at depths 0.4 m (a); 6.7 m (b); 9.9 m (c); 14.9 m (d) below the surface and 1.2 m (e) above the bottom surface. The beginning of the arrow represents the actual location of the

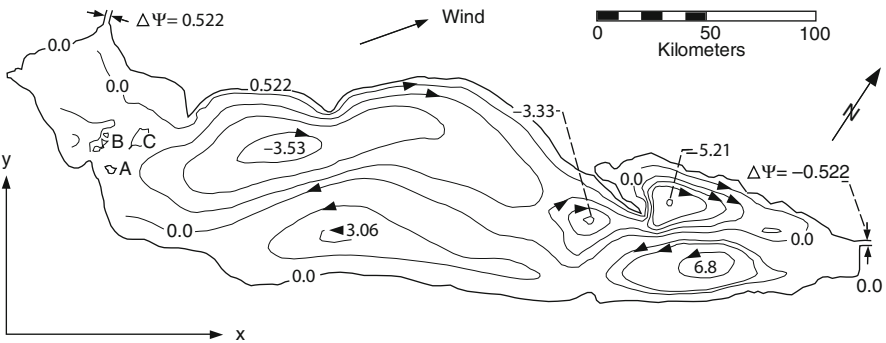


Fig. 9.15 Isoline plot of the steady volume transport stream function for Lake Erie for a uniform steady wind from W 50°S with 10.1 m s^{-1} speed. The ψ -boundary values at the islands are A, -0.375 ; B, -0.087 ; C, -0.432 , adapted from GEDNEY and LICK [20]

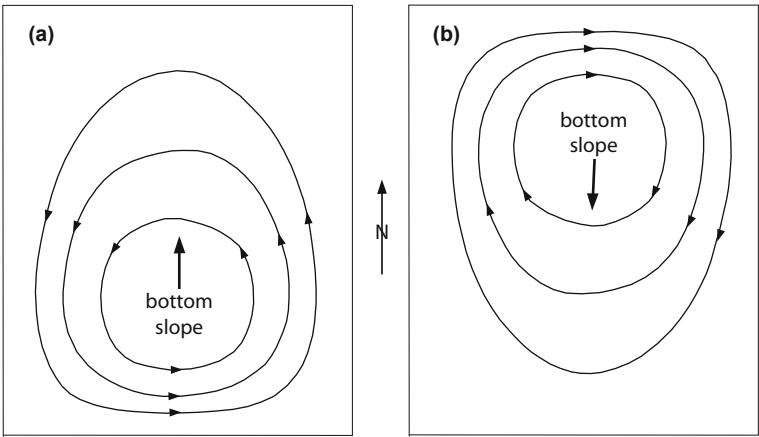
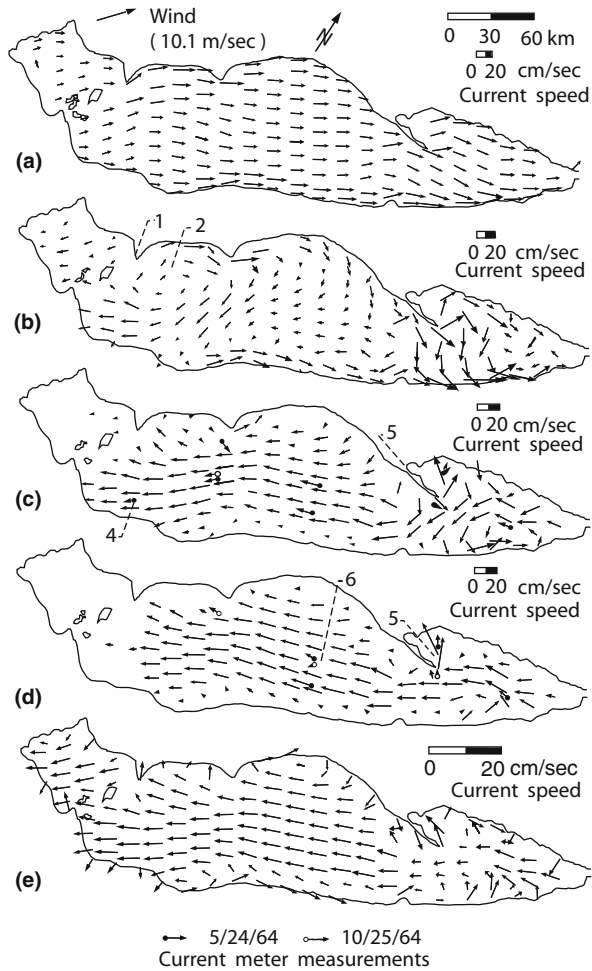


Fig. 9.16 Isolines of the steady volume transport stream function in a rectangular basin with constant North–South bottom slope towards North (a) and towards South (b), respectively (schematic)

Fig. 9.17 Horizontal velocity plots at the depths 0.4 m (a); 6.7 m (b); 9.9 m (c); 14.9 m (d) and 1.2 m above the bottom surface (e). Each panel has its own velocity scale (see *inserts*). Wind direction and geographic North are also indicated as is the length scale (*top*) and the symbols for the measured velocities on 24/25 May 1964 (*bottom*), composed from figures of GEDNEY and LICK [20]



current represented by the arrow. The magnitude of the current is indicated by the velocity scale in each panel. Panels (a) and (b) show that a top surface mass flux is transported towards the Eastern and Southern boundaries. The subsurface return current maintaining mass balance in the opposite direction (towards West) is shown in panels (c) to (e). In the central and Eastern basins, surface currents at 0.4 m are, in general, smaller in the centre of the lake than near the shore. This effect is likely due to the relatively large subsurface return current down the centre of the lake, which is opposite in direction to the surface current. Note also that comparison of velocity plots with the volume transport stream function in Fig. 9.15 is difficult and, generally, fairly inconclusive since horizontal velocities are local, while the stream function is depth averaged.

GEDNEY and LICK [20] used measured velocity data from current metres deployed by the Environmental Protection Agency of the USA (EPA) at the

indicated positions (Fig. 9.17). Such a comparison is critical and perhaps even questionable for steady conditions because steady episodes are unlikely in any lake subjected to wind stress. The EPA data recorded in May 1964 consisted of readings taken every 20 min. To compare the water current measurements with calculations, GEDNEY and LICK summed the 20 min readings over a 24-h period to form a resultant current. The resultant magnitude, divided by the number of readings, and the orientation of the resultant current then ‘define’ the steady counterpart of the time evolving current.

‘The procedure incorporated for determining what wind to use in the numerical calculations for a particular day was to take the average of both the direction and magnitude of the 24-h resultant wind at each of the US Weather Bureau shore stations. This average wind with its magnitude increased by a factor of 1.48 was then used to determine the shear stress at the water surface. The 1.48 factor was determined by comparing shore data with “over-the-lake” wind data taken by the EPA’, GEDNEY and LICK [20]. This determined the 10.1 m s^{-1} speed with wind direction from W 50° S. ‘The current metre data for 24 May 1964, as measured at 10 and 15 m below the surface, is shown in Fig. 9.17c,d. Note that the positions of the measurements are different from those of the calculated current vectors’. GEDNEY and LICK note that ‘the agreement is markedly good in both magnitude and direction. The discrepancy between the magnitude of the measurements and calculations at point 4 at 10 m is believed to be a measurement error since this metre became erratic at a later date. The magnitude of the measurements in the region of point 5 at first appears to be considerably different from the calculated values. However, the agreement between the measurements and calculations is believed to be satisfactory when one considers that the currents are changing rapidly with distance in the point 5 area’.

‘Also, in panels (c), (d) of Fig. 9.17, the current metre measurements are plotted for a W 43° S wind at a speed of 8.6 m s^{-1} . These measurements were taken on May 25, 1964. The agreement is again quite good except for the measurement at point 6 in panel (d). [...] The winds for these measurements differ from the May 24, 1964, case by 1.5 m s^{-1} and 7° in direction. However, both sets of measurements agree quite well with the calculations and with each other’, GEDNEY and LICK [20].

We close this example of application with the following remarks: Given the unsteadiness of the natural wind input and the fact that a steady alternative of the time varying wind velocities is in this case a construct whose validity as a steady wind shear stress is not verified, the agreement between measured and computed velocities is surprising. Beyond this, the model equations have their obvious shortcomings by way of their linearity, EKMAN-type vertical current distribution, slow horizontal variation of the bathymetry and constant (eddy) viscosity. These facts make it even a greater surprise that the agreement between measured and computed velocities is as good as it is. If this is not accidental, one may conclude that the steady circulation is a mode of response for a lake which, on time scales of a day or so, is very robust against fluctuations around the mean wind input. This may be a reason why lakes have their typical circulation structure, which can be observed repeatedly.

9.3.4 Time-Dependent Wind-Induced Currents in Shallow Lakes on the Rotating Earth

9.3.4.1 Development of the Underlying Models

Early theoretical models for calculating time-dependent wind-induced currents have been treated in much the same way as explained above for steady problems. The same simplifying assumptions are invoked – linearity, hydrostatic pressure, only vertical shear stresses are accounted, constant vertical eddy viscosity, no-slip boundary condition at the bottom surface. Thus, re-introducing the time dependence in the momentum equations, subject to the same simplifying assumptions as before, these equations now take the forms (compare with (9.130))

$$\begin{aligned}\frac{\partial u}{\partial t} - f v &= -g \frac{\partial \zeta}{\partial x} + \frac{\partial}{\partial z} \left(\nu \frac{\partial u}{\partial z} \right), \\ \frac{\partial v}{\partial t} + f u &= -g \frac{\partial \zeta}{\partial y} + \frac{\partial}{\partial z} \left(\nu \frac{\partial v}{\partial z} \right), \\ \frac{\partial u}{\partial x} + \frac{\partial v}{\partial y} + \frac{\partial w}{\partial z} &= 0.\end{aligned}\tag{9.152}$$

With the complex notation (9.131) the horizontal momentum equations (9.152)_{1,2} are given by

$$\frac{\partial \mathbf{w}}{\partial t} + i f \mathbf{w} = -g \frac{\partial \zeta}{\partial n} + \frac{\partial}{\partial z} \left(\nu \frac{\partial \mathbf{w}}{\partial z} \right).\tag{9.153}$$

Boundary and initial conditions to which this equation is subjected are the prescription of the wind shear stress at the free surface, the no-slip condition at the bottom surface and the condition of a state of rest at the start $t = 0$, viz.,

$$\left. \begin{aligned} -\rho \nu \frac{\partial \mathbf{w}}{\partial z} &= \tau_s, & \text{at } z = 0, \\ \mathbf{w} &= 0, & \text{at } z = h, \\ \mathbf{w} &= 0, & \text{at } t = 0. \end{aligned} \right\}\tag{9.154}$$

The linear initial boundary value problem has been solved for constant ν by constructing the GREEN's functions of two different problems. The first gives the dynamic response, $\mathbf{w}_1(z, t)$ to unit wind stress in the x -direction, suddenly created at $t = 0$ and maintained; with a constant vertical eddy viscosity, \mathbf{w}_1 satisfies the equations

$$\left. \begin{aligned} \frac{\partial w_1}{\partial t} + ifw_1 &= v \frac{\partial^2 w_1}{\partial z^2}, & z \in (0, h), \quad t \geq 0, \\ -\rho v \frac{\partial w_1}{\partial z} &= 1, & \text{at } z = 0, \quad t > 0, \\ w_1 &= 0, & \text{at } z = h, \quad t > 0, \\ w_1 &= 0, & \text{at } z \in [0, h], \quad t = 0. \end{aligned} \right\} \quad (9.155)$$

The second solution, $w_2(z, t)$ gives the response to a unit surface slope in the x -direction, suddenly created at $t = 0$ and maintained; it satisfies the equations

$$\left. \begin{aligned} \frac{\partial w_2}{\partial t} + ifw_2 &= -g \cdot 1 + v \frac{\partial^2 w_2}{\partial z^2}, & z \in (0, h), \quad t \geq 0, \\ -\rho v \frac{\partial w_2}{\partial z} &= 0, & \text{at } z = 0, \quad t > 0, \\ w_2 &= 0, & \text{at } z = h, \quad t > 0, \\ w_2 &= 0, & \text{at } z \in [0, h], \quad t = 0. \end{aligned} \right\} \quad (9.156)$$

Analytical solutions for w_1 and w_2 have been constructed by FJELDSTAD (1930) [15] and HIDAKA (1933) [26]. Because of linearity of the three problems (9.153), (9.154), (9.155), (9.156), a solution to a general distribution of τ_s and $\partial\zeta/\partial n$ is obtained by superposing a succession of surface increments of differential wind stress and surface slope making up the temporal variation of those quantities, see Fig. 9.18,

$$w(z, t) = \underbrace{\int_0^t w_1(z, t') \frac{\partial \tau_s}{\partial t'}(t - t') dt'}_{\text{solution to a single stress increment}} + \underbrace{\int_0^t w_2(z, t') \frac{\partial^2 \zeta}{\partial t' \partial n}(t - t') dt'}_{\text{solution to a single surface slope increment}}, \quad (9.157)$$

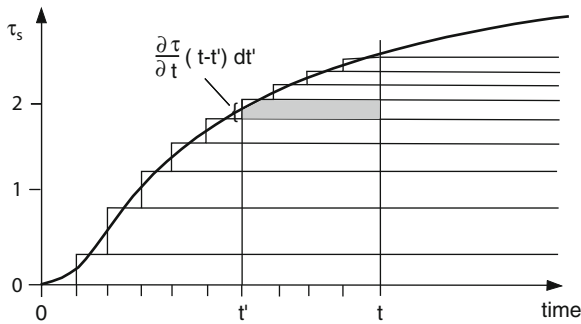


Fig. 9.18 Function $\tau_s(z, t)$ (here real valued) interpreted as a composition of incremental HEAVY-SIDE steps. An analogous interpretation also holds for $\partial\zeta/\partial n(z, t)$

in which it has been assumed that τ_s and $\partial\zeta/\partial n$, defined in (9.131), start from zero values at $t = 0$. The under-braced terms are the contributions of differential single-step responses of (complex-valued) shear stress and surface slope increments at time t' , respectively (which identifies w_1 and w_2 as the corresponding GREEN's functions). Adding these contributions over time from $t' = 0$ to $t' = t$ yields the total wind shear stress and surface slope contributions, which accumulate from time 0 to time t . Performing an integration by parts in (9.157) and imposing the initial conditions $w_{1,2}(z, 0) = 0$, $\tau_s(0) = 0$, $\partial\zeta/\partial n(0) = 0$ gives

$$w(z, t) = \int_0^t \left\{ \tau_s(t - t') \frac{\partial w_1}{\partial t'}(z, t') + \frac{\partial \zeta}{\partial n}(t - t') \frac{\partial w_2}{\partial t'}(z, t') \right\} dt'. \quad (9.158)$$

Vertically integrating (9.158) over depth yields for the complex-valued volume transport the expression

$$W(t) = \int_0^t \left\{ \tau_s(t - t') \frac{\partial W_1}{\partial t'}(t') + \frac{\partial \zeta}{\partial n}(t - t') \frac{\partial W_2}{\partial t'}(t') \right\} dt', \quad (9.159)$$

where

$$W_1(t) = \int_0^h w_1(z, t) dz, \quad W_2(t) = \int_0^h w_2(z, t) dz. \quad (9.160)$$

Here, W_i and $\partial W_i / \partial t$ ($i = 1, 2$) are known and can be computed from the GREEN's functions w_i ($i = 1, 2$). From the continuity equation (9.152)₃ and the kinematic boundary conditions

$$\begin{aligned} \frac{\partial \zeta}{\partial t} + \frac{\partial \zeta}{\partial x} u + \frac{\partial \zeta}{\partial y} v - w &= 0 & \text{at } z = 0, \\ \frac{\partial h}{\partial x} u + \frac{\partial h}{\partial y} v - w &= 0 & \text{at } z = h, \end{aligned} \quad (9.161)$$

the linearised kinematic equation

$$\frac{\partial \zeta}{\partial t} + \frac{\partial U}{\partial x} + \frac{\partial V}{\partial y} = 0 \quad (9.162)$$

can be derived, where $W = U + iV$. Equation (9.159) when substituted into (9.162) comprises an integro-differential equation for ζ , which, in principle, can be solved numerically proceeding step-by-step through time. At each step, a boundary condition on $\partial\zeta/\partial n$ must be satisfied along the lake shore by, e.g. requesting that the component of W normal to the shore is zero. At each time, the vertical structure of the horizontal current may then be determined from (9.157) as the calculations advance. Finally, the vertical structure of the vertical velocity then follows from a z -integration of the continuity equation (9.152)₃.

9.3.4.2 Alternative Integration Procedures

This integration method was suggested by WELANDER [52] but was never put into practice. The obstacle seems to be the use of the integral equation; systems of differential equations seem to be preferable. Such approaches generally start by integrating (9.153) over depth, leading to

$$\frac{\partial \mathbf{W}}{\partial t} + \mathbf{i}f\mathbf{W} = -gh \frac{\partial \zeta}{\partial n} + \frac{\tau_s - \hat{\tau}_b}{\rho}, \quad (9.163)$$

which may be complemented by the volume (mass) balance equation (9.162). Once $\mathbf{W}(x, y, t)$ is numerically determined with the use of (9.162) and (9.163) (for the methodology, see [47, pp. 112–168]), the vertical structure of the current can be determined as above. However, (9.163) has a missing link, the parameterisation of τ_b . The difficulty is that

$$\hat{\tau}_b = -\rho\nu \left(\frac{\partial \mathbf{W}}{\partial z} \right)_{z=h}$$

is given in terms of the horizontal shear at $z = h$ and not in terms of \mathbf{W} (and perhaps τ_s and $\partial\zeta/\partial n$). An approximation of it could be $\hat{\tau}_b = -\rho\nu\mathbf{W}/h$, but this is not accurate. JELESNIANSKI [29] evaluates $\partial\mathbf{W}/\partial z$ from (9.157) and finds for τ_b a convolution integral involving the past history of τ_s and $\partial\zeta/\partial n$, see [23]. His method has been applied very effectively by FORISTALL [16], [17] and FORISTALL et al. [18] to evaluate the storm-generated currents in the Gulf of Mexico. A different procedure has been employed by KIELMANN and KOWALIK [31].

The most elegant method has, however, been proposed by PLATZMAN⁸ [43]. He treats the time derivative $\partial(\cdot)/\partial t$ in (9.153) as if it were a real (or complex) number and writes (9.153) for constant ν as

$$\frac{\partial^2 \mathbf{W}}{\partial z^2} = \frac{1}{\nu} \left(\mathbf{i}f + \frac{\partial}{\partial t} \right) \mathbf{W} + \frac{g}{\nu} \frac{\partial \zeta}{\partial n}. \quad (9.164)$$

Introducing

$$\bar{z} = \frac{z}{h}, \quad \sigma^2 = \sigma_0^2 + \lambda, \quad \sigma_0^2 := \frac{\mathbf{i}fh^2}{\nu}, \quad \lambda := \frac{h^2}{\nu} \frac{\partial}{\partial t}, \quad (9.165)$$

(9.164) takes the form

$$\frac{d^2 \mathbf{W}}{d\bar{z}^2} - \sigma^2 \mathbf{W} = \frac{gh^2}{\nu} \frac{\partial \zeta}{\partial n}. \quad (9.166)$$

⁸ This is sometimes simply called ‘PLATZMAN’s *integration method*’. PLATZMAN was a meteorologist, Professor of Geological Sciences at the University of Chicago. For a biographical sketch, see Fig. 9.1.

Problem 9.6 Equation (9.166), in which σ^2 is treated as if it were a real or complex number, must be solved subject to a prescribed surface shear stress τ_s at $z = 0$ and the no-slip condition at $z = h$. Prove that with the boundary conditions (9.154)_{1,2}, (9.166) possesses the solution

$$w(\bar{z}, t) = \frac{\sinh[\sigma(1 - \bar{z})]}{\sigma \cosh(\sigma)} \frac{h\tau_s}{\rho\nu} + \frac{1}{\sigma^2} \left\{ \frac{\cosh(\sigma\bar{z})}{\cosh(\sigma)} - 1 \right\} \frac{gh^2}{\nu} \frac{\partial \zeta}{\partial n}. \quad (9.167)$$

Prove, moreover, that an integration over depth from $\bar{z} = 0$ to $\bar{z} = 1$ transforms (9.167) into

$$\frac{\nu}{h^2} \left(\sigma^2 + G(\sigma) \right) W = -gh \frac{\partial \zeta}{\partial n} + (1 + H(\sigma)) \frac{\tau_s}{\rho}, \quad (9.168)$$

where

$$G(\sigma) = \frac{\sigma \tanh \sigma}{1 - \frac{1}{\sigma} \tanh \sigma}, \quad H(\sigma) = \frac{\frac{1}{\sigma} \tanh \sigma - \operatorname{sech} \sigma}{1 - \frac{1}{\sigma} \tanh \sigma}. \quad \blacklozenge$$

The solution (9.167) has been constructed as if (9.166) would be an ordinary differential equation; however, (9.168)₁ is not an explicit expression for w , but an operator equation which one wishes to transform into a differential equation that looks similar to (9.163). This can be achieved, if it is assumed that $|\lambda| \ll \sigma_0^2$ and the functions $G(\sigma)$ and $H(\sigma)$ are expanded into TAYLOR series and truncated at the linear terms. This then yields approximately

$$\begin{aligned} G(\sigma) &\simeq G_0(\sigma_0) + \lambda G_1(\sigma_0), \\ H(\sigma) &\simeq H_0(\sigma_0) + \lambda H_1(\sigma_0). \end{aligned} \quad (9.169)$$

It is a straightforward matter to evaluate these functions:

$$\begin{aligned} G_0(\sigma_0) &= \frac{\sigma_0^2 \xi_0}{1 - \xi_0}, \\ G_1(\sigma_0) &= \frac{1 + \xi_0 - (2 + \sigma_0^2) \xi_0^2}{2(1 - \xi_0)^2}, \end{aligned} \quad (9.170)$$

$$\begin{aligned} H_0(\sigma_0) &= \frac{\xi_0 - \eta_0}{1 - \xi_0}, \\ H_1(\sigma_0) &= \frac{(1 - \xi_0 - \sigma_0^2 \xi_0^2) - [1 - (1 + \sigma_0^2) \xi_0] \eta_0}{2\sigma_0^2(1 - \xi_0)^2}, \end{aligned} \quad (9.171)$$

in which

$$\xi := \frac{1}{\sigma} \tanh \sigma, \quad \eta := \operatorname{sech} \sigma. \quad (9.172)$$

If the expressions (9.169) are substituted in (9.168)₁ and the definitions (9.165) are used, then

$$\frac{\partial \mathbf{W}}{\partial t} + i f \mathbb{A} \mathbf{W} = -gh \mathbb{B} \frac{\partial \zeta}{\partial n} + \left(\mathbb{C} + \frac{\mathbb{D}}{i f} \frac{\partial}{\partial t} \right) \frac{\tau_s}{\rho} \quad (9.173)$$

is obtained, in which

$$\begin{aligned} \mathbb{A} &= \frac{1 + \frac{1}{\sigma_0^2} G_0}{1 + G_1}, & \mathbb{B} &= \frac{1}{1 + G_1}, \\ \mathbb{C} &= \frac{1 + H_0}{1 + G_1}, & \mathbb{D} &= \frac{\sigma_0^2 H_1}{1 + G_1}. \end{aligned} \quad (9.174)$$

Equation (9.173) is in the desired form. The four coefficient functions have been plotted by PLATZMAN [43] as functions of σ_0 . These graphs show that $|\mathbb{D}|$ is small in comparison to the moduli of the other coefficients for all values of σ_0 . So

$$\frac{\partial \mathbf{W}}{\partial t} + i f \mathbb{A} \mathbf{W} = -gh \mathbb{B} \frac{\partial \zeta}{\partial n} + \mathbb{C} \frac{\tau_s}{\rho} \quad (9.175)$$

is an approximation which can be used for all practical applications. The distinguished feature of this equation is that it has been obtained without taking side boundaries into account. In PLATZMAN's [43] words: 'An important step in delineating predictive characteristics of this equation is the determination of frequencies of free modes of vibration. In general, it is very difficult to do this if one requires that boundary conditions be met on the sides of a basin of even the simplest shape.' For a rotating rectangular basin of uniform depth but without friction this problem has been solved by RAO [48]: it is given in Volume II of this book series; for circular and elliptical cylinders with constant depth the corresponding solutions are constructed by LAMB [34] and GOLDSTEIN [21], also given in Volume II. Two limits are of practical interest:

- For large depths, $h \rightarrow \infty$, $|\sigma_0| \gg 1$, we have $\mathbb{A} = \mathbb{B} = \mathbb{C} = 1$ and (9.175) reduces to

$$\frac{\partial \mathbf{W}}{\partial t} + i f \mathbf{W} = -gh \frac{\partial \zeta}{\partial n} + \frac{\tau_s}{\rho}. \quad (9.176)$$

In this case $\tau_b = 0$, which was to be expected.

- For small depths ($|\sigma_0| \ll 1$, relating to a shallow lake), the explicit formulae yield

$$\begin{aligned}\mathbb{A} &= \frac{5}{2}\sigma_0^{-2} + \frac{43}{42} = 2.5\sigma_0^{-2} + 1.02, \\ \mathbb{B} &= \frac{5}{6} = 0.833..., \quad \mathbb{C} = \frac{5}{4} = 1.25\end{aligned}\tag{9.177}$$

and (9.175) becomes

$$\frac{\partial \mathbf{W}}{\partial t} + i f \left(\frac{43}{42} \right) \mathbf{W} = -gh \frac{\partial \zeta}{\partial n} + \frac{\tau_s - \hat{\tau}_b}{\rho},\tag{9.178}$$

where

$$\hat{\tau}_b = \frac{5\rho\nu}{2h} \left(\frac{\mathbf{W}}{h} \right) - \frac{1}{6}\rho gh \frac{\partial \zeta}{\partial n} - \frac{\tau_s}{4}.\tag{9.179}$$

It is seen that (9.178) has been put into the form (9.163) with a basal shear stress formula given by (9.179). Accordingly, $\hat{\tau}_b$ depends on (i) \mathbf{W}/h with a coefficient that is inversely proportional to h , (ii) the slope gradient with a coefficient proportional to h and (iii) surface shear stress τ_s . The CORIOLIS acceleration is affected only slightly by a factor $1/42$.

An equation similar to (9.175) with coefficients (9.177) was derived also by NOMITSU [41] more than 30 years earlier. PLATZMAN [43] writes ‘NOMITSU obtained an approximate, two-dimensional rendition of the EKMANN equations by an entirely different method, but his result is remarkably similar to (9.177). NOMITSU’s procedure is based upon a series representation of the influence [GREEN’s] functions for slope and wind transports, along the lines of FJELDSTAD’s [15] work. He found that if only the leading term is retained in each series, the resulting approximate total transport will satisfy an equation of exactly the form (9.175)’, but with the coefficients (9.177) replaced by (index N for NOMITSU)

$$\mathbb{A}_N = 2.47\sigma_0^{-2} + 1, \quad \mathbb{B}_N = \frac{8}{\pi^2} = 0.81, \quad \mathbb{C}_N = 1.27.\tag{9.180}$$

‘Evidently none of the coefficients of NOMITSU’s equation differs from the corresponding coefficients of (9.177) by as much as 7%’. Incidentally, FISCHER [14] used a prediction equation of the form (9.175) with (index F for FISCHER)

$$\mathbb{A}_F = 2.47\sigma_0^{-2} + 1, \quad \mathbb{B}_F = 1.0, \quad \mathbb{C}_F = 1.0.\tag{9.181}$$

Equation (9.178) together with (9.162) can be applied to a particular lake to determine $\partial \zeta / \partial n$ and \mathbf{W} , incorporating thereby the effects of bottom friction. Once these quantities are determined, the vertical structure of the horizontal current follows from (9.158), while ζ follows from an integration in time. PLATZMAN [43] did

apply this procedure to Lake Erie. JELESNIANSKI [29] generalised the method by employing a slip condition at the bottom surface; he applied it to the computation of hurricane surges.

9.3.5 The Dynamical Prediction of Wind Tides on Lake Erie

PLATZMAN's [43] interest in the computation of wind tides on Lake Erie has been stimulated (i) by the practical relevance that high and low water levels (on the East and West shores, respectively) may cause considerable damage and hindrance to shipping, (ii) by the existence of earlier, cruder analyses of the problem,⁹ (iii) by the availability of satisfactory hydrographic and meteorological observations over a long period and (iv) by the large amplitude of the principal wind tide, which at least four times in a 20-year period has exceeded 3.5 m in the set-up between Buffalo and Toledo, a distance of about 385 km. PLATZMAN's work on the computation of wind tides on Lake Erie is likely the first, in which high speed computers have been used in a problem of this mathematical complexity.

9.3.5.1 Wind data and lake-level data

PLATZMAN decided to use exclusively wind data and lake-level data that were available at hourly intervals from anemometers located not more than 32 km from the Lake shore which are maintained by the US Weather Bureau and by the Meteorological Service of Canada. This led to the selection of six stations: Toledo, Sandusky, Cleveland, Erie, Buffalo (all USA) and Clear Creak (Canada), see Fig. 9.19a. With the exception of the station at Sandusky the data available are wind speed and direction, taken over a 1-min interval each hour. At Sandusky, the hourly wind data are values averaged over a 1-h interval (which is probably more adequate for the characterisation of wind-tide computations).

PLATZMAN used lake-level data from records of continuous stage recorders maintained by the US Lake Survey and by the Canadian Hydrographic Survey; these agencies provide a long and continuous period of records and are easily accessible. The data were available as 'hourly scaled values' for each hour of the day, each 'scaled value' being the instantaneous water level (with an accuracy of about 3 mm). Hourly scaled values are well suited for studies of annual and secular variations of lake level. For lake-level *surges* produced by meso-scale atmospheric disturbances, one must have recourse to the continuous record because the time scale of such surges usually is less than 1 h. PLATZMAN, however, concludes that the middle latitude cyclones cause lake surface fluctuations – referred to generally as 'wind tides' – that have characteristic time scales of the duration of several hours. In a way, PLATZMAN was left with no other choice since the water-level gages used are located in stilling wells which suppress short-period wave action.

⁹ See, e.g. [22, 25, 27, 30].

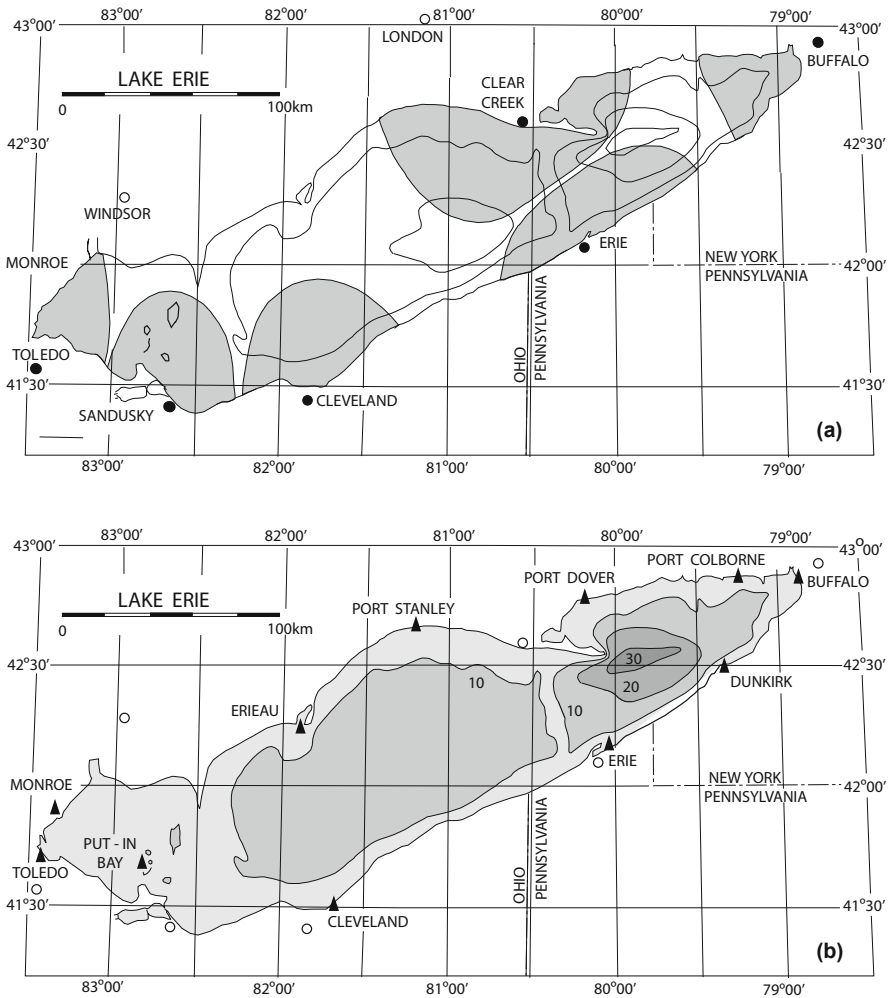


Fig. 9.19 (a) Locations (●) of six first-order weather stations that provided hourly wind data used to compute wind stress. Areas in grey identify regions of predominant influence ($\lambda_m > 0.5$) in wind stress analysis; (b) locations (▲) of lake-level recorders (limnigraphs) for which continuous records are available during at least 1 year in the 20-year period 1940–1959 and weather stations (○) of panel (a). Reproduced from PLATZMAN [43], ©American Meteorological Society, reprinted with permission

According to PLATZMAN, ‘for the purpose of examining records of lake level and wind, the 20-year period 1940–1959 was selected rather arbitrarily. During this period, each of the 11 recording gages was in operation during the entire 20-year period for at least 1 year. The locations of these gages are shown in Fig. 9.19b. Five of these stations were in operation during the entire 20-year period; they provide the main source of data and are located at Toledo, Cleveland, Buffalo, Port Colborne

and Port Stanley'. Some of the gages are 'sheltered' behind breakwaters, within docking slips, etc., which causes certain features (resonances, reflections) of local nature and typical for the location and less for the global response to the wind tide. These have been accordingly taken into account.

9.3.5.2 Characterisation of Lake Erie wind tides

'IRISH and PLATZMAN [28] examined hourly scaled values of Buffalo and Toledo lake levels for the 20-year period 1940–1959 and tabulated the dates of incidence in which the difference in level between these stations exceeded 1.83 m (= 6 ft). During this period 76 cases were found in which Buffalo lake level exceeded that at Toledo by 1.83 m or more', and three cases where it was reverse. Out of these cases PLATZMAN selected 10 for computations for which 'the relevant interval for numerical computation was taken to be the 5-day period centred on the day of occurrence of peak set-up. In all cases this interval spans the storm surge period and also induces the principal resurgences if any occur'. The corresponding inclusive dates are given in Table 9.5. PLATZMAN further states 'that during the 24-h preceding the time of peak set-up, most low-pressure centres move from Southwest to Northeast along tracks that lie within a band about 1000 km (600 miles) wide, the right edge of which coincides with the longitudinal axis of the Lake. Figure 9.20 shows such antecedent tracks in the nine cases' that were considered by PLATZMAN for computations. For all these cases he plotted the observed Buffalo-minus-Toledo set-up time series and compared these with the corresponding time series of the wind-speed squared component along the major lake axis at Clear Creak, demonstrating in all but one case very good coincidence. 'Clear Creak was selected for comparison with the set-up curves because of its good exposure to Southwest winds [...]'. In Fig. 9.21 an excerpt of the nine panels of PLATZMAN's [43] Fig. 9 is given.

Table 9.5 Date and year of peak Buffalo-minus-Toledo set-up (based upon hourly scaled values) and inclusive dates, for the 10 cases selected to provide wind data dynamical computation of lake level. Reproduced from PLATZMAN [43] by permission of American Meteorological Society

Case ^a	Date	Hour (EST)	Peak set-up (feet / m)	Inclusive dates
26	7 Oct 1951	19	7.6/2.32	5–9 Oct 1951
28	21 Dec 1951	18	9.5/2.90	19–23 Dec 1951
31	21 Feb 1953	12	10.8/3.29	19–23 Feb 1953
33	21 Sep 1954	19	9.4/2.87	19–23 Sep 1954
35	22 Mar 1955	18	12.9/3.93	20–24 Mar 1955
36	3 Nov 1955	10	8.1/2.42	1–5 Nov 1955
37	17 Nov 1955	08	12.9/3.93	15–19 Nov 1955
39	16 Nov 1956	10	8.9/2.71	14–18 Nov 1956
40	21 Nov 1956	15	11.1/3.38	19–23 Nov 1956
46	22 Jan 1959	05	7.1/2.16	20–24 Jan 1959

^aThis number pertains to the case numeration used by PLATZMAN. They have no other meaning than to identify the storm case studied by him. ETS = Eastern Standard Time

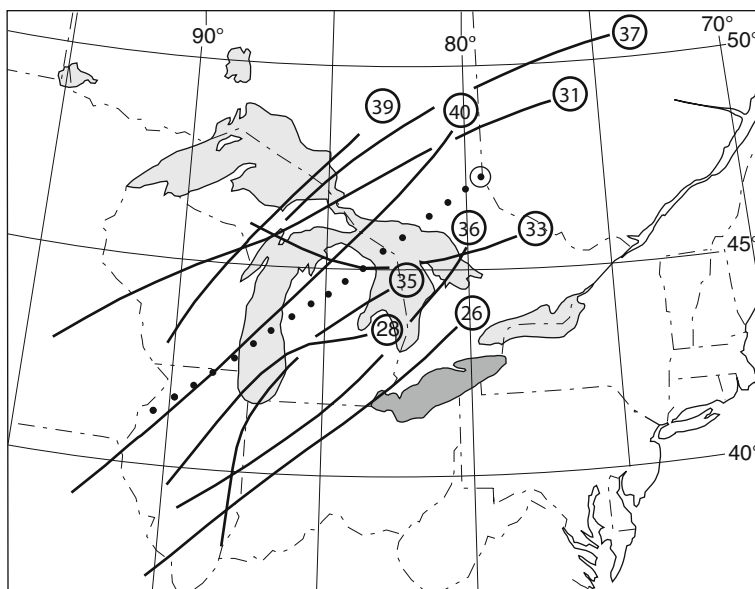


Fig. 9.20 Antecedent tracks of low-pressure centres in the nine cases selected by PLATZMAN for numerical wind-tide computation. Each stream track is for a 24-h period and terminates on position of low-pressure centre at time of peak set-up on Lake Erie. This position is shown by *circle* that encloses the corresponding case number. *Dotted line* is mean track. Reproduced from PLATZMAN [43], ©American Meteorological Society, reprinted with permission

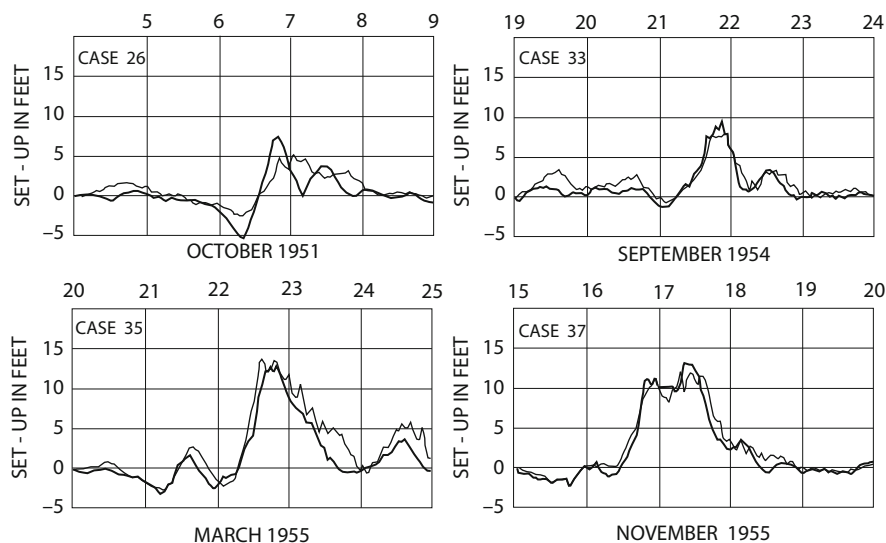


Fig. 9.21 Observed (*heavy curves*) and computed (*light curves*) time series of Buffalo-minus-Toledo set-up for storm surge Cases 26, 33, 35 and 37. The 5-day period is centred on the day of occurrence of maximum set-up, given in feet (1 ft = 0.3048 m); for station positions, see Fig. 9.19b. Reproduced from Fig. 14 of PLATZMAN [43] but differently arranged, © American Meteorological Society, reprinted with permission

9.3.5.3 Wind stress analysis

A notoriously difficult problem for any realistic computation of wind-induced currents in lakes is the transfer of the measurements of the wind speed and direction at a number of wind stations to wind shear stress values at any location on the lake surface. A popular approach is to construct the surface shear stress as a linear combination of $\rho_a k_m |\mathbf{W}_m(t)| \mathbf{W}_m(t)$, where $\mathbf{W}_m(t)$ denotes the wind vector at time t at anemometer station m . ρ_a is the density of air and k_m a dimensionless skin friction coefficient, assumed to adjust the wind shear at the anemometer height through the PRANDTL layer to the surface. Thus,

$$\tau_s(x, y, t) = \sum_m \lambda_m(x, y) \rho_a k_m |\mathbf{W}_m(t)| \mathbf{W}_m(t) \quad (9.182)$$

achieves this transfer, in which $\lambda_m(x, y)$ is a second correcting factor which accounts for corrections due to interpolation between land stations and arbitrary lake surface position, obstacle effects, difference in roughness, fetch, etc. PLATZMAN writes instead of (9.182)

$$\frac{\tau_s}{\rho}(x, y, t) = \sum_m \lambda_m(x, y) K_m |\mathbf{W}_m(t)| \mathbf{W}_m(t), \quad K_m = \frac{\rho_a}{\rho} k_m, \quad (9.183)$$

where K_m is a dimensionless ‘stress factor’; moreover, he chose (rather arbitrarily) the same value for all stations, $K_m = K$, yielding

$$\frac{\tau_s}{\rho}(x, y, t) = K \sum_m \lambda_m(x, y) |\mathbf{W}_m(t)| \mathbf{W}_m(t). \quad (9.184)$$

Of special interest is the specification of the interpolation function $\lambda_m(P)$, where P denotes an arbitrary point (x, y) . The function $\lambda_m(P)$ may be regarded as the ‘influence’ at P of data at P_m . The following conditions are imposed upon λ_m

$$\begin{aligned} \text{(a)} \quad \lambda_m(P_n) &= \begin{cases} 1 & \text{if } m = n, \\ 0 & \text{if } m \neq n, \end{cases} \\ \text{(b)} \quad \sum_m \lambda_m(P) &= 1, \\ \text{(c)} \quad \lambda_m(P) &\geq 0, \\ \text{(d)} \quad \lim_{P \rightarrow P_\infty} (P) &= w_m. \end{aligned} \quad (9.185)$$

Condition (a) means that interpolation at any data point P_n gives exactly the data at P_n , the influence there of data at all other points $P_m (m \neq n)$ being zero. Condition (b) is needed to ensure correct interpolation of uniform data. Condition (c) prevents data at any P_m from giving a negative contribution to the interpolated value at any P ; this excludes most types of polynomial interpolation. Finally, in (d) the notation

$P \rightarrow P_\infty$ signifies that if P approaches the point at infinity (P_∞), w_m is the weight factor that expresses quality or confidence level of the data at P_m [. . .].’

‘Many functions may be synthesised to satisfy (9.185). The following construction gave reasonable results. Define with

$$a_m(P) \equiv (x - x_m)^2 + (y - y_m)^2 \quad (9.186)$$

the square of the distance between P and P_m . Further, let

$$f_m(P) \equiv w_m \prod_{n \neq m} a_n(P) \quad (9.187)$$

be the product of all $a_n(P)$ except $a_m(P)$, with the weight factor w_m of (d). Then,

$$\lambda_m(P) \equiv \frac{f_m(P)}{\sum_k f_k(P)} \quad (9.188)$$

meets all four conditions (a)–(d). To see this, note first $a_m(P_m) = 0$ and $a_m(P) \neq 0$ when $P \neq P_m$, so $f_m(P_m) \neq 0$; hence (9.188) meets (a). Condition (b) obviously is satisfied by (9.188), and (c) is secured by the fact that $a_m \geq 0$. To establish (d), divide numerator and denominator on the right in (9.188) by the product of all factors $a_n(P)$; then

$$\begin{aligned} \lambda_m(P) &= \frac{\frac{f_m(P)}{\prod_k a_k(P)}}{\frac{\sum_k f_k(P)}{\prod_j a_j(P)}} = \frac{\frac{1}{a_m(P)} \left(\frac{f_m(P)}{\prod_{k \neq m} a_k(P)} \right)}{\sum_k \frac{1}{a_k(P)} \left(\frac{f_k(P)}{\prod_{j \neq k} a_j(P)} \right)} \\ &\stackrel{(9.187)}{=} \frac{\frac{w_m}{a_m(P)}}{\sum_k \frac{f_k(P)}{a_k(P)}}. \end{aligned} \quad (9.189)$$

In the limit $P \rightarrow P_\infty$, the definition (9.186) makes $a_m(P) \rightarrow R^2$, where $R(\rightarrow \infty)$ is the distance between P and the centroid of the data point configuration. It follows that in the limit $P \rightarrow P_\infty$ the factors $a_k(P)$ approach equality for all k and may be cancelled in (9.189); application of (b) to the denominator then leads at once to (d).¹⁰

This is PLATZMAN’s [43] parameterisation of the function $\lambda_m(x, y)$. ‘For each data point P_m (that is, for each wind station) one may construct contours of the function $\lambda_m(P)$.’ The contour lines $\lambda_m(P) = 0.5$ for the six stations around Lake

¹⁰ This construction can be generalised by taking for $a_m(P)$ any monotone function of the distance between P and P_m , such that $a_m(P_m) = 0$ and $a_m(P)$ approaches a limit independent of the location of P_m as $P \rightarrow P_\infty$.

Erie are shown in Fig. 9.19a. The regions $\lambda_m(P) \geq 0.5$ thus delineated show the domain of predominant influence for each station.

9.3.5.4 Prerequisites of wind-tide computation

The prediction equations for the wind-tide computation are described in Sect. 9.3.1 of this chapter and comprise (9.175) and (9.177) which have been numerically solved by PLATZMAN in the lake domain for the volume transport vector $\mathbf{W}(x, y, t) = (U + iV)(x, y, t)$; once these are known, (9.162) is numerically integrated in time for the free surface elevation $\zeta(x, y, t)$. This latter function, in particular, delivers the time series $\zeta_m(t)$ at the limnigraph stations around the Lake and allows computation of the temporal evaluation of the set-up between the Buffalo and Toledo stations. We omit the presentation of the numerical scheme, which is outlined by PLATZMAN [43]. To this end, a square lattice for the finite difference approximation has been judiciously chosen with grid size Δs and time step Δt . These and the pertinent physical parameters are collected in Table 9.6. In addition, the input consisted of the following wind data:

- Hourly wind speed and direction at each of the six wind stations;
- Stress factor K_m for each wind station (adjusted to $K = 4 \times 10^{-6}$ for all stations).

Computations were done by PLATZMAN for the *5-day period* centred on the day of occurrence of maximum set-up for each of nine cases of storm events that generated lake-level differences between Buffalo and Toledo larger than 1.83 m (6 ft). The computation delivered time-dependent space-distributed fields of lake level, volume transport vectors and surface current speed and direction. PLATZMAN's [43] paper, however, 'only' reports on lake-level time series at grid points closest to the limnigraph stations.

9.3.5.5 Verification analysis

In what follows, we shall only present a small fraction of the results discussed by PLATZMAN [43]. He showed this comparison for nine storm episodes. The subsequent figures display time series over 5 days of the set-up at selected water-level stations; here 'set-up' means the surface displacement at a particular station above the still water datum. PLATZMAN writes 'For verification of computed wind tides, one must compare computed and observed set-up. This comparison is shown for

Table 9.6 Parameter choices for the wind-tide computations in Lake Erie

Mesh size (7.5 min of arc of the meridian of mean latitude $42^\circ 10'N$)	$\Delta s = 1388.4 \text{ m}$
Time step	$\Delta t = 6 \text{ min}$
Gravity constant	$g = 9.8036 \text{ m s}^{-2}$
Angular velocity of Earth	$\Omega = 7.2921 \times 10^{-5} \text{ s}^{-1}$
Coriolis parameter ($f = 2\Omega \sin \phi$ for $\phi = 42^\circ 10'N$)	$f = 0.97902 \times 10^{-4} \text{ s}^{-1}$
Vertical eddy viscosity	$\nu = 4 \times 10^{-3} \text{ m}^2 \text{ s}^{-1}$

Buffalo-minus-Toledo set-up in Fig. 9.21 [which is a subset of PLATZMAN's, [43], Fig. 14] (heavy curves: observed set-up, light curves: computed set-up). Computed set-up is on the whole in good agreement with that observed, notably in Cases 33, 35 and 37. Case 26 is somewhat anomalous'; agreement between observed and computed set-up for the seven cases not shown here lies in between Cases 26 and 37.

PLATZMAN also examined the computed set-up at individual stations. For this purpose, computed and observed set-up curves for the nine cases are shown in PLATZMAN's article in his figure 16a-i, of which we reproduce here just Case 35 in Fig. 9.22. 'Six stations are represented in an arrangement such that the two on

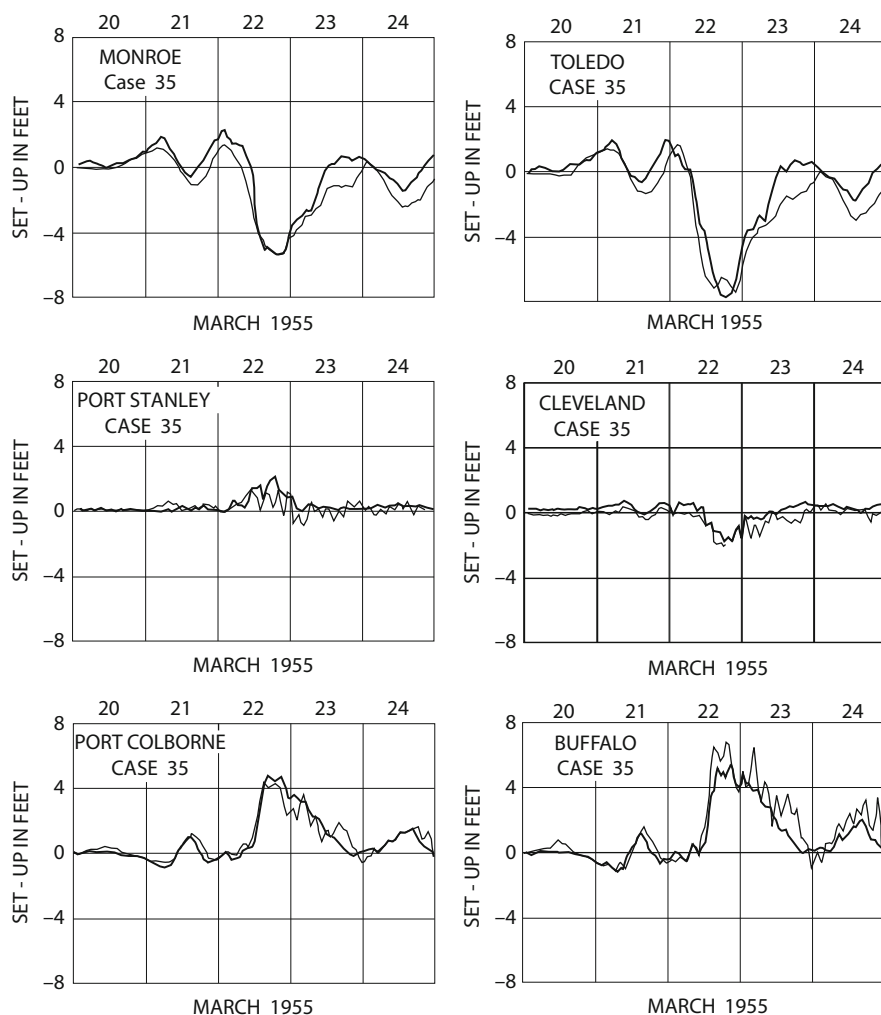


Fig. 9.22 Set-up, observed (*heavy curves*) and computed (*light curves*) for storm Case 35. The 5-day period is centred on the day of occurrence of maximum set-up, given in feet (1 ft = 0.3048 m); for station positions, see Fig. 9.19b. Reproduced from Fig. 16e of PLATZMAN [43] but differently arranged, © American Meteorological Society, reprinted with permission

the top are located at the Western end of the Lake (Monroe, Toledo), the two on the bottom are at the Eastern end (Buffalo and Port Colborne), and the two in the middle are located about midway between the Western and Eastern ends of the Lake (Cleveland and Port Stanley), see Fig. 9.19b for the station locations. Since the two latter stations are near the principal set-up node, the records there show only relatively minor fluctuations and not much coherence'. Agreement between computed and observed set-up is remarkable in this case and it is good in all other cases not reproduced here. PLATZMAN also notes that 'in Case 35, the computed set-up at Buffalo is much more "ragged" than the observed. The same can also be seen at other stations [...] and in other cases. There are two reasons for this. First, the curves of computed set-up are drawn from half-hourly values, while the curves of observed set-up are drawn from hourly values [...]. Second, the frequency spectrum of computed set-up closely mirrors that of the hourly input winds. Since the latter are 1-min values [...], they tend to be very ragged, and since only six stations are used in the wind stress analysis, the interpolation procedure is not very effective in reducing high-frequency components.'

9.4 Final Remarks

This chapter was devoted to the mathematical–numerical determination of the vertical distribution of wind-induced currents in homogeneous lakes and lakes stratified in two layers, when these lakes are subjected at their free surface to wind shear. The theory has been constructed from simple to complex; nevertheless, the non-linear cases, in which the complete three-dimensional bounded geometry of natural lakes that are embedded in a topography influenced external wind field remained untouched and are reserved for close inspection in Volume 3 of this monograph.

The key ideas, which made the high analyticity of the formulation possible, were (i) omission of the temperature as an evolving field, (ii) the tacit acceptance of the shallow-water assumption and (iii) restriction to linearity. Assumption (i) implied that any stratification was considered to be 'frozen' into a vertical-layered structure; (ii) meant that the entire lake was considered a boundary layer for which only the shear stresses τ_{xz} and τ_{yz} survive and (iii) led to the omission of all convective acceleration terms and the application of the free surface boundary conditions at the undeformed surface. These assumptions are all physically transparent – at least they provide a rough delineation of the validity of the emerging model equations. Mathematically, they imply that the differential equations for the horizontal current decouple from the vertical velocity component. Together with the vertically integrated mass balance equation and adequate stress boundary conditions at the free surface and the no-slip condition at the basal surface (which is assumed to be horizontal at all positions of the basin, a prerequisite that the de-coupling of the horizontal and the vertical problems is possible) form a well-posed initial boundary value problem. The solution of this problem which, for a homogeneous water basin, was set up as a set of linear integral equations as early as 1933, was, however, out of reach prior to electronic computation. Further rather ingenious mathematical steps were needed to transform the integral equation formulation into a system of differential equations.

This was achieved in the 1960s of the last century – we have pointed out several variants in the description of the storm surge problem for Lake Erie.

PLATZMAN [43] applied his formulation of the problem to several storm surges as was described in the last subsection to this chapter. He employed early electronic computation and demonstrated good agreement of the computed set-up time series at limnigraph positions around Lake Erie with the measured ones. Good agreement was also obtained in other cases of storm surge events. It is noteworthy that these computations are among those activities, which did not only provide verification of the model equations for storm surges but also acted as inception of the rapid evolution of computational methods in meteorology and oceanography.

References

1. Abramowitz, M. and Stegun, I.A. (eds.): *Handbook of Mathematical Functions*. Dover, New York, NY (1965)
2. Bonham-Carter, G. and Thomas, J.H.: Numerical calculation of steady wind-driven currents in Lake Ontario and the Rochester embayment. *Proceedings of 16th Conference on Great Lakes Research International Association Great Lakes Research*, 640–662 (1973)
3. Bowden, K.F., Fairbairn, L.A. and Hughes, P.: The distribution of shearing stresses in a tidal current. *Geophys. J. R. Astr. Soc.* **2**, 288–305 (1959)
4. Bye, J.A.T.: Wind-driven circulation in unstratified lakes. *Limnol. Oceanogr.* **10**, 451–458 (1965)
5. Csanady, G.T.: Mean circulation in shallow seas. *J. Geophys. Res.* **81**, 5389–5399 (1976)
6. Csanady, G.T.: Turbulent interface layers. *J. Geophys. Res.* **83**, 2329–2342 (1978)
7. Csanady, G.T.: A developing turbulent surface shear layer model. *J. Geophys. Res.* **84**, 4944–4948 (1979)
8. Csanady, G.T.: The evolution of a turbulent Ekman layer. *J. Geophys. Res.* **85**, 1537–1547 (1980)
9. Csanady, G.T.: *Circulation in the Coastal Ocean*. D. Reidel, Dordrecht, 245 p. (1982)
10. Defant, A.: *Physical Oceanography*. Vol. 1, Oxford, Pergamon (1961)
11. Dombroklonskiy, S.V.: Drift current in the sea with an exponentially decaying eddy viscosity coefficient. *Oceanology* **9**, 19–25 (1969)
12. Ekman, V.W.: On the influence of the Earth's rotation on the ocean currents. *Ark. Mat. Astr. Fys.* **2**(11), 1–52 (1905)
13. Ellison, T.H.: Atmospheric turbulence. In: *Surveys in Mechanics* (eds. Batchelor G.K. and Davies R.M.), Cambridge University Press, Cambridge, 400–430 (1956)
14. Fischer, G.: Ein numerisches Verfahren zur Errechnung von Windstau und Gezeiten in Randmeeren. *Tellus* **11**, 60–76 (1959)
15. Fjeldstad, J.D.: Ein Beitrag zur Theorie der winderzeugten Meeresströmungen. *Gerlands Beitr. Geophys.* **23**, 237–247 (1930)
16. Foristall, G.Z.: Three-dimensional structure of storm-generated currents. *J. Geophys. Res.* **79**, 2721–2729 (1974)
17. Foristall, G.Z.: A two-layer model for Hurricane-driven currents on an irregular grid. *J. Phys. Oceanogr.* **9**, 1417–1438 (1980)
18. Foristall, G.Z., Hamilton, R.C. and Cardone, V.J.: Continental shelf currents in tropical storm Delia: Observations and theory. *J. Phys. Oceanogr.* **7**, 2714–2723 (1974)
19. Gedney, R.T.: *Numerical Calculations of Wind-Driven Currents in Lake Erie*. Ph.D. Thesis, Case Western Reserve University, Cleveland, OH (1971)
20. Gedney, R.T. and Lick, W.: Wind driven currents in Lake Erie. *J. Geophys. Res.* **77**, 2714–2723 (1972)

21. Goldstein, S.: Tidal motion in rotating elliptical basins of constant depth. *Mon. Notices R. Astron. Soc. (Geophys. Suppl.)* **2**, 213–231 (1929)
22. Hayford, J.F.: *Effects of Wind and of Barometric Pressures on the Great Lakes*. Carnegie Institution of Washington, Washington, DC, 133 p. (1922)
23. Heaps, N.S.: Vertical structure of current in homogeneous and stratified waters. In: *Hydrodynamics of Lakes*. CISM Lectures No 286 (ed. Hutter, K.), Springer, New York, NY, 152–207 (1984)
24. Heaps, N.S. and Jones, J.E.: Development of a three-layered spectral model for the motion of a stratified sea. II. Experiments with a rectangular basin representing the Celtic Sea. In: *Physical Oceanography of Coastal and Shelf Seas*. (ed. Johns, B.), Elsevier, Amsterdam, 401–465 (1984)
25. Hellström, B.M.O.: *Wind Effects on Lakes and Rivers*. Ingeniörsvetenskaps-akademien, Hand-
ingar 158. 191 p. (1941)
26. Hidaka, K.: Non-stationary ocean currents. *Mem. Imp. Mar. Obs., Kobe* **5**, 141–266 (1933)
27. Hunt Ira, A., Jr.: *Wind, Wind Set-up and Seiches on Lake Erie, Part 2*. US Corps of Engineers, Lake Survey, 58 p. (1959)
28. Irish, S.M. and Platzman, G.W.: An investigation of meteorological conditions associated with extreme wind tides on Lake Erie. *Mon. Wea. Rev.* **90**, 39–47 (1962)
29. Jelesnianski, C.P.: Bottom stress time history in linearized equations of motion for storm surges. *Mon. Weather Rev.* **98**, 462–478 (1967)
30. Keulegan, G.H.: Hydrodynamic effects of gales on Lake Erie. *J. Res. Natl. Bur. Stand.* **50**, 99–109 (1953)
31. Kielmann, J. and Kowalik, Z.: A bottom stress formulation for storm surge problems. *Oceanol. Acta* **3**, 51–58 (1980)
32. Lacomb, H.: *Cours d' Oceanographie Physique*. Gauthier-Villars, Paris (1965)
33. Lai, R.Y.S. and Rao, D.B.: Wind drift currents in deep sea with variable eddy viscosity. *Arch. Met. Geophys. Bioklim* **A25**, 131–140 (1976)
34. Lamb, H.: *Hydrodynamics* (6th Edition). Cambridge University Press, Cambridge (1932)
35. Laska, M.: Characteristics and modelling of physical limnology processes. Mitt. Versuchsanstalt für Wasserbau, Hydrologie und Glaziologie an der ETH Zürich, Nr. 54, 1–230 (1981)
36. Madsen, O.S.: A realistic model of the wind-induced Ekman boundary layer. *J. Phys. Oceanogr.* **7**, 248–255 (1977)
37. Miles, J.W.: On the stability of heterogeneous shear flows. *Fluid Mech.* **10**, 496–508 (1967)
38. Mortimer, C.H.: Motion in thermoclines. *Verh. Internat. Verein. Limnol.* **14**, 79–83 (1961)
39. Mortimer, C.H.: Lake hydrodynamics. *Verh. Internat. Verein. Limnol.* **20**, 124–197 (1974)
40. Munk, W.H. and Andersen, E.R.: Notes on a theory of the thermocline. *J. Mar. Res.* **7**, 276–295 (1948)
41. Nomitsu, T.: Coast effect upon the ocean current and the sea level. *Memoirs, College of Science, Kyoto Imperial University* (Series A). I. (with T. Takegami) Steady state, **17**, 93–141, II. Changing state, **17**, 249–280 (1934)
42. Pearce, B.R. and Cooper, C.K.: Numerical circulation model for wind induced flow. *J. Hydraul. Div. Am. Soc. Civ. Engrs*: **107**(HY3), 285–302 (1981)
43. Platzman, G.W.: The dynamic prediction of wind tides on Lake Erie. *Meteorol. Monographs, Am. Meteorol. Soc.* **4**(26), 44 p. (1963)
44. Pond, S. and Pickard, G.L.: *Introductory Dynamic Oceanography*. Pergamon Oxford, (1978)
45. Prandtl, L.: Neuere Ergebnisse der Turbulenzforschung. *Zeitschrift VDI* **77**, 105–113 (1933)
46. Proudman, J.: *Dynamical Oceanography*. Methuen, London, (1953)
47. Ramming, H.-G. and Kowalik, Z.: *Numerical Modelling of Marine Hydrodynamics*. Elsevier, Amsterdam (1980)
48. Rao, D.B.: Free gravitational oscillations in rotating rectangular basins. *J. Fluid Mech.* **25**, 523–555 (1966)
49. Svensson, U.: Ph.D. Thesis (1979), see in HEAPS [24]

50. Sverdrup, H.U., Johnson, M.M. and Fleming, R.H.: *The Oceans, their Physics, Chemistry and Biology*. Prentice Hall, New York NY, (1946)
51. Thomas, J.H.: A theory of steady wind-driven currents in shallow water with variable eddy viscosity. *J. Phys. Oceanogr.* **5**, 136–142 (1975)
52. Welander, P.: Wind action on a shallow sea: some generalizations of Ekman's theory. *Tellus* **9**, 45–52 (1957)
53. Wilson, B.W.: Note on surface wind stress over water at low and high wind speeds. *J. Geophys. Res.* **65**, 3377–3382 (1960)
54. Witten, A.J. and Thomas, J.H.: Steady wind driven currents in a large lake with depth-dependent eddy viscosity. *J. Phys. Oceanogr.* **6**, 85–92 (1976)

Chapter 10

Phenomenological Coefficients of Water

This chapter is based on the work done by HUTTER and TRÖSCH [35] and extensions of it. We shall list the phenomenological coefficients which describe water as a heat-conducting viscous fluid. Such fluids are described phenomenologically by the following coefficients:

ρ	density,
ν, μ, ζ	kinematic and dynamic viscosities,
c_p, c_v	specific heats at constant pressure and constant volume, respectively,
κ, χ	heat conductivity, thermal diffusivity.

Other parameters, e.g. the coefficients of thermal expansion, are derivable from these fundamental coefficients. It is known that the viscosities, specific heats and coefficient of thermal expansion are, in general, functions of the temperature, pressure, density and the content of impurities, e.g. salts and suspended organic and inorganic matter.

When studying the material properties of water, one quickly recognises that ‘water’ is not a fluid with uniquely defined properties. For one, both hydrogen and oxygen have isotopes. The hydrogen atom exists in three different stable forms (protium, deuterium and tritium) and two radioactive ones (^4H and ^5H). The oxygen has also five isotopes, of which two (^{14}O and ^{15}O) are radioactive ones. Thus, overall, 18 stable different kinds of water exist, with slightly different density, melting and boiling temperatures, specific heats, surface tension, viscosity, electrical conductivity, etc. As a result, ‘pure water’ is a mixture of all of them presented in different proportions. Moreover, investigations of the last decades have shown that water has a clustered structure: individual water molecules are joined together via hydrogen bonds so that water should not be considered as a collection of separate molecules but as a united association of clusters. This cluster structure is the reason for many important water anomalies, including the existence of the density maximum and the sharp increase of its specific volume while freezing. Via its cluster structure and isotopic composition, water has a certain ‘memory’: one can easily distinguish, say, (i) rain water, just condensed from vapour, by its larger deuterium concentration or (ii) water just melted out of ice by its large and ice-structured water clusters. We,

however, shall here not discuss these anomalous properties, but rather present the material properties of ‘usual’ natural water and their dependency on temperature, pressure, salinity and suspended matter.

10.1 Density of Water

Density measurements of water have been conducted separately for *pure* and *natural* water. We shall differentiate between three forms of water: (i) *pure* water, (ii) *natural* water and (iii) *salt water*. *Pure* water consists of distilled H_2O molecules with a certain unspecified but small proportion of deuterium and tritium water; however, these heavy water molecules are so few that they are assumed not to affect the density in any measurably significant proportion. *Salt water* is pure water mixed with salt. The salt in the ocean water is composed of several different minerals, mostly Na^+ and Cl^- ions but also Mg^{++} and Ca^{++} , SO_4^{--} , etc., and, depending on the proportions of these the salts will differently affect the density function. In many applications these variations of salt compositions are not very significant, because they exercise an influence on the density that is too small to become observable in the lake physics results. In such cases one defines a standard composition and uses *salinity* as the variable characterising the salt content and measures it in terms of *electrical conductivity* in a gross fashion. Finally, *natural* water is fresh water as it arises in rivers and lakes. It also contains salts, but because their concentration is small, one speaks of *mineralisation* rather than salinity. Differences of the mineralisation of natural waters of different lakes are sometimes so large that the density function needs separate calibration for such lakes (e.g. for Lake Baikal [59]). However, in lakes, which often possess a small, nearly constant mineral content, which does not affect the density function, also the pressure dependence may be ignored down to 200–300 m. In this case, there only remains the temperature that affects the value of the density. For more information on principles of measurement of water temperature, electrical conductivity and density, as well as on other classifications of water due to the salinity concentration, the reader is advised to read part ‘Observations and measurements’ in Volume 3, of this treatise.

In the temperature range of $T_f \leq T \leq 100^\circ\text{C}$, where T_f is the freezing temperature, the density is not a monotonous function of the temperature. For almost all other substances an increase of the density is measured when the temperature decreases. This monotonic behaviour holds for fresh water only for temperatures above approximately 4°C ; as this temperature is crossed water shows an abnormal behaviour. Pure water has a density maximum at approximately 4°C (3.98°C more accurately), i.e. the density decreases when the temperature falls below this value. This property has important implications for the state of the Earth and its living populations. If this density maximum would not exist above the freezing point, a lake would freeze in winter starting from the bottom with its lowest temperature and eventually freeze through its entire depth. The solar irradiation would be too small to melt the ice. The living creatures would be without nutrients and

would mostly die. Instead, a lake freezes from its surface due to the non-monotonic density–temperature relationship; the ice floats on the surface because of an additional density decrease at freezing from water to ice. The ice cover at the surface forms an insulator of the cold from above for the entire lake below, which in winter assumes a temperature between 0 and 4°C. The density variation of pure water as a function of temperature in the interval $0^\circ\text{C} \leq T \leq 40^\circ\text{C}$ is shown in Fig. 10.1. Despite the fact that this non-monotonicity of the density as a function of temperature is obviously very small (the relative density change in the temperature range of 20°C is of the order of 10^{-3}) it is of immense significance.

Measurements of the density of pure water date back to the NAPOLEONIAN times when the standard litre was introduced as the unit of volume into the metric system. According to BOWMAN and SCHOONOVER [11], the first successful density measurements date back to the beginning of the 20th century and have been collected by TILTON and TAYLOR [65] from the US National Bureau of Standards. They give tables for the density of ‘normal’ water as a function of temperature and account for the content of air in solution, but ignore the influence of the pressure. This correction was accounted for by BOWMAN and SCHOONOVER [11]. Their formula is

$$\rho = \left\{ \left[1 - \frac{(T - 3.9863)^2}{508929.2} \frac{T + 288.9414}{T + 68.12963} \right] \times 0.99973 \right\} \times P_L \times A_L,$$

$$P_L = \frac{1}{1 - c \left(\frac{B_a}{760} + \frac{I}{1033} - 1 \right)} = \frac{1}{1 - c(p - 1)},$$

$$A_L = 1 - (2.11 - 0.053T) \times \left(1 - \frac{1}{1 + t} \right) \times 10^{-6}. \quad (10.1)$$

In this formula, T is the temperature in degree CELSIUS, c is a measure of compressibility ($= 47.7 \text{ ppm atm}^{-1}$), B_a is the barometric pressure (measured in mm

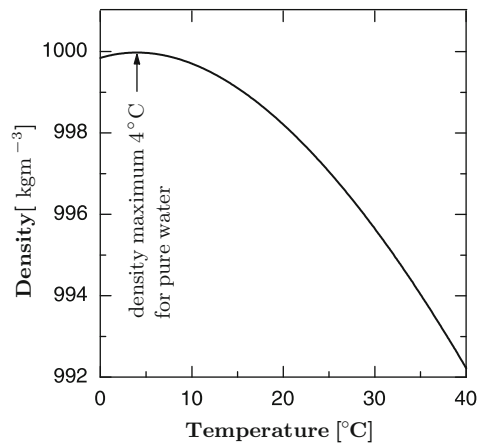


Fig. 10.1 Density variation of pure water as a function of the temperature, obtained with the formula of CHEN and MILLERO [19] with $s = 0$, $p = 1 \text{ atm}$

mercury column), I is the depth below the free water surface and p the absolute pressure (measured in bar); finally, t is the time (measured in days) since the last de-aeration. The value of the density computed this way is in CGS units, i.e. g cm^{-3} . The term in braces is the density formula by TILTON and TAYLOR in g cm^{-3} , P_L is the correction factor that accounts for the compressibility and A_L that for the de-aeration. Formula (10.1) is valid for ‘normal’ water, i.e. water of a ‘mean’ composition of isotopes. A consequence of this composition is, according to BOWMAN and SCHOONOVER, corroborated by modern experimentalists, but measurable only at density differences of somewhat more than one-millionth part. The term in braces

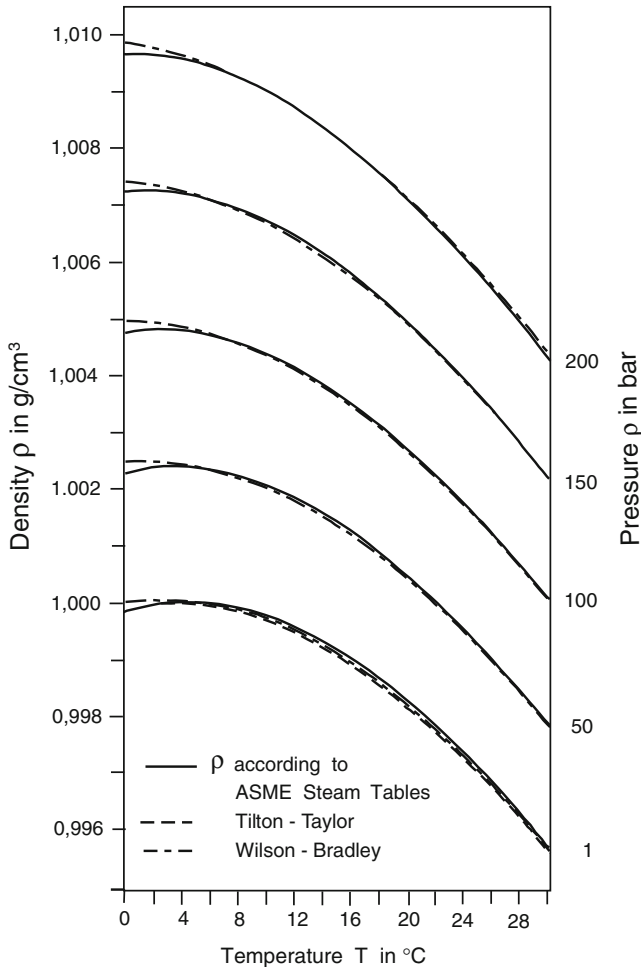


Fig. 10.2 Density of pure water as a function of the temperature and the pressure in the ranges $T \in [0, 30]^\circ\text{C}$ and $p \in [1, 200]$ bar, corresponding to water depths between 0 and 2200 m, from [23], © Laboratory of Hydraulics, Hydrology and Glaciology at ETH Zurich, with permission

of formula (10.1) can be approximated by a polynomial of the third degree. This cubic approximation is said to be valid for $T \in [0, 24]^\circ\text{C}$ and reads

$$\rho = \left\{ \left[0.059385T^3 - 8.56272T^2 + 65.4891T \right] \times 10^{-6} + 0.99984298 \right\} \times P_L \times A_L. \quad (10.2)$$

The values of ρ obtained with (10.2) differ from those of (10.1) at the sixth digit only. Formula (10.2) without the factors P_L and A_L has been published by BÜHRER and AMBÜHL [15].

An additional very complicated formula can be found in the ASME Steam Tables [1]. The formulae shown in these tables are also said to hold for high temperatures and pressures; they are for this reason not very accurate in the temperature range $T \in [0, 30]^\circ\text{C}$ and at pressures $p \in [10^5, 10^7]$ Pa. The tolerance is approximately 0.1 per thousand (0.1 ppt).¹

The density variation of pure water as a function of temperature and pressure (without the account of dissolved air, $A_L = 1$) is shown in Fig. 10.2 as computed by the formulae (i) of the ASME Steam Tables, (ii) the TILTON and TAYLOR formula and (iii) a formula of WILSON and BRADLEY [69], see later formula (10.3). All three formulae show the typical non-linearity of the density function on the temperature in the limnologically significant range, but the non-monotonicity of the density function as a function of temperature for $T \in [0, 4]^\circ\text{C}$ is not reproduced by all formulae. The TILTON and TAYLOR and WILSON and BRADLEY formulae do not show the density maximum for $T \approx 4^\circ\text{C}$. Because in limnology change of the convective flow regime due to the non-monotonicity of the thermal equation of state is significant (e.g. see Fig. 1.9 in Chap. 1), the parameterisation of the density function is of utmost importance in order that the associated flow instabilities and convective processes can properly be captured.

10.1.1 Natural Water and Sea Water

Natural water and sea water are distinguished from pure water by the addition of salts. So-called *standard sea water* contains the following ions (see [2]) in ppt:

K ⁺	0.388
Ca ⁺⁺	0.400
Mg ⁺⁺	1.272
SO ₄ ⁻⁻	2.649
Na ⁺	10.556
Cl ⁻	18.980
H ₂ O	965.675
Not identified	0.188

¹ We shall use ‘ppt’ as the standard symbol for ‘parts per thousand’. So 1 ppt = 0.001.

with mass proportions as indicated (they add up to 1000.008). The NaCl proportions are obviously contributing the largest mass.

Density measurements with sea water have been conducted by KNUDSEN [43], EKMAN [25], NEWTON and KENNEDY [53] and WILSON and BRADLEY [69]. Their measurements comprise the temperature interval $T \in [0, 40]^\circ\text{C}$ and the salinity interval $s \in [0, 40]$ ppt. For higher salinity, see [37]. WILSON and BRADLEY did not analyse the mineral composition and call their water ‘natural sea water’, taken from the Atlantic Ocean, Bermuda Key West Region. They only state that organic tracers were removed. For this sea water they derived the following density–temperature–salinity–pressure formula:

$$\begin{aligned} \frac{1}{\rho} &= 0.70200 + \frac{N(T, s)}{D(p, T, s)}, \\ N(T, s) &= 100(17.5273 + 0.1101T - 0.000639T^2 \\ &\quad - 0.0399986s - 0.000107Ts), \\ D(p, T, s) &= p + 5880.9 + 37.592T - 0.34395T^2 + 2.2524s. \end{aligned} \quad (10.3)$$

In this formula, p is the pressure (measured in bar), T is the temperature (measured in degree CELSIUS) and s is the salinity (measured in g cm^{-3}). For $s = 0$, (10.3) should generate the same results as formulae (10.1) and (10.2) and the formula of the ASME Steam Tables [1]. Figure 10.2 shows that differences are particularly large in the temperature range $[0, 4]^\circ\text{C}$. In particular, it seems to generate for all pressures a monotonic behaviour of the density as a function of the temperature. The formula is therefore not recommended for limnological applications when $T \in [0, 4]^\circ\text{C}$.

Today, the thermal equation of state that is universally accepted in limnology and oceanography is the standard formula proposed by CHEN and MILLERO [19]. It reads

$$\begin{aligned} \rho(T, s) &= \rho_1(T) + \rho_2(T)s, \quad [\text{kg m}^{-3}], \\ \rho_1(T) &= 999.8395 + 6.7914 \times 10^{-2} T - 9.0894 \times 10^{-3} T^2 \\ &\quad + 1.0171 \times 10^{-4} T^3 - 1.2846 \times 10^{-6} T^4 \\ &\quad + 1.1592 \times 10^{-8} T^5 - 5.0125 \times 10^{-11} T^6, \\ \rho_2(T) &= 8.181 \times 10^{-1} - 3.85 \times 10^{-3} T + 4.96 \times 10^{-5} T^2, \end{aligned} \quad (10.4)$$

in which the temperature must be given in degree CELSIUS² and the salinity in grams of solved substance per kilogram of pure water. The values of the density are listed in Table 10.1. A somewhat simpler formula in which the temperature is expressed as a polynomial of third degree is

$$\begin{aligned} \rho(T, s) &= 999.8395 + 6.7914 \times 10^{-2} T \\ &\quad - 9.0894 \times 10^{-3} T^2 \\ &\quad + 1.0171 \times 10^{-4} T^3. \end{aligned} \quad (10.5)$$

² In all subsequent formulae it is understood that the temperature is given in degree CELSIUS.

Table 10.1 Properties of pure water in the temperature range of 0–35°C

°C, temp [°C]	ρ , density [kg m ⁻³]	c_p , specific heat [J kg ⁻¹ K ⁻¹]	α_T , coefficient of thermal expansion [K ⁻¹]	ν , kinematic viscosity [m ² s ⁻¹]
0	999.8395	4217.4	-6.8×10^{-5}	1.78029×10^{-6}
1	999.89843	4213.8683	-5.00943×10^{-5}	1.72178×10^{-6}
2	999.93976	4210.58612	-3.27746×10^{-5}	1.66633×10^{-6}
3	999.96408	4207.54076	-1.60112×10^{-5}	1.61372×10^{-6}
4	999.97192	4204.71986	2.24665×10^{-5}	1.56375×10^{-6}
5	999.96378	4202.11143	1.59601×10^{-5}	1.51624×10^{-6}
6	999.94016	4199.70382	3.1221×10^{-5}	1.47102×10^{-6}
7	999.90151	4197.48579	4.6032×10^{-5}	1.42793×10^{-6}
8	999.84827	4195.44641	6.04165×10^{-5}	1.38685×10^{-6}
9	999.78086	4193.57514	7.43968×10^{-5}	1.34764×10^{-6}
10	999.69967	4191.8618	8.79937×10^{-5}	1.31018×10^{-6}
11	999.60508	4190.29657	1.01227×10^{-4}	1.27437×10^{-6}
12	999.49745	4188.86998	1.14117×10^{-4}	1.24011×10^{-6}
13	999.3771	4187.57294	1.26679×10^{-4}	1.2073×10^{-6}
14	999.24437	4186.39671	1.38932×10^{-4}	1.17587×10^{-6}
15	999.09957	4185.33292	1.5089×10^{-4}	1.14573×10^{-6}
16	998.94297	4184.37356	1.6257×10^{-4}	1.1168×10^{-6}
17	998.77486	4183.51098	1.73984×10^{-4}	1.08903×10^{-6}
18	998.59551	4182.73788	1.85147×10^{-4}	1.06235×10^{-6}
19	998.40516	4182.04734	1.9607×10^{-4}	1.03671×10^{-6}
20	998.20405	4181.4328	2.06765×10^{-4}	1.01203×10^{-6}
21	997.99242	4180.88805	2.17242×10^{-4}	9.88287×10^{-7}
22	997.77048	4180.40726	2.27513×10^{-4}	9.65418×10^{-7}
23	997.53844	4179.98494	2.37586×10^{-4}	9.43384×10^{-7}
24	997.2965	4179.61598	2.4747×10^{-4}	9.22143×10^{-7}
25	997.04486	4179.29562	2.57174×10^{-4}	9.01654×10^{-7}
26	996.7837	4179.01948	2.66705×10^{-4}	8.81883×10^{-7}
27	996.51319	4178.78351	2.7607×10^{-4}	8.62795×10^{-7}
28	996.2335	4178.58405	2.85276×10^{-4}	8.44358×10^{-7}
29	995.9448	4178.4178	2.9433×10^{-4}	8.26542×10^{-7}
30	995.64725	4178.2818	3.03237×10^{-4}	8.09317×10^{-7}
31	995.34099	4178.17348	3.12002×10^{-4}	7.92658×10^{-7}
32	995.02618	4178.09061	3.20631×10^{-4}	7.76539×10^{-7}
33	994.70295	4178.03133	3.29129×10^{-4}	7.60936×10^{-7}
34	994.37144	4177.99415	3.375×10^{-4}	7.45828×10^{-7}
35	994.03178	4177.97792	3.45749×10^{-4}	7.31191×10^{-7}

This formula was used by BÜHRER and AMBÜHL [15]; it describes the density of water in the interval 0°C < *T* < 30°C accurate to six significant figures.

The ambient pressure is accounted for by a multiplicative factor according to

$$\rho(T, p) = \rho(T, p = 1 \text{ bar}) \times \frac{1}{1 - p/\Phi}, \quad p \text{ in [bar]}, \quad (10.6)$$

in which the pressure must be expressed in bar, and the function Φ is given by

$$\Phi(T) = 19652.17 + 148.133 T - 2.293 T^2 + 1.256 \times 10^{-2} T^3 - 4.180 \times 10^{-5} T^4. \quad (10.7)$$

A somewhat simpler description, which is adequate for lakes, uses instead of salinity the electrical conductivity of water, κ ; in terms of this one has

$$\rho(T, \kappa) = \rho(T) (1 + \beta_\kappa \times \kappa_{20}(T)), \quad (10.8)$$

in which the conductivity of water is given in $\mu \text{ S m}^{-1}$ and referred to a standard value of 20°C,

$$\kappa_{20} = \kappa (1.72228 - 0.0541369T + 0.00114842T^2 - 0.0000222651T^3). \quad (10.9)$$

In this formula κ is the value of the conductivity measured at the temperature T [°C]. IMBODEN and WÜEST [36] give for β_κ the value

$$\beta_\kappa = 0.705 \times 10^{-4} \mu \text{ S m}^{-1}. \quad (10.10)$$

In limnology, the temperature range is between 0 and 30°C; larger temperatures virtually never arise. For computational purposes the rather complicated formulae given above can then also be replaced by a quadratic equation

$$\rho(T) = \rho_0 (1 - \tilde{\alpha}(T - T_0)^2). \quad (10.11)$$

The reference temperature is chosen as that of the density maximum, $T_0 = 4^\circ\text{C}$ with the corresponding density $\rho_0 = \rho(4^\circ\text{C})$; $\tilde{\alpha}$ has the value

$$\tilde{\alpha} = 6.493 \times 10^{-6} [\text{K}^{-1}]. \quad (10.12)$$

If one also needs the coefficient of thermal expansion,

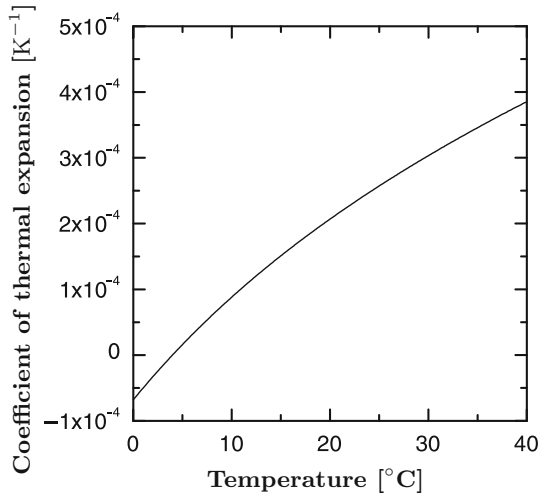
$$\alpha_T = -\frac{1}{\rho} \frac{d\rho}{dT}, \quad (10.13)$$

then for (10.11) α_T is given by

$$\alpha_T = \frac{2\tilde{\alpha}(T - T_0)}{1 - \tilde{\alpha}(T - T_0)^2} \approx 2\tilde{\alpha}(T - T_0). \quad (10.14)$$

Table 10.1 and Fig. 10.3 display the variation of the coefficient of thermal expansion as a function of temperature. One recognises that the temperature dependence of α_T is nearly linear, so that the approximation (10.14) is justified.

Fig. 10.3 Coefficient of thermal expansion for pure water computed with the data generated by formula (10.4) of CHEN and MILLERO [19] for $s = 0$ and $p = 1$ bar



It should be recognised that the coefficient of thermal expansion does not change sign at high pressure and high salinity. According to the CHEN and MILLERO formula the zeros of the coefficient of thermal expansion are given by zeros of the equation

$$\left(\frac{d\rho_1}{dT} + \frac{d\rho_2}{dT}s \right) - \frac{\rho_1(T) + \rho_2(T)s}{1 - p/\Phi(T)} \frac{p}{\Phi^2} \frac{d\Phi}{dT} = 0. \quad (10.15)$$

These zeros for various values of the pressure and salinity are graphically illustrated in Fig. 10.4.

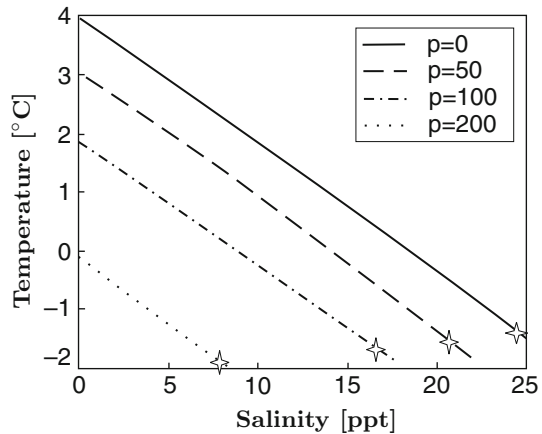


Fig. 10.4 Zeros of the coefficient of thermal expansion (or temperatures of maximum density) for water as a function of the salinity for the selected hydrostatic pressures (in bar), which correspond to water depths of 0, 500, 1000 and 2000 m. The stars indicate the corresponding freezing points

10.1.2 Suspended Matter

In the above, water was regarded as a fluid which is only loaded by minerals in chemical solution. Here, we give estimates of density changes, if water also contains tracers in solid particular form. The size of particles that can be kept in suspension depends principally on the degree of turbulence which exists in the water body at a particular position in a fluid at rest; the particles must be buoyant in order not to fall or rise in the fluid. Very small, slightly non-buoyant particles can be kept in suspension by the BROWNIAN motion.

Consider a mixture of water with a number of solid particles (distinguished by the identifier) α of partial density ρ_α and true density $\bar{\rho}_\alpha$. Then

$$\rho_\alpha = n_\alpha \bar{\rho}_\alpha \quad (10.16)$$

where n_α is the volume fraction of component α . The density of the compound water plus suspended particles is then given by

$$\rho = \sum_{\alpha} n_{\alpha} \bar{\rho}_{\alpha}. \quad (10.17)$$

For the admixture of only one sort of particles, we obtain from (10.17)

$$\rho = n_1 \bar{\rho}_{\text{H}_2\text{O}} + n_2 \bar{\rho}_2 = n_1 \bar{\rho}_{\text{H}_2\text{O}} + (1 - n_1) \bar{\rho}_2. \quad (10.18)$$

This simple formula is graphically interpreted in Fig. 10.5.

To estimate the influence of a suspended tracer, consider water with true density of 1000 kg m^{-3} and a sediment with $\bar{\rho}_2 = 2500 \text{ kg m}^{-3}$. Then formula (10.18) implies the following compound densities:

$(1 - n_1) $	10^{-4}	10^{-3}	10^{-2}	10^{-1}
ρ	1000.25	1002.5	1015	1150

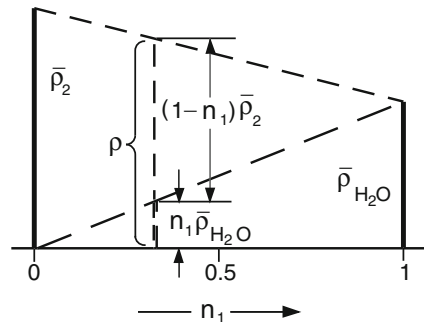


Fig. 10.5 Determination of the density of a binary composition of water and a suspended component of constant true density $\bar{\rho}_2$

This implies that the influence of suspended sediments on the density of the compound fluid at a volume fraction of 1% or more exceeds the influence of the temperature by far. This is important for the intrusion of river water that is loaded with sediments into lakes.

10.2 Specific Heat of Water

One of the anomalous properties of liquid water is its specific heat. It is more than twice as large as that of ice and 5–30 times larger than that of other substances. Moreover, the specific heat of all substances increases with growing temperature – except only that of water (in the temperature range 0–35°C) and mercury.

The specific heat or the *molecular heat capacity of water at constant pressure* shows both a dependence on temperature, which is weak, and a dependence on pressure, which is stronger. This dependence can be written as (see [34])

$$c_p = 4190.0 + \exp(46.40 - 0.156T) [\text{J kg}^{-1} \text{K}^{-1}], \quad T [^\circ\text{C}], \quad (10.19)$$

or when pressure p (depth) [bar] and salinity s [g kg⁻¹] are taken into account

$$\begin{aligned} c_p = & 4217.4 - 3.6608 T + 0.13129 T^2 \\ & - 2.210 \times 10^{-3} T^3 + 1.508 \times 10^{-5} T^4 \\ & + s (-6.616 \times 10^{-2} + 9.28 \times 10^{-3} T - 2.39 \times 10^{-5} T^2) \\ & + p (-4.917 \times 10^{-1} + 1.335 \times 10^{-2} T - 2.177 \times 10^{-4} T^2) \\ & + s p 3.441 \times 10^{-3} \\ & + p^2 1.50 \times 10^{-4}, \end{aligned} \quad (10.20)$$

see [19]. Table 10.1 lists numerical values and Fig. 10.6 displays the pressure dependence of c_p for pure water constructed with formulae of the ASME Steam Tables [1]. It is evident that both pressure and temperature dependencies are rather weak, namely less than 2% for $T \in [0, 30]^\circ\text{C}$ and $p \in [1, 500]$ bar.

10.2.1 Specific Heat of Salty Water

The specific heat of water of different salinities in [ppt] at normal atmospheric pressure [10⁵ Pa] has been compiled from different sources by POPOV et al. [57]. Their table is reproduced below as Table 10.2. It shows c_p in [kJ kg⁻¹ K⁻¹] at various temperatures $T \in [-2, 40]^\circ\text{C}$ and salinities $s \in [0, 40]$ ppt. Note that most data are

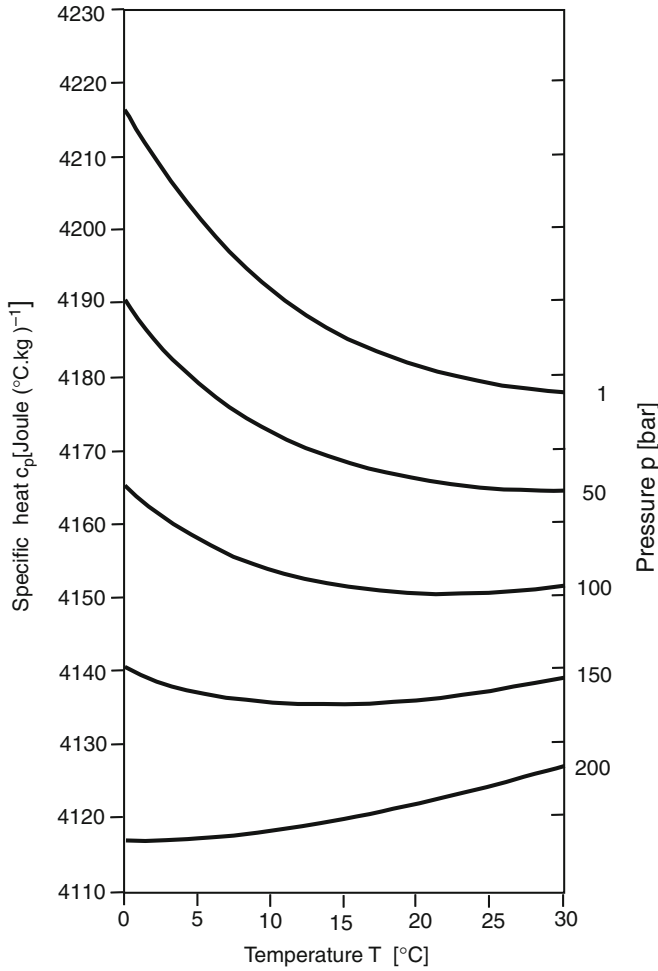


Fig. 10.6 Specific heat at constant pressure, c_p , of pure water as a function of temperature and pressure according to ASME Steam Tables [1]

taken from various experimental sources as indicated; they are printed in the table in regular type. Numbers in bold type have been obtained by using the formulae

$$\begin{aligned}
 c_p [\text{cal g}^{-1} \text{K}^{-1}] &= 1.005 - 4.226 \times 10^{-4}T + 6.321 \times 10^{-6}T^2, \\
 c_p [\text{cal g}^{-1} \text{K}^{-1}] &= 1.005 - 4.136 \times 10^{-3}s + 1.098 \times 10^{-4}s^2 \\
 &\quad - 1.324 \times 10^{-6}s^3.
 \end{aligned}
 \tag{10.21}$$

Table 10.2 Specific heat c_p [$\text{kJ kg}^{-1} \text{K}^{-1}$] at normal atmospheric pressure [10^5 Pa] for $T \in [-2, 10]^\circ\text{C}$ and $s \in [0, 40] \text{ ppt}$

s (ppt)		T ($^\circ\text{C}$)																References	
		0	5	10	15	20	25	30	32	34	35	36	38	40					
-2	-	-	-	-	-	-	-	-	-	-	3.984	3.979	3.968	3.957					[20] *1
	-	-	-	-	-	4.075	4.043	4.013	4.001	3.990	3.984	3.979	3.968	3.957					[20] *1
	0	4.2174	4.1812	4.1466	4.1130	4.0804	4.0484	4.0172			3.9865		3.968	3.9564					[50] *1
1	4.2205			4.1497		4.0831		4.0199						3.9601					[14, 13] *1
	4.217	4.179	4.142	4.107	4.107	4.074	4.043	4.013	4.002	3.990	3.985	3.979	3.968	3.957					[20] *1
	4.208	4.132	4.074	4.032	4.003	4.003	3.973	3.952			3.927			3.894					[71] *2
2	4.214	4.176	4.140	4.106	4.074	4.043	4.013	4.013	4.002	3.991	3.985	3.980	3.968	3.958					[20] *1
	4.210	4.174	4.138	4.105	4.073	4.042	4.013	4.013	4.002	3.991	3.985	3.980	3.969	3.958					[20] *1
	4.2019	4.1679	4.1354	4.1038	4.0730	4.0428	4.0132				3.9842			3.9556					[50] *1
5	4.202	4.168	4.135	4.103	4.072	4.042	4.014	4.014	4.003	3.992	3.986	3.981	3.970	3.959					[20] *1
	4.199	4.124	4.055	4.024	3.994	3.969	3.944				3.919			3.885					[71] *2
	4.1919	4.1599	4.1292	4.0994	4.0702	4.0417	4.0136				3.9861			3.9590					[20] *1
10	4.1949		4.1334			4.0741	4.0178							3.9638					[14, 13] *1
	4.192	4.161	4.130	4.100	4.071	4.042	4.015	4.004	4.004	3.993	3.988	3.983	3.972	3.962					[20] *1
	4.191	4.116	4.061	4.019	3.986	3.960	3.936				3.911			3.881					[71] *2
15	4.1855	4.1553	4.1263	4.0982	4.0706	4.0437	4.0172				3.9912			3.9655					[50] *1
	4.186	4.157	4.128	4.099	4.071	4.0437	4.016	4.006	4.006	3.995	3.990	3.985	3.975	3.965					[20] *1
	4.187	4.112	4.053	4.011	3.982	3.957	3.931				3.906			3.877					[71] *2
17.5	4.187	4.112	4.053	4.011	3.982	3.957	3.931	3.902			3.902			3.877					[44, 64] *1
	4.1816	4.1526	4.1247	4.0975	4.0709	4.0448	4.0190				3.9937			3.9688					[50] *1
	4.1849		4.1280			4.0741	4.0220							3.9718					[14, 13] *1
20	4.182	4.154	4.126	4.098	4.071	4.045	4.018	4.008	4.008	3.998	3.993	3.988	3.978	3.968					[20] *1
	4.182	4.107	4.049	4.007	3.978	3.952	3.927				3.902			3.873					[71] *2
	4.159	4.131	4.105	4.078	4.050	4.023	4.012	3.998	3.993	3.988	3.985	3.978	3.968	3.957					[57] *3

Table 10.2 (continued)

s (ppt)															References
T (°C)	0	5	10	15	20	25	30	32	34	35	36	38	40		
25	4.1793	4.1513	4.1242	4.0977	4.0717	4.0462	4.0210			3.9962			3.9718	[50] *1	
	4.179	4.153	4.126	4.099	4.072	4.046	4.020	4.010	4.000	3.995	3.991	3.981	3.972	[20] *1	
30	4.179	4.103	4.049	4.007	3.943	3.948	3.923			3.898			3.869	[71] *2	
	4.1782	4.1510	4.1248	4.0992	4.0770	4.0494	4.0251			4.0011			3.9775	[50] *1	
	4.1815		4.1279		4.0767		4.0270						3.9788	[14, 13] *1	
	4.178	4.152	4.126	4.100	4.074	4.048	4.023	4.013	4.003	3.999	3.994	3.985	3.976	[20] *1	
35	4.179	4.103	4.075	4.003	3.973	3.948	3.923			3.898			3.865	[71] *2	
	4.1779	4.1511	4.1252	4.0999	4.0751	4.0508	4.0268			4.0031			3.9797	[50] *1	
40	4.1783	4.1515	4.1256	4.1003	4.0754	4.0509	4.0268			4.0030			3.9795	[50] *1	
	4.180		4.128		4.078		4.030						3.983	[14, 13] *1	

*1 are experimental data. Bold types indicate calculated values according to formulae (10.21). *3 (slanted numbers) give interpolated values as computed by POPOV et al. [57] via formula (10.22)

Table 10.3 Specific heat c_v [$\text{kJ kg}^{-1} \text{K}^{-1}$] at constant volume for saline water at atmospheric pressure [10^5 Pa] and $T \in [0, 40]^\circ\text{C}$ and $s \in [0, 40] \text{ ppt}$, calculated by MILLERO and KUBINSKI [49], as compiled by POPOV et al. [57]

T [$^\circ\text{C}$]	s [ppt]								
	0	5	10	15	20	25	30	35	40
0	4.2149	4.1800	4.1461	4.1129	4.0804	4.0482	4.0165	3.9851	3.9540
5	4.2019	4.1673	4.1341	4.1016	4.0697	4.0382	4.0071	3.9765	3.9641
10	4.1873	4.1538	4.1215	4.0899	4.0589	4.0284	3.9982	3.9686	3.9392
15	4.1715	4.1391	4.1080	4.0777	4.0478	4.0186	3.9898	3.9614	3.9332
20	4.1543	4.1229	4.0929	4.0631	4.0341	4.0056	3.9773	3.9495	3.9221
25	4.1356	4.1053	4.0759	4.0470	4.0186	3.9906	3.9630	3.9357	3.9087
30	4.1152	4.0864	4.0580	4.0302	4.0026	3.9756	3.9488	3.9222	3.8957
35	4.0945	4.0659	4.0381	4.0106	3.9835	3.9568	3.9302	3.9038	3.8775
40	4.0724	4.0440	4.0163	3.9890	3.9618	3.9348	3.9079	3.8810	3.8541

Table 10.4 Specific heat c_p [$\text{kJ kg}^{-1} \text{K}^{-1}$] at different constant pressures for sea water at $s \in [34.8, 35] \text{ ppt}$ in the temperature range $T \in [-2, 20]^\circ\text{C}$ as compiled by POPOV et al. [57] from the indicated sources. Values are computed ones

T [$^\circ\text{C}$]	p 10^4 Pa	s [ppt]			T [$^\circ\text{C}$]	p 10^4 Pa	$s = 34.8 \text{ ppt}$ [21, 26]
		34.8 [21, 26]	35 [68, 12]	35 [68, 12]			
-2	1000	3.906			5	1000	3.894
	2000	3.873				2000	3.869
	3000	3.810				3000	3.823
	6000	3.760				6000	3.785
0	1000	3.906			10	8000	3.752
	2000	3.873				1000	3.890
	3000	3.819				2000	3.865
	6000	3.772	3.834	3.698		3000	3.823
	8000	3.735				1000	3.886
2	10000		3.776	3.318	20	2000	3.860
	6000		3.839	3.709		3000	3.820
	2000		3.929	3.919		1000	3.881
	4000		3.883	3.834		2000	3.856
	6000		3.844	3.718			
	10000		3.788	3.343			

Note: The pressure at the bottom of a water column of 1 m is approximately 10^4 Pa , so that numbers in the columns for pressure are approximately the water depth in metres

Formula $(10.21)_1$ is given by JÄGER and STEINWEHR [39] and $(10.21)_2$ by KUWAHARA [45]. For $T = 20^\circ\text{C}$ the figures identified by *3 are computed values by POPOV et al. [57] using the formula by PONIZOVSKY et al. [56]

$$c_p [\text{cal g}^{-1} \text{K}^{-1}] = 1 - 1.307 \times 10^{-2} s [\text{ppt}]. \tag{10.22}$$

POPOV et al. [57] give also tables for the specific heats at constant (higher than atmospheric) pressure, c_p , and constant volume, c_v . Their data are taken from relatively early sources prior to 1975 and are all calculated from formulae, given in

DEFANT [21], EKMAN [26], WANG and MILLERO [68], BRADSHAW and SCHLEICHER [12] and FOFONOFF [31]. Table 10.3 lists c_v [$\text{kJ kg}^{-1} \text{K}^{-1}$] for saline water at normal atmospheric pressure and for $T \in [0, 40]^\circ\text{C}$ and $s \in [0, 40]$ ppt. This table is based on MILLERO and KUBINSKI [49]. Table 10.4, on the other hand, lists c_p [$\text{kJ kg}^{-1} \text{K}^{-1}$] for sea water at $s = 34.8$ ppt, $T \in [-2, 20]^\circ\text{C}$ and a selection of pressures. It is seen from these tables that variations of the specific heats are generally very small. The relative difference between the maximum value and minimum value

$$\Delta c = \frac{c(\text{max}) - c(\text{min})}{c(\text{max})} = 12\%$$

is no more than 12%. A comparison between Tables 10.2 and 10.3 for $s = 0$ ppt also shows that differences between c_v and c_p are generally only a few percent, certainly less than 5%.

10.3 Viscosity of Water

As a compressible fluid, water possesses two dynamic viscosities, a *shear* viscosity and a *bulk* viscosity. If \mathbf{T} is the CAUCHY stress tensor and \mathbf{D} the stretching tensor, then the stress-stretching relation for a NEWTONian fluid is given by

$$\mathbf{T} = \zeta(\text{tr } \mathbf{D})\mathbf{1} + 2\mu\left(\mathbf{D} - \frac{1}{3}(\text{tr } \mathbf{D})\mathbf{1}\right), \quad (10.23)$$

in which μ is the shear viscosity and ζ the bulk viscosity. For volume-preserving fluids, (10.23) reduces to $\mathbf{T} = 2\mu\mathbf{D}$, with only one phenomenological quantity, the shear viscosity.

Values for the viscosities are determined with the aid of *viscometers*, in which a controlled flow of the substance of which the viscosity is to be determined is generated as a consequence of equally controlled applied forces. An ideal flow configuration is POISEUILLE flow, the steady flow in an infinitely long circular pipe. In reality such flows can, however, not exactly be generated, because of ‘defects’ of the idealised situation, e.g. transients at flow initiation and entrance and exit conditions, because of the finiteness of the pipe in the experimental set-up, etc. The POISEUILLE flow formula must, therefore, be corrected for these effects, see [47]. This method is restricted to volume-preserving fluids. WHITE and KEARSLEY [70] employ a different experimental set-up. They measure the period of a torsion pendulum, which carries at its end a spherical shell whose spherical gap is filled with the fluid for which the viscosity (μ) is to be measured. The oscillations of the pendulum generate in the spherical gap an (asymptotically) periodic motion. The dissipation generated by this motion (a function of μ !) requires a power of working input for the steady maintenance of the oscillation, which can be measured via the externally applied torque and which allows determination of the viscosity, see [42]. Channel flows in specially formed canals have also been used to find values for the shear viscosities [54] as have been free fall experiments of rigid bodies of well-defined shapes in a

viscous fluid [38]. Further experimental methods for the measurement of the shear viscosity of salt water have been reported by FABUSS [28] and STOKES and MILLS [62].

It is known from the kinetic theory of a *monatomic* gas that the bulk viscosity of such gases is zero, a fact which follows already from MAXWELL's kinetic theory of gases, see [18, 66]. Non-vanishing bulk viscosity must, therefore, be traced back to the complexity (i.e. non-sphericity of the molecular structure). HALL [32] has presented such a statistical model for the water molecule in the temperature interval $T \in [0, 180]^\circ\text{C}$ and his values for ζ are the only ones known to us.

10.3.1 Pure Water

An early formula for the shear viscosity of pure water is by POISEUILLE [55] and reads

$$\mu = \frac{17.8}{1 + 0.0377T + 0.00022T^2} \quad (10.24)$$

in which T is in degrees CELSIUS and μ appears in millipoise³. Reliable values of μ for pure water have been collected by DORSEY [22]. They are based on results obtained by BINGHAM and JACKSON in 1917 [10] and were summarised in the formula:

$$\frac{1}{\mu} + 120 = 2.1482 \left\{ (T - 8.435) + \sqrt{80784 + (T - 8.435)^2} \right\}. \quad (10.25)$$

Here, T is given in degree CELSIUS and μ^{-1} is then obtained in 1/millipoise. No pressure dependence is indicated, and so (10.24) and (10.25) are assumed to hold for $p = 1$ bar. The measurements of WHITE and KEARSLEY [70] have corroborated these formulae. Figure 10.7 displays the viscosities in the temperature regime $T \in [0, 30]^\circ\text{C}$, and Table 10.5 lists values as given by three different sources.

The pressure dependence of the dynamic viscosity of pure water has been parameterised from a large number of data by STEIN [60, 61]. HUTTER and TRÖSCH [35] present the graph of Fig. 10.8; it is based on STEIN's formulae. These authors also report that for $p \in [1, 200]$ bar, values for the dynamic viscosity vary by less than 1%. This justifies to ignore such dependencies in lake physics applications.

Experimental data for the *bulk viscosity* are sparse. The values computed by HALL [32] in the temperature range $T \in [0, 50]^\circ\text{C}$ are as follows:

$T [^\circ\text{C}]$	0	4	5	10	20	30	40	50
ζ [cpoise]	8.0	7.0	6.8	6.0	4.7	3.7	2.9	2.4

³ 1 millipoise equals 10^{-3} poise. $1 [\text{poise}] = 0.1 [\text{kg m}^{-1} \text{s}^{-1}]$.

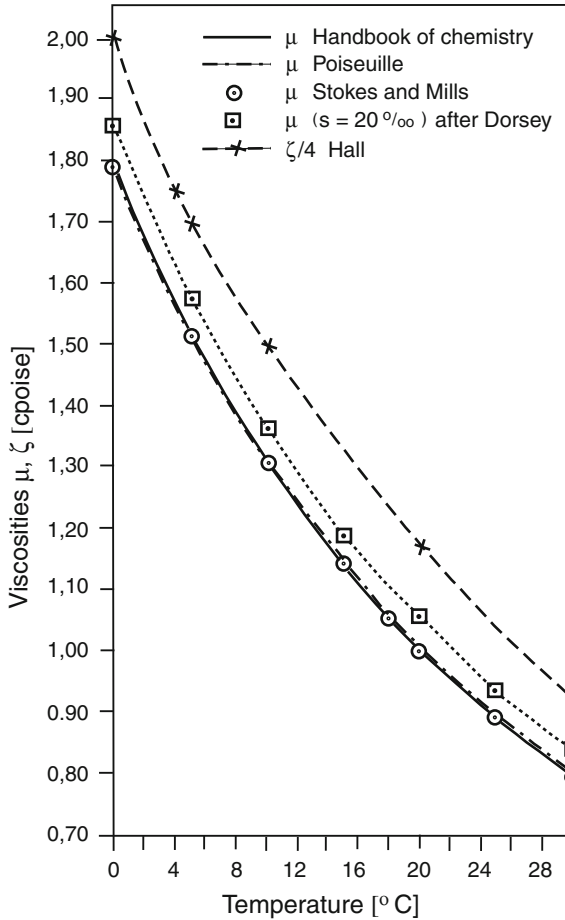


Fig. 10.7 Dynamic viscosities for pure water as functions of temperature as given by the sources in the inset, from [35], © Laboratory of Hydraulics, Hydrology and Glaciology at ETH Zurich, with permission

and a graph of ζ is given in Fig. 10.7. Note that ζ does not vanish; its values are rather about four times larger than those for the shear viscosity μ . This is due to the non-sphericity of the water molecule.

10.3.2 Sea Water

First measurements of the dynamic viscosity for sea water go back to KRÜMMEL and RUPIN (see [44]) and embrace the temperature regime $T \in [0, 30]^\circ\text{C}$ and a salinity $s \in [0, 40]$ ppt. MIYAKE and KOIZUMI [51] determined the dynamic viscosity of salt water for $T \in [0, 30]^\circ\text{C}$ and $s \in [0, 20]$ ppt with a mean error of

Table 10.5 Dynamic viscosity μ of pure water in poise as a function of temperature $T \in [0, 30]^\circ\text{C}$, given by (i) *Handbook of Chemistry and Physics* [33], (ii) CAMP [16] and (iii) STOKES and MILLS [62]

T	Handbook of chemistry and physics	Poiseuille	Stokes and mills
0	1.7921	1.78	1.787
1	1.7313	1.72	
2	1.6728	1.67	
3	1.6191	1.61	
4	1.5674	1.56	1.516
5	1.5188	1.52	
6	1.4728	1.47	
7	1.4284	1.43	
8	1.3860	1.39	1.306
9	1.3462	1.35	
10	1.3077	1.31	
11	1.2713	1.27	
12	1.2363	1.24	1.138
13	1.2028	1.21	
14	1.1709	1.17	
15	1.1404	1.14	
16	1.1111	1.12	1.053
17	1.0828	1.09	
18	1.0559	1.06	
19	1.0299	1.04	
20	1.0050	1.01	1.002
21	0.9810	0.99	
22	0.9579	0.96	
23	0.9358	0.94	
24	0.9142	0.92	0.8903
25	0.8937	0.90	
26	0.8737	0.88	
27	0.8545	0.86	
28	0.8360	0.84	0.7975
29	0.8180	0.82	
30	0.8007	0.81	

± 0.25 ppt. Their experiments were conducted with ‘natural’ sea water (for unmentioned salinity $s = 34$ ppt). FABUSS and KOROSI [30], as well as ISDALE et al. [37, 38], use artificial salt solutions and include regimes $T \in [0, 180]^\circ\text{C}$ and $s \in [0, 180]$ ppt.

A simple way to account for a salinity dependence of the viscosity of water is to write the *kinematic* viscosity as

$$\nu(T, s) = \nu_0(T)(1 - \alpha s), \quad \alpha = 2.5. \tag{10.26}$$

Note that such a formula does not hold for the dynamic viscosity, since $\mu(T, s)$ grows with growing s , while the kinematic viscosity decreases. More accurate

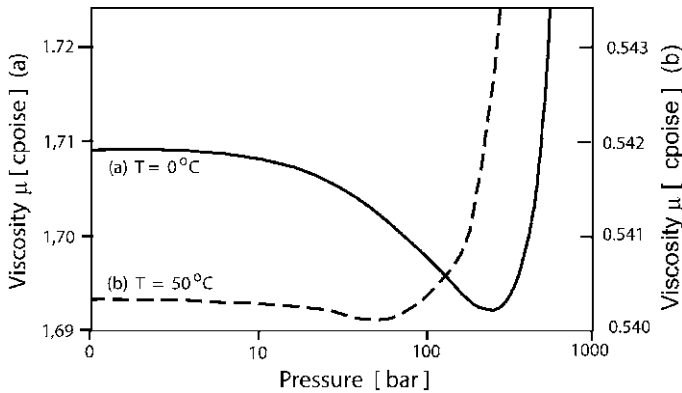


Fig. 10.8 Dynamic viscosity of pure water as a function of the pressure for (a) $T = 0^\circ\text{C}$ and (b) $T = 50^\circ\text{C}$, composed from figures in [35], © Laboratory of Hydraulics, Hydrology and Glaciology at ETH Zurich, with permission

formulae have also been presented. While MIYAKE and KOIZUMI write the dynamic viscosity as

$$\mu(T, s) = \frac{\mu_0}{1 + \alpha(s)T + \beta(s)T^2}, \quad (10.27)$$

where $\mu_0 = \mu(T=0, s)$, and α and β are salinity dependent, but only known in tabular form. ISDALE et al. [37, 38] adjusted an empirical formula to their experiments as follows:

$$\log_{10} \left(\frac{\mu_{20}}{\mu} \right) = \frac{T - 20}{T + 109} \left\{ \mathcal{A} (1 + a_1 s + a_2 s^2) + \mathcal{B} (1 + b_1 s + b_2 s^2) (T - 20) \right\}, \quad (10.28)$$

in which

$$\begin{aligned} \mu_{20} &= 1.002 + c_1 s + c_2 s^2, \\ \mathcal{A} &= 1.37220, \quad \mathcal{B} = 0.000813, \\ a_1 &= -0.001015, \quad b_1 = 0.006102, \quad c_1 = 0.001550, \\ a_2 &= 0.000005, \quad b_2 = -0.000040, \quad c_2 = 0.0000093, \end{aligned}$$

and T is the temperature in degree CELSIUS, s is the salinity in ppt of weight; μ is obtained in (10.28) as cpoise.

Figure 10.9 summarises graphically results of the dynamic viscosity determined by the indicated authors. It is recognised that the values of $\mu(T, s)$ differ from one another more and more as the salinity increases. This may be a consequence of the

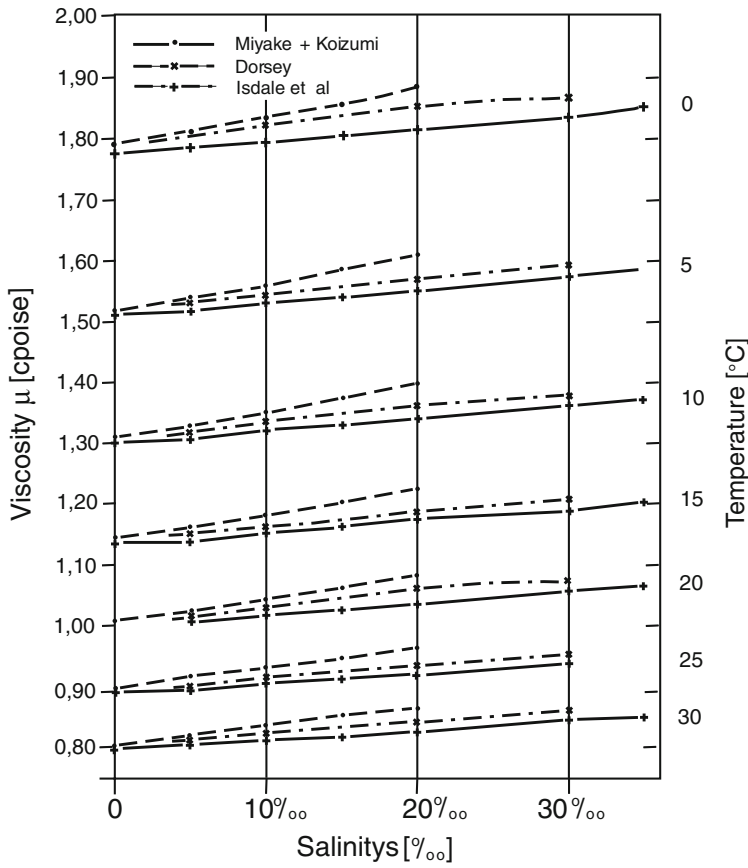


Fig. 10.9 Dynamic viscosity of salt water as a function of the salinity $s \in [0, 30]$ ppt ($= \text{‰}$) for a selection of temperatures $T \in (0, 5, 10, 15, 20, 25, 30)^\circ\text{C}$, from [35]. © Laboratory of Hydraulics, Hydrology and Glaciology at ETH Zurich, with permission

experimental method or the fact that different salt solutions were used. Unfortunately, the papers do not report the exact composition of the solutions. For application in computations we recommend the formulae by DORSEY [22] and ISDALE et al. [38], since viscosities based on the formulae by MIYAKE and KOIZUMI [51] deviate from those of DORSEY by no more than 5%.

10.3.3 Natural Water

Since the dynamic viscosity changes only slightly with the degree of mineralisation, computations according to DORSEY [22] or ISDALE et al. [37, 38] are likely accurate enough. Deviations of numerical values for the shear viscosity from that of pure water are less than 5 ppt. Caution may only have to be observed for problems

of convection in the buoyancy-sensitive temperature regime $T \in [0, 8]^\circ\text{C}$. Here, it is important that the value of the temperature at maximum density is correctly reproduced.

10.3.4 *Suspended Matter*

The preceding analysis has not yet accounted for suspended matter also called particulate tracers. In what follows, we shall regard the material as a mixture of a NEWTONian fluid (water) and rigid particles of compact form. If these suspended particles are spheres and statistically homogeneously distributed, then also the viscosity of the mixture – treated as a NEWTONian fluid – behaves as that of an isotropic fluid. When the suspended particles are platelets or rods, then an anisotropy of the viscous stresses is to be expected.

A first determination of the shear viscosity of a NEWTONian fluid with rigid spherical inclusions goes back the EINSTEIN [23] with a correction in [24]. His focus in this chapter – incidentally his Ph.D. dissertation at the University of Zürich, published after his famous papers on special relativity, photoelectric effect, BROWNIan motion – was an estimation of the dimension of sugar molecules, which are in solution in a NEWTONian fluid. The computations are based on the assumption of STOKESian viscous flow around rigid spheres which are sufficiently far from one another so that the influence of the flow on a particular sphere by the flow around all other spheres can be ignored.

EINSTEIN's computation of the slow viscous flow around the sphere led him to the following formula for the dynamic viscosity:

$$\mu = \mu_0(1 + 2.5n), \quad (10.29)$$

in which μ , μ_0 , n are the dynamic viscosity of the mixture treated as a NEWTONian fluid, μ_0 is that of the bearer fluid, here water, and n is the *volume fraction* of suspended particles in the mixture. (EINSTEIN's second paper corrects the numerical value of the pre-factor of the volume fraction term.) Formula (10.29) has been generalised in various directions. Most of these generalisations are written in the form

$$\mu = \mu_0(1 + \Phi(n, \mathcal{R}_e, \dots)), \quad (10.30)$$

in which Φ accounts for the suspended particles in a more subtle way than had been done by EINSTEIN.

1. JEFFREY [41] assumed that particles are rotational ellipsoids and derived for these the formula

$$\mu = \mu_0(1 + \varphi n), \quad (10.31)$$

with values of φ as shown in Table 10.6 for the indicated cases of the axis of rotational symmetry.⁴ For prolate and oblate ellipsoids the limits φ correspond to long rods and penny-shape particles; φ has nearly the same value for these cases, namely $\varphi = 2$ and 2.06. Of course, to obtain in these two limits the same values of the dynamic viscosity, different number densities of the particles are applied.

2. TAYLOR [63] computed the dynamic viscosity for a NEWTONian mixture consisting of two NEWTONian components, i.e. water with suspended air or oil bubbles of spherical geometry. For small concentrations of such suspended deformationless particles the dynamic viscosity reads

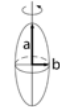
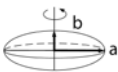
$$\mu = \mu_0 \left\{ 1 + 2.5n \frac{\mu'_0 + \frac{2}{3}\mu_0}{\mu_0 + \mu'_0} \right\}, \quad (10.32)$$

in which μ_0 is the viscosity of the bearer fluid and μ'_0 that of the bubbles. This formula is interesting, because in the two limits $\mu'_0 \rightarrow 0$ and $\mu'_0 \rightarrow \mu_0$ one obtains

$$\begin{aligned} \mu'_0 = 0 &\implies \mu = \mu_0 \left\{ 1 + \frac{2}{3} \times 2.5n \right\}, \\ \mu'_0 = \mu_0 &\implies \mu = \mu_0 \left\{ 1 + \frac{5}{6} \times 2.5n \right\}. \end{aligned} \quad (10.33)$$

Both formulae do not reduce to (10.29). This is not a discrepancy, because in (10.33)₁ the bubbles are filled with an inviscid fluid and in (10.33)₂ the bubbles are filled with a fluid with the same viscosity as the bearer fluid. In EINSTEIN's case the particles are rigid; this corresponds in (10.32) to the limit $\mu'_0 \rightarrow \infty$ for which case (10.32) reduces to (10.29).

Table 10.6 Values of φ for the dynamic viscosity (10.30) for ellipsoids with rotational symmetry about the large and small semi-axes, respectively

	$\varepsilon = (a - b)/a$	φ
 prolate	0	2.5
	0.2	2.36
	0.5	2.17
	0.8	2.04
	1.0	2.00
 oblate	0	2.5
	0.2	2.43
	0.5	2.31
	0.8	2.17
	1.0	2.06

⁴ Formula (10.31) shows that the orientation distribution of the ellipsoids is statistically homogeneous, as the bulk viscosity is isotropic.

3. Formulae (10.29), (10.31) and (10.32) have been derived on the basis of the assumptions that (i) the particles have a well-defined rigid form, (ii) the particle concentration is so sparse that the particles' interaction can be ignored, (iii) convective accelerations are neglected (STOKES flow with no OSEEN correction) and (iv) the particles are effectively buoyant, i.e. buoyancy forces are small and do not demix the suspension. Such prerequisites do practically not exist for the transport of suspended matter. LIN et al. [46] account for the convective acceleration term in the momentum equation and find for this OSEEN-type correction

$$\mu = \mu_0 \left\{ 1 + n \left[\frac{5}{2} + 1.34 \mathcal{R}_e^{3/2} \right] \right\}, \quad (10.34)$$

where

$$\mathcal{R}_e = \frac{a^2 G}{\mu_0 / \rho}$$

is the REYNOLDS number formed with the radius a of the spherical particle, G is the modulus of the velocity gradient of the shear flow ($= \frac{1}{2} J_2$, where $J_2 = \|\text{grad } \mathbf{v}\|$). Unfortunately, formula (10.34) only holds for small REYNOLDS numbers.

4. In the above formulae the volume fraction n is assumed small to the extent that the particles do not interact. BATCHELOR [4–6] and BATCHELOR and GREEN [8, 9] and others account for such interactions. For spherical particles they derive a formula for the dynamic viscosity that is accurate to $\mathcal{O}(n^2)$:

$$\mu = \mu_0 \left(1 + 2.5n + 7.6n^2 \right). \quad (10.35)$$

For a summary of more recent work, see [6]. Formula (10.35) is accurate for concentrations smaller than $n \approx 0.33$. This value follows from (10.35) by requesting that the third term is smaller than the second term to guarantee convergence. For suspensions a value of the volume fraction of 0.33 is in the regime of dense particle flow, in which particle dynamics is important, so that, dynamically, the binary structure should not be ignored. The validity of (10.35) is certainly guaranteed for $n \leq 0.1$, still larger than what one usually encounters in limnological applications.

10.4 Molecular Heat Conductivity of Water

STEIN [60] presents an equation for the heat conductivity. A further formula is contained in the ASME Steam Tables [1]. The formulae are relatively complex; they show that the pressure dependence can be ignored for $p \in [0, 200]$ bar. Table 10.7 lists values for the thermal conductivity κ as stated in the *Handbook of Chemistry*

Table 10.7 Thermal conductivity κ of pure water as given in the *Handbook of Chemistry and Physics* [33] and thermal diffusivities $\chi/(\rho c_p)$ deduced from them

Temperature T [°C]	Heat conductivity, κ		Thermal diffusivity $\chi = \kappa/(\rho c_p)$ [m ² s ⁻¹] $\times 10^{-7}$
	[cal s ⁻¹ m ⁻¹ K ⁻¹]	[W m ⁻¹ K ⁻¹]	
0	1348	0.56544	1.341
10	1381	0.5783	1.380
20	1420	0.5956	1.427

and *Physics* [33] (column 2) and our equivalence in SI units (column 3) and computed thermal diffusivities $\chi = \kappa/(\rho c_p)$. Quadratic interpolation yields⁵

$$\begin{aligned}\kappa &= 0.56544 + 6.094 \times 10^{-3}T + 2,220 \times 10^{-5}T^2 \quad [\text{W m}^{-1} \text{K}^{-1}], \\ \chi &= 1.341 + 3.50 \times 10^{-3}T + 4.0 \times 10^{-5}T^2 \quad [\text{m}^2 \text{s}^{-1}].\end{aligned}\quad (10.36)$$

Figure 10.10 displays these functions in the temperature regime $T \in [0, 25]^\circ\text{C}$. These results must hold for pure and mineralised water.

10.4.1 Heat Conductivity of Salt Water

POPOV et al. [57] have compiled measured and computed values of the heat conductivity of salt water with salinity $s \in [0, 40]$ ppt. Table 10.8 is taken from their book and references from which they took their information are stated in the last column. Values for $s = 0$ ppt lie exactly on the graph of κ in Fig. 10.10. On the other hand, the values in Table 10.8 show that a dependence of the heat conductivity on salinity is insignificant.

Table 10.9 displays the heat conductivities of ocean water with a salinity of 35 ppt and pressures $p \in [10, 1400] \times 10^5$ [Pa]. The data are taken from CASTELLI et al. [17]. Temperatures, for which the figures apply, are shown in the upper row.

Finally, the thermal diffusivities of salt water at selected values of the temperature $[(0, 20)^\circ\text{C}]$ and salinity $[(5, 35)$ ppt] have been given by MONTGOMERY [52]. The values are listed in Table 10.10.

⁵ The heat conductivity and thermal diffusivity are defined by the equations:

$$\rho c_p \frac{dT}{dt} = \kappa \nabla^2 T + \dots$$

and

$$\frac{dT}{dt} = \chi \nabla^2 T + \dots,$$

respectively. Note that the transformation $\chi = \kappa/(\rho c_p)$ only conforms with these equations for constant κ and c_p .

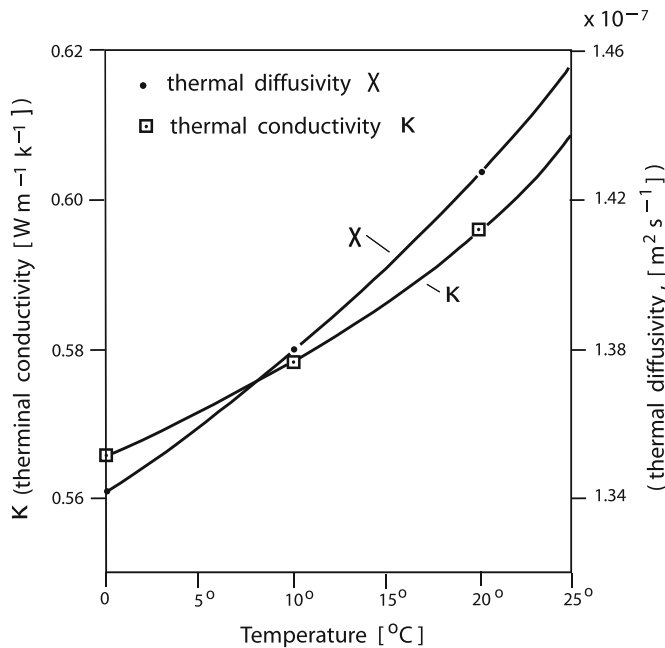


Fig. 10.10 Thermal conductivity and thermal diffusivity for pure water plotted against temperature in the interval $T \in [0, 25]^\circ\text{C}$

Table 10.8 Heat conductivity of salt water κ [$\text{W m}^{-1}\text{K}^{-1}$] at atmospheric pressure [10^5 Pa] and $s \in [0, 40]$ ppt, as compiled by POPOV et al. [57] from the indicated sources

T [°C]	s [ppt]								References
	0	10	17.2	30	33.82	34.4	35	40	
Measured									
0	0.5667				0.561				[27]
	0.5637				0.560				[27]
	0.565						0.565		[67]
20	0.5935						0.5965		[67]
25			0.594			0.583			[29]
	0.611				0.607				[27]
40	0.627						0.6235		[67]
Computed									
0	0.566						0.563		[52, 58]
17.5	0.586	0.572		0.566	0.563		0.561	0.559	[21]
	0.583	0.569		0.563	0.560		0.558	0.557	[3]
20	0.599						0.596		[52, 58]

10.4.2 Impurities

Contrary to the situation for saline water the functional dependence of the mixture thermal conductivity in fluids with suspensions is rather well known. The reason

Table 10.9 Heat conductivity κ [$\text{W m}^{-1}\text{K}^{-1}$] of ocean water at a salinity $s = 35$ ppt and for pressures $p \in [1, 140] \times 10^6$ [Pa] and as measured by CASTELLI et al. [17] and compiled by POPOV et al. [57]

p [10^4 Pa]	1.82°C		10.23°C		20.22°C		30.25°C	
100	0.555	0.558	0.571	0.570	0.558	0.585	0.600	0.598
2000	0.562	0.565	0.578	0.577	0.595	0.592	0.607	0.603
4000	0.569	0.571	0.585	0.584	0.603	0.599	0.614	0.611
6000	0.577	0.573	0.593	0.590	0.610	0.606	0.622	0.616
8000	0.583	0.585	0.599	0.598	0.616	0.613	0.628	0.624
10000	0.590	0.591	0.607	0.604	0.624	0.619	0.636	0.631
12000	0.596	0.595	0.613	0.612	0.629	0.626	0.642	0.638
14000	0.602	0.601	0.619	0.617	0.636	0.632	0.649	0.645

Table 10.10 Thermal diffusivity χ [$\text{m}^2 \text{s}^{-1}$] at atmospheric pressure [10^5 Pa] for $T = (0, 20)^\circ\text{C}$ and $s = (5, 35)$ ppt as given by MONTGOMERY [52]

T [$^\circ\text{C}$]	s [ppt]	
	5	35
0	1.34×10^{-7}	1.39×10^{-7}
20	1.43×10^{-7}	1.49×10^{-7}

is that problems of heat conduction and problems of electrical conduction for solid bodies are analogous and well known for the electrical problem.

Let κ_0 be the heat conductivity of the bearer fluid and $\alpha \kappa_0$ that for the particles in suspension. The heat conductivity, κ , of the mixture that is treated as a heat-conducting fluid is then a function of α , $\kappa = \kappa(\alpha)$ and the shape and constitution of the particles.

MAXWELL [48] solved this electrical conduction problem for rigid spherical inclusions at small concentration to the extent that interaction of particles could be ignored. He found

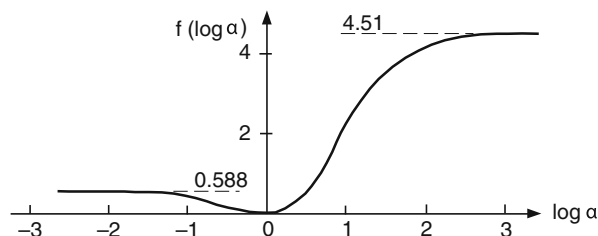
$$\kappa = \kappa_0 \left\{ 1 + \frac{3(\alpha - 1)}{(\alpha + 2)} n \right\}, \quad (10.37)$$

where n is the volume fraction. Hundred years later, JEFFREY [40] improved this formula to include second-order terms in the volume fraction

$$\kappa = \kappa_0 \left\{ 1 + \frac{3(\alpha - 1)}{(\alpha + 2)} n + f(\alpha) n^2 \right\}, \quad (10.38)$$

in which $f(\alpha)$ is plotted in Fig. 10.11 as a function of $\log_{10} \alpha$, as obtained by JEFFREY [40]. BATCHELOR [7] in his review summarises additional results for elliptical particles and spherical particles at any arbitrary concentration.

Fig. 10.11 Coefficient $f(\alpha)$ as a function of $\log_{10}\alpha$ (courtesy of Royal Society of London [40])



References

1. ASME-Steam-Tables.: *Thermodynamic and Transport Properties of Steam*. ASME, New York, NY (1967)
2. Assur, A.: *Composition of Sea Ice and Its Tensile Strength*. National Academy of Sciences, National Research Council, Washington, DC vol. 598 (1958)
3. Barrett, T. and Nettleton, H.R.: Thermal conductivity of liquids and solids. In: Vol. V of *International Critical Tables of Numerical Data, Physics, Chemistry and Technology*, (Ed. E.W. Washburn), McGraw-Hill Book Co. Inc., New York, pp. 218–233 (1929)
4. Batchelor, G.K.: Slender body theory for particles of arbitrary cross section in Stokes-flow. *J. Fluid Mech.* **44**, 419 (1970)
5. Batchelor, G.K.: The stress system in a suspension of forced particles. *J. Fluid Mech.* **41**, 545 (1970)
6. Batchelor, G.K.: Sedimentation in a dilute suspension of spheres. *J. Fluid Mech.* **52**, 245 (1972)
7. Batchelor, G.K.: Transport properties of two-phase materials with random structure. *Annu. Rev. Fluid Mech.* **6**, 227 (1974)
8. Batchelor, G.K. and Green, J.T.: The hydrodynamic interaction of two small freely moving spheres in a linear flow field. *J. Fluid Mech.* **56**, 375 (1972)
9. Batchelor, G.K. and Green, J.T.: The determination of the bulk stress in a suspension of spheres to order c^2 . *J. Fluid Mech.* **56**, 401 (1972)
10. Bingham, E.C. and Jackson, R.F. Standard Substances for the calibration of viscometers. *Bull. US Bur. Stand.* **14**(298), 59 (1917)
11. Bowman, H.A. and Schoonover, R.M.: Procedure for high precision density determinations by hydrostatic weighing. *J. Res. Natl. Bur. Stand.* **71c**(3), 179 (1967)
12. Bradshaw A. and Schleicher K.E.: Direct measurement of thermal expansion of sea water under pressure. *Deep Sea Res.* **17**(4), 691–706 (1970)
13. Bromley, L.A., Desaussure, V.A., Clipp, J.C. and Wright, J.S.: Heat capacities of sea water solutions. *J. Chem. Eng. Data* **12**(2), 202–206 (1967)
14. Bromley L.A., Diamond A.E., Salami E. and Wilkins D.C.: Heat capacities and enthalpies of sea salt solutions to 200 °C. *J. Chem. Eng. Data* **15**(2), 246–253 (1970)
15. Bühner, H. and Ambühl, H.: *Die Einleitung von gereinigtem Abwasser in Seen*. Interner Bericht der Eidg. Anstalt für Wasserversorgung, Abwasserreinigung und Gewässerschutz. Dübendorf, Switzerland (1975)
16. Camp, T.R.: *Water and its Impurities*. Reinhold, New York, NY (1963)
17. Castelli, V.J., Stanley, E.M. and Fischer, E.C.: The thermal conductivity of seawater as a function of pressure and temperature. *Deep Sea Res.* **21**(4), 311–319 (1974)
18. Chapman, S. and Cowling, T.G.: *Mathematical Theory of Non-uniform Gases*. Cambridge University Press, Cambridge (1939)
19. Chen, C.T. and Millero, F.J.: Precise thermodynamic properties for natural waters covering only the limnological range. *Limnol. Oceanogr.* **31**, 657–662 (1986)
20. Cox, R.A. and Smith, N.D.: The specific heat of sea water. *Proc. R. Soc. Lond.* **252A**, 51–62 (1959)

21. Defant, A.: *Physical Oceanography*. Vol. I, Pergamon, New York, NY (1961)
22. Dorsey, N.E.: *Properties of Ordinary Water Substance*. Reinhold, New York, NY (1940)
23. Einstein, A.: Eine neue Bestimmung der Moleküldimensionen. *Ann. d. Phys.* **29**, 298 (1906)
24. Einstein, A.: Berichtigung zu meiner Arbeit Eine neue Bestimmung der Moleküldimensionen. *Ann. d. Phys.* **34**, 591 (1911)
25. Ekman, V.W.: Die Zusammendrückbarkeit des Meerwassers. *Publ. Circonst. Cons. Perm. Inst. Explor. Mer.* **43**, 1 (1908)
26. Ekman, V.W.: Der adiabatische Temperaturgradient im Meere. *Ann. d. Hydrogr. u. Mar. Meteor.* **42**(1), 340–44 (1914)
27. Emerson, W.H. and Jamieson, D.T.: Some physical properties of sea water in various concentrations. *Desalination* **3**(2), 213–224 (1967)
28. Fabuss, B.M.: *Thermophysical Properties of Saline Water System Research and Development Progress*. U.S. Department of the Interior, Office of Saline Water, Report No **189**, May (1966)
29. Fabuss, B.M. and Corosi, A.: *Office Saline Water Research*, Development Progress Report No **384** (1968)
30. Fabuss, B.M. and Corosi, A.: Viscosities of aqueous solutions of several electrolytes present in sea water. *J. Chem. Eng. Data* **14**, 192 (1969)
31. Fofonoff, N.P.: Physical properties of sea water. In: *The Sea, Physical Oceanography*. Vol. 1 (ed. Hill, M. N., London: Interscience, pp. 3–30 (1962)
32. Hall, L.: The origin of excess ultrasonic absorption in water. *Phys. Rev.* **73**, 775 (1948)
33. *Handbook of Chemistry and Physics* (44th Edition) ed. by C.D. Hodgman, Chemical Rubber Publishing Company, Cleveland, OH (1962)
34. Henderson-Sellers, B.: *Engineering Limnology*. Pitman, Boston, MA, 1–265, 356 p. (1984)
35. Hutter, K. and Trösch, J.: *Über die hydrodynamischen und thermodynamischen Grundlagen der Seezirkulation*. Mitteilung Nr 20 der Versuchsanstalt für Wasserbau, Hydrologie und Glaziologie an der ETHZ (ed. Vischer, D.), Zürich, 164 p. (1975)
36. Imboden, D.M. and Wüest, A.: Mixing mechanisms in lakes. In: *Physics and Chemistry of Lakes*. (eds. Lerman, A., Imboden, D.M. and Gat, J.R.), Springer, Berlin, 83–138 (1995)
37. Isdale, J.D. and Morris, R.: Physical properties of sea water solutions. *Desalination* **10**, 329–338 (1972)
38. Isdale, J.D., Spence, C.M. and Thudhope, J.S.: Physical properties of sea water solutions. *Desalination* **10**, 319–328 (1972)
39. Jäger, W. and Steinwehr, H.: Thermal Capacity of Water between 5° and 50°. *Sitzungsber. Preuss. Akad. Wiss.* Berlin, 424–432 (1915)
40. Jeffrey, D.J.: Group expansions for the bulk properties of a statistically homogeneous random suspension. *Proc. R. Soc. Lond.* **338A**, 503 (1974)
41. Jeffrey, G.B.: The motion of ellipsoidal particles immersed in a viscous fluid. *Proc. R. Soc. Lond.*, **102A**, 161 (1922)
42. Kearsley, E.A.: An analysis of an absolute torsional pendulum viscometer. *Trans. Soc. Rheol.* **3**, 69 (1959)
43. Knudsen, M.: *Hydrographical Tables*. Gad. Copenhagen and Williams Margate, London, 1–63 (1901)
44. Krümmel, O.: *Handbuch der Ozeanographie*. Bd. **1**, Engelhorn, Stuttgart (1907)
45. Kuwahara, S.: The velocity of sound in sea water and calculation of the velocity for use in sonic sounding. *Jpn. J. Astron. Geophys.*, **16**(1), 1 (1938)
46. Lin, C.H., Perry, J.H. and Schowalter, W.R.: Simple shear flow round a rigid sphere: Inertial effects and suspension rheology. *J. Fluid Mech.* **44**, 1 (1970)
47. Marvin, R.S.: The accuracy of measurements of viscosity of liquids. *J. Res. Natl. Bur. Stand.* **75A**(6), 535 (1971)
48. Maxwell, J.C.: *Electricity and Magnetism*. (1st Edition), Clarendon Press, Oxford, 365 p. (1873)
49. Millero F.J. and Kubinski T.: Speed of sound in seawater as a function of of temperature and salinity at 1 atm. *J. Acoust. Soc. Am.* **57**(2), 312–319 (1961)

50. Millero, F.J., Perron, G. and Desnoyers, J.E.: Heat capacity of seawater solutions. *J. Geophys. Res.* **78**(21), 4499–4507 (1973)
51. Miyake, Y. and Koizumi, M.: The measurement of the viscosity coefficient of sea water. *J. Mar. Res.* **7**(2), 63 (1948)
52. Montgomery, R.B.: *Oceanographic Data*. American Institute of Physics Handbook. Sec. 2, Mechanics. McGraw Hill, New York, NY, 115–124 (1957)
53. Newton, M. and Kennedy, G.: An experimental study of the P-V-T-S relations in sea water. *J. Mar. Res.* **23**, 88 (1965)
54. Penn, R.W. and Kearsley, E.A.: An absolute determination of viscosity using channel flow. *J. Res. Natl. Bur. Stand.* **75**(6), 553 (1971)
55. Poiseuille, J.: Recherches experimentales sur le mouvement des liquids dans les tubes de très petits diameters. *Compt. Rend.* **11**, 961 (1840), **12**, 1041 (1841)
56. Ponizovsky, A.M., Meleshko, E.P. and Globina, N.I.: Viscosity and specific heat capacity of sea water and natural solutions. *Proc. Crimea Branch Rus. Acad. Sci.* **4**(1), 75–80 (1953) (in Russian)
57. Popov, N.I., Fedorov, K.N. and Orlov, V.M.: *Marine Water*. Nauka, Moscow, 328 p. (1979)
58. Riedel, L.: Die Wärmeleitfähigkeit von wässrigen Lösungen starker Elektrolyte. *Chem. Ing. Technik* **23**(3), 59–64 (1951)
59. Shimaraev M.N., Verbolov V.I., Granin N.G. and Sherstyankin P.P.: *Physical Limnology of Lake Baikal: A Review*. (Eds. Shimaraev, M.N., Okuda, S.) Baikal International Center for Ecological Research Irkutsk-Okayama. 89 p. (1994)
60. Stein, W.A.: Gleichungen für die dynamische Viskosität und Wärmeleitfähigkeit von reinem fluidem Wasser. *Wärme- und Stoffübertragung* **2**, 210 (1969)
61. Stein, W.A.: Das erweiterte Korrespondenzprinzip für die dynamische Idealviskosität und die Idealwärmeleitfähigkeit reiner Stoffe. *Wärme- und Stoffübertragung* **4**, 127 (1971)
62. Stokes, R.H. and Mills, R.: Viscosity of electrolytes and related properties. *Int. Encycl. phys. chem. chem. phys.*, **3**, 16, Pergamon, London (1965)
63. Taylor, G.I.: The viscosity of a fluid containing small drops of another fluid. *Proc. R. Soc. Lond.* **138A**, 41 (1932)
64. Thoulet, J. and Chevallier, A.: Sur la chaleur spécifique de l'eau de mer a divers degres de dilution et de concentration. *C. R. Acad. Sci. Paris* **108**(15), 794–796 (1889)
65. Tilton, L.W. and Taylor, J.K.: Accurate representation of the refractivity and density of distilled water as a function of temperature. *J. Res. Natl. Bur. Stand.* **18**, 205 (1937)
66. Truesdell, C.A. and Muncaster, R.G.: *Fundamentals of Maxwell's Kinetic Theory of a Simple Monatomic Gas*. Academic, New York, NY, XXVIII+593 p. (1980)
67. Tufeu, R.: *Etude expérimentale en fonction de la température et de la conductivité thermique de l'ensemble des gaz rares et de mélanges hélium-argon*. Ph.D. thesis, Université de Paris VI, 120 p., 47 figures, XIV tables (1971)
68. Wang D.P. and Millero F.J.: Precise representation of the P-V-T properties of water and sea water determined from sound speeds. *J. Geophys. Res.* **78**(30), 7122–7128 (1973)
69. Wilson, W. and Bradley, D.: An absolute determination of viscosity using a torsional pendulum. *Deep Sea Res.* **15**, 355 (1968)
70. White, H.S. and Kersley, E.A.: An absolute determination of viscosity using a torsional pendulum. *J. Res. Natl. Bur. Stand.* **75A**(6), 541 (1971)
71. Zubov, N.N.: *Oceanological Tables*. Hydrometeoizdat, Leningrad, 126 p. (1957) (in Russian)

Name Index

A

Ambühl, 393, 395
Anderson, 340
Archimed, 132, 133, 135, 136, 286
ASME, 399, 400, 412

B

Batchelor, 210, 222, 412, 415
Beaufort, 278
Berezin, 153
Bernoulli, 170, 225
Bessel, 352
Betten, 38
Bingham, 405
Bjerknes, 321
Block, 38
Boltzmann, 113
Boussinesq, 109, 110, 127, 128, 141, 145,
147–150, 153, 193, 194, 199, 205, 206,
212, 222, 224, 258, 299
Bowden, 357
Bowen, 38
Bowman, 391, 392
Bradley, 393, 394
Bradshaw, 404
Brown, 100, 398, 410
Brunt, 150, 287, 288, 290, 294, 295, 306
Bryson, 222
Bührer, 393, 395
Burger, 21
Bye, 328

C

Camp, 407
Caratheodory, 69, 79
Carnot, 69, 78, 79
Castelli, 413, 415

Cauchy, 68, 69, 74, 91, 108, 114, 115, 117,
118, 121–123, 125, 138, 139, 157, 404
Celsius, 391, 394, 405, 408
Chadwick, 38
Chen, 391, 394, 397
Choboter, 267
Clausius, 69, 79, 81
Cooper, 270, 357
Coriolis, 20, 21, 98, 151, 162, 165, 175, 195,
264, 267, 297, 319, 322, 323, 328, 330,
349, 357
Cosserat, 113
Csanady, 356, 358

D

d'Alembert, 226, 228, 258
Defant, 345, 346, 404
Descartes, 225
Dietrich, 182
Dirac, 295, 312
Dorsey, 405, 409
Duhem, 69, 79
Dulong, 98

E

Einstein, 221, 410, 411
Ekman, 212, 319–321, 340–348, 350, 351,
353–358, 360, 368, 375, 394, 404
Ellison, 353
Ertel, 172, 177
Euclid, 30, 31
Euler, 68, 74, 76, 86–88, 101, 128, 159, 170,
175, 224, 225, 293, 343, 353

F

Fabuss, 405, 407
Father Louis, 3
Fatio de Duillier, 5

FAVRE, 192, 193, 195

Fer, 269, 271

Fermat, 108

Feynman, 25, 222

Fick, 144, 145, 200, 212

Findenegg, 16

Fischer, 375

Fjeldstad, 370, 375

Fleming, 345

Fofonoff, 404

Forel, 5, 16, 19

Foristall, 372

Foucault, 98

Fourier, 200, 212, 229, 232, 297

Frisch, 210

Froude, 22

G

Galile, 68

Gauss, 60, 103, 106, 108, 136

Gedney, 320, 362, 364–368

Glauert, 188

Goldstein, 374

Green, 62, 91, 369, 371, 375, 412

Gurtin, 38

H

Hall, 405

Hansalic, 203

Heaps, 3, 328, 338, 345–347, 355–358, 363

Heaviside, 370

Helmholtz, 170–172, 175, 177, 179

Hidaka, 370

Hide, 177

Hinze, 210

Hollan, 3, 4

Hooke, 75

Hutchinson, 16, 266

Hutter, 38, 153, 203, 210, 211, 266, 294, 389, 405

I

Imboden, 396

Irish, 378

Isdale, 407–409

Ivanov, 270

J

Jackson, 405

Jäger, 403

Jänichen, 4

Jeffrey, 410, 415

Jelesnianski, 372, 376

Jöhnik, 8, 17, 38, 203, 210, 211, 266

Johnson, 345

Jones, 203, 357

Joule, 81

K

Katz, 177

Kearsley, 404, 405

Kelvin, 69, 79, 80, 82, 160, 161, 170, 255

Kennedy, 394

Kepler, 75

Kielmann, 372

Kirchhoff, 108

Klingbeil, 38

Knudsen, 394

Koizumi, 406, 408, 409

Kolmogorov, 212

Korosi, 407

Kowalik, 372

Kronecker, 32

Krümmel, 406

Kubinski, 403, 404

Kuwahara, 403

L

Lacomb, 350, 360

Lagrang, 86

Lagrange, 75

Lamb, 222, 374

Lanchester, 188

Landau, 222

Langmuir, 268

Laplace, 62, 128, 234, 300

Launder, 203

Lautrup, 222

Leaman, 270

LeBlond, 222, 294

Leibniz, 75, 180, 225

Leibovich, 222

Lesieur, 210

Lick, 320, 362, 364–368

Lifshitz, 222

Lighthill, 222, 294

Lin, 412

Liouville, 302

Liu, 38

Löffler, 16

Lumley, 210

M

Madsen, 351, 353, 355

Maiss, 47

Marshall, 269, 270

Massel, 222

- Maxwell, 405, 415
 Mayer, 69, 78, 81
 McComb, 210
 Mei, 222
 Miles, 339
 Millero, 391, 394, 397, 403, 404
 Mills, 405, 407
 Miyake, 406, 408, 409
 Monin, 210
 Montgomery, 413, 415
 Moore, 99
 Mortimer, 5, 7, 249, 254, 339
 Munk, 213, 214, 218, 219, 340
 Mysak, 222, 294
- N**
- Nansen, 321
 Napoleon, 391
 Navier, 98, 188, 194, 198, 200, 212, 349
 Newton, 67, 68, 70, 74–77, 83, 99, 117, 123,
 124, 128, 140, 166, 225, 279, 286, 319,
 331, 359, 394, 404, 410, 411
 Nomitsu, 375
- O**
- Oseen, 412
- P**
- Papin, 78
 Pascal, 131
 Pearce, 357
 Pedlosky, 165
 Phillips, 222
 Pickard, 345, 346
 Piquet, 210
 Planck, 79
 Platzman, 320, 321, 372, 374–385
 Poincaré, 255
 Pointing, 205
 Poiseuille, 404, 405
 Pond, 345, 346
 Popov, 399, 402, 403, 413–415
 Prandtl, 125, 188, 199–202, 204, 210, 328,
 351, 357, 358, 380
- R**
- Rao, 374
 REYNOLDS, 192
 Reynolds, 21, 103, 119, 136, 137, 185, 187,
 188, 192, 195, 196, 198, 199, 201, 203,
 210–214, 217, 219, 356, 412
 Richardson, 21, 339, 340
 Riemann, 108
 Rodi, 203
- Rossby, 21, 154
 Rotta, 210
 Ruellan, 243, 244
 Rupin, 406
- S**
- Sander, 211
 Sarasin, 5
 Schleicher, 404
 Schmidt, 200, 204
 Schoonover, 391, 392
 Schott, 270
 Schröder, 177
 Schulthaiss, 3
 Seebass, 222
 Send, 269, 270
 Shimaraev, 269
 Spalding, 203
 Spencer, 38
 Stein, 405, 412
 Steinwehr, 403
 Stoker, 222
 Stokes, 62, 64, 159, 164, 169, 188, 194, 198,
 200, 212, 217, 261, 349, 405, 407, 410, 412
 Stommel, 99
 Sturm, 302
 Svensson, 210, 355, 356
 Sverdrup, 345
- T**
- Taylor, 59, 115, 197, 235, 236, 286, 348, 373,
 391–393, 411
 Tennekes, 210
 Thomas, 363
 Tikhomirov, 20
 Tilton, 391–393
 Townsend, 210
 Trösch, 389, 405
 Treder, 177
 Truesdell, 69, 76, 79, 177
- U**
- Umlauf, 203
- V**
- Väisälä, 150, 287, 288, 290, 294, 295, 306
 Van Dyke, 222, 244
 Vaux, 270
 Venn, 225
 von Kármán, 351
- W**
- Wüest, 274, 396
 Walker, 222

Wallet, [243](#), [244](#)

Wang, [38](#), [212](#), [404](#)

Weber, [108](#)

Weis, [203](#)

Weisbach, [6](#)

Welander, [320](#), [363](#), [372](#)

White, [404](#), [405](#)

Whitham, [222](#)

Wilson, [393](#), [394](#)

Witten, [363](#)

Wüest, [141](#)

Y

Yaglom, [210](#)

Z

Zatsepin, [183](#)

Lake Index

A

Amadeus, [12](#)
Aral Sea, [12](#)
Athabaska, [12](#)

B

Baikal, [11](#), [12](#), [19](#), [20](#), [109](#), [141](#), [195](#), [266](#), [273](#),
[390](#)
Balaton, [11](#), [12](#)
Balkhash, [12](#)

C

Caspian Sea, [10–12](#)
Chad, [11](#), [12](#)
Constance, [3](#), [5](#), [11](#), [12](#), [15](#), [18](#), [47](#), [266](#), [269](#),
[275](#), [277–279](#), [307](#)

D

Dead Sea, [10](#), [12](#), [18](#)

E

Edward, [12](#)
Erie, [12](#), [320](#), [363–366](#), [376](#), [382](#), [385](#)
Eyre, [11](#), [12](#)

G

Gairdner, [12](#)
Geneva, [266](#), [269–271](#)
Great Bear, [12](#)
Great Lakes, [20](#)
Great Lakes of America, [266](#)
Great Salt, [12](#)
Great Slave, [12](#)
Green Bay, [3](#)

H

Huron, [12](#)

I

Issyk Kul, [12](#)

K

Kuronian lagoon, [207](#)

L

Lac Léman, [5](#), [7](#)
Ladoga, [12](#), [20](#), [266](#)
Lake of Geneva, [12](#)
Lake of the Four Cantons, [265](#)
Lake of Zürich, [12](#)

M

Manitoba, [12](#)
Maracaibo, [12](#)
Michigan, [3](#), [12](#)
Mweru, [12](#)

N

Neusiedler See, [207](#)
Nicaragua, [12](#)
Nyasa, [12](#)

O

Onega, [12](#), [20](#), [266](#)
Ontario, [12](#), [363](#)

Q

Qinghai, [11](#), [12](#)

R

Reindeer, [12](#)
Rudolf, [12](#)

S

Superior, [12](#)

T

Tanganyika, [11](#), [12](#), [195](#), [266](#)

Tianchi, [10](#)

Titicaca, [12](#)

Tonle, [12](#)

Torrens, [12](#)

Tung Ting, [12](#)

U

Urmia, [12](#)

V

Venern, [12](#)

Victoria, [11](#), [12](#)

Vierwaldstätter See, [265](#), [266](#)

Vistula lagoon, [207](#)

Volta, [12](#)

Vostok, [11](#), [12](#)

W

Winnipeg, [11](#), [12](#)

Winnipegosis, [12](#)

Wuxi, [207](#)

Z

Zürich, [294](#), [295](#), [297](#), [298](#)

Subject Index

A

Absolute acceleration, 97
Absolute system, 95
Absolute temperature, 69
Acceleration, 85, 88
Acoustic waves, 110
Adiabaticity assumption, 148
Algebraic Reynolds stress model, 211
Amictic lake, 17
Amplitude, 244
Angular momentum, 76
Angular velocity, 136
Angular velocity of the Earth, 35
Anisotropic turbulence, 212
Anisotropic turbulent flow state, 210
Anisotropy of viscous stresses, 410
Anisotropy tensor, 211
Anoxia, 266
Antarctica, 17
Anti-nodal lines, 249
Approximation
 constant density layer, 311
 constant-density-two-layer, 313
 long-wave, 239, 246
 rigid lid, 267, 316
 shallow water, 234
 short-wave, 238, 245
 two-layer, 281
Archimedian buoyancy force, 132, 135
Archimedian principle, 132, 133, 136, 286
Aspect ratio, 20, 150, 153
Associative law, 26, 27
Assumption
 hydrostatic pressure, 247
 long-wave, 247
 shallow-water, 247
Assumption of turbulent objectivity, 214
At the bottom surface, 209
At the free surface, 209

Autocorrelation, 197
Average, 185
Averaged density field, 197
Averaging operator, 187

B

Balance
 of energy, 77, 136
 of entropy, 69
 of linear momentum, 74
 of mass, 73, 100
 of moment of momentum, 76
 of momentum, 110
 of momentum of momentum, 110
Balance law, 67, 72, 80
 for dissipation rate
 of the turbulent kinetic energy, 203
 for the mixing length, 202
 for the turbulent kinetic energy, 203
 in a general form, 69
 of energy, 83, 103, 224
 of entropy, 103
 of internal energy, 140
 of linear momentum, 222
 of mass, 83, 103, 222
 of moment of momentum, 111, 112
 of momentum, 83, 103
 of momentum of momentum, 83
Baroclinicity, 311
Barycentric velocity, 193
Basal boundary condition, 208
Basal condition
 no-slip, 329, 332
 perfect sliding, 329, 332
 viscous linear sliding, 332
Basis, 30
Bathymetric profile, 47
Beats, 234
Beaufort's scale, 278

- Bottom slip, 328
- Boundary condition, 207
 - for k and ε , 209
 - for momentum, 207
 - for species concentration, 209
 - for the temperature, 208
- Boundary layer, 334
 - thickness, 243
 - turbulent, 351
- Boussinesq
 - approximated equation, 149
 - approximation, 147
 - assumption, 145
 - fluid, 109, 127, 141, 145, 153
 - number, 153
- Boussinesq fluid, 193, 194, 199, 205, 206, 212, 299
- Brownian motion, 100, 398
- Brunt-Väisälä frequency, 287, 289, 290, 294, 295, 306
- Buoy, 222
- Buoyancy
 - effect, 205
 - force, 132, 133, 193
 - frequency, 150, 287
 - parameter, 153
 - period, 289, 290, 293
- Burger number, 21
- C**
- Cabbeling, 272
- Carrier medium, 221
- Cartesian coordinate system, 30
- Cauchy
 - lemma, 114, 117
 - stress tensor, 125
- Center of gravity (or mass), 274, 276, 278, 280, 281, 316
- Centigrades, 394
- Centrifugal force, 99
- Centripetal acceleration, 97
- Change in potential energy, 281
- Channel flow, 404
- Characteristic equation, 93
- Characteristic turbulent eddy, 192
- Circulation, 58, 264, 319
 - anticyclonic, 273
 - cyclonic, 273
 - steady, 322
 - wind-induced, 330
 - wind induced, 328
- Classical principle of relativity, 68
- Closure relation, 204
- Clusters, 389
- Coefficient
 - constant drag, 332
 - friction (drag), 329
 - of thermal expansion, 389, 396
 - skin friction, 380
- Cold monomictic, 17
- Collinear, 29
- Commutative law, 26
- Complex number, 26
- Component, 141
- Compressibility, 391
- Compressible fluid, 193
- Conductivity, 396
- Conservation
 - of energy, 69
 - of linear momentum, 69
 - of mass, 69
 - of moment of momentum, 69
- Conservation law, 9, 68
- Constituent, 141, 142
- Constitutive theory, 83
- Continuity equation, 106
- Continuous density variation, 280
- Convective acceleration, 323, 330
- Convective chimney, 269, 270
- Convective derivative, 87
- Convergence zone, 272
- Coriolis
 - acceleration, 35, 97, 195
 - force, 20, 99
 - parametre, 21
- Correlation, 190
- Counter phase, 249
- Cross-product, 33
- Curl, 57
- Current
 - drift, 354
 - vertical structure, 353
 - geostrophic, 349
 - gradient, 320, 327, 358, 360
 - slope, 327
 - surface, 353, 382
 - vertical structure, 319, 328, 336, 338
 - wind drift, 327, 346
 - wind-driven
 - steady, 358
 - wind-induced, 319
 - time-dependent, 369
 - vertical structure, 347
- Current meter, 245
- Cyclonic, 20

D

D'Alembert solution, 228
 De-aeration, 392
 Deep ocean convection, 269
 Deflection angle, 348
 Deformation gradient, 90
 Density, 389, 390
 of pure water, 391
 anomaly, 131, 153
 measurement, 391
 preserving, 106, 193
 weighted average, 193
 Density perturbation, 247
 Derivative, 41
 Deuterium, 389
 Differentiation, 41
 Diffusion, 141
 coefficient, 145
 of momentum, 264
 Diffusive mass flux of tracer, 144
 Diffusivity, 145
 Dilatant, 123
 fluid, 124
 Dimension, 29
 Dimictic, 16, 266
 lake, 17
 Dirac pulse, 295
 Direct Numerical Simulation, 194, 210, 212
 Direction of steepest descent, 47
 Dispersion, 232
 Dispersion relation, 228, 242, 245
 finite-depth, 246
 quantised, 257
 Dissipation, 140, 224, 299, 308
 Dissipation rate
 density, 198
 due to the mean velocity, 198
 due to the mean velocity field, 198
 Distance, 29
 Distribution of
 density, 263
 mass, 262, 263
 Distributive law, 27
 Diurnal circulation, 19
 Divergence
 free, 106
 of tensor field, 50
 of vector field, 50, 54
 operator
 for a second rank tensor field, 55
 solenoidal, 106
 theorem, 106
 DNS, 194, 210, 212

Down-stroke, 338
 Down-welling, 338
 Drag coefficient, 277, 290
 Drift, 244
 Dual vector, 57
 Dyadic product, 39
 Dynamic
 bulk, 127
 shear viscosity, 124

E

Early anisotropic closure scheme, 212
 Eddy, 7
 diffusivity, 200
 viscosity, 198
 Eddy viscosity, 331, 346, 351, 355, 357
 E-folding depth, 246
 E-folding time, 293
 Eigenfunctions, 252
 Eigenmodes, 252
 Eigenvalues, 252, 307
 problem, 252
 Ekman
 depth, 319, 342, 346, 348, 351, 360
 layer, 356
 problem, 320, 348
 spiral, 319, 341, 343, 346–348, 350
 theory, 340
 Electrical conductivity, 389, 390, 396
 Electronic recording unit, 296
 Ellipses, 242
 Energy, 68
 balance equation
 in conservative form, 139
 Enthalpy function, 140
 Entropy, 69, 79, 80
 production, 80
 Environment, 71
 Epilimnion, 8, 15, 275, 283, 296, 297, 308,
 310, 311, 330, 333, 337
 Equation
 acoustic, 222
 hydrostatic, 247
 Laplace, 234
 linear wave, 223
 of motion, 121
 kinematic, 236
 of state, 107
 wave, 226, 228
 Equations
 Bessel's differential, 352
 Navier-Stokes, 349
 shallow water, 240
 viscous hydrodynamic, 322

- Equivalent, 31
- Equivalent depth, 313
- Ergodic
 - property, 211
- Ergodic hypothesis, 189
- Ergodicity, 212
- Euclidean space, 31
- Euler acceleration, 97
- Euler's law
 - of angular momentum, 69
 - of moment of momentum, 76
- Eulerian
 - description, 86
 - representation, 86
- External
 - force, 76
 - pressure, 131
- Extinction coefficient, 205
- F**
- Favre average, 193
- Fetch, 277
- Fick's
 - first law, 145
 - of mass flux, 200
 - second law, 144
- Field
 - differentiation, 41
- Filter, 187
- Fingering, 267
- First Coriolis parameter, 36, 151
- First law of thermodynamics, 69, 78, 83, 136
- Fish rope, 241
- Fishline, 222
- Flow
 - simple shear, 339
 - wind-driven, 327
- Fluctuation, 185, 187
- Fluid
 - barotropic, 223
 - elastic, 223
 - Euler, 224
 - homogeneous, 235
 - ideal, 224
 - incompressible, 234
 - linearly stratified, 339
- Fluid body, 123
- Flux, 72
 - of entropy, 80
 - of spin, 76
- Force, 67
 - potential, 129
- Fourier
 - expansions, 229
 - integral, 229
 - series, 229
- Fourier's law
 - of heat conduction, 200
- Free (ideal, frictionless) slip, 337
- Free convection approximation, 147
- Free surface, 208
- Friction, 290
 - coefficient, 291
 - force, 290
- Froude number, 22
- Fundamental equation, 83
- Fundamental equations, 297
- G**
- Gauss
 - law, 136
- Geostrophic motion, 264, 267
- Gradient, 44
 - of tensor field, 50
 - of vector field, 50
- Gradient-type closure, 210
- Gravity, 263
 - current, 18, 268, 269
 - thermally-induced, 271
 - force, 110, 132
 - variation, 263
- Green's functions, 369, 371, 375
- Groundwater accretion, 208
- Group velocity, 232, 238
 - long-wave, 240
- Gyre, 7, 338
- H**
- Harmonic oscillator, 287
- Heat
 - flux, 279
 - latent, 265
 - sensible, 265
 - transfer coefficient, 279
- Heat conduction, 224
- Heat conductivity, 389, 412–415
- Heat flow, 77, 139
- Heat supply
 - radiation, 77
- Hodograph plane, 344, 360
- Holo, 15
- Holomictic, 15–17
- Holomictic lake, 16, 17
- Homogeneous water, 2
- Homogenisation, 276
 - of water masses, 274

Homothermy, 266
 Horizontal exchange coefficient, 213
 Horizontal velocities, 259, 260
 Hydrodynamics of lakes, 1
 Hydrogen, 389
 Hydrogen bonds, 389
 Hydrologic front, 271
 Hydrostatic
 equation, 129
 pressure assumption, 154
 Hydrostatic force balance, 297
 Hydrostatics, 110, 128
 Hypolimnion, 8, 15, 275, 283, 296, 297, 308, 310, 311, 330, 333, 337

I

Ideal fluid, 83, 127
 Impurities, 414
 elliptical particles, 415
 spherical particles, 415
 Incompressibility, 107
 Incompressible, 107
 Inertial reference system, 68
 Infinitesimal cube, 103
 Infrared radiation, 264
 Inland sea, 10
 Instability, 285
 transition to, 339
 Internal
 energy, 77
 oscillations, 2
 pressure, 131
 wave, 18
 Internal oscillations, 294
 Invariant, 93, 94
 Inverse stable
 temperature stratification, 15
 Inversely stably
 stratified, 15
 Irreversibility, 80
 Irreversible, 69
 Irrotational, 58
 Isomorphic, 31
 Isopycnal
 depth-time series, 296
 surfaces, 296
 time series, 297
 Isotherm
 depth-time series, 296, 311
 Isotropic, 190
 tensor, 210
 tensor function
 of tensors of second rank, 214
 turbulence, 190, 192

K

Kelvin
 temperature, 69
 Kinematic
 viscosity, 124, 185
 turbulent, 204
 Kinematics, 84
 Kinetic energy, 77
 Kinetic theory of gases, 405
 Kronecker Delta, 32

L

Lagrangean
 description, 86
 representation, 86
 Lake
 morphology, 5
 narrow homogeneous, 322
 stratified in two layers, 330
 Lake-level data, 376
 Lake-level-time series, 382
 Lake-surface fluctuations, 376
 Laminar, 6
 flow, 185
 Langmuir circulation, 268
 Laplace operator, 128, 300
 Laplacean operator, 223
 Large Eddy Simulation, 210, 212
 Law
 of conservation of energy, 67
 Left Cauchy–Green deformation tensor, 91
 Left stretch tensor, 90
 Length of a vector, 27
 LES, 189, 210, 212
 Limnetic, 18, 20
 Limnigraph, 245, 377, 382, 385
 Limnology, 396
 Linearly independent, 29
 Littoral, 3, 18, 20
 Littoral water, 271
 Local balance law, 103
 of internal energy, 139
 of mass, 105
 of momentum, 118
 Local derivative, 87
 Logarithmic
 singularity, 352, 358
 spiral, 343
 Longitudinal eigenmode, 254
 Longitudinal waves, 110

M

- Mass, 68
 - concentration of tracer, 143
 - density, 100
 - fraction, 143
- Material
 - behavior, 123
 - body, 25
 - particle, 84
 - time derivative, 86
- Matrix of the Cauchy stress tensor, 118
- Mean strain rate tensor, 214
- Mean value, 187
- Mechanics, 68
- Mero, 16
- Meromictic, 16, 266
- Meromictic lake, 17
- Metalimnion, 8, 15, 264, 282, 296, 297, 306, 308, 310–312, 332, 333
 - thickness, 311
- Method of separation of variables, 231
- Mictic, 15
- Mineralization, 390, 409
- Mixing, 274
- Mixing length, 201
- Mode, 305
 - baroclinic, 305, 307, 311
 - higher order, 311, 313
 - internal, 310
 - number, 308
 - of the horizontal velocity component, 311
 - of the vertical velocity component, 311
- Model- $(k - \ell)$, 202
- Model- $(k - \omega)$, 202
- Model- $(k - \varepsilon)$, 202
- Model- $(k - \varepsilon)$, 203
 - for Boussinesq fluids, 203
 - for density preserving, 203
- Molecular
 - heat capacity, 399
 - heat conductivity, 412
- Moment
 - of a force, 37
 - of a vector, 37
 - of flux
 - of linear momentum, 76
 - of supply
 - of linear momentum, 76
- Moment of momentum, 76
- Momentum, 68
 - equation
 - for a Newtonian Boussinesq fluid, 128

- flux, 74
 - of the body, 110
- Mono-lake, 17
- Monomictic, 17
- Mooring, 296
- Motion, 84
 - function, 84
- Munk's turbulence parameterization, 218

N

- Navier-Stokes
 - equation, 200
 - fluid, 198
- Navier-Stokes-Fourier-Fick equation, 212
- Net transport, 307
- Newton's law, 279
 - second, 286
- Newton's second law, 68, 74, 118
 - of motion, 67
- Newtonian Boussinesq fluid, 127
- n^{th} longitudinal mode, 254
- No-slip condition, 208
- Nodal lines, 249
- Nonequilibrium stress, 125
- Norm of a vector, 27
- Normal stress, 114

O

- ODF integrators, 241
- Oil spill trajectories, 355
- Oligomictic, 17
- One equation model, 201, 202
- Orthogonal, 29
- Orthonormal basis, 30
- Oscillations in rectangular basins, 252
- Oseen-type correction, 412
- Out of phase, 249
- Overturn, 266
- Oxygen, 389

P

- Partial derivative, 45
- Particle trajectories, 250, 251
- Particulate tracers, 410
- Pascal paradoxon, 131
- Pelagial, 3, 18
- Perturbation pressure, 234, 237, 246
- Phase
 - speed, 228, 231, 245
 - velocity, 230, 238
 - long-wave, 240
- Phenomenological coefficients, 389
- Photosynthesis, 8
- Physical balance law, 73

Physical law, 68
 Physical limnology, 1
 Physically realizable process, 212
 Physics of lakes, 1
 Phytoplankton population, 205
 Pointing vector, 205
 Poiseuille flow, 404
 Polar decomposition theorem, 90, 91
 Polymictic, 17
 Potential energy, 79, 277
 Power due to the wind action, 278
 Power of working, 277, 404
 Power of working of the pressure, 140
 Prandtl
 layer, 357, 380
 mixing length, 328
 Prandtl number, 204, 210
 Present configuration, 84
 Pressure, 111, 235, 255, 394
 absolute, 392
 barometric, 391
 gauge, 247
 work parameter, 153
 Principia, 124
 Principle of determinism, 67
 Process
 adiabatic, 224
 homotropic, 224
 isentropic, 224
 Process variables, 77
 Processes
 baroclinic, 263, 267
 barotropic, 263, 267
 external, 264, 267
 internal, 264, 267
 Production, 72, 142
 of entropy, 80
 Production rate density
 of species c , 206
 Profundal zone, 18
 Projection, 211
 filter, 211
 Proper value, 252
 problem, 252
 Protium, 389
 Pseudoplastic, 123, 124
 Pure longitudinal mode, 258
 Pure transversal mode, 258

R

Radiating source, 139
 Radiation, 263, 299
 RANS, 189, 210, 211

Real number, 26
 Rectangular basin, 254
 Reference configuration, 84
 Reflection, 244, 247
 Relative
 acceleration, 97
 system, 95
 velocity, 97
 Reynolds
 averaged equation, 211
 averaging procedure, 195
 hypothesis, 198
 number, 21, 185
 stress, 214
 stress tensor, 196, 199, 213, 217
 theorem, 136
 transport theorem, 119, 137
 versus Favre average, 192
 Richardson number, 21, 339
 Right Cauchy–Green deformation tensor, 91
 Right stretch tensor, 90
 Rigid lid, 302
 Rigid spherical inclusions, 410
 River
 inflow, 362
 outflow, 362
 Rossby
 number, 21, 153, 154
 radius of deformation, 21
 Rotation, 57
 of tensor field, 50
 of vector field, 50
 Roughness length, 355

S

Salinity, 390, 394, 396
 Scalar, 25
 product, 27
 Schmidt number, 204
 Seasonal variation
 of the temperature, 3
 of the thermocline, 8
 Second Coriolis parameter, 36, 151
 Second law of thermodynamics, 69
 Second rank tensor, 53
 Second statistical moment, 190
 Seiche, 5
 Separation of variables technique, 302
 Set-up, 325, 378, 379, 382, 383
 current, 327
 Shallow shore region, 246
 Shallow water
 approximation, 20, 150, 154

- equation, 150
 - scaling, 218
 - Shear
 - instability, 339
 - stress, 111, 114
 - vertical structure, 328, 336
 - viscosity, 127
 - Shear traction, 277
 - Sigmoidal curve, 339
 - Sigmoidal density profile, 282, 295
 - Simple shear experiment, 125
 - Skewness, 339
 - Skewsymmetric, 52
 - Slidig friction law, 329
 - Solar irradiation, 2
 - Solar radiation, 264, 266
 - Solid body, 123
 - Space scale, 185
 - Specific density, 131
 - Specific heat, 389, 399
 - at constant pressure, 400, 401, 403
 - at constant volume, 403
 - Speed of sound, 223
 - adiabatic, 224
 - Spin, 76
 - Spin tensor, 57, 89
 - Spring circulation, 15, 18
 - Stability, 285
 - Stable direct summer stratification, 15
 - Standard litre, 391
 - State variables, 77
 - Stationary random process, 187
 - Steady, 106
 - Stokes
 - assumption, 217
 - Strain rate, 126
 - deviator, 126
 - tensor, 89
 - Strain rate tensor, 351
 - Stratification, 17, 264, 312
 - linear, 304, 308
 - neutrally stable, 268
 - stable, 266, 267, 274, 287, 289
 - summer, 308
 - unstable, 267, 268, 287, 289
 - locally, 294
 - Stratified, 2
 - Streaklines, 6
 - Stream
 - line, 243, 250
 - lines, 327, 328, 337, 338
 - Stream function, 364, 367
 - boundary conditions, 364
 - volume transport, 366
 - Stream line, 243, 250
 - Stream track, 379
 - Stress, 110
 - factor, 380
 - turbulent shear, 351
 - vertical shear, 330, 338
 - viscous, 323, 330
 - wind shear, 322, 343, 362
 - Stress tensor, 113, 114
 - Stress vector, 111, 113
 - Stretch tensor
 - left, 91
 - right, 91
 - Stretching deviator, 126
 - Stretching tensor, 89, 126
 - Structural front, 19
 - Sturm-Liouville eigenvalue problem, 302
 - Subgrid behavior, 201
 - Subgrid eddy momentum exchange, 212
 - Summary of $(k - \varepsilon)$ -equation, 206
 - Summer stratification, 14
 - Supply, 72
 - of angular momentum, 76
 - of entropy, 80
 - of spin, 76
 - Surface
 - basal, 235
 - displacement, 246
 - elevation, 245, 255, 259, 260
 - free, 235
 - Surface force, 76, 111
 - Surface gravity waves, 234
 - linearized
 - dispersion relation, 238
 - Surface tension, 389
 - Surface wall layer, 356
 - Surface water
 - penetration to depth, 268
 - Surges, 376
 - Suspended matter, 398, 410
 - Suspended substance, 141
 - Symbolic notation, 31
 - Symmetric, 52
- T**
- Temperature, 394
 - boiling, 389
 - freezing, 390
 - melting, 389
 - of maximum density, 397

- Temperature correlation, 197
 - Tensor, 25, 38
 - product, 39
 - Tetrahedron, 116
 - Thermal
 - bar, 271, 273
 - conductivity, 413, 414
 - of a mixture, 414
 - convection, 268
 - diffusion, 296, 299
 - diffusivity, 389, 413, 415
 - equation of state, 297, 393
 - expansion, 275, 283
 - Thermal bar, 19
 - Thermal equation of state, 107, 126
 - Thermals, 269
 - Thermistor chain, 245, 294, 296
 - Thermobaric effect, 274
 - Thermocline, 15, 264, 295, 330, 339
 - depth, 279
 - Thermodynamic pressure, 126, 140
 - Thermodynamics, 68
 - Thermometry of lakes, 5
 - Tides
 - on Lake Erie, 376
 - Time scale, 185
 - Torsion pendulum, 404
 - Total transport, 344
 - Trace operator, 53
 - Tracer, 2, 141
 - Traction vector, 111
 - Trajectories, 240, 243, 244
 - particle, 242, 250
 - Trajectory, 87
 - Transfer matrix, 314
 - Transport, 2
 - Transport stream function, 361
 - Transport theorem, 103
 - Transpose of tensor, 52
 - Transversal modes, 254
 - Transverse eigenmode, 254
 - Transverse waves, 110
 - Tritium, 389
 - Turbidity, 2
 - Turbidity currents, 269
 - Turbocline, 8, 265, 268
 - Turbulence, 6, 18
 - Turbulence activity, 266
 - Turbulent
 - diffusivity, 201
 - dissipation rate, 198, 201, 202
 - eddies, 268
 - exchange coefficient, 199
 - flow, 185
 - heat flux, 199
 - heat flux vector, 196
 - kinematic viscosity, 199
 - kinetic energy, 190, 198, 201, 202
 - mass flux vector, 196
 - mixing, 268
 - motion, 185
 - Prandtl number, 200
 - Schmidt number, 200
 - shear stress, 199
 - species diffusivity, 204
 - species mass flux, 196, 199
 - thermal diffusivity, 204
 - viscosity, 125, 201
 - vorticity, 202
 - Two equation model, 201, 202
- V**
- Vapour, 389
 - Vector, 25
 - field, 54
 - product, 33
 - space, 26
 - valued field, 50
 - Velocity, 85
 - of the surface current, 348
 - Velocity components, 255
 - Velocity measurements, 311
 - Vertical exchange coefficient, 213
 - Viscometer, 404
 - Viscosity
 - bulk, 404, 405
 - dynamic, 389, 406–412
 - kinematic, 389, 407
 - shear, 404, 405, 409
 - Viscous contribution
 - to the stress, 140
 - Viscous flow, 410
 - Viscous fluid, 83
 - Volume
 - force, 76
 - preserving, 107
 - Volume fraction, 398, 410, 412
 - Volume transport, 348, 361, 371
 - gyre, 366
 - vector, 382
 - Vortex stretching, 95
 - Vortex tilting, 95
 - Vorticity, 89
 - tensor, 89
 - vector, 89

W

Warm monomictic, 17

Water

standard seawater, 393

anomalies, 389

cascade, 19

density maximum, 14

mineralized, 413

natural, 390

pure, 390, 395, 400, 405–409, 413

rainwater, 389

saline, 390, 403, 406, 409, 413, 414

Water waves, 222, 244

Wave, 221

backward moving, 250

crest, 250

forward moving, 250

frequency, 227, 230, 238

length, 238

number, 227, 230, 232, 238

vector, 230, 231

phase, 227, 230, 233

plane, 230

propagation

dispersive, 232

non-dispersive, 232

quasi-standing, 248

standing, 248, 249

gravity, 251

solution, 253

surface, 234

trough, 250

Wave guide, 295

Waves

deep-water, 246

dispersive, 234

linear acoustic, 224

non-dispersive, 234, 247

plane, 224

shallow water, 246, 247

standing, 247, 258

surface water, 253

Weather station, 377

Wind, 263

data, 376–378

factor, 345, 355

induced current, 212

mixing, 268

set-up, 18

stress, 380

vector, 380

Wind-tide, 378

computation, 382

Winter

holomixis, 18

homothermy, 14, 15, 18

stagnation, 15

Winter cascading, 270

Wonder of the rising water, 4